PO Box 2345, Beijing 100023, China
Fax: +86-10-85381893
E-mail: wjg@wjgnet.com www.wjgnet.com

World J Gastroenterol 2004;10(16):2311-2317
World Journal of Gastroenterology
 ISSN 1007-9327

• REVIEW •

Drug therapy for ulcerative colitis

Chang-Tai Xu, Shu-Yong Meng, Bo-Rong Pan

Chang-Tai Xu, Editorial Department, Journal of Fourth Military Medical University, Fourth Military Medical University, Xi'an 710032, Shaanxi Province, China
Shu-Yong Meng, Department of Thoracic and Oncology Surgery, Shaanxi Provincial Textile Hospital, Xi'an 710038, Shaanxi Province, China
Bo-Rong Pan, Department of Oncology, Xijing Hospital, Fourth Military Medical University, Xi'an 710032, Shaanxi Province, China
Supported by the Science Foundation of Health Bureau of Shaanxi province, No.04D26
Correspondence to: Chang-Tai Xu, Editorial Department, Journal of Fourth Military Medical University, Fourth Military Medical University, 17 Changle West Road, Xi'an 710032, Shaanxi Province, China. xuct2001@163.com
Telephone: +86-29-83373804 **Fax:** +86-29-83374499
Received: 2004-03-23 **Accepted:** 2004-04-29

Abstract

Ulcerative colitis (UC) is an inflammatory destructive disease of the large intestine occurred usually in the rectum and lower part of the colon as well as the entire colon. Drug therapy is not the only choice for UC treatment and medical management should be as a comprehensive whole. Azulfidine, Asacol, Pentasa, Dipentum, and Rowasa all contain 5-aminosalicylic acid (5-ASA), which is the topical anti-inflammatory ingredient. Pentasa is more commonly used in treating Crohn's ileitis because Pentasa capsules release more 5-ASA into the small intestine than Asacol tablets. Pentasa can also be used for treating mild to moderate UC. Rowasa enemas are safe and effective in treating ulcerative proctitis and proctosigmoiditis. The sulfa-free 5-ASA agents (Asacol, Pentasa, Dipentum and Rowasa) have fewer side effects than sulfa-containing Azulfidine. In UC patients with moderate to severe disease and in patients who failed to respond to 5-ASA compounds, systemic (oral) corticosteroids should be used. Systemic corticosteroids (prednisone, prednisolone, cortisone, *etc.*) are potent and fast-acting drugs for treating UC, Crohn's ileitis and ileocolitis. Systemic corticosteroids are not effective in maintaining remission in patients with UC. Serious side effects can result from prolonged corticosteroid treatment. To minimize side effects, corticosteroids should be gradually reduced as soon as the disease remission is achieved. In patients with corticosteroid-dependent or unresponsive to corticosteroid treatment, surgery or immunomodulator is considered. Immunomodulators used for treating severe UC include azathioprine/6-MP, methotrexate, and cyclosporine. Integrated traditional Chinese and Western medicine is safe and effective in maintaining remission in patients with UC.

Xu CT, Meng SY, Pan BR. Drug therapy for ulcerative colitis. *World J Gastroenterol* 2004; 10(16): 2311-2317
http://www.wjgnet.com/1007-9327/10/2311.asp

INTRODUCTION

Ulcerative colitis (UC) is an inflammatory destructive disease of the large intestine characterized by motility and secretion disorders. Inflammation usually occurs in the rectum and lower part of the colon, but it may affect the entire colon[1-4]. UC rarely affects the small intestine except for the end section, called the terminal ileum. UC may also be called colitis or proctitis[4, 5].

Inflammation makes the colon empty frequently, causing diarrhea. Ulcers formed in places where the inflammation has killed the cells of colon, bleeding ulcers and pus discharge. UC is an inflammatory bowel disease (IBD) that causes inflammation in the small intestine and colon. UC can be difficult to diagnose because its symptoms are similar to other intestinal disorders and another type of IBD called Crohn's disease (CD). CD differs from UC because it causes deeper inflammation within the intestinal wall[5-7]. Also, CD usually occurs in the small intestine, although it can also occur in the mouth, esophagus, stomach, duodenum, large intestine, appendix, and anus. UC may occur in people of any age, but most often it starts between ages 15 and 30, or less frequently between ages 50 and 70. Children and adolescents sometimes develop the disease. UC affects men and women equally and appears to run in some families.

UC CHARACTERISTICS

Of the estimated two million Americans suffer from IBD, CD is far less common than UC, but currently the incidences of each are estimated to be about equal. The incidence may vary depending on gender, age, and geography[4-6]. Men and women have an equal risk for UC. IBD is diagnosed most often in young people between the ages of 10 and 19, but it can occur at any age. A smaller peak onset occurs between 50 and 80 years. About 2% of IBD cases appear in children below age 10. UC is most common among people of European descent. People of African descent have a lower incidence than Caucasians. Low incidence regions include Asia and South America. Ethnically, Jewish people have a higher risk. UC may disproportionately affect people of higher socioeconomic classes, but evidence for this is inconclusive.

UC shares certain characteristics[4-8]: (1) Symptoms usually appear in young adults. (2) Symptoms can develop gradually or suddenly. (3) Both are chronic. The symptoms may flare up (relapse) after symptom-free periods (remission) or symptoms may be continuous without treatment. (4) The disease can be mild or very severe and disabling. (5) The severity of symptoms and relapse rates of both UC and DC vary with seasons, with the highest risk in winter and autumn and lowest in summer.

Factors associated with UC

Smokers have lower than average rates of UC (but higher than average rates of CD). In fact, it has been reported that some patients with UC had disorders after they gave up smoking, and many studies have stressed the association between smoking and protection against UC. This information is certainly no encouragement to smoke. Rather, patients should ask their physician about trials using nicotine replacement aids. Breast feeding also appears to be associated with lower risk of UC. Left-handed people have a significantly higher risk for both IBDs and other diseases associated with immune abnormalities. A 2001 study reported that patients with UC were more likely to have a history of depression or anxiety than those without IBD. Some researchers suggested that depression might alter the immune system and make people more susceptible to UC[3,4].

Symptoms of UC

General symptoms Fever may occur with severe attacks, usually a low-grade. Spiking fever and chills indicate complications. Loss of appetite, weight loss and impaired growth in children are usually not evidence of mild or moderate or severe UC. Increased frequency, a feeling of incomplete evacuation, tenesmus (a painful urge for a bowel movement even if the rectum is empty) and fecal incontinence may occur in mild or severe stage. Anal ulcers and fistulae, channels that can burrow between organs, loops of intestine or between intestines and skin, may be early symptoms. Recurrent diarrhea is very common, but the onset may be very gradual and mild or silent. Feces may also contain mucus. Recurrent diarrhea is prevalent in developing countries, particularly in tropical regions[6-8]. Blood is always present in stools, it may be readily visible or visible only using a microscope (so-called occult blood). Constipation can be a symptom of UC but not as common as diarrhea. It can occur during flare-ups, and when the inflamed rectum triggers a reflex response in the colon that causes it to retain the stool. But constipation in CD is usually a symptom of obstruction in the small intestine.

Abdominal symptoms Pain is not a prominent symptom but can vary. Vague discomfort may occur in the lower abdomen, an ache around the top of the hipbone, or cramps in the middle of the abdomen. Severe pain can occur during flare-ups. Recurrent episodes of pain in the lower right part of the abdomen or above the pubic bone often precede and are relieved by defecation. Bloating, nausea, and vomiting may also occur. Intestinal pain may also be an indication of serious conditions, such as an abscess, or a perforation of the intestinal wall.

Complications of UC Patients with UC limited to the rectum (proctitis) or colitis limited to the end of the left colon (proctosigmoiditis) usually do quite well. Short periodic treatments using oral medications or enemas may be sufficient. Serious complications are rare in these patients. In those with a more extensive disease, blood loss from the inflamed intestines can lead to anemia, and may require treatment with iron supplements or even blood transfusions. Rarely, the colon can acutely dilate to a large size when the inflammation becomes very severe. This condition is called toxic megacolon. Patients with toxic megacolon are extremely ill with fever, abdominal pain and distention, dehydration, and malnutrition. Unless the patient improves rapidly with medication, surgery is usually necessary to prevent colon rupture[3-5,7,8].

Colon cancer is a recognized complication of chronic UC. The risk for cancer begins to rise significantly after 8 to 10 years of colitis. The risk of a patient with UC developing colon cancer is also related to the location and the extent of the disease. Patients with only ulcerative proctitis probably do not have increased colon cancer risk compared to the general population. Among patients with active pancolitis of 10 years or longer, their risk of colon cancer is 10-20 times higher that of the general population. In patients with chronic left-sided colitis, the risk of colon cancer is increased but not as high as in patients with chronic pancolitis.

Since these cancers have a more favorable outcome when treated at an earlier stage, yearly colon examination is recommended after 8 years of a known extensive disease. During these examinations, samples of tissue (biopsies) should be taken to search for precancerous lesions in the lining cells of the colon. When precancerous lesions are found, removal of the colon may be necessary to prevent colon cancer.

Complications of UC involve other parts of the body. Ten percent of the patients can develop inflammation of the joints (arthritis). Some patients have low back pain due to arthritis of the sacroiliac joints. Rarely, patients may develop painful and red skin nodules (erythema nodosum). Yet others can have painful and red eyes (uveitis, episcleritis). Because these particular complications are a permanent risk in vision impairment, eye pain or redness is symptoms that require a physician's evaluation. Diseases of the liver and bile ducts may associate with UC. For example, in rare patients with a condition called sclerosing cholangitis, repeated infections and inflammation in the bile ducts can lead to recurrent fever, yellowing of skin (jaundice), cirrhosis, and the need for a liver transplant.

DRUG TREATMENT

Both medications and surgery have been used to treat UC[7-21]. However, surgery is reserved for those with severe inflammation and life-threatening complications. There is no medication that can cure UC. Patients with UC will typically experience periods of relapse (worsening of inflammation) followed by periods of remission lasting for mo to years. During relapses, symptoms of abdominal pain, diarrhea, and rectal bleeding can worsen patients' quality of life. During remissions, these symptoms subside. Remissions usually occur because of treatment with medications or surgery, but occasionally they occur spontaneously.

Since UC cannot be cured by medications, the goals of treatment with medications are to induce remissions, maintain remissions, minimize side effects of treatment, and improve the quality of life. The treatment of UC with medications is similar, though not always identical, to the treatment of CD[9-11,16-20].

Medications treating UC include anti-inflammatory agents such as 5-ASA compounds, systemic and topical corticosteroids, and immunomodulators.

Anti-inflammatory medications that decrease intestinal inflammation are analogous to arthritis medications that decrease joint inflammation (arthritis). The anti-inflammatory medications used in the treatment of UC are topical 5-ASA compounds such as sulfasalazine (Azulfidine), olsalazine (Dipentum), and mesalamine (Pentasa, Asacol, Rowasa enema) that need direct contact with the inflamed tissues in order to be effective. Systemic corticosteroids can decrease the inflammation throughout the body without direct contact with the inflamed tissue. Systemic corticosteroids have predictable side effects in long-term treatment. Immunomodulators are medications that suppress the body's immune system either by reducing the cells that are responsible for immunity, or by interfering with proteins that are important in promoting inflammation. Immunomodulators are increasingly becoming important for patients with severe UC who do not respond adequately to anti-inflammatory agents. Examples of immunomodulators include 6-mercaptopurine (6-MP), azathioprine, methotrexate, and cyclosporine.

A somewhat curious new treatment is nicotine. It has long been observed that the risk of UC appears to be higher nonsmokers and in ex-smokers. In certain circumstances, patients could improve clinically when treated with nicotine while they failed to respond to other medications.

5-ASA compounds (azulfidine, asacol, pentasa, dipentum)

5-ASA (5-aminosalicylic acid), also called mesalamine, is chemically similar to aspirin. Aspirin (acetylsalicylic acid) has been used for many years in treating arthritis, bursitis, and tendinitis (conditions of tissue inflammation). Aspirin, however, is not effective in treating UC. On the other hand, 5-ASA is effective in treating UC if the drug can be delivered directly (topically) onto the inflamed colon lining[17-21]. For example, Rowasa for enema is a 5-ASA solution that is effective in treating inflammation in and near the rectum (ulcerative proctitis and ulcerative proctosigmoiditis). However, the enema solution cannot reach high enough to treat inflammation in the upper colon. Therefore, for most patients with UC, 5-ASA must be taken orally. When pure 5-ASA is taken orally, however, the

stomach and upper small intestine absorb most of the drug before it reaches the colon. Therefore, to be effective as an oral agent for UC, 5-ASA has to be modified chemically to escape absorption by the stomach and upper intestines. These modified 5-ASA compounds are sulfasalazine (Azulfidine), mesalamine (Pentasa, Asacol), and olsalazine (Dipentum).

Azulfidine

Sulfasalazine (Azulfidine)[22] has been used successfully for many years in inducing remission among patients with mild to moderate UC. Inducing remission means decreasing intestinal inflammation and relieving symptoms of abdominal pain, diarrhea, and rectal bleeding. Sulfasalazine has also been used for prolonged periods of time to maintain remissions.

Sulfasalazine consists of a 5-ASA molecule linked chemically to a sulfapyridine molecule. (Sulfapyridine is a sulfa antibiotic). Connecting the two molecules together prevents absorption by the stomach and upper intestines prior to reaching the colon. When sulfasalazine reaches the colon, bacteria in the colon will break the linkage between the two molecules. After breaking away from 5-ASA, sulfapyridine is absorbed into the body and then excreted in the urine. Most of the active 5-ASA, however, remains in the colon to treat colitis.

Most of the side effects of sulfasalazine are due to the sulfapyridine molecule. These side effects include nausea, heartburn, headache, anemia, skin rashes, and in rare instances, hepatitis and kidney inflammation. In men, sulfasalazine can reduce the sperm count which sperm count is reversible, and the count usually returns to normal after discontinuing sulfasalazine or by changing to a different 5- ASA compound.

The benefits of sulfasalazine generally are dose related. Therefore, high doses of sulfasalazine may be necessary to induce remission. Some patients cannot tolerate high doses because of nausea and stomach upset. To minimize stomach upset, sulfasalazine is generally taken after or with meals. Some patients find it easier to take Azulfidine-EN (enteric-coated form of sulfasalazine). Enteric-coating helps decrease stomach upset. The newer 5-ASA compounds do not have the sulfapyridine component and have fewer side effects than sulfasalazine.

Asacol

Asacol is a tablet consisting of 5-ASA compound, mesalamine, surrounded by an acrylic resin coating (Asacol is sulfa free)[22,23]. The resin coating prevents 5-ASA from being absorbed as it passes through the stomach and small intestine. When the tablet reaches the terminal ileum and colon, the resin coating dissolves, thus releasing 5-ASA into the colon.

Asacol is effective in inducing remissions in patients with mild to moderate UC. It is also effective when used for prolonged periods of time to maintain remissions. The recommended dose of Asacol to induce remission is two 400-mg tablets three times daily (total of 2.4 g/d). Two tablets of Asacol twice daily (1.6 g/d) are recommended for maintaining remission. Occasionally, the maintenance dose should be higher. As Azulfidine, the benefits of Asacol are dose-related. If patients do not respond to 2.4 g/d of Asacol, the dose is frequently increased to 3.6 g/d (and sometimes even higher) to induce remission. If patients fail to respond to the higher doses of Asacol, then alternatives such as corticosteroids are recommended.

Pentasa

Pentasa is a capsule consisting of 5-ASA compound mesalamine inside controlled-release spheres. Like Asacol, it is sulfa free. As the capsule travels down the intestines, 5-ASA inside the spheres is slowly released into the intestines. Unlike Asacol, mesalamine in Pentasa is released into the small intestine as well as colon. Therefore, Pentasa can be effective in treating inflammation in the small intestine and colon. Pentasa is currently the most logical 5-ASA compound for treating mild to moderate CD involving the small intestine. Pentasa is also used to induce remission and maintain remission among patients with mild to moderate UC[23,24].

Olsalazine (Dipentum)

Olsalazine (Dipentum) consists of two 5-ASA molecules linked together[24,25]. It is sulfa free. The linked 5-ASA molecules travel through the stomach and the small intestine unabsorbed. When the drug reaches the terminal ileum and the colon, normal bacteria in the intestine break the linkage and release the active drug into the colon and terminal ileum. Olsalazine has been used in treating UC and maintaining remissions. A side effect unique to olsalazine is secretory diarrhea (diarrhea resulting from excessive production of fluid in the intestines). This condition occurs in 5-10% of patients, and diarrhea sometimes can be severe.

Colazal

Colazal (balsalazide) is a capsule in which 5-ASA is linked by a chemical bond to another molecule that is inert (without effect on the intestine) and prevents 5-ASA from being absorbed[25-29]. This drug is able to travel through the intestine unchanged until it reaches the end of the small bowel (terminal ileum) and colon. There, intestinal bacteria break apart 5-ASA and the inert molecule, releasing 5-ASA. Because intestinal bacteria are most abundant in the terminal ileum and colon, Colazal is used to treat inflammation predominantly localized to the colon. Colazal recently has been approved by FDA for use in United States of America.

More clinical trials are needed to compare the effectiveness of Colozal to other mesalamine compounds such as Asacol in treating UC. Therefore in United States of Amerrica, 5-ASA, has to be individualized[27,28]. Colozal should be prescribed for patients who cannot tolerate or fail to respond to Asacol, also for patients with predominantly left sided colitis, since some studies seem to indicate that Colozal is effective in treatieng left sided colitis.

Rowasa enema

Rowasa is 5-ASA compound mesalamine in enema form and is effective in the treatment of ulcerative proctitis and ulcerative proctosigmoiditis (two conditions where active 5-ASA drugs taken as enemas can easily reach the inflamed tissues directly)[29,30]. Each Rowasa enema contains 4 g of mesalamine in 60 mL of fluid. The enema is usually administered at bedtime, and patients are encouraged to retain the enema through the night.

The enema contains sulfite and should not be used by patients with sulfite allergy. Otherwise, Rowasa enemas are safe and well tolerated.

Rowasa also comes in suppository form for treating limited proctitis. Each suppository contains 500 mg of mesalamine and usually is administered twice daily. While some patients improve within several days after using Rowasa, the usual course of treatment is 3-6 wk. Some patients may need even longer courses of treatment for optimal benefit. In patients who do not respond to Rowasa, oral 5-ASA compounds (such as Asacol) can be added. Some studies have reported increased effectiveness in treating ulcerative proctitis and proctosigmoiditis by combining oral 5-ASA compounds with Rowasa enemas. Oral 5-ASA compounds are also used to maintain remission in ulcerative proctitis and proctosigmoiditis[30].

Another alternative for patients who fail to respond to Rowasa or who cannot use Rowasa is cortisone enemas (Cortenema). Cortisone is a corticosteroid that is a potent anti-inflammatory agent. Oral corticosteroids are systemic drugs with serious and predictable long-term side effects. Cortenema is a topical corticosteroid that is less absorbed into the body than oral corticosteroids, and therefore, it has fewer and less side effects.

Side effects of 5-ASA compounds

Sulfa-free 5-ASA compounds have fewer side effects than sulfasalazine and also do not impair male fertility. In general, they are safe medications for long-term use and well tolerated[23-28]. Patients allergic to aspirin should avoid 5-ASA compounds because they are chemically similar to aspirin. In a few occasions kidney inflammation has been reported due to the use of 5-ASA compounds. These compounds should be used with caution in patients with known kidney disease. It also is recommended that blood tests of kidney function are obtained before and during the treatment.

A rare instance of acute worsening of diarrhea, cramps, and abdominal pain may occur at times and may be accompanied by fever, rash, and malaise. This reaction is believed to represent an allergy to t5-ASA compounds.

Corticosteroids for UC

Corticosteroids (prednisone, prednisolone, hydrocortisone, *etc*.) have been used for many years in the treatment of patients with moderate to severe CD and UC or who fail to respond to optimal doses of 5-ASA compounds[31-34]. Unlike 5-ASA compounds, corticosteroids do not require direct contact with inflamed intestinal tissues to be effective. Oral corticosteroids are potent anti-inflammatory agents. After absorption, corticosteroids exert prompt anti-inflammatory action throughout the body. Consequently, they are used in treating Crohn's enteritis, ileitis, and ileocolitis, as well as UC and Crohn's colitis. In critically ill patients, intravenous corticosteroids (such as hydrocortisone) can be given in the hospital. Corticosteroids are faster acting than 5-ASA compounds. Patients frequently experience improvement in their symptoms within days after using starting corticosteroids. Corticosteroids, however, do not appear to be useful in maintaining remissions in UC[22-24].

Proper use of corticosteroids

Once the decision is made to use oral corticosteroids, treatment usually is initiated with prednisone, 40-60 mg daily. The majority of patients with UC respond with an improvement in symptoms. Once symptoms improve, prednisone is reduced by 5-10 mg per wk until the dose of 20 mg per day is reached. The dose then is tapered at a slower rate until prednisone ultimately is discontinued. Gradually reducing corticosteroids not only minimizes the symptoms of adrenal insufficiency, but also reduces the chances of abrupt relapse of colitis.

Many doctors use 5-ASA compounds at the same time as corticosteroids. In patients who achieve remission with systemic corticosteroids, 5-ASA compounds such as Asacol are often continued to maintain remissions[10,17-19]. In patients whose symptoms return during reduction of the dose of corticosteroids, the dose of corticosteroids is increased slightly to control the symptoms. Once the symptoms are under control, the reduction can resume at a slower pace. Some patients become corticosteroid dependent and consistently develop symptoms of colitis whenever the corticosteroid dose is below a certain level. In patients who are corticosteroid dependent or unresponsive to corticosteroids, other anti-inflammatory medications, immunomodulator medications or surgery are considered. The management of patients who are corticosteroid dependent or patients with a severe disease which responds poorly to medications is complex. Doctors who are experienced in treating inflammatory bowel disease and in using immunomodulators should evaluate these patients.

Side effects of corticosteroids

Side effects of corticosteroids depend on the dose and duration of treatment. Short courses of prednisone, for example, usually are well tolerated with few and mild side effects. Long term high doses of corticosteroids usually produce predictable and potentially serious side effects. Common side effects include rounding of the face (moon face), acne, increased body hair, diabetes, weight gain, high blood pressure, cataracts, glaucoma, increased susceptibility to infections, muscle weakness, depression, insomnia, mood swings, personality changes, irritability, and thinning of bones (osteoporosis) with an accompanying increased risk of compression fractures of the spine. Children on corticosteroids can experience stunted growth.

The most serious complication of long-term corticosteroid use is aseptic necrosis of the hip joints. Aseptic necrosis means death of bone tissue. It is a painful condition that can ultimately lead to the need for surgical replacement of the hips. Aseptic necrosis also has been reported in knee joints. It is unknown how corticosteroids cause aseptic necrosis. The estimated incidence of aseptic necrosis among corticosteroid users is 3-4%. Patients on corticosteroids who develop pain in hips or knees should report the pain to their doctors promptly. Early diagnosis of aseptic necrosis with cessation of corticosteroids has been reported in some patients to decrease the severity of the disease and possibly help avoid hip replacement.

Prolonged use of corticosteroids can depress the ability of adrenal glands to produce cortisol (a natural corticosteroid necessary for proper functioning of the body). Abruptly discontinuing corticosteroids can cause symptoms due to a lack of natural cortisol (a condition called adrenal insufficiency). Symptoms of adrenal insufficiency include nausea, vomiting, and even shock. Withdrawing corticosteroids too quickly can also produce symptoms of joint aches, fever, and malaise. Therefore, corticosteroids need to be gradually reduced rather than abruptly stopped. Even after corticosteroids are discontinued, the ability of adrenal glands' to produce cortisol can remain depressed for mo to two years. The depressed adrenal glands may not be able to produce enough cortisol to help the body handle stresses such as accidents, surgery, and infections. These patients will need treatment with corticosteroids (prednisone, hydrocortisone, *etc*.) during stressful situations to avoid developing adrenal insufficiency. Because corticosteroids are not useful in maintaining remission in UC and CD and because they have predictable and potentially serious side effects, these drugs should be used for the shortest possible time.

Preventing corticosteroid-induced osteoporosis

Long-term use of corticosteroids such as prednisolone or prednisone can cause osteoporosis, because corticosteroids could decrease calcium absorption from intestines and increase loss of calcium from the kidneys and bones. Increasing dietary calcium intake is important but alone cannot halt corticosteroid-induced bone loss. Management of patients on long-term corticosteroids should include adequate calcium (1 000 mg/d if premenopausal, 1 500 mg/d if postmenopausal) and vitamin D (800 U/d) intake, needs for continued corticosteroid treatment and the lowest effective dose, a bone density study to measure the extent of bone loss in patients taking corticosteroids for more than 3 mo, regular weight-bearing exercise and stopping cigarette smoking, discussion with the doctor regarding the use of alondronate (Fosamax) or risedronate (Actonel) in prevention and treatment of corticosteroid induced osteoporosis.

Immunomodulator medications

Immunomodulators are medications that weaken the body's immune system, which is composed of immune cells and cell-produced proteins. These cells and proteins serve to defend the body against harmful bacteria, viruses, fungi, and other foreign invaders. Activation of the immune system causes

inflammation within the tissues where the activation occurs. Normally, the immune system is activated only when the body is exposed to harmful invaders. In patients with CD and UC, however, the immune system is abnormally and chronically activated in the absence of any known invaders. Immunomodulators decrease tissue inflammation by reducing the population of immune cells and/or by interfering with their production of proteins that promote immune activation and inflammation. Generally, the benefits of controlling moderate to severe UC outweigh the risks of infection due to weakened immunity. Examples of immunomodulators include azathioprine (Imuran), 6-mercaptopurine (6-MP, Purinethol), cyclosporine (Sandimmune), and methotrexate[31-37].

Azathoprine (imuran) and 6-MP (purinethol)

Azathioprine and 6-mercaptopurine (6-MP) are medications that weaken the body's immunity by reducing the population of a class of immune cells called lymphocytes[31]. Azathioprine and 6-MP are related chemically. Specifically, azathioprine is converted into 6-MP inside the body. In high doses, these two drugs are useful in preventing rejection of transplanted organs and in treating leukemia. In low doses, they are used to treat patients with moderate to severe CD and UC. Azathioprine and 6-MP are increasingly recognized by doctors as valuable drugs in treating CD and UC. Some 70% of patients with moderate to severe disease benefit from these drugs. Because of the slow onset of action and the side effects, 6-MP and azathioprine are used mainly in the following situations[31-34], UC and CD patients with severe diseases not responding to corticosteroids, patients experiencing undesirable corticosteroid-related side effects, patients dependent on corticosteroids and unable to discontinue them without developing relapses.

When azathioprine and 6-MP are added to corticosteroids in the treatment of UC patients who do not respond to corticosteroids alone, they may have an improved response to smaller doses, and shorter courses of corticosteroids may be used. Some patients can discontinue corticosteroids without experiencing relapses. The ability to reduce corticosteroid has earned the reputation of 6-MP and azathioprine as "steroid-sparing" medications[32-34]. In severe UC patients with severe disease who suffer frequent relapses, 5-ASA may not be sufficient, and more potent azathioprine and 6-MP will be necessary to maintain remissions. In the doses used for treating UC and CD, the long-term side effects of azathioprine and 6-MP are less serious than long-term oral corticosteroids or repeated courses of oral corticosteroids.

Side effects of 6-MP and azathioprine

Side effects of 6-MP and azathioprine include increased vulnerability to infections, inflammation of the liver (hepatitis) and pancreas (pancreatitis), and bone marrow toxicity (interfering with the formation of cells that circulate in the blood)[31-37].

The goal of treatment with 6-MP and azathioprine is to weaken the body's immune system in order to decrease the intensity of inflammation in intestines. However, weakening the immune system increases the vulnerability to infections. For example, in a group severe CD patients unresponsive to standard doses of azathioprine, raising the dose of azathioprine helped to control the disease, but two patients developed cytomegalovirus (CMV) infection.

Azathioprine and 6-MP-induced inflammation of the liver (hepatitis) and pancreas (pancreatitis) is rare. Pancreatitis typically causes severe abdominal pain and sometimes vomiting. Pancreatitis due to 6-MP or azathioprine occurs in 3-5% of patients, usually during the first several wk of treatment. Patients who develop pancreatitis should not receive either of these two medications again[38,39]. Azathioprine and 6-MP also suppress the bone marrow where red blood cells, white blood cells, and platelets are made. Actually, a slight reduction in white blood cell count during treatment is desirable since it indicates that the dose of 6-MP or azathioprine is high enough to have an effect. However, excessively low red or white blood cell counts indicate bone marrow toxicity. Therefore, patients on 6-MP and azathioprine should have periodic detection of blood counts (usually every two wk initially and then every 3 mo during maintenance) to monitor the effect of the drugs on their bone marrow. 6-MP can reduce the sperm count in men. When the partners of male patients on 6-MP conceive, there is a higher incidence of miscarriages and vaginal bleeding. There also are respiratory difficulties in the newborn. Therefore, it is recommended that whenever feasible, male patients should stop 6-MP and azathioprine for 3 mo before conception. Patients on long-term high dose azathioprine to prevent rejection of the kidney after kidney transplantation have an increased risk of lymphoma. There is no evidence at present that long-term use of azathioprine and 6-MP in low doses used in IBD increases the risk of lymphoma, leukemia or other malignancies[6,40].

6-MP characteristics

One problem with 6-MP and azathioprine is their slow onset of action. Typically, 3 mo or a longer time is required to achieve the full benefit of these drugs. During this time, corticosteroids frequently have to be maintained at high levels to control inflammation[33].

The reason for this slow onset of action is partly due to the way prescribed 6-MP by doctors. Typically, 6-MP is started at a dose of 50 mg/d. The blood count is then checked 2 wk later. If the white blood cell count (specifically the lymphocyte count) is not reduced, the dose is increased. This cautious, stepwise approach helps prevent severe bone marrow and liver toxicity, but delays benefit from the drug.

Studies have shown that giving higher doses of 6-MP early can speed up the benefit of 6-MP without increasing toxicity in most patients, but some patients do develop severe bone marrow toxicity. Therefore, the dose of 6-MP has to be individualized. Scientists now believe that an individual's vulnerability to 6-MP toxicity is genetically inherited. Blood tests can be performed to identify those individuals with increased vulnerability to 6-MP toxicity. In these individuals, lower initial doses can be used. Blood tests can also be performed to measure the levels of certain by-products of 6-MP[32-34]. The levels of these by-products in the blood help doctors more quickly determine whether the dose of 6-MP is right for the patient.

6-MP maintained treatment

Patients on maintainance with 6-MP or azathioprine for years have not any important long-term side effects. Their doctors, however, should closely monitor their patients on long-term 6-MP. There are data suggesting that patients on long-term maintenance with 6-MP or azathioprine fared better than those who stopped these medications. Those who stopped 6-MP or azathioprine were more likely to experience relapses, more likely to need corticosteroids or undergo surgery[22-24,40].

Methotrexate

Methotrexate is an immunomodulator and anti-inflammatory medication. Methotrexate has been used for many years in the treatment of severe rheumatoid arthritis and psoriasis, and is helpful in treating patients with moderate to severe CD who neither respond to 6-MP and azathioprine nor tolerate these two medications. Methotrexate may also be effective in patients with moderate to severe UC who do not respond to corticosteroids or 6-MP and azathioprine. It can be given orally or by weekly

injections under the skin or into the muscles. It is more reliably absorbed with the injections[35-39]. One major complication of methotrexate is the development of liver cirrhosis when the medication is given over a prolonged period of time (years). The risk of liver damage is higher in patients who also abuse alcohol or have morbid (severe) obesity. Generally, periodic liver biopsies are recommended for a patient who has received a cumulative (total) methotrexate dose of 1.5 g and higher[38-40].

Other side effects of methotrexate include low white blood cell counts and inflammation of the lungs.

Methotrexate should not be used in pregnancy.

Cyclosporine

Cyclosporine (Sandimmune) is a potent immunosuppressant used in preventing organ rejection after transplantation. It has also been used to treat patients with severe UC and CD. Because of the approval of infliximab (Remicade) for treating severe CD, cyclosporine will probably be used primarily in severe UC. Cyclosporine is useful in fulminant UC and severely ill patients who do not respond to systemic corticosteroids. Cyclosporine is available as an oral medication, but the relapse rate with oral cyclopsorine is high. Therefore, cyclosporine seems most useful when administered intravenously in acute situations[33-37].

Side effects of cyclosporine include high blood pressure, renal function impairment, and tingling sensations in the extremities. More serous side effects include anaphylactic shock and seizures.

Traditional Chinese medicine

A total of 10 218 patients with UC reported in Chinese medical literature and the cases diagnosed were analyzed according to the diagnostic criteria of Lennard-Jones from 1981 to 2000. The number of cases increased by 3.08 times over the past 10 years (2 506 patients were diagnosed from 1981 to 1990 while 7 512 patients were diagnosed from 1991 to 2000). Lesion range was described in 7 966 patients, 5 592 (70.2%) were proctosigmoiditis or proctitis, 1 792 (22.5%) left-sided colitis, 582 (7.3%) pancolitis. Among the 8 122 patients, 2 826 (34.8%) had first episode, 4 272 (52.6%) had chronic relapse, 869 (10.7%) were of chronic persistent type, 154 (1.9%) were of acute fulminant type. The course of the illness wwas described in 5 867 patients, 4 427 (75.5%) were less than 5 years, 910 (15.5%) between 5 and 10 years, 530 (9.1%) more than 10 years. Six hundred and sixteen patients (6.1%) had extraintestinal manifestations. The mean age at the diagnosis was 40.7 years (range 6-80 years, and the peak age 30-49 years). The male to female ratio was 1.09. Among the 270 patients diagnosed in our hospital, 36 had histories of smoking, there was no negative association between the severity of UC and smoking (P>0.05), 21 smokers were followed up for one year, 15 of them had given up smoking when the disease was diagnosed, and one year later, 7 patients relapsed, another 6 patients continued smoking, and one year later, 2 patients relapsed. Among the 270 UC patients diagnosed in our hospital, 4 patients (1.5%) from 2 families had a familial history of UC. Treatment was done in 6 859 patients, only 5-ASA and/or corticosteroid only in 1 276 patients (18.6%), Chinese herbs alone in 1 377 patients (20.1%), combined Chinese and Western medicine in 4 056 patients (59.1%), surgery was performed in 87 patients (1.3%), other treatments in 63 patients (0.9%). In China, the number of UC patients increased significantly in the past 10 years. Lesions were commonly located to the left side colon. The course was short with rare extraintestinal manifestations. The age of onset was relatively high. Males and females were nearly equally affected. No negative relation was found between smoking and severity of the disease. Familial relatives were rarely involved. Traditional Chinese medicine (TCM) was widely used in the treatment of UC[33].

Langmead *et al*.[41] reported that herbal remedies for the treatment of IBD included slippery elm, fenugreek, devil's claw, Mexican yam, tormentil and *Wei tong ning*, a traditional Chinese medicine. Reactive oxygen metabolites produced by inflamed colonic mucosa may be pathogenic. Aminosalicylates (5-ASA) are antioxidant and other such agents could be therapeutic. Luminol-enhanced chemiluminescence in a xanthine/xanthine oxidase cell-free system was used to detect superoxide scavenging by herbs and 5-ASA. Fluorimetry was used to define peroxyl radical scavenging by using a phycoerythrin degradation assay. Chemiluminescence was used to detect herbal effects on generation of oxygen radicals by mucosal biopsies from patients with active UC. All materials tested scavenged peroxyl dose-dependently. Oxygen radical release from biopsies was reduced after incubation in all herbs except Mexican yam. All six herbal remedies have antioxidant effects. Fenugreek is not a superoxide scavenger, while Mexican yam does not inhibit radical generation of inflamed biopsies. Slippery elm, fenugreek, devil's claw, tormentil and *Wei tong ning* are novel drugs in IBD.

A total of 118 patients with UC were treated by integration of traditional Chinese and Western medicine[42-44]. Another 86 cases of UC were treated by simple Western drugs as controls. The therapeutic effects on both groups were observed and compared after two therapeutic courses of 40 consecutive days. As a result, 39 cases were cured, 60 cases improved and 19 cases failed, with a total effective rate of 84% in the treatment group. In the control group, 15 cases were cured, 37 cases improved and 34 cases failed, with a total effective rate of 60.5%. Statistically, the difference was very significant (P<0.01). It can be concluded that treatment of UC by the integrated method is superior to that by simple Western drugs[40].

Treatment of chronic UC by traditional Chinese and Western medicine is safe and effective in maintaining remission[41-44].

REFERENCES

1 **Daperno M**, Sostegni R, Scaglione N, Ercole E, Rigazio C, Rocca R, Pera A. Outcome of a conservative approach in severe ulcerative colitis. *Dig Liver Dis* 2004; **36**: 21-28

2 **Hurlstone DP**, McAlindon ME, Sanders DS, Koegh R, Lobo AJ, Cross SS. Further validation of high-magnification chromoscopic-colonoscopy for the detection of intraepithelial neoplasia and colon cancer in ulcerative colitis. *Gastroenterology* 2004; **126**: 376-378

3 **Diculescu M**, Ciocirlan M, Ciocirlan M, Pitigoi D, Becheanu G, Croitoru A, Spanache S. Folic acid and sulfasalazine for colorectal carcinoma chemoprevention in patients with ulcerative colitis: the old and new evidence. *Rom J Gastroenterol* 2003; **12**: 283-286

4 **van Staa TP**, Cooper C, Brusse LS, Leufkens H, Javaid MK, Arden NK. Inflammatory bowel disease and the risk of fracture. *Gastroenterology* 2003; **125**: 1591-1597

5 **Winther KV**, Jess T, Langholz E, Munkholm P, Binder V. Survival and cause-specific mortality in ulcerative colitis: follow-up of a population-based cohort in Copenhagen County. *Gastroenterology* 2003; **125**: 1576-1582

6 **Thuraisingam A**, Leiper K. Medical management of ulcerative colitis. *Hosp Med* 2003; **64**: 703-707

7 **Raychaudhuri SP**, Raychaudhuri SK. Role of NGF and neurogenic inflammation in the pathogenesis of psoriasis. *Prog Brain Res* 2004; **146**: 433-437

8 **Lichtenstein GR**. Evaluation of bone mineral density in inflammatory bowel disease: current safety focus. *Am J Gastroenterol* 2003; **98**(12 Suppl): S24-S30

9 **Solem CA**, Loftus EV, Tremaine WJ, Sandborn WJ. Venous thromboembolism in inflammatory bowel disease. *Am J Gastroenterol* 2004; **99**: 97-101

10 **Kane SV**, Bjorkman DJ. The efficacy of oral 5-ASAs in the treatment of active ulcerative colitis: a systematic review. *Rev Gastroenterol Disord* 2003; **3**: 210-218

11 **Teml A**, Kratzer V, Schneider B, Lochs H, Norman GL, Gangl A, Vogelsang H, Reinisch W. Anti-Saccharomyces cerevisiae antibodies: a stable marker for Crohn's disease during steroid and 5-aminosalicylic acid treatment. *Am J Gastroenterol* 2003; **98**: 2226-2231

12 **Gionchetti P**, Rizzello F, Habal F, Morselli C, Amadini C, Romagnoli R,Campieri M. Standard treatment of ulcerative colitis. *Dig Dis* 2003; **21**: 157-167

13 **Sutherland L**, MacDonald JK. Oral 5-aminosalicylic acid for induction of remission in ulcerative colitis. *Cochrane Database Syst Rev* 2003: CD000543

14 **Toubanakis C**, Batziou E, Sipsas N, Galanopoulos G, Tzivras M, Archimandritis A. Acute pancreatitis after long-term therapy with mesalazine, and hyperamylasaemia associated with azathioprine in a patient with ulcerative colitis. *Eur J Gastroenterol Hepatol* 2003; **15**: 933-934

15 **Ustun S**, Dagci H, Aksoy U, Guruz Y, Ersoz G. Prevalence of amebiasis in inflammatory bowel disease in Turkey. *World J Gastroenterol* 2003; **9**: 1834-1835

16 **Diculescu M**, Ciocirlan M, Ciocirlan M, Pitigoi D, Becheanu G, Croitoru A, Spanache S. Folic acid and sulfasalazine for colorectal carcinoma chemoprevention in patients with ulcerative colitis: the old and new evidence. *Rom J Gastroenterol* 2003; **12**: 283-286

17 **Russinko PJ**, Agarwal S, Choi MJ, Kelty PJ. Obstructive nephropathy secondary to sulfasalazine calculi. *Urology* 2003; **62**: 748

18 **Norgard B**, Puho E, Pedersen L, Czeizel AE, Sorensen HT. Risk of congenital abnormalities in children born to women with ulcerative colitis: a population-based, case-control study. *Am J Gastroenterol* 2003; **98**: 2006-2010

19 **Aqel B**, Bishop M, Krishna M, Cangemi J. Collagenous colitis evolving into ulcerative colitis: a case report and review of the literature. *Dig Dis Sci* 2003; **48**: 2323-2327

20 **Moum B**. 5-aminosalicylic acid in the treatment of ulcerative colitis and Crohn's disease. *Tidsskr Nor Laegeforen* 2003; 1**23**: 2565-2567

21 **Wong JM**, Wei SC. Efficacy of Pentasa tablets for the treatment of inflammatory bowel disease. *J Formos Med Assoc* 2003; **102**: 613-619

22 **Loftus EV Jr**, Kane SV, Bjorkman D. Systematic review: short-term adverse effects of 5-aminosalicylic acid agents in the treatment of ulcerative colitis. *Aliment Pharmacol Ther* 2004; **19**: 179-189

23 **Chourasia MK**, Jain SK. Pharmaceutical approaches to colon targeted drug delivery systems. *J Pharm Pharm Sci* 2003; **6:** 33-66

24 **Edmond LM**, Hopkins MJ, Magee EA, Cummings JH. The effect of 5-aminosalicylic acid-containing drugs on sulfide production by sulfate-reducing and amino acid-fermenting bacteria. *Inflamm Bowel Dis* 2003; **9**: 10-17

25 **Foster RA**, Zander DS, Mergo PJ, Valentine JF. Mesalamine-related lung disease: clinical, radiographic, and pathologic manifestations. *Inflamm Bowel Dis* 2003; **9**: 308-315

26 **Farrell RJ**. Epidermal growth factor for ulcerative colitis. *N Engl J Med* 2003; **349**: 395-397

27 **Christodoulou D**, Katsanos K, Baltayannis G, Tzabouras N, Tsianos EV. A report on efficacy and safety of azathioprine in a group of inflammatory bowel disease patients in northwest Greece. *Hepatogastroenterology* 2003; **50**: 1021-1024

28 **Sinha A**, Nightingale J, West KP, Berlanga-Acosta J, Playford RJ. Epidermal growth factor enemas with oral mesalamine for mild-to-moderate left-sided ulcerative colitis or proctitis. *N Engl J Med* 2003; **349**: 350-357

29 **Paoluzi P**, D'Albasio G, Pera A, Bianchi Porro G, Paoluzi OA, Pica R, Cottone M, Miglioli M, Prantera C, Sturniolo G, Ardizzone S. Oral and topical 5-aminosalicylic acid (mesalazine) in inducing and maintaining remission in mild-moderate relapse of ulcerative colitis: one-year randomized multicentre trial. *Dig Liver Dis* 2002; **34**: 787-793

30 **Ebinger M,** Leidl R, Thomas S, Von Tirpitz C, Reinshagen M, Adler G, Konig HH. Cost of outpatient care in patients with inflammatory bowel disease in a German University Hospital. *J Gastroenterol Hepatol* 2004; **19**: 192-199

31 **Card T**, West J, Hubbard R, Logan RF. Hip fractures in patients with inflammatory bowel disease and their relationship to corticosteroid use: a population based cohort study. *Gut* 2004; **53**: 251-255

32 **Quondamcarlo C**, Valentini G, Ruggeri M, Forlini G, Fenderico P, Rossi Z. Campylobacter jejuni enterocolitis presenting as inflammatory bowel disease.*Tech Coloproctol* 2003; **7**: 173-177

33 **Reffitt DM**, Meenan J, Sanderson JD, Jugdaohsingh R, Powell JJ, Thompson RP. Bone density improves with disease remission in patients with inflammatory bowel disease. *Eur J Gastroenterol Hepatol* 2003; **15**: 1267-1273

34 **Katz S**. Update in medical therapy of ulcerative colitis: a practical approach. *J Clin Gastroenterol* 2002; **34**: 397-407

35 **Keven K**, Sahin M, Kutlay S, Sengul S, Erturk S, Ersoz S, Erbay B. Immunoglobulin deficiency in kidney allograft recipients: comparative effects of mycophenolate mofetil and azathioprine. *Transpl Infect Dis* 2003; **5**: 181-186

36 **Corominas H**, Baiget M. Clinical utility of thiopurine s-methyltransferase genotyping. *Am J Pharmacogenomics* 2004; **4**: 1-8

37 **Menachem Y**, Gotsman I. Clinical manifestations of pyoderma gangrenosum associated with inflammatory bowel disease. *Isr Med Assoc J* 2004; **6**: 88-90

38 **Schroder O**, Blumenstein I, Schulte-Bockholt A, Stein J. Combining infliximab and methotrexate in fistulizing Crohn's disease resistant or intolerant to azathioprine. *Aliment Pharmacol Ther* 2004; **19**: 295-301

39 **Feagan BG**. Maintenance therapy for inflammatory bowel disease. *Am J Gastroenterol* 2003; **98**(12 Suppl): S6-S17

40 **Hanauer SB**, Present DH. The state of the art in the management of inflammatory bowel disease. *Rev Gastroenterol Disord* 2003; **3**: 81-92

41 **Langmead L**, Dawson C, Hawkins C, Banna N, Loo S, Rampton DS. Antioxidant effects of herbal therapies used by patients with inflammatory bowel disease: an *in vitro* study. *Aliment Pharmacol Ther* 2002; **16**: 197-205

42 **Chen Q**, Zhang H. Clinical study on 118 cases of ulcerative colitis treated by integration of traditional Chinese and Western medicine. *J Tradit Chin Med* 1999; **19**: 163-165

43 **Meng M**. TCM differential treatment of 57 cases of chronic gastritis complicated by ulcerative colitis. *J Tradit Chin Med* 1999; **19**: 10-15

44 **Wang B**, Ren S, Feng W, Zhong Z, Qin C. Kui jie qing in the treatment of chronic non-specific ulcerative colitis. *J Tradit Chin Med* 1997; **17**: 10-13

Edited by Chen WW and Wang XL **Proofread by** Xu FM

PO Box 2345, Beijing 100023, China
Fax: +86-10-85381893
E-mail: wjg@wjgnet.com www.wjgnet.com

World J Gastroenterol 2004;10(16):2318-2322
World Journal of Gastroenterology
 ISSN 1007-9327

• LIVER CANCER •

Construction and selection of subtracted cDNA library of mouse hepatocarcinoma cell lines with different lymphatic metastasis potential

Li Hou, Jan-Wu Tang, Xiao-Nan Cui, Bo Wang, Bo Song, Lei Sun

Li Hou, Jan-Wu Tang, Xiao-Nan Cui, Bo Wang, Bo Song, Lei Sun, Department of Pathology, Dalian Medical University, Dalian 116027, Liaoning Province, China
Supported by the Natural Science Foundation of Liaoning Province, No. 20022122
Correspondence to: Dr. Jian-Wu Tang, Department of Pathology, Dalian Medical University, Dalian 116027, Liaoning Province, China. houli72@163.net
Telephone: +86-411-4720610
Received: 2003-06-05 **Accepted:** 2003-07-30

Abstract

AIM: In order to elucidate the molecular mechanism of lymphatic metastasis of hepatocarcinoma, we detected the difference of gene expression between mouse hepatocarcinoma cell lines Hca-F and Hca-P with different lymphatic metastasis potential.

METHODS: cDNA of Hca-F cells was used as a tester and cDNA of Hca-P cells was used as a driver. cDNAs highly expressed in Hca-F cells were isolated by the suppression subtractive hybridization (SSH) method. The isolated cDNA was cloned into T/A cloning vector. The ligation products were transformed into DH5 α competent cells. Individual clones were randomly selected and used for PCR amplification. Vector DNA from positive clones was isolated for sequencing.

RESULTS: There were 800 positive clones in amplified subtracted cDNA library. Random analysis of 160 clones with PCR showed that 95% of the clones contained 100-700 bp inserts. Analysis of 20 sequenced cDNA clones randomly picked from the SSH library revealed 4 known genes (mouse heat shock protein 84 ku, DNA helicase, ribosomal protein S13 ,ethanol induced 6 gene) and 3 expressed sequence tags (ESTs). Four cDNAs showed no homology and presumably represent novel genes.

CONCLUSION: A subtracted cDNA library of differentially expressed genes in mouse heptocarcinoma cell lines with different lymphatic metastasis potential was successfully constructed with SSH and T/A cloning techniques. The library is efficient and lays a solid foundation for searching new lymphatic metastasis related genes. The expression of mouse heat shock protein gene, DNA helicase and other 4 novel gene may be different between mouse heptocarcinoma cell lines with different lymphatic metastasis potential.

Hou L, Tang JW, Cui XN, Wang B, Song B, Sun L. Construction and selection of subtracted cDNA library of mouse hepatocarcinoma cell lines with different lymphatic metastasis potential. *World J Gastroenterol* 2004; 10(16): 2318-2322
http://www.wjgnet.com/1007-9327/10/2318.asp

INTRODUCTION

Metastasis is the most lethal attribute of malignant tumors[1]. Ninety percent of malignant tumors are carcinomas, and lymph nodes are often the first organ to develop metastasis[2]. Lymph node metastases form a bridgehead for further metastatic spread. But its molecular mechanism remains poorly understood. A mouse hepatocarcinoma cell line named Hca-F with high lymphogenous metastatic potential and its syngeneic cell line named Hca-P[3] with low lymphogenous metastatic potential have been isolated from hepatocarcinomas in mice. The biological phenotypes between different cells are based on the difference between their phenotypes of gene expression. In this study, we constructed a subtracted cDNA library of differentially expressed genes in these two hepatocarcinoma cell lines using the suppressive subtractive hybridization (SSH)[4-6], which can detect the difference in gene expression between different cells.

MATERIALS AND METHODS

Animals and cell lines

Hepatocarcinoma cell lines, Hca-F and Hca-P, were obtained from our department. Twenty inbred 615-mice maintained in our laboratory were equally divided into 2 groups. Hca-F and Hca-P cells (2×10^6 cells/mouse) were respectively inoculated in 10 mice in each group. On the 28th day post inoculation, the mice were killed and their lymph nodes were collected and stained by HE and examined under microscope. Therefore, the lymph node metastasis rate was calculated.

Isolation of RNA and mRNA

Total RNA was isolated from Hca-F and Hca-P cells (10^8 cells) respectively using Trizol regent (Gibco BRL, USA). And mRNA was isolated from total RNA using the OligotexTM mRNA kit (Qiagen, USA) according to its manufacturer's instructions. The integrity of RNA and mRNA was checked on a 1% agrose gel.

Suppression subtractive hybridization (SSH)

Analysis of differentially expressed genes in Hca-F and Hca-P cells was performed by the suppression subtractive hybridization (SSH) using the CLONTECH PCR-Select™ cDNA subtraction kit (Clotech, USA). In brief[7,8], 2 μg of mRNA from Hca-F and Hca-P cells was used for double strand cDNA synthesis, and the resulting cDNA was digested with Rsa I. The digested cDNA of Hca-F cells(as a Tester) was split into two groups and ligated to either adaptor I or adaptor 2R. Subtractive hybridization was performed by annealing an excess of Hca-P cDNAs (as a Driver) with each sample of adaptor ligated tester cDNAs. The cDNAs were heat denatured and incubated at 68°Cfor 8 h. After the first hybridization, the two samples were mixed together and hybridized again with freshly denatured driver cDNAs for 20 h at 68°C. The two rounds of hybridization would generate a normalized population of tester specific cDNA with different adaptors on each end. After filling in the end, two rounds of PCR amplification were performed to enrich desired cDNAs containing both adaptors by exponential amplification of these products. The optimized cycles for the first and second PCR were 30 and 20, respectively, to increase representation and reduce redundancy of subtracted cDNA libraries. Secondary PCR products were used as templates for

PCR amplification of G3PDH at 20, 25, 30, 35 cycles to assure subtracted efficiency.

Cloning of subtracted cDNA libraries

Products from the secondary PCR were T-A cloned into a T vector (Takara, China). The ligation products were transformed into DH5 α competent cells. The transformed cells were plated on LB plates containing ampicilin, X-Gal and IPTG, which allowed for color selection of colonies. Randomly selected individual white clones were grown for 8 h and then used for PCR amplification of clones.

Sequencing and BLAST homology search

Twenty candidate positive clones from subtracted cDNA library were selected for sequencing. Sequencing was performed by Takara Biotech using a M13 primer. The BLAST program was used to search for the cDNA sequence homology of isolated clones in GeneBank.

RESULTS

The analysis of integrity of RNA and mRNA

The A_{260}/A_{280} of RNA and mRNA from Hca-F and Hca-P was 1.9, which showed extracted RNA and mRNA were pure. Agarose gel electrophoresis showed that RNA was not destroyed by ribonucleases (Figure 1).

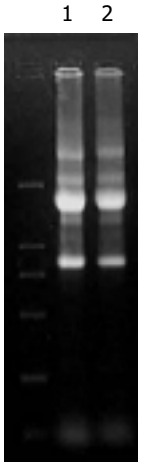

Figure 1 Total RNA from Hca-F and Hca-P cells. Lane 1: RNA from Hca-F cells, Lane 2: RNA from Hca-P cells.

Rsa I digestion

The size of digested cDNA molecular was smaller than undigested in agarose gel electrophoresis, indicating that tester cDNA and driver cDNA were completely digested.

Subtracted cDNA library construction by SSH

In this study, SSH was performed to identify differentially expressed genes among cDNAs of hepatocarcinoma cell lines, Hca-F and Hca-P. One subtracted F-P cDNA library was constructed using Hca-F with high lymphogenous metastatic potential as a tester and its syngeneic cell line named Hca-P with low lymphogenous metastatic potential as a driver. The subtracted cDNA library after secondary PCR amplification looked like smears (Figure 2).

Subtraction efficiency analysis showed that the abundance of non-differentially expressed genes was effectively reduced. In no subtracted cDNA library, the PCR products of housekeeping gene G3PDH were visible after 25 cycles. However, 35 cycles were required in the subtracted cDNA library for G3PDH to be detected (Figure 3).

The subtraction cDNA library contained 800 positive (white) clones. Random analysis of 160 clones with PCR showed that 95% of positive clones contained 100-700 bp inserts (Figure 4).

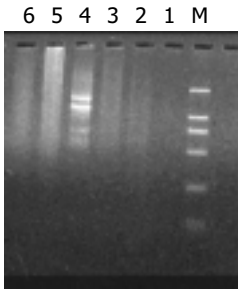

Figure 2 Results of secondary PCR amplification. Lanes 1-3: Product of primary PCR amplification, Lane 4: Secondary PCR amplification product of PCR control cDNA, Lane 5: Secondary PCR amplification product of unsubtracted cDNA ,Lane 6: Secondary PCR amplification product of subtracted cDNA.

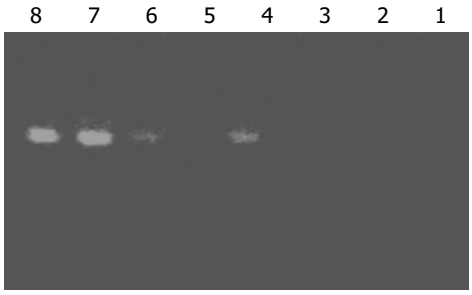

Figure 3 Analysis of subtraction effect. PCR was performed on subtracted (Lanes 1-4) or unsubtracted (Lanes 5-8) secondary PCR product with G3PDH 5'¯Primer and 3'¯primer. Lanes 1, 5: 20 cycles, Lanes 2, 6: 25 cycles, Lanes 3, 7: 30 cycles, Lanes 4, 8: 35 cycles.

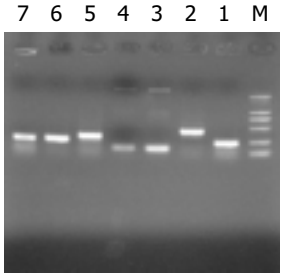

Figure 4 Results of clone PCR amplication. There was a average insert size of 0.1-0.7 kb.

ACCTGATTACGAATTCGAGCTCGGTACCCGGGGATCCTCTAGAG
ATTGGCCGCCCGGGCAGGTCTATAGGGCTCGAGCGGCCG
CCCGGGCAGGTACCATGGTCTAGAGTCGACTAAGTAGGTAAAA
ACTCGAGCCTGCAGGTCTAGATCAGAAAACTCGAGCCTGCA
GGTCTAGATCAGAAAAAAAAAAACTCGAGCCTGCAGG
TCTAGATGGCATCGATGAAGATGAGGTCACTGCAGAGGAGC
CCAGTGCTGCTGTTCCTGATGAGATCCCCCCTCTGGAAGGCGATG
AGGATGCCTCGCGCATGGAAGAGGTGGATTAAAGCCTCCTG
GAAGAAGCCCTGCCCTCTGTATAGTATCCCCGTGGCTCCCCCAGCA
GCCCTGACCCACCTGACTCTCTGCTCATGTCTACAAGAATCTTCT
ATCCTGTCCTGTGCCTTAAGGCAGGAAGATCCCCTCCCACAGAAT
AGCAGGGTTGGGTGTTATGTATTGTGGTTTTTTTGTTTGTCTTAT
TTTGTTCTAAAATTAAAAGTATGCAAAATAAAGAAGATGCA
GTTTCAAAAAAAAAAAAAACTCGAGCCTGCAGGTCTAGATCA
GCGCGTGGTACCTCGGCCGCGACCACGCTAATCGTCGACCT
GCAGGCATGCAAGCT

Figure 5 Sequence of clone 10-3.

Sequencing and homology search

Automatic sequencing proved that most clones were isolated no more than two times (Figures 5-7). BLAST homology search revealed that some sequences were homologous with known gene fragments and others were possibly novel genes, showing few sequence homologies with any known sequences in the GenBank. The results of homology search are shown in Table 1.

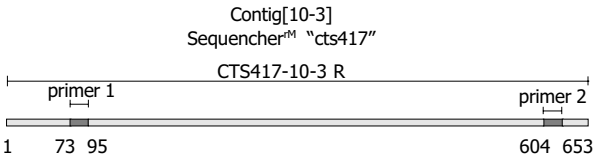

Figure 6 Gene structure of clone 10-3. Both nested primer 1 and nested primer 2R in the cDNA sequence were contained in subtracted library, indicating that only cDNA with both 2 adaptors could be amplified by PCR.

Table 1 Homologue searching of sequenced cDNA fragments from SSH library

Clone number	Size(bp)	Sequence identity
10-3	508	Mus musculus heat shock protein, 84 ku 1 (Hsp84-1)
2-2	385	Mus musculus ribosomal protein S13 (Rps13)
6-2	323	Mouse mRNA for DNA helicase
18-4	226	Mouse, similar to ethanol induced 6, clone MGG51351
11-7	363	Mouse 10 d embryo whole body cDNA, RIKEN full-length enrich library, clone 2610102k11
16-3	403	Mouse 2 d neonate thymus thymic cells cDNA RIKEN full-length library enriched library, clone E430002F13
7-1	570	Mouse chromosome 2 clone RP 24-322M5
15-7	460	Mouse chromosome 12 clone RP23-210N16
1-8	200	EST-mouse
5-8	159	EST-mouse
6-8	216	EST-mouse
2-6	61	Unknown
1-3	132	Unknown
1-6	241	Unknown
16-8	240	Unknown

Analysis of metastasis rate of Hca-F and Hca-P cells

The lymphatic metastasis rate was 80% (8/10) and 10% (1/10), respectively, for Hca-F cells and Hca-P cells.

DISCUSSION

Cancer is the most important cause of death of humans. There is no technique that can selectively kill cancer cells. A wide range of Metastasis leads to the failure of treatment and the death of patients. Therefore, investigation of cancer metastasis, particular the mechanisms, is important in order to improve the efficacy of the treatment. Metastasis[9] is a complex process, which is made up of several steps. However, the molecular mechanism of lymphatic metastasis remains poorly understood because of lack of lymphatic metastasis models. A mouse hepatocarcinoma cell line named Hca-F with a metastasis rate over 70% and its syngeneic cell line named Hca-P with a metastasis rate less than 30% have been separated from hepatocacinomas in mice. The difference in their metastasis potential might be based on the difference in their phenotypes of gene expression. Many different techniques could be used to isolate differentially expressed genes, such as expressed sequencing tag (EST)[10], serial analysis of gene expression (SAGE)[11], subtractive hybridization, mRNA differential display (DD-RTPCR)[12], cDNA representative difference analysis (RDA)[13], suppression subtractive hybridization (SSH), and cDNA microarry[14].

The novel technique named SSH[15-18] has become an ideal subtractive system that combines high subtraction efficiency with normalized representation of differentially expressed genes, and is based on suppression PCR that permits exponential amplification of genes differing in abundance, but suppresses the amplification of sequences of identical abundance genes in two cells at the same time. Therefore, differentially expressed genes of low abundance can be cloned, while differentially expressed genes of high abundance are not excessively isolated. It has been reported that SSH can achieve more than 1 000-fold enrichment of low abundance genes, but only requires 2 μg mRNA instead of the 5-20 μg required in other methods. This method has been successfully used to isolate significant genes in many researches[19-23]. Von Stein *et al.* observed a 94% positive rate in their study, and suggested that confirmation of differential expression by Northern blot analysis for each clone obtained was unnecessary[24].

In the present study, we reported the efficiency of SSH

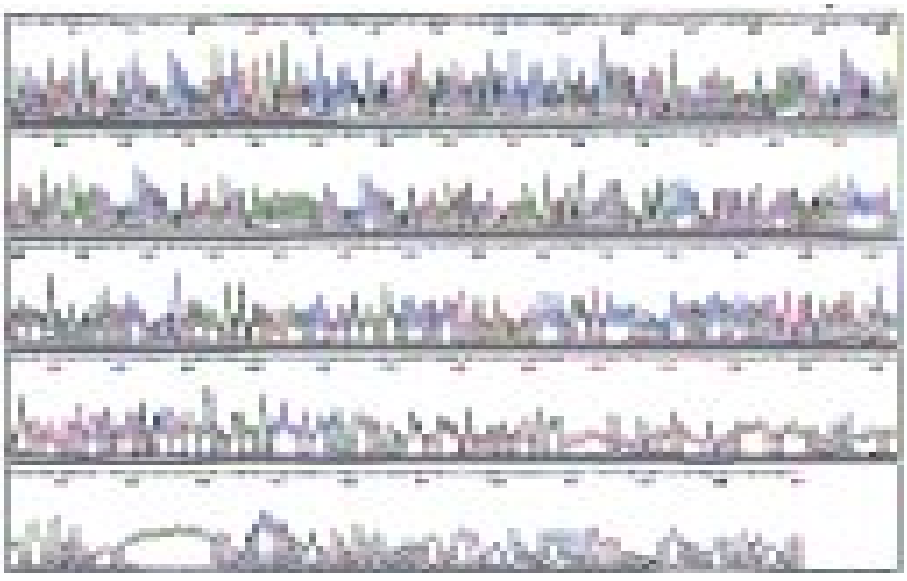

Figure 7 Result of clone 10-3 sequencing.

technique in identifying differentially expressed genes in Hca-F and Hca-P. PCR analysis showed that the subtraction efficiency after subtractive hybridization was effectively reduced. We constructed a subtracted cDNA library between Hca-F cells and Hca-P cells. There were 800 positive clones in the amplified subtracted cDNA library. Random analysis of 160 clones with PCR showed that 95% of clones contained 100-700 bp inserts. After sequencing and BLAST homology search, these clones could be divided into three groups: known genes preciously reported to be related to metastasis and carcinogenesis, known genes never described to be related to metastasis and carcinogenesis, and unknown genes. The identification of the first group of known genes attested to the validity of this method. The library is efficient and lays a solid foundation for searching new lymphatic metastasis related genes.

The No. 10-3 clone obtained in the present study showed homology with mouse heat shock proteins(HSPs). HSPs[25-27] have been found to be ubiquitous molecules expressed in response to stress in all living organisms. The three important roles[28] in regard to cancer development are regulation of apoptosis, modulation of immune response and drug resistance. HSPs are cytoplasmic proteins that could act as molecular chaperones for protein molecules in various intra-cellular processes[29,30]. They are called "heat shock proteins" since they were first discovered in cells exposed to high temperatures. HSPs were also expressed in hepatocarcinoma (HCC)[31-34], and up-regulated in early stage of HCC compared with noncancerous liver tissue. King *et al*.[33] reported that HSPs expressed in HCC (45/58), and its expression was stronger in HCC than in noncancerous liver tissue. HSPs were related to metastasis[35-38]. HSP expression was found in 54 out of 86 (62.7%) gastric carcinomas and was significantly related to more than six metastatic lymph nodes[35]. Over expression of HSPs was related to tumor configuration, lymph node metastasis, and lymphatic vessel invasion in esophageal squamous cell carcinoma[36]. So far, there has no report concerning HSP expression and lymphatic metastasis of HCC. In the present study, we found that HSP expression was different between mouse HCC cell lines Hca-F and Hca-P, indicating that HSP expression might be related to HCC metastasis.

The No. 6-2 clone obtained showed homology with mouse helicase. It has been found that DNA helicases[39-41], because they unwound duplex DNA, have important roles in cellular DNA events such as replication, recombination, repair and transcription. The change in helicases expression could be found in human carcinomas[42], lymphoma[43], leukemia and so on. Helicases were also related to metastasis[44]. B16-F10 and B16-BL6 are B16 mouse melanoma sublines that preferentially metastasize to the lung and their metastasis potential is different. Helicases and ribosomal protein (L37) showed higher expression in B16-BL6 cells than in B16-F10 cells[45]. There has been no report on the association between helicase up-regulation and HCC metastasis. Thus, further investigations are required to elucidate the role of helicase in HCC metastasis.

Besides, two clones obtained in the present study showed homology to mouse ribosomal protein S13 and ethanol induced 6 gene. To our knowledge, there have been no reports on their relation to metastasis. Whether ribosomal protein S13 and ethanol induced 6 gene can be considered as candidate gene of metastasis related gene remains unclear. Clone 11-7 showed homology with mouse of 10-d embryo whole body cDNA library clone 2610102k11, It is important to study the correlation between metastasis and embryo gene expression. Clone 7-1 showed homology with mouse mouse chromosome 2 clone RP 24-322M5 and clone 15-7 showed homology with mouse chromosome 12 clones RP23-210N16. Whether there are candidate metastasis-related genes on chromosome 2 and chromosome 12 needs further investigation. The other three clones showed homology with three EST sequence.

In addition to the known genes, four clones showed no homology with any known sequences, indicating that they were novel genes, although the full-length sequence of these new genes and their function in lymphatic metastasis remain to be determined.

In conclusion, differentially expressed genes in mouse hepatocarcinoma cell lines with different lymphatic metastasis potential can be isolated by SSH method. Comprehensive study of these genes can help understand the molecular mechanism of lymphatic metastasis.

REFERENCES

1 **Yoshida BA**, Sokoloff MM, Welch DR, Rinker-Schaeffer CW. Metastasis-suppressor genes: a riview and perspective on an emerging field. *J Natl Cancer Inst* 2000; **92**: 1717-1730

2 **Sleeman JP.** The lymph node as a bridgehead in the metastatic dissemination of tumors. *Recent Results Cancer Res* 2000; **157**: 55-81

3 **Hou L**, Li Y, Jia YH, Wang B, Xin Y, Ling MY, Lü S. Molecular mechanism about lymphogenous metastasis of hepatocarcinoma cells in mice. *World J Gastroenterol* 2001; **7**: 532-536

4 **Ahmed FE**. Molecular techniques for studying gene expression in carcinogenesis. *J Environ Sci Health Part C Environ Carcinog Ecotoxicol Rev* 2002; **20**: 77-116

5 **Li J**, Han BL, Huang GJ, Qian GS, Liang P, Yang TH, Chen J. Screening and identification for cDNA of differentially expressed genes in human primary hepatocellular carcinoma. *Zhonghua Yixue Yichuanxue Zazhi* 2003; **20**: 49-52

6 **Petersen S**, Petersen I. Expression profiling of lung cancer based on suppression subtraction hybridization (SSH). *Methods Mol Med* 2003; **75**: 189-207

7 **Luo M**, Kong XY, Liu Y, Zhou RH, Jia JZ. cDNA libraries construction and screening in gene expression profiling of disease resistance in wheat. *Yichuan Xuebao* 2002; **29**: 814-819

8 **Liu Y**, Cheng J, Lu YY, Wang G, Mou JS, Li L, Zhang LX, Chen JM. Cloning of genes transactivated by hepatitis B virus X protein. *Zhonghua Ganzangbing Zazhi* 2003; **11**: 5-7

9 **Poste G**, Fidler IJ. The pathogenesis of cancer metastasis. *Nature* 1980; **283**: 139-146

10 **Adams MD**, Kelley JM, Gocayne JD, Dubnick M, Polymeropoulos MH, Xiao H, Merril CR, Wu A, Olde B, Moreno RF, Kerlavage AR, McCombie WR, Verlavage JC. Complementary DNA sequencing: expressed sequence tags and human genome project. *Science* 1991; **252**: 1651-1656

11 **Velculescu VE**, Zhang L, Vogelstein B, Kinzler KW. Serial analysis of gene expression. *Science* 1995; **270**: 484-487

12 **Liang P,** Pardee AB. Differential display of eukaryotic messenger RNA by means of the polymerase chain reaction. *Science* 1992; **257**: 967-971

13 **Lisitsyn N**, Wigler M. Cloning the differences between two complex genomes. *Science* 1993; **259**: 946-951

14 **Schena M**, Shalon D, Davis RW, Brown PO. Quantitative monitoring of gene expression patterns with a complementary DNA microarray. *Science* 1995; **270**: 467-470

15 **Ai JK**, Huang X, Wang YJ, Bai Y, Lu YQ, Ye XJ, Xin DQ, Na YQ, Zhang ZW, Guo YL. Screening of novel genes differentially expressed in human renal cell carcinoma by suppression subtractive hybridization. *Aizheng* 2002; **21**: 1065-1069

16 **Li JY**, Boado RJ, Pardridge WM. Blood-brain barrier genomics. *J Cereb Blood Flow Metab* 2001; **21**: 61-68

17 **Chen I**, Hsieh T, Thomas T, Safe S. Identification of estrogen-induced genes downregulated by AhR agonists in MCF-7 breast cancer cells using suppression subtractive hybridization. *Gene* 2001; **262**: 207-214

18 **Wang H**, Zhan Y, Xu L, Feuerstein GZ, Wang X. Use of suppression subtractive hybridization for differential gene expression in stroke: discovery of CD44 gene expression and localization in permanent focal stroke in rats. *Stroke* 2001; **32**: 1020-1027

19 **Zhou J**, Wang H, Lu A, Hu G, Luo A, Ding F, Zhang J, Wang X, Wu M, Liu Z. A novel gene, NMES1, downregulated in human

esophageal squamous cell carcinoma. *Int J Cancer* 2002; **101**: 311-316

20 **Saito A**, Fujii G, Sato Y, Gotoh M, Sakamoto M, Toda G, Hirohashi S. Detection of genes expressed in primary colon cancers by *in situ* hybridisation: overexpression of RACK 1. *Mol Pathol* 2002; **55**: 34-39

21 **Miyasaka Y**, Enomoto N, Nagayama K, Izumi N, Marumo F, Watanabe M, Sato C. Analysis of differentially expressed genes in human hepatocellular carcinoma using suppression subtractive hybridization. *Br J Cancer* 2001; **85**: 228-234

22 **Roberts D**, Williams SJ, Cvetkovic D, Weinstein JK, Godwin AK, Johnson SW, Hamilton TC. Decreased expression of retinol-binding proteins is associated with malignant transformation of the ovarian surface epithelium. *DNA Cell Biol* 2002; **21**: 11-19

23 **Stassar MJ**, Devitt G, Brosius M, Rinnab L, Prang J, Schradin T, Simon J, Petersen S, Kopp-Schneider A, Zoller M. Identification of human renal cell carcinoma associated genes by suppression subtractive hybridization. *Br J Cancer* 2001; **85**: 1372-1382

24 **von Stein OD**, Thies WG, Hofmann M. A high throughput screening for rarely transcribed differentially expressed genes. *Nucleic Acids Res* 1997; **25**: 2598-2602

25 **Piura B**, Rabinovich A, Yavelsky V, Wolfson M. Heat shock proteins and malignancies of the female genital tract. *Harefuah* 2002; **141**: 969-972

26 **Friedman EJ**. Immune modulation by ionizing radiation and its implications for cancer immunotherapy. *Curr Pharm Des* 2002; **8**: 1765-1780

27 **Parmiani G**, Castelli C, Dalerba P, Mortarini R, Rivoltini L, Marincola FM, Anichini A. Cancer immunotherapy with peptide-based vaccines: what have we achieved? Where are we going? *J Natl Cancer Inst* 2002; **94**: 805-818

28 **Lebret T**, Watson RW, Fitzpatrick JM. Heat shock proteins: their role in urological tumors. *J Urol* 2003; **169**: 338-346

29 **Srivastava P**. Roles of heat-shock proteins in innate and adaptive immunity. *Nat Rev Immunol* 2002; **2**: 185-194

30 **Candido EP**. The small heat shock proteins of the nematode Caenorhabditis elegans: structure, regulation and biology. *Prog Mol Subcell Biol* 2002; **28**: 61-78

31 **Chuma M**, Sakamoto M, Yamazaki K, Ohta T, Ohki M, Asaka M, Hirohashi S. Expression profiling in multistage hepatocarcinogenesis: identification of HSP70 as a molecular marker of early hepatocellular carcinoma. *Hepatology* 2003; **37**: 198-207

32 **Yin Y,** Qin Q, Zhang W, Zhao J, Zhang C, Yu J. Overexpression of heat shock protein 70 and spontaneous cancer cell apoptosis in hepatocellular carcinoma. *Zhonghua Ganzangbing Zazhi* 2001; **9**: 84-85

33 **King KL**, Li AF, Chau GY, Chi CW, Wu CW, Huang CL, Lui WY. Prognostic significance of heat shock protein-27 expression in hepatocellular carcinoma and its relation to histologic grading and survival. *Cancer* 2000; **88**: 2464-2470

34 **Osada T**, Sakamoto M, Nishibori H, Iwaya K, Matsuno Y, Muto T, Hirohashi S. Increased ubiquitin immunoreactivity in hepatocellular carcinomas and precancerous lesions of the liver. *J Hepatol* 1997; **26**: 1266-1273

35 **Kapranos N**, Kominea A, Konstantinopoulos PA, Savva S, Artelaris S, Vandoros G, Sotiropoulou-Bonikou G, Papavassiliou AG. Expression of the 27-kDa heat shock protein (HSP27) in gastric carcinomas and adjacent normal, metaplastic, and dysplastic gastric mucosa, and its prognostic significance. *J Cancer Res Clin Oncol* 2002; **128**: 426-432

36 **Noguchi T**, Takeno S, Shibata T, Uchida Y, Yokoyama S, Muller W. Expression of heat shock protein 70 in grossly resected esophageal squamous cell carcinoma. *Ann Thorac Surg* 2002; **74**: 222-226

37 **Sagol O**, Tuna B, Coker A, Karademir S, Obuz F, Astarcioglu H, Kupelioglu A, Astarcioglu I, Topalak O. Immunohistochemical detection of pS2 protein and heat shock protein-70 in pancreatic adenocarcinomas. Relationship with disease extent and patient survival. *Pathol Res Pract* 2002; **198**: 77-84

38 **Mese H**, Sasaki A, Nakayama S, Yoshioka N, Yoshihama Y, Kishimoto K, Matsumura T. Prognostic significance of heat shock protein 27 (HSP27) in patients with oral squamous cell carcinoma. *Oncol Rep* 2002; **9**: 341-344

39 **Ishiguro H**, Shimokawa T, Tsunoda T, Tanaka T, Fujii Y, Nakamura Y, Furukawa Y. Isolation of HELAD1, a novel human helicase gene up-regulated in colorectal carcinomas. *Oncogene* 2002; **21**: 6387-6394

40 **Fuchsova B**, Novak P, Kafkova J, Hozak P. Nuclear DNA helicase II is recruited to IFN-alpha-activated transcription sites at PML nuclear bodies. *J Cell Biol* 2002; **158**: 463-473

41 **Furuichi Y**. Premature aging and predisposition to cancers caused by mutations in RecQ family helicases. *Ann N Y Acad Sci* 2001; **928**: 121-131

42 **Mohaghegh P,** Hickson ID. DNA helicase deficiencies associated with cancer predisposition and premature ageing disorders. *Hum Mol Genet* 2001; **10**: 741-746

43 **Kaneko H**, Morimoto W, Fukao T, Kasahara K, Kondo N. Telomerase activity in cell lines and lymphoma originating from Bloom syndrome. *Leuk Lymphoma* 2001; **42**: 757-760

44 **Takagi Y**, Suyama E, Kawasaki H, Miyagishi M, Taira K. Mechanism of action of hammerhead ribozymes and their applications *in vivo*: rapid identification of functional genes in the post-genome era by novel hybrid ribozyme libraries. *Biochem Soc Trans* 2002; **30**(Pt 6): 1145-1149

45 **Ishiguro T**, Nakajima M, Naito M, Muto T, Tsuruo T. Identification of genes differentially expressed in B16 murine melanoma sublines with different metastatic potentials. *Cancer Res* 1996; **56**: 875-879

Edited by Xia HHX and Wang XL **Proofread by** Chen WW and Xu FM

PO Box 2345, Beijing 100023, China
Fax: +86-10-85381893
E-mail: wjg@wjgnet.com www.wjgnet.com

World J Gastroenterol 2004;10(16):2323-2326
World Journal of Gastroenterology
 ISSN 1007-9327

• COLORECTAL CANCER •

COX-2 expression and tumor angiogenesis in colorectal cancer

Ai-Wen Wu, Jin Gu, Zhen-Fu Li, Jia-Fu Ji, Guang-Wei Xu

Ai-Wen Wu, Jin Gu, Jia-Fu Ji, Guang-Wei Xu, Department of Surgery, Beijing Cancer Hospital, Beijing Institute for Cancer Research, School of Oncology, Peking University, Beijing 100036, China
Zhen-Fu Li, Department of Biochemistry, Beijing Cancer Hospital, Beijing Institute for Cancer Research, School of Oncology, Peking University, Beijing 100036, China
Correspondence to: Dr. Guang-Wei Xu, Department of Surgery, Beijing Cancer Hospital, Beijing Institute for Cancer Research, School of Oncology, Peking University, 52 Fucheng Road, Haidian District, Beijing 100036, China. gwx@caca.edu.cn
Telephone: +86-10-88122452 **Fax:** +86-10-88122452
Received: 2003-11-17 **Accepted:** 2003-12-22

Abstract

AIM: Cyclooxygenase-2 (COX-2) is one of the rate-limiting enzymes in metabolism of arachidonic acid, and COX-2 inhibitors demonstrate preventive effects on cancer, especially on colorectal cancer. The underlying mechanism remains unclear. The aim of this study was to illustrate the relationship between angiogenesis and COX-2 in carcinogenesis of colorectal cancer.

METHODS: One hundred and seventy patients with colorectal cancer were enrolled in our study from January 1993 to September 2001 in School of Oncology, Peking University. COX-2 and VEGF expression were detected with the immunohistochemistry (IHC) technique. IHC assays were carried out with the aid of tissue microarray (TMA) procedure. Specimens from 35 of these patients were examined with reverse transcriptase PCR (RT-PCR).

RESULTS: COX-2 and VEGF expressions were stronger in colorectal cancer than those in the corresponding normal tissues, at both protein and mRNA levels. One hundred patients were eligible for analysis after IHC assay of COX-2 and VEGF. The positive rate of VEGF was much higher in COX-2 positive group (47/85) than in COX-2 negative group ($\chi^2 = 4.181$, $P = 0.041$). The result was further verified by the result of RT-PCR ($\chi^2 = 8.517$, $P = 0.003$). Correlation coefficient was 0.409 after Spearman correlation analysis ($P = 0.015$).

CONCLUSION: COX-2 may be involved in the course of tumor angiogenesis of colorectal cancer and acts through VEGF.

Wu AW, Gu J, Li ZF, Ji JF, Xu GW. COX-2 expression and tumor angiogenesis in colorectal cancer. *World J Gastroenterol* 2004; 10(16): 2323-2326
http://www.wjgnet.com/1007-9327/10/2323.asp

INTRODUCTION

Cyclooxygenase (COX) is one of the rate-limiting enzymes in metabolism of arachidonic acid, which catalyzes arachidonic acid into a series of products such as prostaglandins and other eicosanoids. It has two isoforms, COX-1 and COX-2. COX-2 acts as superoxidants and transforms arachidonic acid into PGG_2, and then into PGH_2. COX-2 is inducibly expressed in many human tissues by cytokines, oncogenes, and tumor promoters[1-3]. Recent clinical epidemiological studies have demonstrated the preventive effect of COX inhibitors on cancer, especially on colorectal cancer[4-6]. Cellular and animal experimental studies have also indicated its relevance to tumor invasion, metastasis, cell apoptosis, cell cycle, and body immunity[7], and the role of COX-2 in the development of colorectal cancer.

Angiogenesis is among the most important characteristics of tumors and plays an important role in the course of cancer invasion and metastasis. Recent studies have confirmed the hypothesis of tumor growth, which is generally dependent on tumor angiogenesis. Any significant increase in tumor mass must be preceded by an increase in vascular supply to deliver nutrients and oxygen to the tumor[8]. Experimental studies from Seed and Tsujii[9,10] suggested that COX-2 might be involved in angiogenesis. Few reports on the role of COX-2 in tumor angiogenesis of colorectal cancer in clinical settings are available.

MATERIALS AND METHODS

Patients and tissues

A total of 170 patients after surgical treatment in School of Oncology, Peking University, from January 1993 to September 2001 were studied retrospectively. Specimens from these patients were prepared as tissue microarray and then underwent immunohistochemical assays. Specimens from thirty-five patients were prepared for reverse transcriptase PCR (RT-PCR), including 22 male patients and 13 female patients.

Tissue array preparation and immunohistochemical staining

Formalin-fixed and paraffin-embedded tissues were subjected to routine sectioning of 3-5 μm thickness and HE staining. Tissue array block was completed for subsequent sectioning according to the predetermined scheme described before[11]. Two-step immunohistochemical staining was used for COX-2 and VEGF detection. The titer of COX-2 (Cayman Chemical, USA) and VEGF (Zhongshan Biological Inc., Beijing, China) antibody were 1:200 and 1:50 respectively. Human colon adenocarcinoma with strong COX-2 staining served as a positive control, whereas PBS instead of antibody served as a negative control. Two pathologists independently reviewed slides with immunohistochemical staining. Microscopically, the slides with no staining in the negative control and the specific dark yellow staining of cytoplasm and neuclear membrane in the positive control were eligible for a further analysis. Semiquantitative scoring system was adopted according to the staining intensity: 0 for no staining, 1 for weak yellow, 2 for dark yellow, and 3 for brown staining with granular distributions. The mean score was used for statistical analysis and the threshold for positivity was 2[11].

Specimen preparation and RT-PCR

Tumor tissues and the corresponding normal mucosae at least 10 cm away were collected 30 min after removal of the specimens. The tissues were then stored under -70 °C for RNA extraction. Total RNA was prepared from the specimens with Trizol reagent

(Gibco BRL Co.) according to the manufacturer's instructions. cDNA synthesis was carried out with 1μg of total RNA. Sense and antisense primers of 0.5 μL were mixed with 11 μL dd H_2O, 5 μL PCR buffer, 3 μL $MgCl_2$ (25 mmol/L), 2 μL dNTP (10 mmol/L), 2 μL cDNA, and 0.8 μL Taq DNA polymerase for PCR. The primers for PCR were 5' TTC AAA TGA GAT TGT GGG AAA AT 3' (sense primer) and 5' AGA TCA TCT CTG CCT GAG TAT CTT 3' (antisense primer). PCR reactions were processed in a PTC 100 thermocycler under the following conditions: at 94 °C for 5 min, at 94 °C for 30 s, extension at 55 °C for 30 s, then at 72 °C for 30 s for 40 cycles, and then at 72 °C for 5 min. The RT-PCR products were then analyzed on 15 g/L agarose gels. Colon cancer cell line HT-29 and β-actin served as a positive and inner control, respectively. PCR reactions without cDNA were used as blank controls.

Statistical analysis

All statistical analyses were carried out with the SPSS software, 10.0, USA. The relationship between COX-2 expression and categorical variables was compared with χ^2 test or Fisher two-sided exact test. Continuous variables were analyzed with *t* test and $P<0.05$ was considered statistically significant. Correlation analysis was processed via the Spearman method.

RESULTS

Expression of COX-2 protein in colorectal cancer tissues

Of the 170 colorectal cancer patients, 139 were eligible for analysis after COX-2 immunohistochemical assays. Immunohistochemical assays demonstrated that COX-2 protein was located in cytoplasm and nuclear membrane. The staining was weak yellow, dark yellow, and brown at a low-power field and diffuse or granular staining at a high-power field under a microscope (Figure 1A). A weak staining of COX-2 was observed in normal tissue with a positive rate of 24.1% (7/29). COX-2 expression was much stronger in tumor cells with dark yellow or brown staining with occasional granular distributions than in normal tissues. The positive rate of COX-2 in colorectal cancer was 84.9% (118/139).

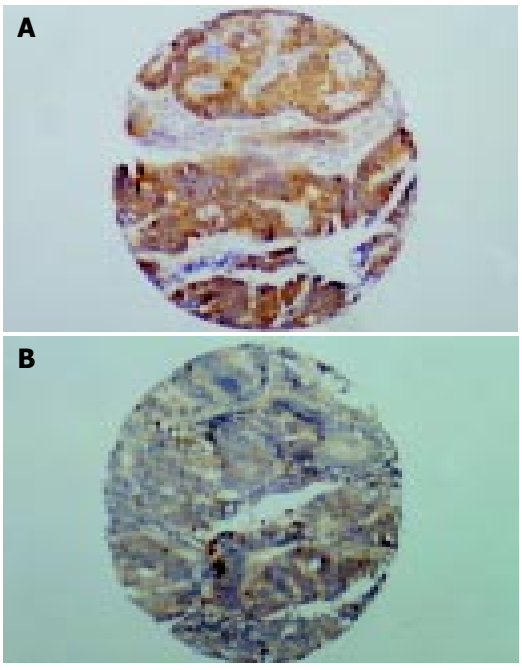

Figure 1 COX-2 and VEGF expressions in colorectal cancer tissues (IHC assay). A: Well-differentiated colonic adenocarcinoma, COX-2 immunostaining, ×100. B: Well-differentiated colonic adenocarcinoma, VEGF immunostaining, ×100.

Expression of VEGF protein in colorectal cancer tissues

For some reasons, only 100 colorectal cancer patients were eligible for further analysis after immunohistochemical assays. VEGF protein was located in cytoplasm of tumor cells and endothelial cells (Figure 1B). About 51.0% (51/100) of the tumors presented with strong VEGF staining, and the rate was much higher than that of normal tissues.

Expression of COX-2 and VEGF mRNA in colorectal cancer tissues

In consistent with the results of IHC assay, RT-PCR revealed stronger expressions of COX-2 and VEGF in tumors than in corresponding normal tissues (Figure 2). Among the 35 paired specimens of colorectal cancer tissues undergoing RT-PCR assays, 27 (77.1%) and 28 (80.0%) were positive with VEGF and COX-2, respectively, compared with 9 (25.7%) and 11 (31.4%) in normal tissues ($P<0.01$).

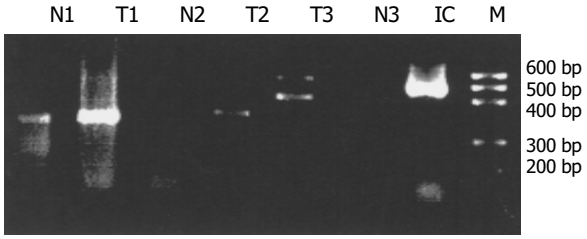

Figure 2 COX-2 and VEGF expressions in colorectal cancer tissues (RT-PCR assay). N: normal T: tumor IC: internal control M: marker. The Arabic number represents the number of samples. The marker has six lanes from 100 bp to 600 bp. The left four lanes stand for the 304 bp products of COX-2 while the right two lanes are the VEGF products of 541 and 408 bp respectively. The internal control of β-actin produced a 496 bp product.

Correlation between COX-2 and VEGF expression in colorectal cancer tissues

For the reason of TMA, a total of 100 cases were eligible for IHC analysis. Among these, 47 COX-2 positive cases presented with a positive VEGF staining (55.3%). The positive rate of VEGF was much higher than that in COX-2 negative group (26.7%). The difference between two groups had a statistical significance ($\chi^2 = 4.181$, $P = 0.041$). Among the 27 cases with COX-2 mRNA expression, 25 had a strong VEGF expression while only 2 in COX-2 negative group ($\chi^2 = 8.517$, $P = 0.003$) (Table 1). COX-2 and VEGF expression demonstrated a tendency to having a positive correlation with correlation coefficient of 0.409 ($P = 0.015$).

Table 1 Expression of COX-2 and VEGF in colorectal cancer tissue (RT-PCR / IHC)[1]

VEGF expression	COX-2 positive	COX-2 negative	Total
Positive	25 / 47	2 / 4	27 / 51
Negative	3 / 38	5 / 11	8 / 49
Total	28 / 85	7 / 15	35 / 100

[1]Fisher double-side exact test ($P = 0.003 / 0.041$).

DISCUSSION

It has been documented that COX-2 plays an important role in the development of human tumors[12-16]. COX-2 could promote the growth and invasion of tumors[17,18] and increase invasiveness and potential of tumor metastasis[19,20]. Recent research results indicated that COX-2 could also induce tumor angiogenesis and was correlated with hematogenous metastasis of tumors[10,21].

Tumor angiogenesis is one of the important characteristics of tumors involving their growth and metastasis. The formation of primary or metastatic lesions and even their further development are dependent on tumor angiogenesis. Newly-formed vessels were in need of nutrition and oxygen when the tumor grew to 2-3 mm in size[8].

It had been found many factors are involved in tumor angiogenesis including bFGF, aFGF, PGE_1, PGE_2, VEGF, TGFα, TGFβ, and TNF[22]. The most important is vessel endothelial growth factor (VEGF), a highly specific mitogen of vessel endothelial cells. The biological functions of VEGF included selective promotion of mitosis of endothelial cells, stimulation of their proliferation and angiogenesis, an increase in vessel transparency and extravasculization of plasma large molecules[23-26]. It was reported that COX-2 might interact with VEGF[27,28]. Therefore, the relationship of COX-2 and angiogenesis (VEGF as the marker of angiogenesis) was then investigated at protein and mRNA levels.

The positive rate of COX-2 mRNA and COX-2 protein were 80% (28/35) and 84.9% in colorectal cancer. Both were much higher than those in normal tissues (P<0.01), which indicated the role of COX-2 in carcinogenesis of colorectal cancer. The expressions of COX-2 and VEGF were studied through RT-PCR and IHC assays. The result of RT-PCR showed that 25 were VEGF positive among the 28 COX-2 positive patients, and only 2 were VEGF positive in the COX-2 negative group. Correspondingly, of the 85 patients with COX-2 positive staining, 47 (55.3%) expressed VEGF while only 26.7% in the COX-2 negative group, indicating the correlationship between the expressions of COX-2 and VEGF, which was further verified by the Spearman correlation analysis. Cianchi[28] recently found a close correlation between COX-2 and VEGF as well as microvessel density (MVD) in their studies on 31 colorectal cancer patients by Western blot and Northern blot analysis, and immunohistochemical assays, which was consistent with our results.

The mechanism underlying the role of COX-2 in tumor angiogenesis has been unclear[29]. Preliminary results showed that angiogenesis occurred when endothelial cells were cultured with cancer cells over-expressing COX-2[10]. It could be inhibited by selective COX-2 inhibitors in endothelial cells *in vitro*[29]. It was proved that the activity of COX-2 in interstitial cells was necessary for secretion of VEGF, proliferation of endothelial cells and new vessel formation[30]. These experimental results suggested that such metabolic products might induce the expression of VEGF via pathways of paracrine, autocrine or intracrine, and stimulate proliferation of vessel endothelial cells and formation of tumor vessels[29].

The regulatory effect of COX-2 on VEGF production and tumor angiogenenesis suggested that COX-2 expression might be an upstream event in tumor angiogenesis[10,29]. We also found that COX-2 expression was positively correlated with expression of VEGF, one of the most important factors for tumor angiogenesis. The expression rate of VEGF was high in patients with positive COX-2 expression (25/28) while low in COX-2 negative patients (2/7). In addition, staining intensity of COX-2 was correlated with that of VEGF. Management of the murine animal model of lung and prostate cancers with the gene knockout technique or COX-2 inhibitor resulted in not only tumor shrinkage but also inhibition of tumor angiogenesis. Endothelial cells were scattered without formation of an ordered tubular structure. The MVD of tumor and expression of VEGF were significantly decreased, further suggesting the role of COX-2 on VEGF expression and tumor angiogenesis[31,32].

Great progresses have been made in the research of tumor angiogenesis. Trials on targeted therapy against angiogenesis have been ongoing to block or postpone tumor angiogenesis so as to cure cancer[33,34]. More than twenty drugs are in their phase I or II and even III clinical trials in the United States of America. Though preliminary results were promising, there is still a long way to go. Therefore, as an upper-stream event, COX-2 might be a potential target of the cancer gene therapy worthy of further research.

REFERENCES

1 **Williams CS**, Mann M, DuBios RN. The role of cyclooxygenases in inflammation, cancer, and development. *Oncogene* 1999; **18**: 7908-7916

2 **Egil F**. Biochemistry of cyclooxygenase (COX-2) inhibitors and molecular pathology of COX-2 in neoplasia. *Crit Rev Clin Lab Sci* 2000; **37**: 431-502

3 **Subbaramaiah K**, Dannenberg AJ. Cyclooxygenase 2: a molecular target for cancer prevention and treatment. *Trends Pharmaco Sci* 2003; **24**: 96-102

4 **Thun MJ**, Hennekenn CH. Aspirin and other non-steroidal antiinflammatory drugs and the risk of cancer development. *In*: DeVitt VT, Hellman S, Rosenberg SA. Cancer: principles and practice of oncology. 6th edition. Philadelphia: *Lippincott Williams Wilkins Press U S A* 2001: 601-607

5 **Kawamori T**, Rao CV, Seibert K, Reddy BS. Chemopreventive activity of celecoxib, a specific cyclooxygenase-2 inhibitor, against colon carcinogenesis. *Cancer Res* 1998; **58**: 409-412

6 **Reddy BS**, Rao CV, Seibert K. Evaluation of cyclooxygenase-2 inhibitor for potential chemopreventive properties in colon carcinogenesis. *Cancer Res* 1996; **56**: 4566-4569

7 **Dannenberg AJ**, Zakim D. Chemoprevention of colorectal cancer through inhibition of cyclooxygenase-2. *Semin Oncol* 1999; **26**: 499-504

8 **Folkman J**. What is the evidence that tumors are angiogenesis dependent? *J Natl Cancer Inst* 1990; **82**: 4-6

9 **Seed MP**, Brown JR, Freematle CN, Papwoeth JL, Colville-Nash PR, Willis D, Somerville KW, Asculai S, Willoughby DA. The inhibition of colon-26 adenocarcinoma development and angiogenesis by topical diclofenac in 2.5% hyaluronan. *Cancer Res* 1997; **57**: 1625-1629

10 **Tsujii M**, Kawano S, Tsuji S, Sawaoka H, Hori M, DuBios RN. Cyclooxygenase regulates angiogenesis induced by colon cancer cells. *Cell* 1998; **93**: 705-716

11 **Wu AW**, Gu J, Ji JF, Li ZF, Xu GW. Role of COX-2 in carcinogenesis of colorectal cancer and its relationship with tumor biological characteristics and patients' prognosis. *World J Gastroenterol* 2003; **9**: 1990-1994

12 **Eberhart CE**, Coffey RJ, Radhika A, Giardiello FM, Ferrenbach S, DuBois RN. Up-regulation of cyclooxygenase 2 gene expression in human colorectal adenomas and adenocarcinomas. *Gastroenterology* 1994; **107**: 1183-1188

13 **Ohno R**, Yoshinaga K, Fujita T, Hasegawa K, Iseki H, Tsunozaki H, Ichikawa W, Nihei Z, Sugihara K. Depth of invasion parallels increased cyclooxygenase-2 levels in patients with gastric carcinoma. *Cancer* 2001; **91**: 1876-1881

14 **Saukkonen K**, Nieminen O, van Rees B, Vilkki S, Harkonen M, Juhola M, Mecklin JP, Sipponen P, Ristimaki A. Expression of cyclooxygenase-2 indysplasia of the stomach and in intestinal-type gastric adenocarcinoma. *Clin Cancer Res* 2001; **7**: 1923-1931

15 **Wolff H**, Saukkonen K, Anttila S, Karjalainen A, Vainio H, Ristimaki A. Expression of cyclooxygenase-2 in human lung carcinoma. *Cancer Res* 1998; **58**: 4997-5001

16 **Shamma A**, Yamamoto H, Doki Y, Okami J, Kondo M, Fujiwara Y, Yano M, Inoue M, Matsuura N, Shiozaki H, Monden M. Up-regulation of cyclooxygenase-2 in squamous carcinogenesis of the esophagus. *Clin Cancer Res* 2000; **6**: 1229-1238

17 **Tsujii M**, Kawano S, DuBois RN. Cyclooxygenase-2 expression in human colon cancer cells increases metastatic potential. *Proc Natl Acad Sci U S A* 1997; **94**: 3336-3340

18 **Attiga FA**, Fernandez PM, Weeraratna AT, Manyak MJ, Patierno SR. Inhibitors of prostaglandin synthesis inhibit human prostate tumor cell invasiveness and reduce the release of matrix metalloproteinases. *Cancer Res* 2000; **60**: 4629-4637

19 **Tomazawa S**, Nagawa H, Tsuno NH, Hatano K, Osada T, Kitayama J, Osada T, Saito S, Tsuruo T, Shibata Y, Nagawa H.

Inhibition of haematogenous metastasis of colon cancer in mice by a selective COX-2 inhibitor, JTE-522. *Br J Cancer* 1999; **81**: 1274-1279

20 **Tomozawa S**, Tsuno NH, Sunami E, Hatano K, Kitayama J, Osada T, Saito S, Tsuruo T, Shibata Y, Nagawa H. Cyclooxygenase-2 overexpression correlates with tumour recurrence, especially haematogenous metastasis, of colorectal cancer. *Br J Cancer* 2000; **83**: 324-328

21 **Masunaga R**, Kohno H, Dhar DK, Ohno S, Shibakita M, Kinugasa S, Yoshimura H, Tachibana M, Kubota H, Nagasue N. Cyclooxygenase-2 expression correlates with tumor neovascularization and prognosis in human colorectal carcinoma patients. *Clin Cancer Re*s 2000; **6**: 4064-4068

22 **Fidler IJ.** Molecular biology of cancer: invasion and metastasis *In*: DeVita SH, Rosenberg SA, eds. Cancer: Principles and Practice of Oncology, 5th edition. Philadelphia: *Lippincott Raven Publishers* 1997: 135-152

23 **Yancopoulos GD**, Klagsbrun M, Folkman J. Vasculogenesis, angiogenesis, and growth factors: ephrins enter the fray at the border. *Cell* 1998; **93**: 661-664

24 **Krishnan J**, Kirkin V, Steffen A, Hegen M, Weih D, Tomarev S, Wilting J, Sleeman JP. Differential *in vivo* and *in vitro* expression of vascular endothelial growth factor (VEGF)-C and VEGF-D in tumors and its relationship to lymphatic metastasis in immunocompetent rats. *Cancer Res* 2003; **63**: 713-722

25 **Furudoi A**, Tanaka S, Haruma K, Kitadai Y, Yoshihara M, Chayama K, Shimamoto F. Clinical significance of vascular endothelial growth factor C expression and angiogenesis at the deepest invasive site of advanced colorectal carcinoma. *Oncology* 2002; **62**: 157-166

26 **Li CY**, Shan S, Huang Q, Braun RD, Lanzen J, Hu K, Lin P, Dewhirst MW. Initial stages of tumor cell-induced angiogenesis: evaluation via skin window chambers in rodent models. *J Natl Cancer Inst* 2000; **92**: 143-147

27 **Leung WK**, To KF, Go MY, Chan KK, Chan FK, Ng EK, Chung SC, Sung JJ. Cyclooxygenase-2 upregulates vascular endothelial growth factor expression and angiogenesis in human gastric carcinoma. *Int J Oncol* 2003; **23**: 1317-1322

28 **Cianchi F**, Cortesini C, Bechi P Fantappie O, Messerini L, Vannacci A, Sardi I, Baroni G, Boddi V, Mazzanti R, Masini E. Up-regulation of cyclooxygenase 2 gene expression correlates with tumor angiogenesis in human colorectal cancer. *Gastroenterology* 2001; **121**: 1339-1347

29 **Prescott SM**. Is cyclooxygenase-2 the alpha and the omega in cancer? *J Clin Invest* 2000; **105**: 1511-1513

30 **Tsujii M**, DuBois RN. Alterations in cellular adhesion and apoptosis in epithelial cells overexpressing prostaglandin endoperoxide synthase 2. *Cell* 1995; **83**: 493-501

31 **Williams CS**, Tsujii M, Reese J, Dey SK, DuBois RN. Host cyclooxygenase- 2 modulates carcinoma growth. *J Clin Invest* 2000; **105**: 1589-1594

32 **Liu XH**, Kirschenbaum A, Yao S, Lee R, Holland JF, Levine AC. Inhibition of cyclooxygenase-2 suppresses angiogenesis and the growth of prostate cancer *in vivo*. *J Urol* 2000; **164**(3 Pt1): 820-825

33 **Ruggeri B**, Singh J, Gingrich D, Angeles T, Albom M, Chang H, Robinson C, Hunter K, Dobrzanski P, Jones-Bolin S, Aimone L, Klein-Szanto A, Herbert JM, Bono F, Schaeffer P, Casellas P, Bourie B, Pili R, Isaacs J, Ator M, Hudkins R, Vaught J, Mallamo J, Dionne C. CEP-7055: a novel, orally active pan inhibitor of vascular endothelial growth factor receptor tyrosine kinases with potent antiangiogenic activity and antitumor efficacy in preclinical models. *Cancer Res* 2003; **63**: 5978-5991

34 **Ellis LM**. A targeted approach for antiangiogenic therapy of metastatic human colon cancer. *Am Surg* 2003; **69**: 3-10

Edited by Wang XL and Chen ZR **Proofread by** Xu FM

PO Box 2345, Beijing 100023, China
Fax: +86-10-85381893
E-mail: wjg@wjgnet.com www.wjgnet.com

World J Gastroenterol 2004;10(16):2327-2329
World Journal of Gastroenterology
 ISSN 1007-9327

• VIRAL HEPATITIS •

New serum biomarkers for detection of HBV-induced liver cirrhosis using SELDI protein chip technology

Xiao-Dong Zhu, Wei-Hua Zhang, Cheng-Lin Li, Yang Xu, Wei-Jiang Liang, Po Tien

Xiao-Dong Zhu, Wei-Jiang Liang, Po Tien, Department of Molecular Virology, Institute of Microbiology, Chinese Academy of Sciences, Beijing 100080, China
Wei-Hua Zhang, Yang Xu, Ciphergen Biosystems, Inc., Beijing, China
Cheng-Lin Li, Department of Pathology, Beijing You'an Hospital, Beijing 100054, China
Supported by the Major State Basic Research Development Program of China (973 Program), No. 2001CB510001
Co-first-authors: Xiao-Dong Zhu and Wei-Hua Zhang
Correspondence to: Professor Po Tien, Department of Molecular Virology, Institute of Microbiology, Chinese Academy of Sciences, Zhongguancun Beiyitiao, Beijing 100080, China. tienpo@sun.im.ac.cn
Telephone: +86-10-62554247 **Fax:** +86-10-62622101
Received: 2003-12-12 **Accepted:** 2004-02-18

Abstract

AIM: To find new serum biomarkers for liver cirrhosis (LC) in chronic carriers of hepatitis B virus (HBV).

METHODS: Surface enhanced laser desorption/ionization time-of-flight (SELDI-TOF) mass spectrometry was used to discover biomarkers for differentiating HBV induced LC from non-cirrhotic cohorts. A training population of 25 patients with HBV-induced LC, 20 patients with HCC, and 25 closely age-matched healthy men, was studied.

RESULTS: Two biomarkers with M_r 7 772 and 3 933 were detected in sera of non-cirrhotic cohorts, but not in patients with HBV-induced LC. A sensitivity of 80% for all LC patients, a specificity of 81.8% for all non-cirrhotic cohorts and a positive predictive value of 75% for the study population were obtained.

CONCLUSION: These two serum biomarkers for HBV-induced LC might be used for diagnosis and assessment of disease progression.

Zhu XD, Zhang WH, Li CL, Xu Y, Liang WJ, Tien P. New serum biomarkers for detection of HBV-induced liver cirrhosis using SELDI protein chip technology. *World J Gastroenterol* 2004; 10(16): 2327-2329
http://www.wjgnet.com/1007-9327/10/2327.asp

INTRODUCTION

Liver cirrhosis (LC), the end-stage of liver fibrosis, is generally irreversible. Patients with LC caused by chronic infection of HBV are at high risks of hepatocellular carcinoma and high death rate[1,2]. Although some serum assays are on the way to differentiate chronic HBV infection or LC from HCC, pretreatment liver biopsy has been considered as the "gold standard" for assessing the grade of liver injury and stage of liver fibrosis. Clinicians relying on liver biopsy are able to correctly diagnose the stage of fibrosis or presence of cirrhosis in 80% patients[3]. However, liver biopsy can be associated with significant expense, manpower issues, and risk of patient injury. As a result, we still need to identify noninvasive tests that could replace liver biopsy.

Protein profiles might reflect the pathological state of HBV infection. The relationship between protein profile and disease progression could be achieved by analyzing the complex serum proteomic patterns[4,5]. We used a protein biochip surface-enhanced laser desorption/ionization time-of-flight (SELDI-TOF) mass spectrometry coupled with an artificial intelligence learning algorithm to differentiate HBV induced LC from non-cirrhosis cohorts. A blinded test was used to determine the sensitivity and specificity of the established pattern.

MATERIALS AND METHODS

Samples

Of the 107 serum samples selected, 40 were from patients with HBV-induced LC and 30 from patients with HCC from You'an Hospital, Beijing, China, 37 from healthy men provided by Center of Cancer Prevention and Treatment, Zhongshan University, China. All HBV infected patients with LC were examined by ELISA and were HBeAg positive in serum. The final diagnoses were pathologically confirmed and specimens were obtained before treatment. All samples were fresh and stored at -70 °C and closely age-matched.

Protein chip array analysis

Three different chip chemistries (cationic, anionic, and Cu metal binding, Ciphergen Biosystems, Inc, Fremont, CA) were tested to determine which provided the best serum profiles in terms of number and resolution of protein peaks. It showed that WCX2 weak cationic chip gave the best result. A total of 10 μL of each sample was diluted into 20 μL with U9 buffer (1×PBS, 9 mol/L urea, 1% CHAPS) and mixed. The mixing step was repeated several times on ice for a total of 30 min. An eight-spot WCX chip was washed with 50 mmol/L sodium acetate (pH 4.0) twice. Then sodium acetate buffer was added to U9-treated sample to make a further 1:13 dilution. The diluted serum mixture (100 μL) was applied to a protein chip array and incubated for 1 h on a shaker. After washing with the same sodium acetate buffer three times followed by a quick water rinse, 0.5 μL of saturated sinapinic acid (SPA) solution was applied onto each spot and allowed to air-dry. Then chips were performed on Protein Biological System II(c) mass spectrometer reader (PBSII, Ciphergen Biosystems, Inc).

Bioinformatics and biostatistics

Classification model was built up with Biomarker Pattern's Software (BPS, Ciphergen Biosystems, Inc). Training data set consisted of 70 serum samples (25 from patients with LC, 20 from patients with liver cancer, and 25 from healthy individuals). A classification tree was set up to divide the data set into two bins based on the intensities of peaks. At each bin a peak intensity threshold was set. If the peak intensity of a sample was lower than or equal to the threshold, this sample would go to the left-side bin. Otherwise, the sample would go to the right-side bin. The process would go on until a blind sample entered a final bin, either labeled at Con (control sample) or LC (LC serum). Peaks selected by the process to form the model

were the ones that yielded the least classification error when they were combined to use.

Data set from double-blind trials consisted of 37 serum samples (15 from patients with LC, 10 from patients with liver cancer, and 12 from healthy individuals) and was used to test the model.

Specificity and sensitivity were respectively calculated as the proportion of the number of non-cirrhotic samples correctly identified to the total number of non-cirrhotic samples. Positive predictive value gives the probability of disease if a test result is positive.

RESULTS

Evaluation of SELDI protein chip

As various chip array chemistries provided different serum protein profiles in terms of number and resolution of protein peaks, WCX2, SAX2 and IMAC3-Cu metal binding chip arrays were tested, respectively. WCX2 binding chip was observed to give the best results. To demonstrate the reproducibility of the mass spectra, 8 independently obtained spectra of a serum sample of a healthy man were performed by between-run assay. We calculated that the coefficient of variance for seven selected M/Z peaks whose relative intensities were above 25 with the highest amplitude <10%. As shown in Figure 1, serum spectra from patients and healthy men do not show large variations. Therefore, small variations between different sample groups could be used for biomarker discovery. SELDI-TOF spectra of randomly selected serum samples of patients with HBV induced LC, patients with HCC, and healthy individuals are shown in Figures 1 and 2. Two proteins of M_r 7 772 and 3 933 were down-regulated in LC or up-regulated in non-cirrhotic group (healthy/HCC).

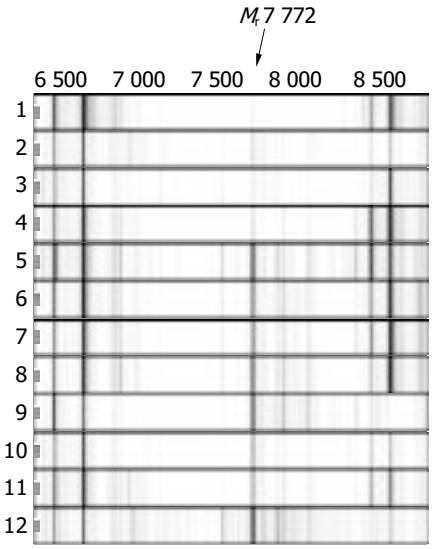

Figure 1 SELDI-TOF mass spectra. Spectra 1-4 from HBV-induced LC patients, 5-8 from healthy men, and 9-12 from HCC patients. A biomarker of M_r 7 772 was present in non-cirrhotic group, but not in LC serum samples.

Data analysis

Peak labeling was performed with Biomarker Wizard of Ciphergen ProteinChip software 3.1.1. The peak intensities were then transferred to Biomarker Pattern's software. Totally 35 peaks from M_r 2 000 to 30 000 were selected to construct the classification model. Figure 3 shows the tree structure and sample distribution. Two peaks, M_r 7 772 and 3 933, were chosen to set up the decision tree, respectively. At Node 1, samples of M_r 7 772 with peak intensities lower than or equal to 7.514 went to Terminal Node 1, which had 9 control samples and 21 LC samples. Otherwise, samples entered Node 2, which had 40 samples. At Node 2, samples of M_r 3 933 with peak intensities lower than or equal to 8.217 went to Terminal Node 2, which had 1 control sample and 3 LC samples. The other samples entered Terminal Node 3, which had 35 control samples and l LC sample. The model identified 70 samples, 36 in control and 34 in LC, and yielded a sensitivity of 96% and specificity of 77.8%. When the double-blind sample data set was used to challenge the model, the model predicted a sensitivity of 80% and specificity of 81.8%. The positive predictive value was 75%.

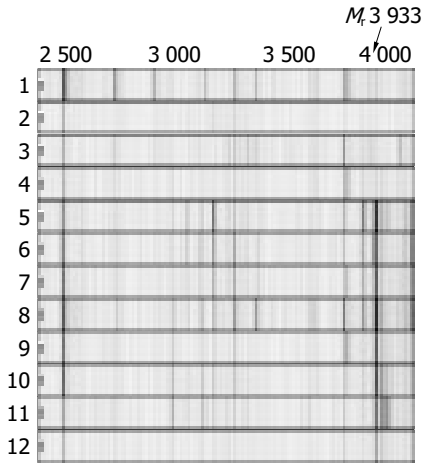

Figure 2 SELDI-TOF mass spectra. Spectra 1-4 from HBV induced LC patients, 5-8 from healthy men, and 9-12 from HCC patients. A biomarker of M_r 3 933 was present in non-cirrhotic group, but not in LC serum samples.

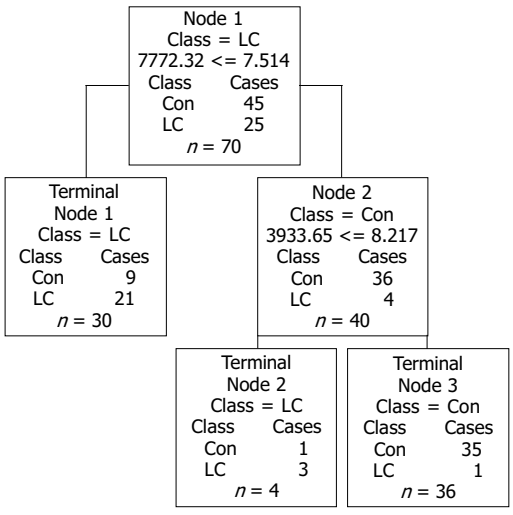

Figure 3 Tree structure and sample distribution. The root node and descendant nodes are indicated in gray, and the terminal nodes are shown in black. Peaks with M_r 7 772 and 3 933 were chosen to set up the decision tree.

DISCUSSION

HBV infection often leads to a prolonged active viral replication, HBV DNA integration and eventually LC[6]. About 55-85% of LC patients will develop hepatocellular carcinoma, which always has bad prognosis. It is estimated that HCC may be responsible for more than 1 million deaths annually and it is the fifth most frequent cause of cancer death worldwide[7]. Liver biopsy has remained the gold standard for identification of patients with liver diseases. However, the differential diagnosis between HCC

and LC is sometimes difficult and new biochemical markers for HCC are required. In recent years, several non-invasive serum biomarkers have been considered to diagnose LC associated with HBV, including hyaluronic acid (HA)[8,9], type III procollagen peptide, laminin and type IV collagen[10].

Among the non-invasive serum biomarkers for liver fibrosis and cirrhosis, HA was reported to be the best marker for diagnosis[11]. HA with a molecular mass of several million is present in most tissues as a component of the extracellular matrix. Elevated levels of serum HA have been reported in various diseases including liver diseases. Increases in serum HA correspond to the progression of liver diseases, including viral and non-viral diseases. Ding *et al*. demonstrated that the elevated serum HA levels were closely related to the severity of liver fibrosis, particularly in LC[12]. In addition, Procollagen III peptide, laminin, and type IV collagen with molecular masses of 45 000, 400 000 and 67 000, respectively, are also extracellular matrix glycoproteins and have been reported to be correlated to necrosis and inflammation as well as fibrosis in patients with chronic hepatitis and LC[13]. However, the diagnostic value, i.e. sensitivity and specificity, of these markers for patients with cirrhosis has not been satisfactory so far. Use of multiple markers led to 90% sensitivity at most in diagnosing cirrhosis, but variable specificity was about 60%[14].

SELDI-TOF mass spectrometry is a recently described affinity-based mass spectrometric method that combines chromatography and mass spectrometry. This novel technology has been used for protein or peptide biomarker identification, biomolecular interactions and post-translational modifications. Protein chip technology has proven to be useful in the discovery of potential diagnostic markers for prostate[15-17], bladder[18], ovarian[19], breast[20-22], lung cancers[23], and pancreatic ductal adenocarcinoma. However, using it to discover new biomarkers of HBV induced diseases has not been addressed before. To identify potential biomarkers that can detect HBV induced LC, protein profiles of serum samples from LC patients were compared with those from the non-cirrhotic controls. Biomarker Pattern's Software was used to identify two peaks differentially presented in control healthy and HCC serum samples compared with LC samples. The top-scored two peaks with M_r 7 772 and 3 933 were finally selected. These two proteins generated a sensitivity of 96% and specificity of 77.8%. It is difficult to find a good single marker associated with diseases because of the differences among patients' age, gender, diet and genes. Furthermore, double-blind test was used to determine the sensitivity and specificity of the model. A sensitivity of 80%, specificity of 81.8% and positive predictive value of 75% for the study population were obtained when comparing LC versus non-cirrhotic (HCC/healthy men) groups. The low-molecular-mass serum proteins are apparently different from known non-invasive serum biomarkers for LC in many aspects and might be acceptable for diagnosis and assessment of HBV associated LC.

REFERENCES

1 **Lai CL,** Lok A, Wu PC, Ng M. Risk factors and hepatocellular cancer. *Lancet* 1985; **2**: 329-330
2 **Colombo M,** de Franchis R, Del Ninno E, Sangiovanni A, De Fazio C, Tommasini M, Donato MF, Piva A, Di Carlo V, Dioguardi N. Hepatocellular carcinoma in Italian patients with cirrhosis. *N Engl J Med* 1991; **325**: 675-680
3 **Poniachik J,** Bernstein DE, Reddy KR, Jeffers LJ, Coelho-Little ME, Civantos F, Schiff ER. The role of laparoscopy in the diagnosis of cirrhosis. *Gastrointest Endosc* 1996; **43**: 568-571
4 **Issaq HJ,** Veenstra TD, Conrads TP, Felschow D. The SELDI-TOF MS approach to proteomics: protein profiling and biomarker identification. *Biochem Biophys Res Commun* 2002; **292**: 587-592
5 **He QY,** Lau GK, Zhou Y, Yuen ST, Lin MC, Kung HF, Chiu JF. Serum biomarkers of hepatitis B virus infected liver inflammation: a proteomic study. *Proteomics* 2003; **3**: 666-674
6 **Torbenson M,** Thomas DL. Occult hepatitis B. *Lancet Infect Dis* 2002; **2**: 479-486
7 **Yu AS,** Keeffe EB. Management of hepatocellular carcinoma. *Rev Gastroenterol Disord* 2003; **3**: 8-24
8 **Xiang** Y, Qian L, Wang B. Reversion of HBV-related liver fibrosis and early cirrhosis by baicao rougan capsule. *Zhongguo Zhongxiyi Jiehe Zazhi* 1999; **19**: 709-711
9 **Kozlowska** J, Loch T, Jablonska J, Cianciara J. Biochemical markers of fibrosis in chronic hepatitis and liver cirrhosis of viral origin. *Przegl Epidemiol* 2001; **55**: 451-458
10 **Chang TT,** Lin HC, Lee SD, Tsai YT, Lee FY, Jeng FS, Wu JC, Yeh PS, Lo KJ. Clinical significance of serum type-III procollagen aminopropeptide in hepatitis B virus-related liver diseases. *Scand J Gastroenterol* 1989; **24**: 533-538
11 **Luo R,** Yang S, Xie J, Zhao Z, He Y, Yao J. Diagnostic value of five serum markers for liver fibrosis. *Zhonghua Ganzangbing Zazhi* 2001; **9**: 148-150
12 **Ding H,** Chen Y, Feng X, Liu D, Wu A, Zhang L. Correlation between liver fibrosis stage and serum liver fibrosis markers in patients with chronic hepatitis B. *Zhonghua Ganzangbing Zazhi* 2001; **9**: 78-80
13 **Castera L,** Hartmann DJ, Chapel F, Guettier C, Mall F, Lons T, Richardet JP, Grimbert S, Morassi O, Beaugrand M, Trinchet JC. Serum laminin and type IV collagen are accurate markers of histologically severe alcoholic hepatitis in patients with cirrhosis. *J Hepatol* 2000; **32**: 412-418
14 **Oh S,** Afdhal NH. Hepatic fibrosis: are any of the serum markers useful? *Curr Gastroenterol Rep* 2001; **3**: 12-18
15 **Qu Y,** Adam BL, Yasui Y, Ward MD, Cazares LH, Schellhammer PF, Feng Z, Semmes OJ, Wright GL Jr. Boosted decision tree analysis of surface-enhanced laser desorption/ionization mass spectral serum profiles discriminates prostate cancer from noncancer patients. *Clin Chem* 2002; **48**: 1835-1843
16 **Adam BL,** Qu Y, Davis JW, Ward MD, Clements MA, Cazares LH, Semmes OJ, Schellhammer PF, Yasui Y, Feng Z, Wright GL Jr. Serum protein fingerprinting coupled with a pattern-matching algorithm distinguishes prostate cancer from benign prostate hyperplasia and healthy men. *Cancer Res* 2002; **62**: 3609-3614
17 **Banez LL,** Prasanna P, Sun L, Ali A, Zou Z, Adam BL, McLeod DG, Moul JW, Srivastava S. Diagnostic potential of serum proteomic patterns in prostate cancer. *J Urol* 2003; **170**: 442-446
18 **Adam BL,** Vlahou A, Semmes OJ, Wright GL Jr. Proteomic approaches to biomarker discovery in prostate and bladder cancers. *Proteomics* 2001; **1**: 1264-1270
19 **Petricoin EF,** Ardekani AM, Hitt BA, Levine PJ, Fusaro VA, Steinberg SM, Mills GB, Simone C, Fishman DA, Kohn EC, Liotta LA. Use of proteomic patterns in serum to identify ovarian cancer. *Lancet* 2002; **359**: 572-577
20 **Li J,** Zhang Z, Rosenzweig J, Wang YY, Chan DW. Proteomics and bioinformatics approaches for identification of serum biomarkers to detect breast cancer. *Clin Chem* 2002; **48**: 1296-1304
21 **Paweletz CP,** Trock B, Pennanen M, Tsangaris T, Magnant C, Liotta LA, Petricoin EF 3rd. Proteomic patterns of nipple aspirate fluids obtained by SELDI-TOF: potential for new biomarkers to aid in the diagnosis of breast cancer. *Dis Markers* 2001; **17**: 301-307
22 **Coombes KR,** Fritsche HA Jr, Clarke C, Chen JN, Baggerly KA, Morris JS, Xiao LC, Hung MC, Kuerer HM. Quality control and peak finding for proteomics data collected from nipple aspirate fluid by surface-enhanced laser desorption and ionization. *Clin Chem* 2003; **49**: 1615-1623
23 **Xiao XY,** Tang Y, Wei XP, He DC. A preliminary analysis of non-small cell lung cancer biomarkers in serum. *Biomed Environ Sci* 2003; **16**: 140-148

Edited by Chen WW **Proofread by** Zhu LH and Xu FM

PO Box 2345, Beijing 100023, China
Fax: +86-10-85381893
E-mail: wjg@wjgnet.com www.wjgnet.com

World J Gastroenterol 2004;10(16):2330-2333
World Journal of Gastroenterology
 ISSN 1007-9327

• VIRAL HEPATITIS •

Association of interleukin-12 *p40* gene 3'-untranslated region polymorphism and outcome of HCV infection

Li-Min Yin, Wan-Fu Zhu, Lai Wei, Xiao-Yuan Xu, De-Gui Sun, Yan-Bin Wang, Wen-Mei Fan, Min Yu, Xiu-Lan Tian, Qi-Xin Wang, Yan Gao, Hui Zhuang

Li-Min Yin, Wan-Fu Zhu, Wen-Mei Fan, Hui Zhuang, Department of Microbiology, School of Basic Medical Sciences, Peking University, Beijing 100083, China
Xiao-Yuan Xu, Min Yu, Xiu-Lan Tian, Department of Infectious Disease, First Hospital, Peking University, Beijing 100034, China
Lai Wei, Qi-Xin Wang, Yan Gao, Hepatology Institute, People's Hospital, Peking University, Beijing 100044, China
De-Gui Sun, Gu'an Station of Disease Prevention and Control, Gu'an 102700, Hebei Province, China
Yan-Bin Wang, Beijing Ditan Hospital, Beijing 100730, China
Supported by the National Key Technologies Research and Development Program of China during the 10th Five-Year Period, No. 2001BA705B06
Correspondence to: Professor Wan-Fu Zhu, Department of Microbiology, School of Basic Medical Sciences, Peking University, Beijing 100083, China. zhuwanfu@sun.bjmu.edu.cn
Telephone: +86-10-82801599 **Fax:** +86-10-82801599
Received: 2004-01-15 **Accepted:** 2004-02-21

Abstract

AIM: To investigate the effect of interleukin-12 *p40* gene (*IL12B*) 3'-untranslated region polymorphism on the outcome of HCV infection.

METHODS: A total of 133 patients who had been infected with HCV for 12-25 (18.2±3.8) years, were enrolled in this study. Liver biochemical tests were performed with an automated analyzer and HCV RNA was detected by fluorogenic quantitative polymerase chain reaction. B-mode ultrasound was used for liver examination. Polymerase chain reaction-restriction fragment length polymorphism (PCR-RFLP) was used for the detection of *IL12B* (1188A/C) polymorphism.

RESULTS: Self-limited infection was associated with AC genotype (OR = 3.48; $P = 0.001$) and persistent infection was associated with AA genotype (OR = 0.34; $P = 0.014$) at site 1188 of *IL12B*. In patients with persistent HCV infection, no significant differences were found regarding the age, gender, duration of infection and biochemical characteristics ($P>0.05$). According to B-mode ultrasound imaging and clinical diagnosis, patients with persistent infection were divided into groups based on the severity of infection. No significant differences were found in the frequency of IL-12 genotype (1188A/C) between different groups ($P>0.05$).

CONCLUSION: The polymorphism of *IL12B* (1188A/C) appears to have some influence on the outcome of HCV infection.

Yin LM, Zhu WF, Wei L, Xu XY, Sun DG, Wang YB, Fan WM, Yu M, Tian XL, Wang QX, Gao Y, Zhuang H. Association of interleukin-12 *p40* gene 3'-untranslated region polymorphism and outcome of HCV infection. *World J Gastroenterol* 2004; 10(16): 2330-2333
http://www.wjgnet.com/1007-9327/10/2330.asp

INTRODUCTION

Hepatitis C virus (HCV) is the major cause of post-transfusion hepatitis. As is estimated by WHO, approximately 170 million people globally may have been infected with HCV[1]. Although chronic HCV infections are often clinically silent for decades, an estimated 85% of individuals infected with HCV develop persistent infection, and these patients are likely to end up with cirrhosis and liver cancer[1-3]. HCV infection persists despite the presence of specific humoral and cellular immune responses, and the factors leading to viral clearance or persistence are poorly understood. But some researches showed that the outcome might already be determined at an early time point following infection[4-7]. Patients with acute HCV infection presenting a self-limited acute hepatitis develop a strong Th1 response. In contrast, patients developing a chronic infection show a predominant Th2 response, but a weak Th1 response. These findings suggest that the imbalance or skewness between responses of Th1 and Th2 cells is involved in disease progression and in the incapability to eradicate HCV[8-10]. Interleukin 12 (IL-12) is a key cytokine presented with the initiation of immune response, which is one of the most clearly defined factors determining Th1 and Th2 differentiation[11,12]. IL-12 might, therefore, play an important role in the pathogenesis of HCV infection by affecting the Th1/Th2 balance. Single nucleotide polymorphism (SNP) (1188A/C) was identified at position 1188 in the 3'-untranslated region (UTR) of IL-12 *p40* gene (*IL12B*) and was found to correlate with many diseases[13-15].

In this study, we proposed that some genotypes of SNP (1188A/C) might associate with either disease outcome or the state of illness in chronic HCV infection. To test this hypothesis, we determined the frequency of genotypes at the SNP site using polymerase chain reaction-restriction fragment length polymorphism (PCR-RFLP) in HCV infected patients, as well as the relationship between *IL12B* and outcome of HCV infection.

MATERIALS AND METHODS

Subjects

A total of 133 patients with confirmed diagnoses of HCV infection in Gu'an County, Hebei Province, China, who had been infected with HCV for 12-25 (18.2±3.8) years, were enrolled in this study. All the patients were investigated in January 2002. There were 61 (45.9%) male and 72 (54.1%) female patients ranging from 30 to 69 years old (mean age, 46.5±8.3 years). All subjects had no access to antivirus treatment.

Laboratory examination

Venous blood was drawn from each individual and genomic DNA was extracted from clotted blood with a protocol by using silica (Sigma, S-5631). Genotyping of SNP (1188A/C) was carried out by PCR-RFLP according to Hall *et al*.[13]. Liver biochemistry tests including alanine aminotransferase (ALT), aspartate aminotransferase (AST), γ-glutamyltransferase (γ-GT), alkaline phosphatase (ALP), total bilirubin (TBil), direct bilirubin (DBil), total protein (Tp), albumin (ALB) and serum albumin/globulin ratio (A/G) were measured with HITACHI 7170 automatic

biochemistry analyzer. The B-mode ultrasound was performed for liver examination. HCV RNA was detected with quantitative fluorogenic PCR.

Statistical analysis

Data were expressed as mean±SD. Student's *t*-test, one-way analysis of variance and Chi-square tests were used for statistical analysis according to the data obtained. Logistic regression was used to assess the impact of variables on the odds of the outcome of HCV infection. Multivariate analysis of variance was used to analyze the difference of clinical characteristics among patients with persistent infection. All univariate and multivariable calculations, including odds ratios (OR), 95% confidence intervals (95% CI), and *P* values were calculated using the SPSS (version 10).

RESULTS

Of 133 cases investigated in this study, 91 (68.4%) were HCV RNA positive and 42 (31.6%) were HCV RNA negative. SNP typing of DNA samples from all the subjects is shown in Table 1. The proportions of male subjects were 31.0% in self-limited infection and 52.7% in persistent infection. Female gender was closely related to self-limited infection ($P<0.05$). All patients were HCV infected as a consequence of plasma donation. The mean durations of infection were 17.76 and 18.44 years for patients with self-limited infection and matched patients with persistent infection, respectively. HCV genotype 1b was found in all the patients except two. In addition, the two groups were indistinguishable with respect to age, source of infection, duration of infection and HCV genotype ($P>0.05$).

Table 1 Features of subjects enrolled in the study

Group	*n*	Gender (male/female)	Age (yr)	Duration of infection (yr)
Self-limited infection	42	13/29	45.71±7.68	17.76±3.82
Persistent infection	91	48/43	46.85±8.56	18.44±3.82

Agarose gel electrophoresis result of three genotypes of SNP (1188A/C) is shown in Figure 1. Genotype frequencies at SNP (1188A/C) are listed in Table 2. There was significant difference in genotype distribution between subjects with self-limited infection and subjects with persistent infection ($P<0.01$). The distribution of genotype showed a good fit to Hardy-Weinberg equilibrium. At SNP (1188A/C) locus, the AC homozygous genotype was found more frequently in subjects with self-limited infection compared to those with persistent infection: 64.3% *vs* 34.1% (OR = 3.48; 95% CI: 1.52-8.10; $P = 0.001$). The AA genotype was more frequent in individuals with persistent infection compared to those with self-limited infection: 40.7% *vs* 19.0% (OR = 0.34; 95% CI: 0.12-0.87; $P = 0.014$).

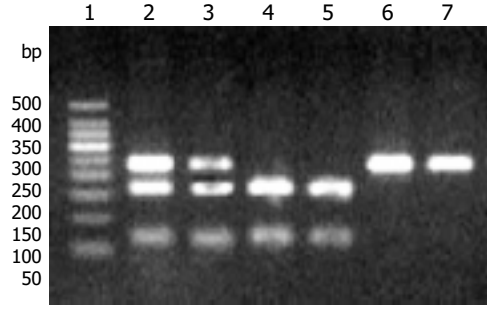

Figure 1 2% agarose gel electrophoresis of restriction enzyme digested products. Lane 1: 50 bp DNA ladder; lanes 2 and 3: AC genotype; lanes 4 and 5: CC genotype; lanes 6 and 7: AA genotype.

Table 2 Genotype frequencies of 1188A/C SNP of *IL12B* in patients

Genotype	Self-limited infection (%) *n* = 42	Persistent infection (%) *n* = 91	OR	95% CI	*P*
AA	8 (19.0)	37 (40.7)	0.34	0.12-0.87	0.014
CC	7 (16.7)	23 (25.3)	0.59	0.20-1.61	0.270
AC	27 (64.3)	31 (34.1)	3.48	1.52-8.10	0.001

Comparisons of genotype distribution using chi square test showed significant difference between self-limited infection and persistent infection ($P = 0.004$).

Effects of variables on the outcome of HCV infection were investigated by means of binary logistic regression analysis (Table 3). Both genotypes of SNP (1188A/C) and gender were independently associated with the outcome of HCV infection (OR 0.43, $P = 0.001$; OR 0.41, $P = 0.029$, respectively).

Table 3 Multivariate analysis of the effects of variables on the outcome of HCV infection

Variable	*P*	Multivariate odds ratio (95% CI)
Genotype	0.001	0.43 (0.27-0.70)
Gender	0.029	0.41 (0.18-0.91)
Duration of infection	NS	-

The general features, biochemical characteristics and HCV RNA levels in patients with persistent infection grouped by the genotype of SNP (1188A/C) of *IL12B* were analyzed (Table 4). No significant differences were found in age, gender or the duration of infection between three groups. And no significant differences were found in ALT, AST, γ-GT, ALP, TBil, DBil, Tp, ALB, A/G or HCV RNA levels between three groups ($P>0.05$). According to the result from B-mode ultrasound and clinical diagnosis, patients with persistent infection were divided into groups based on severity. No significant differences were found in genotype frequencies between different groups ($P>0.05$). Multivariate analysis of variance was used to analyze the different biochemical characteristics between three groups, and no difference was found ($P>0.05$) (data not shown).

Table 4 Characteristics of patients with different SNP (1188A/C) genotypes during persistent infection

Characteristics	AA *n* = 38	CC *n* = 23	AC *n* = 30
Age (yr)	46.9±8.2	46.7±9.7	46.8±8.4
Gender (male/female)	21/17	12/11	15/15
Duration of disease (yr)	18.0±3.8	18.8±4.0	18.1±3.8
ALT (U/L)	51±44	51±60	44±26
AST (U/L)	50±30	51±34	47±20
γ-GT (U/L)	24±26	35±33	28±34
ALP (U/L)	88±26	92±28	93±22
Tbil (μmol/L)	29±11	8.95±2.59	10.1±4.2
Dbil (μmol/L)	5.8±2.0	5.3±2.2	5.4±2.4
Tp (g/L)	75.3±3.9	72.24±5.95	75.0±5.8
ALB (g/L)	44.4±2.3	43.8±2.3	44.5±2.6
A/G	1.46±0.21	1.59±0.32	1.51±0.30
HCV RNA[1]	5.07±1.49	4.95±1.52	5.58±1.24

[1]Values are expressed as $\log_{10}$ RNA copies per mL.

DISCUSSION

For the first time, we investigated here the polymorphism of

SNP (1188A/C) of *IL12B* in patients with HCV infection and demonstrated that AA genotype decreased and AC genotype increased in self-limited infection. Although there was no significant difference in allele distribution between patients with self-limited infection and patients with persistent infection, A allele tended to be decreased and C genotype to be increased in self-limited infection. In this study, however, there was no association between genotype of SNP (1188A/C) of *IL12B* and biochemical characteristics of subjects with persistent infection. And no association was found between genotype of SNP (1188A/C) and the severity of subjects with persistent infection.

HCV infection is characterized by a broad spectrum of possible outcomes. Infection is self-limited in a fortunate minority, while the majority of patients develop persistent infection[16,17]. Patients with acute HCV infection presenting a self-limited acute hepatitis and with eradication of the virus develop a strong Th1 response but a weak or absent Th2 response. In contrast, patients developing a chronic infection show a predominant Th2 response, but a weak Th1 response. These observations suggest that Th1 cytokine effect is essential for protection against HCV infection, while the production of Th2 cytokine seems to have an inhibiting effect on the patient's immunological system[8,10]. IL-12 is a key regulator of the polarization of immune responses to T helper 1 or 2 categories and plays a role in autoimmune and infectious diseases[11,12,18]. IL-12 might, therefore, have effects on the pathogenesis of HCV infection by affecting Th1/Th2 balance.

IL-12 is comprised of two disulphide-linked protein subunits designated p35 and p40, which are encoded by two different genes, *IL12A* and *IL12B*[19,20]. IL-12 *p40* expression is restricted to the production of *p70* because *p35* is expressed ubiquitously and constitutively at low levels. Thus, secretion of the biologically active p70 heterodimer appears to be predominantly regulated at the level of *IL12B*[12]. IL-12 is secreted mainly by antigen-presenting cells and plays a key role in innate resistance and adaptive immunity. IL-12 acts on T cells and NK cells by enhancing generation and activity of cytotoxic lymphocytes and inducing proliferation and production of cytokines, especially IFN-γ. IL-12 is also the major cytokine responsible for differentiation of T helper 1 cells, which are potent producers of IFN-γ[12,19]. And IFN-γ plays important roles in the immune response to HCV infection. Some studies have been reported that the deletions of IL-12 *p40* lead to serious impairment of immunity to intracellular bacteria[21]. The SNP at position 1188 in the untranslated region of IL-12 *p40* gene mapped to chromosome 5q31-33. Although SNP is located in UTR and does not alter the coding sequence, some researches showed that this SNP site was associated with immune-mediated disease[13,22].

Many studies showed that there was close relationship between IL-12 and hepatitis C. Nelson *et al*. reported that patients with chronic HCV infection had elevated IL-12, which correlated with serum ALT and intrahepatic HCV-specific CTL activity. These data indicate that IL-12 is involved in the immunopathogenesis of chronic HCV infection, especially in cell-mediated immunity, which might be important in spontaneous or interferon mediated viral clearance[23,24]. Another study reported the impairment in allostimulatory capacity of peripheral blood dendritic cells in HCV- infected individuals, which is likely due to low IL-12 expression and restored by endogenous IL-12[25]. Some studies have found that IL-12 can produce lower HCV-RNA level[26-31].

Studies on functional characteristics of this polymorphism suggest that they influence the secretion of cytokines. Morahan *et al*. reported the 3'-UTR alleles showed different levels of *IL12B* mRNA expression in cell lines. They identified EBV-transformed cell lines homozygous for each allele. Expression of *IL12B* mRNA was significantly reduced in the C/C genotype cell line in contrast to the A/A line[32]. But Seegers *et al*. found that a TaqI polymorphism (C/C) in IL12 *p40* 3'-UTR correlated with increased IL-12 *p70 in vitro*[33]. The results were complicated and the functional characteristics of this polymorphism still need to be evaluated. Currently our group is working on the IL-12 mRNA and protein levels of three different genotypes to clarify how SNP (1188A/C) influences the course of hepatitis C.

In summary, we have reported that the frequency of A/A genotype of *IL12B* 3'-UTR SNP was decreased in self-limited HCV infection. It suggests that this SNP is associated with different outcomes of HCV infection, presumably by affecting Th1/Th2 balance. Nevertheless, since the outcome of HCV infection is a complicated polygenic trait, the interactive effects between SNP (1188A/C) of *IL12B* and other factors involved in the outcome of hepatitis C still need to be evaluated.

ACKNOWLEDGEMENT

We are very grateful to Professor Shu-Lin Liu for his critical revision of this paper.

REFERENCES

1 Global surveillance and control of hepatitis C. Report of a WHO Consultation organized in collaboration with the Viral Hepatitis Prevention Board, Antwerp, Belgium. *J Viral Hepat* 1999; **6**: 35-47
2 **Villano SA,** Vlahov D, Nelson KE, Cohn S, Thomas DL. Persistence of viremia and the importance of long-term follow-up after acute hepatitis C infection. *Hepatology* 1999; **29**: 908-914
3 **Alter HJ,** Seeff LB. Recovery, persistence, and sequelae in hepatitis C virus infection: a perspective on long-term outcome. *Semin Liver Dis* 2000; **20**: 17-35
4 **Thimme R,** Bukh J, Spangenberg HC, Wieland S, Pemberton J, Steiger C, Govindarajan S, Purcell RH, Chisari FV. Viral and immunological determinants of hepatitis C virus clearance, persistence, and disease. *Proc Natl Acad Sci U S A* 2002; **99**: 15661-15668
5 **Alberti A,** Chemello L, Benvegnu L. Natural history of hepatitis C. *J Hepatol* 1999; **31**(Suppl 1): 17-24
6 **Diepolder HM,** Zachoval R, Hoffmann RM, Jung MC, Gerlach T, Pape GR. The role of hepatitis C virus specific CD4+ T lymphocytes in acute and chronic hepatitis C. *J Mol Med* 1996; **74**: 583-588
7 **Lechner F,** Wong DK, Dunbar PR, Chapman R, Chung RT, Dohrenwend P, Robbins G, Phillips R, Klenerman P, Walker BD. Analysis of successful immune responses in persons infected with hepatitis C virus. *J Exp Med* 2000; **191**: 1499-1512
8 **Montano-Loza A,** Meza-Junco J, Remes-Troche JM. Pathogenesis of hepatitis C virus infection. *Rev Invest Clin* 2001; **53**: 561-568
9 **Boyer N,** Marcellin P. Pathogenesis, diagnosis and management of hepatitis C. *J Hepatol* 2000; **32**(1 Suppl): 98-112
10 **Pape GR,** Gerlach TJ, Diepolder HM, Gruner N, Jung M, Santantonio T. Role of the specific T-cell response for clearance and control of hepatitis C virus. *J Viral Hepat* 1999; **6**(Suppl 1): 36-40
11 **Trinchieri G.** Interleukin-12 and the regulation of innate resistance and adaptive immunity. *Nat Rev Immunol* 2003; **3**: 133-146
12 **Watford WT,** Moriguchi M, Morinobu A, O'Shea JJ. The biology of IL-12: coordinating innate and adaptive immune responses. *Cytokine Growth Factor Rev* 2003; **14**: 361-368
13 **Hall MA,** McGlinn E, Coakley G, Fisher SA, Boki K, Middleton D, Kaklamani E, Moutsopoulos H, Loughran TP Jr, Ollier WE, Panayi GS, Lanchbury JS. Genetic polymorphism of IL-12 p40 gene in immune-mediated disease. *Genes Immun* 2000; **1**: 219-224
14 **Tsunemi Y,** Saeki H, Nakamura K, Sekiya T, Hirai K, Fujita H, Asano N, Kishimoto M, Tanida Y, Kakinuma T, Mitsui H, Tada Y, Wakugawa M, Torii H, Komine M, Asahina A, Tamaki K. Interleukin-12 p40 gene (IL12B) 3'-untranslated region polymorphism is associated with susceptibility to atopic dermatitis and psoriasis vulgaris. *J Dermatol Sci* 2002; **30**: 161-166
15 **Davoodi-Semiromi A,** Yang JJ, She JX. IL-12 p40 is associated with type 1 diabetes in Caucasian-American families. *Diabetes* 2002; **51**: 2334-2336

16 **Alter MJ,** Margolis HS, Krawczynski K, Judson FN, Mares A, Alexander WJ, Hu PY, Miller JK, Gerber MA, Sampliner RE. The natural history of community-acquired hepatitis C in the United States. The Sentinel Counties Chronic non-A, non-B Hepatitis Study Team. *N Engl J Med* 1992; **327**: 1899-1905
17 **Zhu WF,** Yin LM, Li P, Huang J, Zhuang H. Pathogenicity of GB virus C on virus hepatitis and hemodialysis patients. *World J Gastroenterol* 2003; **9**: 1739-1742
18 **Romani L,** Puccetti P, Bistoni F. Interleukin-12 in infectious diseases. *Clin Microbiol Rev* 1997; **10**: 611-636
19 **Trinchieri G.** Interleukin-12: a proinflammatory cytokine with immunoregulatory functions that bridge innate resistance and antigen-specific adaptive immunity. *Annu Rev Immunol* 1995; **13**: 251-276
20 **Gately MK,** Renzetti LM, Magram J, Stern AS, Adorini L, Gubler U, Presky DH. The interleukin-12/interleukin-12-receptor system: role in normal and pathologic immune responses. *Annu Rev Immunol* 1998; **16**: 495-521
21 **Altare F,** Lammas D, Revy P, Jouanguy E, Doffinger R, Lamhamedi S, Drysdale P, Scheel-Toellner D, Girdlestone J, Darbyshire P, Wadhwa M, Dockrell H, Salmon M, Fischer A, Durandy A, Casanova JL, Kumararatne DS. Inherited interleukin 12 deficiency in a child with bacille Calmette-Guerin and Salmonella enteritidis disseminated infection. *J Clin Invest* 1998; **102**: 2035-2040
22 **Alloza I,** Heggarty S, Goris A, Graham CA, Dubois B, McDonnell G, Hawkins SA, Carton H, Vandenbroeck K. Interleukin-12 p40 polymorphism and susceptibility to multiple sclerosis. *Ann Neurol* 2002; **52**: 524-525
23 **Nelson DR,** Marousis CG, Ohno T, Davis GL, Lau JY. Intrahepatic hepatitis C virus-specific cytotoxic T lymphocyte activity and response to interferon alfa therapy in chronic hepatitis C. *Hepatology* 1998; **28**: 225-230
24 **Quiroga JA,** Martin J, Navas S, Carreno V. Induction of interleukin-12 production in chronic hepatitis C virus infection correlates with the hepatocellular damage. *J Infect Dis* 1998; **178**: 247-251
25 **Kanto T,** Hayashi N, Takehara T, Tatsumi T, Kuzushita N, Ito A, Sasaki Y, Kasahara A, Hori M. Impaired allostimulatory capacity of peripheral blood dendritic cells recovered from hepatitis C virus-infected individuals. *J Immunol* 1999; **162**: 5584-5591
26 **Zeuzem S,** Hopf U, Carreno V, Diago M, Shiffman M, Grune S, Dudley FJ, Rakhit A, Rittweger K, Yap SH, Koff RS, Thomas HC. A phase I/II study of recombinant human interleukin-12 in patients with chronic hepatitis C. *Hepatology* 1999; **29**: 1280-1287
27 **O'Brien CB,** Moonka DK, Henzel BS, Caufield M, DeBruin MF. A pilot trial of recombinant interleukin-12 in patients with chronic hepatitis C who previously failed treatment with interferon-alpha. *Am J Gastroenterol* 2001; **96**: 2473-2479
28 **Pockros PJ,** Patel K, O'Brien C, Tong M, Smith C, Rustgi V, Carithers RL, McHutchison JG, Olek E, Debruin MF. A multicenter study of recombinant human interleukin 12 for the treatment of chronic hepatitis C virus infection in patients nonresponsive to previous therapy. *Hepatology* 2003; **37**: 1368-1374
29 **Zeuzem S,** Carreno V. Interleukin-12 in the treatment of chronic hepatitis B and C. *Antiviral Res* 2001; **52**: 181-188
30 **Barth H,** Klein R, Berg PA, Wiedenmann B, Hopf U, Berg T. Analysis of the effect of IL-12 therapy on immunoregulatory T-cell subsets in patients with chronic hepatitis C infection. *Hepatogastroenterology* 2003; **50**: 201-206
31 **Lee JH,** Teuber G, von Wagner M, Roth WK, Zeuzem S. Antiviral effect of human recombinant interleukin-12 in patients infected with hepatitis C virus. *J Med Virol* 2000; **60**: 264-268
32 **Morahan G,** Huang D, Ymer SI, Cancilla MR, Stephen K, Dabadghao P, Werther G, Tait BD, Harrison LC, Colman PG. Linkage disequilibrium of a type 1 diabetes susceptibility locus with a regulatory IL12B allele. *Nat Genet* 2001; **27**: 218-221
33 **Seegers D,** Zwiers A, Strober W, Pena AS, Bouma G. A TaqI polymorphism in the 3'UTR of the IL-12 p40 gene correlates with increased IL-12 secretion. *Genes Immun* 2002; **3**: 419-423

Edited by Chen WW **Proofread by** Zhu LH and Xu FM

PO Box 2345, Beijing 100023, China
Fax: +86-10-85381893
E-mail: wjg@wjgnet.com www.wjgnet.com

World J Gastroenterol 2004;10(16):2334-2339
World Journal of Gastroenterology
 ISSN 1007-9327

Helicobacter pylori enhances tumor necrosis factor-related apoptosis-inducing ligand-mediated apoptosis in human gastric epithelial cells

Yi-Ying Wu, Hwei-Fang Tsai, We-Cheng Lin, Ai-Hsiang Chou, Hui-Ting Chen, Jyh-Chin Yang, Ping-I Hsu, Ping-Ning Hsu

Yi-Ying Wu, Hwei-Fang Tsai, We-Cheng Lin, Ai-Hsiang Chou, Hui-Ting Chen, Ping-Ning Hsu, Graduate Institute of Immunology, College of Medicine, National Taiwan University, Taiwan, China
Jyh-Chin Yang, Ping-I Hsu, Department of Internal Medicine, National Taiwan University Hospital, Taipei, Taiwan, China
Supported by the Grants from the National Health Research Institute, Taiwan, NHRI-GI-EX89S942C and the National Science Council, NSC-90-2314B-075B003, NSC 91-2320B-002 and the National Taiwan University Hospital, NTUH 89S2011
Correspondence to: Dr. Ping-Ning Hsu, Graduate Institute of Immunology, College of Medicine, National Taiwan University, No. 1, Sec. 1, Jen-Ai Road, Taipei, Taiwan, China. phsu@ha.mc.ntu.edu.tw
Telephone: +886- 223123456 **Fax:** +886- 223217921
Received: 2004-03-15 **Accepted:** 2004-04-15

Abstract

AIM: To investigate the relations between tumor necrosis factor-related apoptosis-inducing ligand (TRAIL) and *Helicobacter pylori* (*H pylori*) infection in apoptosis of gastric epithelial cells and to assess the expression of TRAIL on the surface of infiltrating T-cells in *H pylori*-infected gastric mucosa.

METHODS: Human gastric epithelial cell lines and primary gastric epithelial cells were co-cultured with *H pylori in vitro,* then recombinant TRAIL proteins were added to the culture. Apoptosis of gastric epithelial cells was determined by a specific ELISA for cell death. Infiltrating lymphocytes were isolated from *H pylori*-infected gastric mucosa, and expression of TRAIL in T cells was analyzed by flow cytometry.

RESULTS: The apoptosis of gastric epithelial cell lines and primary human gastric epithelial cells was mildly increased by interaction with either TRAIL or *H pylori* alone. Interestingly, the apoptotic indices were markedly elevated when gastric epithelial cells were incubated with both TRAIL and *H pylori* (Control *vs* TRAIL and *H pylori*: 0.51±0.06 *vs* 2.29±0.27, $P = 0.018$). A soluble TRAIL receptor (DR4-Fc) could specifically block the TRAIL-mediated apoptosis. Further studies demonstrated that infiltrating T-cells in gastric mucosa expressed TRAIL on their surfaces, and the induction of TRAIL sensitivity by *H pylori* was dependent upon direct cell contact of viable bacteria, but not CagA and VacA of *H pylori*.

CONCLUSION: *H pylori* can sensitize human gastric epithelial cells and enhance susceptibility to TRAIL-mediated apoptosis. Modulation of host cell sensitivity to apoptosis by bacterial interaction adds a new dimension to the immunopathogenesis of *H pylori* infection.

Wu YY, Tsai HF, Lin WC, Chou AH, Chen HT, Yang JC, Hsu PI, Hsu PN. *Helicobacter pylori* enhances tumor necrosis factor-related apoptosis-inducing ligand-mediated apoptosis in human gastric epithelial cells. *World J Gastroenterol* 2004; 10(16): 2334-2339
http://www.wjgnet.com/1007-9327/10/2334.asp

INTRODUCTION

Helicobacter pylori (*H pylori*), which infects about 50% of the world's population, is the leading cause of chronic gastritis and peptic ulcer diseases. Recent studies have shown that apoptosis of gastric epithelial cells is increased during *H pylori* infection[1-4]. The enhanced gastric epithelial cell apoptosis in *H pylori* infection has been suggested to play an important role in the pathogenesis of chronic gastritis, peptic ulcer and gastric neoplasia. There are a number of mechanisms that may be involved, including the direct cytotoxic effects of the bacteria, as well as inflammatory responses elicited by the infection[4-7]. Recent studies have suggested that T helper type 1 (Th1) cells are selectively increased during *H pylori* infection[8-11]. Th1 cytokines, such as gamma interferon (IFN-) and tumor necrosis factor alpha (TNF-), can increase the release of proinflammatory cytokines, augmenting apoptosis induced by *H pylori*[7]. *H pylori* infection could also induce gastric mucosa damage by increasing expression of Fas in gastric epithelial cells, leading to gastric epithelial cell apoptosis through Fas/FasL interaction with infiltrating T cells[6,12]. These findings suggest a role for immune-mediated apoptosis of gastric epithelial cells during *H pylori* infection.

TRAIL, a novel TNF superfamily member with strong homology to FasL, is capable of inducing apoptosis in a variety of transformed cell lines *in vitro*[13,14]. Recent studies indicated that TRAIL-induced apoptosis occurred through a caspase signaling cascade[15-17]. It has been shown that T cells can kill target cells via TRAIL/TRAIL receptor interaction[18-23], suggesting that TRAIL might serve as a cytotoxic effector molecule in activated T cells *in vivo*. In addition to its role in inducing apoptosis by binding to death receptors, TRAIL itself can stimulate T cells and augment IFN- secretion[24]. These findings have led us to hypothesize that TRAIL/TRAIL receptor interaction was involved in the apoptosis of gastric epithelial cells in *H pylori* gastritis. We therefore designed the study to investigate the interactions between TRAIL and *H pylori* in apoptosis of human gastric epithelial cells. Additionally, we assessed the expression of TRAIL on the surface of infiltrating T-cells in *H pylori*-infected gastric mucosa.

MATERIALS AND METHODS

Bacterial strains, cell lines, and media

H pylori standard strain ATCC43504 (CagA+, VacA+) and the mutant strain ATCC51932 (CagA-, VacA-), obtained from American Type Culture Collections (ATCC) were used. *H pylori* strain NTUH-C1 (CagA+, VacA+) was isolated from a patient with duodenal ulcer in National Taiwan University Hospital. Before each experiment, *H pylori* was passaged on 5% sheep blood agar plates by incubation in an atmosphere consisting

of 5% O_2, 15% CO_2, and 80% N_2 for 2-4 d at 37 °C. Bacteria were cultured in Brucella broth (Difco Labs, Inc. Detroit, MI) supplemented with 5% FBS, vancomycin and amphotericin B under the same conditions for 30 h at 37 °C with agitation (80-100 rpm/min). Cells were then pelleted and resuspended in phosphate-buffered saline at a concentration of 10^8 CFU/mL. Human gastric adenocarcinoma cell line AGS was obtained from ATCC and maintained in DMEM, supplemented with 10% FBS.

Generation of cagA or vacA gene knock out H pylori mutant strains

For generation of *H pylori* isogenic mutant strains with *cagA* or *vacA* gene defect, we introduced mutations into *cagA* or *vacA* gene in *H pylori* strain NTUH-C1. *cagA* and *vacA* genes were amplified by PCR with the following primer pairs, *cagA*: 5'-ATGACTAACGAAACTATTGATCAAACA-3' and 5'-AGATTTTTGGAAACCACCTT TTGTATTA-3'; *vacA*: 5'-GCTGGGATTGGGGGAATG-3' and 5'-TTGCGCGCTA TTGGGTGG-3'. The PCR fragments were purified and then cloned on pGEM-T easy vector by a TA cloning kit (Promega, Madison, WI, USA). The cloned *cagA* or *vacA* gene was digested with *Nhe* I, after which the chloramphenicol resistant marker (CAT cassette) was ligated with recombinant *Nhe* I sites at both ends. The plasmid pGEM-T Easy Vector with *cagA* or *vacA* inserted by the CAT cassette was used for the natural transformation of *H pylori* strain NTUH-C1. The *cagA* gene or *vacA* gene isogenic knockout mutants were selected by the BHI agar plate with 40 ppm chloramphenicol and confirmed with PCR.

Expression and purification of recombinant TRAIL protein and soluble TRAIL receptor (DR4-Fc)

Recombinant TRAIL proteins were expressed in *E. coli* expression system and purified with Ni column as described[24]. In brief, the coding portion of the extracellular domain of TRAIL (amino acid 123-314) was PCR amplified, subcloned into pRSET B vector (Invitrogen, Groningen, the Netherlands) and expressed in *E. coli* expression system. Purification of recombinant His-TRAIL fusion protein was performed by metal chelate column chromatography using Ni-NTA resin according to the manufacturer's recommendations (Qiagen, Hilden, Germany). His-TRAIL was quantified by the Bradford method and protein assay reagent (BioRad, Richmond, CA, USA). To generate soluble recombinant DR4-Fc fusion molecules, the coding sequence for the extracellular domain of human DR4 was isolated by RT-PCR using the forward primer, CGGATTTCATGGCGCCACCACCA, and the reverse primer, GAAGATCTATTATGTCCATTGCC. The amplified product was ligated in-frame into *Bam*HI-cut pUC19-IgG1-Fc vector containing the human IgG1 Fc coding sequence. The fusion gene was then subcloned into pBacPAK9 vector (Clontech, Palo Alto, CA). DR4-Fc fusion protein was recovered from the filtered supernatants of the recombinant virus-infected Sf21 cells using protein G-sepharose beads (Pharmacia, Piscataway, NJ). The bound DR4-Fc protein was eluted with glycine buffer (pH 3) and dialyzed into PBS. The DR4-Fc is a soluble TRAIL receptor, which could bind to TRAIL and block its effect.

Culture of primary human gastric epithelial cells

The culture of human gastric epithelial cells was adapted from the methods described by Smoot *et al*.[25]. Gastric biopsies were obtained from patients undergoing gastric endoscopy in National Taiwan University Hospital for dyspepsia with informed consents. Specimens were collected in Leibowitz's L-15 medium (Life Technologies, Grand Island, NY). Gastric cells were isolated enzymatically after mechanically mincing the tissue, into pieces less than or equal to 1 mm in size. The tissue was then pelleted by centrifugation at 1 500 rpm for five minutes at 4 °C, the collagenase/dispase was discarded, then the tissue was washed once in 10 mL of PBS and pelleted again by centrifugation. The cells were resuspended in the cell culture medium. The gastric epithelial cells obtained above were suspended in 2 mL of Ham's F12 cell culture medium (Life Technologies, Grand Island, NY) with 10% FBS and placed into a 6-well tissue culture cluster well.

Apoptosis assay

A sensitive ELISA which detects cytoplasmic histone-associated DNA fragments was performed according to the manufacturer's protocol (Cell Death Detection ELISA^{PLUS}; Roche Mannheim Biochemicals, Mannheim Germany). Human gastric epithelial cells were cultured in a 96-well plate (10^4 cells/well) overnight, then treated with TRAIL recombinant protein, harvested by centrifugation at 200 g. The cells were lysed by incubation with lysis buffer for 30 min, followed by centrifugation at 200 g for 10 min at room temperature. The supernatant was collected and incubated with immunoreagent pre-prepared for 2 h. After washed gently, the supernatant was pipetted into each well with a substrate solution and kept in the dark until development of the color was sufficient for photometric analysis. The reaction was determined in a spectrophotometer at 405 nm.

Effects of TRAIL and H pylori on apoptosis in human gastric epithelial cells

AGS cells or primary human gastric epithelial cells 5×10^4/well were incubated with *H pylori* (ATCC strain 43504 or strain 51932) under the concentration of 4×10^7 CFU for 12 h. Recombinant TRAIL proteins were added into the culture at the concentration of 1.0 g/mL for 4 h in the absence or presence of soluble TRAIL receptor, DR4-Fc (30 g/mL), which could block the function of TRAIL proteins. Apoptosis of gastric epithelial cells was determined by a specific ELISA as described.

Effects of lipopolysaccharide (LPS) and Campylobacter jejuni on induction of TRAIL sensitivity in human gastric epithelial cells

To exclude the possibility that the effect of induction of TRAIL sensitivity in AGS cells by *H pylori* was a general phenomenon in Gram-negative bacteria, possibly via interaction with LPS on cell wall, we further studied the TRAIL-mediated apoptosis in AGS cells following contact with LPS and *Campylobacter jejuni*. AGS cells were incubated with LPS from *E. coli*, *Campylobacter jejuni*, and *H pylori* (domestic strain NTUH-C1) for 12 h. Recombinant TRAIL proteins were added into the culture. Apoptosis was measured with ELISA as described.

Effects of direct cell contact of bacteria on TRAIL-mediated apoptosis of epithelial cells

AGS cells were incubated with *H pylori* (ATCC strain 43504; CagA+, VacA+) concentrated culture supernatant or with live bacteria separated by a membrane filter (Nunc Tissue Culture; Nunc, Roskilde, Denmark) under the concentration of 4×10^7 CFU/5×10^4 cells for 12 h. Recombinant TRAIL proteins were added into the culture. Cell death was measured with ELISA as described.

Effects of CagA and VacA on TRAIL-mediated apoptosis of epithelial cells

AGS cells (5×10^4 cells) were incubated with a CagA-negative and VacA-negative *H pylori* mutant strain (ATCC strain 51932) as well as the *cagA* or *vacA* gene defect NTUH-C1 isogenic mutant strains for 12 h. Recombinant TRAIL proteins were then added into the culture. Apoptosis was measured with ELISA assay as described.

Expressions of TRAIL on surface of T-lymphocytes in gastric mucosa

For isolation of gastric infiltrating lymphocytes from endoscopic biopsy specimens, the collected tissues were immediately placed in ice-cold RPMI 1640 complete medium (GIBCO BRL, Gaithersburg, MD, USA) containing 10% fetal calf serum (FCS) supplemented with penicillin (50 IU/mL), streptomycin (50 mg/mL), L-glutamine (2 mmol/L) and sodium pyruvate (1 mmol/L). The tissues were washed, diced into 1 mm^3 pieces and treated with collagenase (Type I, 5 g/mL; Sigma Co. St. Louis, MO) and heparin (5 U/mL) in RPMI 1640 complete medium at 37 °C for 60 min. After the samples were washed twice with RPMI 1640 medium, mononuclear cells were collected and then stained with anti-CD3 and anti-TRAIL mAb. The expression of TRAIL on the surface of T cells was detected by flow cytometry according to our previous study[24].

Statistical analysis

The values of apoptosis assay were presented as mean±SD. The results were compared by Student's *t* test. A *P* value less than 0.05 was regarded as statistically significant.

RESULTS

Effects of TRAIL and H pylori on apoptosis in human gastric epithelial cell line

Figure 1 shows the effects of *H pylori* and TRAIL on apoptosis in AGS cells. The apoptosis of AGS cells was slightly increased by TRAIL proteins or *H pylori* alone. Interestingly, the apoptotic index was dramatically increased when AGS cells were incubated with both TRAIL and *H pylori* ($P<0.01$ as compared with control medium, TRAIL or *H pylori* alone). Further studies disclosed that TRAIL-induced apoptosis in AGS cells was increased by *H pylori* in a dose-dependent manner (data not shown).

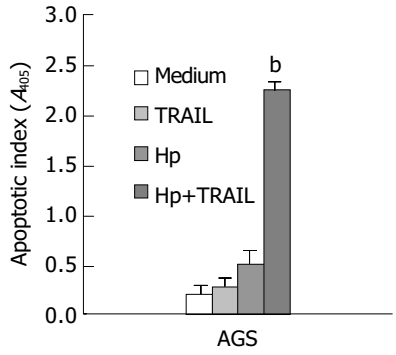

Figure 1 Effects of TRAIL and *H pylori* on apoptosis in human gastric epithelial cell line AGS ($^bP<0.01$ when compared with medium control, TRAIL or *H pylori* alone).

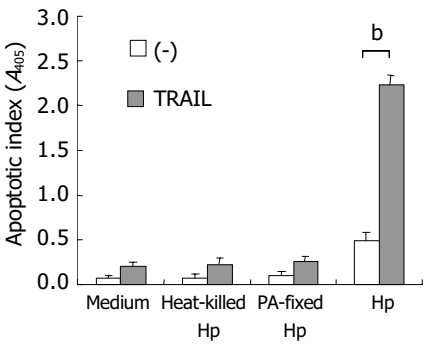

Figure 2 AGS cells incubated with heat killed, paraformaldehyde-fixed (PA-fixed) or live *H pylori* (ATCC strain 43504) under the concentration of 4×10^7 CFU / 5×10^4 cells for 12 h. Open bar: without TRAIL; filled bar: with TRAIL ($^bP<0.01$).

Figure 2 shows that the TRAIL-induced apoptosis depended on viable *H pylori* because exposure of the host cells to heat-killed *H pylori* and paraformaldehyde-fixed *H pylori* did not induce sensitivity to TRAIL-mediated apoptosis.

Impacts of TRAIL and H pylori on apoptosis in primary human gastric epithelial cells

We further isolated and cultured primary human gastric epithelial cells from 23 different human cases (*H pylori*-positive: 12 cases; *H pylori*-negative: 11 cases) to investigate the effects of *H pylori* and TRAIL on apoptosis. The apoptosis of primary human gastric epithelial cells was mildly elevated by either TRAIL or *H pylori* alone (Table 1). However, the apoptotic indices were markedly elevated when the primary gastric epithelial cells were incubated with both *H pylori* and TRAIL. The apoptosis induced by *H pylori* and TRAIL was specifically blocked by adding soluble TRAIL receptor, DR4-Fc, indicating that the cell death was resulted from interaction between TRAIL and TRAIL receptor on the cell surface. Figure 3 shows the representative responses of four cases. All the gastric epithelial cells tested were sensitive to TRAIL after interaction with *H pylori in vitro*.

Table 1 Effects of TRAIL and *H pylori* on apoptosis in primary human gastric epithelial cells

	Apoptotic index[1] (n=23)	P value[2]
Medium	0.512±0.064	-
TRAIL	0.812±0.109	0.425
HP	0.684±0.085	0.779
HP+TRAIL	2.286±0.268	0.018
HP+TRAIL+DR4	0.816±0.129	0.216

[1]mean±SD; [2]Compared with medium alone samples.

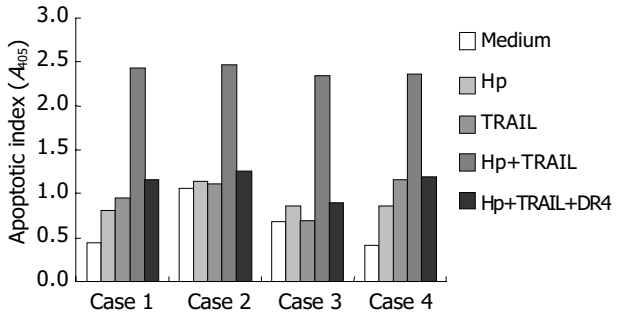

Figure 3 Enhancement of TRAIL-mediated apoptosis by *H pylori* in primary human gastric epithelial cells.

Effects of LPS and Campylobacter jejuni on induction of TRAIL sensitivity in human gastric epithelial cells

To exclude the possibility that the effect of induction of TRAIL sensitivity by *H pylori* was a general phenomenon in Gram-negative bacteria, possible via interaction with lipopolysaccharide (LPS) on cell walls, we further studied the induction of sensitivity to TRAIL-mediated apoptosis in AGS cells after interaction with LPS from *E. coli* and with *Campylobacter jejuni*, a Gram-negative bacterial pathogen in gastrointestinal tract. The results in Figure 4 demonstrate that *H pylori* enhanced TRAIL-mediated apoptosis in AGS cells. However, neither LPS from *E. coli* nor *Campylobacter jejuni* was able to induce TRAIL-sensitivity. Moreover, similar to ATCC strains, domestic *H pylori* strain NTUH-C1 was also capable of inducing TRAIL-sensitivity in AGS cells (Figure 4). These results indicated the ability to sensitize human gastric epithelial cells to TRAIL-induced apoptosis was *H pylori*-specific and not a general phenomenon in Gram-negative bacteria.

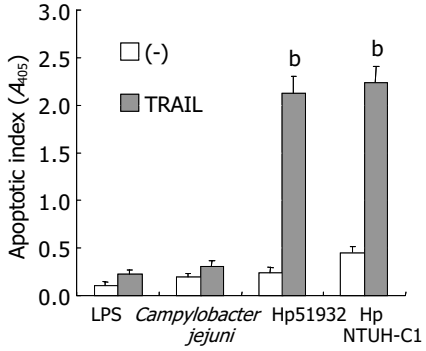

Figure 4 Induction of TRAIL sensitivity specific for *H pylori* in human gastric epithelial cells ($^bP<0.01$ when compared with *H pylori* alone without adding TRAIL samples).

Effects of direct cell contact of bacteria on TRAIL-mediated apoptosis of gastric epithelial cells

To investigate the effects of direct bacteria-epithelial cell contact in induction of TRAIL sensitivity by *H pylori*, AGS cells and bacteria were separated by a membrane filter (Nunc Tissue Culture; Nunc, Roskilde, Denmark). Figure 5 shows the effects of direct cell contact of bacteria on TRAIL-mediated apoptosis in human gastric epithelial cells. The enhancement of TRAIL sensitivity by *H pylori* was abrogated when AGS cells were separated by the filter without direct bacteria-cell contact or co-cultured with concentrated *H pylori* culture supernatant without viable bacteria, indicating that direct contact with viable bacteria was required for induction of TRAIL sensitivity by *H pylori*.

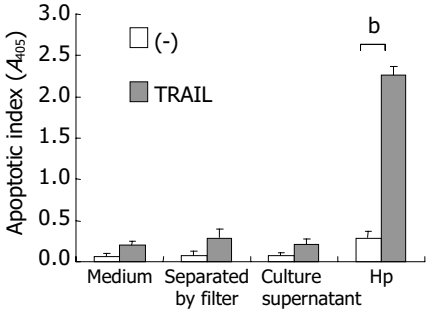

Figure 5 Enhancement of direct bacteria-cell contact dependent TRAIL sensitivity by *H pylori* ($^bP<0.01$).

Effects of cagA and vacA on TRAIL-mediated apoptosis of epithelial cells

To exclude the possibility that the death of gastric epithelial cells induced by TRAIL was related with vacA cytotoxin of *H pylori*, and to elucidate the role of *cagA* gene products in onset of the apoptotic process, we examined the abilities to enhance TRAIL-mediated apoptosis in *H pylori* mutant strain, ATCC 51932, which is deficient of cytotoxin vacA and cagA, and *H pylori* NTUH-C1 *cag A*, *vacA* gene knock out isogenic mutant strains. Figure 6 shows the effects of CagA-negative and VacA-negative *H pylori* strains on TRAIL-mediated apoptosis in gastric epithelial cells. *H pylori* strain 51932 significantly enhanced sensitivity to TRAIL-mediated apoptosis in gastric epithelial cell lines in a dose-dependent manner. *cagA* or *vacA* gene knock out NTUH-C1 mutant strain was also capable of inducing TRAIL sensitivity in gastric epithelial cells. Taken together, these results suggested that *vac* A and *cag*A proteins of *H pylori* were not required for induction of TRAIL-sensitivity in human gastric epithelial cells.

Expression of TRAIL on surface of T-lymphocytes in gastric mucosa

To confirm the expression of TRAIL in gastric infiltrating lymphocytes, gastric biopsy specimens were collected from subjects and examined by flow cytometry. Figure 7 demonstrates the expression of TRAIL on surface of T-lymphocytes isolated from gastric mucosa. Flow cytometry confirmed the presence of TRAIL on the surface of gastric infiltrating T-lymphocytes.

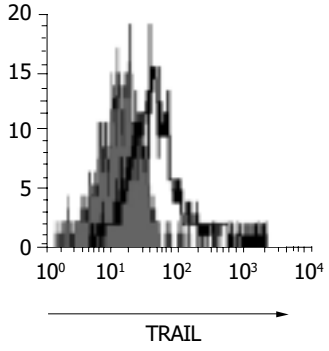

Figure 7 Expression of TRAIL on surface of T cells isolated from gastric mucosa.

DISCUSSION

In this study, we investigated the effects of *H pylori* and TRAIL on apoptosis in human gastric epithelial cells. The apoptosis of primary human gastric epithelial cells was mildly increased after incubated with either *H pylori* or TRAIL alone. Interestingly, the apoptotic indices of gastric epithelial cells were markedly increased when the primary gastric epithelial cells were incubated with both TRAIL and *H pylori*. The

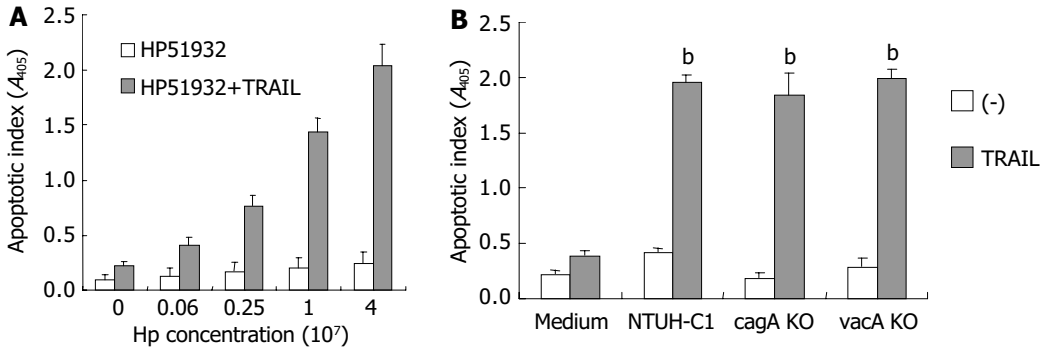

Figure 6 Effects of *vac*A and *cag*A on induction of TRAIL sensitivity by *H pylori*. A: AGS cells (5×10^4 cells) were incubated with a different concentration of *H pylori* (ATCC strain 51932) for 12 h. B: AGS cells were incubated with *H pylori* NTUH-C1 and its *cagA*, *vacA* gene knock out mutant strains (cagA KO, vacA KO) in the concentration of 4×10^7 CFU / 5×10^4 cells for 12 h ($^bP<0.01$ when compared with *H pylori* alone without adding TRAIL samples).

induction of TRAIL-mediated apoptosis by *H pylori* was specifically blocked by adding soluble TRAIL receptor, DR4-Fc. The results implicated that *H pylori* could directly trigger apoptosis in gastric epithelial cells as previously described[26-28] Additionally, the microorganism was also capable of enhancing TRAIL sensitivity in gastric epithelial cells. Most of the apoptosis in gastric epithelial cells after exposure to both *H pylori* and TRAIL was resulted from interaction between TRAIL and TRAIL receptor on the surface of gastric epithelial cells, but not due to direct cytotoxicity induced by *H pylori*.

To confirm the expression of TRAIL in infiltrating T-lymphocytes of gastric mucosa, we isolated the gastric infiltrating lymphocytes from gastric biopsy specimens of *H pylori*-infected subjects. Our data confirmed that TRAIL was expressed on the surface of gastric infiltrating T-cells. This important finding further supports the hypothesis that TRAIL/TRAIL-R interaction is involved in epithelial cell damage during *H pylori* infection. Furthermore, it implicates that infiltrating T-cells in gastric mucosa may play a crucial role in the sequential changes of *H pylori*-related chronic gastritis.

In this study, we also demonstrated that neither *Campylobacter jejuni* nor LPS from *E. coli* was able to induce TRAIL-sensitivity in AGS cells. In contrast, *H pylori* standard strain ATCC43504 (CagA+, VacA+), mutant strain ATCC51932 (CagA-, VacA-) and our domestic strain NTUH-C1 (CagA+, VacA+) were capable of inducing TRAIL-sensitivity in AGS cells. The results indicate the ability to enhance TRAIL sensitivity of gastric epithelial cells is specific for *H pylori* and not a general phenomenon of Gram-negative Bacteria.

It has been demonstrated recently that *H pylori* could directly trigger cell death by cytotoxins after interaction with gastric epithelial cells[26,27,29]. Other reports have shown that *H pylori* could secrete *cag*A into gastric epithelial cells by Type IV secretion, thus inducing intracellular protein phosphorylation in host cells[30-33]. To elucidate the role of *cagA* gene products and *vac*A in TRAIL-mediated apoptosis, we examined the ability to induce TRAIL of a CagA-negative and vacA-negative *H pylori* mutant strain, ATCC 51932 as well as *cagA*, *vacA* gene knock out mutants of NTUH-C1 strain. All the *H pylori* wild type and mutant strains significantly enhanced sensitivity to TRAIL-mediated apoptosis in gastric epithelial cell lines. These findings suggest that expression of *cag*A and *vac*A is not mandatory for induction of TRAIL-sensitivity in gastric epithelial cells.

To investigate the effects of direct bacteria-epithelial cell contact in induction of TRAIL sensitivity by *H pylori*, AGS cells were separated by the filter without direct bacteria-cell contact or co-cultured with concentrated *H pylori* culture supernatant without viable bacteria. The enhanced TRAIL sensitivity was only observed when AGS cells were co-cultured with viable *H pylori*, but not with bacteria culture supernatant or with viable bacteria separated by a permeable membrane, indicating that direct contact with viable bacteria is necessary for induction of TRAIL sensitivity of gastric epithelial cells.

We demonstrated here that human gastric epithelial cells sensitized to *H pylori* conferred susceptibility to TRAIL-mediated apoptosis. Although the induction of TRAIL sensitivity by *H pylori* in gastric epithelial cells was independent of *H pylori* virulent factors CagA and VacA, the degree of apoptosis was linked to the presence of *H pylori* and the associated inflammatory response. Therefore, the degree of mucosal damage was also determined by the inflammatory response induced by *H pylori* within gastric epithelium. Our results suggest a role for immune-mediated apoptosis of gastric epithelial cells by infiltrating T cells during *Helicobacter* infection.

In conclusion, *H pylori* enhance susceptibility of gastric epithelial cells to TRAIL-mediated apoptosis. The induction of TRAIL sensitivity by *H pylori* is dependent upon direct contact of viable bacteria with gastric epithelial cells, but independent of expression of *H pylori* virulent factors *vac*A and *cag*A. Gastric infiltrating T-lymphocytes can express TRAIL on their cell surfaces. Modulation of host cell apoptosis by bacterial interaction adds a new dimension to the immune pathogenesis in chronic *Helicobacter* infection.

ACKNOWLEDGEMENTS

We thank Dr. N Sutkowski for the critical review of the manuscript, Dr. SB Wang and JM Wong (Department of Medicine, National Taiwan University Hospital) for supporting endoscopic biopsy specimens, Ms. WI Tsai and WH Wu for assistance with *H pylori* cultures.

REFERENCES

1 **Jones NL**, Shannon PT, Cutz E, Yeger H, Sherman PM. Increase in proliferation and apoptosis of gastric epithelial cells early in the natural history of *Helicobacter pylori* infection. *Am J Pathol* 1997; **151**: 1685-1703
2 **Mannick EE**, Bravo LE, Zarama G, Realpe JL, Zhang XJ, Ruiz B, Fontham ET, Mera R, Miller MJ, Correa P. Inducible nitric oxide synthase, nitrotyrosine and apoptosis in *Helicobacter pylori* gastritis: effect of antibiotics and antioxidants. *Cancer Res* 1996; **56**: 3238-3243
3 **Moss SF**, Calam J, Agarwal B, Wang S, Holt PR. Induction of gastric epithelial apoptosis by *Helicobacter pylori*. *Gut* 1996; **38**: 498-501
4 **Rudi J**, Kuck D, Strand S, von Herbay A, Mariani SM, Krammer PH, Galle PR, Stremmel W. Involvement of the CD95 (APO-1/Fas) receptor and ligand system in *Helicobacter pylor*i-induced gastric epithelial apoptosis. *J Clin Investig* 1998; **102**: 1506-1514
5 **Fan X**, Crowe SE, Behar S, Gunasena H, Ye G, Haeberle H, Van Houten N, Gourley WK, Ernst PB, Reyes VE. The effect of class II major histocompatibility complex expression on adherence of *Helicobacter pylori* and induction of apoptosis in gastric epithelial cells: a mechanism for T helper cell type 1-mediated damage. *J Exp Med* 1998; **187**: 1659-1669
6 **Jones NL**, Day AS, Jennings HA, Sherman PM. *Helicobacter pylori* induces gastric epithelial cell apoptosis in association with increased Fas receptor expression. *Infect Immun* 1999; **67**: 4237-4242
7 **Wagner S**, Beil W, Westermann J, Logan RP, Bock CT, Trautwein C, Bleck JS, Manns MP. Regulation of epithelial cell growth by *Helicobacter pylori*: evidence for a major role of apoptosis. *Gastroenterology* 1997; **113**: 1836-1847
8 **Bamford KB**, Fan X, Crowe SE, Leary JF, Gourley WK, Luthra GK, Brooks EG, Graham DY, Reyes VE, Ernst PB. Lymphocytes in the human gastric mucosa during *Helicobacter pylori* have a T helper cell 1 phenotype. *Gastroenterology* 1998; **114**: 482-492
9 **D'Elios MM**, Manghetti M, De Carli M, Costa F, Baldari CT, Burroni D, Telford JL, Romagnani S, Del Prete G. T helper 1 effector cells specific for *Helicobacter pylori* in gastric antrum of patients with peptic ulcer disease. *J Immunol* 1997; **158**: 962-967
10 **Karttunen R**, Karttunen T, Ekre HP, MacDonald TT. Interferon gamma and interleukin 4 secreting cells in the gastric antrum in *Helicobacter pylori* positive and negative gastritis. *Gut* 1995; **36**: 341-345
11 **Lindholm C**, Quiding-Jarbrink M, Lonroth H, Hamlet A, Svennerholm AM. Local cytokine response in *Helicobacter pylori-infected* subjects. *Infect Immun* 1998; **66**: 5964-5971
12 **Wang J**, Fan X, Lindholm C, Bennett M, O'Connoll J, Shanahan F, Brooks EG, Reyes VE, Ernst PB. *Helicobacter pylori* modulates lymphoepithelial cell interactions leading to epithelial cell damage through Fas/Fas Ligand interactions. *Infect Immun* 2000; **68**: 4303-4311
13 **Wiley SR**, Schooley K, Smolak PJ, Din WS, Huang CP, Nicholl JK, Sutherland GR, Smith TD, Rauch C, Smith CA. Identification and characterization of a new member of the TNF family that induces apoptosis. *Immunity* 1995; **3**: 673-682
14 **Griffith TS**, Lynch DH. TRAIL: a molecule with multiple re-

ceptors and control mechanisms. *Curr Opin Immunol* 1998; **10**: 559-563
15 **Sheridan JP**, Marsters SA, Pitti RM, Gurney A, Skubatch M, Baldwin D, Ramakrishnan L, Gray CL, Baker K, Wood WI, Goddard AD, Godowski P, Ashkenazi A. Control of TRAIL-induced apoptosis by a family of signaling and decoy receptors. *Science* 1997; **277**: 818-821
16 **Pan G**, Ni J, Wei YF, Yu G, Gentz R, Dixit VM. An antagonist decoy receptor and a death domain-containing receptor for TRAIL. *Science* 1997; **277**: 815-818
17 **LeBlanc H**, Lawrence D, Varfolomeev E, Totpal K, Morlan J, Schow P, Fong S, Schwall R, Sinicropi D, Ashkenazi A. Tumor-cell resistance to death receptor-induced apoptosis through mutational inactivation of the proapoptotic Bcl-2 homolog Bax. *Nat Med* 2002; **8**: 274-281
18 **Kayagaki N**, Yamaguchi N, Nakayama M, Eto H, Okumura K, Yagita H. Type I interferons (IFNs) regulate tumor necrosis factor-related apoptosis-inducing ligand (TRAIL) expression on human T cells: A novel mechanism for the antitumor effects of type I IFNs. *J Exp Med* 1999; **189**: 1451-1460
19 **Kayagaki N**, Yamaguchi N, Nakayama M, Kawasaki A, Akiba H, Okumura K, Yagita H. Involvement of TNF-related apoptosis-inducing ligand in human CD4+ T cell-mediated cytotoxicity. *J Immunol* 1999; **162**: 2639-2647
20 **Thomas WD**, Hersey P. TNF-related apoptosis-inducing ligand (TRAIL) induces apoptosis in Fas ligand-resistant melanoma cells and mediates CD4 T cell killing of target cells. *J Immunol* 1998; **161**: 2195-2200
21 **Nieda M**, Nicol A, Koezuka Y, Kikuchi A, Lapteva N, Tanaka Y, Tokunaga K, Suzuki K, Kayagaki N, Yagita H, Hirai H, Juji T. TRAIL expression by activated human CD4(+)V alpha 24NKT cells induces *in vitro* and *in vivo* apoptosis of human acute myeloid leukemia cells. *Blood* 2001; **97**: 2067-2074
22 **Kaplan MJ**, Ray D, Mo RR, Yung RL, Richardson BC. TRAIL (Apo2 ligand) and TWEAK (Apo3 ligand) mediate CD4+ T cell killing of antigen-presenting macrophages. *J Immunol* 2000; **164**: 2897-2904
23 **Dorr J**, Waiczies S, Wendling U, Seeger B, Zipp F. Induction of TRAIL-mediated glioma cell death by human T cells. *J Neuroimmunol* 2002; **122**: 117-124
24 **Chou AH**, Tsai HF, Lin LL, Hsieh SL, Hsu PI, Hsu PN. Enhanced proliferation and increased IFN-gamma production in T cells by signal transduced through TNF-related apoptosis-inducing ligand. *J Immunol* 2001; **167**: 1347-1352
25 **Smoot DT**, Sewchand J, Young K, Desbordes BC, Allen CR, Naab T. A method for estabilishing primary cultures of human gastric epithelial cells. *Methods Cell Sci* 2000; **22**: 133-136
26 **Kuck D**, Kolmerer B, Iking-Konert C, Krammer PH, Stremmel W, Rudi J. Vacuolating cytotoxin of *Helicobacter pylori* induces apoptosis in the human gastric epithelial cell line AGS. *Infect Immun* 2001; **69**: 5080-5087
27 **Le'Negrate G**, Ricci V, Hofman V, Mograbi B, Hofman P, Rossi B. Epithelial intestinal cell apoptosis induced by *Helicobacter pylori* depends on expression of the cag pathogenicity island phenotype. *Infect Immun* 2001; **69**: 5001-5009
28 **Domek MJ**, Netzer P, Prins B. *Helicobacter pylori* induces apoptosis in human epithelial gastric cells by stress activated protein kinase pathway. *Helicobacter* 2001; **6**: 110-115
29 **Domek MJ**, Netzer P, Prins B, Nguyen T, Liang D, Wyle FA, Warner A. Induction of gastric epithelial cell apoptosis by *Helicobacter pylori* vacuolating cytotoxin. *Cancer Res* 2003; **63**: 951-957
30 **Odenbreit S**, Puls J, Sedlmaier B, Gerland E, Fischer W, Haas R. Translocation of *Helicobacter pylori* CagA into gastric epithelial cells by type IV secretion. *Science* 2000; **287**: 1497-1501
31 **Asahi M**, Azuma T, Ito S, Ito Y, Suto H, Nagai Y, Tsubokawa M, Tohyama Y, Maeda S, Omata M, Suzuki T, Sasakawa C. *Helicobacter pylori* CagA protein can be tyrosine phosphorylated in gastric epithelial cells. *J Exp Med* 2000; **191**: 593-602
32 **Stein M**, Rappuoli R, Covacci A. Tyrosine phosphorylation of the *Helicobacter pylori* CagA antigen after *cag*-driven host cell translocation. *Proc Natl Acad Sci U S A* 2000; **97**: 1263-1268
33 **Higashi H**, Tsutsumi R, Muto S, Sugiyama T, Azuma T, Asaka M, Hatakeyama M. SHP-2 Tyrosine phosphatase as an intracellular target of *Helicobacter pylori* CagA. *Science* 2002; **295**: 683-686

Edited by Wang XL **Proofread by** Chen WW and Xu FM

PO Box 2345, Beijing 100023, China
Fax: +86-10-85381893
E-mail: wjg@wjgnet.com www.wjgnet.com

World J Gastroenterol 2004;10(16):2340-2343
World Journal of Gastroenterology
 ISSN 1007-9327

Antigen epitope of *Helicobacter pylori* vacuolating cytotoxin A

Xiu-Li Liu, Shu-Qin Li, Chun-Jie Liu, Hao-Xia Tao, Zhao-Shan Zhang

Xiu-Li Liu, Shu-Qin Li, Chun-Jie Liu, Hao-Xia Tao, Zhao-Shan Zhang, Bejing Institute of Biotechnology, Beijing 100071, China
Supported by the National High Technology Research and Development Program of China (863 Program), No. 2001AA215161
Correspondence to: Zhao-Shan Zhang, Bejing Institute of Biotechnology, 20 Dongdajie Street, Fengtai District, Beijing 100071, China. zhangzs@nic.bmi.ac.cn
Telephone: +86-10-66948834 **Fax**: +86-10-63833521
Received: 2004-02-11 **Accepted:** 2004-02-24

Abstract

AIM: To construct and select antigen epitopes of vacuolating cytotoxin A (VacA) for nontoxic VacA vaccine against *Helicobacter pylori* (*H pylori*) infection.

METHODS: Eleven VacA epitopes were predicted according to VacA antigenic bioinformatics. Three candidates of VacA epitope were constructed through different combined epitopes. The candidate was linked with *E. coli* heat-labile enterotoxin B (LTB) by a linker of 7 amino acids, and cloned into plasmid pQE-60 in which fusion LTB-VacA epitope was efficiently expressed. To test the antigencity of the candidate, 6 BALB/c mice were treated with the fusion LTB-VacA epitope through intraperitoneal injection. To explore the ability of inhibiting the toxicity of VacA,cantiserum against the candidate was used to counteract VacA that induced HeLa cells to produce cell vacuoles *in vitro*.

RESULTS: Serum IgG against the candidate was induced in the BALB/c mice. *In vitro*, the three antisera against the candidate efficiently counteracted the toxicity of VacA, and decreased the number of cell vacuoles by 14.17%, 20.20% and 30.41% respectively.

CONCLUSION: Two of the three candidates, LZ-VacA1and LZ-VacA2, can be used to further study the mechanism of vacuolating toxicity of VacA, and to construct nontoxic VacA vaccine against *H pylori* infection.

Liu XL, Li SQ, Liu CJ, Tao HX, Zhang ZS. Antigen epitope of *Helicobacter pylori* vacuolating cytotoxin A. *World J Gastroenterol* 2004; 10(16): 2340-2343
http://www.wjgnet.com/1007-9327/10/2340.asp

INTRODUCTION

Pathogenic strains of *Helicobacter pylori (H pylori)* release a M_r 95 000 protein toxin in the growth medium. Growing evidence indicates that VacA is a major virulence factor in *H pylori* long-term infection leading to gastroduodenal ulcers[1-5]. This toxin induces formation of vacuoles in the cytosol of cells, therefore it has been named vacuolating toxin[6-11]. VacA is thus considered as a therapeutic vaccine for individuals infected with *H pylori*. The *VacA* gene encodes a protoxin approximately M_r 140 000, which belongs to the family of secreted proteins. During the process of VacA secretion, a M_r 95 000 mature toxin is exported. A large oligomeric complex appear as 'flower' with M_r 900 000 which is composed of 6-7 VacA monomers[12-15]. When exposed to the acidic situation, the oligomeric complexes were assembled into monomers and the toxicity of VacA was enhanced[16-18]. After VacA exerted its effect on the cells for 90 min, vacuoles were formed[19]. The vacuoles induced by VacA were acidic. Intracellular vacuolation is believed to induce cell damage and eventually apoptosis, which might lead to release of necrotic factors *in vivo* and therefore contribute to the establishment of a chronic inflammatory response. Because vacuolating cytotoxin A is difficult to express, purify and construct the combined vaccine, we studied the antigen epitopes to reduce the toxin.

MATERIALS AND METHODS

E. coli JM109, pFS2.2 and Hela cell were preserved in our laboratory; pQE-60 was a gift of professor Hou-Chu Zhu, Bejing Institute of Biotechnology, Beijing, China; *H pylori* Sydney strain (*HP SS1*), was a gift of professor Min-Hu Chen, Sun Yat-sen University, Guangzhou, China.

*Bam*H I, *Eco*R V, *Nco* I, *Hin*d III, Pyrobest Taq DNA polymerase and T_4 DNA ligase were purchased from TaKaRa Biotechnology corporations.

Isopropyl β-D-thiogalactoside (IPTG), Freund's adjuvant and sheep anti-mouse IgG-HRP were purchased from Sigma corporations, RPMI 1640 and newborn calf serum were purchased from Hyclone corporations.

BALB/c female mice: 6-8 wk old, SPF.

Bioinformatic analysis and design for candidates of VacA antigen epitope

According to the protein characteristics of hydrophilicity, hydrophobicity, secondary structure, accessibility, flexibility and antigenicity, 9 VacA antigen epitopes in the amino acid site of 34-810 were predicted by the antigen-analyzing software GOLDKEY (Table 1).

Table 1 Site and amino acid sequences of predicted VacA epitopes

Site of amino acid	Amino acid sequences of predicted epitopes
35-46	AEEANKTPDKPD
61-66	PHKEYD
146-154	KDSADRTTR
297-317	GYKDKPKDKPSNTTQNNANNN
335-338	NSAQ
446-450	TDTKN
566-568	SGE
734-737	NNNR
746-748	TDD
766-768	DNY
799-806	TPTENGGN

Three candidates of VacA antigen epitope were designed by combining part of 9 predicted epitopes. The candidate LZ-VacA1 was composed of amino acids 35-36 and 146-154, LZ-VacA2 included amino acids 297-317, and LZ-VacA3 contained

amino acids 61-66, 446-450, 734-737, 746-748, 766-768, and 799-806. The gene sequence of candidate epitope was fused with a 7-amino acid linker (YPQDPSS). The nucleotide acid and amino acid sequences of three candidate epitopes were as following.

The sequence of LZ-VacA1 was:

```
TAC  CCT  5'---CAG  GAT  CCG  TCT  TCC  gcc  gaa  gaa  gcc
 Y    P       Q     D    P    S    S    A    E    E    A
aat   aaa  acc cca   gat  aaa  ccc  gat  aag  gat  agt  gct  gat
 N    K    T   P     D    K    P    D    K    D    S    A    D
cgc   acc  acg  aga   GAT---3'
 R    T    T    R     D
```

The sequence of LZ-VacA2 was

```
TAC  CCT  5'---CAG  GAT  CCG  TCT  TCC  ggt  tat  aag  gat
 Y    P       Q     D    P    S    S    G    Y    K    D
aaa   cct  aag  gat   aaa  cct  agt  aac  acc  acg  caa  aat  aat
 K    P    K    D     K    P    S    N    T    T    Q    N    N
gct   aat  aat  aac   GAT---3'
 A    N    N    N     D
```

The sequence of LZ-VacA3 was

```
TAC  CCT  5'---CAG  GAT  CCG  TCT  TCC  cct  cac  aag  gaa
 Y    P       Q     D    P    S    S    P    H    K    E
tac   gac  acg  gat  acc  aaa  aac  aac  aat  aac  cgc  act  gat
 Y    D    T    D    T    K    N    N    N    N    R    T    D
gac   gac  aat  tac  acg  cct  act  gag  aat  ggt  ggc  aat  GAT---3'
 D    D    N    Y    T    P    T    E    N    G    G    N    D
```

Synthesis of DNA sequence of candidate epitopes and insertion of plasmid pFS2.2

Two splicing sequences were designed according to the nucleotide acid sequences of the candidate epitope and linker. These sequences were synthesized artificially and spliced by PCR reaction. PCR reaction solution containing 5 μL 10× PCR buffer, 0.25 μL pyrobest Taq polymerase (5 U/μL), 1 μL P1 and P2 primer (50 ng/μL), 4 μL dNTP, H_2O to 50 μL. Five PCR cycles were performed, each at 95 °C for 30 s, at 60 °C for 30 s, at 72 °C for 15 s.

LZ-VacA1 primer sequence was P1: 5'--cag gat ccg tct tcc gcc gaa gaa gcc aat aaa acc cca gat aaa ccc gat aag--3', P2: 5'---atc tct cgt ggt gcg atc agc act atc ctt atc ggg ttt atc tgg gg---3'.

LZ-VacA2 primer sequence was P1: 5'--cag gat ccg tct tcc ggt tat aag gat aaa cct aag gat aaa cct agt aac acc--3', P2: 5'---atc gtt att att agc att att ttg cgt ggt gtt act agg ttt atc c---3'.

LZ-VacA3 primer sequence was, P1: 5'--cag gat ccg tct tcc cct cac aag gaa tac gac acg gat acc aaa aac aac aat aac cgc act gat--3', P2: 5'---atc att gcc acc att ctc agt agg ggt gta att gtc gtc atc agt gcg gtt att gtt gt---3'.

The DNA sequences of the candidate epitope and plasmid pFS2.2 containing LTB, were digested with restriction endonucleases *Bam*HI and *Eco*RV, and ligated with T_4 ligase. The recombinant plasmid, which included LTB-VacA gene was transformed to JM109. The positive clones were screened and named them as pLZ-SV1, pLZ-SV2 and pLZ-SV3, respectively.

Construction of expression vector and purification of LTB-VacA protein

To improve the efficiency of expression, two primers with the cloning sites *Nco*I and *Hind*III were designed to construct plasmid pQE-60 with LTB-VacA gene. The recombinant plasmid was transformed to JM109. The positive clones were screened and named them as pLZ-QV1, pLZ-QV2 and pLZ-QV3 respectively.

The primers was

P1 5'---cagccatggGTGAATAAAGTAAAATG---3'
Nco I

P2 5'---ggcaagcttGCTCGGTACTAATTAATTAG---3'
Hind III

The strain with recombinant plasmid was cultured in the Luria-Bertani broth for 3 h, induced by IPTG for 4 h, and then harvested. The targeted protein of LTB-VacA was an inclusion body by SDS-PAGE test. The inclusion body was denatured with 6 mol/L guanidine hydrochloride, and natured with dialysis. LTB-VacA infused protein was purified through the anti-LTB antibody affinity chromatography.

Immunization

Twenty-four female BALB/c mice were randomly and averagely divided into control (LTB), LTB-VacA1, LTB-VacA2 and LTB-VacA3 groups. The mice of each group were immunized through intraperitoneal injection of 200 μL (100 μg protein) LTB, LTB-VacA1, LTB-VacA2 or LTB-VacA3 on days 0, 14 and 28. On days 7, 21 and 35, blood of each mouse was collected and antibody titer was determined.

Cell Vacuolization test

VacA was purified from *H pylori* strain SS1 culture supernatant with ammonia sulfate precipitation. The preliminary experiment was performed to show the amount of *H pylori* strain SS1 culture supernatant was added when cell vacuoles were formed. HeLa cells were cultured as monolayers in flasks in RPMI 1640 containing NCS under 50 mL/L CO_2 at 37 °C. Twenty-four hours before experiment, the cells were released with trypsin/EDTA and seeded in 96-well plates in 10^3/well. After the VacA protein was incubated with antibody to LTB-VacA1, 2, 3 and LTB for 4 h at 37 °C, we added the fixture and VacA protein onto the cell surface for 6 h. Then we calculated the total cell number and cell number of vacuolization.

Statistical analysis

Data are presented as mean±SD. Analysis of variance with a two-tailed students *t*-test was used to identify significant differences. $P<0.05$ was considered statistically significant.

RESULTS

Construction of recombinant plasmid

Recombinant plasmids pLZ-VacA1, 2, 3 encoded the infused gene of LTB and VacA1, 2, 3. It was shown from the digestion map of restriction endonucleases *Nco*I and *Hin*d III, the infused gene was successfully cloned to PQE-60 (Figure 1). LTB-VacA1 had the nucleotide acid number of 465 bp (LTB387+LZ-VacA1 78). LTB-VacA2 had the nucleotide acid number of 465 bp (LTB387+LZ-VacA2 78). LTB-VacA3 had the nucleotide acid number of 489 bp (LTB387+LZ-VacA3 102). The amino acids of three LTB-VacA were deduced from the nucleotide acid sequences. LTB-VacA1 and LTB-VacA2 had 155 amino acids, and the M_r was about 17 000. LTB-VacA3 had 163 amino acids, and the molecular weight was about 17 900. The sequences of the three genes were correct by sequencing analyses.

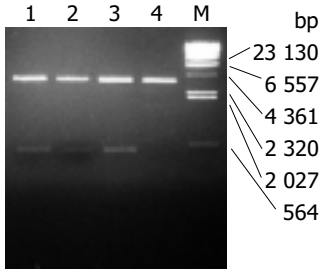

Figure 1 Digestion of recombinant plasmid. M: λDNA / *Hin*d III; Lane 1: pLZ-QV3 / *Nco* I+*Hin*d III; Lane 2: pLZ-QV2 / *Nco* I+*Hin*d III; Lane 3: pLZ-QV1 / *Nco* I+*Hin*d III; Lane 4: pQE-60 / *Nco* I+*Hin*d III.

Expression and purification of infused protein

The LTB-VacA1, 2, 3 proteins were expressed in the JM109 strain. In the SDS-PAGE, the three proteins were 14.13%, 15.51% and 14.79% of the total protein respectively. After purification with anti-LTB antibody affinity chromatography, the percentage of three proteins in the total proteins was improved to 69.26%, 70.18% and 75.35% respectively (Figure 2).

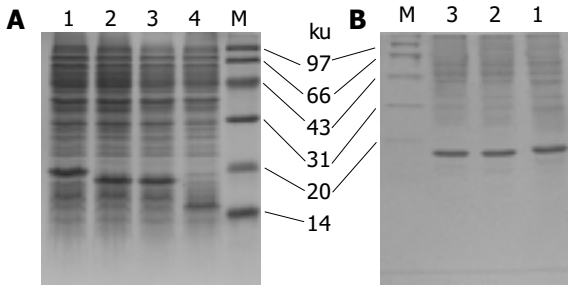

Figure 2 SDS-PAGE of LTB-VacA protein. M: Marker; Lane 1: LTB-VacA3; Lane 2: LTB-VacA2; Lane 3: LTB-VacA1; Lane 4: LTB. A: LTB-VacA proteins were expressed in the JM109; B: Purification with anti-LTB antibody affinity chromatography.

Serum antibody levels in infused protein

Intraperitoneal immunization with the infused protein and Freund's adjuvant resulted in a marked elevation of serum IgG antibody in all the 6 mice after three immunizations (Figure 3).

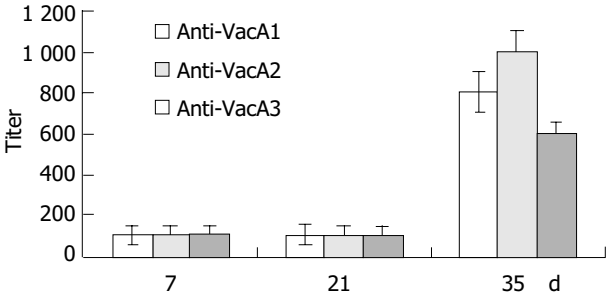

Figure 3 IgG against VacA induced by different LTB-VacA.

Seven days after the first immunization, the Level of antibody was lower. The titer of the antibody was about 1:100. Seven days after the second immunization, the titer of the antibody had no remarkable changes. But 14 d after the third immunization, the titer of the anti-LTB-VacA1 antibody, the titer of the anti-LTB-VacA2 antibody and the titer of the anti-LTB-VacA1 antibody was increased to 1:800, 1:1 000 and 1:600 respectively. The biggest value of positive and negative in the three antibodies was 3.8, 4.2 and 3.2.

HeLa cell vacuolization

The preliminary experimental results showed when we added 10, 30, 40, 80 and 100 μL culture supernatant, the cell vacuolization was produced. Because the space of wells in flasks well was limited, 100 μL VacA protein was added into the culture medium. The ratio of cell vacuolization after we added 100 μL protein was 49.52% (Figure 4).

The control serum, anti-VacA1 serum, anti-VacA2 serum and anti-VacA1 serum were incubated with 100 μL VacA antigen for 4 h. Then we added the fixture and VacA protein in the flasks wells for 6 h. The result showed the control serum and 100 μL VacA antigen could not reduce the ratio of cell vacuolization, but anti-VacA1 serum, anti-VacA2 serum, anti-VacA3 serum could decrease the ratio of cell vacuolization. The change rate of cell vacuolization is 30.41%, 20.20% and 14.17% respectively (Table 2).

Table 2 Inhibition of anti-LTB-VacA antibody on VacA toxin

Group	HeLa cells with vacuoles in total cells (%)	Change rate (%)
VacA toxin	49.52±2.77	0
Anti-LTBantibody (Control)	47.51±1.31	-4.05±1.61
Anti-LTB-VacA1 antibody	34.47±1.97	-30.41±2.41[b]
Anti-LTB-VacA2 antibody	39.52±1.69	-20.20±2.07[b]
Anti-LTB-VacA3 antibody	42.51±1.84	-14.17±2.27[a]

[a]$P<0.05$, [b]$P<0.01$ *vs* control.

DISCUSSION

Many methods could predict the epitopes of protein known as the primary structure, for example hydrophilicity scheme[20], accessibility scheme[21], antigenicity scheme[22], flexibility scheme[23,24] and secondary structure scheme[17]. The antigenic epitopes are correlated with the characteristics, number, sequence of amino acid and protein conformation. Because the different prediction methods emphasize different biological information of antigens, several methods are considered in practice. In this study we chose the GOLDKEY software developed by the Experimental Group led by professor Jia-Jin Wu to analyse the characteristics of VacA protein including hydrophilicity, hydrophobicity, secondary structure, accessibility, flexibility and antigenicity. This software could predict the liner B epitope. At last we got 11 VacA candidate epitopes.

Due to the small molecular weight and the weakness of antigenicity of the antigen epitopes, the carrier or adjuvant must be linked to the epitopes[25,26]. Several epitopes were joined in series and at last got 3 VacA candidate epitopes. LTB is an excellent protein adjuvant to facilitate the organism to produce the antibody epitopes, so we chose LTB to link the 3 epitopes.

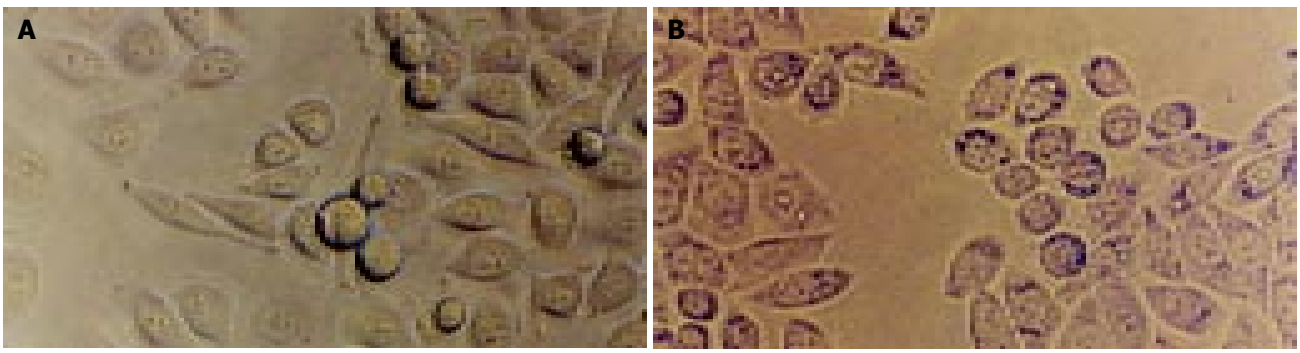

Figure 4 Microscopy of large vacuoles induced by VacA in HeLa cells. A: Normal HeLa cells; B: Vacuolated HeLa cells (Origingal magnification: ×400).

The experiment of Schodel enucleate that plasmid pFS2.2 was a carrier in which *LTB* gene could express soluble LTB and carry outer polypeptides. The experiment of Zhang showed that 21-bp nucleotide acids between LTB and the epitopes could enhance the antigencity of the epitopes. In our study, 7 peptides were used as a linker to join LTB with the epitopes.

At the beginning, LTB-VacA was cloned into plasmid pFS2.2, but the gene could not express these proteins, and then the genes were cloned into plasmid pET22b (+) again. There was a signal peptide in plasmid pET22b (+) in which the gene could express the soluble protein and secrete the protein into periplasm. The soluble proteins would be purified through the anti-LTB antibody affinity chromatography. Contrary to our wishes, the proteins in pFS2.2 were not expressed as expected. Finally, infused proteins were cloned into plasmid pQE-60 and expressed in JM109, but the expressed proteins were inclusion bodies. The inclusion bodies were denatured with guanidine hydrochloride and natured with dialysis, and LTB-VacA was purified through the anti-LTB antibody affinity chromatography.

Protein vacuolating toxin A is the only known virulence factor of *H pylori*. Ninety minutes after VacA activation, the acidic vacuoles were induced in cells. Scientific researches showed that VacA was integrated with receptors in membranes to form an anionic channel. This channel could change the permeation characteristics of the membranes, so that the cells were damaged would undergo apoptosis. In this study, all the 3 antigen epitopes of VacA could induce antibody in mice. Although the antibody could inhibit the vacuolation of Hela cells at a certain extent, they did not inhibit the vacuoles entirely. There are two reasons for this result. First, these epitopes were a part of the neutralized epitopes of VacA, antibody to these epitopes combined with VacA did not destroy the toxicity of VacA, only suppressed the toxin partly. Second, the titer of the antibody was not enough to neutralize the toxin of VacA. Next we are going to settle the problem. First, these epitopes will be joined in series for several copies so that the titer of the antibody will be improved to inhibit the toxin of VacA. Second, we will construct deficient mutations to farther verify the neutralized epitopes of VacA.

REFERENCES

1 **Telford JL,** Ghiara P, Dell'Orco M, Comanducci M, Burroni D, Bugnoli M, Tecce MF, Censini S, Covacci A, Xiang Z. Gene structure of the *Helicobacter pylori* cytotoxin and evidence of its key role in gastric disease. *J Exp Med* 1994; **179**: 1653-1658

2 **van Amsterdam K,** van Vliet AH, Kusters JG, Feller M, Dankert J, van der Ende A. Induced *Helicobacter pylori* vacuolating cytotoxin VacA expression after initial colonisation of human gastric epithelial cells. *FEMS Immunol Med Microbiol* 2003; **39**: 251-256

3 **Inui T,** Mizuno S, Takai K, Nakagawa M, Uchida M, Fujimiya M, Asakawa A, Inui A. *Helicobacter pylori* cytotoxin: a novel ligand for receptor-like protein tyrosine phosphatase beta. *Int J Mol Med* 2003; **12**: 917-921

4 **Cho SJ,** Kang NS, Park SY, Kim BO, Rhee DK, Pyo S. Induction of apoptosis and expression of apoptosis related genes in human epithelial carcinoma cells by *Helicobacter pylori* VacA toxin. *Toxicon* 2003; **42**: 601-611

5 **Toro Rueda C,** Garcia-Samaniego J, Casado Farinas I, Rubio Alonso M, Baquero Mochales M. Clinical importance of the CagA and VacA proteins and of the host factores in the development of peptic ulcer in patients infected by *Helicobacter pylori*. *Rev Clin Esp* 2003; **203**: 430-433

6 **Parsonnet J,** Hansen S, Rodriguez L, Gelb AB, Warnke RA, Jellum E, Orentreich N, Vogelman JH, Friedman GD. *Helicobacter pylori* infection and gastric lymphoma. *N Engl J Med* 1994; **330**: 1267-1271

7 **Yuan JP,** Li T, Shi XD, Hu BY, Yang GZ, Tong SQ, Guo XK. Deletion of *Helicobacter pylori* vacuolating cytotoxin gene by introduction of directed mutagenesis. *World J Gastroenterol* 2003; **9**: 2251-2257

8 **Gebert B,** Fischer W, Weiss E, Hoffmann R, Haas R. *Helicobacter pylori* vacuolating cytotoxin inhibits T lymphocyte activation. *Science* 2003; **301**: 1099-1102

9 **Qiao W,** Hu JL, Xiao B, Wu KC, Peng DR, Atherton JC, Xue H. cagA and vacA genotype of *Helicobacter pylori* associated with gastric diseases in Xi'an area. *World J Gastroenterol* 2003; **9**: 1762-1766

10 **Caputo R,** Tuccillo C, Manzo BA, Zarrilli R, Tortora G, Blanco Cdel V, Ricci V, Ciardiello F, Romano M. *Helicobacter pylori* VacA toxin up-regulates vascular endothelial growth factor expression in MKN 28 gastric cells through an epidermal growth factor receptor-, cyclooxygenase-2-dependent mechanism. *Clin Cancer Res* 2003; **9**: 2015-2021

11 **Wang J,** van Doorn LJ, Robinson PA, Ji X, Wang D, Wang Y, Ge L, Telford JL, Crabtree JE. Regional variation among vacA alleles of *Helicobacter pylori* in China. *J Clin Microbiol* 2003; **41**: 1942-1945

12 **Cover TL,** Blaser MJ. Purification and characterization of the vacuolating toxin from *Helicobacter pylori*. *J Biol Chem* 1992; **267**: 10570-10575

13 **Lupetti P,** Heuser JE, Manetti R, Massari P, Lanzavecchia S, Bellon PL, Dallai R, Rappuoli R, Telford JL. Oligomeric and subunit structure of the *Helicobacter pylori* vacuolating cytotoxin. *J Cell Biol* 1996; **133**: 801-807

14 **Nguyen VQ,** Caprioli RM, Cover TL. Carboxy-terminal proteolytic processing of *Helicobacter pylori* vacuolating toxin. *Infect Immun* 2001; **69**: 543-546

15 **Lanzavecchia S,** Bellon PL, Lupetti P, Dallai R, Rappuoli R, Telford JL. Three-dimensional reconstruction of metal replicas of the *Helicobacter pylori* vacuolating cytotoxin. *Struct Biol* 1998; **121**: 9-18

16 **Cover TL,** Hanson PI, Heuser JE. Acid-induced dissociation of VacA, the *Helicobacter pylori* vacuolating cytotoxin, reveals its pattern of assembly. *J Cell Biol* 1997; **138**: 759-769

17 **Yahiro K,** Niidome T, Kimura M, Hatakeyama T, Aoyagi H, Kurazono H, Imagawa K, Wada A, Moss J, Hirayama T. Activation of *Helicobacter pylori* VacA toxin by alkaline or acid conditions increases its binding to a 250-kDa receptor protein-tyrosine phosphatase beta. *J Biol Chem* 1999; **274**: 36693-36699

18 **McClain MS,** Cao P, Cover TL. Amino-terminal hydrophobic region of *Helicobacter pylori* vacuolating cytotoxin (VacA) mediates transmembrane protein dimerization. *Infect Immun* 2001; **69**: 1181-1184

19 **Cover TL,** Halter SA, Blaser MJ. Characterization of HeLa cell vacuoles induced by *Helicobacter pylori* broth culture supernatant. *Hum Pathol* 1992; **23**: 1004-1010

20 **Hopp TP,** Woods KR. Prediction of protein antigenic determinants from amino acid sequences. *Proc Natl Acad Sci U S A* 1981; **78**: 3824-3828

21 **Scott JK,** Smith GP. Searching for peptide ligands with an epitope library. *Science* 1990; **249**: 386-390

22 **Welling GW,** Weijer WJ, van der Zee R, Welling-Wester S. Prediction of sequential antigenic regions in proteins. *FEBS Lett* 1985; **188**: 215-218

23 **Zhao S,** Goodsell DS, Olson AJ. Analysis of a data set of paired uncomplexed protein structures: new metrics for side-chain flexibility and model evaluation. *Proteins* 2001; **43**: 271-279

24 **Kolibal SS,** Brady C, Cohen SA. Definition of epitopes for monoclonal antibodies developed against purified sodium channel protein: implications for channel structure. *J Membr Biol* 1998; **165**: 91-99

25 **Thomson SA,** Sherritt MA, Medveczky J, Elliott SL, Moss DJ, Fernando GJ, Brown LE, Suhrbier A. Delivery of multiple CD8 cytotoxic T cell epitopes by DNA vaccination. *J Immunol* 1998; **160**: 1717-1723

26 **Mateo L,** Gardner J, Chen Q, Schmidt C, Down M, Elliott SL, Pye SJ, Firat H, Lemonnier FA, Cebon J, Suhrbier A. An HLA-A2 polyepitope vaccine for melanoma immunotherapy. *J Immunol* 1999; **163**: 4058-4063

Edited by Wang XL and Chen WW **Proofread by** Xu FM

PO Box 2345, Beijing 100023, China
Fax: +86-10-85381893
E-mail: wjg@wjgnet.com www.wjgnet.com

World J Gastroenterol 2004;10(16):2344-2351
World Journal of Gastroenterology
 ISSN 1007-9327

• BASIC RESEARCH •

4-hydroxy-2, 3-nonenal activates activator protein-1 and mitogen-activated protein kinases in rat pancreatic stellate cells

Kazuhiro Kikuta, Atsushi Masamune, Masahiro Satoh, Noriaki Suzuki, Tooru Shimosegawa

Kazuhiro Kikuta, Atsushi Masamune, Masahiro Satoh, Noriaki Suzuki, Tooru Shimosegawa, Division of Gastroenterology, Tohoku University Graduate School of Medicine, Sendai 980-8574, Japan
Supported by Grant-in-Aid for Encouragement of Young Scientists from Japan Society for the Promotion of Science (to A.M.), by Pancreas Research Foundation of Japan (to A.M.), and by the Kanae Foundation for Life and Socio-Medical Science (to A. M.)
Correspondence to: Atsushi Masamune, M. D., Division of Gastroenterology, Tohoku University Graduate School of Medicine, 1-1 Seiryo-cho, Aoba-ku, Sendai 980-8574, Japan. amasamune@int3.med.tohoku.ac.jp
Telephone: +11-81-22-717-7171 **Fax:** +11-81-22-717-7177
Received: 2004-02-06 **Accepted:** 2004-02-21

Abstract

AIM: Activated pancreatic stellate cells (PSCs) are implicated in the pathogenesis of pancreatic inflammation and fibrosis, where oxidative stress is thought to play a key role. 4-hydroxy-2,3-nonenal (HNE) is generated endogenously during the process of lipid peroxidation, and has been accepted as a mediator of oxidative stress. The aim of this study was to clarify the effects of HNE on the activation of signal transduction pathways and cellular functions in PSCs.

METHODS: PSCs were isolated from the pancreas of male Wistar rats after perfusion with collagenase P, and used in their culture-activated, myofibroblast-like phenotype unless otherwise stated. PSCs were treated with physiologically relevant and non-cytotoxic concentrations (up to 5 μmol/L) of HNE. Activation of transcription factors was examined by electrophoretic mobility shift assay and luciferase assay. Activation of mitogen-activated protein (MAP) kinases was assessed by Western blotting using anti-phosphospecific antibodies. Cell proliferation was assessed by measuring the incorporation of 5-bromo-2′-deoxyuridine. Production of type I collagen and monocyte chemoattractant protein-1 was determined by enzyme-linked immunosorbent assay. The effect of HNE on the transformation of freshly isolated PSCs in culture was also assessed.

RESULTS: HNE activated activator protein-1, but not nuclear factor κB. In addition, HNE activated three classes of MAP kinases: extracellular signal-regulated kinase, c-Jun N-terminal kinase, and p38 MAP kinase. HNE increased type I collagen production through the activation of p38 MAP kinase and c-Jun N-terminal kinase. HNE did not alter the proliferation, or monocyte chemoattractant protein-1 production. HNE did not initiate the transformation of freshly isolated PSCs to myofibroblast-like phenotype.

CONCLUSION: Specific activation of these signal transduction pathways and altered cell functions such as collagen production by HNE may play a role in the pathogenesis of pancreatic disorders.

Kikuta K, Masamune A, Satoh M, Suzuki N, Shimosegawa T. 4-hydroxy-2, 3-nonenal activates activator protein-1 and mitogen-activated protein kinases in rat pancreatic stellate cells. *World J Gastroenterol* 2004; 10(16): 2344-2351
http://www.wjgnet.com/1007-9327/10/2344.asp

INTRODUCTION

In 1998, star-shaped cells in the pancreas, namely pancreatic stellate cells (PSCs), were identified and characterized[1,2]. They are morphologically similar to the hepatic stellate cells that play a central role in inflammation and fibrogenesis of the liver[3]. In normal pancreas, stellate cells are quiescent and can be identified by the presence of vitamin A-containing lipid droplets in the cytoplasm. In response to pancreatic injury or inflammation, they are transformed ("activated") from their quiescent phenotype into highly proliferative myofibroblast-like cells which express the cytoskeletal protein α-smooth muscle actin (α-SMA), and produce type I collagen and other extracellular matrix components. Many of the morphological and metabolic changes associated with the activation of PSCs in animal models of fibrosis also occur when these cells are grown in serum-containing medium in culture on plastic. There is accumulating evidence that PSCs, like hepatic stellate cells, are responsible for the development of pancreatic fibrosis[1,2,4]. It has also been suggested that PSCs may participate in the pathogenesis of acute pancreatitis[4,5]. In view of their importance in pancreatic fibrosis and inflammation, it is of particular importance to elucidate the molecular mechanisms underlying their activation. The activation of signaling pathways such as p38 mitogen-activated protein (MAP) kinase[6] and Rho-Rho kinase pathway[7] is likely to play a central role in PSC activation. However, the precise intracellular signaling pathways in PSCs are largely unknown.

The role of oxidative stress in the development of acute and chronic pancreatitis has been clarified[8,9]. Reactive oxygen species and aldehydic end-products of lipid peroxidation, such as 4-hydroxy-2,3-nonenal (HNE), could act as mediators affecting signal transduction pathways, proliferation, and functional responses of target cells[10-12]. HNE is a specific and stable end product of lipid peroxidation. It could be produced in response to oxidative insults[13], and has been regarded to be responsible for many of the effects during oxidative stress *in vivo*[13,14]. It reacts with DNA and proteins, generating various forms of adducts (cysteine, lysine, and histidine residues) that are capable of inducing cellular stress responses such as cell signaling and apoptosis[14]. It has been shown that alcoholic chronic pancreatitis is characterized by the co-localization of evident lipid peroxidation, as assessed by immunoreactivity of HNE inside acinar cells, and the deposition of collagen type I in the fibrous septa and fibrotic stroma surrounding the pancreatic acini[15]. The stronger HNE immunoreactivity at the periphery of acini raised the possibility that HNE might affect the cell functions of PSCs, but the effects of HNE on the signaling pathways and the regulation of cell functions in PSCs are unknown. We here report that HNE at physiologically relevant and non-cytotoxic concentrations activated activator protein-1 (AP-1) and three classes of MAP kinases in PSCs. In addition, HNE increased type I collagen production from PSCs. Specific

activation of these signal transduction pathways and altered cell functions such as collagen production by HNE may play a role in the pathogenesis of pancreatic disorders.

MATERIALS AND METHODS

Materials

3-(4, 5-dimethylthiazole-2-yl)-2, 5-diphenyltetrazolium bromide (MTT) was obtained from Dojindo (Kumamoto, Japan). Poly (dI.dC)-poly (dI.dC) and [γ-^{32}P] ATP were purchased from Amersham Biosciences UK, Ltd. (Buckinghamshire, England). Collagenase P and recombinant human interleukin (IL)-1β were from Roche Applied Science (Mannheim, Germany). Double-stranded oligonucleotide probes for AP-1 and nuclear factor κB (NF-κB) were purchased from Promega (Madison WI). Rat recombinant platelet-derived growth factor (PDGF)-BB was from R&D Systems (Minneapolis, MN). Rabbit antibodies against phosphospecific MAP kinases, total MAP kinases, and inhibitor of NF-κB (IκB-α) were purchased from Cell Signaling Technologies (Beverly, MA). Rabbit antibody against glyceraldehyde-3-phosphate dehydrogenase (G3PDH) was from Trevigen (Gaithersburg, MD). HNE, SB203580, SP600125, and U0126 were from Calbiochem (La Jolla, CA). All other reagents were from Sigma-Aldrich (St. Louis, MO) unless specifically described.

Cell culture

All animal procedures were performed in accordance with the National Institutes of Health Animal Care and Use Guidelines. Rat PSCs were prepared from the pancreas tissues of male Wistar rats (Japan SLC Inc., Hamamatsu, Japan) weighing 200-250 g as previously described using the Nycodenz solution (Nycomed Pharma, Oslo, Norway) after perfusion with 0.3 g/L collagenase P[16]. The cells were resuspended in Ham's F-12 containing 100 mL/L heat-inactivated fetal bovine serum (ICN Biomedicals, Aurora, OH), penicillin sodium, and streptomycin sulfate. Cell purity was always more than 90% as assessed by a typical star-like configuration and by detecting vitamin A autofluorescence. All experiments were performed using cells between passages two and five except for those using freshly isolated PSCs. Unless otherwise stated, we incubated PSCs in serum-free medium for 24 h before the addition of experimental reagents.

Cell viability assay

Cell viability was assessed by the MTT assay as previously described[17]. After treatment with HNE for 24 h, MTT solution was added to the cells at a final concentration of 500 μg/mL and the incubation continued at 37 °C for 4 h. After the incubation period, the medium was aspirated and the formazan product was solubilized with dimethylsulfoxide. Cell viability was determined by the differences in absorbance at wavelengths of 570 min 690 nm.

Intracellular peroxide production assay

Intracellular peroxide production was examined as previously described[14]. Briefly, cells were incubated with 2',7'-dichlorofluorescin diacetate (DCF-DA) at 50 μmol/L for 30 min at 37 °C, and then treated with experimental reagents for an additional 30 min at 37 °C. After chilled on ice, cells were washed with ice-cold PBS, scraped from the plate, and resuspended at 1×10^6 cells/mL in PBS containing 10 mmol/L EDTA. The fluorescence intensities of 2', 7'-dichlorofluorescin formed by the reaction of DCF-DA with peroxides of more than 10 000 viable cells from each sample were analyzed by FACSCaliber flow cytometer (Becton Dickinson Co. Ltd., Tokyo, Japan) with excitation and emission settings of 488 and 525 nm, respectively. Prior to data collection, propidium iodide was added to the sample to gate out dead cells. Experiments were repeated at least twice with similar results. The data are expressed as one representative histogram.

Cell proliferation assay

Serum-starved PSCs (approximately 80% density) were treated with HNE at the indicated concentrations in the absence or presence of PDGF-BB (25 ng/mL). Cell proliferation was assessed using a commercial kit (Cell proliferation ELISA, BrdU; Roche Applied Science) according to the manufacturer's instruction. This is colorimetric immunoassay based on the measurement of 5-bromo-2'-deoxyuridine (BrdU) incorporation during DNA synthesis[18]. After 24-hour-incubation with experimental reagents, cells were labeled with BrdU for 3 h at 37 °C, fixed, and incubated with peroxidase-conjugated anti-BrdU antibody. Then the peroxidase substrate 3,3',5,5'-tetramethylbenzidine was added, and BrdU incorporation was quantitated by differences in absorbance at wavelength 370 min 492 nm.

Nuclear extracts preparation and electrophoretic mobility shift assay

Nuclear extracts were prepared and electrophoretic mobility shift assay was performed as previously described[19]. Double-stranded oligonucleotide probes for AP-1 (5'-CGCTTGATGAGT CAGCCGGAA-3') and NF-κB (5'-AGTTGAGGGGACTT TCCCAGGC-3') were endlabeled with [γ-^{32}P]ATP. Nuclear extracts (approximately 5 μg) were incubated with the labeled oligonucleotide probe for 20 min at 22 °C, and electrophoresed through a 40 g/L polyacrylamide gel. Gels were dried, and autoradiographed at -80 °C overnight. A 100-fold excess of unlabeled oligonucleotide was incubated with nuclear extracts for 10 min prior to the addition of the radiolabeled probe in the competition experiments.

Luciferase assay

Luciferase assays were performed as previously described[20] using luciferase expression vectors containing two consensus AP-1 binding sites (TGACTCA), or two consensus NF-κB binding sites (GGGACTTTCC), which were kindly provided by Dr. Naofumi Mukaida (Kanazawa University, Japan). Approximately 1×10^6 PSCs were transfected with 2 μg of each luciferase expression vector, along with 40 ng of pRL-TK vector (Promega) as an internal control, using the FuGENE6 reagent (Roche Applied Science). After 24 h, the transfected cells were treated with HNE at 1 μmol/L for an additional 24 h. At the end of the incubation, cell lysates were prepared using Pica Gene kit (Toyo Ink Co., Tokyo, Japan), and the light intensities were measured using a model Lumat LB9507 Luminescence Reader (EG&G Berthold, Bad Wildbad, Germany).

Western blot analysis

Activation of MAP kinases was examined by Western blot analysis using anti-phosphospecific MAP kinase antibodies as previously described[21]. Cells were treated with HNE, and lysed in sodium dodecyl sulfate buffer (62.5 mmol/L Tris-HCl at pH 6.8, 20 g/L sodium dodecyl sulfate, 100 mL/L glycerol, 50 mmol/L dithiothreitol, 1 g/L bromphenol blue) for 15 min on ice. The samples were then sonicated for 2 s, heated for 5 min, and centrifuged at 12 000 *g* for 5 min to remove insoluble cell debris. Whole cell extracts (approximately 100 μg) were fractionated on a 100 g/L sodium dodecyl sulfate-polyacrylamide gel. They were transferred to a nitrocellulose membrane (Bio-Rad, Hercules, CA), and the membrane was incubated overnight at 4 °C with rabbit antibodies against phosphorylated MAP kinases (extracellular signal-regulated kinase (ERK)1/2, c-Jun N-terminal kinase (JNK), or p38 MAP kinase). After incubation with peroxidase-conjugated goat anti-rabbit secondary

antibody for 1 h, proteins were visualized by using an ECL kit (Amersham Biosciences UK, Ltd.). Levels of total MAP kinases, IκB-α, α-SMA, and G3PDH were examined in a similar manner.

Enzyme-linked immunosorbent assay

After a 24-h incubation, cell culture supernatants were harvested and stored at -80 °C until the measurement. Monocyte chemoattractant protein-1 (MCP-1) levels in the culture supernatants were measured by enzyme-linked immunosorbent assay (Pierce Biotechnology, Rockford, IL) according to the manufacturer's instructions.

Collagen assay

PSCs were incubated with HNE in serum-free medium for 48 h. Type I collagen released into the culture supernatant was quantified by enzyme-linked immunosorbent assay, as previously described[22]. Briefly, immunoassay plates (Becton Dickinson, Franklin Lakes, NJ) were coated with diluted samples overnight at 4 °C. After blocking with 50 g/L dry milk in PBS, plates were incubated with goat anti-rat type I collagen antibody (SouthernBiotech, Birmingham, AL). After washing of the plate, rabbit anti-goat IgG antibody conjugated with alkaline phosphatase was added, and incubated. Finally, P-nitrophenylphosphate was added as a substrate, and the collagen levels were determined by differences in absorbance at wavelength 405 min 690 nm. Rat tail collagen type I was used as a standard. The collagen levels in each sample were normalized to the cellular DNA content, which was determined by a fluorometric assay, according to the method of Brunk *et al*.[23]. The results are expressed as a percentage of the untreated control.

Activating effect of HNE on PSCs in culture

Freshly isolated PSCs were incubated with HNE (at 1 μmol/L) in serum-free medium or 50 mL/L fetal bovine serum-containing medium. After 7-d incubation, morphological changes characteristic of PSC activation were assessed after staining with glial acidic fibrillary protein (GFAP) as previously described[24] using a streptavidin-biotin-peroxidase complex detection kit (Histofine Kit; Nichirei, Tokyo, Japan). Briefly, cells were fixed with 100 mL/L methanol for 5 min at -20 °C, and then endogenous peroxidase activity was blocked by incubation in methanol with 3 mL/L hydrogen peroxide for 5 min. After immersion in normal goat serum for 1 h, the slides were incubated with rabbit anti-GFAP antibody at a dilution of 1:100 overnight at 4 °C. The slides were incubated with biotinylated goat anti-rabbit antibody for 45 min, followed by peroxidase-conjugated streptavidin for 30 min. Finally, color was developed by incubating the slides for several minutes with diaminobenzidine (Dojindo, Kumamoto, Japan). In addition, total cellular proteins (approximately 25 μg) were prepared, and the levels of α-SMA and G3PDH were determined by Western blotting.

Statistical analysis

The results were expressed as mean±SD. Luminograms and autoradiograms are representative of at least three experiments. Differences between experimental groups were evaluated by the two-tailed unpaired Student's *t* test. A *P*-value less than 0.05 was considered statistically significant.

RESULTS

HNE was cytotoxic at high concentrations

Because HNE has been shown to be cytotoxic at high concentrations in several types of cells[25], we first examined the effect of HNE on the cell viability of PSCs. PSCs were incubated with increasing concentrations of HNE for 24 h, and the cell viability was assessed by MTT assay. HNE up to 5 μmol/L did not alter the cell viability, but above 5 μmol/L, HNE was cytotoxic (Figure 1). The results were also confirmed by trypan blue dye exclusion test (data not shown). Based on these results, we used HNE up to 5 μmol/L in the subsequent experiments.

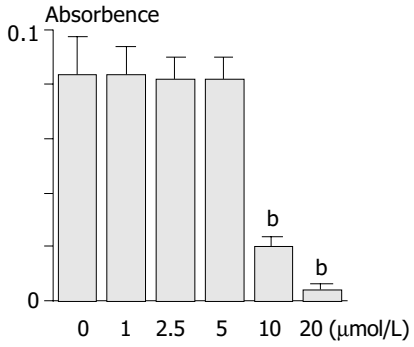

Figure 1 PSCs were incubated with HNE at the indicated concentrations in serum-free medium for 24 h. Cell viability was determined by the MTT assay, and the absorbance at 570 min 690 nm ("*A*.") of the sample is given. Data are shown as mean±SD (n = 6). $^aP<0.05$ *vs* control, $^bP<0.01$ *vs* control.

HNE was a potential inducer of oxidative stress

We examined the production of pro-oxidants using a peroxide-sensitive fluorescent probe, DCF-DA. This chemical is freely permeable to cells. Once inside the cells, it is hydrolyzed to DCF and trapped intracellularly. In the presence of peroxides, especially hydrogen peroxide, DCF is oxidized to fluorescent 2',7'-dichlorofluorescin, which can then be readily detected by flow cytometry[14]. Treatment with HNE (at 5 μmol/L) increased the peroxide-activated fluorescence intensity, indicating that HNE was a potential inducer of intracellular oxidative stress in PSCs (Figure 2).

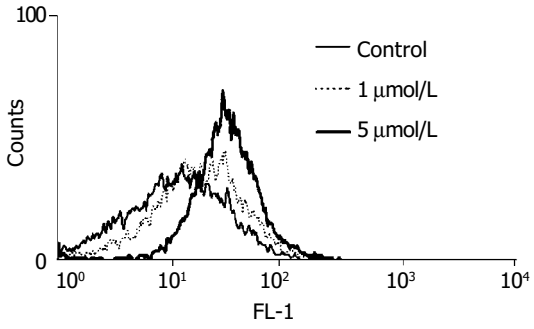

Figure 2 PSCs were incubated with DCF-DA (at 50 μmol/L) for 30 min and then treated with HNE (at 1 or 5 μmol/L) for 30 min. The fluorescence intensity of more than 10 000 cells was analyzed using a flow cytometer.

HNE increased AP-1, but not NF-κB binding activity

We next examined the effects of HNE on the activation of the transcription factors NF-κB and AP-1. These transcription factors are important regulators of gene expression in response to many stimuli including proinflammatory cytokines and growth factors[26,27]. PSCs were incubated with HNE, or IL-1β for 1 h. Nuclear extracts were prepared, and the specific binding activities of AP-1 and NF-κB were examined by electrophoretic mobility shift assay. HNE, as well as IL-1β, increased the AP-1 binding activity (Figure 3A). The specificity of AP-1-specific DNA binding activity was demonstrated by the addition of a 100-fold molar excess of unlabeled AP-1 oligonucleotide, but not by unrelated NF-κB oligonucleotide in competition assays (data not shown). In contrast, NF-κB binding activity was induced by IL-1β, but not by HNE (Figure 3B).

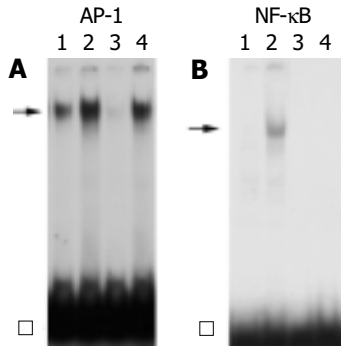

Figure 3 PSCs were treated with IL-1β (at 2 ng/mL, lane 2) or HNE (at 5 μmol/L, lane 4) in serum-free medium for 1 h. Nuclear extracts were prepared and subjected to electrophoretic mobility shift assay using AP-1 (panel A) or NF-κB (panel B) oligonucleotide probes. Arrows denote specific inducible complexes competitive with cold double-stranded oligonucleotide probes (lane 3). Lane 1: control (serum-free medium only). □: free probe.

HNE increased AP-1, but not NF-κB dependent transcriptional activity

To confirm that AP-1 activation observed by electrophoretic mobility shift assay was functional, the effect of HNE on AP-1 dependent transcriptional activity was examined. PSCs were transiently transfected with NF-κB- or AP-1-luciferase gene reporter constructs and assayed for the luciferase activity. As shown in Figure 4, HNE increased AP-1-dependent, but not NF-κB-dependent luciferase activity. Phosphorylation and degradation of the inhibitory protein IκB-α, and subsequent dissociation of this protein from NF-κB were thought to be necessary for the activation[26]. We also examined the effect of HNE on the degradation of IκB-α by Western blotting. IL-1β, but not HNE, induced transient degradation of IκB-α, further supporting that HNE did not activate NF-κB (Figure 4B).

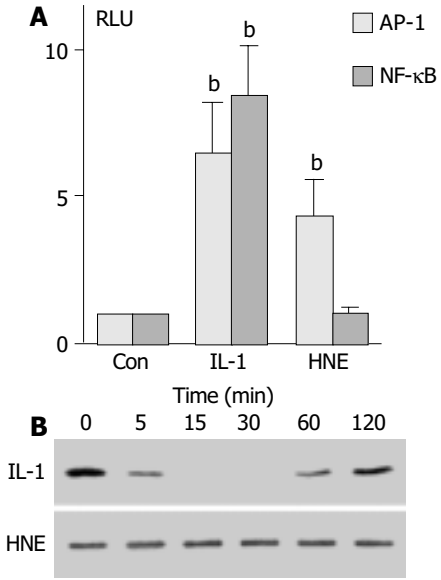

Figure 4 HNE increased AP-1, but not NF-κB, -dependent transcriptional activity. A: PSCs were transfected with the luciferase vectors (2 X AP-1 or 2 X NF-κB) along with pRL-TK vector as an internal control. After 24 h, the transfected cells were treated with IL-1β (at 2 ng/mL) or HNE (at 1 μmol/L). After another 24-h incubation, intracellular luciferase activities were determined. The data represent mean mean±SD, calculated from three independent experiments as fold induction compared with the activity observed in control (serum-free medium only, "Con"). $^{b}P<0.01$ *vs* control. RLU: relative light units. B: PSCs were treated with IL-1β (at 2 ng/mL) or HNE (at 1 μmol/L) in serum-free medium for the indicated times. Total cell lysates were prepared, and the level of IκB-α was determined by Western blotting.

HNE activated MAP kinases

Induction of the expression of AP-1 components c-Fos and c-Jun by a variety of stimuli such as growth factors and cytokines is mediated by the activation of three distinct MAP kinases: ERK1/2, JNK, and p38 MAP kinase[27,28]. Activation of these kinases occurs through phosphorylation[27,28]. We determined the activation of these MAP kinases in HNE-treated cells by Western blotting using anti-phosphospecific MAP kinase antibodies. These antibodies recognize only phosphorylated forms of MAP kinases, thus allowing the assessment of activation of these kinases. HNE activated these three classes of MAP kinases in a time-dependent manner with peaking around 5 to 15 min (Figure 5).

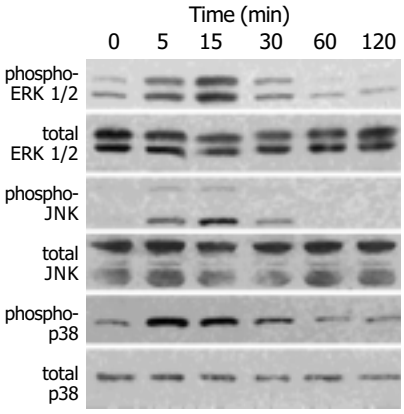

Figure 5 PSCs were treated with HNE (at 1 μmol/L) for the indicated times. Total cell lysates (approximately 100 μg) were prepared, and the levels of activated, phosphorylated MAP kinases were determined by Western blotting using anti-phosphospecific antibodies. Levels of total MAP kinases were also determined.

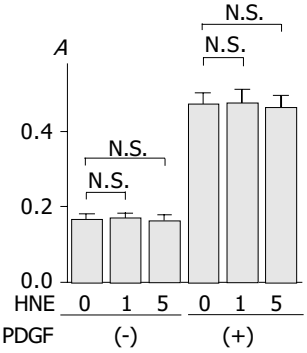

Figure 6 PSCs were treated with HNE (at 0, 1, or 5 μmol/L) in the absence or presence of PDGF (at 25 ng/mL) in serum-free medium. After 24-h incubation, cells were labeled with BrdU for 3 h. Cells were fixed, and incubated with peroxidase-conjugated anti-BrdU antibody. Then the peroxidase substrate 3,3', 5,5'-tetramethylbenzidine was added, and BrdU incorporation was quantitated by differences in absorbance at wavelength 370 min 492 nm ("*A*.", optical density). Data are shown as mean±SD ($n = 6$). $^{b}P<0.01$ versus control (serum-free medium only), N.S.: not significant.

HNE did not alter basal and PDGF-BB-induced proliferation

We then examined the effects of HNE on basal and PDGF-induced proliferation. As previously reported[16], PDGF-BB significantly increased proliferation. HNE did not affect either

basal or PDGF-BB-induced proliferation of PSCs (Figure 6).

HNE did not induce MCP-1 production

Activated PSCs acquired the proinflammatory phenotype; they might modulate the recruitment and activation of inflammatory cells through the expression of MCP-1[29]. IL-1β induced MCP-1 production, but HNE did not (Figure 7).

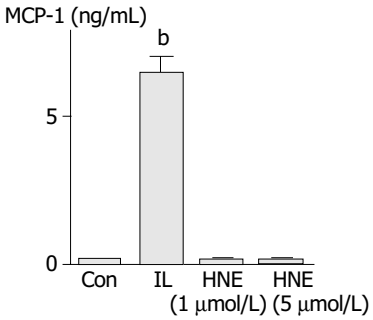

Figure 7 PSCs were treated with IL-1β (2 ng/mL, "IL") or HNE (at 1 or 5 μmol/L) in serum-free medium. After 24 h, culture supernatant was harvested, and the MCP-1 level was determined by enzyme-linked immunosorbent assay. Data shown are expressed as mean±SD (n = 6). ^{b}P<0.01 versus control ("Con", serum-free medium only).

HNE increased type I collagen production

It has been shown that culture-activated PSCs express α-SMA and produce type I collagen. Indeed, α-SMA expression has been accepted as a marker of PSC activation[1], and *in situ* hybridization techniques showed that α-SMA-positive cells were the principal source of collagen in the fibrotic pancreas[4]. HNE increased the production of type I collagen (Figure 8). Our previous finding that ethanol and acetaldehyde induced collagen production through p38 MAP kinase[30] prompted us to examine the role of MAP kinases in HNE-induced type I collagen production. Thus we employed specific inhibitors to block these pathways. A selective p38 MAP kinase inhibitor SB203580[31], and a JNK inhibitor SP600125[32] decreased type I collagen production. In contrast, U0126, a specific inhibitor of MAP kinase kinase activation and consequent ERK1/2 activation[33], did not affect the collagen production. These results suggested that HNE induced type I collagen production through the activation of p38 MAP kinase and JNK, but not ERK pathway.

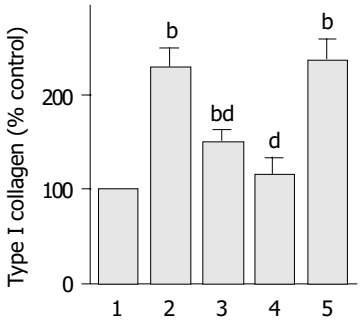

Figure 8 PSCs were treated with HNE (at 1 μmol/L , lane 2) in the absence or presence of SB203580 (at 25 mmol/L , lane 3), SP600125 (at 10 μmol/L, lane 4), or U0126 (at 5 μmol/L, lane 5). After 48-h incubation, type I collagen released into the cultute supernatant was quantified by enzyme-linked immunosorbent assay. The collagen levels in each sample were normalized to the cellular DNA content. The results are expressed as a percentage of the untreated control ("Con"). Data are shown as mean±SD (n = 6). ^{b}P<0.01 *vs* control (serum-free medium only, lane 1). ^{d}P<0.01 *vs* HNE only (lane 2).

HNE did not initiate the transformation of freshly isolated PSCs to activated phenotype

Finally, we examined whether HNE initiated the transformation of PSCs from quiescent to myofibroblast-like phenotype in culture. Freshly isolated PSCs were incubated with HNE in serum-free medium or 50 mL/L serum-containing medium for 7 d. Morphological changes characteristic of PSC activation were assessed after staining with GFAP. After 7 d, PSCs cultured with 50 mL/L serum showed transformation into cells with a myofibroblast-like phenotype (Figure 9A). In contrast, PSCs treated with HNE were small and circular, with lipid droplets presenting in many cells and slender dendritic processes (Figure 9B), as PSCs treated with serum-free medium only (Figure 9C). In agreement with the morphological changes, significant expression of α-SMA was observed on d 7 in serum-treated PSCs, whereas HNE did not induce α-SMA expression.

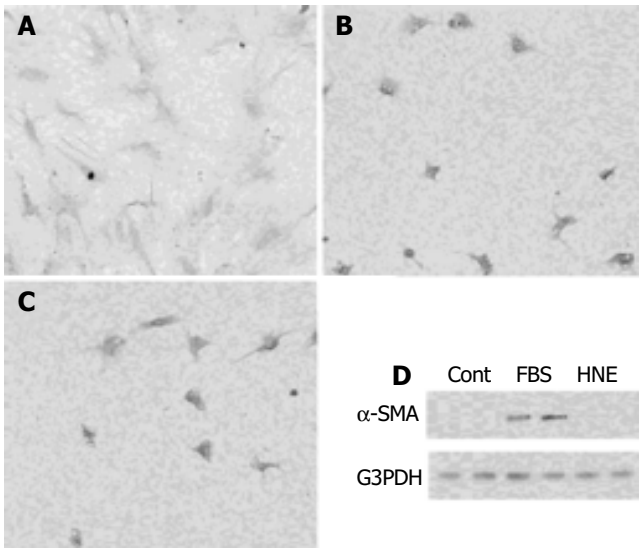

Figure 9 A,B,C: Freshly isolated PSCs were incubated with 50 mL/L serum (panel A), HNE (at 1 μmol/L, panel B), or serum-free medium (panel C) for 7 d. Morphological changes characteristic of PSC activation were assessed after staining with GFAP. Original magnification: ×10 objective. D: Total cell lysates (approximately 25 μg) were prepared from cells treated with serum-free medium ("Cont"), 50 mL/L serum ("FBS"), or HNE (at 1 μmol/L) for 7 d, and the levels of α-SMA and G3PDH were determined by Western blotting.

DISCUSSION

It has been established that oxidative stress plays a critical role in the pathogenesis of both acute and chronic pancreatitis[8,9]. HNE, an aldehydic end product of lipid peroxidation, is believed to be largely responsible for pathological effects observed during oxidative stress[13]. The major effects of HNE produced during oxidative stress are believed to be damage to cellular components such as glutathione and proteins. However, recent studies have revealed that HNE at non-cytotoxic levels could potently activate a stress response mechanism[14]. In this study, we have shown for the first time that HNE, at non-cytotoxic concentrations, activated AP-1, but not NF-κB, in PSCs. This selective pattern of activation was distinct from that elicited by IL-1β and tumor necrosis factor-α, which also activated NF-κB[5]. In addition, HNE activated three classes of MAP kinases (ERK1/2, JNK, and p38 MAP kinase). HNE-induced type I collagen production was inhibited by SB203580, a p38 MAP kinase inhibitor, and by SP600125, a JNK inhibitor, suggesting

a role of p38 MAP kinase and JNK in the type I collagen production. The concentrations of HNE used in this study (up to 5 μmol/L) could be easily reached *in vivo* in conditions of mild to moderate oxidative stress, and were considered to be physiologically relevant[13].

It has been shown that ethanol increased HNE protein adduct accumulation in the pancreas of rats[34]. During pancreatic injury *in vivo*, PSCs might be exposed to HNE via two pathways: (1) exogenous exposure as a result of the generation of HNE by surrounding cells (e.g. acinar cells and inflammatory cells) or (2) endogenous exposure as a result of the generation of HNE within the cells. Casini *et al*.[15] have shown that stronger HNE immunoreactivity was observed at the periphery of acini in chronic alcoholic pancreatitis. Under such a circumstance, it is likely that PSCs exogenously expose to HNE. Our present study is exclusively concerned with the effect of exogenously-delivered HNE on cell biology, and it remains to be clarified how results of this study correlated with the potential effect of HNE formed endogenously in the cell. It is likely that PSCs were exposed to endogenous HNE during ethanol consumption, because PSCs, in addition to pancreatic acinar cells[35], had the capacity to metabolize ethanol to acetaldehyde via alcohol dehydrogenase-mediated oxidation of ethanol[36].

Activated PSCs acquire the proinflammatory phenotype; they may modulate the recruitment and activation of inflammatory cells. We have reported that activated PSCs expressed MCP-1[29] in response to IL-1β and tumor necrosis factor-α *in vitro*. Indeed, MCP-1 expression by activated PSCs was shown to be increased in fibrous tissue sections from patients with chronic pancreatitis[37]. In this study, HNE failed to induce NF-κB activation and consequent MCP-1 production. The failure of HNE to induce MCP-1 expression is not surprising because the activation of NF-κB has been shown to play a central role in MCP-1 expression in PSCs[29]. This is in contrast to human endothelial cells where the AP-1 proteins c-Fos and c-Jun directly induce MCP-1 expression independently of the NF-κB pathway[38]. The effects of HNE on the activation of NF-κB and AP-1 appeared to depend on the types of cells. In a similar manner to PSCs, HNE activated AP-1, but not NF-κB, in murine and human macrophages[39] and human hepatic stellate cells[40]. On the other hand, HNE did not activate AP-1, but did attenuate IL-1β- and phorbol ester-induced NF-κB activation in human monocytic THP-1 cells[41]. The inhibition of NF-κB activation was mediated through the inhibition of IκB phosphorylation and subsequent proteolysis[41]. Recent reviews[42,43] have emphasized that redox-dependent activation of NF-κB was cell and stimulus specific as opposed to the concept that oxidative stress was a common mediator of diverse NF-κB activators. Li and Karin[42] reported that when a redox-regulated effect on NF-κB was observed, it appeared to occur downstream from the IκB kinase, at the level of ubiquitination and/or degradation of IκB.

In this study, HNE activated three classes of MAP kinases in PSCs. This is in agreement with the previous study showing that HNE activated these three classes of MAP kinases in rat liver epithelial RL34 cells[14]. In human hepatic stellate cells, Parola *et al*.[40] reported that HNE formed adducts with the p46 and p54 isoforms of JNK, leading to the nuclear translocation and activation of these signaling molecules, and, in turn, the induction of the transcription factors c-jun and AP-1. Unlike human hepatic stellate cells, we showed that HNE induced phosphorylation of p46 and p54 JNK in rat PSCs. On the other hand, we have shown that activation of ERK played a central role in PDGF-BB-induced proliferation of PSCs[16]. In spite of the ability to activate ERK, HNE failed to alter the proliferation regardless of the presence or absence of PDGF-BB, suggesting that activation of ERK is required but not sufficient for the proliferation of PSCs. This is in agreement with the concept that activation of ERK, although necessary, may not be sufficient to justify the mitogenic properties of an agonist[44].

We here showed that HNE did not initiate the transformation of quiescent PSCs. This is in disagreement with the previous reports showing that ethanol and acetaldehyde activated quiescent PSCs through the generation of oxidative stress[36]. However, it should be noted that previous studies examining the effects of oxidative stress on the activation of hepatic stellate cells have reported conflicting results. Lee *et al*.[45] reported that quiescent hepatic stellate cells were activated upon exposure to the pro-oxidant compound ascorbate/ferrous sulfate or the lipid peroxidation product malondialdehyde. Maher *et al*.[46] reported that stimulatory effects of malondialdehyde only occurred after hepatic stellate cells had been preactivated by culture on plastic. Olynyk *et al*.[47] reported that malondialdehyde and HNE decreased α-SMA expression in hepatic stellate cells at d 3 when compared to controls not incubated with the compounds. Previous studies have suggested that cytokines and growth factors such as transforming growth factor-β1 and tumor necrosis factor-α induced the transformation of quiescent PSCs[48,49]. These mediators were released or produced from inflammatory cells, platelets, and pancreatic acinar cells, during the course of pancreatitis[48,49], leading to the activation of PSCs. Once activated, PSCs were sensitive to HNE, and showed profibrogenic responses, thus playing a role in the pathogenesis of pancreatic fibrosis.

In agreement with the previous study in human hepatic stellate cells[40], HNE increased type I collagen production in PSCs. Lee *et al*.[45] reported that oxidative stress-induced collagen synthesis in hepatic stellate cells was associated with induction of transcription factors NF-κB and c-myb[45]. In rat PSCs, the role of NF-κB was unlikely because HNE failed to activate NF-κB. Although the molecular mechanisms by which HNE increased type I collagen production in hepatic stellate cells were not further pursued, we have shown that HNE-induced type I collagen production was mediated by the activation of JNK and p38 MAP kinase. Along this line, it has been reported that malondialdehyde increased α2 (I) collagen gene activity through JNK activation in hepatic stellate cells[50]. It should be noted that the biological action of HNE may result in multiple effects within the complex network of events occurring in the process of fibrosis following reiterated pancreatic injury, with the resulting overall biological effects being influenced by the actual HNE concentration, the target cell or cells available, and the presence of growth factors and other mediators in the microenvironment. Nevertheless, our findings that HNE induced type I collagen production suggest possible links between oxidant stress, aldehyde-adduct formation, and pancreatic fibrosis. Very recently, it has been reported that HNE acted as a potent pro-fibrogenic stimulus in the expression of genes involved in extracellualr matrix deposition in activated hepatic stellate cells[51]. Indeed, we have found that HNE increased the transcriptional activity of prolyl 4-hydroxylase (α), a key enzyme that catalyzes the formation of 4-hydroxyproline (Satoh *et al*. manuscript in preparation). Elucidation of the functions of PSCs would provide better understanding and rational approaches for the control of pancreatic inflammation and fibrosis.

ACKNOWLEDGEMENT

The authors thank Dr. Naofumi Mukaida for the luciferase vectors.

REFERENCES

1 **Apte MV**, Haber PS, Applegate TL, Norton ID, McCaughan GW, Korsten MA, Pirola RC, Wilson JS. Periacinar stellate

shaped cells in rat pancreas: identification, isolation, and culture. *Gut* 1998; **43**: 128-133
2 **Bachem MG**, Schneider E, Gross H, Weidenbach H, Schmid RM, Menke A, Siech M, Beger H, Grunert A, Adler G. Identification, culture, and characterization of pancreatic stellate cells in rats and humans. *Gastroenterology* 1998; **115**: 421-432
3 **Friedman SL**. Molecular regulation of hepatic fibrosis, an integrated cellular response to tissue injury. *J Biol Chem* 2000; **275**: 2247-2250
4 **Haber PS**, Keogh GW, Apte MV, Moran CS, Stewart NL, Crawford DH, Pirola RC, McCaughan GW, Ramm GA, Wilson JS. Activation of pancreatic stellate cells in human and experimental pancreatic fibrosis. *Am J Pathol* 1999; **155**: 1087-1095
5 **Masamune A**, Sakai Y, Kikuta K, Satoh M, Satoh A, Shimosegawa T. Activated rat pancreatic stellate cells express intercellular adhesion molecule-1 (ICAM-1) *in vitro*. *Pancreas* 2002; **25**: 78-85
6 **Masamune A**, Satoh M, Kikuta K, Sakai Y, Satoh A, Shimosegawa T. Inhibition of p38 mitogen-activated protein kinase blocks activation of rat pancreatic stellate cells. *J Pharmacol Exp Ther* 2003; **304**: 8-14
7 **Masamune A**, Kikuta K, Satoh M, Satoh K, Shimosegawa T. Rho kinase inhibitors block activation of pancreatic stellate cells. *Br J Pharmacol* 2003; **140**: 1292-1302
8 **Sanfey H**, Bulkley GB, Cameron JL. The pathogenesis of acute pancreatitis. The source and role of oxygen-derived free radicals in three different experimental models. *Ann Surg* 1985; **201**: 633-639
9 **Braganza JM**. The pathogenesis of chronic pancreatitis. *QJM* 1996; **89**: 243-250
10 **Droge W**. Free radicals in the physiological control of cell function. *Physiol Rev* 2002; **82**: 47-95
11 **Hensley K**, Robinson KA, Gabbita SP, Salsman S, Floyd RA. Reactive oxygen species, cell signaling, and cell injury. *Free Radic Biol Med* 2000; **28**: 1456-1462
12 **Uchida K**. 4-Hydroxy-2-nonenal: a product and mediator of oxidative stress. *Prog Lipid Res* 2003; **42**: 318-343
13 **Esterbauer H**, Schaur RJ, Zollner H. Chemistry and biochemistry of 4-hydroxynonenal, malonaldehyde and related aldehydes. *Free Rad Biol Med* 1991; **11**: 81-128
14 **Uchida K**, Shiraishi M, Naito Y, Torii Y, Nakamura Y, Osawa T. Activation of stress signaling pathways by the end product of lipid peroxidation. 4-hydroxy-2-nonenal is a potential inducer of intracellular peroxide production. *J Biol Chem* 1999; **274**: 2234-2242
15 **Casini A**, Galli A, Pignalosa P, Frulloni L, Grappone C, Milani S, Pederzoli P, Cavallini G, Surrenti C. Collagen type I synthesized by pancreatic periacinar stellate cells (PSC) co-localizes with lipid peroxidation-derived aldehydes in chronic alcoholic pancreatitis. *J Pathol* 2000; **192**: 81-89
16 **Masamune A**, Kikuta K, Satoh M, Kume K, Shimosegawa T. Differential roles of signaling pathways for proliferation and migration of rat pancreatic stellate cells. *Tohoku J Exp Med* 2003; **199**: 69-84
17 **Mosmann T**. Rapid colorimetric assay for cellular growth and survival: application to proliferation and cytotoxicity assays. *J Immunol Methods* 1983; **65**: 55-63
18 **Porstmann T**, Ternynck T, Avrameas S. Quantitation of 5-bromo-2-deoxyuridine incorporation into DNA: an enzyme immunoassay for the assessment of the lymphoid cell proliferative response. *J Immunol Methods* 1985; **82**: 169-179
19 **Masamune A**, Igarashi Y, Hakomori S. Regulatory role of ceramide in interleukin(IL)-1 beta-induced E-selectin expression in human umbilical vein endothelial cells. Ceramide enhances IL-1 beta action, but is not sufficient for E-selectin expression. *J Biol Chem* 1996; **271**: 9368-9375
20 **Masamune A**, Shimosegawa T, Masamune O, Mukaida N, Koizumi M, Toyota T. *Helicobacter pylori*-dependent ceramide production may mediate increased interleukin 8 expression in human gastric cancer cell lines. *Gastroenterology* 1999; **116**: 1330-1341
21 **Masamune A**, Satoh K, Sakai Y, Yoshida M, Satoh A, Shimosegawa T. Ligands of peroxisome proliferator-activated receptor-gamma induce apoptosis in AR42J cells. *Pancreas* 2002; **24**: 130-138
22 **Moshage H**, Casini A, Lieber CS. Acetaldehyde selectively stimulat collagen production in cultured rat liver fat-storing cells but not in hepatocytes. *Hepatology* 1990; **12**(3 Pt1): 511-518
23 **Brunk CF**, Jones KC, James TW. Assay for nanogram quantities of DNA in cellular homogenates. *Anal Biochem* 1979; **92**: 497-500
24 **Masamune A**, Satoh M, Kikuta K, Suzuki N, Shimosegawa T. Establishment and characterization of a rat pancreatic stellate cell line by spontaneous immortalization. *World J Gastroenterol* 2003; **9**: 2751-2758
25 **Kruman I**, Bruce-Keller AJ, Bredesen D, Waeg G, Mattson MP. Evidence that 4-hydroxynonenal mediates oxidative stress-induced neuronal apoptosis. *J Neurosci* 1997; **17**: 5089-5100
26 **Grilli M**, Chiu JJ, Lenardo MJ. NF-kappa B and Rel: participants in a multiform transcriptional regulatory system. *Int Rev Cytol* 1993; **143**: 1-62
27 **Karin M**, Liu Z, Zandi E. AP-1 function and regulation. *Curr Opin Cell Biol* 1997; **9**: 240-246
28 **Robinson MJ**, Cobb MH. Mitogen-activated protein kinase pathways. *Curr Opin Cell Biol* 1997; **9**: 180-186
29 **Masamune A**, Kikuta K, Satoh M, Sakai Y, Satoh A, Shimosegawa T. Ligands of peroxisome proliferator-activated receptor-gamma block activation of pancreatic stellate cells. *J Biol Chem* 2002; **277**: 141-147
30 **Masamune A**, Kikuta K, Satoh M, Satoh A, Shimosegawa T. Alcohol activates activator protein-1 and mitogen-activated protein kinases in rat pancreatic stellate cells. *J Pharmacol Exp Ther* 2002; **302**: 36-42
31 **Cuenda A**, Rouse J, Doza YN, Meier R, Cohen P, Gallagher TF, Young PR, Lee JC. SB 203580 is a specific inhibitor of a MAP kinase homologue which is stimulated by cellular stresses and interleukin-1. *FEBS Lett* 1995; **364**: 229-233
32 **Bennett BL**, Sasaki DT, Murray BW, O'Leary EC, Sakata ST, Xu W, Leisten JC, Motiwala A, Pierce S, Satoh Y, Bhagwat SS, Manning AM, Anderson DW. SP600125, an anthrapyrazolone inhibitor of Jun N-terminal kinase. *Proc Natl Acad Sci U S A* 2001; **98**: 13681-13686
33 **Favata MF**, Horiuchi KY, Manos EJ, Daulerio AJ, Stradley DA, Feeser WS, Van Dyk DE, Pitts WJ, Earl RA, Hobbs F, Copeland RA, Magolda RL, Scherle PA, Trzaskos JM. Identification of a novel inhibitor of mitogen-activated protein kinase kinase. *J Biol Chem* 1998; **273**: 18623-18632
34 **McKim SE**, Uesugi T, Raleigh JA, McClain CJ, Arteel GE. Chronic intragastric alcohol exposure causes hypoxia and oxidative stress in the rat pancreas. *Arch Biochem Biophys* 2003; **417**: 34-43
35 **Haber PS**, Apte MV, Applegate TL, Norton ID, Korsten MA, Pirola RC, Wilson JS. Metabolism of ethanol by rat pancreatic acinar cells. *J Lab Clin Med* 1998; **132**: 294-302
36 **Apte MV**, Phillips PA, Fahmy RG, Darby SJ, Rodgers SC, McCaughan GW, Korsten MA, Pirola RC, Naidoo D, Wilson JS. Does alcohol directly stimulate pancreatic fibrogenesis? Studies with rat pancreatic stellate cells. *Gastroenterology* 2000; **118**: 780-794
37 **Saurer L**, Reber P, Schaffner T, Buchler MW, Buri C, Kappeler A, Walz A, Freiss H, Mueller C. Differential expression of chemokines in normal pancreas and in chronic pancreatitis. *Gastroenterology* 2000; **118**: 356-367
38 **Wang N**, Verna L, Hardy S, Forsayeth J, Zhu Y, Stemerman MB. Adenovirus-mediated overexpression of c-Jun and c-Fos induces intercellular adhesion molecule-1 and monocyte chemoattractant protein-1 in human endothelial cells. *Arterioscler Thromb Vasc Biol* 1999; **19**: 2078-2084
39 **Camandola S**, Scavazza A, Leonarduzzi G, Biasi F, Chiarpotto E, Azzi A, Poli G. Biogenic 4-hydroxy-2-nonenal activates transcription factor AP-1 but not NF-kappa B in cells of the macrophage lineage. *Biofactors* 1997; **6**: 173-179
40 **Parola M**, Robino G, Marra F, Pinzani M, Bellomo G, Leonarduzzi G, Chiarugi P, Camandola S, Poli G, Waeg G, Gentilini P, Dianzani MU. HNE interacts directly with JNK isoforms in human hepatic stellate cells. *J Clin Invest* 1998; **102**:

1942-1950

41 **Page S**, Fischer C, Baumgartner B, Haas M, Kreusel U, Loidl G, Hayn M, Ziegler-Heitbrock HW, Neumeier D, Brand K. 4-Hydroxynonenal prevents NF-kappaB activation and tumor necrosis factor expression by inhibiting IkappaB phosphorylation and subsequent proteolysis. *J Biol Chem* 1999; **274**: 11611-11618

42 **Li N**, Karin M. Is NF-kappaB the sensor of oxidative stress? *FASEB J* 1999; **13**: 1137-1143

43 **Bowie A**, O'Neill LA. Oxidative stress and nuclear factor-kappaB activation: a reassessment of the evidence in the light of recent discoveries. *Biochem Pharmacol* 2000; **59**: 13-23

44 **Blenis J**. Signal transduction via the MAP kinases: proceed at your own RSK. *Proc Natl Acad Sci U S A* 1993; **90**: 5889-5892

45 **Lee KS**, Buck M, Houglum K, Chojkier M. Activation of hepatic stellate cells by TGF alpha and collagen type I is mediated by oxidative stress through c-myb expression. *J Clin Invest* 1995; **96**: 2461-2468

46 **Maher JJ**, Tzagarakis C, Gimenez A. Malondialdehyde stimulates collagen production by hepatic lipocytes only upon activation in primary culture. *Alcohol Alcohol* 1994; **29**: 605-610

47 **Olynyk JK**, Khan NA, Ramm GA, Brown KE, O'Neill R, Britton RS, Bacon BR. Aldehydic products of lipid peroxidation do not directly activate rat hepatic stellate cells. *J Gastroenterol Hepatol* 2002; **17**: 785-790

48 **Apte MV**, Haber PS, Darby SJ, Rodgers SC, McCaughan GW, Korsten MA, Pirola RC, Wilson JS. Pancreatic stellate cells are activated by proinflammatory cytokines: implications for pancreatic fibrogenesis. *Gut* 1999; **44**: 534-541

49 **Schneider E**, Schmid-Kotsas A, Zhao J, Weidenbach H, Schmid RM, Menke A, Adler G, Waltenberger J, Grunert A, Bachem MG. Identification of mediators stimulating proliferation and matrix synthesis of rat pancreatic stellate cells. *Am J Physiol Cell Physiol* 2001; **281**: C532-C543

50 **Anania FA**, Womack L, Jiang M, Saxena NK. Aldehydes potentiate alpha(2)(I) collagen gene activity by JNK in hepatic stellate cells. *Free Radic Biol Med* 2001; **30**: 846-857

51 **Zamara E**, Novo E, Marra F, Gentilini A, Romanelli RG, Caligiuri A, Robino G, Tamagno E, Aragno M, Danni O, Autelli R, Colombatto S, Dianzani MU, Pinzani M, Parola M. 4-Hydroxynonenal as a selective pro-fibrogenic stimulus for activated human hepatic stellate cells. *J Hepatol* 2004; **40**: 60-68

Edited by Zhu LH and Xu FM

PO Box 2345, Beijing 100023, China
Fax: +86-10-85381893
E-mail: wjg@wjgnet.com www.wjgnet.com

World J Gastroenterol 2004;10(16):2352-2356
World Journal of Gastroenterology
 ISSN 1007-9327

• BASIC RESEARCH •

Structure prediction and activity analysis of human heme oxygenase-1 and its mutant

Zhen-Wei Xia, Wen-Pu Zhou, Wen-Jun Cui, Xue-Hong Zhang, Qing-Xiang Shen, Yun-Zhu Li, Shan-Chang Yu

Zhen-Wei Xia, Yun-Zhu Li, Shan-Chang Yu, Department of Pediatrics, Rui Jin Hospital, Shanghai Second Medical University, Shanghai 200025, China
Wen-Pu Zhou, Wen-Jun Cui, Xue-Hong Zhang, College of Life Science and Biotechnology, Shanghai Jiaotong University & Chinese Academy of Sciences, Shanghai Branch, Shanghai 200030, China
Qing-Xiang Shen, Shanghai Institute of Planned Parenthood Research, Shanghai 200032, China
Supported by the National Natural Science Foundation of China, No. 30170988, Shanghai Municipal Education Commission Foundation, No.2000B06, and Shanghai Jiaotong University-Shanghai Second Medical University Cooperative Foundation
Correspondence to: Dr. Xia Zhen Wei, Department of Pediatrics, Rui Jin Hospital, Shanghai Second Medical University, 197 Rui Jin Er Road, Shanghai 200025, China. xzw63@hotmail.com
Telephone: +86-21-64333414 **Fax:** +86-21-64333414
Received: 2004-01-02 **Accepted:** 2004-02-03

Abstract

AIM: To predict wild human heme oxygenase-1 (whHO-1) and hHO-1 His25Ala mutant (△hHO-1) structures, to clone and express them and analyze their activities.

METHODS: Swiss-PdbViewer and Antheprot 5.0 were used for the prediction of structure diversity and physical-chemical changes between wild and mutant hHO-1. hHO-1 His25Ala mutant cDNA was constructed by site-directed mutagenesis in two plasmids of *E. coli* DH5α. Expression products were purified by ammonium sulphate precipitation and Q-Sepharose Fast Flow column chromatography, and their activities were measured.

RESULTS: rHO-1 had the structure of a helical fold with the heme sandwiched between heme-heme oxygenase-1 helices. Bond angle, dihedral angle and chemical bond in the active pocket changed after Ala25 was replaced by His25, but Ala25 was still contacting the surface and the electrostatic potential of the active pocket was negative. The mutated enzyme kept binding activity to heme. Two vectors pBHO-1 and pBHO-1(M) were constructed and expressed. Ammonium sulphate precipitation and column chromatography yielded 3.6-fold and 30-fold higher purities of whHO-1, respectively. The activity of △hHO-1 was reduced 91.21% after mutation compared with whHO-1.

CONCLUSION: Proximal His25 ligand is crucial for normal hHO-1 catalytic activity. △hHO-1 is deactivated by mutation but keeps the same binding site as whHO-1. △hHO-1 might be a potential inhibitor of whHO-1 for preventing neonatal hyperbilirubinemia.

Xia ZW, Zhou WP, Cui WJ, Zhang XH, Shen QX, Li YZ, Yu SC. Structure prediction and activity analysis of human heme oxygenase-1 and its mutant. *World J Gastroenterol* 2004; 10(16): 2352-2356
http://www.wjgnet.com/1007-9327/10/2352.asp

INTRODUCTION

Heme oxygenase (HO) is responsible for the physiological breakdown of heme into equimolar amounts of biliverdin, carbon monoxide, and iron. Three isoforms (HO-1, HO-2, and HO-3) have been identified. HO-1 is ubiquitous, its mRNA levels and activity can be increased several-fold by heme, other metalloporphyrins, transition metals, and stress-inducing stimuli. In contrast, HO-2 is present chiefly in brain and testes and is virtually uninducible. HO-3 has very low activity; its physiological functions probably include heme binding. The HO system has been strongly highlighted for its potential significance in maintaining cellular homeostasis. Nevertheless the physiological correlations of the three isoforms and their reciprocal interrelation have been poorly understood[1-4].

HO-1 regulates the levels of serum bilirubin as the rate-limiting enzyme in heme degradation pathway. Recent reports showed that HO-1 was identified as an ubiquitous stress protein and it had important physiological roles. Overexpression of HO-1 gene resulted in protection from cytokine-induced oxidative stress[5], inflammation[6-9], apoptosis[10-17] and proliferation[18-25].

It has been reported that histidine (His) residues at positions 25, 84, 119 and 132 in HO-1 sequence are conserved in rat, human, mouse and chicken. These histidines may be important for heme-binding[26]. His25 and His132 mutants were reported for the proximal heme iron ligand in rat heme oxygenase-1 (rHO-1)[27]. The unambiguous spectroscopic demonstration that His25 is the proximal iron ligand leaves the role of His132 uncertain. His 25 is essential for heme degradation activity of the enzyme. The research on human HO-1 (hHO-1) structure has been shown that hHO-1 embodies a novel protein fold that consists primarily of α-helices, and the heme is held between two of these helices[28].

It is unclear whether hHO-1 mutant has the same characteristics and displays catalytic inactivity but binding heme as Ala replacing His 25. In this study, the characteristics of wild hHO-1 (whHO-1) and its mutant were predicted by bio-informatics method. On the basis of the results, the truncated hHO-1 cDNA mutant was constructed by site-directed mutagenesis. Two expression plasmids, pBHO-1 and pBHO-1 (M) containing whHO-1 and hHO-1 His25Ala mutant (△hHO-1), respectively, were constructed and expressed in *E.coli*, and then isolated, purified and analyzed of their activities analysis.

MATERIALS AND METHODS

Materials

Swiss-PdbViewer and Antheprot 5.0 were from GlaxoSmithKline R&D and the Swiss Institute of Bioinformatics and CBI, BeiJin University respectively. Plasmid pBHO-1 was provided by Lightning and Ortiz de Montellano (Department of Pharmaceutical Chemistry, University of California). Mutation primer was synthesized by Boya Company. Anti-HO-1 antibody, RNase and DNase were purchased from Sigma. Restriction endonucleases were from Haojia Company, Q-Sepharose Fast Flow Anion exchange column was from Amersham Pharmacia. pBS II KS+/-, pGEM3Z and *E. coli* strain DH5α were stored in author's laboratory.

Methods

Structure analysis of hHO-1 and its mutant Swiss-PdbViewer and Antheprot 5.0 were used to analyze the structure diversity and physical-chemical changes between whHO-1 and △hHO-1. Then the prime structure was refined by energy minimization. Gromos96 was used as force field. The molecular surfaces and electrostatic potential were calculated. The rationality of the resulted model was validated by Ramachandran plot.

Construction of △hHO-1 expression vector pBHO-1 (M) *Eco*RI/*Sal*I digested fragment of pBHO-1, which is from expression vector containing the truncated hHO-1 cDNA (804 bp), was cloned into the *Eco*RI/*Sal*I sites of plasmid pBSKS II to construct plasmid pBSHO-1. hHO-1 His25Ala mutant cDNA could be amplified by PCR using pBSHO-1 as template. The mutation primer (5'-GACAGCATGCCCCAGGATTTGTCAG AGGCCCTGAAGGAGGCCACCAAGGAGGTGGCCACCC-3') and reverse primer (5'-AACAGCTATGACCATG-3') were chosen, which have changed the His 25 codon CAC into Ala codon GCC. The reaction conditions were: at 94 °C for 5 min, followed by 94 °C for 1 min, at 55 °C for 1 min, 72 °C for 2 min, with amplification repeated for 30 cycles, and finally at 72 °C for 10 min. The mutant cDNA was gel-purified and digested with *Sph*I/*Sal*I and then cloned into *Sph*I/*Sal*I sites of plasmid pGEM3Z. hHO-1 His25Ala mutant cDNA was screened by restriction digestion and confirmed by sequencing in pGEM3ZHO-1(M). Verified hHO-1 mutant cDNA was obtained from *Sph*I/*Sal*I digested fragment of pGEM3ZHO-1 (M) and then cloned into pBHO-1, thus the expression vector containing △hHO-1 was designated as pBHO-1 (M) (Figure 1).

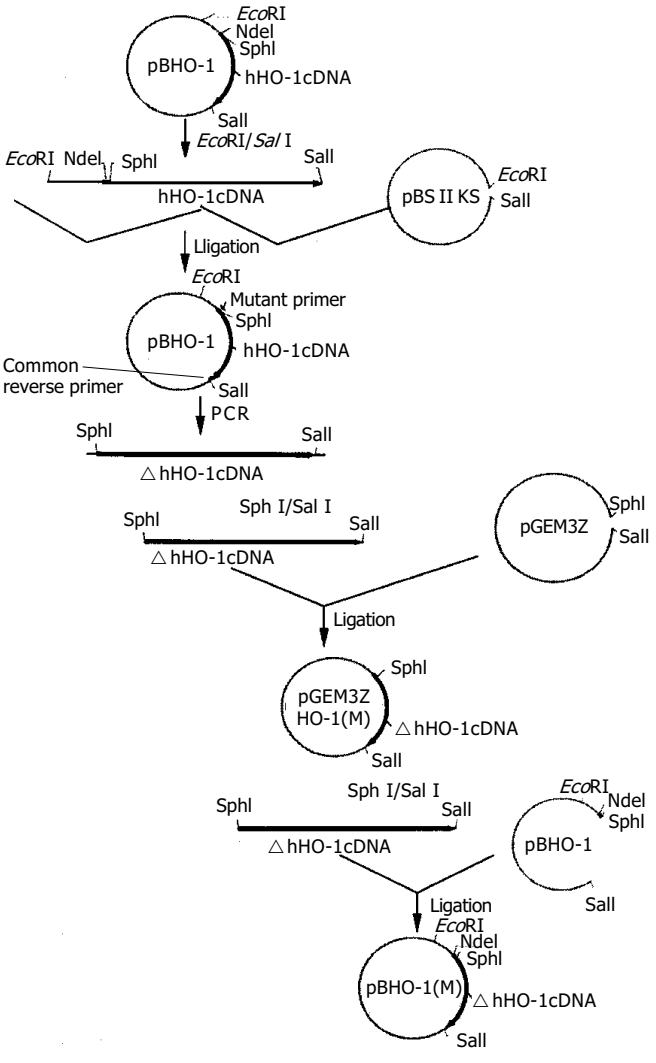

Figure 1 Construction of expression vector pBHO-1(M).

Expression and purification of whHO-1 and △hHO-1 A total of 5.0 mL inoculum was set up from plates with fresh colonies of transformed *E. coli* DH5α and incubated at 37 °C for 12-16 h. From the fresh cultures 400 μL was used to inoculate into 40 mL cultures of the same media. The cells were grown at 37 °C until A_{600} reached 0.3-0.5, then added with 0.5 mmol/L IPTG for 18 h. The expression products were harvested and analyzed with sodium dodecyl sulfate-polyacrylamide gel (SDS-PAGE) and Western blotting at the time points of 7, 9 and 11 h, respectively, after addition of IPTG. Then 500 mL inoculum in medium was incubated under same condition. The harvested cells were centrifuged at 6 000 r/min for 20 min at 4 °C, washed once in PBS, and then centrifuged at 6 000 r/min for 10 min at 4 °C. The cells were lysed in 50 mmol/L Tris buffer (pH 8.0) containing 1 mmol/L dithiothreitol, 1 mmol/L EDTA, 1 mmol/L phenylmethanesulfonyl fluoride (PMSF) and sonicated for 10 min. Then the cells were centrifuged at 13 000 r/min for 1 h at 4 °C. The supernatant was collected and ammonium sulfate was added to a final concentration of 30%, and the solution was stirred for 60 min. Following centrifugation (13 000 r/min for 20 min), ammonium sulfate concentration was raised to 60% of saturation. The pellets precipitated by ammonium sulfate were collected and resuspended in 0.1 mol/L potassium phosphate (pH 7.4) and then dialyzed against 1 g/L NH_4HCO_3 for 4 h (×4-times). Protein 130 mg was applied to a Q-Sepharose Fast Flow anion column and eluted with a step gradient of 50 mmol/L Tris-HCl (pH 7.4) (buffer A) containing 0-0.5 mol/L NaCl (buffer B). The fractions containing hHO-1 protein were pooled together and applied to Q-Sepharose Fast Flow anion column again. The protein was eluted with a step gradient of 50 mmol/L Tris-HCl (pH 8.4) (buffer C) containing 0-0.5 mol/L NaCl (buffer B). The gradient was increased linearly from 0-100% buffer B. Fractions containing hHO-1 protein were pooled and dialyzed against 1 g/L NH_4HCO_3 for 4 h (×4 times).

Western blotting Blot analysis was carried out as previously described[29]. Microsomal protein samples were fractionated by SDS-PAGE under denaturing conditions. The separated proteins were electrophoretically transferred to a nitrocellulose membrane. Western blotting was carried out using monoclonal antibody to hHO-1 and the immunoreactive bands were visualized by staining (1 mol/L Tris-HCl pH 9.5, 1 mol/L $MgCl_2$, 0.1 mg/mL nitro-blue tetrazolium, 0.1 mg/mL 5-bomo-4-chloro-3-indolyphosphate-toluidine salt).

Analysis of whHO-1 and △hHO-1 activities Protein samples were incubated with heme (50 μmol/L), rat liver cytosol (5 mg/mL), $MgCl_2$ (2 mmol/L), glucose-6-phosphate dehydrogenase (1 unit), glucose-6-phosphate (2 mmol/L), and NADPH (0.8 mmol/L) in 0.5 mL of 0.1 mol/L potassium phosphate buffer (pH 7.4), for 60 min at 37 °C. Reaction was stopped by putting the tubes on ice, and reaction solution was extracted with chloroform. The rate of bilirubin formation was monitored at 464 nm by a spectrophotometer and then calculated using an extinction coefficient of 40.0 mmoL/(L.cm)[29].

RESULTS

Whole structure comparison between whHO-1 and △hHO-1

In heme-heme oxygenase-1 complex, heme is sandwiched in whHO-1. When Ala 25 replaces His 25, the complex structure does not change. In the heme-binding pocket, Ala 25 loses contacting with heme as His 25 does. The molecular surface has a catalytic reaction pocket, which includes Thr 21, His 25, Ala 28, Glu 29, Gly 139, Asp140, Gly 143. After binding heme, His 25 still lies on the surface but Gly139, Asp140 and Gly143 are covered by heme. When Ala 25 replaces His 25, Ala 25 still lies in the surface (Figure 2). In activity domain, the bond angle, dihedral angle and chemical bond appear differently after Ala 25 replacing His 25 (Table 1, Figure 3).

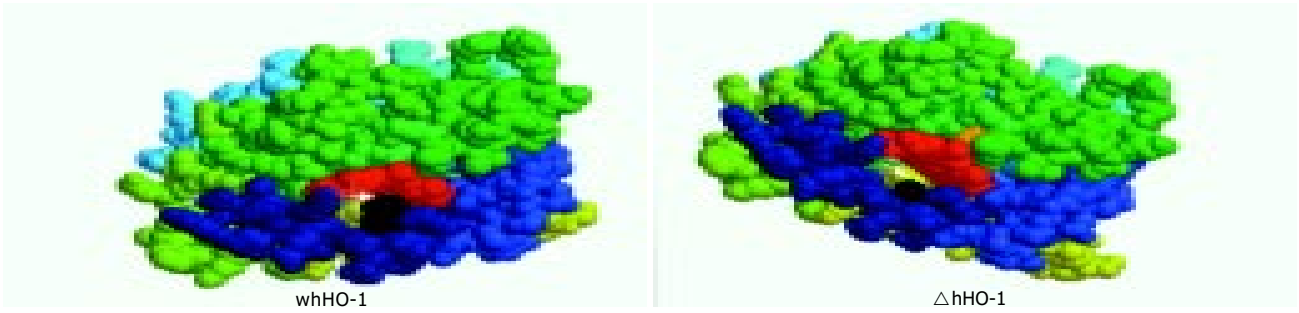

Figure 2 Prime simulated structure of whHO-1 and △hHO-1. Red: heme; Black: His 25 and Ala 25. Ala 25 loses contacting with heme as His 25 does in the heme-binding pocket.

Figure 3 Changes of bond angle, dihedral angle and chemical bond.

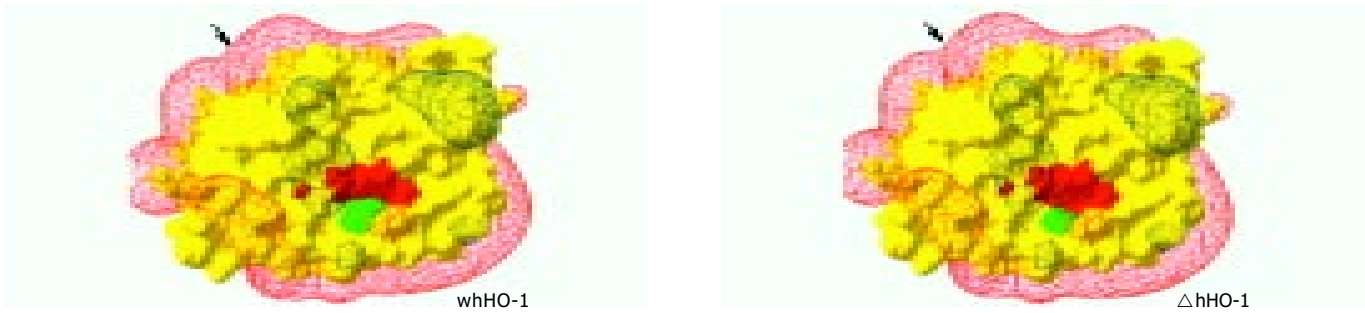

Figure 4 Molecular surfaces and electrostatic potential of whHO-1 and △hHO-1. The electrostatic potential of active pocket is –1.800.

Table 1 Bond angle, dihedral angle and the distance between atoms of △hHO-1

		Prime simulation	Optimized simulation
Bond angle	C24-N-CA	119.12	121.79
	CA-C-N26	115.92	115.12
Distance	CB-FE	5.55	5.58
between atoms	CA-FE	6.28	6.26
Dihedral angle	ω	175.40	175.61
	φ	-40.78	-34.45
	ψ	-60.70	-62.89

Though Ala 25 replaces His 25, the molecular surfaces and electrostatic potential changed little (Figure 4). The electrostatic potential of active pocket was still negative. The mutagenesis had no apparent effect on molecular surface. Ramachandran plot showed that dihedral angles φ (-33.98) and ψ (-64.46) were in rational range.

Antheprot 5.0 analysis also showed that there was no alteration in the secondary structure between whHO-1 and △hHO-1. Garnier, Gibrat, DPM and homology predicted the same results. Physical-chemical characteristics showed somewhat alteration. Hydrophobicity increased, while hydrophilicity decreased. There was no change in antigenicity, helical membranous regions and solvent accessibility.

Construction of pBHO-1(M) containing △hHO-1

hHO-1 cDNA was site mutated at His 25 (to Ala) by PCR with pBSHO-1 as the template. The 866-bp PCR product showed that nucleotide 3-773 sequences encoded hHO-1 domain from 25-265 AA. The mutant cDNA was cloned into the *Sph*I/*Sal*I sites of plasmid pGEM3Z for constructing plasmid pGEM3ZHO-1 (M). hHO-1 His25Ala mutant cDNA was confirmed by sequencing in pGEM3ZHO-1(M). The verified hHO-1 mutant cDNA from the *SphI*/*Sal*I digested fragment of pGEM3ZHO-1 (M) was cloned into pBHO-1, thus the expression vector containing △hHO-1 was designated as pBHO-1 (M) (Figure1). Both whHO-1 and △hHO-1 cDNAs equally encoded the proteins containing 265 amino acids with a M_r 30 500.

Expression and identification of whHO-1 and △hHO-1 in E.coli DH5α

E.coli DH5α was transformed by pBHO-1 and pBHO-1 (M), respectively, and treated with 0.5 mmol/L IPTG for 18 h at 37 . Equal quantities of cells transformed with different expression vectors were lysed by protein electrophoresis buffer. Untransformed *E.coli* sample was used as the negative control. As shown in Figure 5, *E.coli* DH5α transformed pBHO-1 or pBHO-1 (M) highly expressed whHO-1 and △hHO-1 with a M_r 30 500. Meanwhile, *E. coli* DH5α not treated with IPTG also expressed whHO-1 and △hHO-1, but its expression yield

was significantly lower than that of transformed cells. Analysis of cell lysates showed that whHO-1 and △hHO-1 were mainly present in the supernatants.

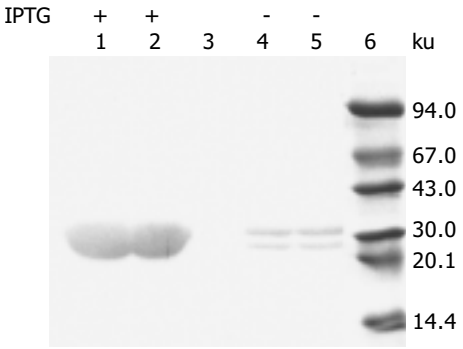

Figure 5 Western blotting of whHO-1 and △hHO-1 expressed in DH5α. Lanes 1, 2: Expression products of pBHO-1 and pBHO-1(M) in DH5α induced with IPTG; lane 3: Control; lanes 4, 5: Expression products of pBHO-1 and pBHO-1(M) in DH5α not treated with IPTG; lane 6: Marker.

Purification of whHO-1 and △hHO-1

The protein with a M_r 30 500 was purified by 30-60% ammonium sulphate precipitation and analyzed by SDS-PAGE.

After precipitated with ammonium sulphate, whHO-1 sample was applied to Q-Sepharose Fast Flow anion column (pH 7.4). The first peak containing whHO-1 (No. 1-3 tubes) was collected (Figure 6A) and loaded on Q-Sepharose Fast Flow anion column (pH 8.4) again. whHO-1 was shown to be eluted in the second peak (No. 49-63 tubes) (Figure 6B). All samples were analyzed by SDS-PAGE and Western blotting in order to identify the separation efficiency. The activity of whHO-1 after purification was 30-fold higher than that in the initial lysates (Table 2).

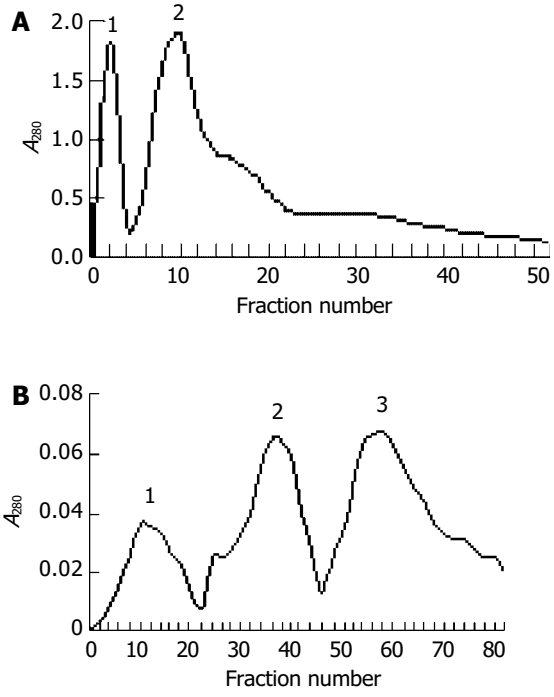

Figure 6 Q-Sepharose Fast Flow column chromatography. A: pH 7.4 buffer; B: pH 8.4 buffer.

Precipitated △hHO-1 was further purified in the same way as described above. One purified protein's M_r was 30 500. The purified whHO-1 and △hHO-1 are shown on SDS-PAGE (Figure 7).

Table 2 whHO-1 activities after different purification

	Supernatant of DH5α lysates	30-60% $(NH_4)_2SO_4$	Q-Sepharose fast flow
whHO-1 activity ($U \cdot mg^{-1} \cdot h^{-1}$)	0.5	1.8	15
Purification fold	1.0	3.6	30

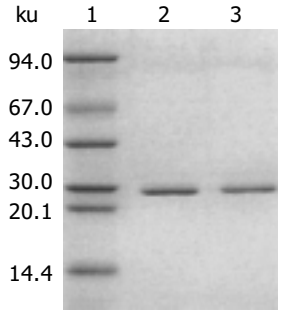

Figure 7 SDS-PAGE analysis of purified whHO-1 and △hHO-1. Lane 1: Marker; lane 2: whHO-1; lane 3: △hHO-1.

DISCUSSION

An understanding of the structure and function of hHO-1 is of importance in the context of human diseases, but due to limited accessibility and difficulties associated with their purification from microsomal membranes, little direct information has been available until the expression of rHO-1 in *E. coli* was achieved. The protein thus obtained is soluble, easily purified, and fully active. Encouraged by this result, the research on HO-1 including hHO-1 has been thriving.

hHO-1 is anchored to the endoplasmic reticulum membrane via a stretch of hydrophobic residues at the C-terminus. While full-length hHO-1 consists of 288 residues, a truncated version with residues 1-265 has been expressed as a soluble active enzyme in *E. coli*. This recombinant enzyme precipitated from ammonium sulfate solution but without a high purity for studies[30].

In the present studies, we acquired the structures of hHO-1 with residues 1-265 and its mutant using Swiss-PdbViewer. Due to the high similarity between hHO-1 and its mutant, the hHO-1 structure was used as template. Through homology modeling, template selection and target-template alignment, a molecular backbone and side chains were built in one step. Results demonstrated that the refined model, as well as the entire assay, was valid. Predictions of the structure showed that hHO-1 and its mutant had similar electrostatic potential suggesting that they have similar affinity to heme in electrostatic potential. Ala is a hydrophobic amino acid without chemical activity, and its side chain is short. So it has no interference with binding through steric hindrance.

Rat His25Ala HO-1 provides a new approach to construct hHO-1 mutant. hHO-1 mutants were prepared in which residue His25 was replaced by Ala using site-directed mutagenesis to understand the role of hHO-1 His25 in keeping the activity of this enzyme. In this study, the synthesized forward primer was applied in which His25 codon was replaced by the Ala codon. This cDNA was cloned into the expression vector pBHO-1, then pBHO-1 and pBHO-1(M) were transformed into *E. coli*, which were used to express whHO-1 and △hHO-1. Although the endogenous protein expression of *E. coli* could disturb the measurement of whHO-1 and its mutants by SDS-PAGE, hHO-1 and its mutant expression could be detected by anti-HO-1 antibody in Western blotting.

Our study shows that precipitation with ammonium sulfate can enrich whHO-1 and △hHO-1 in the lysates. Compared with the whHO-1 activity, △hHO-1 activity was reduced by

91.21%. It suggests that His25 is crucial for the catalytic activity of whHO-1, the proximal His25 ligand is critically required for normal hHO-1 catalysis. The results are similar to previous reports[31-35].

hHO-1 has anti-inflammatory[6-9], antiapoptotic[10-17], and antiproliferative[18-25] effects, and salutary effects on neonatal hyperbilirubinemia[36]. The results show a valid way to control the concentration of bilirubin in human, since hHO-1 is the rate-limiting enzyme in the catabolic reaction of heme, which ultimately produces bilirubin in human body. High-level bilirubin in newborns, patients with the Crigler-Najjar type I syndrome and certain hepatic disorders can result in hyperbilirubinemia, especially in patients whose bilirubin is impaired for developmental or genetic reasons. Currently clinical methods are only to eliminate formed bilirubin. There is no effective way to inhibit bilirubin production, and △hHO-1 would be a potential inhibitor for bilirubin production.

REFERENCES

1 **Elbirt KK**, Bonkovsky HL. Heme oxygenase: recent advances in understanding its regulation and role. *Proc Assoc Am Physicians* 1999; **111**: 438-447
2 **Scapagnini G**, D'Agata V, Calabrese V, Pascale A, Colombrita C, Alkon D, Cavallaro S. Gene expression profiles of heme oxygenase isoforms in the rat brain. *Brain Res* 2002; **954**: 51-59
3 **Montellano PR**. The mechanism of heme oxygenase. *Curr Opin Chem Biol* 2000; **4**: 221-227
4 **Chu GC**, Katakura K, Zhang X, Yoshida T, Ikeda-Saito M. Heme degradation as catalyzed by a recombinant bacterial heme oxygenase (Hmu O) from Corynebacterium diphtheriae. *J Biol Chem* 1999; **274**: 21319-21325
5 **Immenschuh S**, Ramadori G. Gene regulation of heme oxygenase-1 as a therapeutic target. *Biochem Pharmacol* 2000; **60**: 1121-1128
6 **Kushida T**, Li Volti G, Quan S, Goodman A, Abraham NG. Role of human heme oxygenase-1 in attenuating TNF-alpha-mediated inflammation injury in endothelial cells. *J Cell Biochem* 2002; **87**: 377-385
7 **Alcaraz MJ**, Fernandez P, Guillen MI. Anti-inflammatory actions of the heme oxygenase-1 pathway. *Curr Pharm Des* 2003; **9**: 2541-2551
8 **Wagener FA**, van Beurden HE, von den Hoff JW, Adema GJ, Figdor CG. The heme-heme oxygenase system: a molecular switch in wound healing. *Blood* 2003; **102**: 521-528
9 **Chok Mk**, Senechal M, Dorent R, Mallat Z, Leprince P, Bonnet N, Pavie A, Ghossoub JJ, Gandjbakhch I. Apoptosis and expression of heme oxygenase-1 in heart transplant recipients during acute rejection episodes. *Transplant Proc* 2002; **34**: 3239-3240
10 **Rothfuss A**, Speit G. Overexpression of heme oxygenase-1 (HO-1) in V79 cells results in increased resistance to hyperbaric oxygen (HBO)-induced DNA damage. *Environ Mol Mutagen* 2002; **40**: 258-265
11 **Takata K**, Kitamura Y, Kakimura J, Shibagaki K, Taniguchi T, Gebicke-Haerter PJ, Smith MA, Perry G, Shimohama S. Possible protective mechanisms of heme oxygenase-1 in the brain. *Ann N Y Acad Sci* 2002; **977**: 501-506
12 **Katori M**, Busuttil RW, Kupiec-Weglinski JW. Heme oxygenase-1 system in organ transplantation. *Transplantation* 2002; **74**: 905-912
13 **Cornelussen RN**, Knowlton AA. Heme-oxygenase-1: versatile sentinel against injury. *J Mol Cell Cardiol* 2002; **34**: 1297-1300
14 **Ke B**, Shen XD, Zhai Y, Gao F, Busuttil RW, Volk HD, Kupiec-Weglinski JW. Heme oxygenase 1 mediates the immunomodulatory and antiapoptotic effects of interleukin 13 gene therapy *in vivo* and *in vitro*. *Hum Gene Ther* 2002; **13**: 1845-1857
15 **Abraham NG**, Kushida T, McClung J, Weiss M, Quan S, Lafaro R, Darzynkiewicz Z, Wolin M. Heme oxygenase-1 attenuates glucose-mediated cell growth arrest and apoptosis in human microvessel endothelial cells. *Circ Res* 2003; **93**: 507-514
16 **Colombrita C**, Lombardo G, Scapagnini G, Abraham NG. Heme oxygenase-1 expression levels are cell cycle dependent. *Biochem Biophys Res Commun* 2003; **308**: 1001-1008
17 **Pandya HC**, Snetkov VA, Twort CH, Ward JP, Hirst SJ. Oxygen regulates mitogen-stimulated proliferation of fetal human airway smooth muscle cells. *Am J Physiol Lung Cell Mol Physiol* 2002; **283**: L1220-1230
18 **Perrella MA**, Yet SF. Role of heme oxygenase-1 in cardiovascular function. *Curr Pharm Des* 2003; **9**: 2479-2487
19 **Morse D**. The role of heme oxygenase-1 in pulmonary fibrosis. *Am J Respir Cell Mol Biol* 2003; **29**(3 Suppl): S82-86
20 **Stanford SJ**, Walters MJ, Hislop AA, Haworth SG, Evans TW, Mann BE, Motterlini R, Mitchell JA. Heme oxygenase is expressed in human pulmonary artery smooth muscle where carbon monoxide has an anti-proliferative role. *Eur J Pharmacol* 2003; **473**: 135-141
21 **Li L**, Grenard P, Nhieu JT, Julien B, Mallat A, Habib A, Lotersztajn S. Heme oxygenase-1 is an antifibrogenic protein in human hepatic myofibroblasts. *Gastroenterology* 2003; **125**: 460-469
22 **Bauer I**, Rensing H, Florax A, Ulrich C, Pistorius G, Redl H, Bauer M. Expression pattern and regulation of heme oxygenase-1/heat shock protein 32 in human liver cells. *Shock* 2003; **20**: 116-122
23 **Hancock WW**, Buelow R, Sayegh MH, Turka LA. Antibody-induced transplant arteriosclerosis is prevented by graft expression of anti-oxidant and anti-apoptotic genes. *Nat Med* 1998; **4**: 1392-1396
24 **Zhang M**, Zhang BH, Chen L, An W. Overexpression of heme oxygenase-1 protects smooth muscle cells against oxidative injury and inhibits cell proliferation. *Cell Res* 2002; **12**: 123-132
25 **Soares MP**, Lin Y, Anrather J, Csizmadia E, Takigami K, Sato K, Grey ST, Colvin RB, Choi AM, Poss KD, Bach FH. Expression of heme oxygenase-1 can determine cardiac xenograft survival. *Nat Med* 1998; **4**: 1073-1077
26 **Liu Y**, Moenne-Loccoz P, Hildebrand DP, Wilks A, Loehr TM, Mauk AG, Ortiz de Montellano PR. Replacement of the proximal histidine iron ligand by a cysteine or tyrosine converts heme oxygenase to an oxidase. *Biochemistry* 1999; **38**: 3733-3743
27 **Ito-Maki M**, Ishikawa K, Matera KM, Sato M, Ikeda-Saito M, Yoshida T. Demonstration that histidine 25, but not 132, is the axial heme ligand in rat heme oxygenase-1. *Arch Biochem Biophys* 1995; **317**: 253-258
28 **Schuller DJ**, Wilks A, Ortiz de Montellano PR, Poulos TL. Crystal structure of human heme oxygenase-1. *Nat Struct Biol* 1999; **6**: 860-867
29 **Xia Z**, Shao J, Shen Q, Wang J, Li Y, Chen S, Yu S. The preparation of rat heme oxygenase-1 mutant to reduce the level of bilirubin. *Chin Med J* 2001; **114**: 348-351
30 **Schuller DJ**, Wilks A, Ortiz de Montellano P, Poulos TL. Crystallization of recombinant human heme oxygenase-1. *Protein Sci* 1998; **7**: 1836-1838
31 **Auclair K**, Moenne-Loccoz P, Ortiz de Montellano PR. Roles of the proximal heme thiolate ligand in cytochrome p450 (cam). *J Am Chem Soc* 2001; **123**: 4877-4885
32 **Wilk A**, Medzihradsky KF, Ortiz de Montellano PR. Heme oxygenase active-site residues identified by heme-protein cross-linking during reduction of CBrC13. *Biochemistry* 1998; **37**: 2889-2896
33 **Lad L**, Schuller DJ, Shimizu H, Friedman J, Li H, Ortiz de Montellano PR, Poulos TL. Comparison of the heme-free and -bound crystal structures of human heme oxygenase-1. *J Biol Chem* 2003; **278**: 7834-7843
34 **Foresti R**, Motterlini R. The heme oxygenase pathway and its interaction with nitric oxide in the control of cellular homeostasis. *Free Radic Res* 1999; **31**: 459-475
35 **Chang SH**, Barbosa-Tessmann I, Chen C, Kilberg MS, Agarwal A. Glucose deprivation induces heme oxygenase-1 gene expression by a pathway independent of the unfolded protein response. *J Biol Chem* 2002; **277**: 1933-1940
36 **Maines MD**. The heme oxygenase system: a regulator of second messenger gases. *Annu Rev Pharmacol Toxixol* 1997; **37**: 517-554

Edited by Chen WW and Zhu LH **Proofread by** Xu FM

PO Box 2345, Beijing 100023, China
Fax: +86-10-85381893
E-mail: wjg@wjgnet.com www.wjgnet.com

World J Gastroenterol 2004;10(16):2357-2360
World Journal of Gastroenterology
 ISSN 1007-9327

• BASIC RESEARCH •

Effect of SNPs in protein kinase *Cz* gene on gene expression in the reporter gene detection system

Zhuo Liu, Hong-Xia Sun, Yong-Wei Zhang, Yun-Feng Li, Jin Zuo, Yan Meng, Fu-De Fang

Zhuo Liu, Hong-Xia Sun, Yong-Wei Zhang, Yun-Feng Li, Jin Zuo, Yan Meng, Fu-De Fang, National Laboratory of Medical Molecular Biology, Institute of Basic Medical Sciences, Chinese Academy of Medical Sciences & Peking Union Medical College, Beijing 100005, China
Supported by the National High Technology Research and Development Program of China, No. 2002BA711A05, No. 2002BA711A10-02 and the National Natural Science Foundation of China, No. 30170441, No. 30370668 and the Natural Science Foundation of Beijing, No. 7032033 and the Foundation of Ministry of Education of China, No. 20030023020, No. 20010023024
Co-first-authors: Zhuo Liu and Yong-Wei Zhang
Co-correspondents: Yan Meng and Fu-De Fang
Correspondence to: Fu-De Fang, National Laboratory of Medical Molecular Biology, Institute of Basic Medical Sciences, Chinese Academy of Medical Sciences & Peking Union Medical College, Beijing 100005, China. fangfd@public3.bta.net.cn
Telephone: +86-10-65253005 **Fax:** +86-10-65253005
Received: 2003-12-10 **Accepted:** 2004-01-12

Abstract

AIM: To investigated the effects of the SNPs (rs411021, rs436045, rs427811, rs385039 and rs809912) on gene expression and further identify the susceptibility genes of type 2 diabetes.

METHODS: Ten allele fragments (49 bp each) were synthesized according to the 5 SNPs mentioned above. These fragments were cloned into luciferase reporter gene vector and then transfected into HepG2 cells. The activity of the luciferase was assayed. Effects of the SNPs on RNA splicing were analyzed by bioinformatics.

RESULTS: rs427811T allele and rs809912G allele enhanced the activity of the reporter gene expression. None of the 5 SNPs affected RNA splicing.

CONCLUSION: SNPs in protein kinase *Cz* (*PKCZ*) gene probably play a role in the susceptibility to type 2 diabetes by affecting the expression level of the relevant genes.

Liu Z, Sun HX, Zhang YW, Li YF, Zuo J, Meng Y, Fang FD. Effect of SNPs in protein kinase *Cz* gene on gene expression in the reporter gene detection system. *World J Gastroenterol* 2004; 10(16): 2357-2360
http://www.wjgnet.com/1007-9327/10/2357.asp

INTRODUCTION

Type 2 diabetes is a highly heterogeneous chronic disease characterized by metabolic disorder of blood glucose, its onset involves a number of susceptibility genes. Since 1996, locating and cloning the predisposing genes of type 2 diabetes, as well as the functional investigation, has become one of the hot spots worldwide in type 2 diabetes research. Based on genomic screening technology, it was reported firstly among Western population in succession that type 2 diabetes susceptibility genes located on different chromosomes[1-23]. The susceptibility genes were localized on chromosome 9 in Chinese population[24]. According to the case-control analysis in the region of 1p36.33-1p36.23, our research group found that one SNP locus, rs436045 in protein kinase *Cz* (*PKCZ*) gene, was linked to type 2 diabetes in Chinese population, and the haplotype block has been identified. While analyzing the haplotype which consists of the 5 SNPs (rs411021, rs436045, rs427811, rs385039, rs809912), we noticed that, in the case group, the haplotype CGTAG showed a significantly higher frequency than that in control group, whereas the frequency of haplotype TAGGA decreased significantly ($P<0.01$, OR = 1.625), it implied that the changes of those haplotypes related to the onset of type 2 diabetes in Chinese[25]. However, it is still unclear weather haplotypes play a role during the episode of the disease.

To determine the biological function of those haplotypes, we investigated their influence on gene expression by bioinformatics approach and reporter gene activity determination system, which would provide a basis for further research.

In the previous work, we found that the 5 SNPs at the introns of *PKCZ* gene located in the same haplotype block in case group, and the haplotype they formed was clearly associated with type 2 diabetes mellitus. In order to determine the susceptibility loci associated with type 2 diabetes, we performed functional analysis on 5 SNPs.

MATERIALS AND METHODS

Identification of SNPs in the coding region of PKCZ gene

Coding region (from exon 4 to exon 13 or from rs1878745 to rs262642) of *PKCZ* gene was investigated for SNPs (cSNP) by sequencing. Ten unrelated type 2 diabetic patients and 10 control subjects from Han population in China were enrolled in a case-control study. Primers were designed by Primer 3.0 program (http://zeno.well.ox.ac.uk:8080/gitbin/ primer3_www.cgi) and each PCR product was limited within about 500 base pairs. The sequencing results from ABI377 sequencer were analyzed through PhredPhrap/consed program to identify functional SNPs.

Analysis of the effect of 5 intron SNPs on mRNA splicing

The distance from the SNP to the splicing point in exon was determined based on the published genome sequence. According to this information, we preliminarily estimated whether the SNP site influences gene splicing.

Search of the information on PKC family member

The location and sequence of other PKC family members were obtained by means of bioinformatics. Then, different spliceosomes from other family members residing in the sequence of *PKCZ* were analyzed.

Analysis of the introns where 5 SNPs located

Each SNP and the intron sequence around the loci were compared with the data in cDNA database (www.sanbi.ac.za) to reveal the sequence homology. The open reading frames in this sequence were analyzed, and then the amino acid was

blast using the (www.ncbi.nlm.nih.gov) protein database in search of the sequence homology.

Effects of SNPs on gene expression by transient transfection

Ten alleles corresponding to the 5 SNPs in *PKCZ* gene were cloned into pGL3-promoter vector in the direction from 5' to 3' (Table 1). Meanwhile, HepG2 cells were cultured with DMEM (Gibco, LOS angeles, USA) containing 100 mL/L fetal bovine serum. Then, the cells (1.5×10^5-2×10^5) were transfected with pGL3-promoter vector (1 uL) or recombinant vector with Lipofectamine transfection reagent (Promega, madison, USA). The transfection rate was assayed by using pRL-SV40 DNA (100 ng, Promega, madison, USA) as an internal control. Forty-eight hours post transfection, the luciferase activity was determined by the Dual-Luciferase® Reporter Assay System using pRL-SV40 as an internal control.

Table 1 Sequence of ten 49-bp fragments containing each allele of 5 SNPs

Fragment name	Sequence
rs809912G-forward	5' ggggtaccccagccatcctccacc c gcccattctccatcc 3'
rs809912G-reverse	3' gtcggtaggaggtgg g cgggtaagaggtaggttctagaag 5'
rs809912A-forward	5' ggggtaccccagccatcctccacc t gcccattctccatcc 3'
rs809912A-reverse	3' ggggtaccccagccatcctccacc a gcccattctccatcc 5'
rs436045A-forward	5' ggggtacccagcagtgcctgtcag a tttggtccaagcagt 3'
rs436045A-reverse	3' tcgtcacggacagtc t aaaccaggttcgtcactctagaag 5'
rs436045G-forward	5' ggggtacccagcagtgcctgtcag g tttggtccaagcagt 3'
rs436045G-reverse	3' tcgtcacggacagtc c aaaccaggttcgtcactctagaag 5'
rs427811T-forward	5' ggggtaccgctcagtgtcctcttt t gagaaggtataggtg 3'
rs427811T-reverse	3' gagtcacaggagaaa a ctcttccatatccacatctagaag 5'
rs427811G-forward	5' ggggtaccgctcagtgtcctcttt g gagaaggtacaggtg 3'
rs427811G-reverse	3' gagtcacaggagaaa c ctcttccatgtccacatctagaag 5'
rs385039G-forward	5' ggggtacctgtttacagaagctac g ttgtaacacctgctc 3'
rs385039G-reverse	3' caaatgtcttcgatg c aacattgtggacgagatctagaag 5'
rs385039A-forward	5' ggggtacctgtttacagaagctac a ttgtaacacctgctc 3'
rs385039A-reverse	3' caaatgtcttcgatg t aacattgtggacgagatctagaag 5'
rs411021C-forward	5' ggggtaccgggggttgcggtgagc c gagattgtgccactg 3'
rs411021C-reverse	3' ccccaacgccactcg g ctctaacacggtgacctctagaag 5'
rs411021T-forward	5' ggggtaccgggggttgcggtgagc t gagattgtgccactg 3'
rs411021T-reverse	3' ccccaacgccactcg a ctctaacacggtgacctctagaag 5'

RESULTS

SNPs in the coding region of PKCZ gene

While seeking for functional SNPs by sequencing the exons around the 13 intron SNPs discovered in the previous work, we found no new ones except for the rs1878745 corresponding to NCBI database. It suggested that the disease loci probably did not exist in the coding region.

Influence of positive SNP on the PKCZ gene expression

To locate the disease SNP, we investigated the effect of the 5 positive SNPs (rs411021, rs436045, rs427811, rs385039, and rs809912) lying in the same haplotype block on *PKCZ* gene expression. The influence of the 5 SNPs over RNA splicing was evaluated since all the 5 SNPs lay in the introns. The distance of the SNPs from the upstream and downstream of the splicing site are respectively as the following: rs411021 (3 535 bp, 5 283 bp), rs436045 (4 770 bp, 4 048 bp), rs427811 (8 729 bp, 89 bp), rs385039 (1 629 bp, 57 bp), and rs809912 (>2 kb, 2 057 bp). Those are comparatively long distant to 5' splice donor site, 3' receptor site and the internal vertex, suggesting that they have little association with pre-mRNA splicing. In addition, we estimated if differential splicing occurs between *PKCZ* gene and other PKC family members. Although there are at least 11 family members besides *PKCZ*, none of them locate on chromosome 1, which negates the 'differential splicing supposition'. The location of introns where 5 SNPs located was analyzed. As a first step, we compared the intron sequence around the loci of each of the 5 SNPs with the data in cDNA database (www.sanbi.ac.za) in order to reveal the sequence homology. Result showed that the introns had no coding function because neither cDNA sequence homology nor protein sequence homology by ORF analysis was found. But this result needs to be further confirmed by Northern blotting. And finally, the effects of the SNPs on gene expression were investigated. Transfected HepG2 cell containing pGL3-promoter reporter gene vector was used to detect the activity of the reporter gene that could reflect indirectly whether the fragment inserted affected gene expression. Statistical analysis showed a significant difference between the two SNPs of rs4278111 and rs809912. In rs4278111, the reporter gene activity of T allele was 1.5 times that of the G allele, while in rs809912, in G allele it was 1.7 times that of A allele (Table 2). Therefore, these two SNPs will probably affect the expression level of *PKCZ* gene.

Table 2 Transcriptional regulatory activity of each construct of PKCZ in HepG2 cells

Construct	Relative luciferase activity	*P*
pGL3-promoter	0.3533±0.040	
pGL3-rs411021C	0.5167±0.064	
pGL3-rs411021T	0.5100±0.102	0.928
pGL3-rs436045A	0.3433±0.051	
pGL3-rs436045G	0.3767±0.023	0.363
pGL3-rs427811T	0.6233±0.064[a]	
pGL3-rs427811G	0.4433±0.068	0.029
pGL3-rs385039A	0.3500±0.044	
pGL3-rs385039G	0.3467±0.015	0.907
pGL3-rs809912A	0.1800±0.017[a]	
pGL3-rs809912G	0.3033±0.042	0.009

[a]$P<0.05$ in comparison between construct and pGL3-promoter vector.

DISCUSSION

PKCZ is a member of serine/threonine protein kinase family, belonging to atypical PKC, and independent of both calcium and diacylglycerol (DAG)[26]. It is insensitive to PKC inhibitors and cannot be activated by phorbol ester. *PKCZ* protein is thought to function downstream of phosphatidylinositol 3-kinase (PI 3-kinase) in insulin signaling pathway and plays a role in promoting the translocation and activation of GluT4 from the cytosol to membranes which will accelerate the glucose transport in skeletal muscle and adipocytes[27-30]. In addition, *PKCZ* can induce negative feedback to the signaling pathway through phosphorylating IRS-1[31,32]. Insulin-stimulated glucose transport is defective in type 2 diabetes mellitus, and this defect can be ameliorated via correcting PRKC-zeta/lambda activation defect[33], suggesting that the transport deficiency is at least partly associated with the activation defect of *PKCZ*. Our previous research showed that *PKCZ* is related to susceptibility to type 2 diabetes mellitus in Chinese population. If so, whether genetic polymorphism of *PKCZ* gene will influence the pathways associated with blood glucose regulation by affecting its gene expression, and increase the susceptibility to this disease ultimately? Based on bioinformatics research and reporter gene activity determination system, our data provide first evidence that intron SNP loci in *PKCZ* gene affect gene expression. Horikawa[34] has reported that gene expression was under the influence of the 3 intron SNPs in *CAPN10* gene, the

susceptibility gene of type 2 diabetes in Mexican American. Such kind of result was also reported by other groups, for example, an SNP in *COL1N1* gene can change the binding site of transcription factor Sp1 thereby influencing the gene expression, resulting in the decline of bone density as well as osteoporosis[35].

In our experiment, we found the two alleles (rs427811T and rs809912G) that had a relatively high frequency in type 2 diabetic patients could improve the reporter gene expression, apparently in conflict with our predicted result. This phenomenon might be explained by the hypothesis that *PKCZ* gene was involved in other signaling pathways and its relation to the disease was more complicated than we had estimated. Till now, there have been no reports that *PKCZ* gene expression is changed in the tissues of type 2 diabetic patients. But PED/PEA-15, a substrate of PKC, was reported to increase *PKCZ* gene expression in the patient's tissues[36], which inhibited insulin stimulated glucose transportation. Thus, the high expression of PED/PEA-15 gene probably plays a role in insulin resistance of type 2 diabetes. Our next goals are to determine whether *PKCZ* interacts with PED/PEA-15 in insulin signaling pathway, and whether PED/PEA-15 or its analogue is involved in the inhibition of the insulin stimulated glucose transport via another signal pathway.

REFERENCES

1 **Hanis CL**, Boerwinkle E, Chakraborty R, Ellsworth DL, Concannon P, Stirling B, Morrison VA, Wapelhorst B, Spielman RS, Gogolin-Ewens KJ. A genome-wide search for human non-insulin-dependent (type 2) diabetes genes reveals a major susceptibility locus on chromosome 2. *Nat Genet* 1996; **13**: 161-166

2 **Mahtani MM**, Widen E, Lehto M, Thomas J, McCarthy M, Brayer J, Bryant B, Chan G, Daly M, Forsblom C, Kanninen T, Kirby A, Kruglyak L, Munnelly K, Parkkonen M, Reeve-Daly MP, Weaver A, Brettin T, Duyk G, Lander ES, Groop LC. Mapping of a gene for type 2 diabetes associated with an insulin secretion defect by a genome scan in Finnish families. *Nat Genet* 1996; **14**: 90-94

3 **Ghosh S**, Watanabe RM, Hauser ER, Valle T, Magnuson VL, Erdos MR, Langefeld CD, Balow J Jr, Ally DS, Kohtamaki K. Type 2 diabetes: evidence for linkage on chromosome 20 in 716 Finnish affected sib pairs. *Proc Natl Acad Sci U S A* 1999; **96**: 2198-2203

4 **Vionnet N**, Hani El H, Dupont S, Gallina S, Francke S, Dotte S, De Matos F, Durand E, Lepretre F, Lecoeur C, Gallina P, Zekiri L, Dina C, Froguel P. Genomewide search for type 2 diabetes-susceptibility genes in French whites: evidence for a novel susceptibility locus for early-onset diabetes on chromosome 3q27-qter and independent replication of a type 2-diabetes locus on chromosome 1q21-q24. *Am J Hum Genet* 2000; **67**: 1470-1480

5 **Elbein SC**, Hoffman MD, Teng K, Leppert MF, Hasstedt SJ. A genome-wide search for type 2 diabetes susceptibility genes in Utah Caucasians. *Diabetes* 1999; **48**: 1175-1182

6 **Watanabe RM**, Ghosh S, Langefeld CD, Valle TT, Hauser ER, Magnuson VL, Mohlke KL, Silander K, Ally DS. The Finland-United States investigation of non-insulin-dependent diabetes mellitus genetics (FUSION) study. II. An autosomal genome scan for diabetes-related quantitative-trait loci. *Am J Hum Genet* 2000; **67**: 1186-1200

7 **Wiltshire S**, Hattersley AT, Hitman GA, Walker M, Levy JC, Sampson M, O'Rahilly S, Frayling TM, Bell JI, Lathrop GM, Bennett A, Dhillon R, Fletcher C, Groves CJ, Jones E, Prestwich P, Simecek N, Rao PV, Wishart M, Bottazzo GF, Foxon R, Howell S, Smedley D, Cardon LR, Menzel S, McCarthy MI. A genomewide scan for loci predisposing to type 2 diabetes in a U.K. population (the Diabetes UK Warren 2 Repository): analysis of 573 pedigrees provides independent replication of a susceptibility locus on chromosome 1q. *Am J Hum Genet* 2001; **69**: 553-569

8 **Permutt MA**, Wasson JC, Suarez BK, Lin J, Thomas J, Meyer J, Lewitzky S, Rennich JS, Parker A, DuPrat L, Maruti S, Chayen S, Glaser B. A genome scan for type 2 diabetes susceptibility loci in a genetically isolated population. *Diabetes* 2001; **50**: 681-685

9 **Lindgren CM**, Mahtani MM, Widen E, McCarthy MI, Daly MJ, Kirby A, Reeve MP, Kruglyak L, Parker A, Meyer J, Almgren P, Lehto M, Kanninen T, Tuomi T, Groop LC, Lander ES. Genomewide search for type 2 diabetes mellitus susceptibility loci in Finnish families: the Botnia study. *Am J Hum Genet* 2002; **70**: 509-516

10 **Busfield F**, Duffy DL, Kesting JB, Walker SM, Lovelock PK, Good D, Tate H, Watego D, Marczak M, Hayman N, Shaw JTE. A genomewide search for type 2 diabetes-susceptibility genes in indigenous Australians. *Am J Hum Genet* 2002; **70**: 349-357

11 **Demenais F**, Kanninen T, Lindgren CM, Wiltshire S, Gaget S, Dandrieux C, Almgren P, Sjogren M, Hattersley A, Dina C, Tuomi T, McCarthy MI, Froguel P, Groop LC. A meta-analysis of four European genome screens (GIFT Consortium) shows evidence for a novel region on chromosome 17p11.2-q22 linked to type 2 diabetes. *Hum Mol Genet* 2003; **12**: 1865-1873

12 **Lakka TA**, Rankinen T, Weisnagel SJ, Chagnon YC, Rice T, Leon AS, Skinner JS, Wilmore JH, Rao DC, Bouchard C. A quantitative trait locus on 7q31 for the changes in plasma insulin in response to exercise training: the HERITAGE Family Study. *Diabetes* 2003; **52**: 1583-1587

13 **Daimon M**, Ji G, Saitoh T, Oizumi T, Tominaga M, Nakamura T, Ishii K, Matsuura T, Inageda K, Matsumine H, Kido T, Htay L, Kamatani N, Muramatsu M, Kato T. Large-scale search of SNPs for type 2 DM susceptibility genes in a Japanese population. *Biochem Biophys Res Commun* 2003; **302**: 751-758

14 **Laivuori H**, Lahermo P, Ollikainen V, Widen E, Haiva-Mallinen L, Sundstrom H, Laitinen T, Kaaja R, Ylikorkala O, Kere J. Susceptibility loci for preeclampsia on chromosomes 2p25 and 9p13 in Finnish families. *Am J Hum Genet* 2003; **72**: 168-177

15 **Thameem F**, Yang X, Permana PA, Wolford JK, Bogardus C, Prochazka M. Evaluation of the microsomal glutathione S-transferase 3 (MGST3) locus on 1q23 as a Type 2 diabetes susceptibility gene in Pima Indians. *Hum Genet* 2003; **113**: 353-358

16 **Reynisdottir I**, Thorleifsson G, Benediktsson R, Sigurdsson G, Emilsson V, Einarsdottir AS, Hjorleifsdottir EE, Orlygsdottir GT, Bjornsdottir GT, Saemundsdottir J, Halldorsson S, Hrafnkelsdottir S, Sigurjonsdottir SB, Steinsdottir S, Martin M, Kochan JP, Rhees BK, Grant SF, Frigge ML, Kong A, Gudnason V, Stefansson K, Gulcher JR. Localization of a susceptibility gene for type 2 diabetes to chromosome 5q34-q35.2. *Am J Hum Genet* 2003; **73**: 323-335

17 **van Tilburg JH**, Sandkuijl LA, Strengman E, van Someren H, Rigters-Aris CA, Pearson PL, van Haeften TW, Wijmenga C. A genome-wide scan in type 2 diabetes mellitus provides independent replication of a susceptibility locus on 18p11 and suggests the existence of novel Loci on 2q12 and 19q13. *J Clin Endocrinol Metab* 2003; **88**: 2223-2230

18 **Duggirala R**, Almasy L, Blangero J, Jenkinson CP, Arya R, DeFronzo RA, Stern MP, O'Connell P. American Diabetes Association GENNID Study Group.Further evidence for a type 2 diabetes susceptibility locus on chromosome 11q. *Genet Epidemiol* 2003; **24**: 240-242

19 **Frayling TM**, Wiltshire S, Hitman GA, Walker M, Levy JC, Sampson M, Groves CJ, Menzel S, McCarthy MI, Hattersley AT. Young-onset type 2 diabetes families are the major contributors to genetic loci in the Diabetes UK Warren 2 genome scan and identify putative novel loci on chromosomes 8q21, 21q22, and 22q11. *Diabetes* 2003; **52**: 1857-1863

20 **Duggirala R**, Almasy L, Blangero J, Jenkinson CP, Arya R, DeFronzo RA, Stern MP, O'Connell P. American Diabetes Association GENNID Study Group.Further evidence for a type 2 diabetes susceptibility locus on chromosome 11q. *Genet Epidemiol* 2003; **24**: 240-242

21 **Hsueh WC**, St Jean PL, Mitchell BD, Pollin TI, Knowler WC, Ehm MG, Bell CJ, Sakul H, Wagner MJ, Burns DK, Shuldiner AR. Genome-wide and fine-mapping linkage studies of type 2

diabetes and glucose traits in the Old Order Amish: evidence for a new diabetes locus on chromosome 14q11 and confirmation of a locus on chromosome 1q21-q24. *Diabetes* 2003; **52**: 550-557

22 **Kim SH**, Ma X, Klupa T, Powers C, Pezzolesi M, Warram JH, Rich SS, Krolewski AS, Doria A. Genetic modifiers of the age at diagnosis of diabetes (MODY3) in carriers of hepatocyte nuclear factor-1alpha mutations map to chromosomes 5p15, 9q22, and 14q24. *Diabetes* 2003; **52**: 2182-2186

23 **Sellick GS**, Garrett C, Houlston RS. A novel gene for neonatal diabetes maps to chromosome 10p12.1-p13. *Diabetes* 2003; **52**: 2636-2638

24 **Luo TH**, Zhao Y, Li G, Yuan WT, Zhao JJ, Chen JL, Huang W, Luo M. A genome-wide search for type II diabetes susceptibility genes in Chinese Hans. *Diabetologia* 2001; **44**: 501-506

25 **Li YF, Sun HX**, Wu GD, Du WN, Zuo J, Shen Y, Qiang BQ, Yao ZJ, Wang H, Huang W, Chen Z, Xiong MM, Meng Y, Fang FD. Protein kinase C/zeta (*PRKCZ*) gene is associated with type 2 diabetes in Han population of North China and analysis of its haplotypes. *World J Gastroenterol* 2003; **9**: 2078-2082

26 **Nishizuka Y**. Protein kinase C and lipid signaling for sustained cellular responses. *FASEB J* 1995; **9**: 484-496

27 **Standaert ML**, Galloway L, Karnam P, Bandyopadhyay G, Moscat J, Farese RV. Protein kinase C-zeta as a downstream effector of phosphatidylinositol 3-kinase during insulin stimulation in rat adipocytes. Potential role in glucose transport. *J Biol Chem* 1997; **272**: 30075-30082

28 **Standaert ML**, Bandyopadhyay G, Perez L, Price D, Galloway L, Poklepovic A, Sajan MP, Cenni V, Sirri A, Moscat J, Toker A, Farese RV. Insulin activates protein kinases C-zeta and C-lambda by an autophosphorylation-dependent mechanism and stimulates their translocation to GLUT4 vesicles and other membrane fractions in rat adipocytes. *J Biol Chem* 1999; **274**: 25308-25316

29 **Etgen GJ**, Valasek KM, Broderick CL, Miller AR. *In vivo* adenoviral delivery of recombinant human protein kinase C-zeta stimulates glucose transport activity in rat skeletal muscle. *J Biol Chem* 1999; **274**: 22139-22142

30 **Tremblay F**, Lavigne C, Jacques H, Marette A. Defective insulin-induced GLUT4 translocation in skeletal muscle of high fat-fed rats is associated with alterations in both Akt/protein kinase B and atypical protein kinase C (zeta/lambda) activities. *Diabetes* 2001; **50**: 1901-1910

31 **Ravichandran LV**, Esposito DL, Chen J, Quon MJ. Protein kinase C-zeta phosphorylates insulin receptor substrate-1 and impairs its ability to activate phosphatidylinositol 3-kinase in response to insulin. *J Biol Chem* 2001; **276**: 3543-3549

32 **Liu YF**, Paz K, Herschkovitz A, Alt A, Tennenbaum T, Sampson SR, Ohba M, Kuroki T, LeRoith D, Zick Y. Insulin stimulates PKCzeta -mediated phosphorylation of insulin receptor substrate-1 (IRS-1). A self-attenuated mechanism to negatively regulate the function of IRS proteins. *J Biol Chem* 2001; **276**: 14459-14465

33 **Kanoh Y**, Bandyopadhyay G, Sajan MP, Standaert ML, Farese RV. Rosiglitazone, insulin treatment, and fasting correct defective activation of protein kinase C-zeta/lambda by insulin in vastus lateralis muscles and adipocytes of diabetic rats. *Endocrinology* 2001; **142**: 1595-1605

34 **Horikawa Y**, Oda N, Cox NJ, Li X, Orho-Melander M, Hara M, Hinokio Y, Lindner TH, Mashima H, Schwarz PE, del Bosque-Plata L, Horikawa Y, Oda Y, Yoshiuchi I, Colilla S, Polonsky KS, Wei S, Concannon P, Iwasaki N, Schulze J, Baier LJ, Bogardus C, Groop L, Boerwinkle E, Hanis CL, Bell GI. Genetic variation in the gene encoding calpain-10 is associated with type 2 diabetes mellitus. *Nat Genet* 2000; **26**: 163-175

35 **Uitterlinden AG**, Burger H, Huang Q, Yue F, McGuigan FE, Grant SF, Hofman A, van Leeuwen JP, Pols HA, Ralston SH. Relation of alleles of the collagen type Ialpha1 gene to bone density and the risk of osteoporotic fractures in postmenopausal women. *N Engl J Med* 1998; **338**: 1016-1021

36 **Condorelli G**, Vigliotta G, Iavarone C, Caruso M, Tocchetti CG, Andreozzi F, Cafieri A, Tecce MF, Formisano P, Beguinot L, Beguinot F. PED/PEA-15 gene controls glucose transport and is overexpressed in type 2 diabetes mellitus. *EMBO J* 1998; **17**: 3858-3866

Edited by Zhu LH and Chen WW **Proofread by** Xu FM

PO Box 2345, Beijing 100023, China
Fax: +86-10-85381893
E-mail: wjg@wjgnet.com www.wjgnet.com

World J Gastroenterol 2004;10(16):2361-2368
World Journal of Gastroenterology
 ISSN 1007-9327

• BASIC RESEARCH •

Prolongation of liver allograft survival by dendritic cells modified with NF-κB decoy oligodeoxynucleotides

Ming-Qing Xu, Yu-Ping Suo, Jian-Ping Gong, Ming-Man Zhang, Lü-Nan Yan

Ming-Qing Xu, Jian-Ping Gong, Ming-Man Zhang, Lü-Nan Yan, Department of General Surgery, West China Hospital, Sichuan University, Chengdu 610041, Sichuan Province, China
Yu-Ping Suo, West China Second University Hospital, Sichuan University, Chengdu 610041, Sichuan Province, China
Supported by the Postdoctoral Science Foundation of China, No. 2003033531
Correspondence to: Professor Lü-Nan Yan, Department of General Surgery, West China Hospital, Sichuan University, Chengdu 610041, Sichuan Province, China. xumingqing0018@163.com
Telephone: +86-28-85582968
Received: 2003-07-04 **Accepted:** 2003-09-25

Abstract

AIM: To induce the tolerance of rat liver allograft by dendritic cells (DCs) modified with NF-κB decoy oligodeoxynucleotides (ODNs).

METHODS: Bone marrow (BM)-derived DCs from SD rats were propagated in the presence of GM-CSF or GM-CSF+IL-4 to obtain immature DCs or mature DCs. GM-CSF+IL-4-propagated DCs were treated with double-strand NF-κB decoy ODNs containing two NF-κB binding sites or scrambled ODNs to ascertain whether NF-κB decoy ODNs might prevent DC maturation. GM-CSF-propagated DCs, GM-CSF+NF-κB decoy ODNs or scrambled ODNs-propagated DCs were treated with LPS for 18 h to determine whether NF-κB decoy ODNs could prevent LPS-induced IL-12 production in DCs. NF-κB binding activities, costimulatory molecule (CD40, CD80, CD86) surface expression, IL-12 protein expression and allostimulatory capacity of DCs were measured with electrophoretic mobility shift assay (EMSA), flow cytometry, Western blotting, and mixed lymphocyte reaction (MLR), respectively. GM-CSF-propagated DCs, GM-CSF+IL-4 -propagated DCs, and GM-CSF+NF-κB decoy ODNs or scrambled ODNs-propagated DCs were injected intravenously into recipient LEW rats 7 d prior to liver transplantation and immediately after liver transplantation. Histological grading of liver graft rejection was determined 7 d after liver transplantation. Expression of IL-2, IL-4 and IFN-γ mRNA in liver graft and in recipient spleen was analyzed by semiquantitative RT-PCR. Apoptosis of liver allograft-infiltrating cells was measured with TUNEL staining.

RESULTS: GM-CSF-propagated DCs, GM-CSF+NF-κB decoy ODNs-propagated DCs and GM-CSF+ scrambled ODNs-propagated DCs exhibited features of immature DCs, with similar low level of costimulatory molecule(CD40, CD80, CD86) surface expression, absence of NF-κB activation, and few allocostimulatory activities. GM-CSF+IL-4-propagated DCs displayed features of mature DCs, with high levels of costimulatory molecule (CD40, CD80, CD86) surface expression, marked NF-κB activation, and significant allocostimulatory activity. NF-κB decoy ODNs completely abrogated IL-4-induced DC maturation and allocostimulatory activity as well as LPS-induced NF-κB activation and IL-12 protein expression in DCs. GM-CSF+NF-κB decoy ODNs-propagated DCs promoted apoptosis of liver allograft-infiltrating cells within portal areas, and significantly decreased the expression of IL-2 and IFN-γ mRNA but markedly elevated IL-4 mRNA expression both in liver allograft and in recipient spleen, and consequently suppressed liver allograft rejection, and promoted liver allograft survival.

CONCLUSION: NF-κB decoy ODNs-modified DCs can prolong liver allograft survival by promoting apoptosis of graft-infiltrating cells within portal areas as well as down-regulating IL-2 and IFN-γ mRNA and up-regulating IL-4 mRNA expression both in liver graft and in recipient spleen.

Xu MQ, Suo YP, Gong JP, Zhang MM, Yan LN. Prolongation of liver allograft survival by dendritic cells modified with NF-κB decoy oligodeoxynucleotides. *World J Gastroenterol* 2004; 10(16): 2361-2368
http://www.wjgnet.com/1007-9327/10/2361.asp

INTRODUCTION

Dendritic cells (DC) play a critical role in the initiation and regulation of immune response and are instrumental in the induction and maintenance of tolerance[1-7]. The function of DCs is regulated by their state of maturation. Immature DCs resident in nonlymphoid tissues such as normal liver are deficient at antigen capture and progressing[8,9], whereas mature DCs, resident in secondary lymphoid tissues, are potent antigen-presenting cells (APC), which can induce naive T-cell activation and proliferation[9-13]. The ability of DCs to initiate immune responses is determined by their surface expression of major histocompatibility complex (MHC) gene products and costimulatory molecules (CD40, CD80, CD86), and the secretion of the immune regulator, interleukin (IL)-12[9-18]. Immature DCs that express surface MHC class II, but deficient in surface costimulatory molecules and few expressions of IL-12, can induce T-cell anergy[8,19,20], and inhibit immune reactivity[21,22].

Immature donor-derived DCs that are deficient in surface costimulatory molecules freshly isolated from commonly transplanted organs, can induce alloAg-specific T cell anergy *in vitro*[23]. These DCs prolong survival of fully allogeneic grafts in rodents, in same cases, indefinitely[24,25]. In addition, pharmacologic inhibition of DC maturation in nonhuman primates is associated with the induction of organ transplant tolerance[26]. Moreover, immature human DCs have been shown to induce T regulatory cells *in vitro*[27] and to promote Ag-specific T cell tolerance in healthy volunteers[28]. Thus, DCs offer potential both for therapy of allograft rejection and promotion of transplant tolerance.

The inherent ability of DCs to traffic exquisitely to T cell areas of secondary lymphoid tissues[8,29] and to regulate immune responses makes them attractive targets for manipulation with genes encoding immunosuppressive molecules, such as IL-4, IL-10, CTLA4Ig, Fas ligand (CD95L), or transforming growth factor (TGF)-β1, that suppress T cell response by various

mechanisms. A potential obstacle to the successful use of genetically engineered DCs for therapeutic immunosuppression is their maturation/activation *in vivo* following interactions with proinflammatory factors that may overcome the desired effect of transgene products. Recent studies showed that both DC maturation and immunostimulatory ability depended on NF-κB-dependent gene transcription[29-34], inhibition of NF-κB activation could suppress DC maturation/activation induced by IL-4 or LPS stimulation[29,34,35], and DCs treated with NF-κB decoy oligodeoxynucleotides(ODNs) containing specific NF-κB binding sites could induce tolerance of cardiac allograft[29,34].

Although genetically engineered DCs have been used in tolerance induction of cardiac allograft, there are few evidences that genetically engineered DCs can be used to induce tolerance of liver allograft. In the present study, whether NF-κB decoy ODNs-treated DCs could prolong liver allograft survival in rats was studied.

MATERIALS AND METHODS

NF-κB decoy ODNs

Double-stranded NF-κB decoy ODNs or scrambled ODNs (as a control for NF-κB decoy ODNs) were generated using equimolar amounts of single-stranded sense and antisense phosphorothioate-modified oligonucleotide containing two NF-κB binding sites (sense sequence 5'-AGGGACTTTCCGCTG-GGGACTTTCC-3', NF-κB binding sites bold lines and underlined)[34] and scrambled oligonucleotide (sense sequence 5'-TTGCCGTACCTGACTTAGCC-3')[36]. Sense and antisense strands of each oligonucleotide were mixed in the presence of 150 mmol/L PBS, heated to 100 °C, and allowed to cool to room temperature to obtain double-stranded DNA.

Propagation of bone marrow-derived DC populations

Bone marrow cells harvested from femurs of normal SD rats were cultured in 24-well plates (2×10^6 per well) in 2 mL of RPMI 1640 complete medium supplemented with antibiotics,10 mL/L fetal calf serum (FCS) and 4.0 ng/mL recombinant rat GM-CSF to obtain immature DCs. In addition to GM-CSF, 10 ng/mL recombinant rat IL-4 was added to cultures to obtained mature DCs. To select plates, 10 μmol/L NF-κB decoy or scrambled ODNs was added at the initiation of culture of DCs[34] to test the ability of NF-κB decoy ODNs to inhibit IL-4-induced DC maturation. Cytokine-enriched medium was refreshed every 2 d, after gentle swirling of the plates, half of the old medium was aspirated and an equivalent volume of fresh, cytokine-supplemented medium was added. Thus, nonadherent granulocytes were depleted without dislodging clusters of developing DC attached loosely to a monolayer of plastic-adherent macrophages. Nonadherent cells released spontaneously from the clusters were harvested after 7 d. In certain experiments, after propagation for 7 d, GM-CSF-propagated DCs, GM-CSF+ NF-κB decoy ODNs - propagated DCs and GM-CSF + scrambled ODNs - propagated DCs were cultured with 10 μg/mL LPS for 18 h to test the ability of NF-κB decoy ODNs to prevent LPS-induced IL-12 production in DCs.

Phenotypical features of DCs

Expression of cell surface molecules was quantitated by flow cytometry as described in our previous study. Aliquots of 2×10^5 DCs propagated for 7 d *in vitro* were incubated with the following primary mouse anti-rat mAbs against CD40, CD80, CD86, or rat IgG as an isotype control for 60 min on ice [1 μg/mL diluted in PBS/(10 mL/L FCS)]. Cells were washed with PBS/(10 mL/L FCS) and labeled with FITC-conjugated goat anti-mouse IgG, diluted 1/50 in PBS/(10 mL/L FCS) for 30 min on ice. At the end of this incubation, the cells were washed, propidium iodide/PBS were added, and the cells were subsequently analyzed by a FACS-4 200 flow cytometer.

DCs allostimulatory capacity

One-way mixed leukocyte reactions (MLR) were performed in 96-well, round-bottomed microculture plates. Graded doses of γ-irradiated (20Gy) allogeneic(SD) stimulator cells (DCs) were added to 2×10^5 nylon wool-eluted LEW rat splenic T cells (responders) and maintained in complete medium for 72 h in 50 mL/L CO_2 in air at 37 °C. [^{3}H]thymidine(1 μCi/well) was added for the last 18 h of culture. Cells were harvested onto glass fiber mats using an automatic system, and [^{3}H]thymidine incorporation was determined by a liquid scintillation counter. Results were expressed as mean±SD.

Isolation of nuclear proteins

Nuclear proteins were isolated from DC extract by placing the sample in 0.9 mL of ice-cold hypotonic buffer [10 mmol/L HEPES (pH7.9), 10 mmol/L KCl, 0.1 mmol/L EDTA, 0.1 mmol/L ethylene glycol tetraacetic acid, 1 mmol/L DTT, protease inhibitors (aprotinin, pepstatin, and leupeptin, 10 mg.mol/L each)]. Homogenates were incubated on ice for 20 min, vortexed for 20 s after adding 50 μL of 100 g/L Nonidet P-40, and then centrifuged for 1 min at 4 °C in an Eppendorf centrifuge. Supernatants were decanted, nuclear pellets after a single wash with hypotonic buffer without Nonidet-P40 were suspended in an ice-cold hypertonic buffer [20 mmol/L HEPES (pH7.9), 0.4 mol/LNaCl , 1 mmol/LEDTA, 1 mol/L DTT, protease inhibitors], incubated on ice for 30 min at 4 °C, mixed frequently, and centrifuged for 15 min at 4 °C. Supernatants were collected as nuclear extracts and stored at -70 °C. Concentrations of total proteins in the samples were determined according to the method of Bradford.

Electrophoretic mobility shift assay (EMSA) for NF-κB activation of DCs

NF-κB binding activity was performed in a 10-μL binding reaction mixture containing 1×binding buffer [50 mg/L of double-stranded poly (dI-dC), 10 mmol/L Tris-HCl (pH7.5), 50 mmol/LNaCl, 0.5 mmol/L EDTA, 0.5 mmol/LDTT, 1 mmol/L $MgCl_2$, and 100 mL/L glycerol], 5 μg of nuclear protein , and 35 fmol of double-stranded NF-κB consensus oligonucleotide (5'-AGT TGAGGGGACTTT CCCAGGC -3') that was endly labeled with γ-^{32}P (111TBq /mmol at 370 GBq^{-1}) using T4 polynucleotide kinase. The binding reaction mixture was incubated at room temperature for 20 min and analyzed by electrophoresis on 70 g/L nondenaturing polyacrylamide gels. After electrophoresis, the gels were dried by a gel-drier and exposed to Kodak X-ray films at -70 °C.

Western blotting for IL-12 protein expression in DCs stimulated with LPS

GM-CSF-propagated DCs, GM-CSF+ NF-κB decoy ODNs-propagated DCs and GM-CSF + scrambled ODNs-propagated DCs were cultured with 10 μg/mL LPS for 18 h. DCs were starved in serum-free medium for 4 h at 37 °C. These cells were washed twice with cold PBS, resuspended in 100 μL lysis buffer (1 mL/L Nonidet P-40, 20 mmol/L Tris-HCl, pH8.0, 137 mmol/L NaCl, 100 mL/L glycerol, 2 mmol/L EDTA, 10 μg/mL leupeptin, 10 μg/mL aprotinin, 1 mmol/L PMSF, and 1 mmol/L sodium orthovanadate), and total cell lysates were obtained. Homogenates were centrifuged at 10 000 *g* for 10 min at 4 °C. Cell lysates (20 μg) were electrophoresed on SDS-PAGE gels, and transferred to PVDC membranes for Western blot analysis. Briefly, PVDC membranes were incubated in a blocking buffer for 1 h at room temperature, then incubated for 2 h with Abs against IL-12 p35 and IL-12 p40 and IL-12 p70. Membranes were washed and incubated for 1 h with HRP-labeled horse anti-goat or goat anti-rabbit IgG. Immunoreactive bands were visualized by ECL detection reagents. The binding bands were quantified by a

scanning the densitometer of a bio-image analysis system. The results were expressed as a relative optical density.

Liver transplantation

Sixty male LEW rats and sixty male SD rats weighing 250 -300 g were used in all experiments. Allogeneic liver transplantation model was established using a combination of SD rats with LEW rats. All operations were performed under ether anesthesia in sterile conditions. Orthotopic liver transplantation was performed according to the method described in our previous study. Normal saline (group A), 1×10^7 GM-CSF-propagated DCs (group B), 1×10^7 GM-CSF+IL-4-propagated DCs (group C), and 1×10^7 GM-CSF+ NF-κB decoy ODNs or scrambled ODNs-propagated DCs (group D or group E) were injected intravenously through the penile vein into recipient LEW rats 7 d prior to liver transplantation and immediately after liver transplantation, respectively. Liver graft tissues and recipient spleen samples ($n = 8$) were harvested 7 d after liver transplantation and immediately frozen in liquid nitrogen and kept at -80 °C until use. Part of the liver graft tissues was sectioned and preserved in 40 g/L formaldehyde.

Histology

Part of liver tissues was sectioned and preserved in 40 g/L formaldehyde, embeded in paraffin, and stained with hematoxylin and eosin. Histological grading of rejection was determined according to the criteria described by Williams.

Apoptosis of liver graft-infiltrating cells (GIC)

Apoptotic cells in tissue sections were detected with the *in situ* cell death detection kit. Liver graft tissue sections were dewaxed and rehydrated according to standard protocols. Tissue sections were incubated with proteinase K(20 μg/mL in 10 mmol/L Tris/HCl, pH 7.4-8.0) for 15 to 30 min at 21-37 °C. Endogenous peroxidase activity was quenched with blocking solution (3 mL/LH_2O_2 in methanol) for 30 min at room temperature before exposure to TUNEL reaction mixture at 37 °C for 60 min. After washed in stop wash buffer, peroxidase(POD) was added to react for 30 min at 37 °C. DAB-substrate was used for color development, and the sections were counterstained with Harrs' hematoxylin. TUNEL staining was mounted under glass coverslip and analysed under a light microscope.

Semiquantitative RT -PCR assay for expression of IL-2, IL-4 and IFN-γmRNA in liver graft and spleen

IL-2, IL-4 and IFN-γ mRNA expression was determined by semiquantitative RT-PCR amplification in contrast with housekeeping gene β-actin, respectively. Total RNA from 10 mg liver allograft and recipient spleen tissue was extracted using Tripure™ reagent. First-strand cDNA was transcribed from 1 μg RNA using AMV and an Oligo(dT_{15}) primer. PCR was performed in a 25 μL reaction system containing 10 μL cDNA, 2 μL 10 mmol/L dNTP, 2.5 μL 10×buffer, 2.5 μL 25 mmol/L $MgCl_2$, 2 μL specific primer, 5 μL water and 1 μL Taq (35 cycles: at 95 °C for 60 s, at 59 °C for 90 s, and at 72 °C for 10 s). Primers[37-39] used in PCR reactions were as follows: IL-2, 5' primer 5'-CAT GTA CAGCA TGCAGCTCGCATCC-3', 3' primer 5'-CCACCACAGTTGCTG GCTCATCATC-3', to give a 410-bp PCR product; IL-4, 5' primer 5'-TGATGGGTCTCAGCCCCCACCTTGC-3', 3' primer 5'-CTT TCAGTGTTGTGAGCGTGGACTC-3', to give a 378-bp PCR product; IFN-γ, 5' primer 5'-AAGACA ACCAGGCCATCAGCA-3', 3' primer 5'-AGCCACAGTGTGAGTTCAGTC-3', to give a 547-bp product; β-actin, 5' primer 5'-ATGCCATCC TGCGT CTGGACCTGGC-3', 3' primer 5'-AGCATTTGCGGTGCAC GATGGAGGG-3', to give a 607-bp product. PCR products of each sample were subjected to electrophoresis in a 15 g/L agarose gel containing 0.5 mg/L ethidium bromide. Densitometrical analysis using NIH image software was performed for semiquantification of PCR products, and mRNA expression was evaluated by the band-intensity ratio of IL-2, IL-4 and IFN-γ to β-actin, and presented as percent of β-actin (%).

Statistical analysis

Statistic analysis of data was performed using the *t*-test and rank sum test, $P<0.05$ was considered statistically significant.

RESULTS

NF-κB decoy ODNs inhibited IL-4 or LPS - induced NF-κB activation in DCs

To confirm whether NF-κB decoy ODNs might specifically bind to NF-κB, analysis of NF-κB activity was performed with nuclear extracts obtained from GM-CSF-propagated DCs, GM-CSF+IL-4-propagated DCs, GM-CSF+LPS-propagated DCs, GM-CSF+IL-4+ODNs-propagated DCs and GM-CSF+LPS +ODNs - propagated DCs by EMSA. As shown in Figure 1, EMSA analysis showed no NF-κB activation in GM-CSF - propagated DCs but significant NF-κB activation in IL-4 or LPS -stimulated DCs. NF-κB decoy ODNs completely inhibited IL-4 or LPS-induced NF-κB activation in DCs, whereas scrambled ODNs had little effect on inhibition of IL-4 or LPS - induced NF-κB activation in DCs.

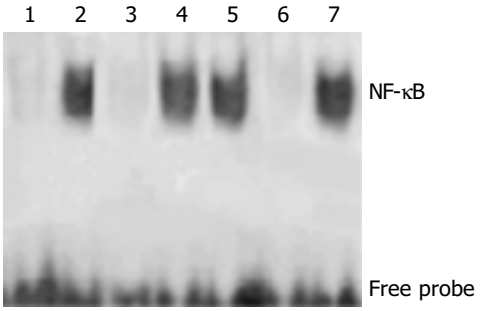

Figure 1 Inhibition of IL-4 or LPS -induced NF-κB activation in DCs by NF-κB decoy ODNs. Nuclear proteins of GM-CSF DCs, GM-CSF + IL-4 DCs, GM-CSF+IL-4 + NF-κB decoy ODNs DCs, GM-CSF+IL-4 + scrambled ODNs DCs, GM-CSF + LPS DCs, GM-CSF+LPS+ NF-κB decoy ODNs DCs and GM-CSF+LPS+ scrambled ODNs DCs were measured by EMSA (lanes 1-7).

NF-κB decoy ODNs inhibited IL-4 - induced costimulatory molecule surface expression in DCs

Functional maturation of DCs was associated with up-regulation of costimulatory molecules (CD40, CD80, and CD86). To test the ability to inhibit DC maturation, NF-κB decoy ODNs or scrambled ODNs were added at the initiation of culture of GM-CSF+IL-4 - stimulated SD rat BM-derived DCs. After culture for 7 d, surface expression of CD40, CD80, and CD86 was analyzed by flow cytometry. Figure 2 shows the effects of ODNs on phenotype of the cultured DCs in the presence of GM-CSF+IL-4. Flow cytometric analysis showed GM-CSF-propagated DCs exhibited immature phenotypical features with very low levels of CD40, CD80 and CD86 surface expression, GM-CSF+IL-4-propagated DCs displayed mature phenotypical features with high level of CD40, CD80, and CD86 surface expression. NF-κB decoy ODNs prevented IL-4-induced DCs maturation, and maintained DCs in the immature state, with low levels of surface costimulatory molecule expression. Whereas the scrambled ODNs could not prevent IL-4-induced DCs maturation, and maintained DCs in the mature state, with similar high levels of surface costimulatory molecule expression compared with GM-CSF+IL-4-propagated DCs (data not shown) .

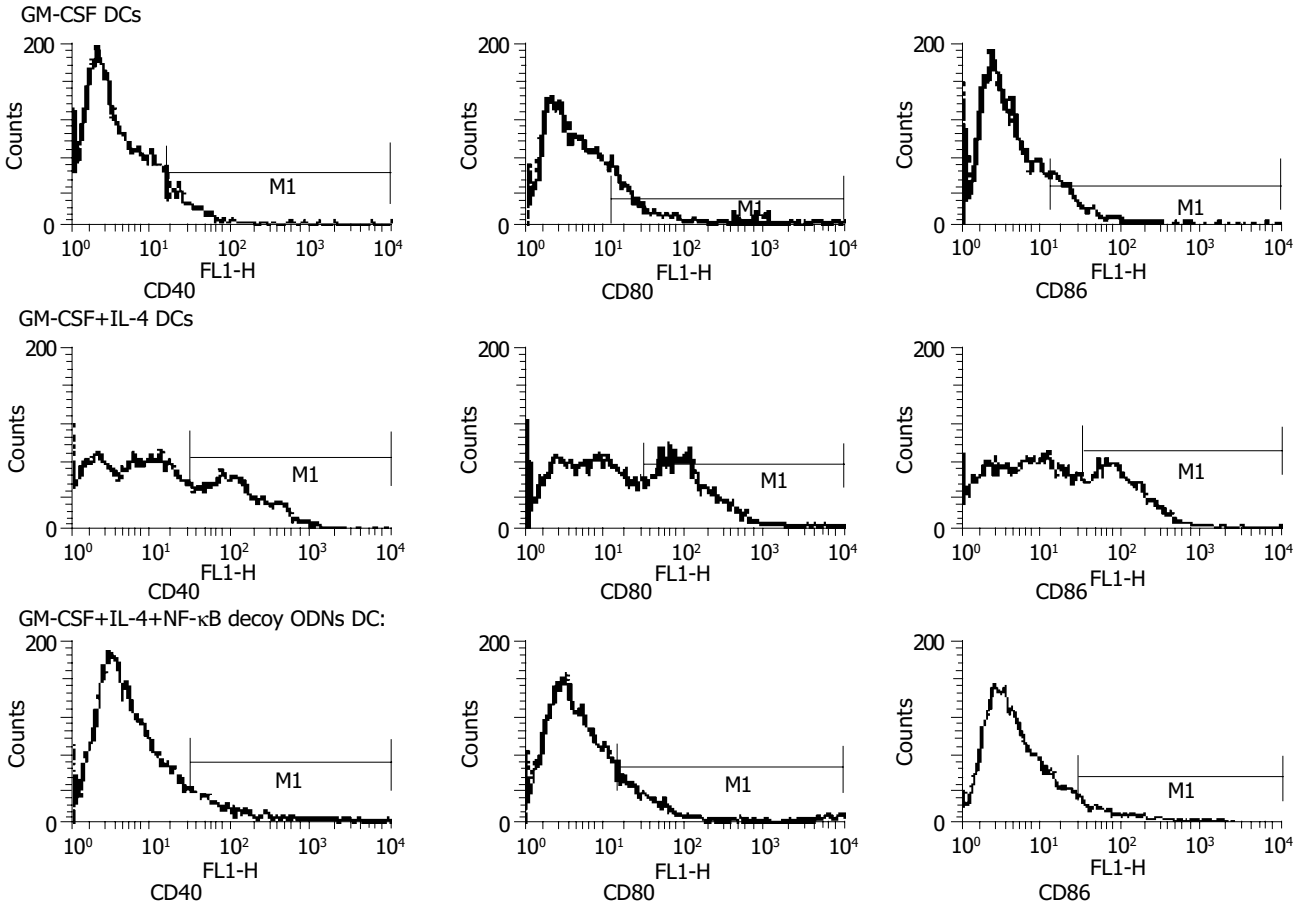

Figure 2 Suppression of IL-4-induced costimulatory molecule expression in DCs by NF-κB decoy ODNs.

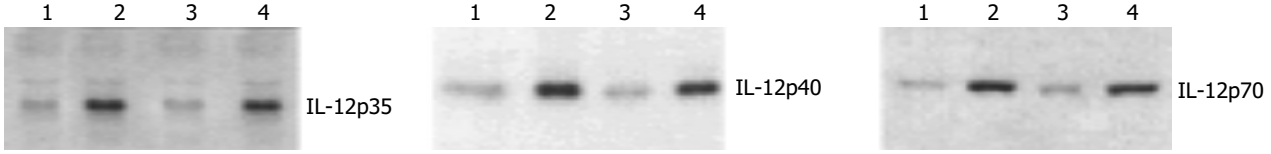

Figure 3 Suppression of IL-12 protein expression in LPS-stimulated DCs by NF-κB decoy ODNs. Protein extracts from GM-CSF DCs, GM-CSF+LPS DCs, GM-CSF+LPS +NF-κB decoy ODNs DCs and GM-CSF+LPS +scrambled ODNs DCs were measured by Western blot (lane 1-4).

NF-κB decoy ODNs abrogated LPS- induced IL-12 protein expression in DCs

Previous studies showed that IL-12 protein expression was significantly up-regulated in mature DCs[10,17,19,40]. To further confirm whether NF-κB decoy ODNs might prevent DC maturation, LPS-induced IL-12 protein (p35, p40 and p70) expression in DCs was measured. As shown in Figure 3, very low level of IL-12 protein was detected in GM-CSF DCs, and markedly high level of IL-12 protein was detected in LPS-stimulated DCs (P<0.001). NF-κB decoy ODNs completely abrogated the LPS-induced production of IL-12 protein in DCs, whereas scrambled ODNs had almost no effect on down-regulation of LPS - induced IL-12 protein expression in DCs.

DCs allostimulatory capacity was inhibited by NF-κB decoy ODNs

The effect of NF-κB decoy ODNs on DCs immunostimulatory activity was evaluated by *in vitro* MLR. Graded number of γ-irradiated DCs (SD) was cultivated for 72 h with a fixed number of allogeneic (LEW) splenic T cells in MLR. The results of a representative experiment are shown in Figure 4. In comparison with IL-4 stimulated mature DCs or IL-4 + scrambled ODNs-propagated DCs, which were potent inducers of DNA synthesis and consistent with their mature surface phenotype, IL-4+NF-κB decoy ODNs- propagated DCs induced only a minimal T cell proliferation. The poor stimulatory capacity of IL-4 +NF-κB decoy ODNs DCs remained unchanged after a longer incubation with allogeneic T cells (4- or 5-d MLR, data not shown). The results suggested that allostimulatory capacity of DCs was inhibited by NF-κB decoy ODNs.

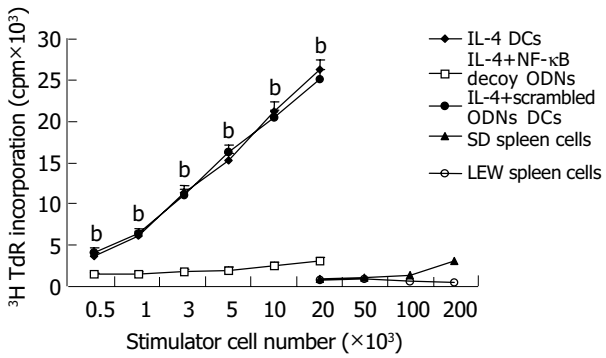

Figure 4 Suppression of allostimulatory function of IL-4-stimulated DCs by NF-κB decoy ODNs. ^bP<0.001 *vs* IL-4+NF-κB decoy ODNs -propagated DCs.

NF-κB decoy ODNs- treated DCs prolonged donor-specific liver allograft survival

To examine the effect of NF-κB decoy ODNs-treated DCs on liver allograft survival *in vivo*, 1×10^7 unmodified immature bone marrow-derived DCs from SD rats (GM-CSF DCs), GM-CSF+IL-4-propagated mature DCs, and GM-CSF+NF-κB decoy ODNs or scrambled ODNs-propagated immature DCs were injected intravenously through the penile vein into recipient LEW rats 7 d prior to liver transplantation and immediately after liver transplantation, respectively. Table 1 and Figure 5 show the effect of DCs on liver allograft rejection and recipient survival. GM-CSF+IL-4-propagated mature DCs accelerated the liver allograft rejection and shorted the survival time of recipient animals. Immature donor DCs (GM-CSF or GM-CSF+scrambled ODNs-propagated DCs) significantly suppressed liver allograft rejection and prolonged graft survival compared with untreated controls. In comparison with GM-CSF or GM-CSF +scrambled ODNs-propagated DCs, NF-κB decoy ODNs-treated DCs exerted a marked effect on liver allograft rejection and recipient survival, and significantly suppressed the liver allograft rejection and prolonged survival time of recipient animals.

Table 1 Rejection stages of liver allografts

Rejection stages	Group A (*n*)	Group B (*n*)	Group C (*n*)	Group D (*n*)	Group E (*n*)
0	0	1	0	6	2
1	2	6	0	2	6
2	6	1	2	0	0
3	0	0	6	0	0

Group B *vs* group A, $u = 2.475$, $P<0.05$; Group C *vs* group A, $u = 2.951$, $P<0.01$; Group D *vs* group A, $u = 3.298$, $P<0.01$; Group D *vs* group B, $u = 2.416$, $P<0.05$; Group E *vs* group A, $u = 0.901$, $P>0.05$.

NF-κB decoy ODNs-treated DCs promoted apoptosis of liver allograft-infiltrating cells in portals

Although the precise mechanisms remain unclear, spontaneous acceptance of liver grafts in mice has been associated with high levels of apoptosis in GIC population[41]. In contrast, FL liver gllografts that were rejected acutely showed reduced apoptotic activity in GIC within portal areas and enhanced apoptosis of hepatocytes[42]. These data suggested a critical immunoregulatory role of apoptosis in determining the outcome of hepatic allografts. To determine whether the prolongation of liver allografts survival induced by NF-κB decoy ODNs-treated DCs was associated with enhanced apoptosis of GIC, apoptotic activity in the graft was examined by TUNEL staining with immunohistochemistry analysis. *In situ* TUNEL staining of liver graft sections revealed that a certain level of apoptosis of GIC was induced by immature DCs (GM-CSF or GM-CSF+scrambled ODNs-propagated DCs), and mature DCs appeared to protect GIC from apoptosis. The greatest degree of apoptosis of GIC within portal areas of liver grafts was induced by NF-κB decoy ODNs-treated DCs (Figure 6). These data strongly suggested that augmentation of apoptosis of activated GIC within portal areas of liver grafts might be critical in promoting the tolerance of liver allografts.

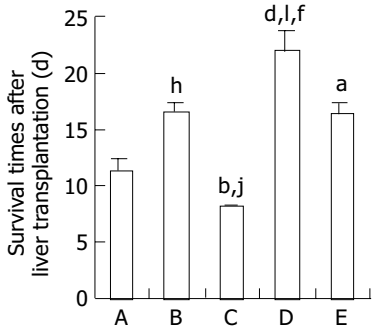

Figure 5 Prolongation of survival of liver allograft recipient by NF-κB decoy ODNs-treated DCs. $^bP<0.001$ *vs* group A, $^dP<0.001$ *vs* group A, $^fP<0.001$ *vs* group C, $^hP<0.001$ *vs* group A, $^jP<0.001$ *vs* group B, $^lP<0.001$ *vs* group B, $^aP>0.05$ *vs* group B.

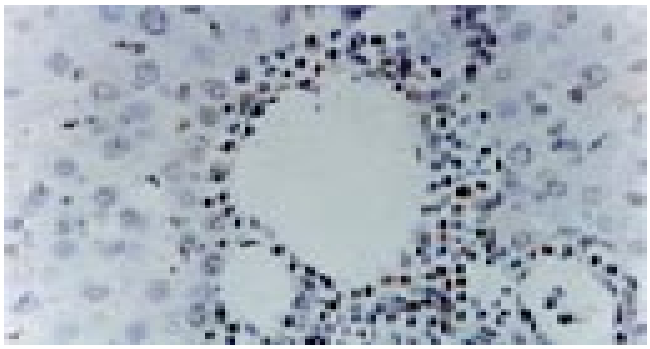

Figure 6 Augmentation of apoptosis of liver allograft-infiltrating cells in portals. by NF-κB decoy ODNs-treated DCs (×400).

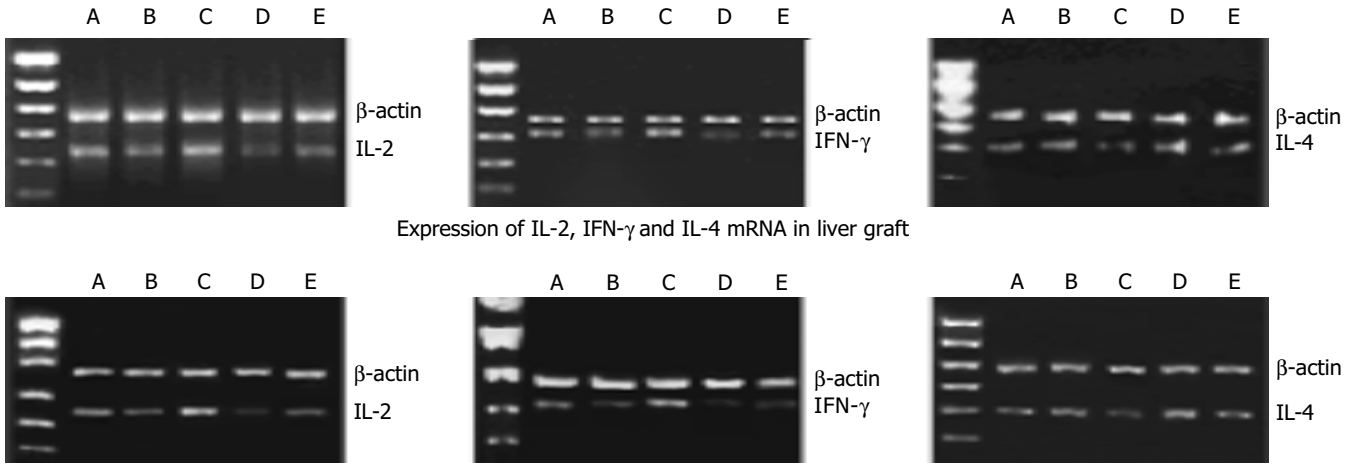

Figure 7 Suppression of IL-2 and IFN-γ mRNA expression and up-regulation of IL-4 mRNA expression both in liver graft and in recipient spleen by NF-κB decoy ODNs-modified DCs.

NF-κB decoy ODNs-treated DCs suppressed IL-2 and IFN-γ mRNA but elevated IL-4 mRNA expression both in liver graft and in recipient spleen

To determine the relationship of specific cytokine production to the outcome of liver transplantation, cytokine mRNA expression in liver graft and recipient spleen 7 d after liver transplantation was examined by RT-PCR assay. IL-2, IL-4 and IFN-γ mRNA were readily detected both in liver graft and in recipient spleen 7 d after liver transplantation in animals from group A. Administration of immature DCs (group B and group E) partially down-regulated IL-2 mRNA and INF-γ mRNA expression and partially up-regulated IL-4 mRNA expression in liver graft and recipient spleen. Administration of IL-4 stimulated mature DCs (Group C) significantly up-regulated expression of IL-2 and IFN-γ mRNA but markedly down-regulated IL-4 mRNA expression in liver graft and recipient spleen ($P<0.001$ *vs* group A, B, D, E. Statistic data not shown). However, administration of NF-κB decoy ODNs-modified DCs (groupD) significantly suppressed expression of IL-2 and IFN-γ mRNA and significantly elevated expression of IL-4 mRNA both in liver grafts and in recipient spleen ($P<0.001$ *vs* group A, B, C, E. Statistic data not shown). Taken together, these results suggested that prolongation of liver allograft survival induced by NF-κB decoy ODNs-modified DCs might be associated with down-regulation of IL-2 and IFN-γ production and up-regulation of IL-4 production in liver graft and recipient lymphoid tissue.

DISCUSSION

It is accepted that both donor and recipient DCs mediate the rejection of graft in organ transplantation. Thus, conversion of these two sets of DCs to specifically inactivate recipient alloreactive T cells should allow the long-term acceptance of graft in the absence of continuous immunosuppression. In the present study, we showed that stably immature DCs modified with NF-κB decoy ODNs markedly suppressed the rejection of liver allograft and prolonged liver allograft survival.

The ability of DCs to traffic to T cell areas of secondary lymphoid tissues and subsequently direct immune responses makes them ideal candidates for cell-based therapies of allograft rejection. Several studies showed that immature donor DCs, deficient in surface costimulatory molecules, could induce T-cell hyporesponsiveness[20-22] and prolong graft survival in unmodified hosts[43,44].

Several strategies have been used to arrest the maturation of DCs and to potentiate their tolerogenicity. While some have shown their promising, all have significant disadvantages. CsA could inhibit DC function, but its effect was weak and temporary, easily to be overcome by cytokines such as IL-4[45]. CsA may inhibit DC maturation *in vivo*, but also interferes with signal transduction through the T cell receptor complex, thus impairing the development of antigen-specific tolerance. Indeed, CsA interferes with T cell maturation and selection and can lead to generation of autoreactive T cells. Additionally, CsA is associated with significant toxicity. Antibodies to fusion proteins specific for cell-surface molecules (anti-CD40, CTLA4Ig) could prevent DC costimulation of T cells[46]. However, antibodies and fusion proteins have a limited half-life. Late up-regulation of DC costimulatory molecules upon encountering the host microenvironment requires treatment of multiple antibodies. Expression of immunosuppressive gene products such as IL-10, TGF-β and CTLA4-Ig by DCs could result in further inhibition of alloimmune responses *in vitro*[20,29,47,48]. However, adenoviral vectors used to efficiently deliver transgene expression could simultaneously activate DCs[20,29]. Thus, transgene expression was overcome by the vigorous upregulation of costimulatory molecules on the transfected DC surface. Antisence oligodeoxynucleotides to molecules such as ICAM-1 could prolong kidney and heart allograft survival[49]. However, effects were not donor specific, nor did grafts survive indefinitely. To date, strategies using genetically DCs alone in experimental organ transplantation have failed to induce tolerance. In the setting of transplantation, proinflammatory cytokines and other factors were capable of promoting DC maturation abound within recipient tissues. Thus, late maturation and inherent T cell stimulatory potential of genetically engineered DCs may overcome the effects of localized immunosuppressive transgene expression. However, our and other data indicated that preconditioning donor DCs *in vitro* with ODN to block NF-κB nuclear translocation were sufficient to stably suppress the up-regulation of costimulatory molecules and IL-12 production in response to potent activating stimuli, such as LPS and IL-4.

NF-κB is an important transcriptional regulator of the immune response in a variety of cell types, but its precise function in DCs has not been extensively evaluated. Nonetheless, interference with its actions, either by CsA or using ODN decoy approach, could result in significant suppression of immune function at the level of cytokine production, effector function, and costimulation capacity.

Although long-term allograft survival has been achieved after infusion of costimulatory molecule-deficient DCs in a few specific mouse strain combinations, the ability of immature DCs to prolong allograft survival in most models is still not satisfactory.

In this study, by targeting the NF-κB pathway in DCs with short NF-κB decoy ODNs, DCs were maintained in an immature phenotype associated with significantly reduced allostimulatory capacity *in vitro*. More importantly, with administration of NF-κB decoy ODNs-treated donor DCs, significant suppression of liver allograft rejection and marked prolongation of recipient survival were achieved in the absence of immunosuppression. *In vivo*, only the effect of NF-κB decoy ODNs-treated donor DCs on liver allograft survival was maximal, although some suppression of liver allograft rejection and survival prolongation were observed in recipients injected with immature DCs without NF-κB decoy ODNs modification.

The mechanisms by which NF-κB decoy ODNs-treated DCs prolong survival of liver allografts are unclear. We found *in vitro* and *in vivo* evidence that stably immature NF-κB decoy ODNs-treated DCs could suppress T cell allostimulatory ability, promote apoptosis of graft-infiltrating cells, and inhibit Th1 immunostimulatory cytokines such as IL-2 and IFN-γ mRNA expression and increase Th2 cytokine (IL-4) mRNA expression both in liver graft and in recipient spleen. Apoptosis of alloreactive T cells appears to be an important mechanism underlying the survival prolongation of organ graft, apoptosis of immunoreactive T cells within the graft and host secondary lymphoid tissue plays a pivotal role in determining the balance between liver transplant tolerance and rejection. Previous studies showed that blockade of costimulation by donor-derived DCs markedly promoted apoptosis of alloreactive T cells in host lymphoid tissue and prolonged organ graft survival[50,51]. However, prevention of apoptosis of alloreactive T cells could block the induction of peripheral transplant tolerance[42,52]. In the present study, *in situ* TUNEL staining of liver grafts from NF-κB decoy ODNs-modified DCs-treated recipients showed the greatest degree of apoptosis of lymphocytes within portal areas of liver grafts. The result strongly suggested that the enhanced apoptosis of liver allograft-infiltrating lymphocytes might be an important mechanism for survival prolongation of liver allograft induced by NF-κB decoy ODNs-treated DCs.

Another important mechanism by which NF-κB decoy ODNs-treated DCs prolong survival of liver allografts may be the alteration of immunoregulatory cytokines (such as IL-2, IL-4 and IFN-γ) mRNA expression both in liver graft and in recipient spleen. In the present study, high level expression of IL-2, IL-4 and IFN-γ mRNA was observed in grafts and recipient spleen

of untreated recipient animals, which was consistent with immune activation. Administration of immature DCs (GM-CSF DCs or GM-CSF + scrambled ODNs DCs) partially down-regulated IL-2 mRNA and IFN-γ mRNA expression and partially up-regulated IL-4 mRNA expression both in liver graft and in recipient spleen. NF-κB decoy ODNs-treated DCs appeared to skew cytokine expression toward Th2 cytokines (IL-4), and significantly suppressed Th1 cytokines (INF-γ and IL-2) mRNA expression both in liver graft and in recipient spleen. The suppressed expression of IFN-γ and IL-2 mRNA both in liver graft and in spleen might be associated with the enhanced apoptosis of T cells and the skewing toward Th2. Although there is evidence that IL-10 could exacerbate organ allograft rejection and its neutralization could modestly prolong transplant survival[53,54], the predominant expression of Th2 cytokines, such as IL-4 and IL-10, was implicated in long term survival of the allograft in general. In contrast to Th2 cytokines, expression of Th1 cytokines, especially IFN-γ, in graft models has been shown to be associated with acute rejection[29,50,55]. Thus, significantly decreased expression of Th1 cytokines such as IL-2 and IFN-γ mRNA, as well as the relatively high level of IL-4 mRNA both in liver allograft and in recipient spleen may be an important mechanism underlying the tolerance of liver allograft induced by NF-κB decoy ODNs-treated DCs.

REFERENCES

1 **Zhang JK**, Chen HB, Sun JL, Zhou YQ. Effect of dendritic cells on LPAK cells induced at different times in killing hepatoma cells. *Shijie Huaren Xiaohua Zazhi* 1999; **7**: 673-675
2 **Li MS**, Yuan AL, Zhang WD, Chen XQ, Tian XH, Piao YT. Immune response induced by dendritic cells induce apoptosis and inhibit proliferation of tumor cells. *Shijie Huaren Xiaohua Zazhi* 2000; **8**: 56-58
3 **Luo ZB**, Luo YH, Lu R, Jin HY, Zhang PB, Xu CP. Immunohistochemical study on dendritic cells in gastric mucosa of patients with gastric cancer and precancerous lesions. *Shijie Huaren Xiaohua Zazhi* 2000; **8**: 400-402
4 **Li MS**, Yuan AL, Zhang WD, Liu SD, Lu AM, Zhou DY. Dendritic cells *in vitro* induce efficient and specific anti-tumor immune response. *Shijie Huaren Xiaohua Zazhi* 1999; **7**: 161-163
5 **Wang FS**, Xing LH, Liu MX, Zhu CL, Liu HG, Wang HF, Lei ZY. Dysfunction of peripheral blood dendritic cells from patients with chronic hepatitis B virus infection. *World J Gastroenterol* 2001; **7**: 537-541
6 **Banchereau J**, Briere F, Caux C, Davoust J, Lebecque S, Liu YJ, Pulendran B, Palucka K. Immunobiology of dendritic cells. *Annu Rev Immunol* 2000; **18**: 767-811
7 **Banchereau J**, Steinman RM. Dendritic cells and the control of immunity. *Nature* 1998; **392**: 245-252
8 **Khanna A**, Morelli AE, Zhong C, Takayama T, Lu L, Thomson AW. Effects of liver-derived dendritic cell progenitors on Th1- and Th2-like cytokine responses *in vitro* and *in vivo*. *J Immunol* 2000; **164**: 1346-1354
9 **Morelli AE,** O'Connell PJ, Khanna A, Logar AJ, Lu L, Thomson AW. Preferential induction of Th1 responses by functionally mature hepatic (CD8alpha- and CD8alpha+) dendritic cells: association with conversion from liver transplant tolerance to acute rejection. *Transplantation* 2000; **69**: 2647-2657
10 **Mehling A**, Grabbe S, Voskort M, Schwarz T, Luger TA, Beissert S. Mycophenolate mofetil impairs the maturation and function of murine dendritic cells. *J Immunol* 2000; **165**: 2374-2381
11 **Stuart LM**, Lucas M, Simpson C, Lamb J, Savill J, Lacy-Hulbert A. Inhibitory effects of apoptotic cell ingestion upon endotoxin-driven myeloid dendritic cell maturation. *J Immunol* 2002; **168**: 1627-1635
12 **Ismaili J**, Rennesson J, Aksoy E, Vekemans J, Vincart B, Amraoui Z, Van Laethem F, Goldman M, Dubois PM. Monophosphoryl lipid A activates both human dendritic cells and T cells. *J Immunol* 2002; **168**: 926-932
13 **Sato K**, Nagayama H, Enomoto M, Tadokoro K, Juji T, Takahashi TA. Autocrine activation-induced cell death of T cells by human peripheral blood monocyte-derived $CD4^+$ dendritic cells. *Cell Immunol* 2000; **199**: 115-125
14 **Zheng H**, Dai J, Stoilova D, Li Z. Cell surface targeting of heat shock protein gp96 induces dendritic cell maturation and anti-tumor immunity. *J Immunol* 2001; **167**: 6731-6735
15 **Morel Y**, Truneh A, Sweet RW, Olive D, Costello RT. The TNF superfamily members LIGHT and CD154 (CD40 ligand) costimulate induction of dendritic cell maturation and elicit specific CTL activity. *J Immunol* 2001; **167**: 2479-2486
16 **Kobayashi M**, Azuma E, Ido M, Hirayama M, Jiang Q, Iwamoto S, Kumamoto T, Yamamoto H, Sakurai M, Komada Y. A pivotal role of Rho GTPase in the regulation of morphology and function of dendritic cells. *J Immunol* 2001; **167**: 3585-3591
17 **Hertz CJ**, Kiertscher SM, Godowski PJ, Bouis DA, Norgard MV, Roth MD, Modlin RL. Microbial lipopeptides stimulate dendritic cell maturation via Toll-like receptor 2. *J Immunol* 2001; **166**: 2444-2450
18 **Thoma-Uszynski S**, Kiertscher SM, Ochoa MT, Bouis DA, Norgard MV, Miyake K, Godowski PJ, Roth MD, Modlin RL. Activation of toll-like receptor 2 on human dendritic cells triggers induction of IL-12, but not IL-10. *J Immunol* 2000; **165**: 3804-3810
19 **Hirano A**, Luke PP, Specht SM, Fraser MO, Takayama T, Lu L, Hoffman R, Thomson AW, Jordan ML. Graft hyporeactivity induced by immature donor-derived dendritic cells. *Transpl-Immunol* 2000; **8**: 161-168
20 **Lee WC**, Zhong C, Qian S, Wan Y, Gauldie J, Mi Z, Robbins PD, Thomson AW, Lu L. Phenotype, function, and *in vivo* migration and survival of allogeneic dendritic cell progenitors genetically engineered to express TGF-beta. *Transplantation* 1998; **66**: 1810-1817
21 **Hayamizu K**, Huie P, Sibley RK, Strober S. Monocyte-derived dendritic cell precursors facilitate tolerance to heart allografts after total lymphoid irradiation. *Transplantation* 1998; **66**: 1285-1291
22 **Khanna A**, Steptoe RJ, Antonysamy MA, Li W, Thomson AW. Donor bone marrow potentiates the effect of tacrolimus on nonvascularized heart allograft survival: association with microchimerism and growth of donor dendritic cell progenitors from recipient bone marrow. *Transplantation* 1998; **65**: 479-485
23 **Lu L**, McCaslin D, Starzl TE, Thomson AW. Bone marrow-derived dendritic cell progenitors (NLDC 145+, MHC class II+, B7-1dim, B7-2-) induce alloantigen-specific hyporesponsiveness in murine T lymphocytes. *Transplantation* 1995; **60**: 1539-1545
24 **Fu F**, Li Y, Qian S, Lu L, Chambers F, Starzl TE, Fung JJ, Thomson AW. Costimulatory molecule-deficient dendritic cell progenitors (MHC class II+, CD80dim, CD86-) prolong cardiac allograft survival in nonimmunosuppressed recipients. *Transplantation* 1996; **62**: 659-665
25 **Lutz MB**, Suri RM, Niimi M, Ogilvie AL, Kukutsch NA, Rossner S, Schuler G, Austyn JM. Immature dendritic cells generated with low doses of GM-CSF in the absence of IL-4 are maturation resistant and prolong allograft survival *in vivo*. *Eur J Immunol* 2000; **30**: 1813-1822
26 **Thomas JM**, Contreras JL, Jiang XL, Eckhoff DE, Wang PX, Hubbard WJ, Lobashevsky AL, Wang W, Asiedu C, Stavrou S, Cook WJ, Robbin ML, Thomas FT, Neville DM Jr. Peritransplant tolerance induction in macaques: early events reflecting the unique synergy between immunotoxin and deoxyspergualin. *Transplantation* 1999; **68**: 1660-1673
27 **Jonuleit H**, Schmitt E, Schuler G, Knop J, Enk AH. Induction of interleukin 10-producing, nonproliferating CD4(+) T cells with regulatory properties by repetitive stimulation with allogeneic immature human dendritic cells. *J Exp Med* 2000; **192**: 1213-1222
28 **Dhodapkar MV**, Steinman RM, Krasovsky J, Munz C, Bhardwaj N. Antigen-specific inhibition of effector T cell function in humans after injection of immature dendritic cells. *J Exp Med* 2001; **193**: 233-238
29 **Bonham CA**, Peng L, Liang X, Chen Z, Wang L, Ma L, Hackstein H, Robbins PD, Thomson AW, Fung JJ, Qian S, Lu L. Marked prolongation of cardiac allograft survival by dendritic cells genetically engineered with NF-kappa B oligodeoxyribonucleotide decoys and adenoviral vectors encoding CTLA4-Ig. *J Immunol* 2002; **169**: 3382-3391
30 **Ouaaz F**, Arron J, Zheng Y, Choi Y, Beg AA. Dendritic cell

development and survival require distinct NF-κB subunits. *Immunity* 2002; **16**: 257-270

31 **Rescigno M**, Martino M, Sutherland CL, Gold MR, Ricciardi-Castagnoli P. Dendritic cell survival and maturation are regulated by different signaling pathways. *J Exp Med* 1998; **188**: 2175-2180

32 **Verhasselt V**, Vanden Berghe W, Vanderheyde N, Willems F, Haegeman G, Goldman M. N-acetyl-L-cysteine inhibits primary human T cell responses at the dendritic cell level: association with NF-κB inhibition. *J Immunol* 1999; **162**: 2569-2574

33 **Mann J**, Oakley F, Johnson PW, Mann DA. CD40 induces interleukin-6 gene transcription in dendritic cells: regulation by TRAF2, AP-1, NF-kappa B, AND CBF1. *J Biol Chem* 2002; **277**: 17125-17138

34 **Giannoukakis N**, Bonham CA, Qian S, Chen Z, Peng L, Harnaha J, Li W, Thomson AW, Fung JJ, Robbins PD, Lu L. Prolongation of cardiac allograft survival using dendritic cells treated with NF-kB decoy oligodeoxyribonucleotides. *Mol Ther* 2000; **1**(5 Pt 1): 430-437

35 **Nouri-Shirazi M**, Guinet E. Direct and indirect cross-tolerance of alloreactive T cells by dendritic cells retained in the immature stage. *Transplantation* 2002; **74**: 1035-1044

36 **Abeyama K**, Eng W, Jester JV, Vink AA, Edelbaum D, Cockerell CJ, Bergstresser PR, Takashima A. A role for NF-kappaB-dependent gene transactivation in sunburn. *J Clin Invest* 2000; **105**: 1751-1759

37 **Sun J**, McCaughan GW, Matsumoto Y, Sheil AG, Gallagher ND, Bishop GA. Tolerance to rat liver allografts. I. Differences between tolerance and rejection are more marked in the B cell compared with the T cell or cytokine response. *Transplantation* 1994; **57**: 1394-1357

38 **McKnight AJ**, Barclay AN, Mason DW. Molecular cloning of rat interleukin 4 cDNA and analysis of the cytokine repertoire of subsets of CD4+ T cells. *Eur J Immunol* 1991; **21**: 1187-1194

39 **Ikejima K**, Enomoto N, Iimuro Y, Ikejima A, Fang D, Xu J, Forman DT, Brenner DA, Thurman RG. Estrogen increases sensitivity of hepatic Kupffer cells to endotoxin. *Am J Physiol* 1998; **274**(4 Pt 1): G669-G676

40 **Stober D**, Schirmbeck R, Reimann J. IL-12/IL-18-dependent IFN-gamma release by murine dendritic cells. *J Immunol* 2001; **167**: 957-965

41 **Qian S**, Lu L, Fu F, Li Y, Li W, Starzl TE, Fung JJ, Thomson AW. Apoptosis within spontaneously accepted mouse liver allografts: evidence for deletion of cytotoxic T cells and implications for tolerance induction. *J Immunol* 1997; **158**: 4654-4661

42 **Qian S**, Lu L, Fu F, Li W, Pan F, Steptoe RJ, Chambers FG, Starzl TE, Fung JJ, Thomson AW. Donor pretreatment with Flt-3 ligand augments antidonor cytotoxic T lymphocyte, natural killer, and lymphokine-activated killer cell activities within liver allografts and alters the pattern of intragraft apoptotic activity. *Transplantation* 1998; **65**: 1590-1598

43 **Lu L**, Li W, Zhong C, Qian S, Fung JJ, Thomson AW, Starzl TE. Increased apoptosis of immunoreactive host cells and augmented donor leukocyte chimerism, not sustained inhibition of B7 molecule expression are associated with prolonged cardiac allograft survival in mice preconditioned with immature donor dendritic cells plus anti-CD40L mAb. *Transplantation* 1999; **68**: 747-757

44 **Lutz MB**, Suri RM, Niimi M, Ogilvie AL, Kukutsch NA, Rossner S, Schuler G, Austyn JM. Immature dendritic cells generated with low doses of GM-CSF in the absence of IL-4 are maturation resistant and prolong allograft survival *in vivo*. *Eur J Immunol* 2000; **30**: 1813-1822

45 **Lee JI**, Ganster RW, Geller DA, Burckart GJ, Thomson AW, Lu L. Cyclosporine A inhibits the expression of costimulatory molecules on *in vitro*-generated dendritic cells: association with reduced nuclear translocation of nuclear factor kappa B. *Transplantation* 1999; **68**: 1255-1263

46 **Yin D**, Ma L, Zeng H, Shen J, Chong AS. Allograft tolerance induced by intact active bone co-transplantation and anti-CD40L monoclonal antibody therapy. *Transplantation* 2002; **74**: 345-354

47 **Takayama T**, Kaneko K, Morelli AE, Li W, Tahara H, Thomson AW. Retroviral delivery of transforming growth factor-beta1 to myeloid dendritic cells: inhibition of T-cell priming ability and influence on allograft survival. *Transplantation* 2002; **74**: 112-119

48 **Takayama T**, Nishioka Y, Lu L, Lotze MT, Tahara H, Thomson AW. Retroviral delivery of viral interleukin-10 into myeloid dendritic cells markedly inhibits their allostimulatory activity and promotes the induction of T-cell hyporesponsiveness. *Transplantation* 1998; **66**: 1567-1574

49 **Stepkowski SM**, Wang ME, Condon TP, Cheng-Flournoy S, Stecker K, Graham M, Qu X, Tian L, Chen W, Kahan BD, Bennett CF. Protection against allograft rejection with intercellular adhesion molecule-1 antisense oligodeoxynucleotides. *Transplantation* 1998; **66**: 699-707

50 **Li W**, Lu L, Wang Z, Wang L, Fung JJ, Thomson AW, Qian S. IL-12 antagonism enhances apoptotic death of T cells within hepatic allografts from Flt3 ligand-treated donors and promotes graft acceptance. *J Immunol* 2001; **166**: 5619-5628

51 **Li W**, Lu L, Wang Z, Wang L, Fung JJ, Thomson AW, Qian S. Costimulation blockade promotes the apoptotic death of graft-infiltrating T cells and prolongs survival of hepatic allografts from FLT3L-treated donors. *Transplantation* 2001; **72**: 1423-1432

52 **Li Y**, Li XC, Zheng XX, Wells AD, Turka LA, Strom TB. Blocking both signal 1 and signal 2 of T-cell activation prevents apoptosis of alloreactive T cells and induction of peripheral allograft tolerance. *Nat Med* 1999; **5**: 1298-1302

53 **Li W**, Fu F, Lu L, Narula SK, Fung JJ, Thomson AW, Qian S. Differential effects of exogenous interleukin-10 on cardiac allograft survival: inhibition of rejection by recipient pretreatment reflects impaired host accessory cell function. *Transplantation* 1999; **68**: 1402-1409

54 **Li W**, Fu F, Lu L, Narula SK, Fung JJ, Thomson AW, Qian S. Systemic administration of anti-interleukin-10 antibody prolongs organ allograft survival in normal and presensitized recipients. *Transplantation* 1998; **66**: 1587-1596

55 **Shirwan H**, Barwari L, Khan NS. Predominant expression of T helper 2 cytokines and altered expression of T helper 1 cytokines in long-term allograft survival induced by intrathymic immune modulation with donor class I major histocompatibility complex peptides. *Transplantation* 1998; **66**: 1802-1809

Edited by Wang XL and Xu FM

PO Box 2345, Beijing 100023, China
Fax: +86-10-85381893
E-mail: wjg@wjgnet.com www.wjgnet.com

World J Gastroenterol 2004;10(16):2369-2372
World Journal of Gastroenterology
 ISSN 1007-9327

• BASIC RESEARCH •

Grey scale enhancement of rabbit liver and kidney by intravenous injection of a new lipid-coated ultrasound contrast agent

Ping Liu, Yun-Hua Gao, Kai-Bin Tan, Zheng Liu, Song Zuo

Ping Liu, Yun-Hua Gao, Kai-Bin Tan, Zheng Liu, Song Zuo, Department of Ultrasound, Xinqiao Hospital, Third Military Medical University, Chongqing 400037, China
Supported by the National Natural Science Foundation of China, No. 30270384
Correspondence to: Professor Yun-hua Gao, Department of Ultrasound, Xinqiao Hospital, Third Military Medical University, Chongqing 400037, China. gaoyunhua116@hotmail.com
Telephone: +86-23-68774698 **Fax:** +86-23-68755631
Received: 2003-12-12 **Accepted:** 2004-01-15

Abstract

AIM: To assess the grey scale enhancement of a new lipid-coated ultrasound contrast agent in solid abdominal organs as liver and kidney.

METHODS: Size distribution and concentration of the lipid-coated contrast microbubbles were analyzed by a Coulter counter. Two-dimensional (2D) second harmonic imaging of the hepatic parenchyma, the inferior vena cava and the right kidney of the rabbits were acquired before and after contrast agent injection. Images were further quantified by histogram in Adobe Photoshop 6.0. Time-intensity curves of hepatic parenchyma, inferior vena cava and renal cortex were generated from the original grey scale.

RESULTS: The 2D images of hepatic parenchyma and cortex of the kidney were greatly enhanced after injection and the peak time could last more than 50 min.

CONCLUSION: This new lipid ultrasound contrast agent could significantly enhance the grey scale imaging of the hepatic parenchyma and the renal cortex for more than 50 min.

Liu P, Gao YH, Tan KB, Liu Z, Zuo S. Grey scale enhancement of rabbit liver and kidney by intravenous injection of a new lipid-coated ultrasound contrast agent. *World J Gastroenterol* 2004; 10(16): 2369-2372
http://www.wjgnet.com/1007-9327/10/2369.asp

INTRODUCTION

New ultrasound contrast consisting of perfluorocarbon microbubbles could enhance grey scale images of parenchymal organs. It provided a new method in diagnosis[1-10]. The development of new ultrasound contrast agent (UCA) has become one of the most promising fields in ultrasound medicine. So far, several UCAs, like Optison[11,12] and Definity[13], have been approved for treatment and become commercially available; many others are still in clinical trials[14-16]. Based on the chemical components of bubble film, UCAs could be divided into four different types: Surfactants[17-19], human albumin[20,21], polymer[22] and lipids[23-25]. The lipids are superior to the others in many aspects: no risk of blood transmitted infection, excellent stability and some tissue-specific targeting, like the reticuloendothelial system. This study was aimed to investigate the effectiveness, reproducibility of a new lipid contrast agent in the enhancement of abdominal parenchymal organs. All the protocols were approved by IRB (Internal Review Board) of Xinqiao Hospital.

MATERIALS AND METHODS

Preparation and analysis of lipid-coated microbubble agent

Liposome, which consists of two kinds of phospholipids and polyethylene glycol, was prepared by lyophilization. Then the lipids were rehydrated with certain media, like glucose and deionized water. The resultant suspension was sonicated by an ultrasound sonicator (YJ 92-II Xinzhi Corp. Hang-zhou, Zhejiang Province). The perfluoropropane was introduced into the suspension during sonication, then it was kept still, until it was separated into two layers, the upper layer was still in white colloid whereas the lower layer was slowly defecated. Then the upper layer of the agent was extracted and analyzed. To acquire size distribution data of the new contrast agent, the milky microbubbles suspension was analyzed by Sysmex KX-21 (Sysmex Corporation, Japan). The surface electric potential and pH of UCA were measured by Zeta 3 000 (Malvern Ltd., United Kingdom).

Animal models

Ten healthy rabbits, weighing 2.0-2.2 kg, were enrolled in this study. The body hair at experimental region was removed for liver and renal scan. Rabbits were anesthetized by intramuscular injection of "Xu Mian Xing" (mainly consisted of haloperidol and made by Changchun University of Agriculture and Prologue) at the dose of 0.15 mL/kg bm, and the intravenous infusion was set up through ear veins. Lipid contrast agent was injected at 0.01 mL/kg bm, and followed by 1 mL saline flush.

Settings of ultrasound equipment

A Siemens Sequoia 512 (Siemens Acuson Co., Mountain View, California) ultrasound system was used in this study. The second harmonic imaging of 6L3 probe at 3.0/6.0 MHz was used. The mechanic index and output power were set at 0.11 and -24 dB, respectively. All the other parameters, like gain, depth, TGC, compress and focus, were kept constant during experiment. Experimental images were digitally recorded. Overall, baseline and 60 min contrast images were acquired. All images were transformed from original DICOM files into JPEG format by Viewpro (Acuson Co.). Grey scale was calculated by histogram in Adobe Photoshop 6.0 (Adobe Co.). Sample area used in the histogram had 1 088 pixels in an ellipse. Time-density curve was generated based on the mean pixel grey scale of hepatic parenchyma and renal cortex.

Pathological examination

All animals were sacrificed by intravenous injection of 10% potassium chloride. The liver, kidney and lung tissues were autopsied and fixed in 40 g/L formaldehyde for H&E stain. All tissue slides were reviewed by pathologists.

Statistical analysis

The grey scale data acquired from liver, inferior vena cava and

renal cortex were expressed as mean±SD. Pre- and post-contrast of liver's and kidney's grey scale data were compared by paired two-tailed Student's *t* test in SPSS 8.0 program. *P* critical value less than 0.05 was considered to be statistically significant.

RESULTS

Contrast agent

The visual appearance of the newly made liposome contrast agent was an opaque milky suspension, and it was slowly delaminated. The microbubble concentration was (7-8)×10^9/mL, and the size distribution was 2 to 10 μm. About 90% of the microbubbles were less than 8 μm (Figure 1). The surface electric potential was -71.2 mV and the pH was 6.42.

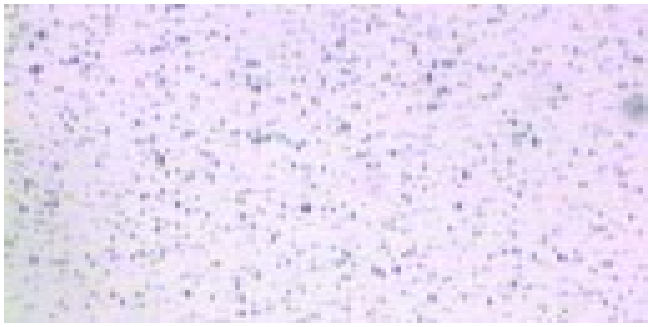

Figure 1 Microbubbles in 400-fold diluted saline (original magnification: ×100).

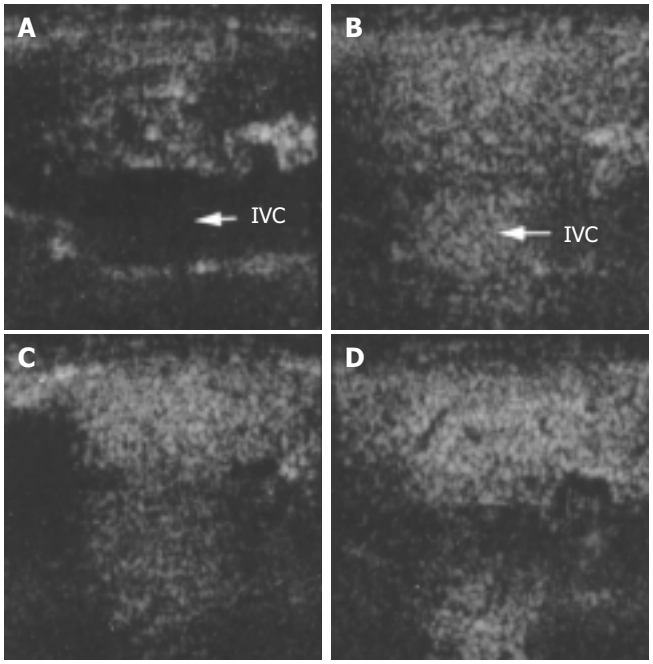

Figure 2 Ultrasound images of liver parenchyma and inferior vena cava (IVC) before and after the injection of microbubbles. A: before injection; B: 30 s after injection; C: 1 min after injection; D: 2 min after injection.

Grey scale enhancement of liver and kidney

The images of both hepatic parenchyma and renal cortex were visually significantly enhanced after intravenous injection of the contrast agent (Figures 2-5). Time-intensity curves of both liver and cortex were elevated and kept at a high level. The grey scale of liver parenchyma (61.2±3.1) 30 s after contrast injection was significantly higher than that of baseline image (38.0±3.0, $P<0.05$). At the time point of 180 s after injection, the grey scale of liver parenchyma reached 83.2±1.8 which was significantly higher than baseline ($P<0.01$). And 54 min after the injection, the liver enhancement remained at 57.8±1.4. One hour after contrast injection, the grey scale dropped to 45.2±1.0, which had no statistical significance. Similar results were observed in the contrast enhancement of renal cortex, and the grey scales were 18.1±3.8 at baseline, 48.8±3.3 ($P<0.01$) 10 s after injection, 27.4±4.1 ($P<0.01$) 56 min after injection, 26.1±3.9 60 min after injection ($P<0.05$). These results confirmed that this lipid microbubbles contrast agent could effectively enhance hepatic parenchyma and renal cortex at a relatively long time.

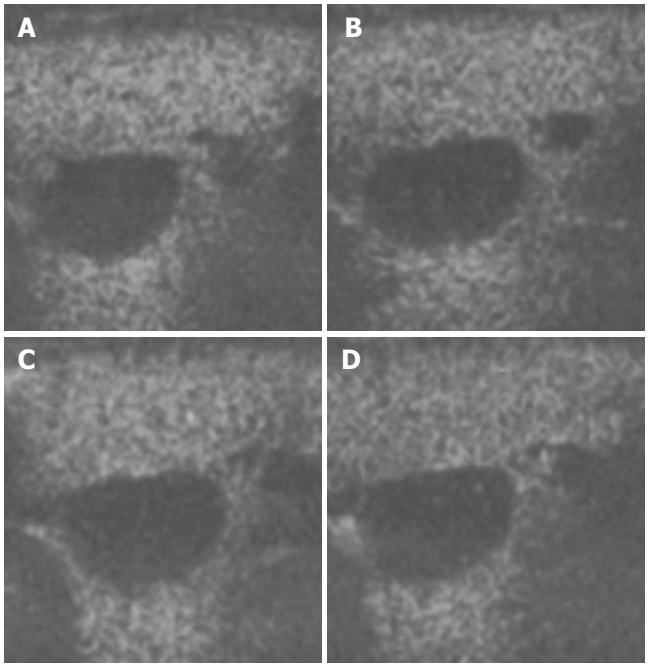

Figure 3 Ultrasound images of liver parenchyma and inferior vena cava (IVC) before and after the injection of microbubbles. A: 15 min after injection; B: 25 min after injection; C: 30 min after the injection; D: 40 min after the injection.

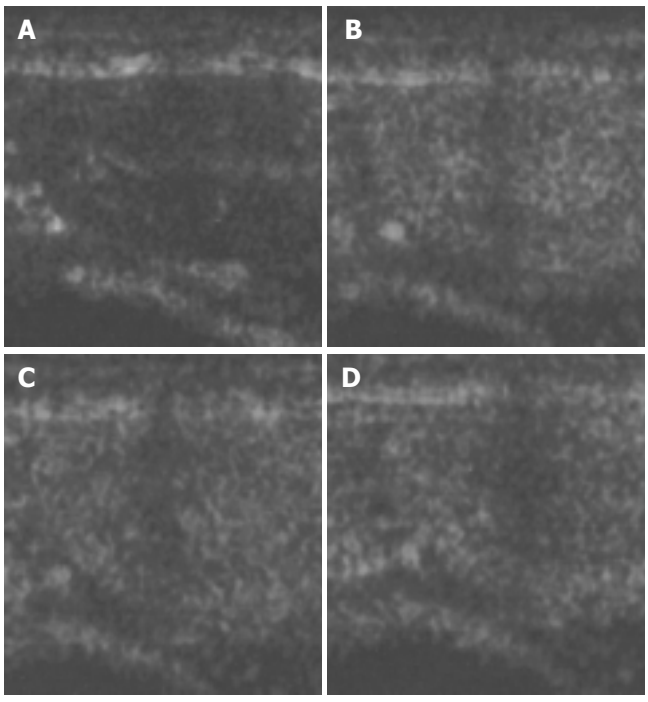

Figure 4 Ultrasound images of renal cortex before and after the injection of microbubbles. A: before injection; B: 30 s after injection; C: 1 min after injection; D: 2 min after injection.

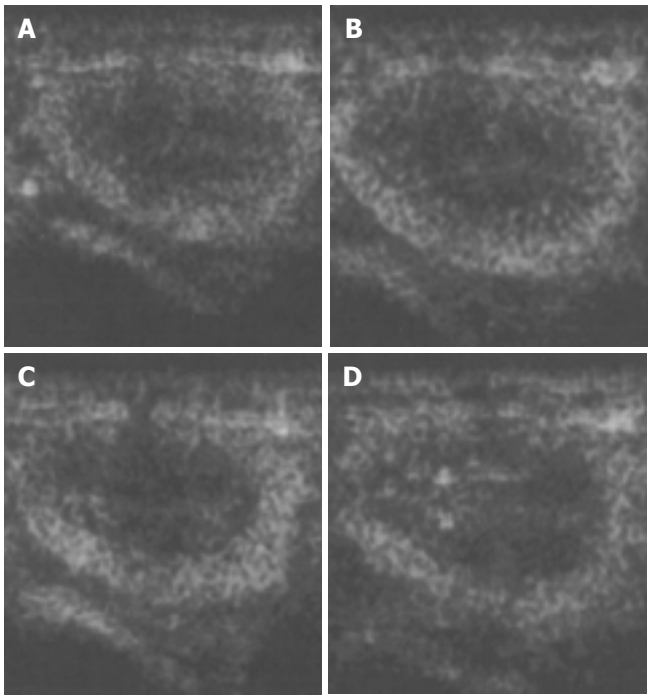

Figure 5 Ultrasound images of the renal cortex after injection of microbubbles. A: 5 min after injection; B: 10 min after injection; C: 30 min after injection; D: 40 min after injection.

At inferior vena cava (IVC), the time-intensity curve was different from that of hepatic parenchyma and renal cortex. The grey scale of IVC significantly rose to 52.5±2.9 20 s after contrast injection which was higher compared with baseline (5.8±1.6). The significant enhancement lasted only 120 s after injection, then diminished gradually and disappeared at 240 s after contrast injection. IVC contrast intensity dropped back to baseline 27 min after injection (17.0±5.2).

Pathological results

All tissues from liver, lung, and kidney were normal in histology, and there was no sign of air embolism or infarction spot.

DISCUSSION

Lipid-coated microbubbles were mainly composed of several biocompatible phospholipids that had excellent stability and non-bioactive components. The lipids had been widely used in the preparation of ultrasound contrast agent, liposome and other drugs. In this study, a new ultrasound contrast agent based on lipids was prepared and showed excellent stability in the enhancement of hepatic parenchyma and renal cortex at a minimal dose of 0.01 mL/kg bm. Grey scale enhancement could last more than 50 min from both visual assessment and quantitative statistical analysis. This enhancement was longer than some previous reports, which were about 5-15 min[19,25,26]. Also, the time-intensity curves of hepatic parenchyma and renal cortex were quite different from that of inferior vena cava. These microbubbles tended to be stable in parenchyma, rather than in circulation, as the time-density curve from IVC showed a 200-s wash-in and wash-out enhancement.

According to some reports[27,28] and our experiment[29], we assumed that the prolonged enhancement was due to the uptake of microbubbles by the reticuloendothelial system in liver. But this could not explain the prolonged enhancement in the kidney, which is not rich of reticuloendothelial system. There might be some other reasons. Since the peak contrast intensities of liver parenchyma and cortex appeared much later than that of inferior vena cava, they were 12 min, 6 min and 30 s, respectively, it indicated that after the peak contrast in circulation there was another peak contrast in solid organs, and it was presumed to be the accumulation of microbubbles in hepatic sinusoids or capillary bed in cortex. As we know, hepatic parenchyma is consisted of hepatic sinusoids and renal cortex is mostly consisted of glomeruli. They are both rich in capillaries. Meanwhile, the blood flow in hepatic sinusoids and glomeruli is much slower than that in inferior vena cava. So, the microbubbles could easily be accumulated in capillary bed, which resulted in the prolonged enhancement of liver and kidney.

As IVC grey scale at 27 min postinjection was lower than that before injection, the hepatic parenchyma might block ultrasound transmission to IVC by condensed bubble's attenuation, and this could produce visually lower IVC echo.

In this study, the new lipids ultrasound contrast agent was long-term stable in enhancement of liver parenchyma and renal cortex. The mean size of the microbubbles was less than 8 μm, which was smaller than that of red blood cell, and thereby it was safe for intravenous injection. Pathologically, all the tissues from liver, lung, and kidney were normal in histology, and there were no signs of air embolism or infarction spot.

In comparison with other lipid-coated microbubbles[30], this contrast agent had a higher bubble concentration and a longer stability in parenchymal organs. The reason for this might attribute to the reconstituted membrane of the microbubbles. Polyethylene glycol could protect phagocytosis from Kupffer cell, and it could exist in hepatic sinusoid longer. Tween 80, a kind of surfactant, which has never been used in other lipid microbubbles contrast agent, may increase the bubbles or microbubbles concentration.

Although this new lipid-based contrast agent exhibited a prolonged enhancement, the true reason has not been clarified. Further studies are needed to investigate the mechanism of long-lasting enhancement.

REFERENCES

1 **Lindner JR,** Song J, Christiansen J, Klibanow AL, Xu F, Ley K. Ultrasound assessment of inflammation and renal tissue injury with microbubbles targeted to P-Selectin. *Circulation* 2001; **104:** 2107-2112
2 **Bang N,** Nielsen MB, Rasmussen AN, Osterhammel PA, Pedersen JF. Hepatic vein transit time of an ultrasound contrast agent: simplified procedure using pulse inversion imaging. *Br J Radiol* 2001; **74:** 752-755
3 **Ramnarine KV**, Kyriakopoulou K, Gordon P, McDicken NW, McArdle CS, Leen E. Improved characterisation of focal liver tumours: dynamic power Doppler imaging using NC100100 echo-enhancer. *Eur J Ultrasound* 2000; **11:** 95-104
4 **Marelli C.** Preliminary clinical experience in cardiology with sonazoid. *Am J Cardiol* 2000; **86**(Suppl): 10G-13G
5 **Albrecht T,** Blomley MJK, Cosgrove DO, Taylor-Robinson SD, Jayaram V, Eckersley R, Urbank A, Butler-Barnes J, Patel N. Non-invasive diagnosis of hepatic cirrhosis by transit-time analysis of an ultrasound contrast agent. *Lancet* 1999; **353:** 1579-1583
6 **Du WH,** Yang WX, Wang X, Xiong XQ, Zhou Y, Li T. Vascularity of hepatic VX2 tumors of rabbits: Assessment with conventional power Doppler US and contrast enhanced harmonic power Doppler US. *World J Gastroenterol* 2003; **9:** 258-261
7 **Lindner JR.** Detection of inflamed plaques with contrast ultrasound. *Am J Cardiol* 2002; **90**(Suppl): 32L-35L
8 **Wang WP,** Ding H, Qi Q, Mao F, Xu ZZ, Kudo M. Characterization of focal hepatic lesions with contrast-enhanced C-cube gray scale ultrasonography. *World J Gastroenterol* 2003; **9:** 1667-1674
9 **Eyding J,** Wilkening W, Postert T. Brain perfusion and ultrasonic imaging techniques. *Eur J Ultrasound* 2002; **16:** 91-104
10 **Feril LB,** Kondo T, Zhao QL, Ogawa R, Tachibana K, Kudo N, Fujimoto S, Nakamura S. Enhancement of ultrasound-induced

apoptosis and cell lysis by echo-contrast agents. *Ultrasound Med Biol* 2003; **29:** 331-337

11 **Yamaya Y**, Niizeki K, Kim J, Entin PL, Wagner H, Wagner PD. Effects of optison® on pulmonary gas exchange and hemodynamics. *Ultrasound Med Biol* 2002; **28:** 1005-1013

12 **Masugara H**, Petcrs B, Lafittc S, Strachan MG, Ohmori K, DcMarin AN. Quantitative assessment of myocardial perfudion during graded coronary stenosis by real-time myocardial contrast echo refilling curves. *J Am Coll Cardiol* 2001; **37:** 262-269

13 **Kitzman DW,** Goldman ME, Gillam LD, Cohen JL, Aurigemma GP, Gottdiener JS. Efficacy and safety of the novel ultrasound contrast agent perflutren (definity) in patients with suboptimal baseline left ventricular echocardiographic images. *Am J Cardiol* 2000; **86:** 669-674

14 **Driven HA,** Rasmussen H, Johnson H, Videm S, Walday P, Grant D. Intestinal and hepatic lesions in mice, rats, and other laboratory animals after intravenous administration of gas-carrier contrast agents used in ultrasound imaging. *Toxicol Appl Pharmacol* 2003; **188:** 165-175

15 **Moran CM,** Anderson T, Pye SD, Sboros V, McDicken WN. Quantification of microbubble destruction of three fluorocarbon-filled ultrasonic contrast agents. *Ultrasound Med Biol* 2000; **26:** 629-639

16 **Moran CM,** Watson RJ, Fox KAA, McDiken WN. *In vitro* acoustic characterisation of four intravenous ultrasonic contrast agents at 30MHz. *Ultrasound Med Biol* 2002; **28:** 785-791

17 **Marelli C.** Preliminary clinical experience in cardiology with Sonazoid. *Am J Cardiol* 2000; **86**(Suppl): G10-13

18 **Yokoyama N,** Schwarz KQ, Chen X, Steinmetz SD, Becher H, Schimpky C, Schlief R. The effect of echo contrast agent on doppler velocity measurements. *Ultrasound Med Biol* 2003; **29:** 765-770

19 **Basude R,** Duckworth JW, Wheatley MA. Influence of environmental conditions on a new surfactant-based contrast agent: ST68. *Ultrasound Med Biol* 2000; **26:** 621-628

20 **Porter TR,** Xie F, Kricsfeld A, Kilzer K. Noninvasive identification of acute myocardial ischemia and reperfusion with contrast ultrasound using intravenous perfluoropropane-exposed sonicated dextrose albumin. *J Am Coll Cardiol* 1995; **26:** 33-40

21 **Bekeredjian R,** Behrens S, Ruef J, Dinjus E, Unger E, Baum M, Kuecherer HF. Potential of gold-bound microtubules as a new ultrasound contrast agent. *Ultrasound Med Biol* 2002; **28:** 691-695

22 **Wei K,** Crouse L, Weiss J, Villanueva F, Schiller NB, Naqvi TZ, Siegel R, Monaghan M, Goldman J, Aggarwal P, Feigenbaum H, Demaria A. Comparison of usefulness of dipyridamole stress myocardial contrast echocardiography to technetium-99m sestamibi single-photon emission computed tomography for detection of coronary artery disease (PB127 Multicenter Phase 2 Trial results). *Am J Cardiol* 2003; **91:** 1293-1298

23 **Bjerknes K,** Braenden JU, Smistad G, Agerkvist I. Evaluation of different formulation studies on air-filled polymeric microcapsules by multivariate analysis. *Inter J Pharma* 2003; **257:** 1-14

24 **Basilico R,** Blomley MJK, Harvey CJ, Filippone A, Heckemann RA, Eckersley RJ, Cosgrove DO. Which continuous US scanning mode is optimal for the detection of vascularity in liver lesions when enhanced with a second generation contrast agent? *Euro J Radiol* 2002; **41:** 184-191

25 **Bokor D.** Diagnostic efficacy of SonoVue. *Am J Cardiol* 2000; **86**(Suppl): 19G-24G

26 **Totaro R**, Baldassarre M, Sacco S, Marini C, Carolei A. Prolongation of TCD-enhanced doppler signal by continuous infusion of levovist. *Ultrasound Med Biol* 2002; **28:** 1555-1559

27 **Quaia E,** Blomley MJK, Patel S, Harvey CJ, Padhani A, Price P, Cosgrove DO. Initial observations on the effect of irradiation on the liver-specific uptake of Levovist. *Eur J Radiol* 2002; **41:** 192-199

28 **Heckemann RA,** Harvey CJ, Blomley MJK, Eckersley RJ, Butler-Barnes J, Jayaram V, Cosgrove D. Enhancement characteristics of the microbubble agent Levovist: reproducibility and interaction with aspirin. *Eur J Radiol* 2002; **41:** 179-183

29 **Liu P,** Gao YH, Tan KB, Zuo S, Liu Z. Enhanced imaging of the rabbit liver using the self-made liposome contrast agent: an earlier experimental study. *Zhongguo Chaosheng Yixue Zazhi* 2003; **19**: 4-6

30 **Bouakaz A,** Krenning BJ, Vletter WB, Cate FJ, Jong ND. Contrast superharmonic imaging: A feasibility study. *Ultrasound Med Biol* 2003; **29:** 547-553

Edited by Chen WW **Proofread by** Zhu LH and Xu FM

PO Box 2345, Beijing 100023, China
Fax: +86-10-85381893
E-mail: wjg@wjgnet.com www.wjgnet.com

World J Gastroenterol 2004;10(16):2373-2378
World Journal of Gastroenterology
 ISSN 1007-9327

• BASIC RESEARCH •

Intestinal barrier damage caused by trauma and lipopolysaccharide

Lian-An Ding, Jie-Shou Li, You-Sheng Li, Nian-Ting Zhu, Fang-Nan Liu, Li Tan

Lian-An Ding, Jie-Shou Li, You-Sheng Li, Nian-Ting Zhu, Fang-Nan Liu, Li Tan, Jinling Hospital, Nanjing University Medical School, Nanjing 210002, Jiangsu Province, China
Correspondence to: Lian-An Ding, Associate Professor, Jinling Hospital, Nanjing University Medical School, 305 East Zhongshan Road, Nanjing 210002, Jiangsu Province, China. dlahaolq@hotmail.com
Telephone: +86-532-2911324 **Fax:** +86-532-2911840
Received: 2003-08-05 **Accepted:** 2003-10-27

Abstract

AIM: To investigate the intestinal barrier function damage induced by trauma and infection in rats.

METHODS: Experimental models of surgical trauma and infection were established in rats. Adult Sprague-Dawley rats were divided into 4 groups: control group (n = 8), EN group (n = 10), PN group (n = 9) and Sep group (n = 8). The rats in PN and Sep groups were made into PN models that received isonitrogenous, isocaloric and isovolumic TPN solution during the 7-d period. Rats in EN and Sep groups received laparotomy and cervical catheterization on day 1 and received lipopolysaccharide injection intraperitoneally on d 7. On the 7th day all the animals were gavaged with lactulose and mannitol to test the intestinal permeability. Twenty-four hours later samples were collected and examined.

RESULTS: The inflammatory responses became gradually aggravated from EN group to Sep group. The mucosal structure of small intestine was markedly impaired in PN and Sep groups. There was a low response in IgA level in Sep group when compared with that of EN group. Lipopolysaccharide injection also increased the nitric oxide levels in the plasma of the rats. The intestinal permeability and bacterial translocation increased significantly in Sep group compared with that of control group.

CONCLUSION: One wk of parenteral nutrition causes an atrophy of the intestinal mucosa and results in a moderate inflammatory reaction in the rats. Endotoxemia aggravats the inflammatory responses that caused by laparotomy plus TPN, increases the production of nitric oxide in the body, and damages the intestinal barrier function.

Ding LA, Li JS, Li YS, Zhu NT, Liu FN, Tan L. Intestinal barrier damage caused by trauma and lipopolysaccharide. *World J Gastroenterol* 2004; 10(16): 2373-2378
http://www.wjgnet.com/1007-9327/10/2373.asp

INTRODUCTION

Severe infection is still the main cause of death in critical illnesses such as severe trauma, burns and in massive use of immunosuppressive medicines. The endotoxin produced by G- bacilli is the important factor for the impairment of tissues and cells of the body. It could damage the systemic immunity, impair the intestinal barrier function, increase the mucosal permeability, and hence cause enterogenous infection, a phenomenon known as bacteria translocation[1,2]. The impairments aggravate the primary infection, which might cause multiple organ dysfunction syndrome (MODS), and even death. The alterations in pathophysiology and immunology when endotoxemia occurs, are very important for us to evaluate the impaired gut barrier function.

In routine clinical practice, some patients would complicate with infections after operation and trauma. Most of them can be cured, but a few of these infections would last for a longer time. Based on the consideration of the latter being a phenomenon of bacterial translocation as a result of the damage of intestinal barrier function, we conducted this animal experiment so as to investigate if there were gut barrier damage and bacterial translocation in such instances.

MATERIALS AND METHODS

Experimental animals and grouping

Adult, healthy male Sprague-Dawley rats, with body mass of 150-180 g (supplied by Shanghai Experimental Animal Center, Chinese Academy of Sciences) were used. The rats were fed for over 1 wk in our laboratory for adaptation and then put into metabolic cages for 5-7 d. The temperature in the animal rooms was 17-21°C with proper humidity (about 60%) and illumination of 12 h/d (6:00-18:00). During the adaptation period all the rats were fed with regular rat chow and tap water *ad libitum*. When the rat's body mass reached 200-300 g, 33 rats were chosen randomly and divided into 4 groups: (1) control group (n = 8), which were fed rat chow and tap water freely; (2) EN group (n = 10), in which a central venous catheter was inserted into animals' superior vena cava through right jugular vein under anaesthesia, and connected to the swivel apparatus. The rats also received laparotomy and were fed the chow freely; (3) PN group (n = 9), which were infused with a whole nutrients solution through a central venous catheter, and with drinking water ad libitum; (4) Sep group (n = 8) in which an exploratory laparotomy and central venous catheterization served as the trauma. After this, TPN was their sole nutrition source plus drinking water ad lib. On the 7th day 5 mg/kg of lipopolysaccharide was injected intraperitoneally for EN and SEP groups. PN and Sep Groups received isonitrogenous, isocaloric and isovolumic TPN solution during the 7-d period. All the protocols and procedures were approved by our University Committee of Animal Experiment Administration.

Intravenous nutrients and other relevant chemicals

TPN ingredients About 11.4% compound amino acids injection (Novamin), 20% medium-long chain fat emulsion (Lipovenoes MCT), multivitamin mixture (Soluvit, Vitalipid) and a trace element mixture (Addamel) were purchased from Sino-Sweden and Fresenius Pharmaceutical Corp. LTD.

Chemicals and reagents Lipopolysaccharide (LPS, from *E. coli*, 055: B5) was purchased from Sigma Co.; NO Test Kit was purchased from Promega Co., USA. Immunohistochemistry (T cell subgroups measurement) reagents were purchased from Serotec Ltd., Germany and IgA, Bethyl Co., USA.

Experimental model

Operation procedures Under anaesthesia with 100 mg/kg of ketamin injected into the animals intraperitoneally, the TPN model was established and a rotary transfusion apparatus was

used for TPN infusion[3]. For surgical trauma, after shaving the hair on the abdomen, an incision (about 4 cm in length) was made and the whole abdominal cavity was explored and examined for about 5 min from the epigastrium to the pelvic cavity. The incision was sutured in double layers with silk suture No. 1. The operation was done under aseptic conditions.

TPN solution The rats were put in the metabolic cages after surgical recovery. Each rat received 230 kcal/kg body mass of calories and 1.42 g nitrogen/kg each day in 50 mL of TPN solution. The ratio of glucose to lipid in this solution is 2:1, and nonprotein calorie to nitrogen (kcal/g), 137:1. Multivitamins, electrolytes, trace elements and 500 units of heparin were also included in the TPN solution. All the nutrient solutions were prepared under aseptic conditions daily and the infusion was done with an injecting micropump continuously and uniformly during 24 h each day. TPN infusion was started immediately after recovery from the laparotomy. On the first and last days of the experiment, each rat was given half of the total calories without any changes of other TPN ingredients.

Induction of endotoxemia On the 7th d of the experiment, 5 mg/kg of LPS in 5 mL of sterile distilled water was injected into the animals' peritoneal cavity to cause a sepsis state.

Lactulose/mannitol solution gavage On the 7th d of the experiment, 66 mg of lactulose and 50 mg of mannitol dissolved in 2 mL of normal saline were gavaged. Twenty-four hour urine was collected, the volume recorded and 0.2 mL of mercury salicylosulfide added. Then 5 mL of the urine specimen was stored at -20 °C until measurement.

Sample preparation and measurements

Twenty-four hours after gavaging with lactulose and mannitol and injecting endotoxin, 100 mg/kg of ketamine was injected intraperitoneally as an anesthetic. After the laparotomy was done, tissue and blood samples were collected and gross and laboratory examinations were performed.

Bacteriological test Blood 0.5 mL from the portal vein was drawn for culture. One gram of anterior lobe liver tissue and about 0.2-0.5 g mesenteric lymph nodes were excised. Each sample was put in a tissue homogenizer and 1.5 mL of normal saline was added before they were homogenized. The specimens were sent to a microbiological laboratory for aerobic culture and bacterial identification by morphological and bacteriological analyzer.

Bacterial culture (1) 10 μL homogenates of the lymph nodes and liver were separately taken and put on blood agar plates. Another 10 μL lymph nodes and liver homogenates were mixed with 10 mL saline for a dilution and the diluted samples were inoculated also on blood agar plates. (2) 0.5 mL of portal vein blood was inoculated into 4.5 mL of common broth for bacterial enrichment 16-18 h, then 20 μL of the enrichment solution was inoculated on blood agar plates. (3) The cultured media were put in a CO_2 incubator at 35 °C for 24-48 h. If there was no bacterial growth, they would be regarded as negative; but if there was growth, it would be further identified.

Identification of bacteria First, Gram-stained smears were made to determine whether they were cocci or bacilli and G^+ or G^-. Second, identifications were made using bacteriological analyzer of Vitek-32 (Bio Merieux Vitek, Inc., USA). Gram-positive cocci were tested with GPI card, Gram-negative bacilli, with GNI card, and fungi, YBC card.

Preparation of small intestine specimens The whole small intestine below the Treitz ligament was excised and immediately placed on ice cold of 9 g/L saline. The intestine was opened longitudinally and the contents of the intestine were washed out with icy saline. Two cm of proximal jejunum and distal ileum were cut and put into a 40 g/L neutral formaldehyde solution promptly and sent to be examined histologically. About 5 cm intestine segments from the upper, middle and lower sections were resected and then the surfaces of the mucosa were dried with cotton swabs. The mucous membrane of the icy specimens was scraped, weighed and divided into two equal parts. They were immediately put into liquid nitrogen and then stored at -70 °C.

Histological examination of the intestinal mucosa Specimens were embedded in paraffin, 4 μm sections were cut and stained with H.E., analyzed with an HPIAS-1000 Multimedia Color Analysis System. Three low power (10×10) fields in each section were observed. The lengths of 5 villi, the depth of 5 crypts and the thickness of the mucosa at 5 sites were analyzed. The average value was calculated and documented. All the calculation was done double-blindly by two experienced pathologists.

Immunohistochemical analysis of T cell subpopulation[4] Specimens were embedded in paraffin, 4 μm sections were cut and stained with H.E., T cell subsets were examined by immunohistochemical SP method. The total T lymphotocyte and its positive stained subpopulations (CD3, CD4, CD8) were counted in 10 whole villi in each section. The ratios and rates were then calculated. All the calculation was done double-blindly by two experienced pathologists.

Blood sampling Three milliliter blood from the right cardiac ventricle was drawn and 1 250 u heparin added. The blood was centrifuged and the serum stored at -70 °C. Then the animals were sacrificed by exsanguination.

Lactulose/mannitol test The lactulose and mannitol concentrations in the preserved urine sample were measured by a high-performance liquid chromatograph (Waters Co., USA). The ion-exchange column used was purchased from Transgenomic Co., USA. The ratio between the two sugars was then calculated. The test was to measure the amount of excreted dual sugars in urine of 24 h. Because these two kinds of saccharide nearly neither metabolize nor synthesize in the body, amounts of the two sugars being excreted from urine reflect the "leaking" degree of the intestine, or permeable extent of the intestine. The molecular weight of these two saccharides is different. The test error can be reduced when using two sugars of different molecular weight than using one only for the test. If the ratio of the two sugars' percentage in tested group was significantly bigger than that of normal control group, it could be concluded that the intestinal permeability in tested animals increased.

Determination of IgA The frozen samples of blood plasma and mucosa of the small intestine were melted to room temperature and 1 mL normal saline was then added to the melted 100 mg of mucosa before the homogenates were made, and then the concentration of IgA in their supernatants after centrifugation below 4 °C was measured. The results were shown as IgA μg/mL of blood plasma and IgA μg/g of small intestine mucosa.

Determination of NO The frozen samples of blood plasma and mucosa of the small intestine were melted to room temperature and concentration of NO in them was measured with the enzymatic method (Griess Reaction)[5] .The results were shown as NO μmol/L of blood plasma and NO μmol/g of small intestine mucosa.

Statistical analysis

All the values were expressed as the mean±SE. One-way ANOVA was used to check the differences between groups. Chi-square test was used to check the differences of bacterial translocation rates between groups. When P was less than 0.05, the difference was considered statistically significant. The degree of correlation was described using Pearson correlation coefficient. Software SPSS10.0 was used in all statistical tests.

RESULTS

General animal manifestation

All the rats except those in the normal group appeared to have

symptoms in different degrees, such as lethargy, idleness, ruffling of hair, stop drinking and grossly concentrated urine. Some rats appeared very slow in their responses to sound stimulations and also had diarrhea. Their eyes appeared glazed with crusting exudates. These symptoms were prominent during the 5 to 15 h following LPS injection. There was no statistical difference in mortality within 24 h after LPS injection between EN and Sep groups.

Complete blood cell count

The total number of leukocytes and the number of neutrophils in PN group [(14.97±2.704)×10^9/L and (6.82±2.254)×10^9/L] was more than those of control group [(7.59±0.379)×10^9/L and (2.34±0.568)×10^9/L]. On the contrary, Sep group rats showed a low response in cell count [(8.9±0.82)×10^9 and (4.35±0.92)×10^9/L]. Platelet count in groups of EN, PN and Sep [(586.5±65.03)×10^9, (483.33±94.62)×10^9 and (277.5±44.87)×10^9/L respectively] decreased markedly as compared with that of control group [(928.7±33.89)×10^9/L].

Body weight

At the beginning of the experiment there was no difference in the body mass of the animals. At the end of the experiment, the body mass increase was 32.38±3.39 g in the control group. The body mass of other three groups decreased; it was 33.88±3.19 g of loss in Sep group, the greatest among them.

Morphology and morphometry of small intestinal mucous membrane

The degree of damage of the villi and crypts and the thinning of the mucous membrane in jejunum and ileum were most significant in Sep group among the animals (Figures 1, 2).

Concentrations of NO in blood plasma and small intestinal mucosa

Concentrations of NO in blood plasma increased significantly after LPS injection (groups EN and SEP), whereas it was not evident in mucous membrane of small intestine (Table 1).

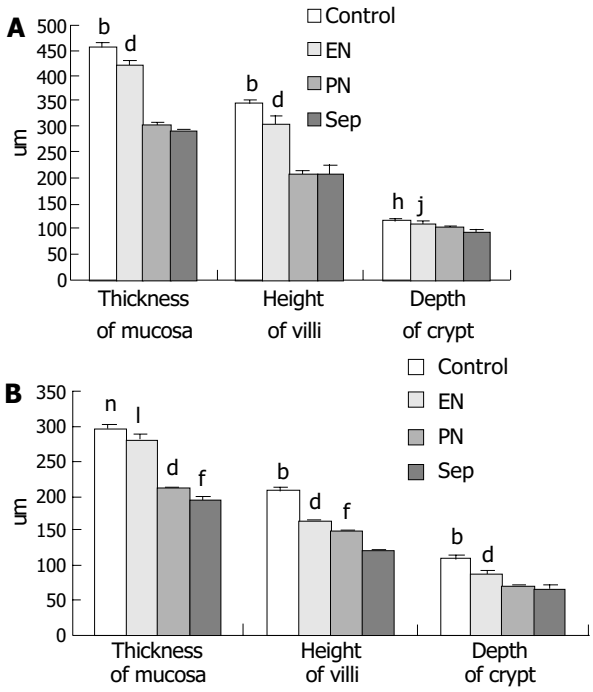

Figure 2 Morphometry for structure of small intestine mucosa (mean±SE). $^bP<0.001$ *vs* EN, PN and Sep gorups; $^dP<0.001$ *vs* PN and Sep gorups; $^fP<0.01$ *vs* Sep gorup; $^hP<0.005$ *vs* PN and Sep gorups; $^jP<0.001$ *vs* Sep group; $^aP<0.02$ *vs* Sep gorup; $^nP<0.01$ *vs* EN gorup; $^lP<0.001$ *vs* PN and Sep groups.

IgA levels in plasma and small intestinal mucosa

IgA level was highest in blood plasma and intestinal mucosa in EN group among the animals (Table 2).

CD3 lymphocyte and CD4/CD8 ratio

There was no difference in CD3 population among the groups

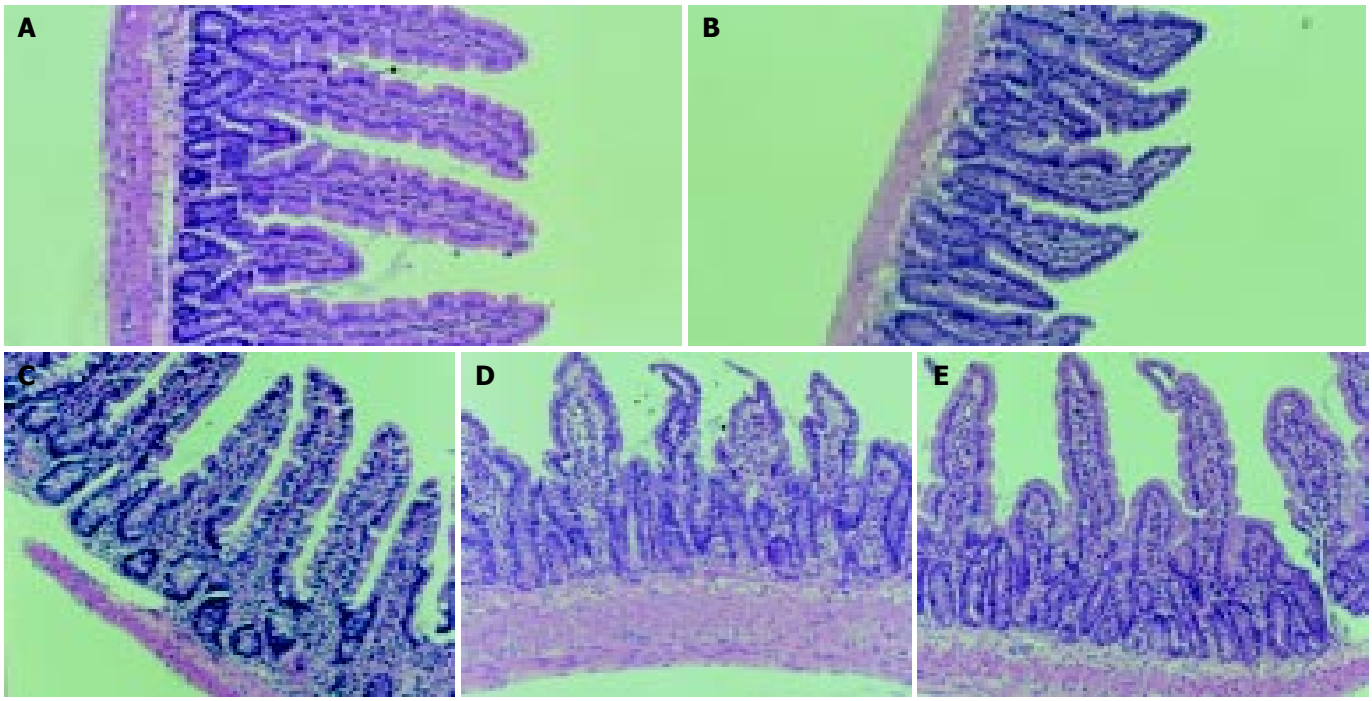

Figure 1 Alterations in architecture of small intestinal mucosa. (HE staining, original magnification: ×100). A: Normal mucous membrane of jejunum in control rats. B: Normal mucous membrane of ileum in control rats. C: Histological changes of jejunal mucosa of group T1 rats. The villi become sparser than those in control. The height and shape of villi are normal on the whole. D: Histological changes of ileal mucosa in PN group rats. The section shows a severe atrophy in mucosal structure. The villi become shorter, blunt and swollen. E: Histological changes of jejunal mucosa of Sep group. The villi are sparse and shorter than those of control group.

but CD4/CD8 ratio in EN and PN groups was higher than that of control group. There was no significant difference in ratio of CD4 to CD8 between Sep group and control group.

Table 1 Concentrations of NO in blood plasma and in intestinal mucosa

Group	*n*	BP(μmol/L)	SIM(μmol/g)[1]
Control	8	38.63±8.75[b]	39.19±2.68
EN	10	103.39±10.18	67.19±6.67
PN	9	63.06±23.33[a]	66.90±6.25
Sep	8	113.33±30.47	53.10±2.16

Values are expressed as mean±SE; BP, blood plasma; SIM, mucous membrane of small intestine; [b]$P<0.01$ *vs* EN group and Sep group; [a]$P<0.05$ *vs* Sep group: [1]There was no statistical significance in NO levels in mucous membrane of small intestine among groups; $r = 0.485$, $P = 0.515$, there was no correlation of NO concentration in mucous membrane with that in blood plasma.

Table 2 IgA levels in blood plasma and small intestinal mucosa

Group	*n*	Blood plasma IgA (μg/mL)	Mucosa tissue IgA (μg/g)
Con	8	146.73±18.03[a]	507.48±59.18[a]
EN	10	260.37±38.54[b]	733.51±81.42[b]
PN	9	133.94±21.47	489.38±14.27
Sep	8	194.52±39.31	511.89±52.33

Data are expressed as mean±SE; [a]$P<0.05$ *vs* EN group; [b]$P<0.01$ *vs* PN group; $r = 0.998$, $P = 0.002$, $P<0.003$, there was a positive correlation in IgA level in blood plasma with that in intestinal mucosa.

Lactulose/mannitol (L/M) test

The L/M ratio showed a significant increment in all rats except those in control group animals (Table 3).

Table 3 Dual sugar (lactulose/mannitol) test

Group	*n*	Rate of lactulose	Rate of mannitol	Ratio of L/M
Control	8	0.0097±0.0027	0.0202±0.0026	0.4789±0.1001
EN	10	0.0213±0.0035	0.0283±0.0020	0.7981±0.1559
PN	9	0.0981±0.0374	0.0723±0.0285	1.4494±0.2670
Sep	8	0.1466±0.0572	0.0361±0.0089	4.0088±0.8893[b]

Data are expressed as mean±SE. Rate of lactulose (or mannitol): denotes the rate of lactulose (mannitol) amount excreted in urine with that gavaged; Ratio of L/M denotes the ratio of the above two rates. [b]$P<0.01$ *vs* control, EN and PN groups.

Table 4 Examination of bacterial translocation

Group	*n*	MLN	Liver	PVB	RBT	Log_{10} TB±SD
Control	8	3/8	0/8	0/8	12.5% (3/24)	0.5414±0.288
EN	10	4/10	2/10	3/10	30.0% (9/30)	1.6444±0.349
PN	9	5/9	4/9	4/9	48.15% (13/27)[b]	2.3279±0.433[b]
Sep	8	6/8	7/8	7/8	83.33% (20/24)[d]	3.2815±0.483[d]

Values are expressed as mean±SE; MLN: Mesenteric lymph node; PVB: Portal venous blood; RBT: Rate of bacterial translocation; TB: Translocated bacteria; 3/8: Numerator represents the positive samples of bacteria culture; denominator represents the number of animals enrolled. [b]$P<0.01$ *vs* Control; [d]$P<0.01$ *vs* control, EN and PN groups; $r=0.979$, $P=0.021$, $P<0.03$, there was a positive correlation of rate of bacterial translocation with the value of Log_{10} translocated bacteria.

Bacterial identification and bacterial translocation

The results of bacterial culture were labeled as positive when the CFU found per gram of tissue (or mL of blood) was more than or equaled to 10^3[6]. In Sep group the rate of bacterial translocation was the highest. The logarithm of the number of translocated bacteria correlated positively with the rate of bacterial translocation (Table 4). The bacteria translocated, in order of frequency, were proteus, *E. coli*, enterococcus and other Gram-negative bacteria. One or two, even three bacterial groups were usually recovered from the same organ when translocation was present.

DISCUSSION

Recent studies have shown that the gastrointestinal tract is not only an organ for nutrient digestion and absorption, but also an organ for systemic immunity and at the same time performs a barrier function. It prevents bacteria and endotoxin in the lumen of the GI tract from entering the blood circulation (bacterial/endotoxin translocation). At the time when body and/or organ tissues are injured by trauma, burns, infection, ischemia/reperfusion and surgical operation strikes, the intestinal barrier malfunction occurs and enterogenous infection ensues. Thus, it aggravates the original illness and makes it persistent, causing multiple organ dysfunction syndrome (MODS) and even death[1, 2,6-9]. Based on these, Wilmore named the GI tract as "a central organ after surgical stress"[3].

Most infections that take place in abdominal surgery are commonly caused by G^- bacilli or polyinfection, which brings harm to body through endotoxin. Endotoxin (LPS) plays a very important role during stress. *In vivo* and *in vitro* studies in animals and humans indicated that LPS could cause damage to the intestinal barrier function and cause bacterial translocation[1,3,6]. The aim of the experiment was to mimic the clinical cases above. In the experiment, we had laparotomy plus parenteral nutrition as trauma. Sick manifestations emerged after a few days' parenteral nutrition. One wk parenteral nutrition was obviously an inflammatory stimulus to rats. Laparotomy was a minor injury, whereas it was an intermediate degree of impairment when administering laparotomy plus 1-wk parenteral nutrition to rats. Clinical manifestations in rats confirmed the point of view. We injected lipopolysaccharide to rats intraperitoneally after 1-wk parenteral nutrition so as to mimic infested clinical situations after trauma. There were two main harmful stimuli, parenteral nutrition and LPS injection, included in our experiment. We have had another two control groups, the group of parenteral nutrition (PN) and the group of LPS injection with enteral feeding (EN) except the normal control one so as to investigate and compare the damage degree of different injury stimuli to gut barrier.

Investigations have reported the relation of TPN with bacterial translocation. Qin and his colleagues[10] discovered that parenteral feeding in a 7-d period in experimental pancreatitis of dogs caused a significant damage of intestinal mucosa and bacterial translocation (BT) when compared with that of given isonitrogenous and isocaloric enteral feeding. Similar results were reported by other scholars[11,12]. A study even revealed that 2-d TPN resulted in BT in SD rats[13]. In their investigation patients underwent thoracic esophagectomy, Takagi *et al*. presented that in patients receiving TPN from 1 wk before operation to 2 wk after operation, serum levels of IL-6, IL-10 and endotoxin were higher than that of receiving isonitrogenous and isocaloric TEN. The result suggested that TPN could increase the endotoxin translocation from the bowel[14].

Our investigation achieved similar results and showed that feeding rats with TPN for 1 wk led to a remarkable atrophy of the intestinal mucous membrane; hence an increase in intestinal permeability and bacterial translocation ensued. The rats were

in a state of systemic inflammatory response, which was shown by clinical manifestations of the animals and analysis of their blood cells. It is known that the cause of increment in intestinal permeability in animals fed with TPN is mainly the atrophy of the intestinal mucous membrane[15,16]. Parenteral nutrition could meet the needs of other organs and tissues of the body, but not that of the intestinal mucosa. Seventy percent of the nutrients that intestinal epithelia need is absorbed directly from the intestinal lumen by mucosa cells[17]. Enteral feeding could prevent the intestinal mucous membrane from atrophy and avoid increment of intestinal permeability[10-12] . Likewise, it could also prevent gut associated lymphatic tissue (GULT) from atrophy, which could increase the intestinal mucosal immunity[16,17]. It could be seen from our investigation that the damage of intestinal mucous membrane in EN rats was greatly attenuated. Enteral feeding led to a better immune reaction in these rats than others. The increase of gut permeability was avoided and the rate of bacterial translocation alleviated. It was shown from the analysis of complete blood cell count in the rats that the total number of leukocytes and the number of neutrophils increased following the stimulus of TPN in PN group, whereas there was a low reaction in Sep group, which suffered from more severe stress injury than PN group. The falling of platelet count may be related to a greater depletion of platelets that was caused by an intravascular coagulation due to the systemic inflammatory reaction[1,18].

A series of symptoms appeared after injecting LPS into laparotomised TPN-rats in our experiment: lethargy, idleness, ruffling of hair, stopping drinking and grossly concentrated urine *etc*. Some rats appeared to have very low reactions to sound and other stimulations and also had diarrhea. Some eyes appeared glazed with crusting exudates. These symptoms were prominent during the 5 to 15 h following LPS injection, and the menifestations were alleviated gradually thereafter. These were in accordance with other reports[1,3,6,18-20]. No statistical difference was found in the mortality within 24 h after LPS injection between the two groups (there were 1 and 3 deaths for EN and Sep groups respectively).

The animals in Sep group responded acutely after being injected with LPS intraperitoneally. LPS aggravated the impairment of the intestinal mucosal barrier and bacterial translocation that was caused by TPN. The aggravation of impairment of the mucosal barrier function might be related to nitric oxide (NO), which was shown by an increased NO level in blood plasma after LPS injection. Some scholars considered that high output of NO after surgical stress could damage the oxygenation metabolism in mitochondria of the intestinal epithelia[3,21].

The increment of intestinal permeability caused by endotoxin is very complicated. It may relate to many inflammatory mediators such as cytokines, vasoactive amines and oxygen free radicals[22,23]. Among them, NO, one of the main oxygen free radicals in the body, is an important inflammatory mediator causing impairment of the intestinal barrier[3,18,24]. Generally, the body could only secrete small amounts of NO under the effects of constructive NO synthase (cNOS) and endothelial NO synthase (eNOS). This low level of NO has protective effects on the body[20], whereas a higher concentration of NO being produced under the effect of inducible NO synthase (iNOS) when the body suffered from harmful stimulations, would impair the functions of cells and tissues of the body, including the intestinal barrier function. It was concluded from a great number of studies that a lower NO level was beneficial and a higher NO level was harmful to the body[3,23,25], and using NO inhibitor when stress occurred could reduce the damage of gut barrier[26,27]. The results from our investigation were in accordance with this hypothesis.

The intestinal immunity is very important in maintaining intestinal barrier function. It is known that the digestive tract is the largest immune organ in the human body. About 80% of humoral immunity and 50% of cellular immunity locate in the digestive tract[25,28]. Intestinal mucosal IgA is the first defense line of the intestinal barrier. It has an important function in preventing bacterial adherence and translocation from intestinal lumens[21]. The IgA secretion in our EN group increased after LPS stimulation, but it had a low reaction in PN group when compared with that of EN group. The ratio of CD4 to CD8 in mucous membrane of small intestine in Sep group was lower than that in groups EN and PN, reflecting a low cellular immune response. This is in accordance with other reports that LPS could stimulate the increment of suppressive T lymphocytes[22]. IgA level in blood plasma is positively correlated with that in the intestinal mucosa, and this accords with a previous report[29]. Our results indicated that the increase of bacterial translocation was not only caused by an increased intestinal permeability, but also by an impairment of the whole intestinal barrier function[16,30]. The kinds and groups of translocated bacteria and the phenomenon that there were 1 to 3 kinds of translocated bacteria in the same organ found in our experiment were in accordance with other reports[3,31].

In summary, one week of parenteral nutrition caused an extreme atrophy of intestinal mucosa and an impairment of intestinal barrier function in SD rats. LPS aggravated this damage and also damaged the systemic immunity of the animals. The aggravation was related to the increased NO produced by the stimulation of LPS.

ACKNOWLEDGEMENT

We would like to thank Professor Hai-Feng Shao and Professor Gen-Bao Xu for their technical guidance and advice; we are grateful to the staff of the Animal Laboratory and the Institute of General Surgery of Nanjing University Medical School for their generous support and assistance to our study.

REFERENCES

1 **van Deventer SJ**, ten Cate JW, Tytgat GN. Intestinal endotoxemia. Clinical significance. *Gastroenterology* 1988; **94**: 825-831
2 **Yu P,** Martin CM. Increased gut permeability and bacterial translocation in Pseudomonas pneumonia-induced sepsis. *Crit Care Med* 2000; **28**: 2573-2577
3 **Dickinson E**, Tuncer R, Nadler E, Boyle P, Alber S, Watkins S, Ford H. NOX, a novel nitric oxide scavenger, reduces bacterial translocation in rats after endotoxin challenge. *Am J Physiol* 1999; **277**(6 Pt 1): G1281-1287
4 **Whiteland JL**, Nicholls SM, Shimeld C, Easty DL, Williams NA, Hill TJ. Immunohistochemical detection of T-cell subsets and other leukocytes in paraffin-embedded rat and mouse tissues with monoclonal antibodies. *J Histochem Cytochem* 1995; **43**: 313-320
5 **Green LC**, Wagner DA, Glogowski J, Skipper PL, Wishnok JS, Tannenbaum SR. Analysis of nitrate, nitrite, and [15N]nitrate in biological fluids. *An Biochem* 1982; **126**: 131-138
6 **O' Dwyer ST**, Michie HR, Ziegler TR, Revhaug A, Smith RJ, Wilmore DW. A single dose of endotoxin increases intestinal permeability in healthy humans. *Arch Surg* 1988; **123**: 1459-1464
7 **Wilmore DW**, Smith RJ, O'Dwyer ST, Jacobs DO, Ziegler TR, Wang XD. The gut: a central organ after surgical stress. *Surgery* 1988; **104**: 917-923
8 **Berg RD**. Bacterial translocation from the gastrointestinal tract. *Trends Microbiol* 1995; **3**: 149-154
9 **Swank GM**, Deitch EA. Role of the gut in multiple organ failure: bacterial translocation and permeability changes. *World J Surg* 1996; **20**: 411-417
10 **Qin HL**, Su ZD, Hu LG, Ding ZX, Lin QT. Effect of early intrajejunal nutrition on pancreatic pathological features and

gut barrier function in dogs with acute pancreatitis. *Clin Nutr* 2002; **21**: 469-473

11 **Mosenthal AC**, Xu D, Deitch EA. Elemental and intravenous total parenteral nutrition diet-induced gut barrier failure is intestinal site specific and can be prevented by feeding nonfermentable fiber. *Crit Care Med* 2002; **30**: 396-402

12 **Li J**, Langkamp-Henken B, Suzuki K, Stahlgren LH. Glutamine prevents parenteral nutrition-induced increases in intestinal permeability. *J Parenter Enteral Nutr* 1994; **18**: 303-307

13 **Pscheidl E**, Schywalsky M, Tschaikowsky K, Boke-Prols T. Fish oil-supplemented parenteral diets normalize splanchnic blood flow and improve killing of translocated bacteria in a low-dose endotoxin rat model. *Crit Care Med* 2000; **28**: 1489-1496

14 **Takagi K**, Yamamori H, Toyoda Y, Nakajima N, Tashiro T. Modulating effects of the feeding route on stress response and endotoxin translocation in severely stressed patients receiving thoracic esophagectomy. *Nutrition* 2000; **16**: 355-360

15 **Sugiura T**, Tashiro T, Yamamori H, Takagi K, Hayashi N, Itabashi T, Toyoda Y, Sano W, Nitta H, Hirano J, Nakajima N, Ito I. Effects of total parenteral nutrition on endotoxin translocation and extent of the stress response in burned rats. *Nutrition* 1999; **15**: 570-575

16 **MacFie J**. Enteral versus parenteral nutrition: the significance of bacterial translocation and gut-barrier function. *Nutrition* 2000; **16**: 606-611

17 **van der Hulst RR**, von Meyenfeldt MF, van Kreel BK, Thunnissen FB, Brummer RJ, Arends JW, Soeters PB. Gut permeability, intestinal morphology, and nutritional depletion. *Nutrition* 1998; **14**: 1-6

18 **Fish RE**, Spitzer JA. Continuous infusion of endotoxin from an osmotic pump in the conscious, unrestrained rat: a unique model of chronic endotoxemia. *Circ Shock* 1984; **12**: 135-149

19 **Wichterman KA**, Baue AE, Chaudry IH. Sepsis and septic shock—a review of laboratory models and a proposal. *J Surg Res* 1980; **29**: 189-201

20 **Schmidt H**, Secchi A, Wellmann R, Bach A, Bohrer H, Gebhard MM, Martin E. Effect of endotoxemia on intestinal villus microcirculation in rats. *J Surg Res* 1996; **61**: 521-526

21 **Unno N**, Wang H, Menconi MJ, Tytgat SH, Larkin V, Smith M, Morin MJ, Chavez A, Hodin RA, Fink MP. Inhibition of inducible nitric oxide synthase ameliorates endotoxin-induced gut mucosal barrier dysfunction in rats. *Gastroenterology*, 1997; **113**: 1246-1257

22 **Marshall JC**, Christou NV, Meakins JL. Small-bowel bacterial overgrowth and systemic immunosuppression in experimental peritonitis. *Surgery* 1988; **104**: 404-411

23 **Mishima S**, Xu D, Deitch EA. Increase in endotoxin-induced mucosal permeability is related to increased nitric oxide synthase activity using the Ussing chamber. *Crit Care Med* 1999; **27**: 880-886

24 **Forsythe RM**, Xu DZ, Lu Q, Deitch EA. Lipopolysaccharide-induced enterocyte-derived nitric oxide induces intestinal monolayer permeability in an autocrine fashion. *Shock* 2002; **17**: 180-184

25 **Nadler EP**, Ford HR. Regulation of bacterial translocation by nitric oxide. *Pediatr Surg Int* 2000; **16**: 165-168

26 **Hsu CM**, Liu CH, Chen LW. Nitric oxide synthase inhibitor ameliorates oral total parenteral nutrition-induced barrier dysfunction. *Shock* 2000; **13**: 135-139

27 **Deitch EA**, Shorshtein A, Houghton J, Lu Q, Xu D. Inducible nitric oxide synthase knockout mice are resistant to diet-induced loss of gut barrier function and intestinal injury. *J Gastrointest Surg* 2002; **6**: 599-605

28 **Hulsewe KW**, van Acker BA, von Meyenfeldt MF, Soeters PB. Nutritional depletion and dietary manipulation: effects on the immune response. *World J Surg* 1999; **23**: 536-544

29 **Brandtzaeg P**, Halstensen TS, Kett K, Krajci P, Kvale D, Rognum TO, Scott H, Sollid LM. Immunobiology and immunopathology of human gut mucosa: humoral immunity and intraepithelial lymphocytes. *Gastroenterology* 1989; **97**: 1562-1584

30 **Deitch EA**, Ma WJ, Ma L, Berg RD, Specian RD. Protein malnutrition predisposes to inflammatory-induced gut-origin septic states. *Ann Surg* 1990; **211**: 560-567

31 **Naaber P**, Smidt I, Tamme K, Liigant A, Tapfer H, Mikelsaar M, Talvik R. Translocation of indigenous microflora in an experimental model of sepsis. *J Med Microbiol* 2000; **49**: 431-439

Edited by Zhang JZ and Chen WW **Proofread by** Zhu LH and Xu FM

PO Box 2345, Beijing 100023, China
Fax: +86-10-85381893
E-mail: wjg@wjgnet.com www.wjgnet.com

World J Gastroenterol 2004;10(16):2379-2382
World Journal of Gastroenterology
 ISSN 1007-9327

• CLINICAL RESEARCH •

DA-9601 for erosive gastritis: Results of a double-blind placebo-controlled phase III clinical trial

Sang Yong Seol, Myung Hwan Kim, Jong Sun Ryu, Myung Gyu Choi, Dong Wook Shin, Byoung Ok Ahn

Sang Yong Seol, Department of Gastroenterology, Inje University of Medicine, Busan, Korea
Myung Hwan Kim, Department of Gastroenterology, Ulsan University of Medicine, Seoul, Korea
Jong Sun Ryu, Department of Gastroenterology, Chunnam University of Medicine, Gwangju, Korea
Myung Gyu Choi, Department of Gastroenterology, Catholic University of Medicine, Seoul, Korea
Dong Wook Shin, Byoung Ok Ahn, Dong-A Pharmaceutical Research Institute, Yongin, Korea
Correspondence to: Byoung Ok Ahn, Dong-A Pharmaceutical Research Institute, 47-5, Sanggal-ri, Kiheung-up, Yongin-shi, Kyunggi-do 449-905, Korea. ahnbo@donga.co.kr
Telephone: +82-31-2801394 **Fax:** +82-31-2828564
Received: 2004-02-06 **Accepted:** 2004-03-02

Abstract

AIM: To determine the efficacy and safety of DA-9601 on erosive gastritis versus cetraxate as a standard drug by gastrointestinal endoscopy.

METHODS: Five hundred and twelve patients with erosive gastritis were divided into three groups. The groups received 180 mg or 360 mg of DA-9601, or 600 mg of cetraxate (Neuer™) t.i.d. for 2 wk, respectively. Endoscopic observations were performed before and 2 wk after the treatment, and the cure and improvement rates were investigated.

RESULTS: Of the 512 intention-to-treat (ITT) population, 457 patients comprised the per protocol (PP) analysis. Endoscopic cure rate was significantly higher in the DA-9601 group than in the cetraxate group in both the PP (56%, 58% *vs* 36%; DA-9601 180 mg, 360 mg and cetraxate, respectively) and ITT (52%, 51% *vs* 35%) populations. Two DA-9601 groups (180 and 360 mg) had significantly higher endoscopic improvement rates than the cetraxate group in both the PP (67%, 65% *vs* 46%) and ITT (63%, 58% *vs* 45%) populations. The percentage of symptom relief over the 2 wk was found not significantly different between groups. During the study, both DA-9601 and cetraxate produced no treatment-associated adverse events.

CONCLUSION: From these results, it appears that DA-9601 has excellent efficacy on erosive gastritis. This study also confirms the safety profile of DA-9601.

Seol SY, Kim MH, Ryu JS, Choi MG, Shin DW, Ahn BO. DA-9601 for erosive gastritis: Results of a double-blind placebo-controlled phase III clinical trial. *World J Gastroenterol* 2004; 10(16): 2379-2382
http://www.wjgnet.com/1007-9327/10/2379.asp

INTRODUCTION

Gastritis is a heterogeneous pathological condition, and is one of the most frequent reasons for medical consultation in Asian countries, including Korea and Japan. However, in Western countries, these conditions are diagnosed as non-ulcer dyspepsia (NUD), which affects approximately one in five Americans[1-4]. Gastritis, the "precursor" lesion to mucosal ulceration is both an important clinical entity and an important cause of abdominal pain in children[5]. Inflammation of the gastric mucosa is the end result of an imbalance between mucosal defensive and aggressive factors (i.e., disturbances in gastric acidity and the mucus-bicarbonate barrier), and recently a great deal of attention has been focused on gastric hormones, specifically gastrin, and pepsinogens I and II[6,7].

Gastritis can be classified into acute or chronic forms based upon Sydney System, and chronic gastritis can be subclassified as nonatrophic, atrophic, and special types[8,9]. Using this Sydney pathologic classification as a guide, Chen *et al*.[10] reported a simplified classification for gastritis based on practical radiologic evaluation, including erosive gastritis (acute and chronic), *Helicobacter pylori* (*H pylori*) gastritis, chronic nonspecific gastritis, hyperplastic gastritis, and miscellaneous types (including granulomatous, phlegmonous, eosinophilic, corrosive, other infectious types and rare types).

At present, the exact pathophysiology of this syndrome is poorly understood. However, current evidence suggests that *H pylori* infection, changes in lifestyles, eating behaviors, and nonsteroidal anti-inflammatory drug (NSAID) ingestion are causative factors in the pathogenesis of gastric mucosal injury in humans[11]. *H pylori* is known to be a particularly important pathogen in gastric and duodenal inflammation by producing excessive mucosal-reactive oxygen species (ROS), which damage the cell membrane and deplete gastric antioxidants[12].

The current rationale for drug treatment in gastritis is similar to other gastrointestinal disorders (eg., non-ulcer dyspepsia), and depends mainly on symptomatic relief using gastroprotective agents (e.g., rebamipide, teprenone, ecabet sodium, sofalcone, cetraxate, *etc*.), H_2 receptor antagonists (e.g., cimetidine, ranitidine, famotidine, *etc*.), and antacids[13]. However, despite many efforts, the pharmacological treatment of patients with gastritis usually achieves only partial symptomatic relief in the majority of cases.

DA-9601 (Stillen™), a phytopharmaceutical derived from *Artemisia asiatica*, has been reported to possess antioxidative and cytoprotective actions in various models of gastric mucosal damage[14-16]. Though the mode of action of DA-9601 has not been fully elucidated, this new antioxidative drug scavenges superoxide and hydroxyl radicals, possesses potent anti-inflammatory activities, regenerates mucosal epithelial cells, and enhances the cytoprotective cytokines[17-19].

The present study was designed to assess the therapeutic effects and safety of DA-9601 on gastritis. Cetraxate, which has been shown to have therapeutic effects on gastritis was selected as the standard drug for comparative purposes.

MATERIALS AND METHODS

Patients

The patients examined in this study consisted of 550 erosive gastritis patients who were diagnosed endoscopically between

August 2000 and December 2001. All patients gave their written consent to this study. Out of 550 initially enrolled patients, 512 completed the study. Those 512 patients were subsequently randomized, of whom 326 were allocated to DA-9601 (186 had 180 mg and 140 had 360 mg daily) and 186 to cetraxate 600 mg. The exclusion criteria were: a history of peptic ulcer disease and reflux esophagitis; the presence of a malignant tumor in the digestive tract; the use of drugs capable of interfering with digestive mucosal integrity, gastric secretion or gastrointestinal motility, including H_2 receptor antagonists, NSAIDs, muscarinic antagonists, gastroprotective agents (within the previous 14 d); thrombotic patients (cerebral thrombosis, myocardial infarction, thrombophlebitis, *etc*.); consumption coagulopathy patients; a history of hypersensitivity to drugs (rash, fever, itching, *etc*.); the presence of major hematological, renal, cardiac, pulmonary, or hepatic abnormalities.

Methods

The study was performed as a randomized, double-blind, placebo-controlled, multicenter trial. Subjects were recruited at the following five Korean centers; Inje University of Medicine (Busan), Ulsan University of Medicine (Seoul), Chunnam University of Medicine (Gwangju), Catholic University of Medicine (Seoul), and Ajou University of Medicine (Suwon). Gastrointestinal endoscopies were performed in all patients before starting therapy, and 2 wk later. Patients diagnosed with erosive gastritis were included and divided into 3 groups following initial symptom assessment, and either treated with DA-9601 180 or 360 mg, or cetraxate 600 mg t.i.d. for 2 wk. After completing the therapy, endoscopic examinations were conducted according to the following grades: score 1, no erosions; score 2 (mild), erosion number between 1 and 2; score 3 (moderate), erosion number between 3 and 5; score 4 (severe), erosion number more than 6, for the evaluation of cure rate and improvement rate (Table 1). In addition, all patients completed a standardized subjective assessment questionnaire, according to Table 2. Safety surveillance was done at the end of therapy, based on responses to a complaint questionnaire, results of physical examinations and laboratory tests. Blood samples were obtained at the end of therapy to determine concentrations of GPT, GOT, and bilirubin. Complaint questionnaires were recorded for the appreciable harmful or unpleasant reactions experienced by a patient as a result of drug therapy.

Table 1 Evaluation of efficacy based on endoscopic observations

Score	Number of erosions
1 (none)	0
2 (mild)	1–2
3 (moderate)	3–5
4 (severe)	6<

Table 2 Evaluation of efficacy in individual symptom

Score	Criteria
1 (none)	No symptom
2 (weak)	Symptoms occurred once a week
3 (moderate)	The symptoms did not affect their life and occurred more than twice a week
4 (strong)	The symptoms affected their everyday life and occurred daily

Statistics analysis

Endoscopic efficacy was analyzed on an intention-to-treat (ITT) and per protocol (PP) basis. Both subjective and objective criteria were analyzed using Duncan's multiple test. Comparisons between treatment groups were performed using the chi-square test. Data were considered to be significant when $P<0.05$.

RESULTS

A total of 512 patients completed the trial. Baseline characteristics of the study populations are detailed in Table 3, which shows that the study groups were comparable with respect to demographics and disease-specific characteristics.

Table 3 Base-line characteristics of the patients (*n*, %)

Characteristic		DA-9601 180 mg (*n* = 186)	DA-9601 360 mg (*n* = 140)	Cetraxate 600 mg (*n* = 186)
Male sex		89 (47.9)	72 (51.4)	92 (49.5)
Age(yr)		45.9±11.2	44.6±12.1	46.4±11.5
History	<1 wk	3 (1.6)	1 (0.7)	3 (1.6)
	1–4 wk	31 (16.7)	28 (20.0)	29 (15.6)
	>4 wk	98 (52.7)	27 (19.3)	97 (52.2)
	Unknown	54 (29.0)	84 (60.0)	57 (30.7)
Type	Erosion	186 (100)	140 (100)	186 (100)
	Bleeding	8 (4.3)	4 (2.9)	10 (5.4)
	Redness	51 (27.4)	47 (33.6)	44 (23.7)
	Edema	2 (1.1)	10 (7.1)	5 (2.7)
Grade	Mild	14 (7.5)	18 (12.9)	21 (11.3)
	Moderate	50 (26.9)	40 (28.6)	54 (29.0)
	Severe	122 (65.6)	82 (58.6)	111 (59.7)

Data values are mean±SD.

Table 4 Number of patients for ITT and PP assays

	Number of patients		
	DA-9601 180 mg	DA-9601 360 mg	Cetraxate 600 mg
ITT analysis	186	140	186
PP analysis	171	120	166

Efficacy evaluation

The ITT population was composed of 512 patients (186 in the DA-9601 180 mg group, 140 in the DA-9601 360 mg group, and 186 in the cetraxate 600 mg group) (Table 4). Endoscopic cure rates in DA-9601 180 mg, 360 mg, and cetraxate 600 mg groups were 52.2%, 51.4%, and 35%, respectively (Figure 1). A significant difference was found between the DA-9601 and cetraxate groups ($P<0.05$), however, no difference in cure rates was found between the DA-9601 groups.

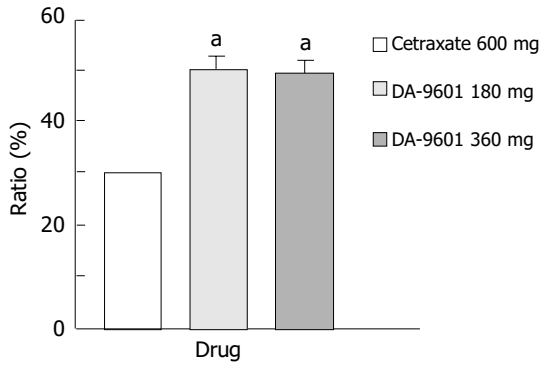

Figure 1 Estimated cure rates of erosive gastritis by intention-to-treat (ITT) analysis among patients treated with DA-9601 (180 mg or 360 mg, t.i.d.) or cetraxate (600 mg, t.i.d.) for 2 wk. [a]$P<0.05$ *vs* 600 mg of cetraxate.

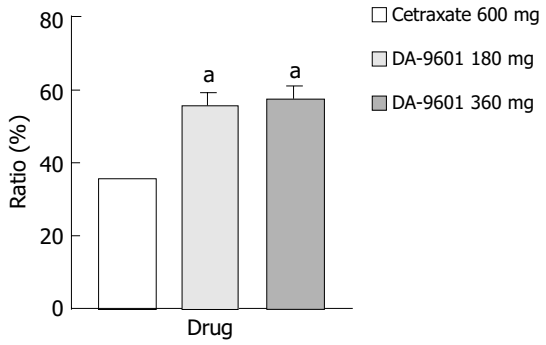

Figure 2 Estimated cure rates of erosive gastritis by per protocol (PP) analysis among patients treated with DA-9601 (180 mg or 360 mg, t.i.d.) or cetraxate (600 mg, t.i.d.) for 2 wk. [a]*P*<0.05 *vs* 600 mg of cetraxate.

The PP assay population comprised 457 patients (171 in the DA-9601 180 mg group, 120 in the DA-9601 360 mg group, and 166 in the cetraxate 600 mg group) (Table 4). The estimated cure rates of erosive gastritis by PP analysis in DA-9601 180 mg, 360 mg, and cetraxate 600 mg groups were 55.6% (95/171), 57.5% (69/120), and 35.5% (59/166), respectively (Figure 2). The cure rates between the DA-9601 and cetraxate groups (P<0.05) were significantly different, however, no difference was found between the DA-9601 groups.

Estimated improvement rates by ITT analysis of erosive gastritis patients treated with cetraxate (600 mg) and DA-9601 (180 or 360 mg) showed statistically significant differences (P<0.05); however, no difference was observed between the DA-9601 treated populations (Figure 3). The improvement rates of those treated with DA-9601 180 mg, 360 mg and cetraxate 600 mg were 63.4% (118/186), 57.9% (81/140), and 44.6% (83/186), respectively.

The estimated improvement rates by PP analysis for erosive gastritis treated with DA-9601 or cetraxate were statistically different (P<0.05) (Figure 4). However, no difference was found between the DA-9601 treated groups. The estimated improvement rates were 67.3% (115/171), 65.0% (78/120), and 46.4% (77/166) in the DA-9601 180 mg, DA-9601 360 mg, cetraxate 600 mg treated groups.

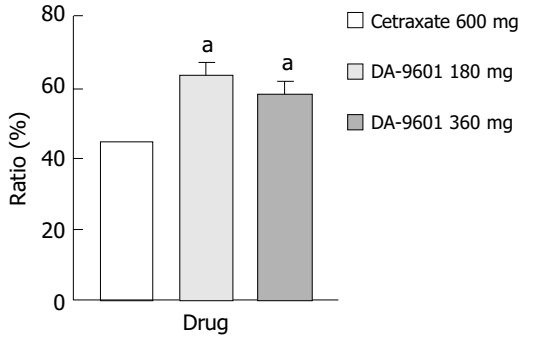

Figure 3 Estimated improvement rates of erosive gastritis by intention-to-treat (ITT) analysis among patients treated with DA-9601 (180 mg or 360 mg, t.i.d.) or cetraxate (600 mg, t.i.d.) for 2 wk. [a]*P*<0.05 *vs* 600 mg of cetraxate.

Symptom relief rates

The symptom relief rates determined by the ITT and PP methods showed no statistically significant difference between the study populations. The overall degrees of symptom reduction by the ITT method in the DA-9601 180 mg, 360 mg, and cetraxate 600 mg groups were 77.4% (144/186), 75.0% (105/140), and 73.1% (136/186), respectively (Figure 5), and by PP analysis these were 81.3% (139/171), 81.7% (98/120), and 76.5% (127/166).

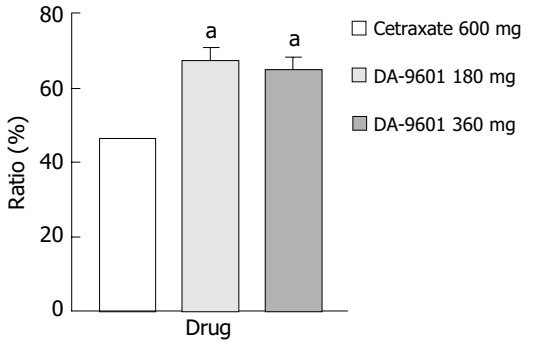

Figure 4 Estimated improvement rates of erosive gastritis by per protocol (PP) analysis among patients treated with DA-9601 (180 mg or 360 mg, t.i.d.) or cetraxate (600 mg, t.i.d.) for 2 wk. [a]*P*<0.05 *vs*. 600 mg of cetraxate.

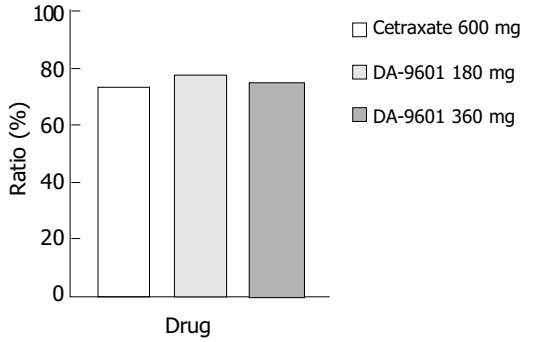

Figure 5 Overall reduction rates of symptoms among patients treated with cetraxate (600 mg, t.i.d.) or DA-9601 (180 mg and 360 mg, t.i.d.) for 2 wk.

Table 5 Incidence of adverse events (*n*, %)

	DA-9601 180 mg	Cetraxate 600 mg
Gastrointestinal		
Dyspepsia	2 (1.08)	0
Nausea	2 (1.08)	0
Diarrhea	2 (1.08)	0
Heartburn	1 (0.54)	1 (0.54)
Abdominal pain	1 (0.54)	1 (0.54)
Acid reflux	0	1 (0.54)
Vomiting	1 (0.54)	1 (0.54)
CNS and ANS		
Dizziness	1 (0.54)	0
Headache	1 (0.54)	1 (0.54)
Skin		
Itching	1 (0.54)	1 (0.54)
Skin redness	1 (0.54)	1 (0.54)
Facial edema	0	1 (0.54)
Liver		
sGPT elevation	1 (0.54)	1 (0.54)
sGOT elevation	0	1 (0.54)
Bilirubin elevation	0	1 (0.54)
Total	14 (7.53)	11 (5.91)

Safety

Serious adverse reactions were not encountered during this study. Of the 186 cetraxate 600 mg treated patients, the incidence of adverse effects was 7.5% (11 cases); including heartburn, abdominal pain, acid reflux, headache, itching, skin redness, facial edema, *etc*. Mild adverse events were observed in 14 of 186 patients treated with DA-9601 180 mg (Table 5). In the case of DA-9601 360 mg group, no notable change was observed

either in subjective assessment questionnaire or in clinical examination at the end of the study as compared to DA-9601 180 mg or cetraxate groups. No statistically significant difference was observed between the cetraxate and DA-9601 treated groups.

DISCUSSION

Although gastritis is the most common complication in the digestive tract, the definition of gastritis is not consensual due to differences in diagnostic criteria. It has been postulated that gastritis contributes to the natural history of ulcer development due to the decreased protection offered by the mucosal barrier lining the stomach, and increased epithelial cell exposure to hydrochloric acid.

The aim of this study was to demonstrate the efficacy and safety of DA-9601 versus cetraxate, a widely used anti-ulcer drug, for the treatment of erosive gastritis. Cetraxate, which has a mucosal protective effect, was first introduced in 1976 as an anti-ulcer drug[20]. It is widely used clinically in Japan and other Asian countries. The mode of action of cetraxate is ascribed to an increased gastric mucosal blood flow through enhanced nitric oxide synthase activity, and the prevention of a decrease in the mucosal prostaglandin content[21]. The results of the present randomized, double-blind, placebo-controlled, multicenter study demonstrate that orally administrated DA-9601 is both effective and well-tolerated in the treatment of erosive gastritis of various etiologies.

Adverse reactions were seen in 7.5% (14/186) of the patients in DA-9601 180 mg treated group and in 5.9% (11/186) of patients in the cetraxate 600 mg treated group. In both groups, the main adverse reactions were vomiting, abdominal pain, headache, skin rash, itching, and sGPT elevation. However, in DA-9601 360 mg treated group, no obvious adverse reactions were observed (0%, 0/140). Therefore, we concluded that there was no drug treatment related adverse reaction based on the lack of dose-response relationship. In the previous four-wk oral toxicity study of DA-9601 in rats at doses of 120, 500, and 2 000 mg/kg.d, no treatment related alternations, including changes in blood biochemistry were observed[22]. In animal experiments, DA-9601 prevented acetaminophen, and CCl_4-induced hepatic GSH depletion and CCl_4-induced increased hepatic MDA (a parameter of lipid peroxidation) in a dose-dependent manner[23,24]. In addition, sGPT and sGOT levels showed a tendency to fall to below the normal range in DA-9601 treated patients (unpublished data).

Conclusively, the present study indicates that DA-9601 has an excellent efficacy and safety profile. Therefore, we believe that DA-9601 is a highly attractive option for the treatment of erosive gastritis, in which a balance between aggressive and defensive factors plays a significant role.

REFERENCES

1 **Talley NJ**. Dyspepsia: how to manage and how to treat? *Aliment Phamacol Ther* 2002; **16**(Suppl 4): 95-104
2 **Talley NJ**. Therapeutic options in nonulcer dyspepsia. *J Clin Gastroenterol* 2001; **32**: 286-293
3 **Talley NJ**, Stanghellini V, Heading RC, Koch KL, Malagelada JR, Tytgat GN. Functional gastroduodenal disorders. *Gut* 1999; **45**: II37-II42
4 **Kurata JH**, Haile BM. Epidemiology of peptic ulcer disease. *Clin Gastroenterol* 1984; **13**: 289-307
5 **Blecker U**, Gold BD. Gastritis and peptic ulcer disease in childhood. *Eur J Pediatr* 1999; **158**: 541-546
6 **Taylor IL**. Gastrointestinal hormones in the pathogenesis of peptic ulcer disease. *Clin Gastroenterol* 1984; **13**: 355-382
7 **Defize J**, Meuwissen SG. Pepsinogens: an update of biochemical, physiological, and clinical aspects. *J Pediatr Gastroenterol Nutr* 1987; **6**: 493-508
8 **Dixon MF**, Genta RM, Yardley JH, Correa P. Classification and grading of gastritis. The updated Sydney System. International Workshop on the Histopathology of Gastritis, Houston 1994. *Am J Surg Pathol* 1996; **20**: 1161-1181
9 **Whitehead R**. The classification of chronic gastritis: current status. *J Clin Gastroenterol* 1995; **21**(Suppl 1): S131-S134
10 **Chen MY**, Ott DJ, Clark HP, Gelfand DW. Gastritis: classification, pathology, and radiology. *South Med J* 2001; **94**: 184-189
11 **Yoshikawa T**, Naito Y. The role of neutrophils and inflammation in gastric mucosal injury. *Free Rad Res* 2000; **33**: 785-794
12 **Kashiwagi H**. Ulcers and gastritis. *Endoscopy* 2003; **35**: 9-14
13 **Talley NJ**. Update on the role of drug therapy in non-ulcer dyspepsia. *Rev Gastroenterol Disord* 2003; **3**: 25-30
14 **Oh TY**, Ryu BK, Yang JI, Kim WB, Park JB, Oh TY, Lee SD, Lee EB. Studies on antiulcer effects of DA-9601, an *Artemisia herba* extract against experimental gastric ulcers and its mechanism. *J Appl Pharmacol* 1996; **4**: 111-121
15 **Lee EB**, Kim WB, Ryu BK, Ahn BO, Oh TY, Kim SH. Studies on protective effect of DA-9601, an *Artemisiae Herba* extract, against ethanol-induced gastric mucosal damage and its mechanism. *J Appl Pharmacol* 1997; **5**: 202-210
16 **Oh TY**, Ryu BK, Ko JI, Ahn BO, Kim SH, Kim WB, Lee EB, Jin JH, Hahm KB. Protective effect of DA-9601, an extract of *Artemisiae Herba*, against naproxen-induced gastric damage in arthritic rats. *Arch Pharm Res* 1997; **20**: 414-419
17 **Lee JJ**, Han BG, Kim MN, Chung MH. The inhibitory effect of eupatilin on *Helicobacter pylori*-induced release of leukotriene D_4 in the human neutrophils and gastric mucosal cells. *Korean J Physiol Pharmacol* 1997; **1**: 573-580
18 **Oh TY**, Lee JS, Ahn BO, Cho H, Kim WB, Kim YB, Surh YJ, Cho SW, Lee KM, Hahm KB. Oxidative stress is more important than acid in the pathogenesis of reflux oesophagitis in rats. *Gut* 2001; **49**: 364-371
19 **Oh TY**, Lee JS, Ahn BO, Cho H, Kim WB, Kim YB, Surh YJ, Cho W, Hahm KB. Oxidative damage are critical in pathogenesis of reflux esophagitis: implication of antioxidants in its treatment. *Free rad Biol Med* 2001; **30**: 905-915
20 **Suzuki Y**, Hayashi M, Ito M, Yamagami I. Anti-ulcer effects of 4'-(2-carboxyetyl) phenyl trans-4-aminomethyl cyclohexanecar boxylate hydrochloride (cetraxate) on various experimental gastric ulcers in rats. *Jpn J Pharmacol* 1976; **26**: 471-480
21 **Tachi K**, Goto H, Hayakawa T, Sugiyama S. Prevention of water immersion stress-induced gastric lesions through the enhancement of nitric oxide synthase activity in rats. *Aliment Pharmacol Ther* 1996; **10**: 97-103
22 **Kim OJ**, Kang KK, Kim DH, Baik NG, Ahn BO, Kim WB, Yang I. Four-week oral toxicity study of DA-9601, an antiulcer agent of *Artemisia* spp. Extract, in rats. *J Appl Pharmacol* 1996; **4**: 354-363
23 **Ryu BK**, Ahn BO, Oh TY, Kim SH, Kim WB, Lee EB. Studies on protective effect of DA-9601, *Artemisia asiatica* extract, on acetaminophen- and CCl_4-induced liver damage in rats. *Arch Pharm Res* 1998; **21**: 508-513
24 **Cheong JY**, Oh TY, Lee KM, Kim DH, Ahn BO, Kim WB, Kim YB, Yoo BM, Hahm KB, Kim JH, Cho SW. Suppressive effects of antioxidant DA-9601 on hepatic fibrosis in rats. *Korean J Hepatol* 2002; **8**: 436-447

Edited by Zhu LH and Xu FM

PO Box 2345, Beijing 100023, China
Fax: +86-10-85381893
E-mail: wjg@wjgnet.com www.wjgnet.com

World J Gastroenterol 2004;10(16):2383-2390
World Journal of Gastroenterology
 ISSN 1007-9327

• CLINICAL RESEARCH •

Impaired gallbladder motility and delayed orocecal transit contribute to pigment gallstone and biliary sludge formation in β-thalassemia major adults

Piero Portincasa, Antonio Moschetta, Massimo Berardino, Agostino Di Ciaula, Michele Vacca, Giuseppe Baldassarre, Anna Pietrapertosa, Rosario Cammarota, Nunzia Tannoia, Giuseppe Palasciano

Piero Portincasa, Antonio Moschetta, Massimo Berardino, Michele Vacca, Giuseppe Palasciano, Section of Internal Medicine, Department of Internal Medicine and Public Medicine (DIMIMP), University Medical School, Bari, Italy
Agostino Di Ciaula, Division of Internal Medicine, Hospital of Bisceglie, Italy
Giuseppe Baldassarre, Division of Geriatrics, Hospital "Miulli", Acquaviva delle Fonti, Bari, Italy
Anna Pietrapertosa, Rosario Cammarota, Nunzia Tannoia, Chair of Hematology II, University of Bari, Italy
Correspondence to: Professor Piero Portincasa, Section of Internal Medicine, Department of Internal and Public Medicine (DIMIMP), University Medical School of Bari, P.zza G. Cesare 11, 70124 Bari, Italy. p.portincasa@semeiotica.uniba.it
Telephone: +39-80-5478227 **Fax:** +39-80-5478232
Received: 2004-02-02 **Accepted:** 2004-03-13

Abstract

AIM: Gallbladder and gastrointestinal motility defects exist in gallstones patients and to a lesser extent in pigment gallstone patients. To investigated the role of gallbladder and gastrointestinal motility disorders in pigment gallstone formation in β-thalassemia major.

METHODS: Twenty-three patients with β-thalassemia major (16 females; age range 18-37 years) and 70 controls (47 females, age range 18-40 years) were studied for gallbladder and gastric emptying (functional ultrasonography), orocecal transit (OCTT, H_2-breath test), autonomic dysfunction (sweat-spot, cardiorespiratory reflex tests), bowel habits, gastrointestinal symptoms and quality of life (all with questionnaires). Gallbladder content (ultrasonography) was examined before and during 8-12 mo follow-up.

RESULTS: Gallstones and/or biliary sludge were found in 13 (56%) patients. β-thalassemia major patients had increased fasting (38.0±4.8 mL *vs* 20.3±0.7 mL, $P = 0.0001$) and residual (7.9±1.3 mL *vs* 5.1±0.3 mL, $P = 0.002$) volume and slightly slower emptying (24.9±1.7 min *vs* 20.1±0.7 min, $P = 0.04$) of the gallbladder, together with longer OCTT (132.2±7.8 min *vs* 99.7±2.3 min, $P = 0.00003$) than controls. No differences in gastric emptying and bowel habits were found. Also, patients had higher dyspepsia (score: 6.7±1.2 *vs* 4.9±0.2, $P = 0.027$), greater appetite ($P = 0.000004$) and lower health perception ($P = 0.00002$) than controls. Autonomic dysfunction was diagnosed in 52% of patients (positive tests: 76.2% and 66.7% for parasympathetic and sympathetic involvement, respectively). Patients developing sludge during follow-up (38%, 2 with prior stones) had increased fasting and residual gallbladder volume.

CONCLUSION: Adult β-thalassemia major patients have gallbladder dysmotility associated with delayed small intestinal transit and autonomic dysfunction. These abnormalities apparently contribute together with haemolytic hyperbilirubinemia to the pathogenesis of pigment gallstones/sludge in β-thalassemia major.

Portincasa P, Moschetta A, Berardino M, Di Ciaula A, Vacca M, Baldassarre G, Pietrapertosa A, Cammarota R, Tannoia N, Palasciano G. Impaired gallbladder motility and delayed orocecal transit contribute to pigment gallstone and biliary sludge formation in β-thalassemia major adults. *World J Gastroenterol* 2004; 10(16): 2383-2390
http://www.wjgnet.com/1007-9327/10/2383.asp

INTRODUCTION

Patients with cholesterol gallstones have impaired gallbladder emptying[1] and may show dyspeptic symptoms with functional defects of both upper and lower gastrointestinal tract[2-4]. Recently, we reported that gallbladder emptying was also defective in patients with black pigment stones and such defect was less severe than in patients with cholesterol stones[2].

β-thalassemia is one of the most widespread single-gene disorders with 3-6% of the world's population carrying the gene. The disease represents a major public health problem in the Mediterranean area, the Middle East, the India subcontinent and the Far East[5]. Increased production of bilirubin from chronic hemolysis is a prerequisite for formation of pigment gallstones[6,7], and black pigment gallstones often accompany thalassemia major[6], However, despite similar biochemical and clinical features, many β-thalassemia major patients with marked hemolysis did not develop gallstones. One might hypothesize that gallbladder stasis and functional gastrointestinal disorders could contribute to gallstone pathogenesis in β-thalassemia major. In the present study, we investigated for the first time the role of gallbladder and gastrointestinal motility in adult β-thalassemia major patients in relation to gallstone/sludge formation. Autonomic neuropathy and gastrointestinal symptoms were also evaluated.

MATERIALS AND METHODS

Subjects

β-thalassemia major patients (*n* = 23) Age 26±1 years (mean±SE, range 18-37 years), body mass index (BMI) of 21.4±0.6 kg/m^2. Sixteen were women. Patients attended regular review from October 2001 until June 2003 at the Referral Center of the University Hospital of Bari. All the patients were homozygous for a mutation β° or β$^+$ or double heterozygous for a mutation β° or β$^+$. The genetic characteristics of the patients seen in Bari have been previously reported[8]. As β-thalassemia major requires regular blood transfusions and chelating therapy to alleviate the harmful accumulation of iron, all patients were on a program consisting of one or two monthly blood transfusion of packed red blood cells and desferrioxamine given as 40-60 mg/(kg·d) subcutaneously overnight using syringe pumps. The program

lasted for 5 nights per week. Mean length of desferrioxamine treatment was 19.2±0.6 years. All patients had various stages of liver involvement, as confirmed by ultrasonography (*e.g.* liver steatosis, hyperechoic parenchyma) and/or liver biopsy (ranging from active/chronic siderotic and fibrotic hepatitis to definite liver cirrhosis, $n = 1$). The analysis of organ involvement confirmed that splenomegaly, hypothyroidism, and heart disease were the most frequent conditions with a prevalence of 39%, 35% and 18%, respectively. Hypogonadism was present in 35% of the patients. Type I insulin-dependent diabetes and a positive oral glucose tolerance test were present in 9% and 22% of the patients, respectively.

Healthy subjects ($n = 70$) Age 28±1 years (range 18-40 years), BMI 22.0±0.3 kg/m^2. Forty-seven were women. They were recruited from local staff members, students, and family practices. None of the healthy subjects complained of gastrointestinal symptoms or had previous gastrointestinal diseases or surgery. All had a negative abdominal ultrasound.

No significant difference existed in age, BMI and gender distribution between the patients and the normal controls. As expected[9], patients had shorter stature than their matched controls (males: 168±2 cm *vs* 178±7 cm, $P = 0.0006$ and females: 158±0.01 cm *vs* 167±6 cm, $P = 0.00005$). All subjects gave their informed consent and the study was approved by the University of Bari Human Subjects Committee.

Study design

After the outpatient clinic evaluation consisting of history, physical examination, and serum analyses, subjects were scheduled for the motility studies and tests for autonomic neuropathy. A clinical and ultrasonographic follow-up was planned within the next 8-12 mo. Ultrasonography was chosen because it was a non-invasive and validated technique allowing to study both gallbladder[1,10] and gastric[11-16] emptying, simultaneously[17]. We also developed a novel, one-day test for studying the upper gastrointestinal motility by simultaneous assessment of gallbladder, stomach, and small bowel transit[18].

Gallbladder and gastric emptying

The gallbladder was studied for content, wall, shape, and motility with standardized methodology[17]. Gallstones were diagnosed by the presence of mobile high-level echoes with acoustic shadows in the gallbladder, and sludge by the presence of mildly echogenic intraluminal sediment in the absence of acoustic shadows[19]. All gallstone patients had a small gallstone burden (*i.e.* less or equal to 20% of fasting gallbladder volume)[20] and a thin gallbladder wall (*i.e.* less than 3 mm in the fasting state) delimiting a regularly pear-shaped organ[17]. Gallbladder motility was assessed by monitoring gallbladder volumes before and at 5-15 min intervals over 2 h after ingestion of a liquid test meal.

Gastric emptying was assessed by monitoring antral areas at the same time points as for the gallbladder[11,13]. The equipment consisted of an Esaote AUC50 equipped with a 3.5 MHz convex probe. The test meal consisted of 200 mL liquid formula containing fat 11.6 g (35%), protein 12 g (16%) and carbohydrate 36.8 g (49%) with a total of 300 kcal, 1 270 kJ, 445 mOsm/L (*Nutridrink*®, Nutricia S.p.A., Lainate Milano, Italy).

Orocecal transit time

Orocecal transit time was measured at the time when ultrasonographic studies were performed by the hydrogen breath test with a portable, previously validated device (EC60-Gastrolyzer, Bedfont, USA)[18,21]. The substrate consisted of 10 g lactulose (Duphalac Dry®, Solvay Pharma, Belgium) which was added directly to the standard liquid test meal. The accuracy of the detector was±2 p.p.m. A rise of 10 p.p.m. above baseline on two consecutive measurements was considered as orocecal transit time and expressed in minute[22].

Autonomic neuropathy

Symptoms and signs of autonomic dysfunction were evaluated by taking the clinical history according to Rangari *et al*.[23]. The questionnaire was scored as "normal", "mild" and "severe" for the presence of orthostatic hypotension, gastric symptoms, bowel disorders, sweating disorders, bladder dysfunction and in males, impotence. A combination of tests including the Sweat-spot-test (SST)[22,24,25] and cardiorespiratory reflex tests[26], were employed as sensitive methods to assess the presence of autonomic neuropathy[27]. The SST was used to investigate the involvement of cholinergic sympathetic fibers by analyzing sweat abnormalities on the dorsum of the foot. An example of positive and negative test is shown in Figure 1.

A portable device was used to measure the "beat-to-beat" modifications of the R-R interval using skin electrodes connected to *Cardionomic*® (Lifescan, Italy). Lying-to-standing and standing-to-lying tests were used for sympathetic involvement. Valsalva maneuver, deep-breathing, cough test, and postural hypotension test were used for parasympathetic

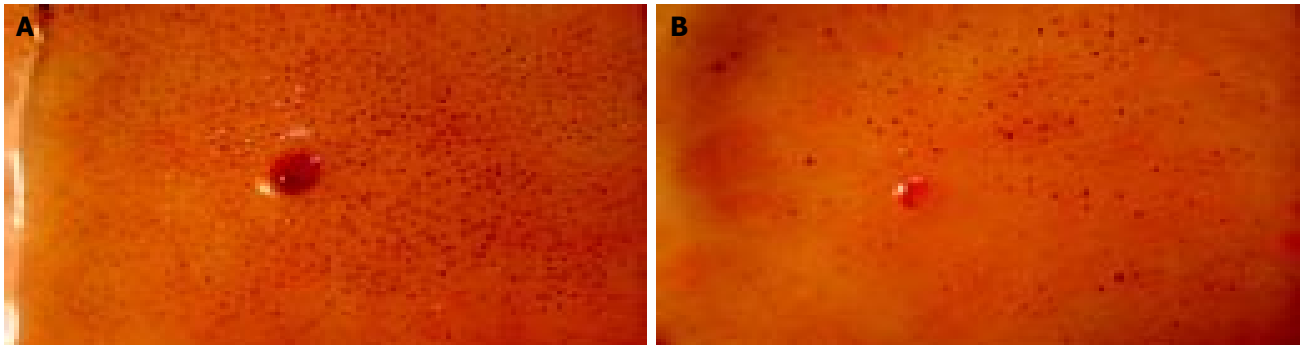

Figure 1 Sweat spot test (SST) for assessment of sympathetic autonomic nervous system[22,24,25]. The skin is coated with iodine and a fine emulsion of starch in arachis oil. Sweat is stimulated by intra-dermal injection of of 0.1 mL acetylcholine (the red dot indicates the point of injection). Denervated glands do not respond to the acetylcholine injection. A colorimetric reaction between starch and iodine is triggered by the sweat from stimulated glands, so that each pore appears as a small black dot after 2-5 min. A digital photo is taken and transferred to a magnifying software to measure the number and distribution of dots appearing in a standard squared grid of 529 mm^2 divided into 64 squared subareas. A normal SST implied a score 12 dots/subarea and/or <8% of abnormal subareas (each square of the grid having less than 6 dots) according to Ryder[24] and to our group[25]. Only patients with both indices (SST score and % abnormal subareas) outside normal limits were considered to have a positive test. A: Normal and even distribution of sweating glands seen as black dots; B: Defective response in a β-thalassemia major patient with sympathetic autonomic neuropathy.

involvement. The results of each test were scored as normal, borderline or abnormal, according to age-controlled values. The overall results for autonomic neuropathy were therefore normal (all tests normal), early involvement (one abnormal test or two borderline abnormal), definite involvement (two or more abnormal tests)[23].

Questionnaires

On the same day of the motility studies, subjects were asked to complete the following questionnaires under the supervision of one operator.

Bristol stool scale form[28] This is a semi-quantitative score to assess the quality of bowel movements. The weekly frequency of evacuations over a time span of one mo was also assessed.

Dyspepsia score[29] This is a semi-quantitative score from four symptoms such as epigastric pain, burning, belching/burping, postprandial fullness. Maximum score was equal to 48 with the upper normal limit equal to 8 and estimated from the mean±2SD of healthy control values.

Visual analogue scales (VAS) of upper gastrointestinal perception[18,30] These are self-assessed 100 mm horizontal lines of upper gastrointestinal perception monitoring appetite, satiety, nausea, abdominal fullness and upper abdominal (epigastric) pain or discomfort. Scores in mm were obtained at baseline (*i.e.* time 0) and at 15, 30, 45, 60, 90 and 120 min postprandially.

Rome criteria for biliary pain[31] Patients with gallstones or sludge were considered "symptomatic" with a history of one or more episodes of colicky pain during the last 12 mo.

Health survey SF-36[18,32,33] This is a short form of questionnaires assessing health-related quality of life (HRQOL). The SF36 includes 36 items which measure eight multi-item variables: general health, physical function, role physical, role emotional, social function, mental health, body pain, and vitality. Healthy subjects in this setting had a HRQOL profile remarkably similar to that derived from subjects across different cultures in USA and UK[34].

Statistical analysis

Results are expressed as mean±SE. Demographic data, as well as baseline characteristics were checked for normal distribution (Kolmogorov-Smirnov goodness of fit test). Statistical significance in contingency tables was evaluated using χ^2 -test or Fisher's exact test when appropriate. Comparison of continuous variables among groups was performed with unpaired Student's *t*-test or Mann-Whitney rank sum test when appropriate. Comparison between multiple groups was assessed using one-way analysis of variance (*ANOVA*) or the Kruskall-Wallis non parametric *ANOVA* on ranks. *Post-hoc* multiple pair wise comparisons were calculated with the Fisher's LSD test. Linear regression analysis was performed by the method of least square and Pearson's coefficient. A multivariate analysis was constructed to study the effect on appetite of motility variables. The variables showing significant correlations in univariate analysis were included in a stepwise multiple regression analysis. All statistical calculations were performed with the NCSS2004 software (Kaysville, UT, USA). Statistical tests were conducted as a two-sided alpha level of 0.05[35,36].

RESULTS

Gallbladder sludge and stones were found in 13 (56%) patients, all asymptomatic for previous episodes of biliary pain. Sludge was detected in 6 (26%) patients, while gallstones were observed in 7 (30%) patients, solitary and small in size (5-9 mm). The other 10 patients (44%) were gallstone/sludge-free.

Routine biochemical analysis

There was no difference in laboratory biochemistry among the three subgroups of thalassemia patients, according to gallbladder content (Table 1). There was a statistically significant relationship between levels of ferritin and AST and ALT in the serum ($0.73< r<0.77$; $P>0.00002$, $P<0.00007$).

Table 1 Laboratory biochemistry in β-thalassemia major patients with gallstones, biliary sludge and gallstone-free

	Gallstones	Sludge	Gallstone/ sludge-free	*P*
No. of subjects	7	6	10	
Total bilirubin (mg/dL)	2.3±0.4	1.4±0.4	1.8±0.3	NS
AST (U/L)	50.9±11.5	32.8±12.5	44.9±9.7	NS
ALT (U/L)	76.7±17.7	42.7±19.1	59.8±14.8	NS
Ferritin (mg/dL)	1 922±445	1 165±481	1 900±372	NS
Hb (g/dL)	9.3±0.1	9.5±0.2	9.5±0.1	NS
Iron (mg/dL)	186.8±16.8	189.6±8.4	156.5±16.8	NS
Total proteins (g/dL)	7.8±0.2	7.9±0.2	7.4±0.2	NS
GGT (U/L)	34.4±5.6	18.3±6.0	19.4±4.7	NS
Alk. Phosphatase (U/L)	1.15±0.2	0.98±0.2	0.9±0.2	NS
LDH (U/L)	331.3±46.7	293.7±36.7	310.7±28.4	NS
Cholesterol (mg/dL)	98.3±10.2	129.4±12.1	96.9±9.0	NS
Tryglicerides (mg/dL)	114.9±23.5	71.6±27.9	84.4±22.0	NS

Data are expressed as mean±SE; NS: Not significant; AST: Aspartate transaminase; ALT: Alanine transaminase; GGT: Gamma-glutamyl transpeptidase; LDH: Lactate dehydrogenase.

Ultrasonographic studies

The study of gallbladder emptying showed that β-thalassemia major patients had increased fasting gallbladder volume (38.0±4.8 mL *vs* 20.3±0.7 mL, $P = 0.0001$), and residual volume (7.9±1.3 mL *vs* 5.1±0.3 mL, $P = 0.002$), decreased percent residual volume (20.3±1.5% *vs* 24.6±1.0%, $P = 0.03$) and slightly slower emptying (24.9±1.7 min *vs* 20.1±0.7 min, $P = 0.04$) than controls, as also suggested by the analysis of the gallbladder emptying curves (Figure 2).

Although all subgroups compared to controls had a significantly greater fasting gallbladder volume, only patients with biliary sludge and normal gallbladder had increased residual volume and delayed emptying. Indeed, relative gallbladder contraction (percent residual volume) was increased in patients with gallstones. β-thalassemia patients and controls showed comparable fasting and postprandial indices of gastric emptying (Table 2).

Orocecal transit time

Mean OCTT was longer in β-thalassemia patients than in controls (132.2±7.8 min *vs* 99.7±2.3 min, $P = 0.00003$) (Figure 3). Seven patients (30.4%) but none of controls had OCTT above the upper normal value of 140 min (*i.e.* mean±2SD) derived from the control group ($P = 0.000026$, χ^2-test). Similar results were found among different subgroups (Table 2).

Autonomic neuropathy

Twenty-one patients agreed to undergo the tests. Symptoms and signs of autonomic dysfunction were found in 11 patients (52%), which were mild in all but 2 cases (asymptomatic). Early or definitive parasympathetic and sympathetic involvement was present in 76.2% and 66.7% of cases, respectively. Early involvement was more frequent in the cases of parasympathetic AN system than those of sympathetic AN system (81.3% *vs* 28.6%, $P = 0.00037$). Overall, there were 3 (14%), 5 (24%), and 13 (62%) patients with normal tests, early involvement (mainly parasympathetic), and definitive involvement (both parasympathetic and sympathetic), respectively. All 5 patients with type I insulin-dependent diabetes or impaired oral glucose tolerance test and all 7 patients with thyroid involvement had

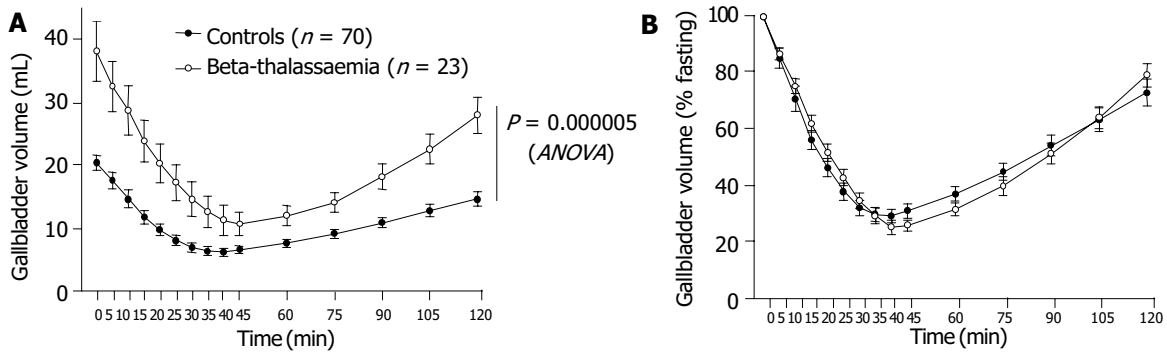

Figure 2 Time-course of fasting and postprandial gallbladder volumes in 23 β-thalassemia major patients and 70 controls and expressed as mL (panel A) or percent fasting gallbladder volume (panel B). Symbols indicate means, while vertical lines indicate SEM. Patients had impaired gallbladder emptying, with significantly increased fasting and postprandial volumes at each time point (panel A), in spite of similar contraction (panel B), compared to controls.

Table 2 Dyspeptic symptoms, bowel habits and gastrointestinal motility indices (gallbladder, stomach, small bowel) in β-thalassemia major patients with or without gallstone/sludge and in controls

	Gallstones	Sludge	GS/sludge-free	Controls	*P*
No. of subjects	7	6	10	70	
Dyspepsia (Buckley score)	5.0±1.0	6.8±2.2	7.8±2.5[a]	4.9±0.2	0.046
Bowel habits (Bristol score)	3.5±0.21	3.4±0.6	3.8±0.2	3.5±0.07	NS
Stomach					
Fasting antral area (cm^2)	2.8±0.2	2.9±0.2	3.4±0.3	3.2±0.1	NS
Postprandial maximal area (cm^2)	10.4±0.2	10.7±0.5	10.9±0.4	11.5±0.2	NS
Postprandial minimal area (%)	0.9±0.5	0.3±0.3	0.4±0.7	2.1±0.4	NS
Postprandial minimal (cm^2)	2.9±0.2	3.0±0.2	3.3±0.2	3.4±0.1	NS
Half-emptying time (min)	28±2	31±2	28±2	27±1	NS
Gallbladder					
Fasting volume (mL)	30.1±3.8[a]	42.9±10.3[a]	40.6±8.9[a]	20.3±0.7	0.000001
Postprandial residual volume (mL)	4.4±0.9	10.0±2.7[ac]	9.1±2.3[ac]	5.1±0.3	0.00030
Postprandial residual volume (%)	14.7±1.6[a]	23.0±2.7	22.6±2.4	24.6±1.0	0.023
Half-emptying time (min)	21±1	27±5[a]	26±2[a]	20±1	0.009
Small bowel					
Orocecal transit Time (min)	128.6±13.4[a]	30.0±15.0[a]	136.0±13.6[a]	99.7±2.3	0.000002

Data are expressed as mean±SE; GS: Gallstones; [a]$P<0.05$ *vs* controls; [c]$P<0.05$ *vs* gallstones (*ANOVA* and Fisher's LSD multiple-comparison test); NS: Not significant.

evidence of autonomic neuropathy. Neither age nor mean duration of desferrioxamine therapy was significantly different in patients with or without autonomic neuropathy (data not shown). Patients with autonomic neuropathy compared with those without it ($n = 3$, scant number might imply a type 2 error), showed a trend towards longer OCTT (132±9 min *vs* 117±3 min, $P = 0.06$), increased fasting volume (39.5±5.7 mL *vs* 19.7±4.3 mL, $P = 0.07$) and decreased contraction (residual volume 8.6±1.6 *vs* 3.2±0.7 mL, $P = 0.044$).

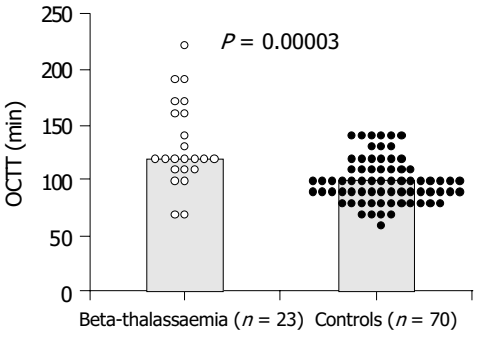

Figure 3 Orocecal transit time (OCTT) by lactulose H_2-breath test in β-thalassemia major patients and controls. Patients had significantly longer OCTT than controls. Data are expressed as individual points and means (bars).

Questionnaires

Overall, bowel habits were comparable in controls and patients (overall: 3.5±0.01 *vs* 3.6±0.2, respectively), while the score for dyspepsia was slightly higher (and statistically significant) in patients than in controls (6.7±1.2 *vs* 4.9±0.2, $P = 0.027$) (Table 2).

The results of VAS for satiety and appetite (as postprandial AUC) showed that the two feelings were strongly and negatively correlated in both patients (r=-0.87, $P<0.0001$ $n = 23$) and controls (r=-0.03, $P<0.0001$, $n = 70$). Profiles for both appetite and satiety, however, were different in patients and controls. Fasting and postprandial appetite scores were invariably greater in patients than in controls. In particular, VAS for appetite was increased at baseline and showed a rapid decrease followed by a rapid and marked postprandial increase, compared to controls (Figure 4). Whereas univariate analysis suggested an inverse relation between appetite and OCTT, gallbladder contraction (as residual volume in percent) and gallbladder half emptying time, multiple regression analysis identified gallbladder half-emptying time as the only predictor ($P<0.002$) of time-related changes of appetite perception in patients. The relationship is shown in Figure 5.

There was no difference in nausea, fullness and abdominal pain between patients and controls either at baseline or postprandially (data not shown).

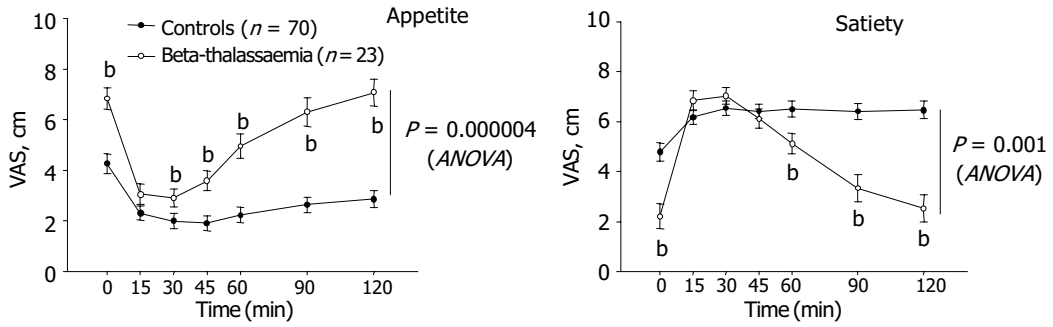

Figure 4 Time-course of visual analogue scale (VAS) for appetite and satiety in β-thalassemia major patients and controls. Data are mean±SE. On the X-axis time "0" is before ingestion of test meal. Asterisks indicate significant differences of controls *vs* patients ($0.0001<P<0.001$, at various time-points and overall *ANOVA*).

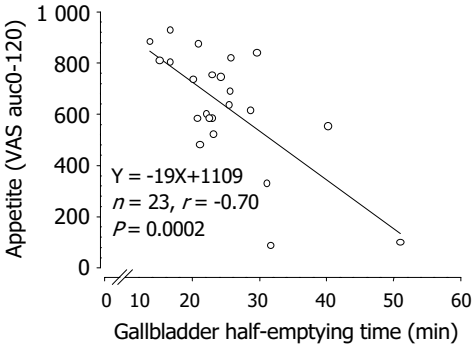

Figure 5 Correlation between appetite sensation (area under curve during 120 min of visual analogues scale) and speed of gallbladder emptying (half-emptying time) in β-thalassemia major patients.

Quality of life

Patients showed a significant deterioration in general health and a lower score than controls (51.7±4 *vs* 73.1±2, $P = 0.00002$, *ANOVA*). All other domains were similar between the two groups.

Follow-up

The follow up was completed after 8-12 mo in 16 out of 23 (69.6%) patients (2 patients were lost at follow-up because one died and the other moved to a different city). All patients remained asymptomatic for biliary symptoms. Gallbladder ultrasound was utilized to identify three subgroups of patients according to gallbladder content: (1) patients with a still anechoic gallbladder bile ($n = 5$), (2) patients who developed biliary sludge alone ($n = 4$) and (3) patients with prior sludge/gallstones who had unchanged gallbladder content ($n = 5$) or had stones and developed additional sludge ($n = 2$) during follow-up.

Table 3 Prior gallbladder motility indices in β-thalassemia major patients according to ultrasonographic appearance of the gallbladder during 8-12 mo follow-up

	Still anechoic	Developed sludge	Prior sludge / gallstones
No. of subjects	5	4	7
Fasting volume (mL), basal	29.2±7.3	60±17[a]	29.2±4.2
Residual volume (mL), basal	5.5±1.4	14.7±4.6[a]	4.9±0.9
Fasting volume at follow-up (mL)	30.9±6.5	72.8±20.1[ac]	36.7±5.1

Data are expressed as mean±SE; [a]$P<0.017$ *vs* still anechoic group; [c]$P<0.05$ *vs* prior sludge / gallstones group (*ANOVA* and Fisher's LSD multiple comparison test).

Variations in individual fasting gallbladder volumes for each subgroup are depicted in Figure 6. Major changes were evident in patients developing biliary sludge (panel A), also when gallbladder volume was expressed as percent increase (panel B). Interestingly, maximum percent increase in fasting gallbladder volume was observed in 2 patients (89% and 130%) who developed sludge in a gallbladder which previously contained only stones and showed normal fasting volume (*i.e.*<cut-off value of 32 mL). These two patients had clinical evidence of diabetes mellitus (and autonomic neuropathy) and hypothyroidism.

Furthermore, patients who developed sludge during follow-up had also significant changes in postprandial gallbladder volume (Table 3), with a trend towards decreased gallbladder contraction (residual volume: 25.6±4.7% *vs* 19.5±2.8% *vs* 17.9 ±3.0%), and longer transit time (OCTT: 150±15.8 *vs* 108±9.7 *vs* 126±12.9 min) when compared with the other two subgroups.

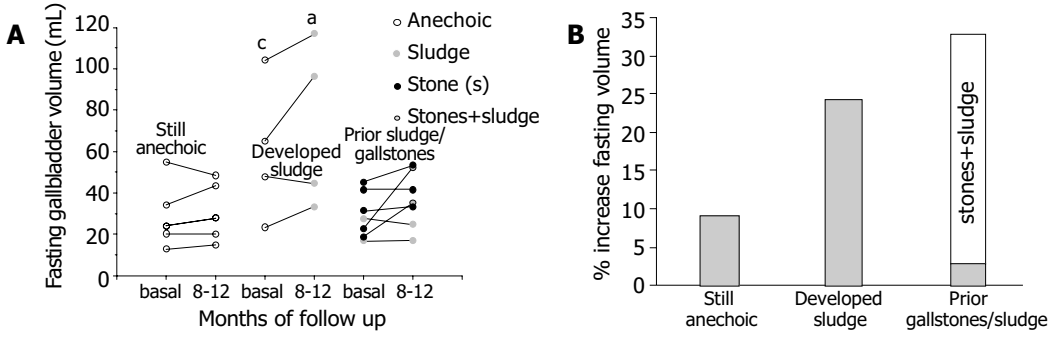

Figure 6 Varations in individual fasting gallbladder volumes for each subgroup in β-thalassemia major patients. A: Major changes in patients who developed biliary sludge: asterisks indicate significant differences, compared to the other two groups of patients ([a]$P<0.05$ *vs* prior sludge / gallstones group and [c]$P<0.017$ *vs* still anechoic group). B: Percent increased fasting gallbladder volume in the three groups of patients. The last bar represents those gallbladders with stones that developed additional sludge ($n = 2$).

DISCUSSION

The present study examined the role of gallbladder and gastrointestinal motility in a well characterized group of adult β-thalassemia major patients in their 3rd decade of life, in relation with the presence of gallstones/biliary sludge. The results suggested the coexistence of impaired gallbladder motility, delayed small intestinal transit, and high prevalence of autonomic neuropathy in β-thalassemia major patients. These abnormalities might contribute, together with haemolytic hyperbilirubinemia to the pathogenesis of gallstones/sludge in β-thalassemia major.

As for other hemolytic disorders including sickle hemoglobinopathy[37], both hyperbilirubinemia and bilirubin overload/precipitation in bile were definite predisposing factors for pigment gallstone in β-thalassemia major patients during chronic hemolysis[6]. Indeed, in this study gallstones and/or biliary sludge were found in 56% of β-thalassemia major patients at entry, increasing to over 80% during follow-up (8-12 mo). A previous study[7] in young patients reported a prevalence of 11.8% and 29.4% for gallstones and sludge, respectively. However, the mean age of β-thalassemia major patients in the present series was 26 years, while it was 12 years in the above mentioned study.

Several pathways might be involved in the pathogenesis of sludge and pigment stones in β-thalassemia. Glucuronidation of excess bilirubin was a predisposing factor in chronic haemolitic diseases[38]. After injection of desferroxamine, both fecal and urinary excretion were observed and there was formation of iron-desferroxamine complex[39] which might potentially interfere with the gallbladder microenviroment, already enriched in calcium bilirubinate. Moreover, increased secretion of glycoproteins by epithelial cells was seen after iron-induced stimulation in the guinea pig gallbladder[40], and this might also take place in β-thalassemia major patients who developed sludge. However, since not all β-thalassemia patients with hemolytic hyperbilirubinemia had gallstones, other pathogenetic mechanisms underlying gallstone formation in β-thalassemia major may play a role.

The present study for the first time suggested that bile stasis and intestinal dysmotility might be key factors in the pathogenesis of pigment gallstones in β-thalassemia major. Pigment stones were common in patients with cirrhosis[41,42], chronic hemolysis[37,43,44], ileal Crohn's disease[45], and conditions associated with impaired gallbladder kinetics[37,44,46-48]. A recent study by our group found a certain degree of impaired motorfunction of the gallbladder also in non-hemolytic pigment stone patients[1]. Compared with controls, there was about 100% increase of fasting gallbladder volume across 3 β-thalassemia major subgroups: *i.e.* patients with stones, sludge and stone-sludge free. Increased fasting gallbladder volume seems to be common in hemolytic conditions leading to pigment stones. Everson *et al.* found a volume of about 27 mL in adolescents and young adults with sickle hemoglobinopathy[37]. Nevertheless, we found that adult "symptomatic" pigment (non hemolytic) stone patients had a fasting volume comparable to controls[2]. In general, fasting gallbladder volume increased with body size[49] and obesity[49,50]. In this respect, the finding of increased fasting gallbladder volume was even more striking if one considered that β-thalassemia major patients had reduced growth with short stature, compared with matched controls[9]. The increment in fasting gallbladder volume in β-thalassemia major, therefore, represents a true phenomenon and seems to point to defective interprandial (fasting) gallbladder motility. It has been found that fluctuations in fasting gallbladder volume (leading to 20-30% contraction) are normally synchronized with the intestinal migrating motor complex (MMC) and release of the intestinal hormone motilin[51]. Patients with cholesterol gallstones had frequently increased fasting gallbladder volume[1] with abnormal MMC and motilin release pattern. Interdigestive gallbladder emptying was reduced, contributing to gallstone formation[52,53]. A similar derangement of fasting gallbladder motility might also develop in β-thalassemia major patients, and contribute to stasis and sludge/stone formation. A mechanical effect on fasting volume due to the physical presence of gallstones in the gallbladder lumen in β-thalassemia major was unlikely since fasting volume was larger in patients with sludge than in those with stones and also greater in patients without gallstone/sludge than in controls. Also, patients were all asymptomatic for biliary colicky pain (excluding an impacted stone within the cystic duct and/or acute cholecystitis). Our data indicate that postprandial gallbladder motility in β-thalassemia major patients is deranged. Not only fasting, but also residual volume was increased and emptying speed was somewhat slower (although still in the normal range) in sludge or gallstone/sludge-free patients, compared to both patients with gallstones and controls. The large residual gallbladder volume might be the consequence of a greater starting fasting volume[1,50,54-58]. By contrast, we found that "crude" contraction was preserved (*i.e.* similar or even smaller percent residual volume than in controls, Table 2). Thus, findings in the present study mimicked those seen in sickle hemoglobinopathy[37], with a smaller contraction index characteristic of β-thalassemia major patients (without mentioning gallbladder emptying speed). Differences in patients' characteristics, age and study protocol might partly account for the discrepancies across studies. Why in our study those patients with gallstones had better gallbladder contraction than controls, remains to be elucidated. Prospective observations are needed to see if, at *equilibrium* (*i.e.* after stone have formed), the gallbladder adapts to a smaller fasting volume and therefore better contraction (smaller residual volume). According to Laplace's law, in fact, the smaller the radius of a given shape (*i.e.* the gallbladder), the smaller the wall tension (from smooth muscle contraction) required to withstand a given internal fluid pressure[59]. It is highly unlikely that release of endogenous cholecystokinin was deranged in this series of pigment gallstone patients, as seen during total parenteral nutrition[60]. Whereas in cholesterol gallstone patients excess biliary cholesterol might alter cholecystokinin smooth muscle receptors[61,62], resulting in secondary impaired gallbladder motility. This possibility has been ruled out in β-thalassemia major patients. In fact, biliary cholesterol saturation did not increase in pigment stone patients and gallbladder smooth muscle contractility *in vitro* was normal[63].

We also found that OCTT was slightly delayed in β-thalassemia major patients, evidently across all subgroups. A clear explanation of the finding is not readily available, but a condition secondary to bacterial overgrowth or delayed colonic transit was highly unlikely, since there was no evidence of bacterial translocation with H_2-breath test and all patients had normal weekly bowel habits and a stool scale form. Small bowel dysmotility might accompany abnormal intestinal migrating motor complexes, as seen in a subgroup of patients with irritable bowel[64] and functional dyspepsia[65]. Also, intestinal mucosal changes have been described in β-thalassemia major patients[66] and might influence some motility patterns in the small bowel. Others have found that small bowel inflammation and/or malabsorption are not more frequent in β-thalassemia major patients[67]. Patients with ileal disease, bypass, or resection were at increased risk for developing pigment gallstones, so were patients with ileal Crohn's disease. Increased bilirubin levels in bile of patients with Crohn disease were caused by lack of functional ileum[45]. One might speculate that delayed OCTT in β-thalassemia major patients might lead to increase of enterohepatic cycling of bilirubin[68], therefore predisponing to pigment gallstone formation.

Autonomic neuropathy might be associated with gastrointestinal dysmotility. As expected, all β-thalassemia major patients with diabetes or abnormal oral glucose tolerance test had impaired tests for autonomic neuropathy (*i.e.* 23% of all patients).

Surprisingly abnormal tests of sympathetic and parasympathetic system were found in 86% of the patients. Potential causes for autonomic neuropathy in β-thalassemia major patients were the coexistence of diabetes mellitus, neurotoxicity of desferroxamine ad iron overload (or both)[69,70] (for example, visual and auditory neurotoxicity were found in 1 patient of this series). The presence of hemolysis might also contribute to neuropathy, as abnormal autonomic cardiovascular response was described in patients with sickle cell anemia[71]. Last but not least, the presence of autonomic dysfunction was also a feature in patients with different types and stages of chronic liver disease,[72] and this might also the case in chronic liver disease of β-thalassemia major patients. Further studies are needed to clarify if the presence of autonomic dysfunction is a useful tool for the prediction of prognosis and outcome of patients with β-thalassemia major.

Positive tests for autonomic neuropathy tended to relate to abnormal gallbladder and small bowel motility. Interestingly, we found delayed OCTT with increased bowel movements in chronic alcoholic patients during abstinence, was associated with dysfunction of autonomic nervous system. A form of subclinical autonomic neuropathy might predispone to a diffuse disorder of smooth muscle, suggesting the multi-organic involvement of the gastrointestinal tract. In the determination of altered OCTT a possible role for dysfunction of autonomic nervous system has been suggested in other series of patients[22] and might deserve further investigations also in β-thalassemia major patients.

In conclusion, the present study shows for the first time that in β-thalassemia major patients in the 3rd decade of life, increased volume and deranged motility of the gallbladder are associated with delayed small intestinal transit and mild dyspeptic symptoms. Such functional abnormalities apparently contribute together with haemolytic hyperbilirubinemia to the pathogenesis of gallstones/sludge in β-thalassemia major.

REFERENCES

1 **Portincasa P,** Di Ciaula A, Baldassarre G, Palmieri VO, Gentile A, Cimmino A, Palasciano G. Gallbladder motor function in gallstone patients: sonographic and *in vitro* studies on the role of gallstones, smooth muscle function and gallbladder wall inflammation. *J Hepatol* 1994; **21**: 430-440

2 **Portincasa P,** Di Ciaula A, Vendemiale G, Palmieri VO, Moschetta A, vanBerge-Henegouwen GP, Palasciano G. Gallbladder motility and cholesterol crystallization in bile from patients with pigment and cholesterol gallstones. *Eur J Clin Invest* 2000; **30**: 317-324

3 **Portincasa P,** Di Ciaula A, Palmieri VO, Velardi A, vanBerge-Henegouwen GP, Palasciano G. Impaired gallbladder and gastric motility and pathological gastro-esophageal reflux in gallstone patients. *Eur J Clin Invest* 1997; **8**: 653-661

4 **van Erpecum KJ,** vanBerge-Henegouwen GP. Gallstones: an intestinal disease? *Gut* 1999; **44**: 435-438

5 **Rodgers GP.** Hemogloblinopathies: The Thalassemias. In: Goldmann L, Bennett JC, editors. Cecil. Textbook of Medicine. Philadelphia: W.B. *Saunders Company* 2000

6 **Sherlock S,** Dooley J. Diseases of the liver and biliary system. *Oxford Blackwell Science* 2002

7 **Kalayci AG,** Albayrak D, Gunes M, Incesu L, Agac R. The incidence of gallbladder stones and gallbladder function in beta-thalassemic children. *Acta Radiol* 1999; **40**: 440-443

8 **Leoni GB,** Rosatelli C, Vitucci A, Addis M, Loi A, Tannoia N, Cao A. Molecular basis of beta-thalassemia intermedia in a southern Italian region (Puglia). *Acta Haematol* 1991; **86**: 174-178

9 **Wonke B.** Clinical management of beta-thalassemia major. *Semin Hematol* 2001; **38**: 350-359

10 **Everson GT,** Braverman DZ, Johnson ML, Kern F Jr. A critical evaluation of real-time ultrasonography for the study of gallbladder volume and contraction. *Gastroenterology* 1980; **79**: 40-46

11 **Hveem K,** Jones KL, Chatterton BE, Horowitz M. Scintigraphic measurement of gastric emptying and ultrasonographic assessment of antral area: relation to appetite. *Gut* 1996; **38**: 816-821

12 **Wedmann B,** Schmidt G, Wegener M, Coenen C, Ricken D, Althoff J. Effects of age and gender on fat-induced gallbladder contraction and gastric emptying of a caloric liquid meal: a sonographic study. *Am J Gastroenterol* 1991; **86**: 1765-1770

13 **Bolondi L,** Bortolotti MSV, Calleti T, Gaiani S, Labo' G. Measurement of gastric emptying by real-time ultrasonography. *Gastroenterology* 1985; **89**: 752-759

14 **Ricci R,** Bontempo I, Corazziari E, La Bella A, Torsoli A. Real-time ultrasonography of the gastric antrum. *Gut* 1993; **34**: 173-176

15 **Bergmann JF,** Chassany O, Petit A, Triki R, Caulin C, Segrestaa JM. Correlation between echographic gastric emptying and appetite: influence of psyllium. *Gut* 1992; **33**: 1042-1043

16 **Darwiche G,** Almer LO, Bjorgell O, Cederholm C, Nilsson P. Measurement of gastric emptying by standardized real-time ultrasonography in healthy subjects and diabetic patients. *J Ultrasound Med* 1999; **18**: 673-682

17 **Portincasa P,** Colecchia A, Di Ciaula A, Larocca A, Muraca M, Palasciano G, Roda E, Festi D. Standards for diagnosis of gastrointestinal motility disorders. Ultrasonography . *Dig Liver Dis* 2000; **32**: 160-172

18 **Portincasa P,** Moschetta A, Baldassarre G, Altomare DF, Palasciano G. Pan-enteric dysmotility, impaired quality of life and alexithymia in a large group of patients meeting the Rome II criteria for irritable bowel syndrome. *World J Gastroenterol* 2003; **9**: 2293-2299

19 **Gallinger S,** Taylor RD, Harvey PRC, Petrunka CN, Strasberg SM. Effects of mucous glycoprotein on nucleation time of human bile. *Gastroenterology* 1985; **89**: 648-658

20 **Portincasa P,** Di Ciaula A, Palmieri VO, Vendemiale G, Altomare E, Palasciano G. Sonographic evaluation of gallstone burden in humans. *Ital J Gastroenterol Hepatol* 1994; **26**: 141-144

21 **Mann NS,** Condon DS, Leung JW. Colonic preparation correlates with fasting breath hydrogen in patients undergoing colonoscopy. *Hepatogastroenterology* 2003; **50**: 85-86

22 **Altomare DF,** Portincasa P, Rinaldi M, Di Ciaula A, Martinelli E, Amoruso AC, Palasciano G, Memeo V. Slow-transit constipation: a solitary symptom of a systemic gastrointestinal disease. *Dis Colon Rectum* 1999; **42**: 231-240

23 **Rangari M,** Sinha S, Kapoor D, Mohan JC, Sarin SK. Prevalence of autonomic dysfunction in cirrhotic and noncirrhotic portal hypertension. *Am J Gastroenterol* 2002; **97**: 707-713

24 **Ryder RE,** Marshall R, Johnson K, Ryder AP, Owens DR, Hayes TM. Acetylcholine sweatspot test for autonomic denervation. *Lancet* 1988; **1**: 1303-1305

25 **Altomare D,** Pilot MA, Scott M, Williams N, Rubino M, Ilincic L, Waldron D. Detection of subclinical autonomic neuropathy in constipated patients using a sweat test. *Gut* 1992; **33**: 1539-1543

26 **Vespasiani G,** Bruni M, Meloncelli I, Clementi L, Amoretti R, Branca S, Carinci F, Lostia S, Nicolucci A, Romagnoli F, Verga S, Benedetti MM. Validation of a computerised measurement system for guided routine evaluation of cardiovascular autonomic neuropathy. *Comput Methods Programs Biomed* 1996; **51**: 211-216

27 **Diem P,** Laederach-Hofmann K, Navarro X, Mueller B, Kennedy WR, Robertson RP. Diagnosis of diabetic autonomic neuropathy: a multivariate approach. *Eur J Clin Invest* 2003; **33**: 693-697

28 **O'Donnell MR,** Virjee J, Heaton KW. Detection of pseudo diarrhoea by simple assessment of intestinal transit rate. *Br Med J* 1990; **300**: 439-440

29 **Buckley MJ,** Scanlon C, McGurgan P, O'Morain C. A validated dyspepsia symptom score. *Ital J Gastroenterol Hepatol* 1997; **29**: 495-500

30 **Portincasa P,** Altomare DF, Moschetta A, Baldassarre G, Di Ciaula A, Venneman NG, Rinaldi M, Vendemiale G, Memeo V, vanBerge-Henegouwen GP, Palasciano G. The effect of acute oral erythromycin on gallbladder motility and on upper gastrointestinal symptoms in gastrectomized patients with and without gallstones: a randomized, placebo-controlled ultrasonographic study. *Am J Gastroenterol* 2000; **95**: 3444-3451

31 **Schoenfield LJ,** Carulli N, Dowling RH, Sama C, Wolpers C. Asymptomatic gallstones: definition and treatment. *Gastroenterol International* 1989; **2**: 25-29

32 **Ware JE,** Snow KK, Kosinski M. SF-36 health survey. Manual

and interpretation guide. Boston: The Health Institute: *New England Medical Center* 1993
33 **Stewart AL,** Greenfield S, Hays RD, Wells K, Rogers WH, Berry SD, McGlynn EA, Ware JE Jr. Functional status and well-being of patients with chronic conditions. Results from the Medical Outcomes Study. *JAMA* 1989; **262**: 907-913
34 **Hahn BA,** Yan S, Strassels S. Impact of irritable bowel syndrome on quality of life and resource use in the United States and United Kingdom. *Digestion* 1999; **60**: 77-81
35 **Armitage P,** Berry G. Statistical methods in medical research. 3rd ed. *Oxford Blackwell Science Ltd* 1994
36 **Dawson B,** Trapp RG. Basic & Clinical Biostatistics. 3rd ed. *New York McGraw Hill* 2001
37 **Everson GT,** Nemeth A, Kourourian S, Zogg D, Leff NB, Dixon D, Githens JH, Pretorius D. Gallbladder function is altered in sickle hemoglobinopathy. *Gastroenterology* 1989; **96**: 1307-1316
38 **Fevery J,** Verwilghen R, Tan TG, de Groote J. Glucuronidation of bilirubin and the occurrence of pigment gallstones in patients with chronic haemolytic diseases. *Eur J Clin Invest* 1980; **10**: 219-226
39 **Faa G,** Crisponi G. Iron chelating agents in clinical practice. *Coodination Chemistry Reviews* 1999; **184**: 291-310
40 **Hale WB,** Turner B, LaMont JT. Oxygen radicals stimulate guinea pig gallbladder glycoprotein secretion *in vitro*. *Am J Physiol* 1987; **253**: G627-G630
41 **Alvaro D,** Angelico M, Gandin C, Ginanni Corradini S, Capocaccia L. Physico-chemical factors predisposing to pigment gallstone formation in liver cirrhosis. *J Hepatol* 1990; **10**: 228-234
42 **Sakata R,** Ueno T, Sata M, Sujacu K, Tamaki S, Torimura T, Tanikawa K. Formation of black pigment gallstone in a hamster model of experimental cirrhosis. *Eur J Clin Invest* 1997; **27**: 840-845
43 **Carey MC.** Pathogenesis of gallstones. *Am J Surg* 1993; **165**: 410-419
44 **Trotman BW.** Pigment gallstone disease. *Gastroenterol Clin North Am* 1991; **20**: 111-126
45 **Brink MA,** Slors JF, Keulemans YC, Mok KS, De Waart DR, Carey MC, Groen AK, Tytgat GN. Enterohepatic cycling of bilirubin: a putative mechanism for pigment gallstone formation in ileal Crohn's disease. *Gastroenterology* 1999; **116**: 1420-1427
46 **Kurihara N,** Ide H, Omata T, Yonamine S, Mashima Y, Tanno M, Chiba K, Yamada H. Evaluation of gallbladder emptying in patients with chronic liver disease by 99 mTc-EHIDA hepatobiliary scintigraphy. *Radioisotopes* 1989; **38**: 269-274
47 **Pompili M,** Rapaccini GL, Caturelli E, Curro D, Montuschi P, D'Amato M, Aliotta A, Grattagliano A, Cedrone A, Anti M. Gallbladder emptying, plasma levels of estradiol and progesterone, and cholecystokinin secretion in liver cirrhosis. *Dig Dis Sci* 1995; **40**: 428-434
48 **Acalovschi M,** Dumitrascu DL, Csakany I. Gastric and gall bladder emptying of a mixed meal are not coordinated in liver cirrhosis - a simultaneous sonographic study. *Gut* 1997; **40**: 412-417
49 **Palasciano G,** Serio G, Portincasa P, Palmieri VO, Fanelli M, Velardi ALM, Calo' Gabrieli B, Vinciguerra V. Gallbladder volume in adults and relationship to age, sex, body mass index and gallstones: a sonographic population study. *Am J Gastroenterol* 1992; **87**: 493-497
50 **Portincasa P,** Di Ciaula A, Palmieri VO, vanBerge-Henegouwen GP, Palasciano G. Effects of cholestyramine on gallbladder and gastric emptying in obese and lean subjects. *Eur J Clin Invest* 1995; **25**: 746-753
51 **Portincasa P,** Peeters TL, Berge-Henegouwen GP, Van Solinge WW, Palasciano G, van Erpecum KJ. Acute intraduodenal bile salt depletion leads to strong gallbladder contraction, altered antroduodenal motility and high plasma motilin levels in humans. *Neurogastroenterol Motil* 2000; **12**: 421-430
52 **Stolk MF,** van Erpecum KJ, Peeters TL, Samsom M, Smout AJ, Akkermans LM, vanBerge-Henegouwen GP. Interdigestive gallbladder emptying, antroduodenal motility, and motilin release patterns are altered in cholesterol gallstone patients. *Dig Dis Sci* 2001; **46**: 1328-1334
53 **Xu QW,** Scott RB, Tan DTM, Shaffer EA. Altered migrating myoelectrical complex in an animal model of cholesterol gallstone disease: the effect of erythromycin. *Gut* 1998; **43**: 817-822
54 **Palasciano G,** Portincasa P, Belfiore A, Baldassarre G, Cignarelli M, Paternostro A, Albano O, Giorgino R. Gallbladder volume and emptying in diabetics: the role of neuropathy and obesity. *J Intern Med* 1992; **231**: 123-127
55 **Portincasa P,** Di Ciaula A, Palmieri VO, vanBerge-Henegouwen GP, Palasciano G. Ultrasonographic study of gallbladder and gastric dynamics in obese people after oral cholestyramine. *Dordrecht Kluwer Academic Publisher* 1994: 323-327
56 **Portincasa P,** Di Ciaula A, Palmieri VO, Baldassarre G, Palasciano G. Enhancement of gallbladder emptying in gallstone patients after oral cholestyramine. *Am J Gastroenterol* 1994; **89**: 909-914
57 **Festi D,** Frabboni R, Bazzoli F, Sangermano A, Ronchi M, Rossi L, Parini P, Orsini M, Primerano AM, Mazzella G, Aldini R, Roda E. Gallbladder motility in cholesterol gallstone disease. Effect of ursodeoxycholic acid administration and gallstone dissolution. *Gastroenterology* 1990; **99**: 1779-1785
58 **van de Meeberg PC,** Portincasa P, Wolfhagen FH, van Erpecum KJ, vanBerge-Henegouwen GP. Increased gall bladder volume in primary sclerosing cholangitis. *Gut* 1996; **39**: 594-599
59 **Shaffer EA.** Abnormalities in gallbladder function in cholesterol gallstone disease: bile and blood, mucosa and muscle—the list lengthens. *Gastroenterology* 1992; **102**: 1808-1812
60 **Sitzmann JV,** Pitt HA, Steinborn PA, Pasha ZR, Sanders RC. Cholecystokinin prevents parenteral nutrition induced biliary sludge in humans. *Surg Gynecol Obstet* 1990; **170**: 25-31
61 **Upp JR Jr,** Nealon WH, Singh P, Fagan CJ, Jonas AS, Greeley GH Jr, Thompson JC. Correlation of cholecystokinin receptors with gallbladder contractility in patients with gallstones. *Ann Surg* 1987; **205**: 641-648
62 **Xu QW,** Shaffer EA. The potential site of impaired gallbladder contractility in an animal model of cholesterol gallstone disease. *Gastroenterology* 1996; **110**: 251-257
63 **Behar J,** Lee KY, Thompson WR, Biancani P. Gallbladder contraction in patients with pigment and cholesterol stones. *Gastroenterology* 1989; **97:** 1479-1484
64 **Pfeiffer A,** Schmidt T, Holler T, Herrmann H, Pehl C, Wendl B, Kaess H. Effect of trospium chloride on gastrointestinal motility in humans. *Eur J Clin Pharmacol* 1993; **44**: 219-223
65 **Jebbink HJ,** Berge-Henegouwen GP, Bruijs PP, Akkermans LM, Smout AJ. Gastric myoelectrical activity and gastrointestinal motility in patients with functional dyspepsia. *Eur J Clin Invest* 1995; **25**: 429-437
66 **Awwad S,** Khalifa AS, Abdel-Fattah S, Mousa S, Sabry F, Eid S. Intestinal mucosal changes in thalassaemia major. *Gaz Egypt Paediatr Assoc* 1975; **23**: 261-265
67 **Sinniah D,** Nagalingam I. D-xylose absorption in B-thalassaemia major. *J Trop Med Hyg* 1978; **81**: 185-187
68 **Vitek L,** Carey MC. Enterohepatic cycling of bilirubin as a cause of 'black' pigment gallstones in adult life. *Eur J Clin Invest* 2003; **33**: 799-810
69 **Triantafyllou N,** Fisfis M, Sideris G, Triantafyllou D, Rombos A, Vrettou H, Mantouvalos V, Politi C, Malliara S, Papageorgiou C. Neurophysiological and neuro-otological study of homozygous beta-thalassemia under long-term desferrioxamine (DFO) treatment. *Acta Neurol Scand* 1991; **83**: 306-308
70 **Zafeiriou DI,** Kousi AA, Tsantali CT, Kontopoulos EE, Augoustidou-Savvopoulou PA, Tsoubaris PD, Athanasiou MA. Neurophysiologic evaluation of long-term desferrioxamine therapy in beta-thalassemia patients. *Pediatr Neurol* 1998; **18**: 420-424
71 **Romero-Vecchione E,** Perez O, Wessolosky M, Rosa F, Liberatore S, Vasquez J. Abnormal autonomic cardiovascular responses in patients with sickle cell anemia. *Sangre* 1995; **40**: 393-399
72 **Oliver MI,** Miralles R, Rubies-Prat J, Navarro X, Espadaler JM, Sola R, Andreu M. Autonomic dysfunction in patients with non-alcoholic chronic liver disease. *J Hepatol* 1997; **26**: 1242-1248

Edited by Wang XL **Proofread by** Chen WW and Xu FM

PO Box 2345, Beijing 100023, China
Fax: +86-10-85381893
E-mail: wjg@wjgnet.com www.wjgnet.com

World J Gastroenterol 2004;10(16):2391-2393
World Journal of Gastroenterology
 ISSN 1007-9327

• CLINICAL RESEARCH •

Clinical features of human intestinal capillariasis in Taiwan

Ming-Jong Bair, Kao-Pin Hwang, Tsang-En Wang, Tai-Cherng Liou, Shee-Chan Lin, Chin-Roa Kao, Tao-Yeuan Wang, Kwok-Kuen Pang

Ming-Jong Bair, Department of Gastroenterology, Mackay Memorial Hospital, Taitung Branch, Taiwan, China
Kao-Pin Hwang, Department of Pediatrics, Kaohsiung Medical College, Taipei, China
Tsang-En Wang, Tai-Cherng Liou, Shee-Chan Lin, Chin-Roa Kao, Department of Gastroenterology, Mackay Memorial Hospital, Taipei, China
Tao-Yeuan Wang, Department of Pathology, Mackay Memorial Hospital, Taipei, China
Kwok-Kuen Pang, Department of Radiology, Mackay Memorial Hospital, Taitung Branch, Taiwan, China
Correspondence to: Dr. Ming-Jong Bair, Department of Gastroenterology, Mackay Memorial Hospital, Taitung Branch, 1, Lane 303 Chang-Sha St. Taitung, Taiwan, China. library@ttms.mmh.org.tw
Telephone: +886-89-310150 **Fax:** +886-89-321240
Received: 2003-09-15 **Accepted:** 2003-11-06

Abstract

Human intestinal capillariasis is a rare parasitosis that was first recognized in the Philippines in the 1960 s. Parasitosis is a life threatening disease and has been reported from Thailand, Japan, South of Taiwan (Kaoh-Siung), Korea, Iran, Egypt, Italy and Spain. Its clinical symptoms are characterized by chronic diarrhea, abdominal pain, borborygmus, marked weight loss, protein and electrolyte loss and cachexia. Capillariasis may be fatal if early treatment is not given. We reported 14 cases living in rural areas of Taiwan. Three cases had histories of travelling to Thailand. They might have been infected in Thailand while stayed there. Two cases had the diet of raw freshwater fish before. Three cases received emergency laparotomy due to peritonitis and two cases were found of enteritis cystica profunda. According to the route of transmission, freshwater and brackish-water fish may act as the intermediate host of the parasite. The most simple and convenient method of diagnosing capillariasis is stool examination. Two cases were diagnosed by histology. Mebendazole or albendezole 200 mg orally twice a day for 20-30 d is the treatment of choice. All the patients were cured, and relapses were not observed within 12 mo.

Bair MJ, Hwang KP, Wang TE, Liou TC, Lin SC, Kao CR, Wang TY, Pang KK. Clinical features of human intestinal capillariasis in Taiwan. *World J Gastroenterol* 2004; 10(16): 2391-2393
http://www.wjgnet.com/1007-9327/10/2391.asp

INTRODUCTION

Capillaria species parasitize many classes of vertebrates, although only 4 species described have been found in humans, namely *Capillaria phillippinensis*, *Capillaria plica*, *Capillaria aerophila*, and *Capillaria hepatica*[1]. *C. philippinensis* is a tiny nematode that was first described in the 1960 s as the causative agent of severe diarrheal syndromes in humans. In 1962, the first case of human intestinal capillariasis occurred in a previously healthy young man from Luzon (Philippines) who subsequently died. At autopsy, a large number of worms, later described as *C. Philippinensis*, were found in the large and small intestines[2]. The disease was first reported by Chitwood *et al.* in 1964[3]. During the Philippine epidemic from 1967 to 1968, more than 1300 persons acquired the illness and 90 patients with parasitologically confirmed infections died[4]. In late 1978 and early 1979, another small outbreak was identified in northeastern Mindanao, the Phillippines, and about 50 persons acquired the infection[4]. Sporadic cases continued to appear in northern Luzon as well as in other areas where epidemics had occurred. The disease is also endemic in Thailand, and was first reported in 1973[5]. Sporadic cases have also been found in Iran[6], Egypt[7,8], Taiwan[9], Japan[10,11], Indonesia[12], Korea[13], Spain (probably acquired in Colombia)[14] and Italy (acquired in Indonesia)[15], indicating that this infection is widespread. Because the infection can result in a severe disease with a high mortality when untreated, early diagnosis is very important. Here we described 14 cases of human intestinal capillariasis found in Taiwan from 1983 to 2001.

MATERIALS AND METHODS

Since 1983, 14 cases have been diagnosed as intestinal capillariasis in Taiwan, all with the symptoms of chronic diarrhea, abdominal pain, borborygmus and marked weight loss. All patients were hospitalized for examination and treatment. Their diagnosis was confirmed by eggs and/or larvae and/or adult *C. philippinensis* found in the feces of 5 patients. Two cases were recognized by a pathologist by histology of jejunum or ileum (Figures 1, 2) with negative stool examination. Bacterial cultures of stool specimens were negative in all patients. The stool specimens were examined by formalin-ether concentration method. *C. Philippinensis* eggs were peanut-shaped with flattened bipolar plugs, 20×40 mm in size (Figure 3).

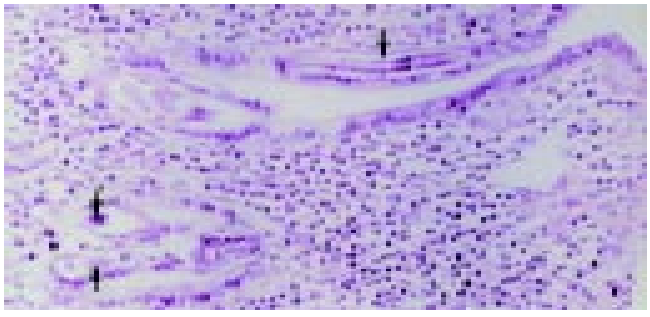

Figure 1 C Philippinensis worms embedded in intestinal mucosa (arrow). Hematoxylin and eosin, ×200.

RESULTS

Fourteen cases, nine males and five females, were 36 to 76 years old when they were diagnosed as intestinal capillariasis (Tables 1, 2). Three lived in Kaohsiung County and eleven in Taitung County. Seven of them were aborigines and two were brother and sister. Two of them had histories of travelling to Thailand. Two patients had history of eating raw or insufficiently cooked fresh-water fish. Four of 14 patients had mixed infection with Clonorchis sinensis or Strongyloides stercoralis whose eggs were also found in the feces.

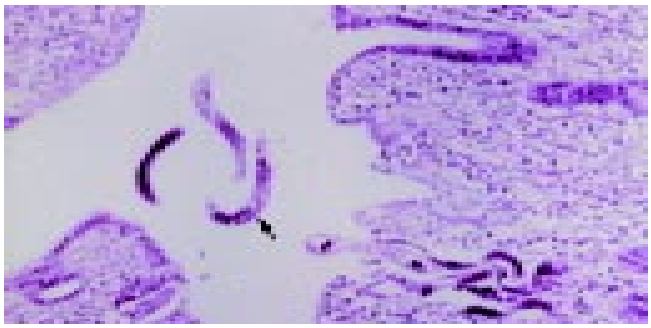

Figure 2 Multiple longitudinal sections of *C. philippinensis* on mucosal surface and lumen. The longitudinal sections shows a row of stichocytes (arrow). Hematoxylin and eosin, ×200.

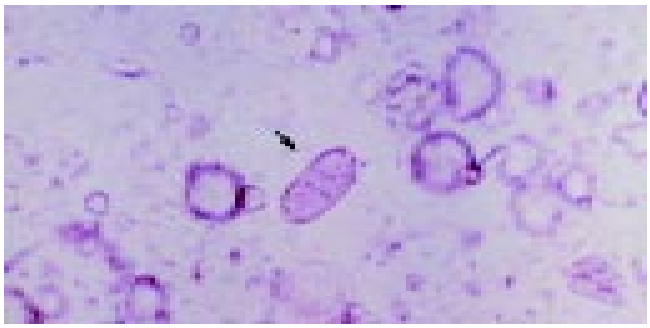

Figure 3 Peanut-shaped eggs of *C. philippinensis* in feces with flattened bipolar plugs. ×160.

Three cases received emergency laparotomy due to peritonitis and two of them were found to have jejunitis cystica profunda. Small bowel series and colonoscopic study revealed mild dilatation and thickened mucosa of jejunum and ileum, which suggested malabsorption. Laboratory findings revealed anemia, malabsorption of fats and carbohydrates and low serum levels of potassium, sodium, calcium and total protein. Mebendazole 200 mg twice a day for 20 d was given to 12 patients, while albendazole was given to the other two patients. All of them were cured and relapses were not observed within 12 mo following chemotherapy and supportive treatment.

DISCUSSION

Capillaria species parasitize many classes of vertebrates, although only 4 species have been found in humans, namely *C. philippinensis*, *C. plica*, *C. aerophila*, and *C. hepatica*[1]. *C. philippinensis* is a tiny nematode first described in the 1960 s as a pathogen inducing severe diarrheal syndromes in humans. In 1962, the first reported case of human intestinal capillariasis occurred in a previously healthy young man from Luzon in the Philippines, who subsequently died. At autopsy, a large number of worms were found in the large and small intestines[2]. Chitwood *et al.* described this case in 1964[3]. There was an epidemic of

Table 1 Characteristics of seven patients with intestinal capillariasis reported in Tai-tung

Case No.	Year Occurred	Occupation	Age (yr)	Sex	Travel history	Associated parasite	Treatment	Outcome
1	1983	Farmer	76	M	-	*Clonorchis sinensis*	Albendazole	Cure
2	1987	Merchant	46	M	-	-	Albendazole	Cure
3	1988	Housewife	58	F	Thailand	-	Mebendazole	Cure
4	1990	Housewife	41	F	-	-	Mebendazole	Cure
5	1991	Housewife	36	F	-	-	Mebendazole	Cure
6	1991	Farmer	62	M	-	*Clonorchis sinensis*	Mebendazole	Cure
7	1991	Housewife	46	F	-	-	Mebendazole	Cure
8	1992	Merchant	53	M	Thailand	-	Mebendazole	Cure
9	1992	Farmer	45	M	-	-	Mebendazole	Cure
10	1995	Farmer	61	M	-	-	Mebendazole	Cure
11	1995	Housewife	45	F	-	*Strongyloides stercoralis*	Mebendazole	Cure
12	1999	Farmer	39	M	-	-	Mebendazole	Cure
13	2000	Fisher-man	69	M	-	-	Mebendazole	Cure
14	2001	Farmer	50	M	-	*Clonorchis sinensis*	Mebendazole	Cure

Table 2 Clinical features and diagnostic method of seven patients with intestinal capillariasis reported in Tai-tung

Case No.	Duration of onset to diagnosis	Diagnostic method	Chronic diarrhea	Abdominal Pain	Abdominal borborygmi	Body weight loss	Anemia	Hypoalbuminemia
1	119 d	Stool ova	+	+	+	+	+	+
2	2Y7 M	Stool ova	+	+	+	+	+	+
3	6 M	Stool ova	+	+	+	+	+	+
4	1Y3 M	Histology	+	+	+	+	+	+
5	120 d	Histology	+	+	+	+	+	+
6	70 d	Stool ova	+	-	-	+	-	+
7	7 d	Stool ova	+	+	-	-	+	+
8	65 d	Stool ova	+	+	+	+	+	+
9	34 d	Stool ova	+	+	+	+	+	-
10	103 d	Stool ova	+	+	+	-	+	+
11	66 d	Stool ova	+	+	+	-	-	+
12	37 d	Histology	+	+	+	+	-	+
13	25 d	Histology	+	-	-	+	-	+
14	17 d	Stool ova	+	+	+	+	-	+

the disease in the Philippines from 1967 to 1968, more than 1 300 persons acquired the illness, and 90 patients with parasitologically confirmed infection died[4]. In late 1978 and early 1979, another small outbreak was identified in northeastern Mindanao, Phillippines, with about 50 persons infected[4]. Sporadic cases continued to appear in northern Luzon and also in other areas where epidemics had occurred. The disease is endemic in Thailand, where it was first reported in 1973[5]. Sporadic cases have also been found in Iran[6], Egypt[7,8], Taiwan[9], Japan[10,11], Indonesia[12], Korea[13], Spain (probably acquired in Colombia)[14], and Italy (acquired in Indonesia)[12]. The parasite thus appears to be widespread. Because infection may result in severe disease with a high mortality when untreated, early diagnosis is very important. Infection with *C. philippinensis* should be considered in the differential diagnosis of malabsorption syndrome[15]. There was often a delay in diagnosis, averaging 4 mo and even longer in Taiwan, especially in non-endemic areas[16]. The delay was over a year in our cases.

It has been found that Capillaria species are closely related to Trichuris and Trichinella species[1], and the eggs of Trichuris trichiura and *C. philippinensis* are similar in appearance, although they can be differentiated by experienced observers[17]. Some individuals could be infected with both parasites, which further confuse the picture. In fact, 10 of the 11 patients described by Whaler *et al*.[18] were infected with both T. trichiura and *C. philippinensis*. An inexperienced observer might confuse the eggs of Capillaria with those of T. trichiuria[1], although a correct parasitologic diagnosis could be made by finding characteristic peanut-shaped eggs with flattened bipolar plugs[2].

The source of *C. philippinensis* infection in our two patients was unclear, particularly as they had no travel history. In Thailand and the Philippines, the infection has been attributed to eating raw or insufficiently cooked fish harboring the larvae[2,19]. Hakka Chinese in Taiwan like to eat raw, freshwater fish, so they might be expected to have a significant incidence of infection if freshwater fish in Taiwan commonly host *C. philippinensis*. This is not the case, however. Our two patients lived in the southeastern part of Taiwan, closest to Luzon, so it was possible that the fish imported from the Philippines were the source of infection. Fish in markets in Taitung County, southeastern Taiwan, have been examined for *C. philippinensis* infection, but the results were negative. Recent findings suggested that fishing-eating birds might be the natural definitive hosts[20], including Bulbulcus ibis, Nyticorax nyticorax, and Ixobrychus sinensis, all of which have been found in Taiwan[21]. Therefore, the possibility of human infection acquired in Taiwan by direct or indirect ingestion of fresh-water fish with a larval stage of the parasite cannot be discounted.

Enteritis cystic profunda is a disorder with mucin-filled cystic spaces lined by non-neoplastic columnar epithelium in the wall of small intestine, predominantly the submucosa. The histology has been found to simulate mucinous carcinoma[22]. It has also been shown to occur in the esophagus[23] and stomach[24,25]. The irregular distribution of the glands and cysts with normal-appearing glandular epithelium containing mucus and Paneth's cells were features suggestive of its benign nature[26].

Albendazole was presently considered the drug of choice for the treatment of human intestinal capilliariasis because it was effective against eggs, larvae, and adult worms[1,26]. However, for a major infection, mebendazole (200 mg orally twice a day for 20 d) was recommended as the treatment of choice. Attempts to reduce the standard schedule of mebendazole treatment (400 mg daily for 3 wk) have failed in Thailand. Our patients responded well to a standard course of mebendazole and had no evidence of relapse.

Convenient international travel and commercial globalization have facilitated the wide dissemination of infectious diseases, whether they are carried by human hosts or non-human vectors. Intestinal capillariasis needs to be considered in the differential diagnosis of patients with chronic diarrhea, borborygmus, abdominal pain, and marked weight loss.

REFERENCES

1 **Cross JH**. Intestinal capillariasis. *Clin Microbiol Rev* 1992; **5**: 120-129
2 **Cross JH**. Intestinal capillariasis. *Parasitol Today* 1990; **6**: 26-28
3 **Chitwood MB**, Valasquez C, Salazar NG. Capillaria phillippinensis sp. N. (Nematoda: Trichinellida) from the intestine of man in the Philippines. *J Parasitol* 1968; **54**: 368-371
4 **Cross JH**, Singson CN, Battad S, Basaca-Sevilla V. Intestinal capillariasis: epidemiology, parasitology and treatment. *Proc R Soc Med Int Cong Symp Ser* 1979; **24**: 81-86
5 **Pradatsundarasar A**, Pecharanond K, Chintanawongs C, Ungthavorn P. The first case of intestinal capillariasis in Thailand. *Southeast Asian J Trop Med Pub Health* 1973; **4**: 131-134
6 **Hoghooghi-Rad N**, Maraghi S, Narenj-Zadeh A. Capilliaria philippinensis infection in Khoozestan Province, Iran: case report. *Am J Trop Med Hyg* 1987; **37**: 135-136
7 **Youssef FG**, Mikhail EM, Mansour NS. Intestinal capillariasis in Egypt: a case report. *Am J Trop Med Hyg* 1989; **40**: 195-196
8 **Mansour NS**, Anis MH, Mikhail EM. Human intestinal capillariasis in Egypt. *Trans R Soc Trop Med Hyg* 1990; **84**: 114
9 **Chen CY**, Hsieh WC, Lin JT, Liu MC. Intestinal capillariasis: report of a case. *J Formosa Med Assoc* 1989; **88**: 617-620
10 **Mukai T**, Shimizu S, Yamamoto M. A case of intestinal capillariasis. *Jpn Arch Int Med* 1983; **3**: 163-169
11 **Nawa Y**, Imai JI, Abe T, Kisanuki H, Tsuda K. A case report of intestinal capillariasis. The second case found in Japan. *Jpn J Parasitol* 1988; **37**: 113-118
12 **Chichino G**, Bernuzzi AM, Bruno A. Intestinal capillariasis (Capillaria philippinensis) acquired in Indonesia: a case report. *Am J Trop Med Hyg* 1992; **47**: 10-12
13 **Lee SH**, Hong ST, Chai JY. A case of intestinal capillariasis in the Republic of Korea. *Am J Trop Med Hyg* 1993; **48**: 542-546
14 **Dronda F**, Chaves F, Sanz A, Lopez-Velez R. Human intestinal capillariasis in an area of nonendemicity: case report and review. *Clin Infect Dis* 1993; **17**: 909-912
15 **Paulino GB**, Wittenberg J. Intestinal capillariasis: a new cause of a malabsorption pattern. *Am J Roentgenol Radiother Nucl Med* 1973; **117**: 340-345
16 **Hwang KP**. Human intestinal capillariasis in Taiwan. *Acta Paed Sin* 1998; **39**: 82-85
17 **Zaman V**, Keong LA. Helminths in: Handbook of medical parasitology. 2nd ed. *Edinburgh: Churchill Livingstone* 1990: 87-217
18 **Whalen GE**, Rosenberg EB, Strickland GT. Intestinal capillariasis: a new disease in man. *Lancet* 1969; **1**: 13-16
19 **Bhaihulaya M**, Indra-Ngarm S, Anathapruit M. Freshwater fishes of Thailand as experimental intermediate host for Capillaria philippinensis. *Int J Parasitol* 1979; **9**: 105-108
20 **Bhaibulaya M**, Indra-Ngarm S. Amaurornis phoenicurus and ardeola bacchus as experimental definite hosts for capillaria philippinensis in Thailand. *Int J Parasitol* 1979; **9**: 321-322
21 **Cross JH**, Basaca-Sevilla V. Experimental transmission of capillaria philippinensis to birds. *Trans R Soc Trop Med Hyg* 1983; **77**: 511-514
22 **Kyriakos M**, Condon SC. Enteritis cystic profunda. *Am J Clin Pathol* 1978; **69**: 77-85
23 **Volrol MW**, Welsh RA, Genet EF. Esophagitis cystica. *Am J Gastroenterol* 1973; **59**: 446-453
24 **Oberman HA**, Lodmell JG, Sower ND. Diffuse heterotopic cystic malformation of the stomach. *N Engl J Med* 1963; **269**: 909-911
25 **Fonde EC**, Rodning CB. Gastritis cystica profunda. *Am J Gastroenterol* 1986; **81**: 459-464
26 **Anderson NJ**, Rivera ES, Flores DJ. Peutz-Jeghers syndrome with cervical adenocarcinoma and enteritis cystica profunda. *West J Med* 1984; **141**: 242-244

Edited by Wang XL and Xu JY **Proofread by** Xu FM

PO Box 2345, Beijing 100023, China
Fax: +86-10-85381893
E-mail: wjg@wjgnet.com www.wjgnet.com

World J Gastroenterol 2004;10(16):2394-2396
World Journal of Gastroenterology
 ISSN 1007-9327

• CLINICAL RESEARCH •

Accuracy of indocyanine green pulse spectrophotometry clearance test for liver function prediction in transplanted patients

Chung-Bao Hsieh, Chung-Jueng Chen, Teng-Wei Chen, Jyh-Cherng Yu, Kuo-Liang Shen, Tzu-Ming Chang, Yao-Chi Liu

Chung-Bao Hsieh, Chung-Jueng Chen, Teng-Wei Chen, Jyh-Cherng Yu, Kuo-Liang Shen, Yao-Chi Liu, Division of General Surgery, Department of Surgery, Tri-Service General Hospital, National Defense Medical Center, Taipei, Taiwan, China
Tzu-Ming Chang, Department of Surgery, Tungs' Taichung Metroharbor Hospital, Taichung, Taiwan, China
Correspondence to: Dr. Chung-Bao Hsieh, 325, sec 2, Cheng-Kung Rd, Taipei, Taiwan, China. albert0920@yahoo.com.tw
Telephone: +886-2-87927191 **Fax:** +866-2-87927372
Received: 2003-11-12 **Accepted:** 2003-12-16

Abstract

AIM: To investigate whether the non-invasive real-time Indocynine green (ICG) clearance is a sensitive index of liver viability in patients before, during, and after liver transplantation.

METHODS: Thirteen patients were studied, two before, three during, and eight following liver transplantation, with two patients suffering acute rejection. The conventional invasive ICG clearance test and ICG pulse spectrophotometry non-invasive real-time ICG clearance test were performed simultaneously. Using linear regression analysis we tested the correlation between these two methods. The transplantation condition of these patients and serum total bilirubin (T. Bil), alanine aminotransferase (ALT), and platelet count were also evaluated.

RESULTS: The correlation between these two methods was excellent (r^2=0.977).

CONCLUSION: ICG pulse spectrophotometry clearance is a quick, non-invasive, and reliable liver function test in transplantation patients.

Hsieh CB, Chen CJ, Chen TW, Yu JC, Shen KL, Chang TM, Liu YC. Accuracy of indocyanine green pulse spectrophotometry clearance test for liver function prediction in transplanted patients. *World J Gastroenterol* 2004; 10(16): 2394-2396
http://www.wjgnet.com/1007-9327/10/2394.asp

INTRODUCTION

Monitoring of liver function is important in patients undergoing liver transplantation. Exact liver function and the extent of the remaining liver function at end-stage liver disease can indicate the appropriate timing of liver transplantation[1-3]. During liver transplantation, immediate liver function evaluation can resolve primary non-functioning of the liver and technical complications[4]. Moreover, post-transplantation early liver function evaluation can detect delayed graft malfunction or acute/chronic graft rejection.

Indocyanine green (ICG) is a synthetic dye that has been used for many years to measure hepatic blood flow and as a test of liver function[5]. It was also used by Makuuchi and his colleagues, based on their experience, as a guide for selecting the type of resection to be performed[6,7]. During liver transplantation, ICG clearance rate has been used for evaluation of the recipient liver[3,8], the donor liver[9,10] and the post-transplant liver graft[3]. Conventional ICG clearance is determined by measuring the rate of elimination using 3 mL venous samples at 0, 5, 10, 15, and 20 min after administering ICG. This invasive technique produces patient discomfort through repeated peripheral venous sampling at exact time intervals. Pulse spectrophotometry is an infrared-based non-invasive technique originally developed for monitoring tissue oxygenation. It has been previously used for the measurement of hepatic ICG concentration by Shinohara *et al*.[11]. In a recent case report, infrared spectrophotometry was sufficiently sensitive to measure the ICG clearance in surgical patients[12].

Even though the ICG clearance test has been used worldwide to predict liver function, there are some limitations for end-stage liver disease in patients with hyperbilirubinemia, intrahepatic shunt or capillarization[13].

ICG pulse spectrophotometry (LiMON) has not been tested in transplanted patients previously.

The aim of this study was to determine the accuracy of ICG spectrophotometry, compared with the conventional invasive method, in predicting liver function in waiting and transplanted patients.

MATERIALS AND METHODS

Thirteen patients who underwent liver transplantation and follow-up at the Tri-Service General Hospital were evaluated in the current study. Eleven male patients were transplanted for chronic liver disease of various etiologies (1 hepatitis C, 2 hepatitis B, and 8 hepatitis B with hepatoma) and 2 patients with end-stage liver disease awaiting transplantation. Patients 7 and 11 were studied in acute rejection during follow up (d36 and 90) and proved by liver biopsy. Patients 3, 4 and 13 were studied immediately post-liver transplantation (within 24, 27 and 12 h) (Table 1).

Invasive ICG measurement

An intravenous (IV) bolus of 0.5 mg/kg ICG was injected rapidly through a central venous catheter or large peripheral venous line, and samples were obtained from another peripheral venous line at 0, 5, 10, 15, 20 min thereafter and kept in an EDTA-treated tube at room temperature until centrifuged at 3 000 r/min for 10 min. Absorbance was measured by a Perkin Elmer spectrophotometer at 805 nm. Direct ICG retention rate at 15 min (ICG_{15D}) and the elimination rate constant ($ICG(K)_D$) values were calculated using a commercial computer program (V-500 Spectra Manager, Jasco, Japan).

ICG pulse spectrophotometry

Pulse-dye densitometry (LiMON, Stahigruburring, Munich, Germany) was used to measure the blood ICG concentration non-invasively in real time. This apparatus makes such measurements possible by continuously monitoring the optical absorption at 805 nm and 890 nm, via an optical probe attached to the patient's finger. During the first 5-10 min after

Table 1 The demographic data of all patients

Diagnosis		Condition (d)	T. Bil	ALT	Cr.	PLT	ICG_{15D}	ICG_{15E}	$ICG(K)_D$	$ICG(K)_E$
1	Alcoholism	Waiting	1.6	121	0.8	16.4	27.2	28.4	0.05	0.08
2	HBV+HCC	Waiting	1.4	47	0.9	12.6	36	38.3	0.03	0.06
3	HBV	During-OLT-(2)	1.6	126	0.8	7.4	3	3.9	0.24	0.22
4	HBV	During-OLT-(2)	1.1	102	1.0	11.8	1	2.5	0.28	0.29
5	HCV+HCC	Post-OLT (43)	0.7	233	2.3	15.1	4	3.7	0.18	0.22
6	HBV	Post-OLT (212)	0.5	8	2.9	12.1	1	2.3	0.35	0.29
7	HBV	Post-OLT (36) Ac. rejection	9.1	131	1.6	7.2	26	24	0.10	0.10
8	HBV+HCC	Post-OLT (142)	0.8	15	1.3	11	6.5	6.8	0.21	0.25
9	HBV+HCC	Post-OLT. (166)	1.1	37	0.7	24.9	2	4	0.32	0.23
10	HBV+HCC	Post-OLT (312)	0.5	16	1.0	18.8	4	4.5	0.24	0.21
11	HBV+HCC	Post-OLT (90) Ac. rejection	2.0	50	2.2	11.5	18	13.7	0.16	0.13
12	HBV+HCC	Post-OLT (367) Ac. renal failure	1.3	46	3.4	6.4	10	11.2	0.28	0.27
13	HBV+HCC	During OLT (1)	3.6	213	3.4	8.5	5.1	5.4	0.31	0.33

HBV: Hepatitis B virus; HCV: Hepatitis C virus; HCC: Hepatocellular carcinoma; OLT: Orthotopic liver transplantation; Ac.: Acute; T. Bil: Total bilirubin; ALT: Alanine aminotransferase; Cr.: Creatinine; PLT: Platelet.

Table 2 The transplanted condition and laboratory data

Patients condition (*n*)	T. Bil	ICG_{15D}	ICG_{15E}	$ICG(K)_D$	$ICG(K)_E$
ESLD (2)	1.50±0.10	29.6±4.4	34.4±4.9	0.04±0.01	0.07±0.01
During-OLT (3)	1.35±0.25	2.0±1.0	3.2±0.7	0.26±0.02	0.25±0.04
Post-OLT (6)	0.86±0.30	3.6±2.1	3.9±0.8	0.26±0.08	0.24±0.03
Acute rejection (2)	5.60±3.60	22.0±4.0	18.9±5.2	0.13±0.03	0.12±0.02

ESLD: End-stage liver disease on waiting list; During-OLT: immediately after liver transplantation within seven days; Post-OLT: > one month after liver transplantation in stable condition; Acute rejection: proved by liver biopsy; the number in brackets means the case number.

ICG was injected, blood ICG concentrations were monitored at every pulse interval via pulse spectrophotometry. The elimination rate constant $ICG(K)_E$ was calculated automatically by the time course of blood ICG concentration. The estimated ICG_{15} retention rate (ICG_{15E}) was obtained via pulse spectrophotometry computer analysis during the first 5-10 min. As the usual measurement time of the Limon is between 5 and 10 min, the (ICG_{15E}) is simply calculated from the ICG plasma disappearance rate[14].

Statistical analysis

Linear regression analysis was used to test the correlation. Statistical significance was considered at $P<0.05$. The statistic software was S-Plus®2000 for Windows (CANdiensten, Amsterdam, The Netherlands).

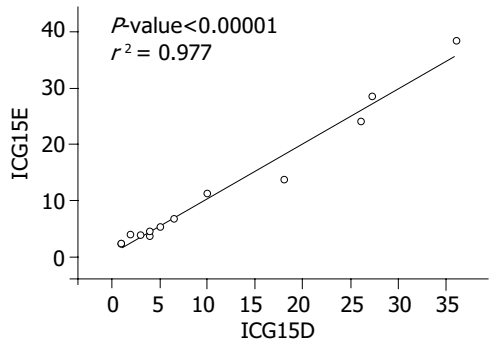

Figure 1 Correlation between the ICG_{15E} and ICG_{15D}. The correlation is excellent, $r^2 = 0.977$.

RESULTS

The correlation between ICG_{15D}, ICG_{15E}, $ICG(K)_D$, $ICG(K)_E$ values for ICG_{15} and ICG(K) by these two methods was excellent ($r^2 = 0.977$, 0.855) (Figures 1, 2). Two patients had poor liver function, elevated T. Bil, and higher ICG_{15} retention rates, and were on the waiting list for transplantation. Three patients who had good liver function immediately post-liver transplantation showed elevated T. Bil. and lower ICG_{15} retention rates. Two patients who were in acute rejection had poor liver function with elevated ALT and higher ICG_{15} retention rates. Five patients, who were in a stable condition with good liver function post-liver transplantation, had low T. Bil. and better ICG_{15} retention rates.

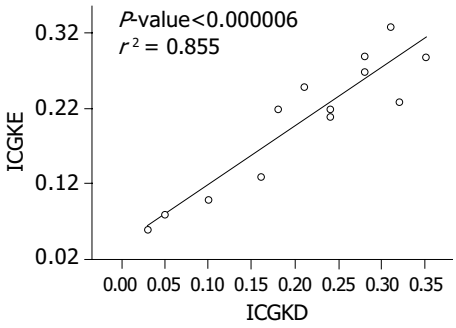

Figure 2 Correlation between ICG $(K)_E$ and ICG $(K)_D$. The correlation is excellent, $r^2 = 0.855$.

DISCUSSION

ICG is a water-soluble tricarbocyanine dye that is extracted by

hepatic parenchyma cells and excreted almost entirely into bile. Hepatic clearance of ICG occurs by two major processes: by uptake across the sinusoidal plasma membrane with a high extraction ratio; and by removal from the hepatocytes via cytoplasmic transport and exclusive biliary excretion with neither intrahepatic conjugation nor enterohepatic circulation[15]. The concentration in the plasma can be measured by spectrophotometry and its rate of elimination has been widely used as a measure of liver blood flow and liver function[16]. Most of the studies assessing liver function before hepatectomy and the postoperative outcome were carried out using the ICG clearance test[17].

Pulse spectrophotometry has been developed in recent years to enable the blood ICG concentration to be measured easily, less invasively, and continuously. The previous method for measuring the ICG concentration by spectrophotometry did not show sufficient accuracy. The new approach, based on pulse spectrophotometry, is able to continuously measure the arterial ICG concentration because of its ability to detect the pulse wave, greatly improving its accuracy.

Pulse spectrophotometry measurements of ICG concentration with each pulse could provide information on ICG liver uptake and excretion. From the concentration, a time curve of the ICG uptake and excretion rates were calculated under different experimental conditions. The experimental study by El-Desoky *et al*.[5] showed the sensitivity of measurement of ICG uptake and excretion rates in hepatic artery occlusion, portal vein occlusion, ischemia-reperfusion injury, hepatic microcirculation, colchicines treatment, and bile duct ligation.

Assessment of liver function remains difficult in transplanted patients because of etiological complexity. The differential diagnosis includes primary non-function of the graft, rejection, virus re-infection, drug intoxication, and thrombosis of hepatic blood vessels. After liver transplantation, liver function tests are often difficult to interpret and non-specific. The diagnosis at present relies on a combination of biochemical, hemodynamic, clinical markers, and occasionally liver biopsy. However, serial observations up to 72 h are required. Measurement of ICG clearance appears to be a simple and safe test to assess early liver graft function. The development of non-invasive pulse spectrophotometry has enabled bedside assessment of the elimination of ICG with immediate results, therefore increasing its clinical usefulness.

A study by Jalan *et al.* showed the ICG measured at 24 h after liver transplantation accurately reflected graft function and predicted graft survival and outcome. In other studies, ICG excretion was a sensitive index of ischemia/reperfusion injury during the early stages post-liver transplantation[17].

The traditional ICG clearance test is invasive and labor-dependent. The whole procedure requires more than 30 min at the bedside for loading dosage and venous puncture. Failure may occur as a result of the patient's underlying disease and medication such as gout, arthritis, and anti-TB drugs. Technical failure may be due to blood hemolysis or laboratory errors. The real-time pulse spectrophotometry ICG clearance test is non-invasive and machine-dependent. Technical failure may be due to detecting probe malpositioning, and patient movement.

In this study, we have chosen two ICG clearance test methods to measure end-stage liver disease, immediately post-liver transplantation or in acute rejection patients. In patients with hyperbilirubinemia, before and after successful liver transplantation, the ICG_{15} clearance test may be very useful in evaluating the new liver's function. ICG pulse spectrophotometry appears to be a sensitive and specific test to predict graft function in ischemia/reperfusion and acute rejection patients. The correlations between ICG(K) and ICG_{15} using these two methods were excellent.

In conclusion, in this study, the correlation between conventional and pulse spectrophotometry ICG clearance tests is excellent in transplanted patients. The ICG pulse spectrophotometry clearance test is a quick, non-invasive, easy, inexpensive, and reliable liver function test in transplantation patients.

REFERENCES

1 **Miyagawa S**, Makuuchi M, Kawasaki S, Kakazu T. Criteria for safe hepatic resection. *Am J Surg* 1995; **169**: 589-594
2 **Oellerich M,** Burdelski M, Lautz HU, Rodeck B, Duewel J, Schulz M, Schmidt FW, Brodehl J, Pichlmayr R. Assessment of pretransplant prognosis in patients with cirrhosis. *Transplant* 1991; **51**: 801-806
3 **Tsubono T,** Todo S, Jabbour N, Mizoe A, Warty V, Demetris AJ, Staezl TE. Indocyanine green elimination test in orthotopic liver recipients. *Hepatology* 1996; **24**: 1165-1171
4 **Plevris JN**, Jalan R, Bzeizi KI, Dollinger MM, Lee A, Garden OJ, Hayes PC. Indocyanine green clearance reflects reperfusion injury following liver transplantation and is an early predictor of graft function. *J Hepatol* 1999; **30**: 142-148
5 **El-Desoky A**, Seifalian AM, Cope M, Delpy DT, Davidson BR. Experimental study of liver dysfunction evaluated by direct indocyanine green clearance using near infrared spectroscopy. *Br J Surg* 1999; **86**: 1005-1011
6 **Lau H,** Man K, Fan ST, Yu WC, Lo CM, Wong J. Evaluation of preoperative hepatic function in patients with hepatocellularcarcinoma undergoing hepatectomy. *Br J Surg* 1997; **84**: 1255-1259
7 **Parks RW,** Garden OJ. Liver resection for cancer. *World J Gastroenterol* 2001; **7**: 766-771
8 **Niemann CU**, Yost CS, Mandell S, Henthorn TK. Evaluation of the splanchnic circulation with indocyanine green pharmacokinetics in liver transplant patients. *Liver Transplant* 2002; **5**: 476-481
9 **Seifalian AM**, Mallet SV, Rolles K, Davidson BR. Hepatic microcirculation during human orthotopic liver transplantation. *Br J Surg* 1997; **84**: 1391-1395
10 **Koneru B**, Leevy CB, Klein KM, Zweil P. Clearance of indocyanine green in the evaluation of liver donors. *Transplantation* 1994; **58**: 729-731
11 **Shinohara H**, Tanaka A, Kitai T, Yanabu N, Inomoto T, Satoh S, Hatano E, Yamaoka Y, Hirao K. Direct measurement of hepatic indocyanine green clearance with near-infrared spectroscopy: separate evaluation of uptake and removal. *Hepatology* 1996; **23**: 137-144
12 **Mandell MS**, Wachs M, Niemann CU, Henthorn TK. Elimination of indocyanine green in the perioperative evaluation of donor liver function. *Anesth Analg* 2002; **95**: 1182-1184
13 **Ott P,** Clemmesen O, Keiding S. Interpretation of simultaneous measurements of hepatic extraction fractions of indocyanine green and sorbitol. Evidence of hepatic shunts and capillarization? *Dig Dis Sci* 2000; **45**: 359-365
14 **Sakka SG**, Meier-Hellmann A. Non-invasive liver function monitoring by indocyanine green plasma disappearance rate in critically ill patients. *International J Intensive Care* 2002: 66-72
15 **Wheeler HO**, Cranston WI, Meltzer JI. Hepatic uptake and biliary excretion of indocyanine green in the dog. *Proc Soc Exp Biol Med* 1958; **99**: 11-20
16 **Caesar J**, Shaldon S, Chiandussi L, Guevara L, Sherlock S. The use of indocyanine green in the measurement of hepatic blood flow and as a test of hepatic function. *Clin Sci* 1961; **21**: 43-47
17 **Kawasaki S**, Makuuchi M, Miyagawa S, Kakazu T, Hayashi K, Kasai H, Milva S, Hui AM, Nishimaki K. Results of hepatic resection for hepatocellular carcinoma. *World J Surg* 1995; **19**: 31-34

Edited by Zhu LH **Proofread by** Xu FM

PO Box 2345, Beijing 100023, China
Fax: +86-10-85381893
E-mail: wjg@wjgnet.com www.wjgnet.com

World J Gastroenterol 2004;10(16):2397-2401
World Journal of Gastroenterology
 ISSN 1007-9327

• CLINICAL RESEARCH •

Prevalence of subclinical hepatic encephalopathy in cirrhotic patients in China

Yu-Yuan Li, Yu-Qiang Nie, Wei-Hong Sha, Zheng Zeng, Fu-Ying Yang, Li Ping, Lin Jia

Yu-Yuan Li, Yu-Qiang Nie, Wei-Hong Sha, Zheng Zeng, Li Ping, Lin Jia, Department of Gastroenterology, First Municipal People's Hospital of Guangzhou 510180, Guangdong Province, China
Fu-Ying Yang, Department of Neurology, First Municipal People's Hospital of Guangzhou 510180, Guangdong Province, China
Supported by Research Funds from Guangzhou Medical College, and Bureau of Public Health of Guangdong Province, China
Correspondence to: Dr. Yu-Yuan Li, Department of Gastroenterology, First Municipal People's Hospital of Guangzhou, #1 Panfu Road, Guangzhou 510180, Guangdong Province, China. liyyliyy@163.net
Telephone: +86-20-81045208 **Fax:** +86-20-81045937
Received: 2003-11-12 **Accepted:** 2003-12-08

Abstract

AIM: Subclinical hepatic encephalopathy (SHE) is a common complication of liver diseases. The aim of this study was to find out the normal value of psychometric test and to investigate the prevalence of SHE in Chinese patients with stabilized hepatic cirrhosis.

METHODS: Four hundred and nine consecutive cirrhotic patients without overt clinical encephalopathy were screened for SHE by using number connection test part A (NCT-A) and symbol digit test (SDT). SHE was defined as presence of at least one abnormal psychometric test. The age-corrected normal values were defined as the mean±2 times standard deviation (2SD), and developed in 356 healthy persons as normal controls. Four hundred and sixteen patients with chronic viral hepatitis were tested as negative controls to assess the diagnostic validity of this test battery.

RESULTS: There was no significant difference in NCT scores and SDT quotients between healthy controls and chronic hepatitis group (P>0.05). In all age subgroups, the NCT and SDT measurements of cirrhotic patients differed significantly from those of the controls (P<0.05). When mean±2SD of SDT and NCT measurements from healthy control group was set as the normal range, 119 cirrhotic patients (29.1%) were found to have abnormal NCT-A and SDT tests, 53 (13.0%) were abnormal only in SDT and 36 (8.8%) only in NCT-A. Taken together, SHE was diagnosed in 208 (50.9%) cirrhotic patients by this test battery. The prevalence of SHE increased from 39.9% and 55.2% in Child-Pugh's grade A and B groups to 71.8% in Child-Pugh's grade C group (P<0.05). After the adjustment of age and residential areas required from the tests, no correlation was found in the rate of SHE and causes of cirrhosis, education level and smoking habit.

CONCLUSION: Psychometric tests are simple and reliable indicators for screening SHE among Chinese cirrhotic patients. By using a NCT and SDT battery, SHE could be found in 50.9% of cirrhotic patients without overt clinical encephalopathy. The prevalence of SHE is significantly correlated with the severity of liver functions.

Li YY, Nie YQ, Sha WH, Zeng Z, Yang FY, Ping L, Jia L. Prevalence of subclinical hepatic encephalopathy in cirrhotic patients in China. *World J Gastroenterol* 2004; 10(16): 2397-2401
http://www.wjgnet.com/1007-9327/10/2397.asp

INTRODUCTION

Subclinical hepatic encephalopathy (SHE) has been defined as a condition in which patients with cirrhosis regardless of its etiology, demonstrates neuro-psychiatric and neuro-physiological defects, yet, having a normal mental and neurological status through global clinical examination[1-3]. SHE could have some disadvantageous influence on patients' daily life, and could be a preceding stage of manifested hepatic encephalopathy (HE) clinically. The prevalence of SHE was reported to vary from 10% to 84%, depending on the diagnostic techniques used and patients selected for the studies[1-10]. Many diagnostic techniques including psychometric test, electro- encephalogram, evoked potentials (EP), have been used to detect SHE. Among these tests, only psychometric test can be administered easily in epidemiological studies. In a variety of psychometric tests listed in the medical literature, SDT and NCT part A (NCT-A) were reported to have the advantages of simplicity and reliability[1,11-15]. The combination of these two tests was commonly applied in epidemiological studies. We evaluated a battery of SDT and NCT tests in a pilot study in Chinese patients with good results[16]. Therefore, it was selected in this big sample size study. By definition, SHE can only be found in cirrhotic patients. In this study, besides the healthy control group for the establishment of normal values of SDT and NCT, we also set up a chronic hepatitis group as negative control to assess the reliability of SDT and NCT test battery. In recent years, studies on the prevalence of SHE have been greatly increased in Western literature, but those from Chinese patients have not been fully documented. The aim of the present study was to establish the normal value of psychometric tests for Chinese people, to determine the prevalence of SHE in stable cirrhotic patients in China by using this test battery, and to explore the features of SHE in these patients.

MATERIALS AND METHODS

Subjects

Four hundred and nine consecutive cirrhotic patients attending the Department of Gastroenterology of Guangzhou Municipal First People's Hospital for screening of SHE from June 1, 1998 to March 31, 2002 were included in the study. Inclusion criteria were: no neurological or mental diseases, no attack of HE in the past or present, no use of sedative or other psychotropic drugs two wk prior to the tests. The following patients were excluded. Those who had portosystemic shunt operation, those who had alcohol consuming more than 150 g daily within 1 wk prior to the study, those who had gastrointestinal bleeding 4 wk previously, those whose hemoglobin level was less than 90 g/L, those who had dehydration or electrolyte imbalance, those whose body temperature was higher than 37.5 , those who had severe cardiac or pulmonary or renal or cerebrovascular

diseases or diabetes mellitus, and those who were illiterates.

Diagnosis of cirrhosis was made according to the criteria revised in 1990 National Symposium on Cirrhosis in China[17]. In this study, 10 patients had liver biopsy. The Child-Pugh's scores were used to assess the severity of liver disease. Special attention was paid to the exclusion of stage 1 HE. The symptoms in this stage included abnormal behavior (exaggeration of normal behavior, euphoria or depression), sleeping disorders (hypersomnia, insomnia or inversion of sleeping pattern), neuromuscular activity (muscular incoordination, impaired handwriting) and changes in mental function (declined alertness or memory, subtle disorientation or impaired calculation). The etiology of the 409 cirrhotic patients consisted of chronic hepatitis B in 322 (78.7%), chronic hepatitis C in 28 (6.9%), and chronic alcoholics in 59 (14.4%). According to the Child-Pugh's grading of liver function, 188 (46.0%) were grade A, 143 (35.0%) grade B and 78 (19.0%) grade C. Two hundred and fourteen patients (52.3%) had no ascites, 72 (17.6%) had mild ascities and 123 (30.1%) had severe ascities. One hundred and sixty-nine patients (41.3%) had normal levels of serum albumin, 102 (24.9%) had mild hypoalbuminemia (30-35 g/L) and 138 (38.8%) had severe hypoalbuminemia (<30 g/L). One hundred and twenty-three patients (30.1%) had normal prothrombin time (PT), 152 (37.2%) had mildly prolonged PT (14-18 s) and 134 (32.7%) severely prolonged PT (>18 seconds). Under endoscopic examination, 28 patients (6.8%) had severe esophageal varices, 152 (37.2%) had mild varices and 229 (56.0%) had no varices.

Normal values of the psychometric tests were obtained from 356 consecutive healthy subjects undergoing routine physical check-up in the hospital between June 1 and July 1, 1998. All of them had no physical and psychological disorders, no neurological or mental diseases and no history of sedatives or alcohol consumption. The negative control group consisted of 416 consecutive outpatients with chronic viral hepatitis in Division of Infectious Diseases of our hospital in the same period. The diagnostic criteria were in accordance with the Chinese National Standards of Viral Hepatitis[18]. Among the 416 cases, 384 (92.3%) had hepatitis B, 32 (7.7%) hepatitis C.

The study was approved by the Ethics Committee of the First Municipal People's Hospital of Guangzhou, Guangzhou Medical College, with written consent from each patient and subject.

Questionnaire

Questionnaire was given to each subject. It included the following items, namely age, sex, smoking habit (smoking cigarette daily, yes/no), alcohol (drinking alcohol daily, yes/no), education (<6 years, 6-12 years, >12 years), residential area (urban/rural), occupation, history of liver diseases, concomitant illness.

Psychometric assessment

Symbol digit test (SDT) was in Chinese version of Wechsler adult intelligence scale revised (WAIS-RC) by Gong[19]. The individuals were given a list of digits from 1 to 9 associated with symbols and asked to fill in blanks with symbols that corresponded to each number. An initial demonstration was performed to familiarize the subjects with the test. The test scores were the total number of correctly sequential matched symbols to the number within a 90-seconds interval. The score was only 0.5, if the symbol was placed upside down. According to age, the total score of each subject was transformed to a quotient from an equivalent form, the subjects were divided into two groups according to their residential areas, either rural or urban area.

In the number connection test (NCT) part A, the subjects were asked to connect the numbers printed on the paper consecutively from 1 to 25 as quickly as possible[20]. After explaination to the subjects, demonstrative tests were given to ensure a correct understanding and then the test was carried on. The test scores included the time required for the test and for correcting the errors.

These two psychometric tests were performed by the patients and subjects with help from medical staffs without awareness of the diagnosis.

Statistical analysis

Student's *t* test and Chi-square test were used to assess the differences among the groups. Multivariate logistic analysis was used to evaluate the influence of the variables in the prevalence. $P<0.05$ was considered statistically significant. Normal cut-off values of SDT and NCT were set at the mean±2SD from the normal control arm, with a low value indicating a poor performance in SDT test and a higher score indicating a poor performance in NCT test. The diagnosis of SHE was made when one or both SDT and NCT appeared abnormal.

RESULTS

The demographic data of three arms are shown in Table 1. There was no significant difference ($P>0.05$) among all variables from the three arms. The results of SDT and NCT in different age subgroups from the three arms are shown in Table 2 and Table 3. In both tests, no significant difference was found between healthy controls and chronic hepatitis arms ($P>0.05$). However, the results in the cirrhotic arm differed significantly from those of the two control arms ($P<0.05$). This finding supported that the Chinese version of SDT and NCT tests could clearly distinguish the neuro-psychiatric defects in SHE. The values of SDT and NCT tests from the healthy control arm could be good parameters for the establishment of normal values of these two tests.

Table 1 Demography in 3 groups

	Control n = 356	Hepatitis n = 416	Cirrhosis n = 409
Age (yr)	44.4±12.7	36.8±18.6	53.4±11.9
Male/female	207/149	330/86	248/161
Education (yr)			
>6	69 (19.4)	69 (16.9)	82 (20.0)
6-12	168 (47.2)	215 (51.7)	190 (46.5)
> 12	119 (33.4)	132 (31.7)	137 (33.5)
Smoking	65 (18.3)	99 (23.8)	88 (21.5)
Alcohol	39 (10.9)	48 (11.5)	123 (30.1)

The influence of the variables on the results of SDT and NCT is shown in Table 4. No significant difference was found in sex, smoking and alcohol drinking habits, and the etiology of cirrhosis ($P>0.05$), but the difference was related to age, education and Child-Pugh's grade ($P<0.05$). However, after adjustment of age and residential areas required for SDT and NCT tests, Child-Pugh's grade was the only risk factor of SHE ($P<0.05$).

The relationships between Child-Pugh's grade and SDT/NCT are shown in Table 5. Although the rate of SHE between Child's grades A and B of liver disease was not significantly different ($P>0.05$), significance was found between grades A and C, and grades B and C ($P<0.05$). One hundred and nineteen patients (29.1%) were abnormal in both NCT and SDT, 53 (13.0%) abnormal in SDT only and 36 (8.8%) in NCT-A only. Taken together, the two-test battery gave the diagnostic rate of SHE in 50.9% of 208 patients.

Table 2 Results of SDT in 3 groups

Age (yr)	Control		Hepatitis		Cirrhosis	
	n	mean±SD	*n*	mean±SD	*n*	mean±SD
</=34	82	12.5±2.2	176	12.7±3.1	52	10.8±2.8[a]
35-44	76	11.9±1.7	114	12.3±3.5	73	9.4±2.7[a]
45-54	74	12.8±2.3	71	12.3±2.2	107	8.9±2.5[a]
55-64	69	11.9±2.1	35	11.5±1.6	87	7.8±2.5[a]
>/=65	54	12.7±2.4	20	9.0±2.2	90	6.7±2.3[a]
Tota	356	12.2±2.3	416	12.2±3.1	409	8.5±2.8[a]

[a]*P*<0.05 *vs* normal control and chronic hepatitis.

Table 3 Results of NCT in 3 groups

Age (yr)	Control		Hepatitis		Cirrhosis[a]	
	n	mean±SD	*n*	mean±SD	*n*	mean±SD
</=34	82	26.7±8.8	176	27.0±6.9	52	46.1±19.2
35-44	76	34.2±12.7	114	35.8±20.3	73	51.4±26.5
45-54	74	39.8±13.8	71	41.9±12.7	107	59.3±30.8
55-64	69	52.7±13.5	35	54.3±7.3	87	71.1±41.8
>/=65	55	69.9±14.8	20	80.1±12.1	90	102.3±48.8
Total	356	47.8±13.2	416	36.8±18.6	409	68.2±41.2

[a]*P*<0.05 *vs* cirrhosis versus normal control and chronic hepatitis.

Table 4 Multivariate logistic analysis for risk factors in cirrhotic group

	n	NCT	DST	SHE(%)	p2	OR
Sex					0.494	0.9
Male	344	67.4±42.1	8.6±2.8	51.2		
Female	65	72.4±36.0	8.7±2.6	52.3		
p1		0.367	0.266	0.866		
Smoking					0.903	1.0
Yes	288	6.2±38.7	8.6±2.6	51.0		
No	121	672.8±46.4	8.3±2.9	52.1		
p1		0.145	0.358	0.850		
Etiology					0.430	0.8
Alcohol	59	71.3±40.1	8.0±2.6	54.2		
Non-alcohol	350	67.7±41.4	8.6±2.9	51.0		
p1		0.541	0.153	0.646		
Education (yr)					0.390	0.9
< 6	72	92.8±50.0	6.9±2.4	51.4		
6-12	199	69.6±41.1	8.2±2.6	55.3		
> 12	138	53.3±27.6	9.7±2.9	45.3		
p1		0.001	0.001	0.221		
Age (yr)					0.779	1.0
< 35	52	46.1±19.2	10.8±2.8	51.9		
35-44	73	51.4±26.5	9.4±2.7	52.1		
45-54	107	59.3±30.8	8.9±2.5	49.5		
55-64	87	71.1±41.8	7.8±2.5	50.0		
> 65	90	102.3±48.8	6.7±2.3	57.8		
p1		0.001	0.001	0.617		
Child-Pugh					0.001	2.0
A	188	58.5±34.9	9.3±2.8	39.9%		
B	143	72.8±41.2	8.1±2.8	55.2%		
C	78	83.1±49.1	7.4±2.6	71.8%		
p1		0.001	0.001	0.001		

p1: *P* value within groups. p2: *P* value among groups in logistic analysis.

Table 5 Relationships between psychometric tests and Child-Pugh's grade

	Child's A	Child's B	Child's C	Total (*n*,%)
n	188	143	78	409
Abnormal in SDT	23	20	10	53 (13.0)
Abnormal in NCT	16	10	10	36 (8.8)
Abnormal in SDT and NCT	35	48	36	119 (29.1)
Total (%)	74 (39.4)	78 (54.5)	56 (71.9)[a]	208 (50.9)

[a]$P<0.05$.

DISCUSSION

The reasons why we selected SDT and NCT part A out of a variety of psychometric tests from the medical literature in this study are as follows. (1) NCT and SDT were simple, inexpensive and sensitive tests and have been well used in many SHE studies on its prevalence, prognosis and treatment[1-15]. NCT part A alone has been shown to be sufficient in detection of SHE in the majority of patients[3,12]. (2) The patients with SHE exhibited selective deficits in reactivity and fine motor skills, with preservation of general intelligence, memory and language speaking. Therefore, it was reasonable to select WAIS performance subtests such as SDT[11,12]. (3) Both SDT and NCT were easy to perform and reproduce in minutes at the outpatient clinics. Moreover more complicated tests would increase the patients' fatigue and mental burden and affect their performance efficiency[11]. In order to evaluate the reliability of SDT/NCT test battery, two control groups were set up. Normal data of each age subgroup in the two tests were obtained from healthy subjects and then assessed with the data from chronic hepatitis negative control and cirrhosis positive control. The corresponding scores of the tests from healthy and chronic hepatitis control groups were very close. By using the normal range drawn from healthy subjects, the total abnormal rate of SDT and NCT in chronic hepatitis group was 5.5% and 7.2% respectively, near marginally statistical range. The results supported that SDT and NCT test battery was a sensitive and specific method for detection of SHE.

Whether or not the patients with alcoholic cirrhosis have a higher prevalence of SHE is still controversial. The higher prevalence of SHE in patients with alcoholic cirrhosis was mostly reported from the studies using EP or electroencephalogram[21], suggesting a diffuse neurological disturbance in alcoholic cirrhotic patients. In China, most cirrhotic patients were caused by chronic hepatitis B. No significant difference in various etiologies was found among the subgroups in this investigation, probably due to the application of psychometric measures only. Some reports supposed that the elder and educational levels might influence the results of psychometric tests[22,23]. No significant correlation was found between the different subgroups in age and education in the present study, since we used age-related normal values to correct the findings.

The selected subjects in this study reflected the real spectrum of cirrhotic patients in Guangzhou. The detected SHE prevalence was 50.9%, with its rate increased from 39.4% in Child-Pugh's grade A to 54.5% and 71.9% in grades B and C. These results agreed well with the data reported from Western literature. The patients with worse liver functions assessed by Child-Pugh's grade had a higher rate of SHE. Child-Pugh's scores were based on patients' symptoms (HE and ascites) and laboratory tests (serum levels of albumin, billirubin, prothrombin). Patients with HE were excluded from this study. We also observed that the patients who had more or severer symptoms and poorer laboratory parameters of cirrhosis whether or not including in Child-Pugh's grade might tend to develop SHE.

Patients with SHE appeared to have no clinical symptoms. However, they might be at risk when they performed complex motor activities as operating a heavy machinery or driveing an automobile[24]. They might have abnormal behaviors such as altered sleeping pattern and impaired cognitive function[25,26]. Patients with SHE were vulnerable to HE[27-29]. However, medical treatment and dietary management in these patients could improve the psychometric tests[28-30]. Early diagnosis and treatment of SHE seem extremely important in China, because of the big population and high prevalence of liver diseases in this country. A high prevalence of SHE in cirrhotic patients should lead us to pay attention to these important findings frequently encountered in our medical practice.

REFERENCES

1 **Ferenci P**, Lockwood A, Mullen K, Tarter R, Weissenborn K, Blei AT. Hepatic encephalopathy- definition, nomenclature, diagnosis, and quantification: final report of the working party at the 11th World Congress of Gastroenterology, Vienna, 1998. *Hepatology* 2002; **35**: 716-721

2 **Rikkers L**, Jenko P, Rudman D, Freides D. Subclinical hepatic encephalopathy: detection, prevalence and relationship to nitrogen metabolism. *Gastroenterology* 1978; **75**: 462-469

3 **Watanabe A**, Sakai T, Sato S, Imai F, Ohto M, Arakawa Y, Toda G, Kobayashi K, Muto Y, Tsujii T, Kawasaki H, Okita K. Clinical efficacy of lactulose in cirrhotic patients with and without subclinical hepatic encephalopathy. *Hepatology* 1997; **26**: 1410-1414

4 **Das A**, Dhiman RK, Saraswat VA, Verma M, Naik SR. Prevalence and natural history of subclinical hepatic encephalopathy in cirrhosis. *J Gastroenterol Hepatol* 2001; **16**: 531-535

5 **Zeng Z**, Li YY, Nie YQ. An epidemiological survey of subclinical hepatic encephalopathy. *Chinese J Hepatol* 2003; **11**: 680-682

6 **Yoo HY**, Edwin D, Thuluvath PJ. Relationship of the model for end-stage liver disease (MELD) scale to hepatic encephalopathy, as defined by eletroencephalography and neuropsychometric testing, and ascites. *Am J Gastroenterol* 2003; **98**: 1395-1399

7 **Kramer L**, Bauer E, Gendo A, Funk G, Madl C, Pidlich J, Gangl A. Neurophysiological evidence of cognitive impairment in patients without hepatic encephalopathy after tranjugular intrahepatic portosystemic shunts. *Am J Gastroenterol* 2002; **97**: 162-166

8 **Scotiniotis IA**, Lucey MR, Metz DC. *Helicobacter pylori* infection is not associated with subclinical hepatic encephalopathy in stable cirrhotic patients. *Dig Dis Sci* 2001; **46**: 2744-2751

9 **Romero-Gomez M**, Boza F, Garcia-Valdecasas MS, Garcia E, Aguilar-Reina J. Subclinical hepatic encephalopathy predicts the development of overt hepatic encephalopathy. *Am J Gastroenterol* 2001; **96**: 2718-2723

10 **Hartmann IJ**, Groeneweg M, Quero JC, Beijeman ST, de Man RA, Hop WC, Schalm SW. The prognostic significance of su [bclinical hepatic encephalopathy. *Am J Gastroenterol* 2000; **95**: 2029-2034

11 **McCrea M**, Cordoba J, Vessey G, Blei AT, Randolph C. Neuropsychological characterization and detection of subclinical hepatic encephalopathy. *Arch Neurol* 1996; **53**: 758-763

12 **Amodio P**, Del Piccolo F, Marchetti P, Angeli P, Iemmolo R, Caregaro L, Merkel C, Gerunda C, Gatta A. Clinical features and survival of cirrhotic patients with subclinical cognitive alteration detected by the number connection test and computerized psychometric tests. *Hepatology* 1999; **29**: 1662-1667

13 **Gitlin N**, Lewis D, Hinkley L. The diagnosis and prevalence of

subclinical hepatic encephalopathy in apparently healthy, ambulant non-shunted patients with cirrhosis. *J Hepatol* 1986; **3**: 75-82
14 **Gilberstadt SJ**, Gilberstadt H, Zieve L, Buegel B, Collier R Jr, McClain CJ. Psychometric performance defects in cirrhotic patients without overt encephalopathy. *Arch Intern Med* 1980; **140**: 519-521
15 **Sood GK**, Sarin SK, Mahaptra J, Broor SL. Comparative efficacy of psychometric tests in detection on subclinical hepatic encephalopathy in nonalcoholic cirrhotics: search for a rational approach. *Am J Gastroenterol* 1989; **84**: 156-159
16 **Jia L**, Li YY. Subclinical hepatic encephalopathy. *Chinese J Intern Med* 1996; **36**: 495-497
17 **Wang JY**. Summary of national symposium on cirrhosis in China. *Zhonghua Xiaohua Bingxue Zazhi* 1991; **11**: 290-291
18 **Wang JY**. Consensus of viral hepatitis prevention and treatment. *Zhonghua Chuanran Bingxue Zazhi* 1995; **13**: 241-247
19 **Gong YX**. Wechsler Adult Intelligence-Revised in China (WAIS-RC). *1st edition, Changsha, China Hunan Atlas Press* 1992: 52-53
20 **Dhiman RK**, Saraswat VA, Verma M, Naik SR. Figure connection: A universal test for assessment of mental state. *J Gastroenterol Hepatol* 1995; **10**: 14-23
21 **Schenker S**, Butterworth R. NMR spectroscopy in portal systemic encephalopathy: are we there yet? *Gastoenterology* 1997; **112**: 1758-1761
22 **Davies AD**. The influence of age on trail making test performance. *J Clin Psychol* 1968; **24**: 96-98
23 **Zeneroli ML**, Cioni G, Ventura P, Russo AM, Venturini I, Casalgrandi G, Ventura E. Interindividual variability of the number connection test. *J Hepatol* 1992; **15**: 263-264
24 **Schomeras H**, Hanster W, Blunck H, Reinhard U, Mayer K, Dolle W. Latent portasystemic encephalopathy, I, Nature of cerebral functional defects and their effection fitness to drive. *Dig Dis Sci* 1981; **26**: 622-630
25 **Tarter RE**, Hegedus AM, Vanthiel DH, Schade RR, Gavaler JS, Starzl TE. Non-alcoholic cirrhosis ascoiated with neuropsycholopathy dysfuntion in the absence of overt evidence of hepatic encephalopathy. *Gastroenterology* 1984; **86**: 1421-1427
26 **Cordoba J**, Cabrera J, Lataif L, Penev P, Zee P, Blei AT. High prevalence of sleep disturbance in cirrhosis. *Hepatology* 1998; **27**: 339-345
27 **Yen CL**, Liaw YF. Somatosensory evoked potentials and number connection test in the detection of subclinical hepatic encephalopathy. *Heptogastroenterology* 1990; **37**: 332-334
28 **Zeng Z**, Li YY. Effects of lactulose trement on the course of subclinical hepatic encephalopathy. *Zhonghua Yixue Zazhi* 2003; **83**: 1126-1129
29 **Saxena N**, Bhatia M, Joshi YK, Garg PK, Dwivedi SN, Tandon RK. Electrophysiological and neuropsychological tests for the diagnosis of subclinical hepatic encephalopathy and pridiction for overt encephalopathy. *Liver* 2002; **22**: 190-197
30 **Dhiman RK**, Sawhney MS, Chawla YK, Das G, Ram S, Dilawari JB. Efficacy of lactulose in cirrotic patients with subclinical hepatic encephalopathy. *Dig Dis Sci* 2000; **45**: 1549-1552

Edited by Wu XN and Wang XL **Proofread by** Xu FM

PO Box 2345, Beijing 100023, China
Fax: +86-10-85381893
E-mail: wjg@wjgnet.com www.wjgnet.com

World J Gastroenterol 2004;10(16):2402-2405
World Journal of Gastroenterology
 ISSN 1007-9327

• CLINICAL RESEARCH •

Prevalence of a newly identified SEN virus in China

Shi-Jie Mu, Juan Du, Lin-Sheng Zhan, Hai-Ping Wang, Rui Chen, Quan-Li Wang, Wen-Ming Zhao

Shi-Jie Mu, Wen-Ming Zhao, School of Life Sciences and Technology, Xi'an Jiaotong University, Xi'an 710049, Shaanxi Province, China
Juan Du, Lin-Sheng Zhan, Hai-Ping Wang, Quan-Li Wang, Institute of Field Transfusion Medicine, Academy of Military Medical Sciences, Beijing 100850, China
Rui Chen, Department of Blood Transfusion, Xijing Hospital, Fourth Military Medical University, Xi'an 710032, Shaanxi Province, China
Supported by the Innovation Foundation of Academy of Military Medical Sciences, No.200104
Correspondence to: Shi-Jie Mu, School of Life Sciences and Technology, Xi'an Jiaotong University, Xi'an 710049, Shaanxi Province, China. musj@nwblood.com
Telephone: +86-29-83375465 **Fax:** +86-29-83244952
Received: 2003-12-23 **Accepted:** 2004-01-08

Abstract

AIM: To establish nested-PCR methods for the detection of SENV-D and SENV-H and to investigate the epidemiology of SEN virus in China.

METHODS: According to published gene sequences, primers from the conserved region were designed. Then, 135 samples from healthy voluntary blood donors and 242 samples from patients with various forms of liver disease were detected by nested-PCR of SENV-D/H. Some PCR products were cloned and sequenced.

RESULTS: By sequencing, the specificity of genotype-specific PCR was confirmed. SENV-D/H DNA was detected in 31% of the blood donors, which was higher than those in America and Italy (2%), and in Japan and Taiwan (15-20%). The prevalence of SENV-D/H viremia was significantly higher in patients with hepatitis B and hepatitis C than in blood donors (59-85% *vs* 31%, $P<0.05$). The prevalence among patients with non-A-E hepatitis was significantly higher than among blood donors (68% *vs* 31%, $P<0.01$), and equivalent to that among patients with hepatitis B and C.

CONCLUSION: Nested-PCR with genotype-specific primers could serve as a useful SENV screening assay. SENV has the same transmission modes as HBV and HCV. The high prevalence in patients with non-A-E hepatitis may attribute to the transmission modes, and SENV may not serve as the causative agents.

Mu SJ, Du J, Zhan LS, Wang HP, Chen R, Wang QL, Zhao WM. Prevalence of a newly identified SEN virus in China. *World J Gastroenterol* 2004; 10(16): 2402-2405
http://www.wjgnet.com/1007-9327/10/2402.asp

INTRODUCTION

Recently, a novel DNA virus designated SEN virus (SENV) was discovered in the serum of a human immunodeficiency virus type 1 (HIV-1)-infected patient[1]. Phylogenetic analysis[2] showed 8 strains (A-H) of SENV. To date, the ninth genotype (SENV-I) has been identified[3]. Among them, 2 SENV strains (SENV-D and SENV-H) were significantly associated with transfusion-associated non-A-E hepatitis[4]. SENV-D and SENV-H were also detected more frequently in patients with chronic liver disease and hepatocellular carcinoma (HCC) than in healthy adults[5,6]. However, the association of SENV infection with liver cell damage is far from clear, and further studies are needed to investigate the clinical relevance of SENV infection worldwide.

The purpose of this study was to develop a nested polymerase chain reaction (nPCR) method for the detection of SENV-D and SENV-H DNA in serum and elucidate its specificity. The presence of SENV-D and SENV-H viremia in patients with various forms of liver diseases and the possible role of SENV infection in non-A-E hepatitis were investigated.

MATERIALS AND METHODS

Patients

A total of 377 serum samples from March 1999 to April 2003 were studied in Xijing Hospital. They were divided into 5 groups as follows: 135 blood donors; 55 patients with acute hepatitis A virus (HAV); 126 with chronic hepatitis B; 20 with chronic hepatitis C; 41 with non-A-E hepatitis defined as negative control for known serologic markers, including I gM anti-HAV, I gM antibody to hepatitis B core antigen (anti-HBc), hepatitis B surface antigen (HBsAg), and antibodies to HCV, HDV and HEV.

Detection of SENV DNA

Viral DNA was extracted from 100 μL serum with the QIAamp blood kit (Qiagen) and resuspended in 20 μL elution buffer. PCR mixture of 20 μL contained 0.4 μmol/L sense primer SENV-P2 (5' -CC[C/G] AAA CTG TTT GAA GAC [C/A]A-3') (designed by ourselves), 0.4 μmol/L antisense primer Lucky2AS (5' -CCT CGG TT[G/T] [C/G]AA A[G/T]G T[C/T]T GAT AGT-3')[1], 200 μmol/L of each dNTP, 2 μL DNA sample, and 1 U *Taq* DNA polymerase. The reactions consisted of preheating at 94 °C for 3 min, 30 cycles of denaturation at 94 °C for 1 min, annealing at 50 °C for 1 min, extension at 72 °C for 40 s, and final incubation at 72 °C for 5 min. The second PCR step was carried out with a 20 μL PCR reaction mixture containing 2 μL of the first-step amplification product, the same PCR buffer used for the first PCR step, 0.4 μmol/L sense primer D10s (5' -GTA ACT TTG CGG TCA ACT GCC-3')[1] and antisense primer Lucky2AS for SENV-D; 0.4 μmol/L sense primer C5s (5' -GGT GCC CCT [A/T] GT [C/T]AG TTG GCG GTT-3') (designed by ourselves) and antisense primer Lucky2AS for SENV-H, 200 μmol/L of each dNTP, and 1 U *Taq* DNA polymerase, PCR consisted of preheating at 94 °C for 1 min, annealing at 58 °C for 1 min, extension at 72 °C for 40 s, and final incubation at 72 °C for 5 min.

Determination of SENV genotypes

Amplicons containing polyA tails and producing visible bands on agarose gel were excised from the gel and ligated to the pGEM vector. DNA extracted from transformed *Escherichia Coli* was sequenced. The sequences excluding primer sequences were aligned with Cluster W to all SENV genotypes, representative of TTV (TA278) and TLMV isolates. The genotype of SENV was determined by the phylogenetic trees.

Table 1 Prevalence of SENV infection in different hepatitis groups in China

Disease	*n*	Single SENV-D	Single SENV-H	Combined SENV-D/-H	Total *n* (%)
Acute hepatitis A	55	2 (3.6)	12 (21)	6 (11)	20 (36)
Chronic hepatitis B	126	17 (13)	16 (12)	41 (32)	74 (59)[b]
Chronic hepatitis C	20	4 (20)	4 (20)	9 (45)	17 (85)[b]
Acute+chronic non-A-E	41	10 (24)	7 (17)	11 (27)	28 (68)[b]
Blood donors	135	9 (6.7)	7 (5)	26 (19)	42 (31)

[b]$P<0.01$ *vs* Blood donors.

Statistical analysis

Data were analyzed by χ^2 test with Yates' correction or Fisher's exact test; $P<0.05$ was considered to be statistically significant.

RESULTS

Genotype-specific PCR with specific primers

PCR products were detected by 20 g/L agarose gel. The results showed that there was a 230-bp band in the gel (Figure 1). The PCR products were inserted into pGEM-T vectors and sequenced. A phylogenetic tree of the SENV-D sequences (Figure 2A) from 8 blood donors (B7, B11, B13, B14, B28, B29, B31 and B33) and 7 patients with non-A-E hepatitis (N4, N9, N10, NC, NF, NG and NK) was constructed. To determine a root of the phylogenetic tree, TLMV was used as an out-group. SENV-D DNA sequences from study subjects clustered in a monophyletic group with the SENV-D prototype sequences. A phylogenetic tree of the SENV-H sequences (Figure 2B) from 7 blood donors (B1, B4, B11, B12, B28, B29 and B30) and 5 patients with non-A-E hepatitis (N4, N8, N10, NA and NF) was constructed. SENV-H DNA sequences from study subjects clustered in a monophyletic group with the SENV-H prototype sequences with the exception of 2 outliers (B1 and B28), which had closer homology to SENV-C.

The specificity of genotype-specific PCR was confirmed by sequencing. Here, all 15 patients diagnosed as SENV-D by the genotype-specific PCR had homology to SENV-D (Figure 2A), while 10 of 12 patients (83%) diagnosed as SENV-H by the genotype-specific PCR had homology to SENV-H, the other 2 had homology to SENV-C which was of the same genotype as SENV-H (Figure 2B).

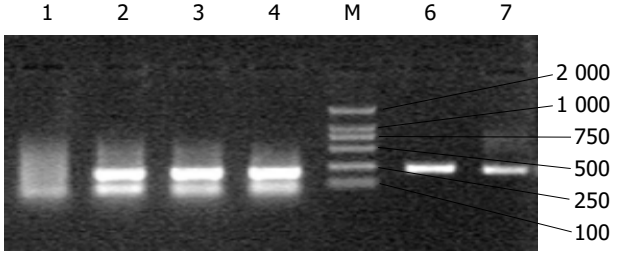

Figure 1 Electrophoresis of PCR products. Lane 1: Negative control; lane 2: Positive control; lanes 3, 4: SENV-D; lane 5: Marker DL2000; lanes 6, 7: SENV-H.

SENV prevalence in patients with liver diseases and in blood donors

SENV-D and/or SENV-H (SENV-D/H) DNAs were positive in 31% of healthy Chinese adults. SENV viremia was identified in 20 (36%) of 55 patients with acute or chronic hepatitis A, in 74 (59%) of 126 patients with chronic hepatitis B, in 17 (85%) of 20 patients with chronic hepatitis C, in 28 (68%) of 41 patients with acute or chronic non-A-E hepatitis. Compared with healthy blood donors, SENV infection was found more frequently in patients with hepatitis B, hepatitis C and non-A-E hepatitis (59-85% *vs* 31%, $P<0.01$, Table 1). However, the prevalence was comparable among patients with acute hepatitis A and healthy adults (31% *vs* 36%). The prevalence of SENV-H was 2-fold higher than that of SENV-D in patients with acute hepatitis A. Mixed SENV-D/H infection was common (Table 1).

DISCUSSION

Viral hepatitis is a worldwide disease[7] and imperils human health gravely. To date, 5 hepatitis viruses from HAV to HEV[8], which account for 8% to 90% hepatitis cases, have been discovered. But we could not find any hepatitis viruses in the left 10% to 20% cases that have typical viral hepatitis manifestations. Scientists speculated that the virus TTV was correlated with non-A-E hepatitis. Chinese scholars studied infection rate of TTV in different populations and its pathogenicity in liver[9-12], and found that TTV had no pathogenicity[13-15]. Afterwards, Primi *et al*.[1] found that SENV and TTV had similar structure. SENV has homogeneity of 55% at nucleotide level with TTV, but they only have homogeneity of 37% at amino acid level[2]. SENV appears to belong to a family of small, circular, non-enveloped, single-stranded DNA viruses that have been designated as circoviruses[16,17]. Phylogenetic analysis of SENV has shown the existence of 8 different variants (A-H). Among them, only SENV-D and SENV-H have higher prevalence ratios, and they are found in 2% of blood donors and >50% of persons with transfusion-associated non-A-E hepatitis in Italy and the United States. Although a strong association of SENV-D/H with transfusion-associated non-A-E hepatitis has been reported, whether SENV-D/H serves as a causative agent of post-transfusion hepatitis remains unknown[18-20].

The results of our present study indicate that nPCR amplified with genotype-specific primers could serve as a useful SENV screening assay. Moreover, because all components of the assay are readily available (specific antibodies are not required), viral testing can be performed in most laboratories that perform PCR. Our recent study indicated that 31% of healthy Chinese adults were positive for SENV-D/H DNA, a rate comparable to that of blood donors in Japan (10-20%)[5,21] and Taiwan (14-20%)[6] (age-specific prevalence), but higher than that of blood donors in the United States and Italy (2%)[22,23]. Co-infection with SENV has been frequently observed in 22-67% of patients with chronic hepatitis B[5,6] and 20-76% of patients with chronic hepatitis C[4-6,24,25]. Our study showed that the prevalence of SENV-D/H infection in patients with chronic hepatitis B and C were 59% and 85% respectively, implying that HCV, HBV and SENV may share common modes of transmission. Our study also indicated that compared with blood donors (31%), SENV-D/H infection was more frequent in patients with non-A-E hepatitis (68%), but comparable to those in patients with chronic hepatitis C and B (85% and 59%, respectively). These results can not support a causal role for SENV-D/H in the development of non-A-E hepatitis. Otherwise, we also documented that the prevalence of SENV-H was comparable to that of SENV-D in different subjects, such as blood donors, patients with chronic

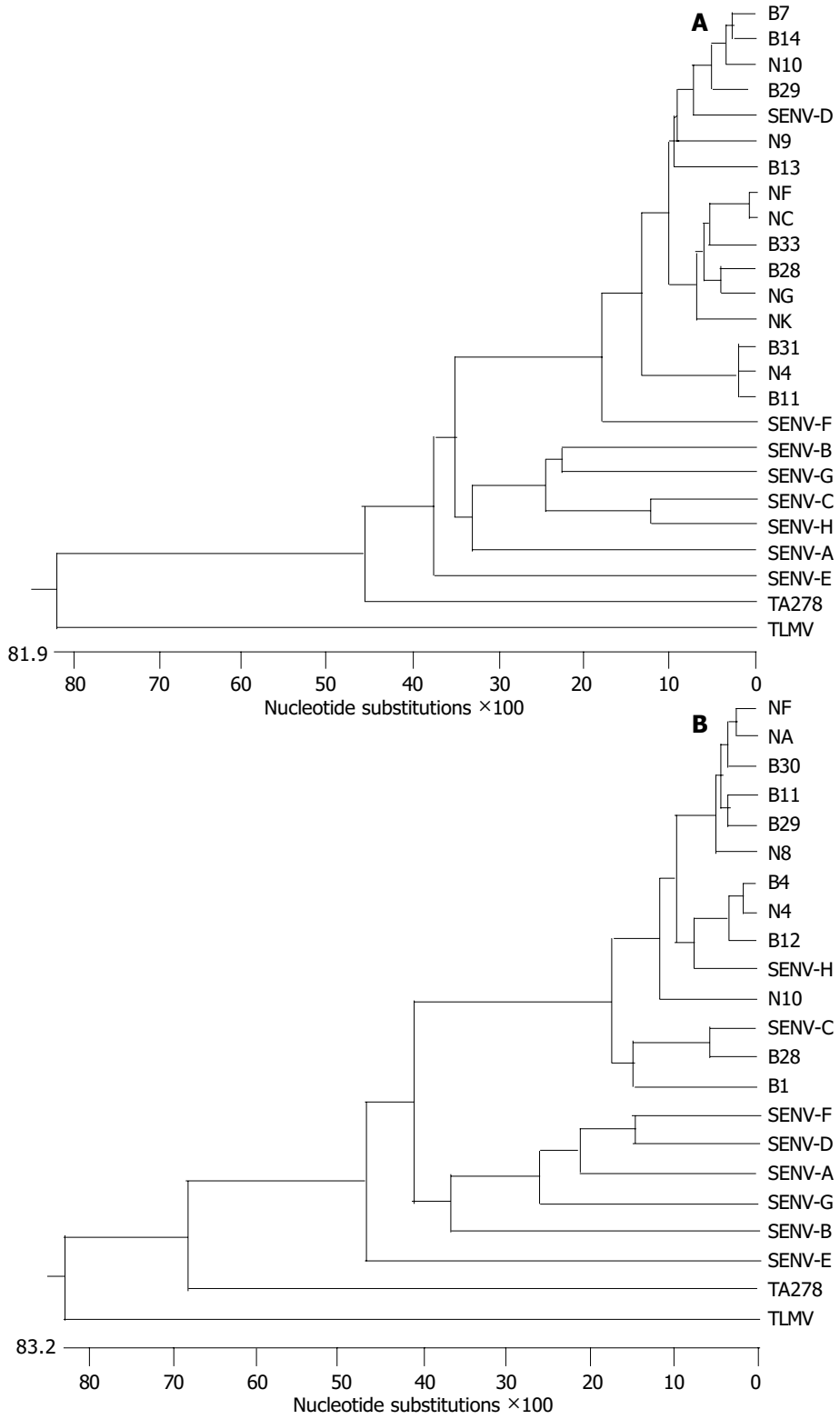

Figure 2 Phylogenetic tree of SENV by neighbor-joining method. A: The tree constructed on basis of 1 prototype TTV isolate (TA278), 1 TTV variant, 8 SEN virus isolates (A-H) and 15 SENV-D Chinese isolates. B: The tree constructed on basis of 1 prototype TTV isolate (TA278), 1 TTV variant, 8 SEN virus isolates (A-H) and 12 SENV-H Chinese isolates.

hepatitis B or C, and patients with non-A-E hepatitis, but among patients with acute hepatitis A, SENV-H was more prevalent than SENV-D ($P<0.05$). This phenomenon awaits further prospective studies.

In summary, the results of this study suggest that SENV has the same transmission modes as HBV and HCV[26]. The high prevalence in patients with non-A-E hepatitis may attribute to the transmission modes, and SENV may not serve as the causative agents. At present, SENV and the larger group of human circoviruses have no established pathogenicity, but they may have disease associations that have not been identified, or they may serve as commensal organisms that have some beneficial role in maintaining homeostasis in the host. They are worthy of more attention, even in the absence of confirmed disease associations.

REFERENCES

1 **Primi D,** Fiordalisi G. Identification of SENV Genotypes. International patent number WO0028039 (http://ep.espacenet.com/)

2 **Tanaka Y,** Primi D, Wang RY, Umemura T, Yeo AE, Mizokami M, Alter HJ, Shih JW. Genomic and molecular evolutionary analysis of a newly identified infectious agent (SEN virus) and its relationship to the TT virus family. *J Infect Dis* 2001; **183:** 359-367

3 **Kojima H,** Kaita KD, Zhang M, Giulivi A, Minuk GY. Genomic analysis of a recently identified virus (SEN virus) and genotypes D and H by polymerase chain reaction. *Antiviral Res* 2003; **60:** 27-33

4 **Umemura T,** Yeo AE, Sottini A, Moratto D, Tanaka Y, Wang RY, Shih JW, Donahue P, Primi D, Alter HJ. SEN virus infection and its relationship to transfusion-associated hepatitis. *Hepatology* 2001; **33:** 1303-1311

5 **Shibata M,** Wang RY, Yoshiba M, Shih JW, Alter HJ, Mitamura K. The presence of a newly identified infectious agent (SEN virus) in patients with liver diseases and in blood donors in Japan. *J Infect Dis* 2001; **184:** 400-404

6 **Kao JH,** Chen W, Chen PJ, Lai MY, Chen DS. Prevalence and implication of a newly identified infectious agent (SEN Virus) in Taiwan. *J Infect Dis* 2002; **185:** 389-392

7 **Zheng RQ,** Wang QH, Lu MD, Xie SB, Ren J, Su ZZ, Cai YK, Yao JL. Liver fibrosis in chronic viral hepatitis: An ultrasonographic study. *World J Gastroenterol* 2003; **9:** 2484-2489

8 **Chang JH,** Wei L, Du SC, Wang H, Sun Y, Tao QM. Hepatitis G virus infection in patients with chronic non-A-E hepatitis. *China Nati J New Gastroenterol* 1997; **3:** 143-146

9 **Liu YL,** Zhu YM, Chen HS, Wang Y. Prevalence and pathogenicity of TT virus infection in patients with liver diseases. *Shijie Huaren Xiaohua Zazhi* 2002; **10**: 1143-1148

10 **Zhang JH,** Chen SZ. An epidemiological study on transfusion transmitted virus infection in China. *Shijie Huaren Xiaohua Zazhi* 2001; **9:** 1384-1390

11 **Zhao Y,** Wang JB. Epidemiological survey on TTV infection and the asso ciation with other viral liver diseases in Changchun area. *Shijie Huaren Xiaohua Zazhi* 2001; **9:** 747-750

12 **Fu EQ**, Bai XF, Pan L, Li GY, Yang WS, Tang YM, Wang PZ, Sun JF. Investigation of TT virus infection in groups of different people in Xi'an. *Shijie Huaren Xiaohua Zazhi* 1999; **7:** 967-969

13 **Abe K,** Inami T, Asano K, Miyoshi C, Masaki N, Hayashi S, Ishikawa K, Takebe Y, Win KM, El-Zayadi AR, Han KH, Zhang DY. TT virus infection is widespread in the general populations from different geographic regions. *J Clin Microb* 1999; **37**: 2703-2705

14 **Ikeuchi T,** Yokosuka O, Kanda T, Imazeki F, Seta T, Saisho H. Roles of TT virus infection in various types of chronic hepatitis. *Intervirology* 2001**; 44:** 219-223

15 **Kadayifci A,** Guney C, Uygun A, Kubar A, Bagci S, Dagalp K. Similar frequency of TT virus infection in patients with liver enzyme elevations and healthy subjects. *Int J Clin Pract* 2001; **55:** 434-436

16 **Adair BM.** Immunopathogenesis of chicken anemia virus infection. *Dev Comp Immunol* 2000; **24:** 247-255

17 **Takahashi K,** Iwasa Y, Hijikata M, Mishiro S. Identification of a new human DNA virus (TTV-like mini virus, TLMV) intermediately related to TT virus and chicken anemia virus. *Arch Virol* 2000; **145:** 979-993

18 **Umemura T,** Tanaka Y, Kiyosawa K, Alter HJ, Shih JW. Observation of positive selection within hypervariable regions of a newly identified DNA virus (SEN virus)(1). *FEBS Lett* 2002; **510**: 171-174

19 **Wilson LE,** Umemura T, Astemborski J, Ray SC, Alter HJ, Strathdee SA, Vlahov D, Thomas DL. Dynamics of SEN virus infection among injection drug users. *J Infect Dis* 2001; **184:** 1315-1319

20 **Schroter M,** Laufs R, Zollner B, Knodler B, Schafer P, Sterneck M, Fischer L, Feucht HH. Prevalence of SENV-H viraemia among healthy subjects and individuals at risk for parenterally transmitted diseases in Germany. *J Viral Hepat* 2002; **9:** 455-459

21 **Umemura T,** Yeo AET, Shih J, Matsumoto A, Orii K, Tanaka E. The presence of SEN Virus infection in Japanese patients with viral hepatitis and liver disease. *Hepatology* 2000; **32:** 381A

22 **Mushahwar IK.** Recently discovered blood-borne viruses: are they hepatitis viruses or merely endosymbionts? *J Med Virol* 2000; **62:** 399-404

23 **Bowden S.** New hepatitis viruses: contenders and pretenders. *J Gastroenterol Hepatol* 2001; **16:** 124-131

24 **Rigas B,** Hasan I, Rehman R, Donahue P, Wittkowski KM, Lebovics E. Effect on treatment outcome of coinfection with SEN viruses in patients with hepatitis C. *Lancet* 2001; **358:** 1961-1962

25 **Umemura T,** Alter HJ, Tanaka E, Orii K, Yeo AE, Shih JW, Matsumoto A, Yoshizawa K, Kiyosawa K. SEN virus: response to interferon alfa and influence on the severity and treatment response of coexistent hepatitis C. *Hepatology* 2002; **35:** 953-959

26 **Tang W,** Peng XM, Zhang Y, Wang H, Jiang XL, Zhou BP. Establishment and application of polymerase chain reaction for detecting D and H subtypes of SEN virus. *Shijie Huaren Xiaohua Zazhi* 2003; **11:** 1540-1543

Edited by Chen WW **Proofread by** Zhu LH and Xu FM

PO Box 2345, Beijing 100023, China
Fax: +86-10-85381893
E-mail: wjg@wjgnet.com www.wjgnet.com

World J Gastroenterol 2004;10(16):2406-2408
World Journal of Gastroenterology
 ISSN 1007-9327

• CLINICAL RESEARCH •

E-cadherin and calretinin as immunocytochemical markers to differentiate malignant from benign serous effusions

Dong-Nan He, Hua-Sheng Zhu, Kun-He Zhang, Wen-Jian Jin, Wei-Ming Zhu, Ning Li, Jie-Shou Li

Dong-Nan He, School of Medicine, Nanjing University, Nanjing 210093, Jiangsu Province, China
Hua-Sheng Zhu, Department of General Surgery, Shanghai Meishan Hospital, Nanjing 210039, Jiangsu Province, China
Kun-He Zhang, Wen-Jian Jin, Digestive Disease Institute of Jiangxi Medical College, Nanchang 330006, Jiangxi Province, China
Wei-Ming Zhu, Ning Li, Jie-Shou Li, Department of General Surgery, Jingling Hospital, Clinical School of Nanjing University, Nanjing 210002, Jiangsu Province, China
Correspondence to: Kun-He Zhang, Digestive Disease Institute of Jiangxi Medical College, Nanchang 330006, Jiangxi Province, China. yfyzkh@sina.com
Telephone: +86-791-8692695
Received: 2003-12-12 **Accepted:** 2004-01-08

Abstract

AIM: To investigate the expressions of E-cadherin and calretinin in exfoliated cells of serous effusions and evaluate their values in distinguishing malignant effusions from benign ones.

METHODS: Fresh serous effusion specimens were centrifuged and exfoliated cells were collected. Cells were then processed with a standardized procedure, including paraformaldehyde fixation, BSA-PBS solution washing and smears preparation. E-cadherin and calretinin were detected by immunocytochemistry (ICC).

RESULTS: In the exfoliated cells of serous effusions, most of carcinoma cells only expressed E-cadherin, and most of mesothelial cells only expressed calretinin, and benign cells (lymphocytes and granulocytes) did not express either of them. For E-cadherin, 85.7% (30/35) of malignant effusions and 8.1% (3/37) of benign fluids were ICC-positive ($P<0.001$). The sensitivity of E-cadherin ICC in the diagnosis of malignant effusions was 85.7%, specificity 91.9%, and diagnostic rate 88.9%. For calretinin, 94.6% (35/37) of benign effusions and 11.4% (4/35) of malignant effusions were ICC-positive ($P<0.001$). The sensitivity of calretinin ICC in the diagnosis of benign effusions was 94.6%, specificity 88.6%, and diagnostic rate 91.7%. For diagnosis of benign and malignant effusions by combining E-cadherin ICC and calretinin ICC, the specificities were up to 100% and 97.1%, respectively.

CONCLUSION: E-cadherin ICC and calretinin ICC are sensitive and specific in differential diagnosis of benign and malignant serous effusion specimens and specificities are evidently improved when both markers are combined.

He DN, Zhu HS, Zhang KH, Jin WJ, Zhu WM, Li N, Li JS. E-cadherin and calretinin as immunocytochemical markers to differentiate malignant from benign serous effusions. *World J Gastroenterol* 2004; 10(16): 2406-2408
http://www.wjgnet.com/1007-9327/10/2406.asp

INTRODUCTION

Serous effusions are common in clinical practice and some cases are caused by metastasis of malignant tumors (malignant effusions). Distinguishing malignant from benign tumors is very important, but sometimes very difficult[1]. Some studies have shown that immunocytochemistry (ICC) of exfoliated cells is valuable in differentiating malignant effusions from benign ones[2-6]. However, the diagnostic value of a single marker was limited, and a panel of markers were more useful[7,8]. Recently, several studies have shown that E-cadherin, an epithelial adhesion molecule, was a useful marker for identifying the carcinoma cells in effusions[9,10], and calretinin, a calcium-binding protein, was a useful marker for identifying the mesothelial cells[11,12]. It is well known that the differentiation between cancer cells and reactive mesothelial cells is the main problem in cytological diagnosis of effusions. In the present study, both E-cadherin and calretinin were used as markers in immunocytochemical staining of exfoliated cells in serous effusions, and their diagnostic values were evaluated.

MATERIALS AND METHODS

Patients and specimens

Seventy-two patients with serous effusions were enrolled in this study (35 male, 37 female, age 14-77 years with an average of 51.8 years). All patients were from the First Affiliated Hospital of Jiangxi Medical College from 2001 to 2002. Effusion specimens were collected and divided into two groups, benign and malignant, according to cytological results. Of these specimens, there were 45 pleural effusions, 24 peritoneal effusions, and 3 malignant pericardial effusions. In the 23 cases of benign pleural effusions, there were 13 cases of tuberculous pleuritis, 2 cases of liver cirrhosis, 1 pulmonary tuberculosis, 1 chyle pleural effusion, and 6 unknown causes. In the 22 cases of malignant pleural effusion, there were 11 cases of lung cancer, 1 submaxillary gland cancer, 1 gastric cancer, 1 primary liver cancer, and 8 cases of unknown origin. In the 14 cases of benign peritoneal effusions, there were 8 cases of liver cirrhosis, 3 tuberculous peritonitis, 1 hepatitis B, 1 Budd-Chiari syndrome, 1 unknown cause. In the 10 cases of malignant peritoneal effusions, there were 4 cases of ovarian cancer, 2 primary liver cancers, 1 gastric cancer, 1 colonic cancer, 1 duodenal papilla cancer, and 1 unknown origin. Three cases of malignant pericardial effusions included 1 case of lung cancer, 1 metastatic squamous cancer and 1 unknown origin.

Specimen processing

About 100 mL fresh effusion was centrifuged at 2 000 r/min for 10 min, and cell pellets were collected. When the effusion was bloody, erythrocytes were destroyed with isotonic ammonium chloride solution (NH_4Cl 4.5 g, $KHCO_3$ 0.5 g, EDTA 0.0186 g, solved in 400 mL distilled water, then distilled water add to a total volume of 500 mL). Same volume of the solution was added to dissolve the cell pellets, which were stirred for 5 min at room temperature, centrifuged at 2 000 r/min for 10 min, and the supernatants removed. Two cell smears were prepared for cytological diagnosis. The remaining cells were processed with a "standardized" procedure[13]: fixed in 40 g/L paraformaldehyde-PBS solution, washed in 10 g/L BSA-PBS solution, the cell concentration was adjusted to 2×10^6/mL, and finally several

cell smears were prepared. The smears were air-dried and stored in a freezer (-85 °C).

Immunocytochemistry and evaluation

Reagents for immunocytochemical staining were provided by Beijing Zhongshan Biotechnology Co. Ltd. Mouse anti-human E-cadherin monoclonal antibody (1:100 dilution) or rabbit anti-human calretinin polyclonal antibody (1:50 dilution) was used as the primary antibody. Biotinylated goat anti-mouse/rabbit IgG was used as the second antibody. The reaction products were visualized by using the streptavidin-horseradish peroxidase and diaminobenzidine. The smears were counterstained with hematoxylin. PBS was used instead of the primary antibodies as negative control.

In E-cadherin ICC, positive cells were stained at cytomembrane, especially in the areas surrounding the cells. In calretinin ICC, whole cells were stained with a "fried eggs" staining pattern. One hundred cells (carcinoma and/or non-carcinoma) were counted under a high power microscope, and the percentage of positive cells was calculated. ICC-positive cells >/= 80% were defined as strong expression (+++), 20-79% as moderate expression (++), 6-19% as weak expression (+), 0-5% as negative expression (-). Specimens with expressions (+)-(+++) were regarded as ICC-positive, and expression (-) as ICC-negative.

Statistical analysis

Qualitative data were analysed with chi-square test, and rank data were tested with rank sum test. Diagnostic values of ICC results were calculated in contrast to that of the cytological results. Diagnostic values of the combination of E-cadherin and calretinin ICC results were calculated in series ways.

RESULTS

E-cadherin expression of exfoliated cells in serous effusions

E-cadherin expression in carcinoma cells was usually strong, with obvious staining at cytomembrane and sometimes in cytoplasm (Figure 1). The areas surrounding the cells had densely stained lines in the clusters of carcinoma cells, but single carcinoma cell was weakly stained. Mesothelial cells were stained occasionally, and no lymphocytes and granulocytes were stained. Thirty of 35 malignant effusion specimens were ICC-positive for E-cadherin (85.7%), and most of them were strong (93.3% was ++-+++). Only 3 of 37 benign effusions were ICC-positive for E-cadherin (8.1%), in which a few mesothelial cells were weakly stained in cytoplasm. The differences in positivity rates and expression intensities between two groups were significant (P<0.001-0.0001) (Table 1).

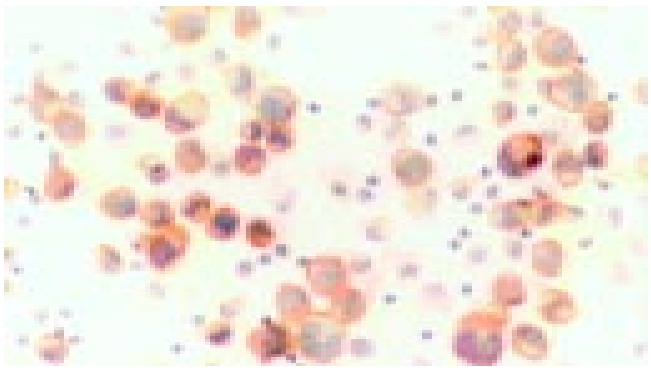

Figure 1 Immunocytochemistry of E-cadherin in the cells from a malignant ascites specimen. Carcinoma cells were mainly stained at cell membranes. Inflammatory cells without staining were as control (Original magnification, ×400).

Table 1 E-cadherin expression in exfoliated cells of serous effusions

Effusion group	*n*	Positivity (%)	Expression intensity			
			–	+	++	+++
Malignant	35	30 (85.7)	5	2	21	7
Benign	37	3 (8.1)	34	1	2	0

χ^2 = 43.633, P<0.001 between the two groups, H = 42.744, P<0.0001 between the two groups.

Calretinin expression of exfoliated cells in serous effusions

Calretinin expression in mesothelial cells was usually high, stained in whole cells (Figure 2). The typical cells looked like "fried eggs". Carcinoma cells were occasionally stained weakly, and no lymphocytes and granulocytes were stained. Thirty-five of 37 benign effusions were ICC-positive for calretinin (94.6%), and all of them were strong positive (+++). Only 4 of 35 malignant effusion specimens were ICC-positive for calretinin (11.4%), with a few carcinoma cells stained weakly. Differences of positivity rates and expression intensities between the two groups were significant (P<0.001-0.0001) (Table 2).

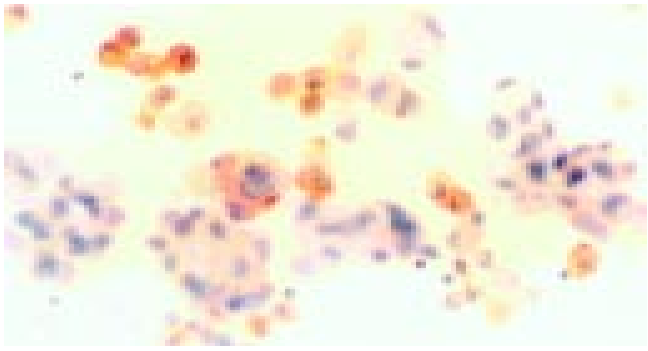

Figure 2 Immunocytochemistry of calretinin in the cells from a malignant ascites specimen. Mesothelial cells were stained strongly and some of them like "fried eggs". Carcinoma cells and inflammatory cells without staining were as control (Original magnification, ×400).

Table 2 Calretinin expression in exfoliated cells of serous effusions

Effusion group	*n*	Positivity (%)	Expression intensity			
			–	+	++	+++
Malignant	35	4 (11.4)	31	1	3	0
Benign	37	35 (94.6)	2	0	0	35

χ^2 = 50.109, P<0.001 between the two groups, H = 59.576, P<0.0001 between the two groups.

Table 3 Diagnostic values of E-cadherin or / and calretinin ICC for serous effusions

Index	Malignant effusion (%)		Benign effusion (%)	
	E-cadherin	E(+) + C(-)	Calretinin	E(-) + C(+)
Sensitivity	85.7	77.1	94.6	86.5
Specificity	91.9	100	88.6	97.1
PV+	90.9	100	89.7	97.0
PV-	87.2	82.2	93.9	87.2
DAR	88.9	88.9	91.7	91.7

E (+) / E (-): E-cadherin (+) / (-); C (+) / C (-): Calretinin (+) / (-); PV+: ICC-positive predictive value; PV-: ICC-negative predictive value; DAR: Accordance rate.

Diagnostic values of E-cadherin ICC or/and calretinin ICC for serous effusions

The diagnostic values (sensitivity, specificity) of both E-cadherin ICC and calretinin ICC for malignant effusions were >/= 90%. Combination analysis of E-cadherin ICC and calretinin ICC could improve the specificities (up to 97.1-100%), while the sensitivities maintained at an acceptable level (Table 3).

DISCUSSION

Serous effusions are common clinical syndromes and can be simply divided into benign and malignant. Differentiation between two kinds of effusions is very important for diagnosis, treatment and prognostic evaluation. The cytological examination is a simple and reliable method for the diagnosis of malignant effusions, but its sensitivity is only 40-60%[14], even lower in clinical practice. Cytological examinations are based on the cellular morphology, which may raise difficulties in distinguishing carcinoma cells from reactive mesothelial cells. Sometimes, carcinoma cells without typical morphological changes or enough number could not be diagnosed cytologically. How to identify the metastatic carcinoma cells and differentiate them from reactive mesothelial cells is key to diagnosing malignant effusions[15]. In the past decade, immunocytochemistry seemed to be a valuable tool in solving the problem, with a complementary value for cytological diagnosis of malignant effusions[16].

The cadherin family consists of more than 16 kinds of molecules that make up a group of phylogenetically and structurally related molecules, with M_r 120 000[17]. E-cadherin, one member of a family of intracellular calcium-dependent adhesion molecules, is a transmembrane protein expressed in epithelial cells. Its extracellular amino terminal binds to the same structure of neighboring homotypic cells when calcium ion exists, mediating the epithelial cell-cell adhesion. Theoretically, only the exfoliated cells originating from epithelial tissues can express E-cadherin, so detection of E-cadherin expression is helpful for determining cells from epithelia. Because no epithelial cells were in benign effusions, the appearance of epithelial cells in effusions means a metastasis of carcinoma developed from epithelia. Our results showed that E-cadherin ICC of the exfoliated cells were valuable for the diagnosis of malignant effusions, with a sensitivity, specificity, positive predictive value, negative predictive value, and diagnostic rate near or over 90% respectively, similar to other studies[1,18]. However, when epithelial cells transformed into malignant cells, E-cadherin expression might decrease to some extent[19,20]. That is the reason why a few carcinoma cells showed weak or negative E-cadherin expression in effusions.

Calretinin is a calcium adhesion protein with M_r 29 000 and mainly expresses in nerve system. Lately, it was found that calretinin selectively expressed in mesotheliomas[21,22], with powerful ability to differentiate mesothelial cells from other cells in effusions[1,5,11,22]. Our results showed that calretinin expression in mesothelial cells was evident, but not in non-mesothelial cells, therefore it is useful in determining the cells from mesothelium, with a sensitivity, specificity, positive predictive value, negative predictive value, and diagnostic rate all near or over 90%. The "fried eggs" staining pattern made calretinin ICC more valuable in differentiating mesothelial cells from carcinoma cells[1].

E-cadherin is an epithelial cell marker, and calretinin is a mesothelial cell marker. Our results showed that the combination of both markers significantly increased their differential diagnostic value with specificities up to 97.1% in serous effusions and 100% in benign and malignant effusions.

REFERENCES

1 **Chhieng DC**, Yee H, Schaefer D, Cangiarella JF, Jagirdar J, Chiriboga LA, Jagirdar J, Chiriboga LA, Cohen JM. Calretinin staining pattern aids in the differentiation of mesothelioma from adenocarcinoma in serous effusions. *Cancer* 2000; **90**: 194-200

2 **Ascoli V**, Scalzo CC, Taccogna S, Nardi F. The diagnostic value of thrombomodulin immunolocalization in serous effusions. *Arch Pathol Lab Med* 1995; **119**: 1136-1140

3 **Ascoli V**, Carnovale-Scalzo C, Taccogna S, Nardi F. Utility of HBME-1 immunostaining in serous effusions. *Cytopathology* 1997; **8**: 328-335

4 **Morgan RL**, De Young BR, McGaughy VR, Niemann TH. MOC-31 aids in the differentiation between adenocarcinoma and reactive mesothelial cells. *Cancer* 1999; **87**: 390-394

5 **Zimmerman RL**, Fogt F, Goonewardene S. Diagnostic utility of BCA-225 in detecting adenocarcinoma in serous effusions. *Anal Quant Cytol Histol* 2000; **22**: 353-357

6 **Afify AM**, Al-Khafaji BM, Paulino AF, Davila RM. Diagnostic use of muscle markers in the cytologic evaluation of serous fluids. *Appl Immunohistochem Mol Morphol* 2002; **10**: 178-182

7 **Davidson B**, Risberg B, Kristensen G, Kvalheim G, Emilsen E, Bjamer A, Berner A. Detection of cancer cells in effusions from patients diagnosed with gynaecological malignancies. Evaluation of five epithelial markers. *Virchows Arch* 1999; **435**: 43-49

8 **Ko EC**, Jhala NC, Shultz JJ, Chhieng DC. Use of a panel of markers in the differential diagnosis of adenocarcinoma and reactive mesothelial cells in fluid cytology. *Am J Clin Pathol* 2001; **116**: 709-715

9 **Schofield K**, D'Aquila T, Rimm DL. The cell adhesion molecule, E-cadherin, distinguishes mesothelial cells from carcinoma cells in fluids. *Cancer* 1997; **81**: 293-298

10 **Schofield K**, D'Aquila T, Rimm DL. E-cadherin expression is a sensitive and specific method for detection of carcinoma cells in fluid specimens. *Diagn Cytopathol* 2000; **22**: 263-267

11 **Barberis MC**, Faleri M, Veronese S, Casadio C, Viale G. Calretinin. A selective marker of normal and neoplastic mesothelial cells in serous effusions. *Acta Cytol* 1997; **41**: 1757-1761

12 **Wieczorek TJ**, Krane JF. Diagnostic utility of calretinin immunohistochemistry in cytologic cell block preparations. *Cancer* 2000; **90**: 312-319

13 **Kuenen-Boumeester V**, van Loenen P, de Bruijn EM, Henzen-Logmans SC. Quality control of immunocytochemical staining of effusions using a standardized method of cell processing. *Acta Cytol* 1996; **40**: 475-479

14 **Fenton KN**, Richardson JD. Diagnosis and management of malignant pleural effusions. *Am J Surg* 1995; **170**: 69-74

15 **Bedrossian CW**. Diagnostic problems in serous effusions. *Diagn Cytopathol* 1998; **19**: 131-137

16 **Delahaye M**, Van der Ham F, Van der Kwast TH. Complementary value of five carcinoma markers for the diagnosis of malignant mesothelioma, adenocarcinoma metastasis, and reactive mesothelium in serous effusions. *Diagn Cytopathol* 1997; **17**: 115-120

17 **Harrington KJ**, Syrigos KN, Harington KJ. The role of E-cadherin-catenin complex: more than an intercellular glue? *Ann Surg Oncol* 2000; **7**: 783-788

18 **Simsir A**, Fetsch P, Mehta D, Zakowski M, Abati A. E-cadherin, N-cadherin, and calretinin in pleural effusions: the good, the bad, the worthless. *Diagn Cytopathol* 1999; **20**: 125-130

19 **Wijnhoven BP**, Dinjens WN, Pignatelli M. E-cadherin-catenin cell-cell adhesion complex and human cancer. *Br J Surg* 2000; **87**: 992-1005

20 **Cai KL**, Wang GB, Xiong LJ. Effects of carbon dioxide and nitrogen on adhesive growth and expressions of E-cadherin and VEGF of human colon cancer cell CCL-228. *World J Gastroenterol* 2003; **9**: 1594-1597

21 **Gotzos V**, Vogt P, Celio MR. The calcium binding protein calretinin is a selective marker for malignant pleural mesotheliomas of the epithelial type. *Pathol Res Pract* 1996; **192**: 137-147

22 **Doglioni C**, Tos AP, Laurino L, Iuzzolino P, Chiarelli C, Celio MR, Viale G. Calretinin: a novel immunocytochemical marker for mesothelioma. *Am J Surg Pathol* 1996; **20**: 1037-1046

Edited by Chen WW and Zhu LH **Proofread by** Xu FM

PO Box 2345, Beijing 100023, China
Fax: +86-10-85381893
E-mail: wjg@wjgnet.com www.wjgnet.com

World J Gastroenterol 2004;10(16):2409-2411
World Journal of Gastroenterology
 ISSN 1007-9327

• BRIEF REPORTS •

Assessment of correlation between serum titers of hepatitis c virus and severity of liver disease

Bhupinder S. Anand, Maria Velez

Bhupinder S. Anand, Maria Velez, Department of Medicine, V. A. Medical Center and Baylor College of Medicine, Houston, Texas 77030, USA
Correspondence to: Bhupinder S. Anand, MD, Digestive Diseases Section (111D), VA Medical Center, 2002 Holcombe Blvd. Houston, Texas 77030, USA. ana0@flash.net
Telephone: +713-794-7273 **Fax:** +713-794-7687
Received: 2003-08-11 **Accepted:** 2004-03-04

Abstract

AIM: The significance of hepatitis C virus (HCV) serum titers has been examined in several clinical situations. There is much evidence that patients with a lower viral load have better response rates to anti-viral therapy compared to those with higher levels. Moreover, a direct association has been observed between serum titers of HCV and transmission rates of the virus. The aim of the present study was to determine if there was any correlation between HCV viral load and the severity of liver disease.

METHODS: Fifty patients with HCV infection were included in the study. These comprised of 34 subjects with a history of alcohol use and 16 non-alcoholics. Quantitative serum HCV RNA assay was carried out using the branched DNA (bDNA) technique. Linear regression analysis was performed between serum viral titers and liver tests. In addition, for the purpose of comparison, the subjects were divided into two groups: those with low viral titers (</=50 genome mEq/mL) and high titers (>50 mEq/mL).

RESULTS: All subjects were men, with a mean±SD age of 47±7.8 years. The mean HCV RNA level in the blood was 76.3×10^5 ±109.1 genome equivalents/mL. There was no correlation between HCV RNA levels and age of the patients (r = 0.181), and the history or amount (g/d) of alcohol consumption (r = 0.07). Furthermore, no correlation was observed between serum HCV RNA levels and the severity of liver disease as judged by the values of serum albumin (r = 0.175), bilirubin (r = 0.217), ALT (r = 0.06) and AST (r = 0.004) levels. Similarly, no significant difference was observed between patients with low viral titers and high titers with respect to any of the parameters.

CONCLUSION: Our results indicate that the severity of liver disease is independent of serum levels of hepatitis C virus. These findings are important since they have a direct impact on the current debate regarding the role of direct cytopathic effect of hepatitis C virus versus immune-mediated injury in the pathogenesis of HCV-related liver damage.

Anand BS, Velez M. Assessment of correlation between serum titers of hepatitis c virus and severity of liver disease. *World J Gastroenterol* 2004; 10(16): 2409-2411
http://www.wjgnet.com/1007-9327/10/2409.asp

INTRODUCTION

Hepatitis C virus (HCV) is a bloodborne pathogen that is endemic in most parts of the world, with an estimated overall prevalence of nearly 3%[1]. Approximately 80% patients with hepatitis C virus develop chronic infection, and progression to cirrhosis occurs in nearly 20% of these subjects[2]. Moreover, patients with HCV-related cirrhosis are at an increased risk of developing hepatocellular carcinoma, which is estimated to occur at the rate of 1.5% to 4% per year[2]. In most individuals, liver disease progresses slowly over several decades, but the rate of progression is highly variable[3-5]. Whereas some patients develop cirrhosis and end-stage liver disease within one to two years of exposure, others may die of old age or an entirely unrelated cause[6]. Although it is mostly unclear why some patients progress more rapidly than others, several factors have been identified as having a role in disease severity. HCV patients co-infected with hepatitis B virus (HBV) have an increased risk of developing cirrhosis and ecompensated liver disease[7] as well as hepatocellular carcinoma[8]. Several researches have noted more severe clinical and histological abnormalities in HCV infected chronic alcoholics compared to non-alcoholics with HCV infection[9-12]. Other factors associated with a more rapid course of liver disease include age at acquisition of HCV infection, gender of the patient and presence of immunodeficiency states[5,6].

Several studies have assessed the correlation between serum HCV viral titers and different clinical and laboratory parameters. Perinatal transmission of HCV from mothers to infants has been found to be related to maternal HCV titers. The risk of HCV transmission was found to be significantly higher (36%) among infants born to women with HCV RNA titers of at least 10^6 per mL compared to none if the titers were $<10^6$ per mL[13]. HCV titers have been found to be associated with responses to anti-viral treatment. Patients with a baseline HCV viral load of $</=2\times10^6$ copies per mL have significantly better responses to anti-viral therapy compared to those with higher viral titers[14]. Patients with HCV genotype 1 have been found in some studies to have higher viral loads than those with HCV genotype 2[15,16], although other studies have failed to observe such an association[17-19]. Previous attempts to assess the effect of viral titers on the severity of liver disease have produced conflicting results and the present study was designed to examine this issue in more detail.

MATERIALS AND METHODS

Patients with chronic hepatitis C virus infection diagnosed on the basis of a positive recombinant immunoblot assay (Riba) were included in the study. All patients were negative for other causes of chronic liver disease including hepatitis B virus infection. Patients were interviewed with respect to alcohol use, and in those with a positive history an assessment was made of the duration of alcohol abuse and amount of daily consumption. Physical findings and results of laboratory tests were recorded. All patients were treatment-naive and were tested before the administration of anti-viral therapy.

Quantitative HCV analysis

Quantitative assay of hepatitis C virus levels was performed by the branched-chain DNA (bDNA) technique (Quantiplex

HCV-RNA; Chiron Corporation, Emeryville, USA). The bDNA assay incorporates a series of steps involving viral nucleic acid hybridizations to obtain signal amplification. This technique is unlike the polymerase chain reaction (PCR)-based assays in which the viral genome is amplified. The results of viral RNA titers in clinical samples are expressed as viral or genome milliequivalents per mL (mEq/mL). When the study was first initiated, only the initial version of the bDNA assay (Quantiplex 1.0), which had a lower limit of detection of 350 000 viral mEq/mL, was available commercially. Subsequently, the Chiron Corporation upgraded the technique and the latest version of the assay (Quantiplex 2.0) was employed which has a lower limit of detection of 200 000 viral mEq/mL.

Statistical analysis

Descriptive statistical analyses were performed, and the results are presented as mean±SD. Comparison of quantitative measurements between groups was performed using Wilcoxon Rank Sum Test. The Students' *t*-test was used to assess changes in HCV RNA levels in the same individual. Linear regression analysis was employed to examine the presence of any correlation between serum HCV RNA levels and different laboratory and clinical parameters including the amount of daily alcohol consumption.

RESULTS

A total of 50 patients were included in the study. These comprised of 34 patients with a history of alcohol use and 16 non-alcoholics. All subjects were men, with a mean±SD age of 47±7.8 years. The mean HCV-RNA level in the blood was 76.3×10^5 ±109.1 genome equivalents/mL. There was no correlation between HCV RNA levels and the age of the patients (r = 0.181), a history of alcohol use or the amount (g/day) of alcohol consumption (r = 0.07). Furthermore, no correlation was observed between HCV RNA levels and the severity of liver disease as judged by the values of serum albumin (r = 0.175), bilirubin (r = 0.217), ALT (r = 0.06) and AST (r = 0.004) levels.

To further assess the effects of viral titers on the severity of liver disease, the study subjects were arbitrarily divided into two groups: patients with low viral titers (</=50 genome mEq/mL) and those with high titers (>50 mEq/mL). The results are shown in Table 1. Again, no difference was observed between the two groups with respect to any of the parameters examined.

Table 1 Comparison of patients with low and high hepatitis C virus serum titers

Parameter	Low HCV RNA level (</=50 genome mEq/L) n = 28	High HCV RNA level (>50 genome mEq/L) n = 22	P value
Age (yr)	48±8.8	45±6	0.35
Alcohol use (g/d)	221±110	274±170	0.27
ALT (U/mL)	77±56	75±41	0.76
AST (U/L)	79±58	93±100	0.96
Albumin (g %)	3.70±0.76	3.90±0.43	0.44
Bilirubin (mg %)	1.35±1.2	0.88±0.32	0.55

Results are expressed as mean±SD.

DISCUSSION

Several factors have been incriminated in predicting the rate of progression of HCV-related chronic liver disease. These include age at acquisition of HCV infection, gender of the patient, alcohol abuse and co-infection with HBV and HIV infections[5-12]. Studies assessing the relationship between serum viral titers and the severity of biochemical and histological abnormalities have produced conflicting results. Some found no correlation between HCV viral loads, and serum ALT values and the extent of histological damage[16,17,19-21]. On the other hand, Kato *et al*. observed significantly higher HCV RNA titers in patients with chronic active hepatitis and cirrhosis compared to those with milder histological abnormalities such as chronic persistent hepatitis[22]. Similarly, Fanning *et al*. in a study on Irish women who acquired their HCV infection through the administration of contaminated anti-D immunoglobulin, obtained a significant correlation between serum HCV viral loads and the degree of hepatic inflammation in liver biopsy specimens[23].

In the present study, we further assessed the association between serum HCV RNA titers and several clinical and laboratory factors. Linear regression analysis showed a complete lack of correlation between the viral loads and age at presentation of the patients and the extent of alcohol consumption. Moreover, none of the laboratory tests showed any correlation with HCV viral count. For the purposes of statistical analysis, we subdivided the patients into those with low (</=50 genome mEq/L) and high (>50 genome mEq/L) viral loads. Again, there was no correlation between any of the clinical and laboratory parameters and HCV viral loads (Table 1).

Our results indicate that the severity of liver disease is independent of serum levels of hepatitis C virus. The precise mechanism by which hepatitis C virus damages the liver remains poorly understood. Until recently, a direct cytopathic effect of the virus was considered as the primary form of liver injury caused by the virus. It has been suggested that the degree of liver damage is the result of a complicated interaction between the virus and immune response of the host[24]. Immune mediated liver damage is believed to be initiated by HCV-specific T cells and is enhanced by HCV-induced HLA-A, B and C and intracellular adhesion molecules[25,26]. The results of the present study are important since they argue against a direct cytopathic effect of HCV and support the hypothesis that the pathogenesis of HCV-related liver damage is immune-mediated.

REFERENCES

1 **Wasley A,** Alter MJ. Epidemiology of hepatitis C: Geographical differences and temporal trends. *Sem Liv Dis* 2000; **20**: 1-16
2 **Alter MJ.** The epidemiology of hepatitis C virus in the west. *Semin Liv Dis* 1995; **15**: 5-14
3 **Kiyosawa D,** Soeyama T, Tanaka E. Interrelationship of blood transfusion non-A, non-B hepatitis and hepatocellular carcinoma: analysis by detection of antibody to hepatitis C virus. *Hepatology* 1990; **12**: 671-675
4 **Tong MJ,** El-Farra NS, Reikes AR, Co RL. Clinical outcomes after transfusion-associated hepatitis C. *N Engl J Med* 1995; **332**: 1463-1466
5 **Poynard T,** Bedossa P, Opolon P. Natural history of liver fibrosis progression in patients with chronic hepatitis C the OBSVIRC, METAVIR, CLINIVIR, and DOSVIRC groups. *Lancet* 1997; **349**: 825-832
6 **Hoofnagle JH**. Hepatitis C: The clinical spectrum of disease. *Hepatology* 1997; **26**(Suppl 1): 15S-20S
7 **Chuang WL,** Chang WY, Lu SN. The role of hepatitis C virus in chronic hepatitis B virus infection. *Gastroenterol Jpn* 1993; 28 (Suppl 5): 23-27
8 **Di Bisceglie AM.** Hepatitis C and hepatocellular carcinoma. *Hepatology* 1997; **26**(Suppl 1): 34S-38S
9 **Coelho-Little ME,** Jeffers LJ, Bernstein DE, Goodman JJ, Reddy KR, de Medina M, Li X. Hepatitis C virus in alcoholic patients with and without clinically apparent liver disease. Alcohol. *Clinical Expt Res* 1995; **19**: 1173-1176
10 **Rosman AS,** Waraich A, Galvin K, Casiano J, Paronetto F, Lieber CS. Alcoholism is associated with hepatitis C but not hepatitis B in an urban population. *Am J Gastroenterol* 1996; **91**: 498-505
11 **Brillanti S,** Masci C, Siringo S, Di Febo G, Miglioli M, Barbara L. Serological and histological aspects of hepatitis C virus in-

fection in alcoholic patients. *J Hepatol* 1991; **13**: 347-350
12 **Zarski JP,** Thelu MA, Moulin C, Rachail M, Seigneurin JM. Interest of the detection of hepatitis C virus RNA in patients with alcoholic liver disease. *J Hepatol* 1993; **17**: 10-14
13 **Ohto H,** Terazewa S, Sasaki N. Transmission of hepatitis C virus from mothers to infants. *N Engl J Med* 1994; **330**: 744-750
14 **McHutchison JG,** Gordon SC, Schiff ER, Shiffman ML, Lee WM, Rustgi VK, Goodman ZD. Interferon alfa-2b alone or in combination with ribavirin as initial treatment for chronic hepatitis C. *N Engl J Med* 1998; **339**: 1485-1492
15 **Lau JYN**, Mizokami M, Kolberg JA, Davis GL, Prescott LE, Ohno T, Perrillo RP. Application of six hepatitis C virus genotyping systems to sera from chronic hepatitis C patients in the United States. *J Infect Dis* 1995; **171**: 281-289
16 **Kao JH,** Lai MY, Chen PJ, Hwang LH, Chen W, Chen DS. Clinical significance of serum hepatitis C virus titers in patients with chronic type C hepatitis. *Am J Gastroenterol* 1996; **91**: 506-510
17 **Nousbaum JB,** Pol S, Nalpas B, Landais P, Berthelot P, Brechot C. Collaborative Study Group. Hepatitis C virus type 1b (II) infection in France and Italy. *Ann Intern Med* 1995; **122**: 161-168
18 **Lau JYN,** Davis GL, Prescott LE, Maertens G, Lindsay KL, Qian K, Mizokami M. Distribution of hepatitis C virus genotypes determined by line probe assay in patients with chronic hepatitis C seen at a tertiary referral center in the United States. *Ann Intern Med* 1996; **124**: 868-876
19 **Zeuzem S,** Franke A, Lee JH, Herrmann G, Ruster B, Roth WK. Phylogenetic analysis of hepatitis C virus isolates and their correlation to viremia, liver function tests, and histology. *Hepatology* 1996; **24**: 1003-1009
20 **Lau JY,** Davis GL, Kniffen J, Qian KP, Urdea MS, Chan CS, Mizokami M. Significance of serum hepatitis C virus RNA levels in chronic hepatitis C. *Lancet* 1993; **341**: 1501-1504
21 **McCormick SE,** Goodman ZD, Maydonovitch CL, Sjogren MH. Evaluation of liver histology, ALT elevation, and HCV RNA titer in patients with chronic hepatitis C. *Am J Gastroenterol* 1996; **91**: 1516-1522
22 **Kato NK,** Hosoda K, Ito Y, Ohto M, Omata M. Quantification of hepatitis C virus by competitive reverse transcription - polymerase chain reaction: increase of the virus in advanced liver disease. *Hepatology* 1993; **18**: 16-20
23 **Fanning L,** Kenny E, Sheehan M, Cannon B, Whelton M, O'Connell J, Collins JK, Shanahan F. Viral load and clinicopathological features of chronic hepatitis C (1b) in a homogenous population. *Hepatology* 1999; **29**: 904-907
24 **Rehermann B.** Interaction between the hepatitis C virus and the immune system. *Semin Liv Dis* 2000; **20**: 127-141
25 **Ballardini G,** Groff P, Pontisso P. Hepatitis C virus (HCV) genotype, tissue HCV antigens, hepatocellular expression of HLA-A, B, C, and intracellular adhesion-1 molecules. *J Clin Invest* 1995; **95**: 2967-2975
26 **Nelson DR,** Marousis CG, Davis GL. The role of hepatitis C virus-specific cytotoxic T lymphocytes in chronic hepatitis C. *J Immunol* 1997; **158**: 1473

Edited by Zhu LH **Proofread by** Xu FM

PO Box 2345, Beijing 100023, China
Fax: +86-10-85381893
E-mail: wjg@wjgnet.com www.wjgnet.com

World J Gastroenterol 2004;10(16):2412-2414
World Journal of Gastroenterology
 ISSN 1007-9327

• BRIEF REPORTS •

Hypertrophied anal papillae and fibrous anal polyps, should they be removed during anal fissure surgery?

Pravin J. Gupta

Pravin J. Gupta, Proctologist, Gupta Nursing Home, D/9, Laxminagar, NAGPUR- 440022, India
Correspondence to: Pravin J. Gupta, M.S., Proctologist, Gupta Nursing Home, D/9, Laxminagar, NAGPUR- 440022, India. drpjg@nagpur.dot.net.in
Received: 2003-07-12 **Accepted:** 2004-03-04

Abstract

AIM: Hypertrophied anal papillae and fibrous anal polyps are not given due importance in the proctology practice. They are mostly ignored being considered as normal structures. The present study was aimed to demonstrate that hypertrophied anal papillae and fibrous anal polyps could cause symptoms to the patients and that they should be removed in treatment of patients with chronic fissure in anus.

METHODS: Two groups of patients were studied. A hundred patients were studied in group A in which the associated fibrous polyp or papillae were removed by radio frequency surgical device after a lateral subcutaneous sphincterotomy for relieving the sphincter spasm. Another group of a hundred patients who also had papillae or fibrous polyps, were treated by lateral sphincterotomy alone. They were followed up for one year.

RESULTS: Eighty-nine percent patients from group A expressed their satisfaction with the treatment in comparison to only 64% from group B who underwent sphincterotomy alone with the papillae or anal polyps left untreated. Group A patients showed a marked reduction with regard to pain and irritation during defecation ($P = 0.0011$), pricking or foreign body sensation in the anus ($P = 0.0006$) and pruritus or wetness around the anal verge ($P = 0.0008$).

CONCLUSION: Hypertrophied anal papillae and fibrous anal polyps should be removed during treatment of chronic anal fissure. This would add to effectiveness and completeness of the procedure.

Gupta PJ. Hypertrophied anal papillae and fibrous anal polyps, should they be removed during anal fissure surgery? *World J Gastroenterol* 2004; 10(16): 2412-2414
http://www.wjgnet.com/1007-9327/10/2412.asp

INTRODUCTION

Hypertrophied anal papillae are essentially skin tags that project up from the dentate line, or the junction between the skin and the epithelial lining of the anus[1]. They are often found as part of the classic triad of a chronic fissure, namely the fissure itself, hypertrophied papilla above and a skin tag below[2,3]. They are also found in isolation, maybe firm and palpable on a digital examination of the anus. In this situation, they must be differentiated from polyps, hemorrhoids, or other growths. Endoscopically they could be differentiated from an adenomatous polyp by their white appearance and their origin from the lower (squamous) aspect of the dentate line in the anal canal. They are usually a symptomatic but occasionally grow large enough to be felt by the patient or are likely to prolapse. Hypertrophied anal papilla should be included in the differential diagnosis of a smooth mass located near the anal verge, especially in a patient with a history of chronic anal irritation or infection[2].

With passage of time, papillae continue to grow in size. A papilla is liable to acquire considerable fibrous thickening over a period of time when it gets a rounded expanded tip, which is known as a fibrous polyp. This is due to piling up and consolidation of chronic inflammatory tissues at the proximal part of the fissure at the dentate line. As many as 16% of the patients having chronic fissure in anus recorded the presence of papillae that turned into fibrous polyps[4]. These papillae are presumed to be caused by edema and low-grade infection.

A fibrosed-hypertrophied papilla is also frequently found at the upper part of a chronic anal fissure or guarding the internal opening of fistula in anus. In the later case however, the symptoms may completely dominate and distort the clinical findings. Dilated veins, white areas, and a large hypertrophied anal papilla are often found in prolapsing types of hemorrhoids[5].

In the past, these structures were not given any importance and were left untreated. Those patients, in whom, the fissure in anus was treated but the concomitant papillae or polyps were left untouched, continued to complain of pruritus, wetness, or an intermittent pricking sensation in the anus. Those with fibrous polyps felt incompletely treated due to a feeling of *something* projecting from the anus. Even a case of giant hypertrophied anal papilla complicated with a massive anal bleeding and prolapse was reported[6].

This study was aimed to assess the impact and utility of attending to these two conditions concurrently while dealing with cases of fissure in ano.

MATERIALS AND METHODS

This study was carried out at Gupta Nursing Home, Nagpur, India, between July 2000 and December 2001.

Two hundred patients suffering from chronic fissure in ano associated with hypertrophied anal papillae or fibrous polyps were selected for the study. All these patients had primarily reported symptoms and complaints of chronic anal fissure. The papillae and polyps were diagnosed preoperatively by using a pediatric anoscope to avoid discomfort during examination. The number of papillae ranged from two to four. However, the fibrous polyp was found to be single in all those patients who were having this pathology.

Only those patients who came for a follow-up after 12 mo of the procedure were included in the study.

Exclusion criteria

Patients having fissure in ano with sentinel tags or hemorrhoids and those who had not signed the informed consent were not included in the study.

The patients were divided into two groups viz: group A and B.

Group A consisted of one hundred patients in whom the anal papillae, anal polyp, or both were treated by radio frequency

procedure along with the fissure. Another hundred patients (group B) were treated only for the fissure and the papillae or polyps were left untreated. The randomization was done by a sealed envelope, which was opened by the operation room nurse upon patient's arrival for the procedure.

An informed consent was obtained from all patients under study. The study was approved by the local ethical committee and was done in accordance with the Declaration of Helsinki. No special pre-operative preparation was carried out. All the patients received a dose of laxative on the prior night. The patient description is given in Table 1.

Table 1 Patient demographic data

Patient characteristics	Group A	Group B
No. of patients	100	100
Mean age yr	37	39
Male: Female	64:36	66:34
Hypertrophied papillae (No. of patients)	100	100
Fibrous anal polyp (No. of patients)	11	8

Statistical analysis

Unpaired Student's *t* test was used to measure postoperative parameters. The level of statistical significance between groups was set at 5 per cent.

Procedures

The procedure was carried out under a short general anesthesia with a muscle relaxant. A lateral subcutaneous sphincterotomy was performed to relieve the sphincter spasm. This was followed by insertion of the anoscope with a proximal illumination. The anal canal was cleaned off the collection. The papillae or polyps were located and were dealt with through a radio frequency surgical technique.

Radio frequency surgery aims at cutting or coagulation of tissues by using a high frequency alternate current. The radiofrequency device performs a simultaneous function of cutting and coagulating of the tissues. The effect of cutting, known as high frequency section, is executed without pressuring or crushing the tissue cells. This is due to the result of heat produced by the tissues' resistance to the passage of the high frequency wave set to motion by the equipment. The heat makes the intracellular water boil, thereby increasing the inner pressure of the cell to the point of breaking it from inside to outside (explosion). This phenomenon is called cellular volatilization[7].

In this procedure, we used the radio frequency generator known as Ellman Dual Frequency 4MHz by Ellman International, Hewlett, N.Y. This instrument produces an electromagnetic wave of a very high frequency that reaches 4 megahertz. The unit is supplied with a handle to which different inter-changeable electrodes could be attached to suit the exact requirement[8]. In our study, we used the ball electrode for coagulation and a round loop electrode for shaving off the desired tissues.

The papillae were directly coagulated with a ball electrode with the radio frequency unit kept on coagulation mode, which resulted in shrinkage and disappearance of the papillae in no time.

For the fibrous anal polyp, we initially coagulated its base circumferentially by a ball electrode and then shaved off the mass by using the round loop electrode. The minor bleeding encountered in some cases was coagulated by touching the bleeding points with the ball electrode. The whole procedure took around 7-10 min to complete.

The patients were prescribed analgesics for one wk and a stool softener for a period of 1 mo.

The first follow up was made after 30 d. The fissures were healed and there was no sphincter spasm in any of the patients from either group. During examination of patients from group A, anoscopies showed total absence of the papillae. Patients who were treated for fibrous polyps did have some amount of edema and mild elevation at the site of destruction. However, patients had fewer complaints of pruritus, pricking, heaviness and a sense of incomplete evacuation as compared to patients from group B.

Follow up on completion of 12 mo of treatment

An independent observer blinded to the procedures made the observations during the follow up. He noted down all the symptoms in a prescribed format specially prepared for the study. The findings are given in Table 2.

RESULTS

The patients from group A who were treated by sphincterotomy followed by radio frequency surgical procedures for removal of hypertrophied anal papillae or fibrous polyps felt far more comfortable as compared to patients in group B who were subjected only to sphincterotomy for treatment of fissure and in whom, as per the prevailing practice, the papillae or anal polyps were left untouched. The other visible advantages experienced by the patients in group A were: a relief of pain and irritation during defecation, absence of pricking or foreign body sensation in the anus and disappearance of pruritus or wetness around the anal verge.

Table 2 One-yr follow-up findings of patients with removal or no removal of hypertrophied anal papillae and fibrous anal polyps (Student's unpaired *t* test)

Findings based on complaints of	Group A	Group B	*P*
Pruritus ani	7 (7%)	32 (32%)	0.0008
Anal pain and irritation	5 (5%)	26 (26%)	0.0011
Discharge per anus	2 (2%)	34 (36%)	0.0005
Sense of incomplete evacuation	5 (5%)	22 (22%)	0.0008
Crawling sensation in anus	8 (8%)	48 (48%)	0.0002
Pricking or foreign body sensation in anus	3 (3%)	32 (32%)	0.0006
Prolapsed per rectum	Nil	4 (4%)	N
Sepsis in the wound	1 (1%)	8 (8%)	0.0044
Recurrence of papillae or polyps	Nil	Not applicable	N
Recurrence of fissure	Nil	Nil	N
Overall satisfaction from the procedures	89%	64%	0.0004

N, not studied.

DISCUSSION

Anal papillae were found in almost 50-60% patients examined by us in regular practice. Usually, they were small, caused no symptoms, and could be regarded as normal structures[9]. However, if it is a case of hypertrophy and the papillae start projecting in the anal canal, it not only requires attention but calls for a suitable treatment also. In such cases, there are chances of increase in the mucus leak resulting in increased anal moisture. These are liable to get traumatized and inflamed during the passage of stool. In addition, on being converted into a fibrous polyp, they tend to project at the anal orifice during defecation, often requiring to be digitally replaced. These polyps are considered as one of the differential diagnoses of rectal prolapse[10]. The patients also reported symptoms like pruritus[11], a foreign body sensation, pricking, a nagging sense of incomplete evacuation and heaviness in the anal region.

As a routine practice, these pathologies were not given any importance[12]. There is very brief reference to this entity in the standard textbooks and other references. Secondary goals of fissure surgery sometimes required the removal of hypertrophied papilla and skin tag as well as the removal of inflammatory and fibrotic tissues surrounding the fissure[13]. Customarily, in the symptomatic papillae or polyps, their removal by crushing of the bases, excision after ligation or electrocautrization has been suggested. All these procedures are time consuming and are associated with complications at times. The use of radio frequency devices to deal with these pathologies has been found to be a quick, easy and significant complication free procedure[14]. The device can ablate the papillae instantly, while the fibrous polyps can be excised after coagulation of the bases and thereafter the pedicles. In the present study, we have specifically excluded those patients of chronic fissure in ano who had sentinel tags or piles, as they were known to cause few of the similar symptoms that were associated with hypertrophied papillae or fibrous anal polyps.

Hypertrophied anal papillae and fibrous anal polyps are important anal pathologies associated with chronic anal fissure and are responsible for symptoms like pruritus, a pricking sensation, heaviness, etc. Their removal should be made an essential part of treatment of chronic fissures in ano. Persistence of these structures leaves behind a sense of incomplete treatment and thereby reducing the overall satisfaction on the part of the patient. radio frequency procedures have been found useful in successfully eradicating these concomitant pathologies of chronic fissure in ano. This procedure should be given a fair chance to prove its utility and long-term efficacy.

REFERENCES

1 **Lenhard B.** Guideline on the disease picture of hypertrophic anal papilla. *Hautarzt* 2002; **53**: 104-105
2 **Heiken JP,** Zuckerman GR, Balfe DM. The hypertrophied anal papilla: recognition on air-contrast barium enema examinations. *Radiology* 1984; **151**: 315-318
3 **Schwartz SI.** In Principles of Surgery, McGraw-Hill international book company, *Singapore, 4th Edition* 1984: 1225
4 **Thomson JPS,** Nicholls RJ, Williams CB. In colorectal diseases, William Heinemann Medical Book Limited, *London, Page 312* 1981
5 **Sadahiro S,** Mukai M, Tokunaga N, Tajima T, Makuuchi H. A new method of evaluating hemorrhoids with the retroflexed fiberoptic colonoscope. *Gastrointest Endosc* 1998; **48**: 272-275
6 **Kusunoki M,** Horai T, Sakanoue Y, Yanagi H, Yamamura T, Utsunomiya J. Giant hypertrophied anal papilla. *Case Report Eur J Surg* 1991; **157**: 491-492
7 **Pfenninger JL.** Modern treatments for Internal Hemorrhoids. *BMJ* 1997; **314**: 1211-1212
8 **Goldberg SN,** Gazelle GS, Dawson SL. Tissue ablation with radiofrequency: effect of probe size, gauge, duration and temperature on lesion volume. *Acad Radiol* 1995; **2**: 399-404
9 **Golighar J,** Duthie H, Nixon H. Surgery of the anus rectum and colon. *Fifth Edition Bailliere Tindal, London* 1992: 151
10 **Euro K W,** Seow-Choen F. Functional problems in adult rectal prolapse and controversies in surgical treatment. *Br J Surg* 1997; **84**: 904-911
11 **Sabiston DC.** In Textbook of Surgery, WB Saunders Company, *London, 12th Edition* 1981: 1130
12 Jensen SL. A randomized trial of simple excision of non-specific hypertrophied anal papillae versus expectant management in patients with chronic pruritus ani. *Ann R Coll Surg Engl* 1988; **70**: 348-349
13 Weaver RM, Ambrose NS, Alexander-Williams J, Keighley MR. Manual dilatation of the anus vs. lateral subcutaneous sphincterotomy in the treatment of chronic fissure-in-ano: results of a prospective, randomized, clinical trial. *Dis Colon Rectum* 1987; **30**: 420-423
14 **Brown JS.** Radio frequency surgery- Minor surgery a text and atlas. *Chap Hall Med* 1997; **42**: 300-326

Edited by Zhu LH **Proofread by** Xu FM

PO Box 2345, Beijing 100023, China
Fax: +86-10-85381893
E-mail: wjg@wjgnet.com www.wjgnet.com

World J Gastroenterol 2004;10(16):2415-2416
World Journal of Gastroenterology
 ISSN 1007-9327

• BRIEF REPORTS •

Lack of evidence for leukocyte maternal microchimerism in primary biliary cirrhosis

Kenichi Nomura, Yoshio Sumida, Takaharu Yoh, Atsuhiro Morita, Yosuke Matsumoto, Sawako Taji, Naohisa Yoshida, Masahito Minami, Yoshito Itoh, Shigeo Horiike, Keisho Kataoka, Masafumi Taniwaki, Takeshi Okanoue

Kenichi Nomura, Yosuke Matsumoto, Shigeo Horiike, Keisho Kataoka, Masafumi Taniwaki, Molecular Hematology and Oncology, Kyoto Prefectural University of Medicine Graduate School of Medical Science, Kyoto 602-0841, Japan
Yoshio Sumida, Department of Internal Medicine, National Nara Hospital, Nara 630-8305, Japan
Takaharu Yoh, Department of Internal Medicine, Aiseikai Yamashina Hospital, Kyoto 607-8086, Japan
Atsuhiro Morita, Ayabe city Hospital, Kyoto 623-0011, Japan
Naohisa Yoshida, Sawako Taji, Masahito Minami, Yoshito Itoh, Takeshi Okanoue, Molecular Gastroenterology and Hepatology, Kyoto Prefectural University of Medicine Graduate School of Medical Science, Kyoto 602-0841, Japan
Masafumi Taniwaki, Clinical Molecular Genetics and Laboratory Medicine, Kyoto Prefectural University of Medicine Graduate School of Medical Science, Kyoto 602-0841, Japan
Supported by the grants of the Ministry of Education, Science, Sports, and Culture of Japan, No.15790497
Correspondence to: Dr. Kenichi Nomura, Molecular Hematology and Oncology, Kyoto Prefectural University of Medicine Graduate School of Medical Science, Kawaramachi-Hirokoji, Kamigyo-ku, Kyoto 602-0841, Japan. nomuken@sun.kpu-m.ac.jp
Telephone: +81-75-251-5521 **Fax:** +81-75-251-0710
Received: 2004-03-11 **Accepted:** 2004-04-09

Abstract

AIM: It is reasonable to assume that microchimerism could also be involved in the induction of primary biliary cirrhosis (PBC). However, previous reports investigated only fetus-microchimerism in women patients. Maternal microchimerism has not been investigated until now. The current study aimed to clear either maternal microchimerism was involved in the pathogenesis of PBC or not.

METHODS: We used fluorescence *in situ* hybridization on paraffin-embedded tissue (We called "Tissue-FISH".) to determine whether maternal cells infiltrated in male patients who were diagnosed as having PBC. Tissue-FISH was performed by using both X and Y specific probes on the biopsy liver sample of 3 male PBC patients.

RESULTS: Infiltrating lymphocytes demonstrated both X and Y signals in all 3 male patients.

CONCLUSION: Maternal microchimerism dose not play a significant role in PBC. PBC may not relate to fetus and maternal microchimerism.

Nomura K, Sumida Y, Yoh T, Morita A, Matsumoto Y, Taji S, Yoshida N, Minami M, Itoh Y, Horiike S, Kataoka K, Taniwaki M, Okanoue T. Lack of evidence for leukocyte maternal microchimerism in primary biliary cirrhosis. *World J Gastroenterol* 2004; 10(16): 2415-2416
http://www.wjgnet.com/1007-9327/10/2415.asp

INTRODUCTION

Molecular biological techniques have shown that fetal cells can be detected in maternal peripheral blood in most pregnancies[1-3]. On this observation, the radical hypothesis of autoimmune disease, proposed in 1996, may be caused by fetal cells that are retained after pregnancies[4]. In systemic sclerosis, it was reported that fetal antimaternal graft-versus-host reactions might be involved in the pathogenesis of systemic sclerosis in some women[5,6]. Thus, the hypothesis that microchimerism might cause the primary biliary cirrhosis (PBC) is very fascinating[7], because it may explain clinical similarities between PBC and chronic graft-versus-host disease (GVHD) in liver after bone marrow transplantation. Some previous reports hypothesized that fetal microchimerism may also play a role in the pathogenesis of PBC[8-11]. However, they concluded that fetal microchimerism was not important in the development of PBC.

Although there is a possibility that PBC may be developed by maternal microchimerism, not fetal microchimerism in female patients, maternal microchimerism has not been considered until now. Thus, we produced one hypothesis that maternal microchimerism might cause PBC.

To test the hypothesis, we investigated 3 male PBC patients by fluorescence *in situ* hybridization (FISH) on paraffin-embedded tissues.

MATERIALS AND METHODS

Patients

Three male patients with PBC were studied after giving informed consent. They were diagnosed at Kyoto Prefectural University of Medicine by liver biopsy and the positivity of serum antimitochondrial antibody (AMA). All patients were compatible with the feature of PBC. None of these patients had scleroderma. They had no experience of blood transfusion.

Methods

We reported tissue-FISH method previously[12-14]. Sections from paraffin-embedded tissues were placed on silane-coated glass slides. The slides were deparaffinized immediately in 2 rinses of 1 000 g/L xylene for 10 min each. Each slide was rehydrated in an ethanol series for 5 min. The slides were then treated with 0.2 mol/L HCl for 20 min, followed by 2×SSC (0.3 mol/L sodium chloride and 0.03 mol/L sodium citrate) for 20 min at 80 °C, treated with 0.05 mg/mL proteinase K in TEN (0.05 mol/L Tris-HCl, pH 7.8, 0.01 mol/L EDTA, and 0.01 mol/L sodium chloride) for 10 min at 37 °C, and placed in 40 g/L formaldehyde in PBS for 10 min. Both FISH probes and target DNA were denatured simultaneously for 10 min at 90 °C, and the slides were incubated overnight at 42 °C, placed in 2×SSC for 10 min at 42 °C, washed twice in 2×SSC/500 g/L formaldehyde formamide for 5 min each at 42 °C, washed 2×SSC for 5 min at 42 °C, and counterstained in 2×SSC/0.03 μg/mL DAPI.

RESULTS

It was easy to recognize the architecture of liver tissues by

fluorescence microscope BX40-RF (Olympus, Tokyo, Japan). The lymphocytes aggregated at the portal zone (Figure 1). We assessed only non-overlapping nuclei having XY or XX signals. Almost infiltrating lymphocytes at septa revealed the XY chromosome pattern (Figure 2). The frequency of nuclei having XY in 3 patients is 96%, 98%, and 97%, respectively. (P<0.01).

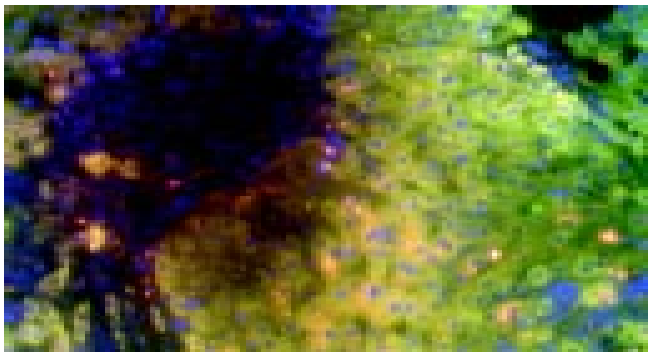

Figure 1 Aggregated lymphocytes at the portal zone.

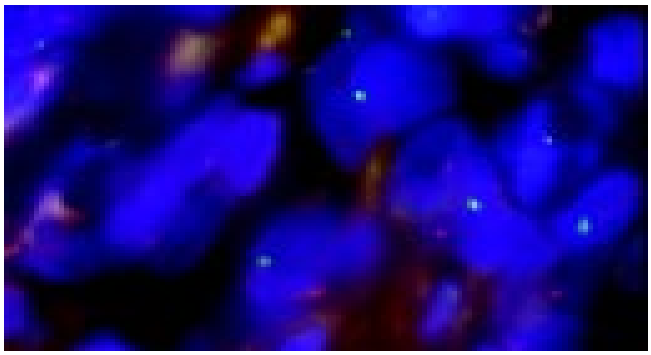

Figure 2 Infiltrating lymphocytes revealed XY chromosome pattern (X; Green, Y; Orange).

DISCUSSION

The hypothesis that fetal microchimerism causing PBC is fascinating. However, this hypothesis does not explain why some cases with PBC were fetal microchimerism negative and why even males and nulliparous women were suffering from PBC. On the other hand, the hypothesis that maternal microchimerism causes PBC is more fascinating, because it resolves the above questions. Every one has the risk of maternal microchimerism, because it has been already established that maternal cells persist for a long-term in immunocompetent offsprings[15]. However, this hypothesis could not be resolved by polymerase chain reaction (PCR), because PCR can only detect the Y-chromosome specific DNA.

To clear whether infiltrating lymphocytes derived from either maternal or fetal cells in male PBC patients, we performed tissue-FISH. Tissue-FISH is able to distinguish infiltrating lymphocytes from hepatocytes, because this method preserves the architecture of liver tissues and the shapes of cells. Tissue-FISH revealed that almost infiltrating lymphocytes were male cells in the liver sample of male patients. These results showed that maternal microchimerism did not play an important role in introducing and maintaining primary biliary cirrhosis.

In conclusion, we were unable to provide the evidence of maternal microchimerism in PBC patients. Although PBC shows the similar histological features with GVHD, PBC may be different from GVHD in etiology.

REFERENCES

1 **Lo YM,** Patel P, Sampietro M, Gillmer MD, Fleming KA, Wainscoat JS. Detection of single-copy fetal DNA sequence from maternal blood. *Lancet* 1990; **335**: 1463-1464
2 **Thomas MR**, Williamson R, Craft I, Yazdani N, Rodeck CH. Y chromosome sequence DNA amplified from peripheral blood of women in early pregnancy. *Lancet* 1994; **343**: 413-414
3 **Bianchi DW**. Prenatal diagnosis by analysis of fetal cells in maternal blood. *J Pediatr* 1995; **127**: 847-856
4 **Nelson JL**. Maternal-fetal immunology and autoimmune disease: is some autoimmune disease auto-alloimmune or allo-autoimmune? *Arthritis Rheum* 1996; **39**: 191-194
5 **Artlett CM,** Smith JB, Jimenez SA. Identification of fetal DNA and cells in skin lesions from women with systemic sclerosis. *N Engl J Med* 1998; **338**: 1186-1191
6 **Nelson JL,** Furst DE, Maloney S, Gooley T, Evans PC, Smith A, Bean MA, Ober C, Bianchi DW. Microchimerism and HLA-compatible relationships of pregnancy in scleroderma. *Lancet* 1998; **351**: 559-562
7 **McDonnell WM**. Is primary biliary cirrhosis a complication of pregnancy? *Hepatology* 1998; **28**: 593-594
8 **Tanaka A**, Lindor K, Gish R, Batts K, Shiratori Y, Omata M, Nelson JL, Ansari A, Coppel R, Newsome M, Gershwin ME. Fetal microchimerism alone does not contribute to the induction of primary biliary cirrhosis. *Hepatology* 1999; **30**: 833-838
9 **Rubbia-Brandt L**, Philippeaux MM, Chavez S, Mentha G, Borisch B, Hadengue A. FISH for Y chromosome in women with primary biliary cirrhosis: lack of evidence for leukocyte microchimerism. *Hepatology* 1999; **30**: 821-822
10 **Invernizzi P**, De Andreis C, Sirchia SM, Battezzati PM, Zuin M, Rossella F, Perego F, Bignotto M, Simoni G, Podda M. Blood fetal microchimerism in primary biliary cirrhosis. *Clin Exp Immunol* 2000; **122**: 418-422
11 **Corpechot C**, Barbu V, Chazouilleres O, Poupon R. Fetal microchi merism in primary biliary cirrhosis. *J Hepatol* 2000; **33**: 696-700
12 **Nomura K**, Sekoguchi S, Ueda K, Nakao M, Akano Y, Fujita Y, Yamashita Y, Horiike S, Nishida K, Nakamura S, Taniwaki M. Differentiation of follicular from mucosa-associated lymphoid tissue lymphoma by detection of t(14;18) on single-cell preparations and paraffin-embedded sections. *Genes Chromosomes Cancer* 2002; **33**: 213-216
13 **Nomura K,** Yoshino T, Nakamura S, Akano Y, Tagawa H, Nishida K, Seto M, Nakamura S, Ueda R, Yamagishi H, Taniwaki M. Detection of t(11;18) (q21;q21) in marginal zone lymphoma of mucosa-associated lymphocytic tissue type on paraffin-embedded tissue sections by using fluorescence *in situ* hybridization. *Cancer Genet Cytogenet* 2003; **140**: 49-54
14 **Matsumoto Y**, Nomura K, Matsumoto S, Ueda K, Nakao M, Nishida K, Sakabe H, Yokota S, Horiike S, Nakamine H, Nakamura S, Taniwaki M. Detection of t(14;18) in follicular lymphoma by dual-color fluorescence *in situ* hybridization on paraffin-embedded tissue sections. *Cancer Genet Cytogenet* 2004; **150**: 22-26
15 **Maloney S**, Smith A, Furst DE, Myerson D, Rupert K, Evans PC, Nelson JL. Microchimerism of maternal origin persists into adult life. *J Clin Invest* 1999; **104**: 41-47

Edited by Wang XL **Proofread by** Chen WW and Xu FM

PO Box 2345, Beijing 100023, China
Fax: +86-10-85381893
E-mail: wjg@wjgnet.com www.wjgnet.com

World J Gastroenterol 2004;10(16):2417-2418
World Journal of Gastroenterology
 ISSN 1007-9327

• BRIEF REPORTS •

Gastrointestinal stromal tumor: Computed tomographic features

Chi-Ming Lee, Hsin-Chi Chen, Ting-Kai Leung, Ya-Yen Chen

Chi-Ming Lee, Hsin-Chi Chen, Ting-Kai Leung, Ya-Yen Chen, Department of Diagnostic Radiology, Taipei Medical University Hospital, Taipei, Taiwan, China
Correspondence to: Chi-Ming Lee, M.D., 252, WuHsing Street, 110, Taipei, Taiwan, China. yayen0220@yahoo.com.tw
Telephone: +886-2-27372181 Ext. 1131 **Fax:** +886-2-23780943
Received: 2004-01-10 **Accepted:** 2004-02-24

Abstract

AIM: Gastrointestinal stromal tumor (GIST) is a rare type of cancer. Computed tomography (CT) is an imaging modality of choice for diagnosing GIST. The aim of this retrospective study was to review the CT imaging features of 17 GIST patients.

METHODS: From 1995 to 2003, there were 47 patients with pathologically proven GISTs at our hospital. Of these, 17 patients underwent preoperative CT. We collected and analyzed these CT images. The CT imaging features included tumor diameter, number and location, tumor margin, location of metastasis, hounsfield units of tumor and effect of contrasts. In addition, we also recorded the surgical findings, including complications, tumor size and location for comparative analysis.

RESULTS: The results showed that 12 (70%) tumors were located in the stomach and five (30%) were located in the jejunum mesentery. GISTs were extraluminal in 12 (70%) patients. The tumor margins of 13 (76%) tumors were well defined and irregular in four (24%). The effect of contrast enhancement on GIST CT imaging was homogenous enhancement in 13 (76%) and heterogeneous enhancement in four (24%). The hounsfield units (HU) were 30.41±5.01 for precontrast images and postcontrast hounsfield units were 51.80±9.24.

CONCLUSION: The stomach was the commonest site of GIST occurrence among our patients. The CT features of GIST were well-defined tumor margins, homogenous enhancement on postcontrast CT images.

Lee CM, Chen HC, Leung TK, Chen YY. Gastrointestinal stromal tumor: Computed tomographic features. *World J Gastroenterol* 2004; 10(16): 2417-2418
http://www.wjgnet.com/1007-9327/10/2417.asp

INTRODUCTION

The term gastrointestinal stromal tumor (GIST) has traditionally been used as a descriptive term for soft tissue tumors of the gastrointestinal tract. Although their exact incidence is still somewhat unclear, it is now estimated that between 5 000 and 10 000 people each year develop GISTs in the world; men and women are equally affected[1]. GISTs were previously thought to be smooth muscle neoplasms, and most were classified as leiomyosarcoma. With the advent of immunohistochemistry and electron microscopy, it has become apparent that GIST may have myogenic features (smooth muscle GIST), neural attributes (gastrointestinal autonomic nerve tumor), characteristics of both muscle and nerve (mixed GIST) or may lack differentiation (GIST not otherwise specified)[2]. GISTs are often discovered incidentally at surgery and should be completely excised. The increasing use of computed tomography (CT) and endoscopy of the upper gastrointestinal tract is a non-or minimally invasive means for the detection of asymptomatic GISTs[3].

In this retrospective study, we analyzed our experience with 17 patients with GISTs who were presurgically investigated by using CT and described the anatomic distribution and imaging features of GIST.

MATERIALS AND METHODS

Patients' data

From 1995 to 2003, there were 47 patients with pathologically proven GISTs at Taipei Medical University Hospital (TMUH) and Wan Fang Hospital (WFH). Of these, 17 (8 males, 9 females, with ages ranging from 33 to 91 years, mean age: 64 years) underwent preoperative CT. We collected and analyzed these CT images.

The abdominopelvic CT scans (HiSpeed CT/I; GE Medical Systems, Milwaukee, WI, USA) were typically obtained after oral administration of 1 000 mL 40 g/L iothalamate meglumine (Mallinckrodt, USA) and intravenous administration of 100 mL (350 mg/mL) iohexol (Nycoveien, Norway) at a flow rate of 2 mL/s, with a section thickness of 10 mm and a pitch of 1.5. The CT imaging features included tumor diameter, number and location, tumor margin (well defined, irregular or clearly invasive), location of metastasis, hounsfield units of tumor and effect of contrast. These characteristics were reviewed blindly by three radiology diplomates. In addition, we also recorded the surgical findings, including complications, tumor size and location for comparison.

RESULTS

The CT imaging findings showed that 14 (82%) patients had one tumor and 3 (18%) patients had two tumors. GIST size ranged from 2 to 19 cm (5.4±1.8 cm). Tumors were located in the stomach in 12 (70%) patients and 5 (30%) patients had tumor located in the jejunal mesentery. GISTs were extraluminal in 12 (70%) patients and intraluminal in 5 (30%). GISTs caused intraluminal bowel obstruction in two patients.

The mean precontrast hounsfield units were 30.41±5.01 and the mean postcontrast hounsfield units were 51.80±9.24. The effect of contrast enhancement on GIST CT imaging was slight enhancement (Figure 1). Thirteen (76%) showed homogenous enhancement and 4 (24%) showed heterogeneous enhancement.

Tumors were well defined in 13 (76%) patients and irregular in 4 (24%) patients. There was no clearly invasive or vascular encasement of tumors among our patients. Three (18%) patients had metastasis, two to the liver and one to the lung. Twelve patients underwent follow-up CT (range of follow-up period from date of diagnosis, 2-40 mo, mean, 22 mo). No patients relapsed.

Operative findings showed that 14 (82%) patients had one tumor and 3 (18%) patients had two tumors. The smallest GIST was 2 cm×2 cm×1.8 cm and the largest was 19 cm×16 cm×8.5 cm in size. The commonest complications among our patients were gastrointestinal tract chronic inflammation, diarrhea and wound

infection. In addition, 17 patients all underwent lymphadenectomies but no metastasis to the lymph nodes was found.

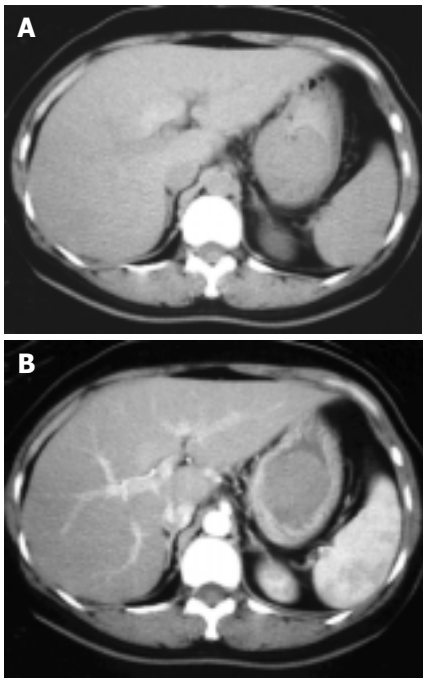

Figure 1 Precontrast and postcontrast CT scans of tumor. A: A precontrast CT scan shows a well-defined intragastric tumor with slightly lower density than the liver. The hounsfield units are 38.77. B: A postcontrast CT scan shows homogenous enhancement of the tumor, with a hounsfield unit of 57.58.

DISCUSSION

The distribution of 725 malignant smooth muscle tumors of the gastrointestinal tract was 47.3% in the stomach, 35.4% in the small intestine, 4.6% in the colon and 7.4% in the rectum, according to Skandalak and Gray[4]. In the report by Akwari *et al*.[5], 68.3% of GISTs were in the stomach, 25.4% were in the small intestine, 2.6% were in the colon and 3.7% were in the rectum. According to a previous study[6], GIST can also occur in the omental and mesenteric tissues, the duodenum and other sites of the gastrointestinal tract. In our study, 12 (70%) patients had tumors located in stomach and five (30%) patients had tumors located in the jejunal mesentery, a distribution more similar to that reported by Akwari *et al*.[5].

According to our results, the precontrast hounsfield units of the tumors were 30.41±5.01 and the postcontrast hounsfield units were 51.80±9.24. The postcontrast hounsfield units were 70% higher than the precontrast hounsfield units. Suster[7] reported hounsfield units of 33.2±1.25 on precontrast imaging and 55.32±5.22 on postcontrast imaging, with 68% enhancement. Ludwig[8] reported hounsfield units of 34.21±1.33 on precontrast imaging and 56.29±3.12 on postcontrast imaging, with 67% enhancement. We believe that precontrast hounsfield units of 30 to 35 and postcontrast hounsfield units of 50 to 60 are indicative of GISTs on CT.

We analyzed the correlation of contrast type and tumor size. Of the 17 patients, 4 (24%) had heterogeneous contrast enhancement and 13 (76%) had homogenous contrast enhancement. The mean tumor diameter of the heterogeneous tumors was 11.6±2.1 cm and that of the homogenous tumors was 3.8±1.3 cm. We found that large tumor sizes appeared to be related to heterogeneous enhancement. Our result is similar to that of Conlon *et al*.[9]. In addition, we found tumors in 13 (76%) of our patients were well-defined, and in Lee's study[10], more than two-thirds of patients also had well-defined GISTs. Thus, well-defined tumors appear to be a feature of GISTs on CT imaging.

Licht *et al*.[11] proposed that the relationship between multiple tumors and metastasis needed further investigation. In our study, we had three patients with multiple tumors and also had three patients with metastases. Only one patient with liver metastasis had multiple tumors; the other two patients with metastasis had only single tumor. Our data appear to indicate that there is no evident correlation between multiple tumors and metastasis. Additionally, 3 (18%) of our patients had metastasis compared to other studies[12,13] in which 20% to 35% of patients had metastasis, but this difference was not statistically significant. Fong *et al*.[13] reported that the metastasis percentage was related to the degree of lymph node involvement. Based on our surgical findings, all the patients who had metastasis had no lymph node involvement. Thus, our results differed from those reported by Fong.

In conclusion, the stomach was the commonest site of GIST tumor location among our patients, with a mean tumor diameter of 5.4±1.8 cm. The CT features of GISTs included well-defined tumor margins and predominantly homogenous contrast enhancement, with precontrast hounsfield units of 30 to 35 and postcontrast hounsfield units of 50 to 60. According to the percentage presented above, we also found a "4 seventy rule" in our GIST images review: 70% tumors were located in the stomach, 70% tumors were extraluminal, 76 % tumor margins were well defined, 76% GIST CT imagings were homogenous enhancement. In addition, metastasis was not related to the degree of lymph node involvement or tumor number in our study.

REFERENCES

1 **Miettien M**, Monihan JM, Sarlamo-Rikala M. Gastrointestinal stromal tumors/smooth muscle tumors (GISTs) primary in the omentum and mesentery: clinicopathologic and immunohistochemical study of 26 cases. *Am J Surg Pathol* 1999; **23**: 1109-1118
2 **Mazur M**, Clark HB. Gastric stromal tumors: Reappraisal of histogenesis. *Am J Surg Pathol* 1983; **7**: 507-519
3 **Pidhorecky I**, Cheney RT, Kraybill WG, Gibbs JF. Gastrointestinal stromal tumors: current diagnosis, biologic behavior, and management. *Ann Surg Oncol* 2000; **7**: 705-712
4 **Skandalakis JE**, Gray SW. Smooth muscle tumors of the alimentary tract. In: Ariel IM, ed. Progress in Clinical Cancer. *New York: Grune and Stratton* 1965: 692-708
5 **Akwari OE**, Dozois RR, Weiland LH, Beahrs OH. Leiomyosarcoma of the small and large bowel. *Cancer* 1978; **42**: 1375-1384
6 **Lewis JJ**, Leung D, Woodruff JM, Brennan MF. Retroperitoneal soft-tissue sarcoma: analysis of 500 patients treated and followed at a single institution. *Ann Surg* 1998; **228**: 355-365
7 **Suster S**. Gastrointestinal stromal tumors. *Semin Diag Pathol* 1996; **13**: 297-313
8 **Ludwig DJ**, Traverso LW. Gut stromal tumors and their clinical behavior. *Am J Surg* 1997; **173**: 390-394
9 **Conlon KC**, Casper ES, Brennan MF. Primary gastrointestinal sarcomas: analysis of prognostic variables. *Ann Surg Oncol* 1995; **2**: 26-31
10 **Lee YT**. Leiomyosarcoma of the gastrointestinal tract: general pattern of metastasis and recurrence. *Cancer Treat Rev* 1983; **10**: 91-101
11 **Licht JD**, Weissmann LB, Antman K. Gastrointestinal sarcomas. *Semin Oncol* 1988; **15**: 181-188
12 **Lindsay PC**, Ordonez N, Raaf JH. Gastric leiomyosarcoma: clinical and pathological review of fifty patients. *J Surg Oncol* 1981; **18**: 399-421
13 **Fong Y**, Coit DG, Woodruff JM, Brennan MF. Lymph node metastasis from soft tissue sarcoma in adults. Analysis of data from a prospective database of 1772 sarcoma patients. *Ann Surg* 1993; **217**: 72-77

Edited by Zhu LH **Proofread by** Xu FM

PO Box 2345, Beijing 100023, China
Fax: +86-10-85381893
E-mail: wjg@wjgnet.com www.wjgnet.com

World J Gastroenterol 2004;10(16):2419-2422
World Journal of Gastroenterology
 ISSN 1007-9327

• BRIEF REPORTS •

Effect of parenteral and enteral nutrition combined with octreotide on pancreatic exocrine secretion of patients with pancreatic fistula

Huan-Long Qin, Zhen-Dong Su, Yang Zou, You-Ben Fan

Huan-Long Qin, Zhen-Dong Su, Yang Zou, You-Ben Fan, Department of Surgery, Sixth People's Hospital, Shanghai Jiaotong University, Shanghai 200233, China
Supported by the Shanghai Science Foundation for Distinguished Young Scholars, No.99QB14010
Correspondence to: Huan-Long Qin, Department of Surgery, Sixth People's Hospital, Shanghai Jiaotong University, Shanghai 200233, China. jiaqc@online.sh.cn
Telephone: +86-21-64368920 **Fax:** +86-21-64368920
Received: 2003-12-10 **Accepted:** 2004-01-15

Abstract

AIM: To evaluate the effect of parenteral and enteral nutrition combined with octreotide on pancreatic exocrine secretion of the patients with pancreatic fistula.

METHODS: Pancreatic juice, drained directly from the pancreatic fistula, was collected, and the volume, protein, amylase, HCO_3^-, K^+, Na^+ and Cl^- were determined on d 1, 4 and 7 before and after 7-d treatment with octreotide, respectively.

RESULTS: No differences in exocrine pancreatic secretion were observed during the enteral and parenteral nutrition period ($t = 2.03$, $P>0.05$); there were significant decreases in pancreatic juice secretion volume, protein, amylase, HCO_3^-, K^+, Na^+ and Cl^- after parenteral and enteral nutrition combined with octreotide compared with octreotide pretreatment ($t = 4.14$, $P<0.05$).

CONCLUSION: There is no stimulatory effect on the pancreatic secretion by intrajejunal nutrition and parenteral nutrition. Octreotide is effective on the reduction of pancreatic fistula output.

Qin HL, Su ZD, Zou Y, Fan YB. Effect of parenteral and enteral nutrition combined with octreotide on pancreatic exocrine secretion of patients with pancreatic fistula. *World J Gastroenterol* 2004; 10(16): 2419-2422
http://www.wjgnet.com/1007-9327/10/2419.asp

INTRODUCTION

Since the 1960 s, parenteral nutrition (PN) has been the dominant mode for administering postoperative nutritional support. PN and enteral nutrition (EN) have been successfully used to treat varied severe diseases[1,2]. But in patients who are recovering from pancreatitis or who have a pancreatic fistula, efforts should be made to avoid stimulation of pancreatic secretion. More recent experimental studies and clinical findings about small intestinal motility and absorption, the development of needle-catheter jejunostomy, and the appearance of new diets have given impetus to the use of enteral feeding for early postoperative nutritional support and the use of octreotide to inhibit pancreatic fistula[3-5]. During application of enteral feeding, the question arises. How the pancreatic secretion was influenced by EN administered into the second jejunal loop? Can the more expensive and less physiological PN be replaced by this method[2]? Since the exocrine function of the pancreas is stimulated by the vagus nerve and the release of gastrointestinal hormones in response to food, there might be no significant increase in the exocrine activity of the pancreas. Animal experiments supported this supposition[6,7]; however, perfusion of distal jejunum with essential amino acids in human and infusion of carbohydrate into the ileum in human and dog enhanced pancreatic enzyme secretion. The present study was to evaluate the effect of parenteral and EN combined with octreotide on pancreatic secretion of the patients with pancreatic fistula by determining the levels of pancreatic secretion, amylase and electrolytes.

MATERIALS AND METHODS

Patients and groups

Seventeen patients (12 male and 5 female; mean age 43 years, range 27 to 71 years) with pancreatic fistula after abdominal injury or operation from July1997 to March 2003 were recruited and randomly divided into PN group ($n = 9$) and EN group ($n = 8$). It included pancreatic fistula after pancreas injury in 8 cases, pancreatic body and tail tumor resection in 5 cases, pancreatoduodenectomy in 4 cases.

Parenteral nutritional support

Nine cases with pancreatic fistula 3-5 d postoperatively were supported by PN for 2 wk. In the first wk, they received only PN. In the second week they received PN and octreotide. The target of nutritional therapy was to provide 20-25 kcal/(kg·d) non-protein diet and 0.12-0.15 g protein/(kg·d), the ratio of calories to nitrogen was (100-120):1.PN was given through continuous infusion (14 h/d) of a mixture of 200 mL/L Intralipid or 200 mL/L Lipofundin (B.Braun), 500 g/L glucose and 70 g/L Vamin and branched-chain amino acid. Seizure energy index of glucose to fat emulsion was 1:1. Multivitamins and electrolytes were also administered into total PN (TPN) solutions. Insulin was supplemented into PN at a ratio of glucose *vs* insulin 6:1. Six patients received TPN through right subclavian vein, 3 cases through right jugular vein. TPN was infused initially at a rate of 40 mL/h and was increased by 20 mL/h every 4 h. Antibiotics were infused by another peripheral vein. The liver and renal function, bicarbonate, serum glucose, fat metabolism were measured every other day. Human albumin, plasma and fresh blood were infused according to the patient's condition. Octreotide 0.3 mg/500 mL saline was infused continuously for 8 h in the second wk and 0.1 mg octreotide was injected subcutaneously at 8:00 pm per day for 7 d.

EN

Eight cases with pancreatic fistula were administered EN 3-5 d postoperatively. Nutrison (Nutricia) was used. Enteral feeding included 2 cases of nasoduodenal tube feeding, 4 cases of jejunectomy, and 2 cases of endoscopically placed nasojejunal tube. The jejunum through jejunostomy catheter was infused 250 mL Nutrison and 500 mL 9 g/L saline during days 1-3; Nutrison 500-1 000 mL and 500 mL milk or vegetable soup were infused for 10-14 d. The infusion rate was controlled by a

microcomputer-pump (Nutricia). During EN, inadequate calories and nitrogen were supplemented by partial PN. Octreotide 0.3 mg/500 mL saline was continuously infused for 8 h in the second week, 0.1 mg octreotide was injected subcutaneously at 8:00 pm per day for 7 d.

Observation samples

Pancreatic juice was collected on ice from the fistula during PN or EN and on d 1, 4, 7 before and after using octreotide, respectively. Samples were stored at -20 until amylase and protein content of the fractions were measured by established methods. Experimental procedures are shown as below.

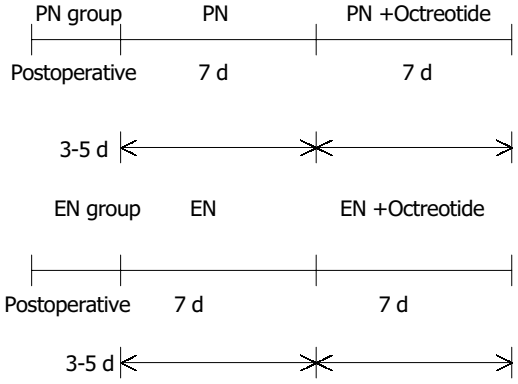

Statistical analysis

Data were collected by two persons blinded to the patients and presented as mean±SD. Statistical significance was evaluated using *t* test by SPSS 10.0 statistical-software, and a *P* value less than 0.05 was considered significant.

RESULTS

Effect of PN and/or EN on pancreatic juice, protein and amylase secretion

Though pancreatic juice, protein and amylase in EN group were slightly increased as compared with PN group, there were no significant changes between the two groups at the first wk ($P>0.05$). During the second wk, the pancreatic juice, protein, amylase decreased markedly from 79.6 mL/d to 60.8 mL/d, 31 mg/L to 22.8 mg/L and 4 220 U/L to 3 270 U/L, respectively, and there was a significant statistical difference as compared with that of pre-using octreotide in PN group ($P<0.05$). During EN combined with octreotide, the pancreatic juice, protein, amylase secretion decreased significantly from 87.9 mL/d to 65.3 mL/d, 36 mg/L to 29.1 mg/L, and 4 440 U/L to 3670 U/L, respectively, and there is a statistical difference as compared with that of pre-using octreotide ($P<0.05$); but there was no statistical difference between two groups after using octreotide ($P>0.05$).

Effect of PN and/or EN combined with octreotide on HCO_3^-, K^+, Na^+, Cl^- secretion in pancreatic juice

During the first wk, there were no differences in HCO_3^-, K^+, Na^+ and Cl^- secretion in pancreatic juice between the two groups. After PN combined with octreotide, HCO_3^-, K^+, Na^+, and Cl^- secretion decreased markedly, from 71 mmol/d to 45 mmol/d, 30 mmol/L to 21 mmol/L, 130 mmol/L to 87 mmol/L, and 60 mmol/L to 45 mmol/L, respectively, and there was a statistical difference as compared with that of pre-using octreotide, respectively ($P<0.05$). During EN supporting, there were no differences in HCO_3^-, K^+, Na^+ and Cl^- secretion in pancreatic juice as compared with PN. During the second wk, HCO_3^-, K^+, Na^+, and Cl^- secretion in EN group decreased significantly, from 79 mmol/d to 52 mmol/d, 35 mmol/L to 25 mmol/L, 135 mmol/L to 94 mmol/L, and 74 mmol/L to 54 mmol/L, respectively, there was a statistical difference as compared with that of pre-using octreotide ($P<0.05$); but there was no statistical difference between two groups after using octreotide ($P>0.05$).

DISCUSSION

As many as 50-70% of patients underwent enterocutaneous pancreatic fistulas after operation[5]. High-out fistulas (more than 200 mL daily) result in significant loss of fluid, alteration in acid-base status and malnutrition. In addition, digestive enzymes, often of extreme pH, can cause inflammation and soft tissue or skin destruction along the fistula tract. These increase the risk of infection and hemorrhage, prolong the time required for spontaneous fistula closure and increase postoperative mortality rates. Conservative management of enterocutaneous pancreatic fistula, including TPN, skin care and infection control, succeeds in a spontaneous closure rate of 24-73%[5-10]. However, such treatment is often of long duration (2-3 mo) and high cost, and is associated with considerable morbidity. In cases in which maximal medical treatment has failed, re-operation for fistula closure is required.

Table 1 Effect of PN and/or EN combined with octreotide on pancreatic juice, protein and amylase secretion

Group	*n*	Pancreatic juice (mL/d)			Protein (mg/L)			Amylase (U/L)		
		d 1	d 4	d 7	d 1	d 4	d 7	d 1	d 4	d 7
PN	9	86±35	77±49	81±31	34±17	30±17	29±17	4 268±1 361	4 026±1 131	4 468±1 487
PN+Oc- treotide	9	64±21[a]	58±19[a]	60±23[a]	25±17[a]	21±17[a]	23±17[a]	3 268±1 031[a]	3 342±1 116[a]	3 081±1 213[a]
EN	8	91±73	81±73	93±73	36±24	37±24	35±24	4 761±987	4 361±1 023	4 276±912
EN+Oc- treotide	8	67±29[c]	61±39[a]	66±34[a]	27±12[a]	31±17	30±10	3 963±1 104[a]	3 566±1 001[a]	3 363±1 221[a]

Oct: Octreotide; [a]$P<0.05$ *vs* PN group ; [c]$P<0.05$ *vs* EN group.

Table 2 Effect of PN and/or EN combined with octreotide on HCO_3^-, K^+, Na^+ and Cl^- secretion in pancreatic juice (mmol/L)

Group	*n*	HCO_3^-			K^+			Na^+			Cl^-		
		d 1	d 4	d 7	d 1	d 4	d 7	d 1	d 4	d 7	d 1	d 4	d 7
PN	9	73±37	69±31	71±32	32±19	28±12	31±17	123±33	133±31	126±43	61±34	63±31	58±24
PN+Oct	9	54±34[a]	57±24[a]	59±31[a]	22±11[a]	19±9[a]	21±17[a]	87±53[a]	78±67[a]	93±55[a]	49±13[a]	42±21[a]	49±17[a]
EN	8	79±44	81±35	83±47	37±17	36±13	34±19	131±44	129±33	139±28	73±37	71±43	68±31
EN+Oct	8	65±23[c]	61±33[c]	57±37[c]	25±15[c]	28±11[c]	28±13	101±63[c]	95±79[c]	91±73[c]	51±15[c]	49±21[c]	53±35[c]

Oct: Octreotide; [a]$P<0.05$ *vs* PN group; [c]$P<0.05$ *vs* EN group.

In theory, reduction of fistula output should promote the chances of spontaneous closure. This is usually achieved by restriction of oral intake, sometimes supplemented with nasogastric suction in order to relieve the burden of gut and pancreas. Pharmacological attempts to decrease intestinal secretions involve using drugs such as somatostatin, loperamide, atropine or pirenzepine, and H_2 blockers such as omeprazole. Although the effectiveness of such treatments has yet to be confirmed[7]. In clinics, PN or EN is usually considered, and they may play an important role in the spontaneous closure of pancreatic fistula, but there is some controversy over their effectiveness and safety.

Effect of PN on pancreatic exocrine secretion

TPN with complete gut rest has been proposed as adjuvant therapy in the treatment of severe acute pancreatitis, to meet metabolic demands and relieve pancreas. A decrease in volume of pancreatic secretion and, in particular, its enzymatic content would likely have a beneficial effect on patient's clinical course. That TPN decreases pancreatic activity is supported by several animal studies. Hamilton *et al*. documented a marked decrease in pancreatic secretions of the normal dog pancreas stimulated maximally by secretion and pancreozymin with the institution of TPN. The volume of pancreatic secretion decreased by 50% and amylase secretion decreased by 71%, but there was a slight increase in bicarbonate excretion. Adler, in 1975, demonstrated that intravenous administration of hypertonic solutions including 50% dextrose resulted in a 24% decrease in pancreatic secretion and a 69% decrease in biliary secretion in a maximally secretin- and pancreozymin-stimulated dog model. PN for patients with pancreatitis has, in general, shown no adverse or beneficial effects on the course of pancreatitis but has provided adequate nutritional support.

The use of intravenous lipid formulations in patients with pancreatic fistula remains controversial despite the evidence that they are not harmful. Kelly and Nahrwold[11] compared the exocrine pancreatic secretory response to intravenous saline and PN in dogs with chronic gastric fistula and found that the latter produced a small but significant increase in the mean volume of pancreatic juice (2.4 *vs* 1.8 mL per 15 min; $P<0.05$) with a slight increase in mean protein and bicarbonate secretions. These differences are minimal compared with the changes found in dogs receiving an intraduodenal infusion of an enteral diet. Hamiloon reported that PN could ameliorate stimulation to the pancreas. The output of the pancreatic juice decreased by 50%, that of amylase by 71% and that of glucose slightly increased. Another canine with chronic pancreatic fistula and stomach ectomy received fat emulsion infusion. Meanwhile, the canine received stimulation of secretin. The results showed that pancreatic juice, protein enzyme, total protein and HCO_3^- did not change during infusion of fat emulsion[12]. Patients with pancreatic fistula postoperative of gastrectomy received PN by administration of 640 mL or 840 mL 100 g/L Liposym for 8 d, the pancreatic juice, protein and HCO_3^- did not increase[13]. Klein *et al*.[14] believed that the effects of different PN contents on the pancreatic juice, HCO_3^- and amylase secretion were different. Intralipid could increase pancreatic juice from 33 mL/h to 39 mL/h, HCO_3^- from 44.5 mmol/L to 54.5 mmol/L, amylase from 25 000 U/L to 32 000 U/L. They held that fat emulsion should be used to supplement essential fatty acid. In the present study, 250 mL 200 mL/L Intralipid or 200 mL/L Lipofundin per day was used as fat energy sources for 2 wk. The results showed that pancreatic juice, protein, amylase, HCO_3^-, K^+, Na^+ and Cl^- secretion did not change. It suggested that PN could not stimulate pancreatic secretion, and supplemental fat emulsion was safety.

Effect of EN on pancreatic secretion

The presence of food in the stomach and duodenum elicits gastropancreatic and duodenopancreatic reflexes that result in stimulation of pancreatic exocrine secretion. However, these effects are not pronounced when nutrients are delivered directly into jejunum.

A study[15] in dogs showed that intragastric delivery of nutrients caused an increase in the volume, and protein and bicarbonate content of pancreatic secretions compared with those in saline-infused controls. Intraduodenal feeding increased the volume of pancreatic secretions but did not affect protein or bicarbonate secretion. Other studies[16] in dogs also showed that the intraduodenal administration of elemental diets or pure amino acid solutions significantly increased pancreatic secretions, suggesting that the amino acid content of elemental diets is responsible for the stimulatory effects. In contrast, intrajejunal delivery of nutrients was not associated with a significant change in the volume, or protein or bicarbonate content of pancreatic secretions compared with controls. These authors also found in one human subject that avoidance of cephalic, gastric, and duodenal stimuli by jejunal tube feeding of acids did not result in pancreatic stimulation. Another canine study[17], in which an elemental diet was fed into the proximal jejunum, demonstrated a brisk pancreatic secretory response. However, the pancreatic juice collected was watery and low in enzyme. They concluded that bypassing the stomach minimized acid secretion, which played an important role in keeping the pancreas at rest. Bodoky *et al*.[18] randomized 12 patients undergoing pylorus-preserving pancreaticoduodenectomy for chronic pancreatitis to receive EN via a needle catheter feeding jejunostomy (7 patients) or PN (5 patients). A catheter placed during operation in the pancreatic duct was used to collect pancreatic secretions. The authors believed that the disease was mainly in the pancreatic head and that the function of the pancreatic remnant was nearly normal. They did not find any difference in the volume of pancreatic secretions or the content of bicarbonate, protein, chymotrypsin or amylase between the two groups.

In the present study, 8 patients received EN for 2 wk, during which the volume of pancreatic juice, protein, amylase and bicarbonate in EN group had a small but not significant increase as compared with PN group. Although there is a paucity of human studies on the effects of oral feeding and EN on pancreatic secretion, one might reasonably conclude from available evidence from human and canine studies that oral, intragastric and intraduodenal feeding produce a significant stimulation of pancreatic secretions. In contrast, intrajejunal feeding has much fewer stimulatory effects and is therefore the route of choice for enteral feeding in pancreatic diseases.

Effect of octreotide on pancreatic juice exocrine secretion

Discovered in 1972, somatostatin is a naturally occurring tetradecapeptide with a wide spectrum of inhibitory biological actions. Within the gastrointestinal tract, somatostatin has been found in the pancreas, stomach, intestinal mucosa and mesenteric neurons. Because of its inhibitory actions, it has been used in the management of upper gastrointestinal haemorrhage, secretory diarrhoea, dumping syndrome and peptide-secreting tumors. Since the mid-1980 s, somatostatin has been advocated as an adjuvant therapy in the conservative treatment of patients with enterocutaneous pancreatic fistula[19,20]. However, its short half-life (1.1-3.0 min) mandates continuous administration. Long-acting somatostatin analogues, such as octreotide acetate and lanreotide, have been developed. Octreotide has a biological half-life of 90-120 min and can be administered subcutaneously two or three times per day. Compared with somatostatin, it not only significantly reduces the secretions of the pancreas and stomach, but also has a more selective range of targets. Both somatostatin and octreotide have been described as effective treatments for

enteric fistulas in adults, with few severe short-term side-effects (mostly diarrhoea, flushing and abdominal pain). These preparations have, therefore, the potential benefit of cutting the cost of treatment and reducing the discomfort of patients by shortening the length of hospital stay. Since 1990, several groups have described favourable results using somatostatin or octreotide for the "conservative" management of enterocutaneous pancreatic fistula. Administration of such drugs has been reported to result in rapid and significant reduction of fistula output (often within 24 h of treatment) and acceleration of fistula closure (from as early as day 2)[21-25].

Martineau *et al*.[4] reviewed the role of octreotide for the management of established enterocutaneous pancreatic fistulas by summarizing the results of 4 randomized trials and 8 case series. They concluded that octreotide significantly decreased enterocutaneous pancreatic fistula output, but did not significantly improve the rate of spontaneous fistula closure. Furthermore, octreotide did not seem to reduce the output, or hasten the time or rate of closure, in fistula of recent onset (less than 8 d). Recently, Berberat *et al*.[8] reviewed six randomized controlled trials and one open randomized trial, and assessed the efficacy of octreotide on preventing postoperative complications in patients underwent major pancreatic operations. They concluded that prophylactic use of octreotide could significantly reduce the complication rate. Sitges-Serra[9] reported that 20 cases with pancreatic fistula received octreotide 10 μg/8 h for 20 d (n = 13). The output of pancreatic juice decreased from 725 mL/24 h to 151 mL/24 h, the rate of spontaneous fistula closure was 78%. Another group (n = 7) used octreotide 100 μg/8 h for 7 d. The output of pancreatic juice increased from 218 mL/24 h to 436 mL/24 h. Torres[26] reported 33 patients with pancreatic fistula received octreotide 75-100 μg/8 h for 10 d, and then stopped. It resulted in increase of pancreatic juice secretion from 228 mL/24 h to 498 mL/24 h. After 6 h, octreotide was used again. Output of pancreatic juice decreased from 828 mL/24 h to 247 mL/24 h, the rate of spontaneous fistula closure was 79%. The time of spontaneous fistula closure of octreotide group was 2-10 d shorter than that of control group. In the present study, the patients with pancreatic fistula received octreotide combined with PN and EN, the secretion of pancreatic juice, protein and amylase was decreased, and secretion of HCO_3^-, K^+, Na^+ and Cl^- was inhibited. These results showed that octreotide can inhibit pancreatic juice, amylase secrete, and maybe beneficial to pancreatic fistula self-repair.

We conclude that administration of nutrient solutions into second jejunal loop does not overstimulate the exocrine function of pancreas, while it produces equivalent results to parenteral administration of nutrients. The enteral feeding combined with octreotide could be effective and safe to reduce pancreatic fistula output.

REFERENCES

1 **Kalfarentzos FE**, Karavias DD, Karatzas TM, Alevizatos BA, Androulakis JA. Total parenteral nutrition in severe acute pancreatitis. *J Am Coll Nutr* 1991; **10**: 156-162

2 **Buchman AL**, Moukarzel AA, Bhutta S, Belle M, Ament ME, Eckhert CD, Hollander D, Gornbein J, Kopple JD, Vijayaroghavan SR. Parenteral nutrition is associated with intestinal morphologic and functional changes in humans. *J Parenter Enteral Nutr* 1995; **19**: 453-460

3 **Dorta G.** Role of octreotide and somatostatin in the treatment of intestinal fistulae. *Digestion* 1999; **60**(Suppl 2): 53-56

4 **Martineau P**, Shwed JA, Denis R. Is octreotide a new hope for enterocutaneous and external pancreatic fistulas closure? *Am J Surg* 1996; **172**: 386-395

5 **De Graef J**, Woussen-Colle MC. Physiological control and pharmacological inhibition of digestive secretions. *Acta Chir Belg* 1985; **85**: 149-153

6 **Qin HL**, Su ZD, Hu LG, Ding ZX, Lin QT. Effect of early intrajejunal nutrition on pancreatic pathological features and gut barrier function in dogs with acute pancreatitis. *Clin Nutr* 2002; **21**: 469-473

7 **Qin HL**, Su ZD, Hu LG, Ding ZX, Lin QT. Parenteral versus early intrajejunal nutrition: Effect on pancreatitic natural course, entero-hormones release and its efficacy on dogs with acute pancreatitis. *World J Gastroenterol* 2003; **9**: 2270-2273

8 **Berberat PO**, Friess H, Uhl W, Buchler MW. The role of octreotide in the prevention of complications following pancreatic resection. *Digestion* 1999; **60**(Suppl 2): 15-22

9 **Sitges-Serra A**, Guirao X, Pereira JA, Nubiola P. Treatment of gastrointestinal fistulas with Sandostatin. *Digestion* 1993; **54** (Suppl 1): 38-40

10 **Voss M**, Ali A, Eubanks WS, Pappas TN. Surgical management of pancreaticocutaneous fistula. *J Gastrointest Surg* 2003; **7**: 542-546

11 **Kelly GA**, Nahrwold DL. Pancreatic secretion in response to an elemental diet and intravenous hyperalimentation. *Surg Gynecol Obstet* 1976; **143**: 87-91

12 **Burns GP**, Stein TA. Pancreatic enzyme secretion during intravenous fat infusion. *J Parenter Enteral Nutr* 1987; **11**: 60-62

13 **Edelman K**, Valenzuela JE. Effect of intravenous lipid on human pancreatic secretion. *Gastroenterology* 1983; **85**: 1063-1066

14 **Klein E**, Shnebaum S, Ben-Ari G, Dreiling DA. Effects of total parenteral nutrition on exocrine pancreatic secretion. *Am J Gastroenterol* 1983; **78**: 31-33

15 **Ragins H**, Levenson SM, Signer R, Stamford W, Seifter E. Intrajejunal administration of an elemental diet at neutral pH avoids pancreatic stimulation. Studies in dog and man. *Am J Surg* 1973; **126**: 606-614

16 **Wolfe BM**, Keltner RM, Kaminski DL. The effect of an intraduodenal elemental diet on pancreatic secretion. *Surg Gynecol Obstet* 1975; **140**: 241-245

17 **Cassim MM**, Allardyce DB. Pancreatic secretion in response to je junal feeding of elemental diet. *Ann Surg* 1974; **180**: 228-231

18 **Bodoky G**, Harsanyi L, Pap A, Tihanyi T, Flautner L. Effect of enteral nutrition on exocrine pancreatic function. *Am J Surg* 1991; **161**: 144-148

19 **Gray M**, Jacobson T. Are somatostatin analogues (octereotide and lanreotide) effective in promoting healing of enterocutaneous fistulas? *J Wound Ostomy Continence Nurs* 2002; **29**: 228-233

20 **Voss M**, Pappas T. Pancreatic fistula. *Curr Treat Options Gastroenterol* 2002; **5**: 345-353

21 **Li-Ling J**, Irving M. Somatostatin and octreotide in the prevention of postoperative pancreatic complications and the treatment of enterocutaneous pancreatic fistulas: a systematic review of randomized controlled trials. *Br J Surg* 2001; **88**: 190-199

22 **Takacs T**, Hajnal F, Nemeth J, Lonovics J, Pap A. Stimulated gastrointestinal hormone release and gallbladder contraction during continuous jejunal feeding in patients with pancreatic pseudocyst is inhibited by octreotide. *Int J Pancreatol* 2000; **28**: 215-220

23 **Duerksen DR**, Bector S, Yaffe C, Parry DM. Does jejunal feeding with a polymeric immune-enhancing formula increase pancreatic exocrine output as compared with TPN? A case report. *Nutrition* 2000; **16**: 47-49

24 **Stabile BE**, Borzatta M, Stubbs RS. Pancreatic secretory responses to intravenous hyperalimentation and intraduodenal elemental and full liquid diets. *J Parenter Enteral Nutr* 1984; **8**: 377-380

25 **Grant JP**, Davey-McCrae J, Snyder PJ. Effect of enteral nutrition on human pancreatic secretions. *J Parenter Enteral Nutr* 1987; **11**: 302-304

26 **Torres AJ**, Landa JI, Moreno-Azcoita M, Arguello JM, Silecchia G, Castro J, Hernandez-Merlo F, Jover JM, Moreno-Gonzales E, Balibrea JL. Somatostatin in the management of gastrointestinal fistulas. A multicenter trial. *Arch Surg* 1992; **127**: 97-99

Edited by Zhu LH and Chen WW **Proofread by** Xu FM

PO Box 2345, Beijing 100023, China
Fax: +86-10-85381893
E-mail: wjg@wjgnet.com www.wjgnet.com

World J Gastroenterol 2004;10(16):2423-2426
World Journal of Gastroenterology
 ISSN 1007-9327

• BRIEF REPORTS •

Risk factors for alcoholic liver disease in China

Xiao-Lan Lu, Jin-Yan Luo, Ming Tao, Yan Gen, Ping Zhao, Hong-Li Zhao, Xiao-Dong Zhang, Nei Dong

Xiao-Lan Lu, Jin-Yan Luo, Ping Zhao, Hong-Li Zhao, Xiao-Dong Zhang, Nei Dong, Department of Gastroenterology, Second Hospital of Xi'an Jiaotong University, Xi'an 710004, Shaanxi Province, China
Ming Tao, Department of Epidemiology, Medical College of Xi'an Jiaotong University, Xi'an 710061, Shaanxi Province, China
Yan Gen, Department of Clinical Laboratory, Second Hospital of Xi'an Jiaotong University, Xi'an 710004, Shaanxi Province, China
Supported by the Scientific Foundation of Ministry of Health of China, No.98-1-236
Correspondence to: Dr. Xiao-Lan Lu, Department of Gastroenterology, Second Hospital of Xi'an Jiaotong University, 157 Xiwulu, Xi'an 710004, Shaanxi Province, China. xiaolan-lu@163.com
Telephone: +86-29-87768926 **Fax:** +86-29-87678758
Received: 2003-11-13 **Accepted:** 2003-03-29

Abstract

AIM: To examine the association of daily alcohol intake, types of alcoholic beverage consumed, drinking patterns and obesity with alcoholic liver disease in China.

METHODS: By random cluster sampling and a 3-year follow-up study, 1 270 alcohol drinkers were recruited from different occupations in the urban and suburban areas of Xi'an City. They were examined by specialists and inquired for information on: Medical history and family medical history, alcohol intake, types of alcoholic beverage consumed, drinking patterns by detailed dietary questionnaires. Routine blood tests and ultrasonography were done.

RESULTS: Multivariate analysis showed that: (1) The risk threshold for developing alcoholic liver disease was ingestion of more than 20 g alcohol per day, keeping on drinking for over 5 years in men. The highest OR was at the daily alcohol consumption >/=160 g, the occurrence rate of ALD amounted to 18.7% (P<0.01). No ALD occurred when ingestion of alcohol was less than 20 g per day. (2) 87.9% of all drank only at mealtimes. The cumulative risk of developing ALD was significantly higher in those individuals who regularly drank alcohol without food than in those who drank only at mealtimes, especially for those who regularly drank hard liquors only and multiple drinks (P<0.05). (3) The alcohol consumption in those with BMI >/=25 was lower than in those with BMI <25, but the risk increased to 11.5%, significantly higher than that of general population, 6.5% (P<0.01). (4) Abstinence and weight reduction could benefit the liver function recovery.

CONCLUSION: In the Chinese population the ethanol risk threshold for developing ALD is 20 g per day, and this risk increases with increased daily intake. Drinking 20 g of ethanol per day and for less than 5 years are safe from ALD. Drinking alcohol outside mealtimes and drinking hard liquors only and multiple different alcohol beverages both increase the risk of developing ALD. Obesity also increases the risk. Abstinence and weight reduction will directly affect the prognosis of ALD. Doctor's strong advice might influence the prognosis indirectly.

Lu XL, Luo JY, Tao M, Gen Y, Zhao P, Zhao HL, Zhang XD, Dong N. Risk factors for alcoholic liver disease in China. *World J Gastroenterol* 2004; 10(16): 2423-2426
http://www.wjgnet.com/1007-9327/10/2423.asp

INTRODUCTION

Alcoholic liver disease (ALD) is a major health and economic problem in the Western world[1-5]. Over 14 million Americans are alcohol abusers or alcohol dependent. The problem in China is not as serious as that in Western world. But in recent years, along with the improved living standard and increased alcohol consumption, the morbidity of ALD has risen quickly. Among drinkers, the morbidity has reached 6.1%[6]. Therefore, ALD has become an increasingly serious disease risk in health care. However, not all drinkers are ALD patients, and there is different susceptibility to damage by alcohol in individuals[5]. As a common problem, some of its risk factors have been reported in Western countries, but recent analyses have confirmed that geographic and racial variations are evident. In China, however, there is no such study to confirm the main risk factors of ALD, such as cumulative alcohol intake, drinking patterns, types of alcoholic beverage ingested and obesity. In the present study, we aimed to analyze these factors according to random cluster sampling data and a 3-year follow-up study.

MATERIALS AND METHODS

Subjects

We recruited 1 270 drinkers from different occupations in the urban and suburban areas of Xi'an City by random cluster sampling. Every participant was examined by medical staff and received detailed inquiry at his or her home. The medical staff members were trained before the beginning of the study in order to be able to administer the questionnaire uniformly. The questions included: (1) An extensive medical history, including previous diagnosis of chronic liver disease and family medical history. (2) Evaluation of alcohol intake, including detailed questions on the use of alcoholic beverages, types of alcoholic beverage consumed, drinking patterns, the duration of use and the time of drinking (at mealtimes or without food). All the questions were also validated by cross-checking with family members. (3) A detailed physical examination, the body mass index (BMI) and ultrasonography were also performed and recorded. (4) Blood samples were taken to check serum alanine aminotransferase (ALT), serum aspartate aminotransferase (AST), γ-glutamyl transferase (GGT), hepatitis B (HBsAg) and anti-hepatitis C virus (anti-HCV). (5) Three years later, all the patients were investigated again, including detailed inquiry about their relevant diseases and alcohol intake in the past 3 years. Meanwhile, the BMI, ultrasonography and blood samples were taken again.

Diagnosis

The diagnosis of ALD was confirmed according to the published data[6].

Statistical analysis

Statistical analysis was performed with SPSS 10.0 statistical

package. A logistic-regression model was used in the multivariate modeling of associations. All the factors for which the *P* value of univariate and discriminant analysis was less than 0.05 were entered in the model. Odds ratios (ORs) and 95% confidence intervals (CI) were also calculated.

RESULTS

Study population

Of the 1 270 drinkers, 83 were ALD patients including 72 cases of alcoholic fatty liver, 6 cases of alcoholic hepatitis, and 4 cases of alcoholic cirrhosis. Only one woman was excluded from the study. None of the patients took any medicine in latest 3 mo. Anti-HCV and HBsAg were all negative. Three years later, 66 of 82 ALD subjects were reinvestigated, constituting 80.5% of all. Of the 66 ALD, 19 subjects had BMI >/= 25 and 47 subjects had BMI less than 25.

Daily alcohol consumption and ALD

Analysis of the data showed that the risk of having ALD was significant with a daily alcohol intake higher than 20 g (Table 1) and the mean duration of drinking longer than 5 years. Above this threshold, the OR for ALD increased proportionally with daily alcohol consumption. The highest OR (10.7, $P<0.01$) occurred when daily consumption exceeded 160 g. At this highest level of alcohol intake, the percentage of subjects with ALD was 18.7%, significantly higher than that of the lowest level of alcohol intake of less than 20 g/d. Among these subjects whose daily alcohol consumption was less than 20 g and the duration of drinking was less than 5 years, no ALD occurred. So we can assume that daily intake of 20 g alcohol for 5 years is the risk threshold. With longer duration of drinking (more than 10-15 years), a few cases occurred even though the daily intake was less than 20 g, but the morbidity was very low, only 2.2%.

Drinking habits and ALD

In our population, beer or wine drinkers were 41.1%, and their alcohol daily intake was less than others. Rural people tended to drink hard liquors. Multiple drinkers were 20.2%, 87.9% of the drinkers consumed alcohol only at mealtimes, the daily alcohol intake was significantly lower than that of alcohol consumed at any time (with and without food) ($P<0.05$). Daily alcohol intake of only hard liquors, also without food was significantly higher than that of all other categories of drinkers, the morbidity of ALD was also the highest, 2.7 times that of drinkers who drank only wine or beer at mealtimes (Table 2).

Obesity and ALD

Among the 1 270 drinkers, 203 had BMI more than 25. Although their average daily alcohol intake was lower than those with BMI less than 25, the ALD morbidity was 11.5%, more than twice that of normal body mass, significantly higher than the average 6.5%. There were no significant differences in drinking habits between the two groups. Multivariate analysis of the data showed that obesity was a risk factor for ALD, (OR: 5.6, $P<0.01$). The difference was significant (Table 3).

Retrospective results

A 3-year follow-up indicated that among 19 cases with BMI>/=25, only 3 cases had a body mass of 20% higher than before, and an increased BMI. Their serum ALT and AST were more than twice the upper normal level. The ultrasonography of the liver also indicated typical alcoholic fatty liver. In 9 of the 19 cases with a significant loss of body weight, their BMI also reduced to below 25. The ultrasonography of liver in several cases also became nearly normal. ALT and AST level was below the upper normal level. Of the remaining 7 subjects, their BMI was the same as before, the “liver function” became nearly normal. Ultrasonography findings became normal in 2 of 7 cases, and

Table 1 Average daily alcohol intake and duration of drinking

Alcohol intake	*n*	<5 yr	> / =5-9 yr	> / =10-14 yr	> / =15-19 yr	> / =20 yr	Total	OR (95% CI)
(g / d)		263	293	233	142	339	1 270	
<20	780	0	1	3	5	8	17 (2.2%)	—
> / =20-39	217	1	2	6	6	10	25 (11.4%)	5.5 (2.9-12.3)
> / =40-79	149	1	6	4	3	6	20 (13.5%)	7.1 (3.5-13.6)
> / =80-159	76	1	3	2	1	4	11 (14.6%)	8.4 (4.1-17.3)
> / =160	48	1	1	2	1	4	9 (18.7%)	10.7 (5.2-23.4)
Total	1 270	4 (1.5%)	13 (4.4%)	17 (6.9%)	16 (11.3%)	32 (9 .4%)	82 (6.5%)	

$P<0.01$, *vs* group of alcohol intake <20 g / d.

Table 2 Different drinking habits and types of alcoholic beverage

Type of beverage	*n*	With meals only			At any time			χ^2
		Daily intake (g)	*n* (%)	Patients (%)	Daily intake (g)	*n* (%)	Patients (%)	
Beer	390	6.1±3.7	351 (90.0)	2 (0.57)	8.9±4.3	39 (10.0)	0 (0.00)	
Wine	132	10.8±5.3	118 (89.4)	1 (0.84)	19.2±9.6	14 (10.6)	1 (7.1)	3.32
Hard liquor	491	45.2±15.9	417 (84.9)	46 (11.0)	67.7±21.1	74 (15.1)	14 (18.9)	3.65
Multiple	257	29.4±11.5	231 (89.9)	14 (6.1)	42.8±13.2	26 (10.9)	4 (15.4)	3.12
Total	1 270		1 117 (87.9)	63 (5.6)		153 (12.1)	19 (12.4)	

$P<0.05$, *vs* Beer.

Table 3 Relationship between BMI and ALD

BMI	*n*	ALD	Years	Daily intake (g)	OR	*P*
> / =25	203	24	13.5±6.2	26.4±13.7	5.6 (3.02-6.21)	<0.01
<25	1 067	58	16.3±5.8	35.7±18.1		

remained the same in the other 5. All these 19 subjects except 3 who drank a little occasionally have already abstained.

Among 47 cases with BMI<25, their body mass did not change significantly. Eleven of them who kept on drinking had ALT and AST more than twice the upper normal level. The ultrasonography of liver revealed no improvement. Of the remaining who abstained from drinking, more than 85% of them had nearly normal "liver function", and better ultrasonographic findings. The percentage of "liver function" recovery was significantly higher than those who went on drinking (P<0.01).

DISCUSSION

Alcohol abuse has been claimed as one important factor leading to chronic liver diseases, as known in other diseases[7-12]. The natural history of alcoholic liver disease ranges from asymptomatic indolent to end stage liver disease. Most patients lack specific clinical features[13,14]. Diagnosis of alcoholic fatty liver and alcoholic steatohepatitis, like non-alcoholic fatty liver, without confirmatory laboratory tests, may involve the history of drinking, ultrasonography and liver biopsy[15-18].

ALD is not only associated with genetic factors, but also involves other factors such as sex, body weight, BMI, the type and pattern of alcoholic beverage consumed, the habit of drinking hard liquors and of consuming alcohol without food, the duration of drinking[19-21]. Yet, as to the risk threshold, in terms of daily alcohol intake and years of duration that can induce alcohol liver damage, there is no uniformed conclusion: with the wide range between 30 g/d and 80 g/d[13,]. Great differences between Western and Eastern countries exist: geographic variations must be present[22,23], especially in China.

Our data suggested that the risk threshold of daily alcohol intake was 20 g; the duration was 5 years for Chinese men. Below the threshold, drinking seldom induced liver damage. If the daily intake exceeded 40 g and the duration was longer than 5 years, the liver damage occurred more frequently. However, with a daily intake higher than 160 g, in some cases the prevalence of alcoholic liver disease was only 18.7%. It means there is significantly different susceptibility among different individuals[24]. It is commonly believed that prevalence of ALD in general population is up to about 15%, and rises with increased alcoholic intake. Our result was a little higher than that, maybe because our subjects were all men. In China, women drinkers are few, and their alcohol consumption is low, so few women develop ALD. There was only one woman case in our data. In spite of that, we believe that there is a great hepatic susceptibility to damage by alcohol in women.

The types of alcoholic beverage and the different drinking and dietary habits are closely related with ALD. Yet, a dose-effect relation between alcohol intake and alcohol-induced hepatic and other organ functional impairment has been demonstrated.

We were able to demonstrate for the first time in China that the habit of drinking hard liquors without food and the consumption of multiple types of drinks were risk factors of alcohol-induced liver damage. Those who drank only wine and beer were at lower risk for ALD. Fortunately, 90% of the Chinese drink wine or alcohol at mealtimes with food. Drinking without food might differentially affect the intragastric metabolism of ethanol by decreasing gastric alcohol dehydrogenase and hepatic glutathione and by accelerating gastric emptying, as it occurs in rats.

Recent studies confirm that the prevalence of alcohol-induced liver disease in obesity is high and serious. Obesity may be a co-risk factor for ALD and accelerate liver damage[25,26]. It is reported that if the body weight is 20% above normal, the risk for ALD will be twice as great as in normal weight one. This is similar to our result. Among those obese patients whose weight was above normal for more than 10 years, the risk for ALD was 2.5-3 times higher. At the same time, the liver damage increases with the increased BMI[27,28]. However, the mechanism is not clear.

All of the patients in this study whose Anti-HCV and HBsAg were negative and with no recent medication history were "pure" ALD. Multivariate analysis showed that each factor was independent of the other variables.

Besides abstaining, which directly affects the prognosis of ALD[29], BMI can also affect the progress of ALD[30]. For the overweight cases, weight loss is an important treatment[31]. Our data have another indication that "education" is also very important for changing patients' lifestyle[32]. Because all the subjects with BMI>/=25 had been told that alcohol and overweight would cause bad prognosis of ALD and strongly recommended complete alcohol abstinence and weight reduction, none of these cases went on drinking heavily. On the other hand, among the men with BMI<25, some did not take the risk of drinking seriously, nearly 15% of them went on drinking during the 3 years, resulting in progress of their ALD.

From the present data we can conclude that the minimum alcohol intake and the duration of years associated with a significant increase in the prevalence of alcohol-related liver disease was 20 g per day and 5 years for men. This risk increases in a dose-related pattern. However, the most striking result is that not only the quantity of alcohol consumed, but also the patterns of drinking are an important determinant of the risk of having ALD. Drinking only hard liquors or multiple types of alcoholic beverages without food, independent of the amount, is associated with an increased prevalence of alcohol-related liver disease. Obesity is also an independent risk factor for ALD. Abstinence and weight loss directly affect the prognosis of ALD. Therefore, we suggest reducing alcohol intake, avoiding drinking outside of mealtimes and consuming only wine or beer, especially for obese people.

REFERENCES

1 **Kerr WC**, Fillmore KM, Marvy P. Beverage-specific alcohol consumption and cirrhosis mortality in a group of English-speaking beer-drinking countries. *Addiction* 2000; **95**: 339-346
2 **Menon KV**, Gores GJ, Shah VH. Pathogenesis, diagnosis, and treatment of alcoholic liver disease. *Mayo Clin Proc* 2001; **76**: 1021-1029
3 **Campollo O**, Martinez MD, Valencia JJ, Segura-Ortega J. Drinking patterns and beverage preferences of liver cirrhosis patients in Mexico. *Subst Use Misuse* 2001; **36**: 387-398
4 **O'Keefee C**, McCormick PA. Severe acute alcoholic hepatitis: an audit of medical treatment. *Ir Med J* 2002; **95**: 108-109
5 **Monzoni A**, Masutti F, Saccoccio G, Bellentani S, Tiribelli C, Giacca M. Genetic determinants of ethanol-induced liver damage. *J Mol Med* 2001; **7**: 255-262
6 **Lu XL**, Tao M, Luo JY, Gen Y, Zhao P, Zhao HL. Epidemiology of alcoholic liver diseases in Xi'an. *Shijie Huaren Xiaohua Zazhi* 2003; **11**: 719-722
7 **Crews FT**, Braun CJ. Binge ethanol treatment causes greater brain damage in alcohol-preferring P rats than in alcohol-nonpreferring NP rats. *Alcohol Clin Exp Res* 2003; **27**: 1075-1082
8 **Schuckit MA**, Smith TL, Danko GP, Isacescu V. Level of response to alcohol measured on the self-rating of the effects of alcohol questionnaire in a group of 40-year-old women. *Am J Drug Alcohol Abuse* 2003; **29**: 191-201
9 **Hezode C**, Lonjon I, Roudot-Thoraval F, Pawlotsky JM, Zafrani ES, Dhumeaux D. Impact of moderate alcohol consumption on histological activity and fibrosis in patients with chronic hepatitis C, and specific influence of steatosis: a prospective study. *Aliment Pharmacol Ther* 2003; **17**: 1031-1037
10 **Rehm J**, Sempos CT, Trevisan M. Alcohol and cardiovascular disease-more than one paradox to consider. Average volume of alcohol consumption, patterns of drinking and risk of coronary heart disease-a review. *J Cardiovasc Risk* 2003; **10**: 15-20

11 **Lip GY**, Beevers DG. Alcohol and cardiovascular disease-more than one paradox to consider. Alcohol and hypertension-does it matter? *J Cardiovasc Risk* 2003; **10**: 11-14

12 **Dal Maso L**, La Vecchia C, Polesel J, Talamini R, Levi F, Conti E, Zambon P, Negri E, Franceschi S. Alcohol drinking outside meals and cancers of the upper aero-digestive tract. *Int J Cancer* 2002; **102**: 435-437

13 **Gordon H**. Detection of alcoholic liver disease. *World J Gastroenterol* 2001; **7**: 297-302

14 **Vaquero J**, Blei AT. Etiology and management of fulminant hepatic failure. *Curr Gastroenterol Rep* 2003; **5**: 39-47

15 **Skelly MM**, James PD, Ryder SD. Findings on liver biopsy to investigate abnormal liver function tests in the absence of diagnostic serology. *J Hepatol* 2001; **35**: 195-199

16 **Angelico F**, Del Ben M, Conti R, Francioso S, Feole K, Maccioni D, Antonini TM, Alessandri C. Non-alcoholic fatty liver syndrome: a hepatic consequence of common metabolic diseases. *J Gastroenterol Hepatol* 2003; **18**: 588-594

17 **Hourigan KJ**, Bowling FG. Alcoholic liver disease: a clinical series in an Australian private practice. *J Gastroenterol Hepatol* 2001; **16**: 1138-1143

18 **Jarque-Lopez A**, Gonzalez-Reimers E, Rodríguez-Moreno F, Santolaria-Fernandez F, Lopez-Lirola A, Ros-Vilamajo R, Espinosa-Villarreal JG, Martinez-Riera A. Prevalence and mortality of heavy drinkers in a general medical hospital unit. *Alcohol Alcohol* 2001; **36**: 335-338

19 **Thurman RG**. Sex-related liver injury due to alcohol involves activation of Kupffer cells by endotoxin. *Can J Gastroenterol* 2000; **14**(Suppl D): 129D-135D

20 **Walsh K**, Alexander G. Alcoholic liver disease. *Postgrad Med J* 2000; **76**: 280-286

21 **Ropero Gradilla P**, Villegas Martinez A, Fernandez Arquero M, Garcia-Agundez JA, Gonzalez Fernandez FA, Benitez Rodriguez J, Diaz-Rubio M, de la Concha EG, Ladero Quesada JM. C282Y and H63D mutations of HFE gene in patients with advanced alcoholic liver disease. *Rev Esp Enferm Dig* 2001; **93**: 156-163

22 **Stewart SH**. Racial and ethnic differences in alcohol-associated aspartate aminotransferase and gamma-glutamyltransferase elevation. *Arch Intern Med* 2002; **162**: 2236-2239

23 **Naveau S**, Giraud V, Ganne N, Perney P, Hastier P, Robin E, Pessione F, Chossegros P, Lahmek P, Fontaine H, Ribard D, Dao T, Filoche B, El Jammal G, Seyrig JA, Dramard JM, Chousterman M, Pillegand B. Patients with alcoholic liver disease hospitalized in gastroenterology. Anational multicenter study. *Gastroenterol Clin Biol* 2001; **25**: 131-136

24 **Diehl AM.** Liver disease in alcohol abusers: clinical perspective. *Alcohol* 2002; **27**: 7-11

25 **Brunt EM**, Ramrakhiani S, Cordes BG, Neuschwander-Tetri BA, Janney CG, Bacon BR, Di Bisceglie AM. Concurrence of histologic features of steatohepatitis with other forms of chronic liver disease. *Mod Pathol* 2003; **16**: 49-56

26 **Clouston AD**, Powell EE. Interaction of non-alcoholic fatty liver disease with other liver diseases. *Best Pract Res Clin Gastroenterol* 2002; **16**: 767-781

27 **Ioannou GN**, Weiss NS, Kowdley KV, Dominitz JA. Is obesity a risk factor for cirrhosis-related death or hospitalization? a population-based cohort study. *Gastroenterology* 2003; **125**: 1053-1059

28 **Mulhall BP**, Ong JP, Younossi ZM. Non-alcoholic fatty liver disease: an overview. *J Gastroenterol Hepatol* 2002; **17**: 1136-1143

29 **Serra MA**, Escudero A, Rodriguez F, del Olmo JA, Rodrigo JM. Effect of hepatitis C virus infection and abstinence from alcohol on survival in patients with alcoholic cirrhosis. *J Clin Gastroenterol* 2003; **36**: 170-174

30 **Bellentani S**, Saccoccio G, Masutti F, Croce LS, Brandi G, Sasso F, Cristanini G, Tiribelli C. Prevalence of and risk factors for hepatic steatosis in Northern Italy. *Ann Intern Med* 2000; **132**: 112-117

31 **Angulo P**, Lindor KD. Treatment of non-alcoholic steatohepatitis. *Best Pract Res Clin Gastroenterol* 2002; **16**: 797-810

32 **Xie X**, Mann RE, Smart RG. The direct and indirect relationships between alcohol prevention measures and alcoholic liver cirrhosis mortality. *J Stud Alcohol* 2000; **61**: 499-506

Edited by Zhu LH **Proofread by** Chen WW and Xu FM

PO Box 2345, Beijing 100023, China
Fax: +86-10-85381893
E-mail: wjg@wjgnet.com www.wjgnet.com

World J Gastroenterol 2004;10(16):2430-2433
World Journal of Gastroenterology
 ISSN 1007-9327

• BRIEF REPORTS •

Receptor binding characteristics and cytotoxicity of insulin-methotrexate

Xiao-Hong Ou, An-Ren Kuang, Zheng-Lu Liang, Xian Peng, Yu-Guo Zhong

Xiao-Hong Ou, An-Ren Kuang, Zheng-Lu Liang, Department of Nuclear Medicine, West China Hospital of Sichuan University, Chengdu 610041, Sichuan Province, China
Xian Peng, Yu-Guo Zhong, Department of Pharmacy, Sichuan University, Chengdu 610041, Sichuan Province, China
Supported by the National Natural Science Foundation of China, No. 30270415
Correspondence to: Anren Kuang, Department of Nuclear Medicine, West China Hospital of Sichuan University, Chengdu 610041, Sichuan Province, China. ouxiaohong2002@xinhuanet.com
Telephone: +86-28-85422696 **Fax:** +86-28-85422696
Received: 2003-09-06 **Accepted:** 2003-10-07

Abstract

AIM: To characterize the receptor binding affinity and cytotoxicity of insulin-methotrexate (MTX) for the potential utilization of insulin as carriers for carcinoma target drugs.

METHODS: MTX was covalently linked to insulin. Insulin-MTX conjugate was purified by Sephadex G-25 column and analyzed by high performance liquid chromatography. Hepatocellular carcinoma cell membrane fractions were isolated by sucrose density gradient centrifugation. Competitive displacement of ^{125}I-insulin with insulin and insulin-MTX binding to insulin receptors were carried out. Cytoreductive effect of insulin-MTX on human hepatoma BEL7402 cells and human hepatocyte cell line HL7702 was evaluated using the MTT assay.

RESULTS: Insulin-MTX competed as effectively as insulin with ^{125}I-insulin for insulin receptors. The values of Kd for insulin-MTX and insulin were 93.82±19.32 nmol/L and 5.01±1.24 nmol/L, respectively. The value of Kd for insulin-MTX was significantly increased in comparison with insulin (t=7.2532, n=4, P<0.005). Insulin-MTX inhibited the growth of human hepatoma cells (BEL7402) almost as potently as MTX. The inhibitory effect reached a peak on the 5 th day when the growth of cells was inhibited by 79% at a concentration of 5.0 μg/mL insulin-MTX. Treatment with 5.0 μg/mL of MTX and 5.0 μg/mL of insulin-MTX merely resulted in inhibition of HL7702 cells by 31.5% and 7.8% on the 5 th day.

CONCLUSION: Insulin-MTX specifically recognizes insulin receptors and inhibits the growth of BEL7402 cells. These results suggest that insulin can be used as a carrier in receptor mediated carcinoma-targeting therapy.

Ou XH, Kuang AR, Liang ZL, Peng X, Zhong YG. Receptor binding characteristics and cytotoxicity of insulin-methotrexate. *World J Gastroenterol* 2004; 10(16): 2430-2433
http://www.wjgnet.com/1007-9327/10/2430.asp

INTRODUCTION

Methotrexate(MTX), a folic acid analog, is a widely used antimetabolite in cancer chemotherapy. It inhibits dihydrofolate reductase, an enzyme necessary for purine and pyrimidine synthesis. However, MTX also acts on other rapidly dividing cells such as trophoblast cells, which comprise the implantation site of early gestation. Other toxic effects include depression of the bone marrow and damage to the epithelium of the gastrointestinal tract. Selective targeting of therapeutic and diagnostic agents may improve MTX's efficacy and reduce its adverse effects. Existing methods for selective targeting are usually based upon chemical conjugation of agents to cell-specific targeting molecules (e.g. ligands, antibodies).

Receptor mediated endocytosis may provide a pathway by which exogenous molecules are transported into the interior of target cells. In recent years a number of receptors have been used for DNA delivery via receptor-mediated endocytosis, including asialoglycoprotein[1-4], transferrin[5-7], epidermal growth factor (EGF) peptides[8-10], as well as insulin receptor[11-13]. It has been shown that expression of insulin receptor is increased on a variety of malignant tumor cells[14-17]. Insulin can be internalized into nuclei of cells possessing insulin receptors[18-21]. These facts indicate that insulin may be an attractive candidate carrier for anticancer drugs in target therapy of carcinomas.

To reduce side effects and increase safety, we planned to delivery MTX via insulin receptor-mediated endocytosis. In the present study, we conjugated MTX to insulin and characterized the binding activity and cytotoxicity of insulin-MTX complex. Our results suggest that insulin is a suitable candidate carrier for anticancer drugs.

MATERIALS AND METHODS

Radioiodination of insulin

Porcine insulin was radioiodinated using the Ch-T method and purified by polyacrylamide gel electrophoresis. Radiochemical purity of the ^{125}I-insulin was measured by thin layer chromatogram (TLC).

The radiochemical purity of ^{125}I-insulin was 98% and remained over 95% 14 d after stored at -20 °C.

Preparation of insulin-MTX

Insulin-MTX was synthesized by the Department of Pharmacy, Sichuan University. Briefly, MTX (50 mg), EDC (100 mg) and HOBt (50 mg) were dissolved in 3 mL of phosphate-buffered saline (pH = 8.9) and mixed with 1 mL of phosphate-buffered saline (pH = 8.9) containing 25 mg of insulin. The mixture was stirred at 4 °C for 48 h. The precipitation was removed by filtration and pH of the solvent was adjusted to 5.5 with 0.5 mol/L HCL. The reaction mixture was kept at 4 °C overnight. Thereafter, the solution was filtered through a 0.25 μm membrane (Millipore, Germany) and the filtrate was evaporated under vacuum. The products were purified over a 3 cm×45 cm Sephadex G-25 column eluted with 2% ammonium carbonate, and fractions which had the maximal absorbance at 276 nm were collected.

Isolated insulin-MTX was analyzed by analytical HPLC (Beckman) with a 4 mm×200 mm ODS column. The mobile phase was 270 mL/L acetonitrile and 730 mL/L 0.1 mol/L NaH_2PO_4 (pH = 0.3) at a flow rate of 0.5 mL/min.

SDS-polyacrylamine gel electrophoresis (SDS-PAGE) was performed in 150 g/L polyacrylamine gel to calculate the molecular weight of insulin-MTX.

Preparation of cell membrane

Hepatocellular carcinoma specimens were obtained from six patients during surgery whose diagnoses were confirmed by histopathology and immediately frozen at -70 °C. Cell membrane fractions were prepared according to established techniques. Tissues were cut into pieces, put into Tris-HCL buffer (pH 7.5) and homogenized. The cell membrane fractions purified by centrifugation in a discontinuity sucrose density gradient were stored at -70 °C. The protein concentration was determined according to Lowrry method.

Receptor binding assay

The conditions of the assay system were modified according to the method reported earlier. In saturation experiments, the cell membrane fractions (80 μg protein) were incubated with increasing concentrations(5×10^3-5×10^5cpm) of ^{125}I-insulin in the absence (total binding) or presence of the same unlabeled insulin (4.3 nmol/L, nonspecific binding). In competition experiment, the cell membrane fractions (80 μg protein) were incubated with 5 nmol/L ^{125}I-insulin in the absence (total binding) and presence of increasing concentrations (10^{-12}-10^{-7} mol/L) of the unlabeled insulin or insulin-MTX. After incubation for 20 h at 4 °C, free ligands were removed by centrifugation at 2 000 r/min for 10 min after addition of 0.1 mL of 3 g/L bovine γ-globulin and 0.8 mL of 15.8% PEG. Radioactivity of the membrane pellets was determined in a gamma counter for 1 min as the total binding. Specific bindings were obtained by subtracting nonspecific bindings from total bindings.

Cell culture

Human hepatoma BEL7402 cells and human hepatocyte HL7702 cells were grown at 37 °C in a humidified incubator with 50 mL/L CO_2 atmosphere in RPMI1640 (GIBCO BRL) medium containing 100 mL/L of decomplemented FBS, penicillin(100 U/mL) and streptomycin (100 U/mL).

Cell treatment and MTT assay

BEL7402 cells and HL7702 cells were seeded at a density of 10^4 cells per well into 96-well plates. After overnight growth, the medium was removed and RPMI containing different concentrations of insulin-MTX or MTX was added .At given time points, 20 μL of MTT (50 mg/mL) was added to each well. After incubation for 4 h at 37 °C in a humidified 50 mL/L CO_2 atmosphere, the medium was removed and 0.2 mL of DMSO was added. Then, the absorbency at 570 nm was read.

Data calculation and statistical analysis

Binding data were calculated with receptor binding analysis software. Values were presented as mean±SD. Statistical comparisons between the means were made with paired *t*-test at a confidence level of 95%.

RESULTS

Analysis of insulin-MTX

The recovery of insulin-MTX was around 71.5%. HPLC assay indicated that isolated insulin-MTX (retention time 12.08 min) yield was approximately 94% (Figure 1). The rest contained insulin (8.81 min) and MTX (4.16 min).

The calculated molecular weight of insulin-MTX was 6 779 u according to its relative position to the molecular mass marker in SDS-PAGE pattern.

Receptor binding

The binding of insulin receptors to unlabelled insulin and the insulin-MTX conjugate derivative were determined by their ability to compete with free radioactively labelled insulin for receptor sites on cell membranes of hepatocellular carcinoma. We first established the normal binding characteristics of ^{125}I-insulin to cell membranes. Binding took place rapidly in the first 2 h, then slowed down and reached its maximum at approximately 18 h. For all subsequent binding experiments, the incubation time was 20 h at 4 °C. As the concentration of ^{125}I-insulin increased, the binding mounted up and plateaued rapidly.

Similar to insulin, the conjugate competed for the binding sites with ^{125}I-insulin on the insulin receptor in a dose-dependent manner (Figure 2). Binding of ^{125}I-insulin (5 nmol/L) was reduced to 50% in the presence of 5.01±1.24 nmol/L of unlabelled insulin or 93.82±19.32 nmol/L of insulin-MTX, respectively. In contrast, MTX did not compete for binding (data not shown).

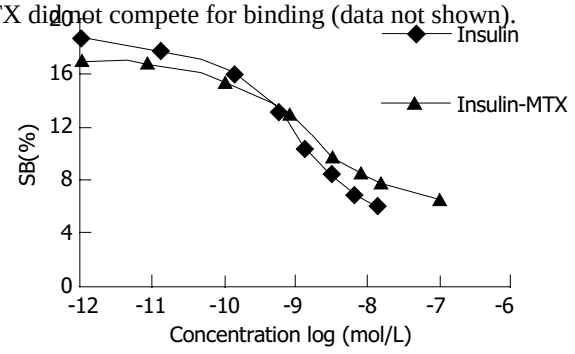

Figure 2 Competitive binding curves of ^{125}I-insulin against insulin-MTX or insulin. The concentration of ^{125}I-insulin was 5 nmol/L. The binding assay was described in the *MATERIALS AND METHODS*.

Inhibition of insulin-MTX complex on cell proliferation

Dose-response curves of insulin-MTX and MTX on BEL7402 and HL7702 cells are shown in Figure 3. Viability was expressed as a percentage of control by dividing the absorbance of each treated well by the average of untreated control. BEL7402 cells

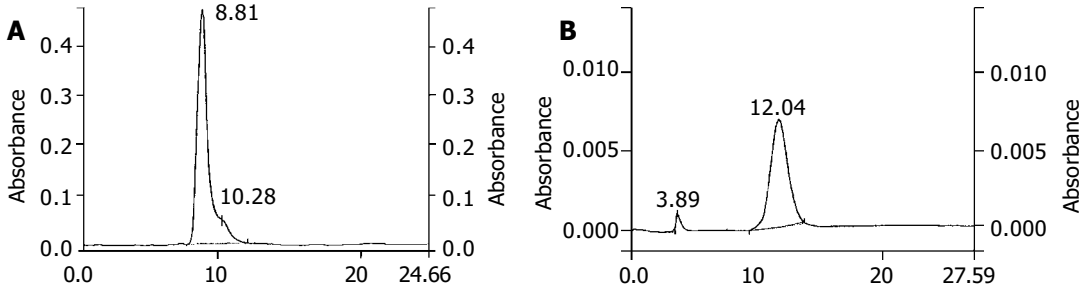

Figure 1 HPLC analysis of insulin and insulin-MTX. The condition was described in *MATERIALS AND METHODS*. Retention time of insulin was 8.81 min. Retention time of insulin-MTX was 12.16 min. A: HPLC analysis of insulin. B: HPLC analysis of insulin-MTX.

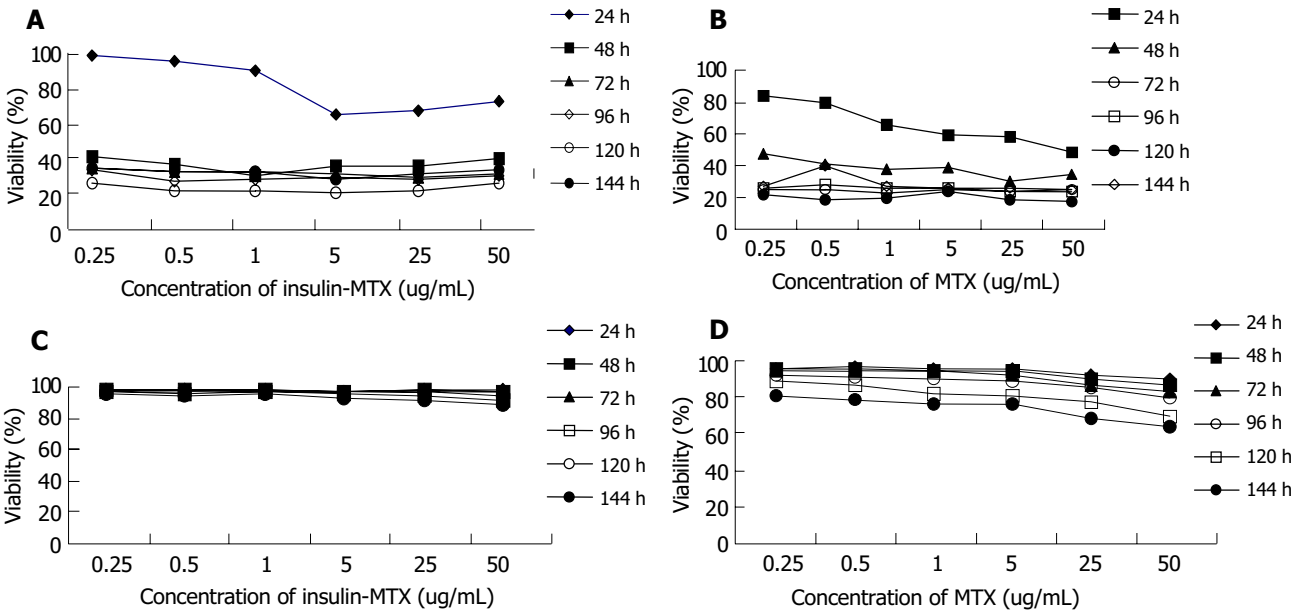

Figure 3 Concentrations of MTX and insulin-MTX in BEL7402 and HL7702 cells. BEL7402 cells and HL7702 cells having cultured overnight were exposed to insulin-MTX or MTX at the indicated concentration for 24 h, 48 h, 72 h, 96 h, 120 h and 144 h respectively. Cell viability was assessed using MTT assay. Viability was expressed as a percentage of control by dividing the absorbance of each treated well by the average of the untreated control. A: Viability of BEL7402 cells treated with insulin-MTX (mean±SD, n = 3), B: Viability of BEL7402 cells treated with MTX (mean±SD, n = 3), C: Viability of HL7702 cells treated with insulin-MTX (mean±SD, n = 3), D: Viability of HL7702 cells treated with MTX (mean±SD, n = 3).

were sensitive to both insulin-MTX and MTX. Cytoreductive effect of MTX and insulin-MTX on BEL7402 cells was concentration-dependent. As early as 24 h, 5.0 μg/mL of insulin-MTX inhibited BEL7402 cell growth by 34.3%, which was relatively lower as compared with 40.6% by 5.0 μg/mL of MTX. The effect reached its peak on the 5 th d, and BEL7402 cells were inhibited by 79% at a concentration of 5.0 μg/mL insulin-MTX and 82.1% at 5.0 μg/mL MTX, respectively. In contrast, treatment with 5.0 μg/mL of MTX and 5.0 μg/mL of insulin-MTX merely resulted in the inhibition of HL7702 cells by 31.5% and 7.8% on the 5th d.

DISCUSSION

The molecule of insulin has sufficient hydroxys and carboxyls that can be used for conjugation with other small molecules. Exploration of the efficiency and specificity of cell entry offered by insulin receptor mediated endocytosis has been proposed previously[22,23]. Here we demonstrated that cross-linking MTX to insulin produced a soluble molecule capable of both specific recognition of the insulin receptors and inhibition of growth of tumor cells, thereby providing a possible tool for target transporting anticancer drugs. The use of insulin as a carrier might offer two advantages. First, most of insulin-MTX could go to tumor cells which overexpress insulin receptors, thus rapidly dividing normal tissues would not be damaged by the drug. Second, tumor cells could develop MTX-resistance frequently via various mechanisms. One of them was due to decreased membrane transport[24-28]. The use of insulin as a carrier might offer an increased MTX transportation into drug-resistant tumor cells.

Since laboratory iodination of insulin with ^{125}I could incur oxidation damage and brings about indiscriminate labelling of tyrosine residues leading to decreased biological activity including aberrant receptor binding, polyacrylamide gel electrophoresis was used to purify monoiodo [^{125}I-Tyr^{A14}] insulin, which was fully active in receptor binding assays[29].Receptor binding analysis showed that insulin-MTX could specifically bind to insulin receptors on human hepatocellular carcinoma. The increased Kd indicated a decreased affinity for receptors, indicating that linking MTX to insulin molecule did interfere with the affinity of insulin-receptor binding. High affinity is one of the most important criteria of tumor-target agents. Decrease in affinity of insulin-MTX for insulin receptors may result from conjugation of MTX with A13 and B17 positions of insulin molecules. These positions are located in the hexamer-forming surface and on the opposite side of the classical binding site, and constitute a second domain of the molecule important for receptor binding[30]. Further studies to improve the affinity of insulin-MTX by modifying the method of conjugation would be needed.

Insulin receptor was considered to play a role in the regulation of hepatocellular carcinoma[31] and there have been reports showing increased insulin receptors expressed on these cells[29,32]. Therefore human hepatoma BEL7402 cell line was selected to measure the cytoreductive effect of insulin-MTX. Our studies showed that BEL7402 cells were sensitive to both insulin-MTX and MTX. However, the molecular weight of insulin-MTX complex was far greater than that of MTX. It was obsered that 0.375 nmoL (1.5×10^{-6} mol/L×0.25 mL) of MTX conjugated to insulin inhibited the growth of BEL7402 cells as effectively as 2.5 nmoL (1×10^{-5} moL /L×0.25 mL) of MTX. HL7702 cells appeared to be less sensitive to both insulin-MTX and MTX, especially to insulin-MTX, when compared with BEL7402 cells. Treatment with 5.0 μg/mL of insulin-MTX resulted in about 10-fold higher toxicity on BEL7402 cells than on HL7702 cells. This may result from the elevated proliferation and the increased expression of insulin receptors of BEL7402 cells. These results indicated that conjugation of insulin could enhance the cytotoxicity of MTX to hepatocarcinoma cells.

Our results showed that the new construct could bind specifically to insulin receptors, but its effect on glucose metabolism depended on the residues with which MTX molecule interacted. An unparalleled relationship of receptor binding and glucose uptake was observed in other insulin analogues and mutants[33,34]. Therefore, it is necessary to test the biological activity of insulin-MTX in glucose metabolism in order to understand its effects on plasma glucose levels. In our study,

SDS-polyacrylamine agarose gel electrophoresis showed the molecular weight of insulin-MTX was 6 779 u, which equaled the mass of one molecule of insulin (M_r = 5 800) and two molecules of MTX (M_r = 454.5). The ratio of insulin molarity to the MTX was estimated to be 1:2. On the basis of this molar ratio, only 20-200 μmoL insulin is required to obtain a high plasma concentration(10-100 μmol/L). Besides, the dose may be reduced because of the targeting ability of insulin-MTX. Even if the conjugates have partial bioactivity in glucose uptake, there is little probability that administration of such a low dose in therapy would result in adverse effects of glucopenia.

In the present study, we demonstrated that insulin-MTX complex could specifically bind to insulin receptors and efficiently inhibit the growth of human hepatoma BEL7402 cells, although the affinity needs to be improved. Receptor-mediated endocytosis has a tremendous potential for delivery of carcinoma target drugs because of the overexpression of insulin receptors on carcinoma tissues.

REFERENCES

1 **Wu J,** Nantz MH, Zern MA. Targeting hepatocytes for drug and gene delivery: emerging novel approaches and applications. *Front Biosci* 2002; **7**: d717-725

2 **Yang Y,** Park Y, Man S, Liu Y, Rice KG. Cross-linked low molecular weight glycopeptide-mediated gene delivery: relationship between DNA metabolic stability and the level of transient gene expression *in vivo*. *J Pharm Sci* 2001; **90**: 2010-2022

3 **Ren T,** Zhang G, Liu D. Synthesis of galactosyl compounds for targeted gene delivery. *Bioorg Med Chem* 2001; **9**: 2969-2978

4 **Han J,** Il Yeom Y**.** Specific gene transfer mediated by galactosylated poly-L-lysine into hepatoma cells. *Int J Pharm* 2000; **202**: 151-160

5 **Qian ZM,** Li H, Sun H, Ho K. Targeted drug delivery via the transferrin receptor-mediated endocytosispathway. *Pharmacol Rev* 2002; **54**: 561-587

6 **Li X,** Fu GF, Fan YR, Shi CF, Liu XJ, Xu GX, Wang JJ. Potent inhibition of angiogenesis and liver tumor growth by administration of an aerosol containing a transferrin-liposome-endostatin complex. *World J Gastroenterol* 2003; **9**: 262-266

7 **Li H,** Q ian ZM. Transferrin / transferrin receptor-mediated drug delivery. *Med Res Rev* 2002; **22**: 225-250

8 **Blessing T,** Kursa M, Holzhauser R, Kircheis R, Wagner E. Different strategies for formation of pegylated EGF-conjugated PEI / DNA complexes for targeted gene delivery. *Bioconjug Chem* 2001; **12**: 529-537

9 **Xu B,** Wiehle S, Roth JA, Cristiano RJ. The contribution of poly-L-lysine, epidermal growth factor and streptavidin to EGF / PLL / DNA polyplex formation. *Gene Ther* 1998; **5**: 1235-1243

10 **Gaidamakova EK,** Backer MV, Backer JM. Molecular vehicle for target-mediated delivery of therapeutics and diagnostics. *J Control Release* 2001; **74**: 341-347

11 **Reddy JA,** Low PS. Folate-mediated targeting of therapeutic and imaging agents to cancers. *Crit Rev Ther Drug Carrier Syst* 1998; **15**: 587-627

12 **Sobolev AS**, Rosenkranz AA, Smirnova OA, Nikitin VA, Neugodova GL, Naroditsky BS, Shilov IN, Shatski IN, Ernst LK. Receptor-mediated transfection of murine and ovine mammary glands *in vivo*. *J Biol Chem* 1998; **273**: 7928-7933

13 **Zhang Y**, Boado RJ, Pardridge WM. Marked enhancement in gene expression by targeting the human insulin receptor. *J Gene Med* 2003; **5**: 157-163

14 **Kalli KR**, Falowo OI, Bale LK, Zschunke MA, Roche PC, Conover CA. Functional insulin receptors on human epithelial ovarian carcinoma cells:implications for IGF-II mitogenic signaling. *Endocrinology* 2002; **143**: 3259-3267

15 **Vella V**, Sciacca L, Pandini G, Mineo R, Squatrito S, Vigneri R, Belfiore A. The IGF system in thyroid cancer: new concepts. *Mol Pathol* 2001; **54**: 121-124

16 **Maune S**, Gorogh T. Detection of overexpression of insulin receptor gene in laryngeal carcinoma cells by using differential display method. *Inootologie* 2000; **79**: 438-441

17 **Frittitta L**, Vignori R, Stampfer MR, Goldfine ID. Insulin receptor overexpression in 184B5 human mamary epithelial cells induces a ligand-dependent transformed phenotype. *J cell Biochem* 1995; **57**: 666-669

18 **Shah N**, Zhang S, Harada S, Smith RM, Jarett L. Electron microscopic visualization of insulin translocation into the cytoplasm and nuclei of intact H35 hepatoma cells using covalently linkedNanogold-insulin. *Endocrinology* 1995; **136**: 2825-2835

19 **Radulescu RT,** Doklea ED, Kehe K, Muckter H. Nuclear colocalization and complex formation of insulin with retinoblastoma protein in HepG2 human hepatoma cells. *J Endocrinol* 2000; **166**: R1-4

20 **Harada S,** Smith RM, Jarett L. Mechanisms of nuclear translocation of insulin. *Cell Biochem Biophys* 1999; **31**: 307-319

21 **Zacksenhaus E,** Jiang Z, Hei YJ, Phillips RA, Gallie BL. Nuclear localization conferred by the pocket domain of the retinoblastoma gene product. *Biochim Biophys Acta* 1999; **1451**: 288-296

22 **Zhang Y,** Jeong Lee H, Boado RJ, Pardridge WM. Receptor-mediated delivery of an antisense gene to human brain cancer cells. *J Gene Med* 2002; **4**: 183-194

23 **Ivanova MM**, Rosenkranz AA, Smirnova OA, Nikitin VA, Sobolev AS, Landa V, Naroditsky BS, Ernst LK. Receptor-mediated transport of foreign DNA into preimplantation mammalian embryos. *Mol Reprod Dev* 1999; **54**: 112-120

24 **Nestle FO,** Alijagic S, Gilliet M, Sun Y, Grabbe S, Dummer R, Burg G, Schadendorf D. Vaccination of melanoma patients with peptide- or tumor lysate-pulsed dendritic cells. *Nat Med* 1998; **4**: 328-332

25 **Thurner B**, Haendle I, Roder C, Dieckmann D, Keikavoussi P, Jonuleit H, Bender A, Maczek C, Schreiner D, von den Driesch P, Brocker EB, Steinman RM, Enk A, Kampgen E, Schuler G. Vaccination with mage-3A1 peptide-pulsed mature, monocyte-derived dendritic cells expands specific cytotoxic T cells and induces regression of some metastases in advanced stage IV melanoma. *J Exp Med* 1999; **190**: 1669-1678

26 **Wu TC,** Guarnieri FG, Staveley-O'Carroll KF, Viscidi RP, Levitsky HI, Hedrick L, Cho KR, August JT, Pardoll DM. Engineering an intracellular pathway for major histocompatibility complex class II presentation of antigens. *Proc Natl Acad Sci U S A* 1995; **92**: 11671-11675

27 **Asai S,** Miyachi H, Kobayashi H, Takemura Y, Ando Y. Large diversity in transport-mediated methotrexate resistance in human leukemia cell line CCRF-CEM established in a high concentration of leucovorin. *Cancer Sci* 2003; **94**: 210-214

28 **Sierra EE,** Goldman ID. Recent advances in the understanding of the mechanism of membrane transport of folates and antifolates. *Semin Oncol* 1999; **26**(2 Suppl 6): 11-23

29 **Kurtaran A**, Li SR, Raderer M, Leimer M, Muller C, Pidlich J, Neuhold N, Hubsch P, Angelberger P, Scheithauer W, Virgolini I. Technetium-99m-galactocyl- neoglycoalbumin combined with iodine-123-Tyr-(A14) insulin visualizes human hepatocellular carcinomas. *J Nucl Med* 1995; **36**: 1875 -1880

30 **Beavis RC**, Kneirman MD, Sharknas D, Heady MA, Frank BH, DeFelippis MR. A novel protein cross-linking reaction in stressed Neutral Protamine Hagedorn formulations of insulin. *J Pharm Sci* 1999; **88**: 331-336

31 **Scharf JG**, Dombrowski F, Ramadori G. The IGF axis and hepatocarcinogenesis. *Mol Pathol* 2001; **54**: 138-144

32 **Spector SA**, Olson ET, Gumbs AA, Friess H, Buchler MW, Seymour NE. Human insulin receptor and insulin signaling proteins in hepatic disease. *J Surg Res* 1999; **83**: 32-35

33 **Guo ZY,** Shen L, Gu W, Wu AZ, Ma JG, Feng YM. *In vitro* evolution of amphioxus insulin-like peptide to mammalian insulin. *Biochemistry* 2002; **41**: 10603-10607

34 **Liao ZY,** Tang YH, Xu MH, Feng YM, Zhu SQ. B9-serine residue is crucial for insulin actions in glucose metabolism. *Acta Pharmacol Sin* 2001; **22**: 939-943

Edited by Zhu LH and Wang XL **Proofread by** Xu FM

PO Box 2345, Beijing 100023, China
Fax: +86-10-85381893
E-mail: wjg@wjgnet.com www.wjgnet.com

World J Gastroenterol 2004;10(16):2434-2438
World Journal of Gastroenterology
 ISSN 1007-9327

• BRIEF REPORTS •

Analysis of multiple factors of postsurgical gastroparesis syndrome after pancreaticoduodenectomy and cryotherapy for pancreatic cancer

Ke Dong, Bo Li, Quan-Lin Guan, Tao Huang

Ke Dong, Bo Li, Quan-Lin Guan, Tao Huang, Department of General Surgery, West China Hospital, Sichuan University, Chengdu 610041, Sichuan Province, China
Supported by the Research Foundation of Department of Health of Sichuan Province, No. 000050
Correspondence to: Dr. Bo Li, Department of General Surgery, West China Hospital, Sichuan University, Chengdu 610041, Sichuan Province, China. cdlibo@medmail.com
Telephone: +86-28-85422476
Received: 2003-11-21 **Accepted:** 2004-02-01

Abstract

AIM: To explore the etiology, pathogenesis, diagnosis, and treatment of postsurgical gastroparesis syndrome (PGS) after pancreatic cancer cryotherapy (PCC) or pancreaticoduodenectomy (PD), and to analyze the correlation between the multiple factors and PGS caused by the operations.

METHODS: Clinical data of 210 patients undergoing PD and 46 undergoing PCC were analyzed retrospectively.

RESULTS: There were 31 (67%, 31/46) patients suffering PGS in PCC group, including 29 with pancreatic head and uncinate tumors and 2 with pancreatic body and tail tumors. Ten patients (4.8%, 10/210) developed PGS in PD group, which had a significantly lower incidence of PGS than PCC group (χ = 145, P<0.001). In PCC group, 9 patients with PGS were managed with non-operative treatment (drugs, diet, nasogastric suction, *etc.*), and one received reoperation at the 16th day, but the symptoms were not relieved. In PD group, all the patients with PGS were managed with non-operative treatment. The PGS in patients undergoing PCC had close association with PCC, tumor location, but not with age, gender, obstructive jaundice, hypoproteinemia, preoperative gastric outlet obstruction and the type and number of gastric biliary tract operations. The mechanisms of PGS caused by PD were similar to those of PGS following gastrectomy. The damage to interstitial cells of Cajal might play a role in the pathogenesis of PGS after PCC, for which multiple factors were possibly responsible, including ischemic and neural injury to the antropyloric muscle and the duodenum after freezing of the pancreatico-duodenal regions or reduced circulating levels of motilin.

CONCLUSION: PGS after PCC or PD is induced by multiple factors and the exact mechanisms, which might differ between these two operations, remain unknown. Radiography of the upper gastrointestinal tract and gastroscopy are main diagnostic modalities for PGS. Non-operative treatments are effective for PGS, and reoperation should be avoided in patients with PGS caused by PCC.

Dong K, Li B, Guan QL, Huang T. Analysis of multiple factors of postsurgical gastroparesis syndrome after pancreaticoduodenectomy and cryotherapy for pancreatic cancer. *World J Gastroenterol* 2004; 10(16): 2434-2438
http://www.wjgnet.com/1007-9327/10/2434.asp

INTRODUCTION

Postsurgical gastroparesis syndrome (PGS) is a complex disorder characterized by postprandial nausea, vomiting, and gastric atony in the absence of mechanical gastric outlet obstruction. Patients frequently suffer marked weight loss and malnutrition that require hospitalization and prolonged parenteral nutrition (PN). These symptoms can be disabling and often fail to be alleviated by drug therapy, for which gastric reoperations usually prove unsuccessful. An identified cause for PGS has not been available, nor is its mechanism quite clarified. PGS after gastrectomy or pancreatoduodenectomy (PD) has been reported in a number of literatures[1-5]. Based on the results of clinical investigations[6-9], cryosurgery targeting at the pancreaticoduodenal region was considered safe and effective for unresectable pancreatic cancer. However, PGS caused by cryotherapy for pancreatic cancer (PCC), to our knowledge, has not been reported. As a unique complication of PCC, gastric stasis occurs in the early postoperative period in most of cases receiving PCC (67%), resulting in long-term loss of a large amount of gastric juice and delayed recovery of oral food intake, and occasionally, excessive gastric juice loss leads to body fluid deficit and metabolic alkalosis. To define the factors contributing to the development of PGS following PD or PCC, we performed this study to retrospectively examine the clinical data of 210 patients undergoing PD and 46 undergoing PCC.

MATERIALS AND METHODS

Subjects

From January 1990 to June 2003, 210 patients (147 male and 63 female patients, aged 35 to 75 years with a mean of 53.6 years) received PD in our hospital for pancreatic cancer or periampullary adenocarcinoma. None of the patients were preoperatively identified to have mechanical gastric outlet obstruction, but 95 had obstructive jaundice and 15 had hypoproteinemia.

During the period between January 1995 to March 2003, another 46 patients (including 31 male and 15 female patients, aged between 39 and 78 years with a mean of 54 years) underwent PCC for unresectable advanced pancreatic cancer, located in the pancreatic head in 21 cases, in the uncinate process in 15 cases, and in the pancreatic body and tail in 10 cases. All the tumors were identified by preoperative helical computed tomography (CT) scan and by intraoperative exploration, including 31 tumors with local involvement and 15 metastatic tumors. Preoperatively, 34 patients were identified to have obstructive jaundice and 6 had hypoproteinemia. All the patients, excluding the 8 with preoperative duodenal obstruction, were free of preoperative mechanical gastric outlet obstruction. Gastrojejunostomy was performed in 37 cases, and cholecystojejunostomy or choledochojejunostomy done in 32 cases during PCC for relief or prevention of the common bile duct and gastric outlet obstruction. Four patients also had concurrent splanchnicectomy with ethanol.

Endoscopy or radiography was employed to identify and exclude cases of mechanical gastric outlet obstruction, and also to detect such problems of anastomotic stricture, efferent

limb obstruction, and jejunogastric intussusception *etc*., as well as food retention after a 4- to 8-h fast, for validating the diagnosis of gastroparesis.

Diagnostic criteria for PGS

At present, consensus has not been reached on the criteria for diagnosis of PGS. Stanciu[10] suggested using gastric scintigraphy with ^{99}Tc-labeled low-fat meal as the gold standard for diagnosing delayed gastric emptying, which utilized gamma camera imaging of the abdomen following the ingestion of a radiolabeled meal, performed at regular intervals of 2 to 4 h to quantify the meal emptying in terms of percentages. Typically, meal emptying of over 50% within 2 h was considered normal, whereas delayed gastric emptying was indicated if gastric retention greater than 10% at 4 h. In this study, we formulated practical diagnostic criteria for PGS after consultation of the previous documentations in the literature[5-7,10], as the following: (1) Absence of mechanical gastric outlet obstruction identified by one or more medical examination modalities; (2) A volume of gastric juice aspirate exceeding 800 mL/d that sustained for more than 10 d; (3) No abnormalities in water, electrolytes, or acid-alkali balance. (4) Absence of underlying diseases causing gastroparesis, such as diabetes, chorionitis, hypothyrosis, *etc*. (5) No history of using such agents as morphine, atropine, *etc*. that affected contraction function of the smooth muscle.

Surgical procedures

In PD group, the organs resected during PD included the gallbladder, common bile duct, head of the pancreas, the entire duodenum, with also subtotal gastrectomy. Proximal jejunum of 10 to 15 cm was also resected. The alimentary and biliary tracts were reconstructed with methods of Child or Whipple.

In patients of PCC group that defied surgical resection of the tumor, cryoprobes were deployed directly into the tumor for freezing to -196 °C twice, lasting for 10-15 min (using LCS 2000 cryogenic surgical system), with the common bile duct, stomach, and jejunum protected by dry cotton pads. Subsequent gastroenteroanastomosis, cholecystojejunostomy, or choledochojejunostomy were performed to reconstruct the alimentary and biliary tracts, according to the findings by intraoperative exploration. Care was taken to avoid freezing of the duodenal wall or causing other iatrogenic injuries such as damage to the biliary system or gastroduodenal artery. Jejunostomy was performed in some cases highly suspected of gastroparesis after PCC for postoperative enteral nutrition (EN) support.

Statistical analysis

The incidence of PGS in the two groups was compared and multiple factors were analyzed using χ^2 test. A P value less then 0.05 was considered statistically significant.

RESULTS

No serious complications took place in the PCC group, nor did operative death or complications occur in relation to the anastomosis. None of the patients developed fistula or pancreatitis. There was only transient elevation of amylase following the operation and the liver function and blood sugar remained normal. In PD group, in contrast, 4 patients developed serious complications after PD, including leakage at the pancreatojejunostomy in 2, bleeding at the anastomosis in 2 cases, stenosis of the anastomosis in 1 and stress peptic ulcer in 1 case. The mortality rate of PD in the perioperative period was 1.5%.

Ten of the 210 patients in PD group presented PGS within 5-10 d postoperatively. PGS developed in 31 of the 46 patients in PCC group, occurring within 5-7 d after the operation, including 29 patients with pancreatic head and uncinate tumors and 2 with pancreatic body and tail tumors. In PD group, 14 patients with PGS received non-operative treatment such as medication, diet therapy, and nasogastric suction *etc*, and 1 patient underwent reoperation on postoperative day 16, which, however, failed to relieve the symptoms. All patients with PGS in PCC group received non-operative treatment. Altogether 41 patients developed PGS in the two groups according to our diagnostic criteria, 15 of these cases were identified 4-7 d after withdrawal of the nasogastric tube and 10 were found to have a gradually increasing volume of gastric juice aspirate to 800 mL/d till 3-7 d after operation. Twenty of the 40 patients developed PGS 2-3 d after intake of liquid or semiliquid diet. Furthermore, the volume of gastric juice suction exceeded 2 000 mL/d in 4 cases following PCC and persisted for ten or more days (Table 1).

PGS following cryosurgery was closely associated with PCC, tumor location, but not with age, gender, obstructive jaundice, hypoproteinemia, preoperative gastric outlet obstruction or the type and number of gastric biliary tract operations (Table 2). PGS following PD was related with age, hypoproteinemia, preoperative gastric outlet obstruction and the type and number of gastric operations performed. Patients undergoing PCC were more likely to develop PGS than those undergoing PD (67% *vs* 4.8%, $\chi = 145$, $P<0.001$).

DISCUSSION

Many debates over the etiology and pathophysiology of PGS remain unresdved. Clinically, the frequency of this complication varies in close association with the type and number of gastric operations performed. Donahue *et al*.[11] reported a 26% incidence of chronic morbidity in patients after truncal vagotomy and antrectomy compared with a 5% incidence after highly selective vagotomy. There also appears to be a greater incidence of PGS associated with antrectomy and Roux-en-Y reconstruction compared with more conventional Billroth I and Billroth II reconstructions. Therefore, the main factor contributing to PGS is denervation and the consequent atony of the gastric remnant rather than disruption of the pacemaker activity in the Roux limb.

The exact mechanisms responsible for PGS after gastric surgery remain unclear but are likely to be multifactorial. The loss of gastric parasympathetic control resulted from vagotomy contributes to PGS via several mechanisms. In the proximal stomach, loss of vagal control leads to accelerated emptying of liquids by disrupting the late-stage tonic contractions responsible for relaxation and accommodation of the gastric fundus. In the distal stomach, vagotomy weakens antral peristaltic contraction responsible for breakdown of chyme. When coupled with the observed decrease in intestinal secretion of prokinetic hormones seen after truncal vagotomy, this leads to delayed emptying of solid substances. Also, the loss of vagal suppression of the ectopic intestinal pacemakers may cause dissociation of the antral pressure waves from the duodenal waves. The consequent disruption of wave sequence prolongs the lag phase of solid food digestion during which food is broken down into small particles by retropulsion and further delays the digestive process[12,13].

Recently, it has been recognized that interstitial cells of Cajal generate electrical pacemaker activity and mediate motor neurotransmission in the stomach. The interstitial cells of Cajal are located in the muscular wall of the gastric corpus and antrum. Gastric dysrhythmias (tachygastrias and bradygastrias) are disturbances of the normal gastric pacesetter potentials and are associated with such symptoms as nausea, epigastric fullness, bloating and delayed gastric emptying. Ordog *et al*.[14] suggest that damage to interstitial cells of Cajal may play a key role in the pathogenesis of diabetic gastropathy. Meanwhile, Zarate *et al*.[15] reported that histological and immunohistochemical

Table 1 Clinical data of the PGS cases

Patient No	Gender	Age (yr)	Operation type	Mean volume of gastric juice aspirate / d (mL)	Period of nasogastric tube aspirate(d)	Period of recovery (d)	Outcome
1	M	53	PCC+A+B	2 200	56	70	Recovery
2	F	39	PCC+B	1 200	13	28	Recovery
3	F	62	PCC+A+C	1 000	10	14	Recovery
4	M	60	PCC+A+C	1 000	21	21	Recovery
5	M	51	PCC+A	850	10	30	Recovery
6	M	61	PCC+A+B	1 250	15	26	Recovery
7	M	62	PCC+A+C	1 200	13	35	Recovery
8	F	60	PCC+C	1 300	11	43	Recovery
9	F	40	PCC+A+B	2 000	25	25	Recovery
10	F	61	PCC +C	1 200	19	14	Recovery
11	M	64	PCC+A+B	1 200	18	Death on d 13 for diabetes complication	Death
12	F	78	PCC	1 500	19	Discharged on d 24[1]	Recovery
13	M	50	PCC+A+C	1 050	12	49	Recovery
14	M	50	PCC+A+C	1 400	15	Transferred to another hospital on d 16	Recovery
15	M	42	PCC	1 450	17	14	Recovery
16	M	46	PCC+A+C	2 000	18	21	Recovery
17	M	43	PCC+A+B	1 200	13	20	Recovery
18	M	73	PCC +B	800	10	19	Recovery
19	M	46	PCC	1 350	14	18	Recovery
20	M	62	PCC+A+B+D	900	11	19	Recovery
21	M	40	PCC+A+C	1 300	15	20	Recovery
22	F	50	PCC +C	2 050	24	32	Recovery
23	F	61	PCC+A+C	1 200	15	20	Recovery
24	M	39	PCC+A+B	1 000	12	Discharged on d 16[1]	Recovery
25	M	53	PCC+A	1 050	13	17	Recovery
26	F	42	PCC+A+B	900	11	18	Recovery
27	M	60	PCC+A+C	1 800	19	25	Recovery
28	M	62	PCC	1 700	20	30	Recovery
29	M	60	PCC+A+C	1 050	12	20	Recovery
30	M	40	PCC+A+C	1 250	12	17	Recovery
31	F	64	PCC+A+B	1 300	13	31	Recovery
32	M	75	PD	1 200	12	16	Recovery
33	F	42	PD	850	10	15	Recovery
34	F	35	PD	1 050	10	19	Recovery
35	M	45	PD	1 250	11	Death on d 16 for complications	Death
36	F	48	PD	1 050	11	17	Recovery
37	M	56	PD	1 450	16	21	Recovery
38	M	60	PD	1 400	14	20	Recovery
39	F	65	PD	1 500	15	20	Reoperation at 16th d
40	M	47	PD	1 250	13	18	Recovery
41	M	63	PD	1 600	16	21	Recovery
mean±SD		53.8±13		1 180±310	15.5±6	23.1±9	

A: Gastroenteroanastomosis; B: Cholecystojejunostomy; C: Choledochojejunostomy; D: Chemical splanchnicectomies. [1]Discharged on request by the patient.

study of the resected specimen showed hypoganglionosis, neuronal dysplasia, and marked reduction in both myenteric and intramuscular interstitial cells of Cajal in patients with idiopathic gastroparesis.

Certainly, PGS after gastric surgery also can be due to muscular, neural, or humoral abnormalities. Hypothyroidism and diabetes[4] have been identified as contributing factors to gastroparesis in some patients. In patients without an identified cause, the gastroparesis is labeled as idiopathic. The mechanisms of PGS following PD is similar to that after gastrectomy.

Table 2 Correlation between multiple factors and PGS after PCC

Group	Age (yr)		Gender		Hypoproteinemia		Jaundice		Surgical procedure		Tumor location		Outlet obstruction	
	60	<60	M	F	Y	N	Y	N	PCC+A (or B, C, D)	PCC	Head and uncinate	Body and tail	Y	N
PGS	15	16	21	10	2	29	22	9	27	4	29	2	5	26
NO PGS	7	8	10	5	4	11	12	3	12	3	7	8	3	12
P	NS		NS		NS		NS		NS		<0.05		NS	

NS: No-significant.

The results of our observations suggest no significant direct relation of PGS following PCC with the types of gastric operations or the loss of gastric parasympathetic control, nor was it related to the patients' age or presence of hypoproteinemia or preoperative gastric outlet obstruction (Table 2), which, however, might be the factors contributing to PGS after gastrectomy or PD[1-5]. We therefore suggest that the mechanism of PGS after PCC may differ, at least partially, from that underlying the PGS following gastrectomy or PD.

Patients with tumors located in the pancreatic head and uncinate process are at higher risk to develop PGS following PCC than those with tumors in the pancreatic body and tail (Table 2). The interstitial cells of Cajal in the muscular wall of the gastric corpus and antrum are exposed to likely damage during the freezing of the pancreatico-duodenal area, which offers a possible explanation for the pathogenesis of PGS after PCC.

Pylorus-preserving pancreatoduodenectomy (PPPD) frequently results in gastric stasis[12,16], which occurs in 20% to 50% of the patients during the early postoperative period. As the duodenum has proved to be important in the initiation and consolidation of phase III activity of the migrating motor complex (MMC) of the stomach, its removal severely undermines the gastric phase III, hence gastric stasis may occur. On the basis of their findings that patients undergoing PPPD had slower recovery of gastric phase III and lower plasma motilin concentrations than those undergoing duodenum-preserving pancreatic head resection, Matsunaga *et al*.[16] concluded that PGS after PPPD might be attributed, at least in part, to delayed recovery of gastric phase III activity due to lowered concentrations of plasma motilin after resection of the duodenum. However, resection of the pancreas does not seem to affect gastrointestinal motility. Malfertheiner and Sarr[17] reported that even a total pancreatectomy failed to obviously affect the motor activity of the entire upper gastrointestinal tract in dogs.

We found in this study that PGS developed in 67% of all patients after PCC through multifactorial mechanisms, which could be at least partially in common with those underlying the PGS resulted from PPPD. The possible factors responsible for PGS after PCC include ischemic and neural injury to the antropyloric muscles and the duodenum after freezing of the pancreatico-duodenal area (but not to direct freezing of the duodenal pacemaker) and reduced circulating levels of motilin originally produced by the enterochromaffin cells in the duodenum and proximal jejunum. The peak plasma motilin concentration occurs in line with phase III activity of the interdigestive MMC in the stomach and duodenum. The phase III starts in the gastroduodenal region and migrates downward along the small intestine, hence its nickname the "housekeeper". The housekeeper function of phase III may be important to empty the gastric juice in the postoperative period after PCC. As the duodenum plays a role in the initiation and consolidation of gastric phase III, the injury of the duodenum by freezing -and thus the interruption of gastric phase III- may be one of the several possible causes of PGS after PCC. But still, the above hypotheses currently have to remain hypothetical, and the exact mechanisms of PGS caused by PCC must await further investigation.

Patients with PGS have non-specific symptoms of early satiety, postprandial bloating, nausea, and vomiting, and the volume of gastric juice suction in most of them can increase gradually during early postoperative period. The diagnosis of PGS is often difficult to confirm. In the absence of identifiable anatomic problems such as anastomotic stricture, efferent limb obstruction, or jejunogastric intussusception, other causes of gastric dystonia must be carefully examined. Hypothyroidism has been identified as a contributing factor to gastroparesis in some patients. Gastroparesis can also occur in patients with diabetes[18,19]. Several complementary diagnostic modalities may be used to confirm the diagnosis of PGS. Fiberoptic endoscopy or radiography of the upper gastrointestinal tract should be performed routinely to exclude anatomical causes of gastric outlet obstruction. Radionuclide GESs can also be necessary, for clinical evaluation and conventional radiographic studies are often unreliable. If endoscopy and radionuclide scintigraphy are inconclusive, a small bowel contrast study should be performed to rule out possible mechanical lesions and/or generalized gut hypomotility. Although not routinely available[20], electromyography of the gastrointestinal tract may provide valuable assistance in the diagnosis of patients with complex motility disturbances.

As the treatment of gastroparesis is far from ideal, nonconventional approaches and nonstandard medications might be of use. Traditional medical therapy consists of behavioral and diet modification, nasogastric tube suction and the use of prokinetic drugs such as bethanecol, metoclopramide, erythromycin and the more recent cisapride[10]. Dietary measures and prokinetic drugs may help relieve the symptoms in most patients, while some patients with severe nausea and vomiting require antiemetic medications. A few patients fail medical therapy and continue to have debilitating symptoms of gastroparesis, who may benefit from a venting gastrostomy[18] or jejunostomy performed surgically, endoscopically, or fluoroscopically[20]. Near-completion gastrectomy (NCG) has proved useful in small series of patients[21], but data on long-term follow-up has been lacking. Gastric electrical stimulation can be of value in the management of gastroparesis[22-24], in which the patients with PGS received continuous high-frequency/low-energy gastric electrical stimulation via electrodes deposited in the muscular wall of the antrum and connected to a neurostimulator in an abdominal wall pocket. This method produced entrainment of the intrinsic slow wave and promoted contractions in phase III with the normal slow wave. This is why a suitable stimulation to the stomach during gastroscopic examination is also helpful for the remission of PGS[3-5]. In this study, 5 patients received gastroscopic examination and the symptoms were markedly relieved. Ten patients with PGS were treated with acupuncture, and the effects were satisfactory.

According to our experience, all patients of PGS caused by PD or PCC need to undergo a long period of nasogastric suction till the clinical symptom relief or recovery occurs. The patients may experience epigastric fullness, nausea, or even vomiting, if

the nasogastric tube is withdrawn too early. Therefore, almost all of the patients with PGS in this study received the gastric juice suction over an average period of 2.2 wk, with the longest exceeding 8 wk. Because of long-term absence of food intake, these patients required nutritional support with a feeding jejunostomy tube or underwent a period of parenteral nutrition. The jejunostomy tube, as we believe, is safe, economic and practical for nutrition support in such patients, because their small intestinal peristaltic contractions and absorption function were normal in spite of PGS. Clinically, almost all of the patients had a concurrent jejunostomy during cryosurgery, considering the likeliness of these patients to develop delayed gastric emptying and for administration of postoperative enteral nutrition support. We consider that the non-operative treatments are effective for PGS after PCC or PD, and gastric reoperations should be avoided.

REFERENCES

1 **Naritomi G,** Tanaka M, Matsunaga H, Yokohata K, Ogawa Y, Chijiiwa K, Yamaguchi K. Pancreatic head resection with and without preservation of the duodenum: Different postoperative gastric motility. *Surgery* 1996; **120**: 831-837

2 **Toyota N,** Takada T, Yasuda H, Amano H, Yoshida M, Isaka T, Hijikata H, Takada K. The effects of omeprazole, a proton pump inhibitor, on early gastric stagnation after a pylorus-preserving pancreaticoduodenectomy: results of a randomized study. *Hepatogastroenterology* 1998; **45**: 1005-1010

3 **Cai YT**, Qin XY. Clinical, analysis of 15 cases with gastroparesis after radicalgastrectomy. *Zhongguo Shiyong Waike Zazhi* 1999; **19**: 338-340

4 **Qin XY**, Lei Y. Functional delayed gastric emptying after gastrectomy. *Zhongguo Weichang Waike Zazhi* 2000; **3**: 7-9

5 **Lui FL**, Qin XY. Clinical analysis of 20 cases with postsurgical gastroparesis syndrome after radical subtotal gastrectomy. *Zhonghua Weichang Waike Zazhi* 2002; **5**: 245-248

6 **Kovach SJ,** Hendrickson RJ, Cappadona CR, Schmidt CM, Groen K, Koniaris LG, Sitzmann JV. Cryoablation of unresectable pancreatic cancer. *Surgery* 2002; **131**: 463-464

7 **Patiutko IuI,** Barkanov AI, Kholikov TK, Lagoshnyi AT, Li LI, Samoilenko VM, Afrikian MN, Savel'eva EV. The combined treatment of locally disseminated pancreatic cancer using cryosurgery. *Vopr Onkol* 1991; **37**: 695-700

8 **Li B**. the current status of combined treatment for pancreatic carcinoma. *Zhongguo Puwai Jichu Yu Linchuang Zazhi* 2000; **7**: 390-392

9 **Chen XL,** Wang D, Yan LN, Li B, Wang XY, Yang BY. Experimental study of cryosurgery for isolated pancreano-duodinal area: a possible therapy for pancreano-duodinal neoplasm. *Zhongguo Puwai Jichu Yu Linchuang Zazhi* 1998; **5:** 324-325

10 **Stanciu GO.** Gastroparesis and its management. *Rev Med Chir Soc Med Nat Iasi* 2001; **105**: 451-456

11 **Donahue PE,** Bombeck CT, Condon RE, Nyhus LM. Proximal gastric vagotomy *versus* selective vagotomy with antrectomy: Results of a prospective, randomized clinical trial after four to twelve years. *Surgery* 1984; **96**: 585-590

12 **Horowitz M,** Dent J, Fraser R, Sun W, Hebbard G. Role and integrationt mechanisms controlling gastric emptying. *Dig Dis Sci* 1994; **39**(Suppl 12): 7S-13S

13 **Schirmer BD.** Gastric atony and the Roux syndrome. *Gastroenterol Clin North Am* 1994; **23**: 327-343

14 **Ordog T,** Takayama I, Cheung WK, Ward SM, Sanders KM. Remodeling of networks of interstitial cells of Cajal in a murine model of diabetic gastroparesis. *Diabetes* 2000; **49**: 1731-1739

15 **Zarate N,** Mearin F, Wang XY, Hewlett B, Huizinga JD, Malagelada JR. Severe idiopathic gastroparesis due to neuronal and interstitial cells of Cajal degeneration: pathological findings and management. *Gut* 2003; **52**: 966-970

16 **Matsunaga H,** Tanaka M, Takahata S, Ogawa Y, Naritomi G, Yokohata K, Yamaguchi K, Chijiiwa K. Manometric evidence of improved early gastric stasis by erythromycin after pylorus-preserving pancreatoduodenectomy. *World J Surg* 2000; **24**: 1236-1242

17 **Malfertheiner P,** Sarr MG, Dimagno EP. Role of the pancreas in the control of interdigestive gastrointestinal motility. *Gastroenterology* 1989; **96**: 200-205

18 **Watkins PJ,** Buxton-Thomas MS, Howard ER. Long-term outcome after gastrectomy for intractable diabetic gastroparesis. *Diabet Med* 2003; **20**: 58-63

19 **Lehmann R,** Honegger RA, Feinle C, Fried M, Spinas GA, Schwizer W. Glucose control is not improved by accelerating gastric emptying in patients with type 1 diabetes mellitus and gastroparesis. A pilot study with cisapride as a model drug. *Exp Clin Endocrinol Diabetes* 2003; **111**: 255-261

20 **Koch KL.** Electrogastrography: physiological basis and clinical application in diabetic gastropathy. *Diabetes Technol Ther* 2001; **3**: 51-62

21 **Jones MP,** Maganti K. A systematic review of surgical therapy for gastroparesis. *Am J Gastroenterol* 2003; **98**: 2122-2129

22 **Abell T**, Lou J, Tabbaa M, Batista O, Malinowski S, Al-Juburi A. Gastric electrical stimulation for gastroparesis improves nutritional parameters at short, intermediate, and long-term follow-up. *J Parenter Enteral Nutr* 2003; **27**: 277-281

23 **Lin Z,** Forster J, Sarosiek I, McCallum RW. Treatment of gastroparesis with electrical stimulation. *Dig Dis Sci* 2003; **48**: 837-848

24 **Lawlor PM,** McCullough JA, Byrne PJ, Reynolds JV. Electrogastrography: a non-invasive measurement of gastric function. *Ir J Med Sci* 2001; **170**: 126-131

Edited by Chen WW **Proofread by** Zhu LH and Xu FM

PO Box 2345, Beijing 100023, China
Fax: +86-10-85381893
E-mail: wjg@wjgnet.com www.wjgnet.com

World J Gastroenterol 2004;10(16):2439-2443
World Journal of Gastroenterology
 ISSN 1007-9327

• BRIEF REPORTS •

Simultaneous detection of HBV and HCV by multiplex PCR normalization

Ning Wang, Xue-Qin Gao, Jin-Xiang Han

Ning Wang, Xue-Qin Gao, Jin-Xiang Han, Shandong Medicinal Biotechnological Center, Shandong Academy of Medical Sciences; Key Laboratory for Biotechdrugs, Ministry of Public Health, Jinan 250062, Shandong Province, China
Supported by the National Key Technology Research and Development Program of China during the 9th Five-Year Plan Period, No. 96C020117
Correspondence to: Professor Jin-Xiang Han, Shandong Medicinal Biotechnological Center, Shandong Academy of Medical Sciences; Key Laboratory for Biotechdrugs, Ministry of Public Health, Jinan 250062, Shandong Province, China. jxhan@sdu.edu.cn
Telephone: +86-531-2919888
Received: 2003-08-23 **Accepted:** 2003-10-07

Abstract

AIM: To design and establish a method of multiplex PCR normalization for simultaneously detecting HBV and HCV.

METHODS: Two pairs of primers with a 20 bp joint sequence were used to amplify the target genes of HBV and HCV by two rounds of amplification. After the two rounds of amplification all the products had the joint sequence. Then the joint sequence was used as primers to finish the last amplification. Finally multiplex PCR was normalized to a single PCR system to eliminate multiplex factor interference. Four kinds of nucleic acid extraction methods were compared and screened. A multiplex PCR normalization method was established and optimized by orthogonal design of 6 key factors. Then twenty serum samples were detected to evaluate the validity and authenticity of this method.

RESULTS: The sensitivity, specificity, diagnostic index and efficiency were 83.3%, 70%, 153.3% and 72.2%, respectively for both HBsAg and anti-HCV positive patients, and were 78.6%, 80%, 258.6% and 79.2%, respectively for HBsAg positive patients, and were 75%, 90%, 165% and 83.3%, respectively for anti-HCV positive patients.

CONCLUSION: The multiplex PCR normalization method shows a broad prospect in simultaneous amplification of multiple genes of different sources. It is practical, correct and authentic, and can be used to prevent and control HBV and HCV.

Wang N, Gao XQ, Han JX. Simultaneous detection of HBV and HCV by multiplex PCR normalization. *World J Gastroenterol* 2004; 10(16): 2439-2443
http://www.wjgnet.com/1007-9327/10/2439.asp

INTRODUCTION

Multiplex PCR uses several pairs of primers that target different genes to simultaneously amplify several different target sequences at a high speed and with a high efficiency. As many amplification factors may interact and produce non-specific amplification, its clinical use is limited. According to the characteristics of a small fragment that did not complement to the genes of PCR primers, we established a multiplex PCR normalization method (This method has been patented in the Chinese Patent Agency). By creating a primary reaction that was appropriate to all target templates, the multiplex was normalized to a single target PCR. This method could overcome the difficulties in establishing and optimizing the multiplex reaction system. In this article the practicality and effectiveness of multiplex PCR were validated by simultaneous detection of HBV and HCV.

MATERIALS AND METHODS

Specimen collection

Twenty-eight serum samples were collected from Jinan Central Hospital and Jinan Infectious Disease Hospital. The samples were all validated by ELISA method, in which 14 cases were HBsAg (+), 8 were anti-HCV (+), and 6 were positive for both HBsAg and anti-HCV. Ten cases were negative for both HBsAg and anti -HCV and used as control.

Reagents and instruments

HBV PCR kits and HCV PCR kits were purchased from Institutes of Liver Diseases, Peking University Medical College. dNTPs, AMV, proteinase K, isothiocyanate guanidine and Triton X –100 were products of TAKARA. PCR Amplification Minicycler™ was from MJ Research, USA. Innotech Imager™ 2200 was from Alpha Innotech Incoporation.

Extraction of virus nucleic acids

Method 1[1]: Proteinase K (10 mg/mL) was added to 150 μL serum and incubated at 50 °C for 2 h. RNA and DNA were extracted with phenol-chloroform at pH4.0 and 8.0 respectively, and then nucleic acids were precipitated with Isopropyl alcohol. The final pellets were dissolved in 10 μL RNase free water and stored at -70 °C.

Method 2[2]: 200 μL guanidine isothiocynate and 20 μL glass powder were added to 200 μL serum and incubated at ambient temperature for 90 min and centrifuged at 12 000 *g*. The supernatant was removed and the pellet was washed and dissolved in reverse transcription buffer PCR detection.

Method 3[3]: 90 μL lytic buffer (120 g GUSCN, 100 mL 0.1mol/L Tris-HCl, pH6.4), 0.2 mol/L EDTA (20 μL, pH8.0) and glass powder were added to 50 μL serum and incubated at room temperature for 10 min, mixed and centrifuged at 12 000 *g* for 15 s, washed 2 times with washing solution (120 g GUSCN, 100 mL 0.1 mol/L Tris-HCl, pH 6.4, 2.6 g Triton ×100), and further washed with 700 mL/L ethanol and acetone. Then acetone was removed and dried at 56 °C for 10 min and TE buffer was added to the pellets and incubate at 56 for 2 min and then centrifuged for 2 min. The supernatant was transferred to another tube for further amplification.

Method 4[4]: 200 μL lytic buffer[6 mol/L guanidine hydrochloride, 10 mmol/L Tris-HCl (pH 7.5), 200 g/L Triton X-100 (pH 4.4)], and 10 mmol/L urea, were added to 200 μL serum, proteinase K 40 μL, glass powder 10 μg, and incubated in 72 °C water bath for 10 min, then 100 μL Isopropyl alcohol was added and centrifuged at 8 000 r/min for 1 min. The supernatant was removed, and washed with 100 μL washing solution [20 mmol/L NaCl, 20 mmol/L Tris-HCl (pH7.5) and 1 000 mL/L ethanol] and

centrifuged at 8 000 r/min for 1 min. The supernatant was removed and washed and centrifuged at 8 000 r/min for 1 min and 13 000 *g* for 10 s, dried and dissolved in 50 μL RNase free water.

Primer design

The primers for the first round of PCR: HBV reverse primer: 5'-GAT GAT GGG ATG GGA ATA CA-3' (position: 2 566-2 586 of P gene), HBV RT primer: 5'-GCT GGT TCA CAT TGT GAG GGG AGT CTA GAC TCG TGG TGG A-3' with the former 20 bp as the joint sequence, and the latter 20 bp in the position of the overlap of genome P region and Pre-S region (position 2 921-2 941). There was a 395 bp between R and RT primers. HCV reverse primer: 5'-ATC ACT CCC CTG TGA GGA A-3' which was located between 47-65 bp. RT –PCR primer: 5'-GCT GGT TCA CAT TGT GAG GGC TAC GAG ACC TCC CGG GGC A-3'. The former 20 bp was the joint sequence, the latter 20 bp was in 313-332 of HBV genome. The product between R and RT primers was a 315 bp fragment. The second round primers: N primer sequence was 5'-GCT GGT TCA CAT TGT GAG GG TAG AGG ACA AAC GGG CAA CA3', the former 20 bp was the joint sequence, and the latter 20 bp was in 2 703-2 723 of HBV genome. RT-PCR primer was the same as that of the first round, the amplification product was a 278 bp fragment between N and RT. The HCV N primer was 5'-GCT GGT TCA CAT TGT GAG GG GGG AGA GCCAT AGT GGT CTG-3', the former 20 bp was the joint sequence, and the latter 20 bp was located between 132-151 of HCV. RT primers were the same as the first round of amplification and the product was a 241 bp fragment. After two rounds of amplification, the third round was amplified with the common primers T: 5'GCT GGT TCA CAT TGT GAG GG3'. The primers were synthesized by phosphoamidite method with 391 DNA synthesizer. The synthesized primers were purified with OPC column[5].

Quality evaluation parameters of designed diagnostic assay

Sensitivity indicated the percent of positive cases by the diagnostic assay in the patient group. It was calculated according to the following formula.

$$\text{Sensitivity} = \frac{\text{True positivity}}{\text{True positive + false negative}} \times 100\%$$

The sensitivity should be 100% for a perfect diagnostic assay.

Specificity indicated the percent of negative cases determined by the diagnostic assay in control group. It was calculated according to the following equation.

$$\text{Specificity} = \frac{\text{True negativity}}{\text{False positivity +true negativity}} \times 100\%$$

The specificity should be 100% for a perfect diagnostic assay.

Diagnostic index was a combined parameter to evaluate the sensitivity and specificity. It was the sum of sensitivity and specificity. The perfect diagnostic index should be 200%, and it should not be lower than 100%.

Agreement rate indicated the ability of a diagnostic assay to correctly discern the patients and control cases. It was calculated by the following method. The perfect agreement rate of a diagnostic assay should be 100%.

$$\text{Agreement rate} = \frac{\text{TP+TN}}{\text{TP+FP+TN+FN}} \times 100\%$$

(TP: true positivity; TN: true negativity; FP: false positivity; FN: false negativity).

Positive predictive value (PPV) indicated the percent of patients in the positive results of diagnostic assay. It was calculated according to the following equation.

$$\text{PPV} = \frac{\text{TP}}{\text{TP+FP}} \times 100\%$$

Negative predictive value (NPV) indicated the percent of non-patients in the negative results of diagnostic assay. It was calculated according to the following equation.

$$\text{NPV} = \frac{\text{TN}}{\text{FN+TN}} \times 100\%$$

(NPV: negative predictive value; TN: true negativity; FN: false negativity; TN: true negativity).

RESULTS

Screening extraction methods for HBV DNA from HBsAg positive serum

Four methods were used to extract HBV DNA from HBsAg positive sera of patients. The results of amplification were compared to that of ELISA (Table 1).

The positive amplification rates were 20%, 60%, 85% and 95% for methods 1 to 4 respectively.

Screening the extracting methods of HCV RNA from anti-HCV positive serum

Fifteen anti-HCV positive sera were extracted with the four methods and the results were compared with ELISA (Table 2).

The positive amplification rates were 6%, 6%, 30% and 95% for methods 1 to 4, respectively compared to the ELISA.

Establishment of simultaneous extraction method of HBVDNA and HCV RNA

Six samples positive for both HBsAg and anti-HCV were extracted and amplified, the simultaneous extraction positive rate was 100% for HBV and 83% for HCV, respectively.

Establishment of RT and first round of amplification method

Orthogonal method was used to select the six common factors

Table 1 Amplification results of HBV DNA from 20 HBsAg positive sera

Method	Sample number																			
	1	2	3	4	5	6	7	8	9	10	11	12	13	14	15	16	17	18	19	20
ELISA	+	+	+	+	+	+	+	+	-	+	+	+	+	+	+	+	+	+	+	+
Method 1	-	-	+	+	+	-	+	-	-	-	-	+	-	-	-	-	-	-	-	-
Method 2	+	-	-	+	+	+	+	+	+	-	+	+	+	-	-	-	+	+	-	-
Method 3	+	+	+	+	+	+	+	+	+	-	-	+	+	+	+	-	+	+	+	+
Mrthod 4	+	+	+	+	+	+	+	+	+	+	+	+	+	+	+	-	+	+	+	+

Note: + represents positive amplification; - represents negative amplification.

Table 2 Amplification results of HCV RNA from 15 anti-HCV positive sera

Method	Sample number														
	1	2	3	4	5	6	7	8	9	10	11	12	13	14	15
ELISA	+	+	+	+	+	+	+	+	+	+	+	+	+	+	+
Method 1	-	-	-	-	-	-	-	-	+	-	-	-	-	-	-
Method 2	-	-	-	+	-	-	-	-	-	-	-	-	-	-	-
Method 3	-	+	+	+	-	-	-	-	+	+	-	-	+	-	-
Method 4	+	+	+	+	+	+	+	+	+	+	-	+	+	+	+

Note: + represents positive amplification; - represents negative amplification.

affecting the amplification, which were the concentrations of dNTPs, Mg^{2+}, Taq polymerase, AMV and primers (including HBV and HCV). Five levels were designed for each factor. The pattern of orthogonal was L 25[5,6]. The PCR reaction was as follows: HBV, 8 μL HCV template, 5 μL 10×buffer, 40 U RNase inhibitor, and other components and finally ddH_2O was added to make the total volume 50 μL. Twenty-five kinds of amplification system were available. After paraffin oil was added, reactions were performed at 50 °C for 30 min, at 95 °C for 2 min,and 30 cycles at 95 °C for 30 s, at 55 °C for 30 s, at 72 °C for 1 min. Then 10 μL amplification product was identified by 15 g/L agarose electrophoresis. The results showed under the condition of protocol 13, that both HBV and HCV targets were successfully amplified, therefore protocol 13 was chosen as the first round protocol. The amplification program was at 50 °C for 30 min, at 95 °C for 2 min, and at 95 °C for 30 s, at 55 °Cfor 30 s and at 72 °C for 1 min for a total of 30 cycles.

Screening of the second round of amplification reaction condition

According to the orthogonal method and experience, 6 protocols were designed. The reaction condition was at 95 °C for 30 s, at 55 °C for 30 s, and at 72 °C for 45 s for a total of 10 cycles. The results showed that the two target bands of HBV and HCV were successfully separated in protocol 1. Therefore the protocol 1 was chosen as the final optimal protocol.

Screening of the third round of amplification reaction

According to the results of the above two rounds of amplification, 7 protocols were designed for the third round of amplification. All the amplification reactions were done at 95 °C for 30 s, at 55 °C for 30 s, at 72 °C for 1 min for a total of 30 cycles. The results showed that the HBV and HCV target bands were discerned more obviously under the condition of protocol 2, which was therefore determined as the optimal protocol.

Comparison of normalized PCR detection results with ELISA method

Twenty-eight samples were detected with both normalized PCR method and ELISA method. In the 14 samples positive for HBsAg, the results of the six antibody-positive amplifications are shown in Figure 1. The concordance of PCR with ELISA was 78.8%. Eight anti-HCV positive samples detected with multiplex PCR had a coincidence rate of 75% compared with ELISA method. When it was used to detect samples positive for both HBsAg and anti-HCV, the coincidence rate was 83.3%. Ten control cases negative for both HBsAg and anti-HCV were also detected with normalized PCR, of which 2 were positive for HBV and 1 for HCV.

Quality evaluation of simultaneous PCR detection of HBV and HCV

Fourteen patients with HBV infection were detected with normalized PCR method. The results showed that the true positivity was 11 and the false negativity was 3 (Table3).

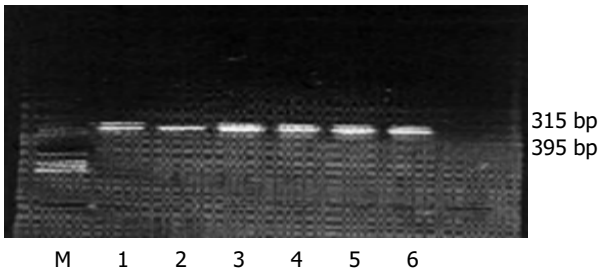

Figure 1 Normalized PCR amplification for patients with both HBsAg and anti-HCV antibodies. M represents X174-hae III marker. Lanes 1 to 6 represent amplification results of six patients who were positive for HBsAg and anti-HCV. Only lane 2 is negative for HCV.

Of the eight HCV patients detected with normalized method, 6 were positive and 2 were negative. Six patients with both HBV and HCV infection were also detected, of which 5 were positive and 1 was negative (Figure 1 and Table 4). Ten patients without HBsAg and anti-HCV infection were also detected with our method, of which 8 were negative for HBV and 2 were positive for HBV (false positivity), 9 were negative for HCV and 1 positive for HCV (false positivity) (Tables 3, 4).

Evaluation of validity and diagnostic power of normalized PCR for detecting HBV DNA

The sensitivity of this method for the detection of HBV DNA was 78.6% (11/14). The specificity was 80% (8/10). The diagnostic index was 158.6% (78.6% plus 80%) and the agreement rate was 79.2%. The positive predictive value was 84.6% (11/13). The negative predictive value was 72.7% (8/11) (Table 3).

Table 3 Evaluation of validity and diagnostic power of normalized PCR for detecting HBV DNA

	HBV patient	Non-HBV control	Total
Positive	11	2	13
Negative	3	8	11
Total	14	10	24

Table 4 Evaluation of validity and diagnostic power of normalized PCR for detecting HCV RNA

	HCV patients	Non-HCV control	Total
Positive	6	1	7
Negative	2	9	11
Total	8	10	18

Quality evaluation of validity and diagnostic power of normalized PCR for detecting HCV RNA

The sensitivity of this method for the detection of HCV RNA

was 75% (6/8). The specificity was 90% (9/10). The diagnostic index was 165% (75% plus 90%) and the diagnostic efficiency was 83.3%. The positive predictive value was 85.7% (6/7). The negative predictive value was 81.8% (9/11) (Table 4).

Evaluation of validity and diagnostic power of normalized PCR for detection of both HBV DNA and HCV RNA

The sensitivity of this method for the detection of superinfection of HBV DNA and HCV RNA was 83.3% (5/6). The specificity was 70% (7/10). The diagnostic index was 153.3% (83.3% plus 70%) and the diagnostic efficiency was 72.2%. The positive predictive value was 62.5%. The negative predictive value was 87.5% (Table 5).

Table 5 Evaluation of validity and diagnostic power of normalized method for detecting HBV and HCV double infection

	HBV(+)and anti-HCV(+)	HBV(-) and anti-HCV(-)	Total
Positive	5	8	13
Negative	1	2	3
Total	6	10	16

DISCUSSION

Virus particles of HBV and HCV are rare in blood and HCV RNA is easily to degrade, therefore selecting protein denaturing agents to quickly dissolve the membrane protein is very important in the process of simultaneous extraction of HBV and HCV nucleic acids. Our results showed that method 4 was the most effective among the four extraction methods. The effective extraction rate was 95% for both HBsAg and anti-HCV positive serum. In method 4, hydrochloride guanine was a potent protein denaturant, it could dissolve the protein and destruct its secondary structure and cell structure, and mad it possible to separate nucleotide protein from nucleic acids. Urea and Triton X-100 are non-detergents and could dissolve cell membrane and precipitate the protein. Proteinase K could further degrade protein. Glass powder had absorptive effect on nucleic acids and therefore could absorb nucleic acids on its surface. Isopropyl alcohol could precipitate nucleic acids and finally the low ion potential solution could elute nucleic acids from the glass powder. This method was confirmed to be effective and authentic, suitable for the separation of virus RNA and DNA. In practice, it was a simple, fast, stable and reproducible method.

Theoretically, there is no limit on the number of target sequences simultaneously amplified by multiplex PCR. But the stringency of specific conditions restricted the number of target sequences amplified. In order to overcome these limits, we established a multiplex normalized amplification method. First a nested PCR amplification was performed with 2 pairs of primers with a joint sequence. Then a normalized amplification was done with joint primers. The effects of competition of primers were the lowest, so that the multiplex PCR became a single target PCR. These measurements could overcome the difficulties in establishing and optimizing the conditions of multiplex PCR. The success of this method has shed some lights on the development of PCR techniques. We used the orthogonal method for the design of experiment[6], and divided the key factors of PCR reaction such as primer concentration, dNTPs, Taq polymerase, AMV and magnesium chloride concentration into different grades, and a factor table was set up. This included all possible arrangements and combination of factors. The results showed that the coordination of proportion of the 6 factors was very important. If the proportion of HBV and HCV primers was not appropriate, and sometimes one of the amplifications was superior to another and only one band could be identified by electrophoresis.

ELISA is a method to detect antibody for the purpose of diagnosis of virus infection. The antibody was only detected 1 to 2 wk after infection, which reflected the immune response of the host, but could not explain the virus replication. PCR method could directly detect the virus nucleic acids. It could reflect the state of virus replication. When the virus was cleaned up, only the antibody was positive, the nucleic acids could not be detected. That is why the detection rate of PCR was lower when ELISA was used as a golden standard. In this study, 1/8 of the anti-HCV patients were negative for HCV RNA, and 1/ 6 patients were positive for both HBsAg and HCV, which were undetectable by our method. This is partly because the patients were in the state of convalescence, and the virus was already cleaned up or was false positive for ELISA due to hyperimmunoglobulinemia, rheumatoid factor and superoxide dismutase. The detection of HCV RNA in non-hepatitis patients could be explained by the fact that the patients might be in the early stage of acute hepatitis, and the antibody had not been produced yet. A close follow-up is needed for the early diagnosis and treatment after the possibility of false positive is excluded.

Currently, the super-infection rate of HBV and HCV was very high, and it was 13.64% to 27.27% reported by Xu[7]. It is important to establish methods that can simultaneously detect combined virus infection. Konomi *et al*.[8] reported a multiplex polymerase chain reaction (PCR) method for simultaneous detection of hepatitis B, C, and G viral genomes. The levels of concordance with the data obtained by conventional single PCR method were 100% for single infection, 98-100% for double infection, and 92% for triple infection. Meng Q and his colleagues[9] established an automatic multiplex system for simultaneously screening hepatitis B virus (HBV), hepatitis C virus (HCV), and human immunodeficiency virus type 1 (HIV-1) in blood donations. The detection limits (95% confidence interval) were 22 to 60 copies/mL for HBV, 61 to 112 IU/mL for HCV, and 33 to 66 copies/mL for HIV-1, using a specimen input volume of 0.2 mL. The AMPLINAT MPX assay could detect a broad range of genotypes or subtypes for all three viruses and had a specificity of 99.6% for all three viruses with sero-negative specimens. In an evaluation of sero-conversion panels, the AMPLINAT MPX assay detected HBV infection an average of 24 d before the detection of HBsAg by enzyme immunoassay. HCV RNA was detected an average of 31 d before HCV antibody appeared. HIV-1 RNA was detected an average of 14 d before HIV-1 antibody and an average of 9 d before p24 antigen. A Chinese group has designed a visual gene-detecting technique using nanoparticle-supported gene probes. With the aid of gold nanoparticle-supported 3'-end-mercapto-derivatized oligonucleotide serving as a detection probe, and 5'-end -amino-derivatized oligonucleotide immobilized on glass surface acting as a capturing probe, target DNA was detected visually by sandwich hybridization based on highly sensitive "nano-amplification" and silver staining. Different genotypes of hepatitis B and C viruses in serum samples from infected patients were detected using home made HBV, HCV, and HBV/HCV gene chips by the gold/silver nanoparticle staining amplification method. The present visual gene-detecting technique might avoid limitations of the reported methods due to for its high sensitivity, good specificity, simplicity, speed, and cheapness[10].

Multiplex PCR assay has been used for the simultaneous detection of many different genes of pathogens including genes related with antibiotic resistance genes in Staphylococcus aureus[11]. A multiplex reverse transcriptase polymerase chain reaction (RT-PCR) was also applied for the simultaneous detection of hepatitis A virus (HAV), poliovirus (PV) and simian rotavirus (RV-SA11), and compared with specific primers for

each genome sequence. Three amplified DNA products representing HAV (192 bp), PV (394 bp) and RV (278 bp) were identified when positive controls were used[12]. A multiplex RT-PCR method was described for the simultaneous detection of all four viruses in combination with a plant mRNA specific internal control which could be used as an indicator of the effectiveness of the extraction and RT- PCR. The upper detection limit for the four viruses was at an extract dilution of 1/200[13]. A multiplex semi-nested PCR was developed for the simultaneous detection and differentiation among porcine circovirus 1 (PCV1), PCV2, and porcine parvovirus (PPV) from boar semen. Primers of PCV1, PCV2 and PPV were specific and did not react with other viruses respectively. Twenty (20.4%) and 42 (42.9%) out of 98 whole semen samples were found to be positive for PCV and PPV using conventional multiplex and semi-nested PCR respectively[14]. Multiplex method for HBV/HCV/HIV-1 has been used for screening 6 805 010 units of serologically negative donation and 112 HBV DNA-positives, 25 HCV RNA positives and 4 HIV-1 RNA positives were screened out and prevented transfusion of the positive blood[15,16].

The sensitivity of our multiplex normalized PCR method was 78.6%, 75% and 83.3% for the detection of HBVDNA, HCVRNA, and super-infection of HBV and HCV respectively. The specificity was 80%, 90% and 70%, respectively. These are good enough for a diagnostic assay. It can detect both DNA and RNA simultaneously and can be completed in one day. It is not only suitable for clinical diagnosis, but also suitable for the screening of HBV and HCV from blood donators to prevent the transmission of these diseases. It can also be used for an epidemiological study. In these respects it needs to be further studied in a large-scale population.

REFERENCES

1 **Hu KQ**, Yu CH, Lee S, Villamil FG, Vierling JM. Simultaneous detection of both hepatitis B virus DNA and hepatitis C virus RNA using a combined one-step polymerase chain reaction technique. *Hepatology* 1995; **21**: 901-907

2 **Yamada O**, Matsumoto T, Nakashima M, Hagari S, Kamahora T, Ueyama H, Kishi Y, Uemura H, Kurimura T. A new method for extracting DNA or RNA for polymerase chain reaction. *J Virol Methods* 1990; **27**: 203-209

3 **Boom R**, Sol CJ, Salimans MM, Jansen CL, Wertheim-van Dillen PM, van der Noordaa J. Rapid and simple method for purification of nucleic acids. *J Clin Microbiol* 1990; **28**: 495-503

4 **Vogelstein B**, Gillespie D. Preparative and analytical purification of DNA from agarose. *Proc Natl Acad Sci U S A* 1979; **76**: 615-619

5 **Han JX**, Zhang C, Yang XC, Tang TH, Wang ML. Investigation on the purification and synthesizing of DNA fragments by OPC methods. *Shandong Yike Daxue Xuebao* 1995; **33**: 173-174

6 **Fang JQ**, Fu CZ, Liao RR. Regression methods of pair -wise data. *Zhongguo Weisheng Tongji* 1996; **13**: 1-5

7 **Xu ZF**, Xu KC, Meng XY. Investigation on the double infection of HBV and HCV. *Nantong Yixueyuan Xuebao* 1994; **14**: 162-165

8 **Konomi N**, Yamaguchi M, Naito H, Aiba N, Saito T, Arakawa Y, Abe K. Simultaneous detection of hepatitis B, C, and G viral genomes by multiplex PCR method. *Jpn J Infect Dis* 2000; **53**: 70-72

9 **Meng Q**, Wong C, Rangachari A, Tamatsukuri S, Sasaki M, Fiss E, Cheng L, Ramankutty T, Clarke D, Yawata H, Sakakura Y, Hirose T, Impraim C. Automated multiplex assay system for simultaneous detection of hepatitis B virus DNA, hepatitis C virus RNA, and human immunodeficiency virus type 1 RNA. *J Clin Microbiol* 2001; **39**: 2937-2945

10 **Wang YF**, Pang DW, Zhang ZL, Zheng HZ, Cao JP, Shen JT. Visual gene diagnosis of HBV and HCV based on nanoparticle probe amplification and silver staining enhancement. *J Med Virol* 2003; **70**: 205-211

11 **Strommenger B**, Kettlitz C, Werner G, Witte W. Multiplex PCR assay for simultaneous detection of nine clinically relevant antibiotic resistance genes in Staphylococcus aureus. *J Clin Microbiol* 2003; **41**: 4089-4094

12 **Coelho C**, Vinatea CE, Heinert AP, Simoes CM, Barardi CR. Comparison between specific and multiplex reverse transcription-polymerase chain reaction for detection of hepatitis A virus, poliovirus and rotavirus in experimentally seeded oysters. *Mem Inst Oswaldo Cruz* 2003; **98**: 465-468

13 **Thompson JR**, Wetzel S, Klerks MM, Vaskova D, Schoen CD, Spak J, Jelkmann W. Multiplex RT-PCR detection of four aphid-borne strawberry viruses in Fragaria spp. in combination with a plant mRNA specific internal control. *J Virol Methods* 2003; **111**: 85-93

14 **Kim J**, Han DU, Choi C, Chae C. Simultaneous detection and differentiation between porcine circovirus and porcine parvovirus in boar semen by multiplex seminested polymerase chain reaction. *J Vet Med Sci* 2003; **65**: 741-744

15 **Ohnuma H**, Tanaka T, Yoshikawa A, Murokawa H, Minegishi K, Yamanaka R, Lizuka HY, Miyamoto M, Satoh S, Nakahira S, Tomono T, Murozuka T, Takeda Y, Doi Y, Mine H, Yokoyama S, Hirose T, Nishioka K. The first large-scale nucleic acid amplification testing (NAT) of donated blood using multiplex reagent for simultaneous detection of HBV, HCV, and HIV-1 and significance of NAT for HBV. *Microbiol Immunol* 2001; **45**: 667-672

16 **Mine H**, Emura H, Miyamoto M, Tomono T, Minegishi K, Murokawa H, Yamanaka R, Yoshikawa A, Nishioka K. High throughput screening of 16 million serologically negative blood donors for hepatitis B virus, hepatitis C virus and human immunodeficiency virus type-1 by nucleic acid amplification testing with specific and sensitive multiplex reagent in Japan. *J Virol Methods* 2003; **112**: 145-151

Edited by Wang XL and Zhang JZ **Proofread by** Xu FM

PO Box 2345, Beijing 100023, China
Fax: +86-10-85381893
E-mail: wjg@wjgnet.com www.wjgnet.com

World J Gastroenterol 2004;10(16):2444-2446
World Journal of Gastroenterology
 ISSN 1007-9327

• BRIEF REPORTS •

Role of endoscopic miniprobe ultrasonography in diagnosis of submucosal tumor of large intestine

Ping-Hong Zhou, Li-Qing Yao, Yun-Shi Zhong, Guo-Jie He, Mei-Dong Xu, Xin-Yu Qin

Ping-Hong Zhou, Guo-Jie He, Xin-Yu Qin, Department of General Surgery, Zhongshan Hospital, Fudan University, Shanghai 200032, China
Li-Qing Yao, Yun-Shi Zhong, Mei-Dong Xu, Endoscopic Center, Zhongshan Hospital, Fudan University, Shanghai 200032, China
Correspondence to: Dr. Ping-Hong Zhou, Department of General Surgery, Zhongshan Hospital, Fudan University, Shanghai 200032, China. chow@zshospital.net
Telephone: +86-21-64043947 **Fax:** +86-21-64038472
Received: 2003-12-10 **Accepted:** 2004-02-01

Abstract

AIM: To evaluate the role of miniprobe ultrasonography under colonoscope in the diagnosis of submucosal tumor of the large intestine, and to determine its imaging characteristics.

METHODS: Thirty-five patients with submucosal tumors of the large intestine underwent miniprobe ultrasonography under colonoscope. The diagnostic results of miniprobe ultrasonography were compared with pathological findings of specimens by biopsy and surgical resection.

RESULTS: Lipomas were visualized as hyperechoic homogeneous masses located in the submucosa with a distinct border. Leiomyomas were visualized as hypoechoic homogeneous mass originated from the muscularis propria. Leiomyosarcomas were shown with inhomogeneous echo and irregular border. Carcinoids were presented as submucosal hypoechoic masses with homogenous echo and distinct border. Lymphangiomas were shown as submocosal hypoechoic masses with cystic septal structures. Malignant lymphomas displayed as hypoechoic masses from mucosa to muscularis propria, while pneumatosis cystoids intestinalis originated from submucosa with a special sonic shadow. One large leiomyoma was misdiagnosed as leiomyosarcoma.

CONCLUSION: Endoscopic miniprobe ultrasonography can provide precise information about the size, layer of origin, border of submucosal tumor of the large intestine and has a high accuracy in the diagnosis of submucosal tumor of the large intestine. Pre-operative miniprobe ultrasonography under colonoscope may play an important role in the choice of therapy for submucosal tumor of the large intestine.

Zhou PH, Yao LQ, Zhong YS, He GJ, Xu MD, Qin XY. Role of endoscopic miniprobe ultrasonography in diagnosis of submucosal tumor of large intestine. *World J Gastroenterol* 2004; 10(16): 2444-2446
http://www.wjgnet.com/1007-9327/10/2444.asp

INTRODUCTION

Due to the development of colonoscope and CT, the reported number of submucosal tumor (SMT) of the large intestine has been increased. SMT of the large intestine includes lipoma, lymphangioma, leiomyoma, carcinoid, metastatic tumor, *etc*. Previous diagnosis depended mainly on barium enema and colonoscope, but none of them could make clear the histological features of SMT, and it was also difficult to differentiate SMT from extramural compression. In the 1980 s, the development of endoscopic ultrasonography (EUS) significantly improved the accuracy of diagnosis of the digestive tract diseases[1]. EUS can provide detailed information about gastrointestinal wall structure and adjacent organs. EUS is highly accurate in the visualization of submucosal lesions and their sonographic layer of origin within gastrointestinal wall. Concerning SMT of the digestive tract, several studies have been published mainly in upper digestive tract[2-4], but there have been few studies on SMT of the lower digestive tract. The aim of this study was to assess the value of EUS in the diagnosis of SMT of the large intestine and determine their imaging characteristics.

MATERIALS AND METHODS

Patients

EUS was performed in 35 patients with elevated lesions which had normal mucosal vision under colonoscope between January 2001 and November 2003. The patient group comprised 19 men and 16 women with a mean age of 54.6 years (range, 32-72 years). The diameter of lesions ranged 0.5-4.2 cm. Of the 35 lesions, 28 were confirmed histologically by endoscopic biopsy and surgical resection, and the histological findings were compared with ultrasonographic imagings. The other 7 patients were observed without resection. The lesion that caused extramural compression of intestinal wall was excluded from this study, which could easily be confused with SMT clinically.

Instruments

A ultrasonic miniprobe (Olympus UM-2R, 12MHz; UM-3R, 20 MHz, Tokyo, Japan) was introduced under electronic colonoscope (Olympus CF-Q240, Tokyo, Japan), as well as an endoscopic ultrasonography system (Olympus EU-M30, Tokyo, Japan). The video image was recorded by ultrasonography image recorder (Sony UP-890, Tokyo, Japan).

Operative procedures

Patients undergoing EUS were prepared with the same method as for conventional colonoscopy. Five mg midazolam was administered intramuscularly and 10 mg scopolamine butylbromide was injected intravenously for sedation before the procedure. When an elevated lesion with normal mucosa was observed endoscopically, the tip of the colonoscope was placed at the distal end of the lesion. The lumen was filled with 100-200 mL water to achieve acoustic coupling between the transducer and the intestinal wall. Subsequently, the miniprobe was introduced through the working channel of the colonoscope and advanced beyond the lesion. The lesion was assessed by real-time ultrasonography while the miniprobe was moved over the lesion region[4].

The layer of origin of SMT was determined according to the continuity between the lesion and adjacent normal colonic wall. The nature of SMT was assessed by its size, layer of origin, border characteristic and internal echogenicity.

Statistical analysis

Values were presented as mean±SD. Analysis of variance with *t* test was used for statistical analysis. *P*</=0.05 was considered statistically significant.

RESULTS

EUS was performed successfully in all 35 patients. The normal wall of the large intestine was displayed in 5 layers (Figure 1). The first 2 layers represented the mucosa (m). The third layer stood for the submucosa (sm). The muscularis propria (mp) was depicted by the 4th layer. Adventitia or serosa (sa) was sometimes displayed as the 5th layer. As the lower part of rectum below the peritoneal reflection had no serosa, the pericolic fat and the mural outer layer constituted the hyperechoic layer. SMT was mostly visualized as hyperechoic, hypoechoic, anechoic lesions within the colorectal wall (Figure 1). The EUS characteristics of SMT are summarized in Table 1.

Lipomas, the most common SMT of the large intestine (accounting for 1/3 in our study), were visualized as hyperechoic homogeneous masses located in the third layer (sm) with a distinct border. Leiomyomas were visualized as hypoechoic homogeneous mass originated from the 4th layer(mp). Two leiomyosarcomas with a mean diameter of 38 mm, inhomogeneous and irregular border were confirmed histologically by surgical resection. One large leiomyoma was misdiagnosed as leiomyosarcoma. Carcinoid was presented as a submucosal hypoechoic mass with a homogenous echo and distinct border. All 3 carcinoids were located in rectus, of which 2 were less than 10 mm in diameter, submucosal continuity was not disrupted, and were resected under colonoscope. Another one was resected by surgery because of large diameter (1.8 cm) and disrupted submucosal continuity. Lymphangiomas were shown with EUS as submucosal anechoic masses with cystic septal structures. Malignant lymphoma displayed as hypoechoic mass from mucosa to mp depending on stage of the disease, while pneumatosis cystoids intestinalis, not real tumor, originated from sm with a special sonic shadow behind mass.

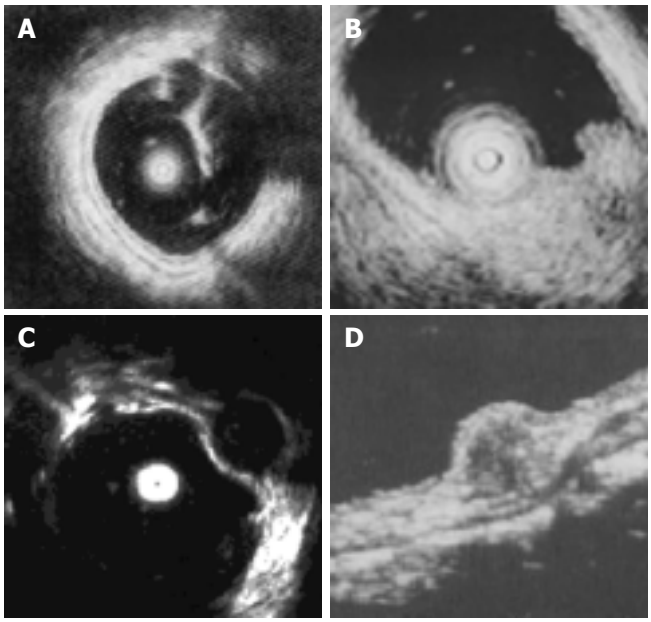

Figure 1 EUS imagines of normal wall and SMT of the large intestine. A: The normal wall was displayed in 5 layers; B: Lipoma imagine showed a hyperechoic homogeneous mass located in the third layer; C: Leiomyoma imagine showed a hypoechoic homogeneous mass originated from the 4th layer; D: Rectal carcinoid imagine showed a submucosal hypoechoic mass with a homogenous echo.

DISCUSSION

Barium enema and colonoscopy are the main widely used examinations in the diagnosis of submucosal lesions of the large intestine. Takada *et al.*[3] classified colonic SMT into five types on the basis of barium enema studies. Typical endoscopic feature of the colonic SMT is an elevated lesion with normal mucosa, and each has its own endoscopic morphologic features. However, it is difficult to determine the real size, layer of the origin and histologic nature of SMT with these procedures alone. In addition, lesions smaller than 10 mm cannot be detected.

Under these circumstances, the development of EUS has provided a brand new dimension in the diagnosis of colorectal lesions[5-11]. EUS can image the entire structure of the colonic wall which corresponds to the histologic layer structure. Normal colonic wall is presented as five-layered structure. By placing high frequency miniprobe on the elevated spot, the layer of the origin of SMT is generally determined by demonstrating continuity between the tumor and the colonic wall. Extraluminal compression is easily differentiated from SMT by EUS. Our study found lipoma, lymphangioma and carcinoid were originated from the third layer (sm). Myogenic tumors were found to be originated from the fourth layer (mp). According to literature, some myogenic tumors were from muscularis mucosa[12].

The size of SMT can be measured with EUS. The biggest SMT we detected in this study was 4.2 cm in diameter. Because of the high frequency employed in this study, it was difficult for miniprobe to observe big lesions. In general, the lower the frequency employed, the better the depth of US penetration and the clearer the image. Therefore, 20 MHz is suitable for clear images of superficial lesions. On the other hand, 12 MHz and 7.5 MHz are more suitable for the evaluation of the big lesions and contiguous tissues. The smallest SMT we detected was 5 mm in diameter, while Sun *et al.*[13] reported that the smallest size detectable was 2 mm in diameter histologically.

The nature of SMT can be determined by the internal echogenicity. In this study, all lipomas were hyperechoic

Table 1 EUS characteristics of SMT of the large intestine

Diagnosis (No.of patients)	EUS findings					
	Size (mm)	Shape	Border	Layer of origin	Echogenicity	Internal echo
Lipoma (*n* = 12)	15±3.1	Round	Regular	Third	Hyperechoic	Homogeneous
Leiomyoma (*n* = 8)	17±4.3	Round	Regular	Fourth	Hypoechoic	Homogeneous
Lymphangioma (*n* = 6)	14±2.3	Round	Regular	Third	Anechoic	Multilocular
Leiomyosarcoma (*n* = 2)	38±2.8	Round Lobulated	Regular	Fourth	Hypoechoic	Inhomogeneous
Carcinoid (*n* = 3)	14±4.2	Round	Regular	Third	Hypoechoic	Homogeneous
Malignant lymphoma (*n* = 2)		Irregular	Irregular	Second to fourth	Hypoechoic	Inhomogeneous
Pneumatosis cystoid intestinalis (*n* = 2)	17±3.6	Irregular	Irregular	Third	Hypoechoic	Inhomogeneous

[a]*P*<0.05 *vs* leiomyoma.

homogeneous and lymphangiomas were anechoic with cystic septal structures[14]. The other SMTs were mostly visualized as hypoechoic masses. Therefore, the former findings are strongly suggestive of lipomas and lymphangiomas.

Leiomyosarcoma of the large intestine is extremely rare, only accounting for 0.1% of colonic malignancy[12]. With regard to differential diagnosis of leiomyomas and leiomyosarcomas, it is suggested to distinguish according to the size and the internal ultrasonsic characteristics of the tumor in literature. For the lesion which has the diameter <30 mm, homogenous resonance and clear borderline, the benign is considered. In contrast, if the lesion has a diameter >30 mm, inhomogeneous resonance and irregular border, it may be diagnosed as malignant. But one case in our study with a diameter of 3.2 cm was eventually diagnosed as leiomyoma by pathology. Endoscopic ultrasonography guided fine needle aspiration (FNA) can further help to diagnose the submucosal masses[15].

EUS is useful in determining the therapy for SMT of the large intestine[16]. Lipoma and lymphangioma are easy to be diagnosed by EUS, and these lesions can be removed endoscopically or observed without resection. Although leiomyoma and leiomyosarcoma are difficult to differentiate, leiomyosarcoma should be strongly suspected, and surgery should be considered when the tumor is over 30 mm in diameter and has an inhomogeneous internal echo. Although myogenic tumor diagnosed by EUS is an indication for surgery at our department, patients are followed up by EUS according to a strict protocol when the size of tumor is smaller than 20 mm and the patient declines surgery.

In conclusion, EUS can provide precise information about the size, layer of origin, and echogenicity of the SMT of the large intestine. It is useful in the diagnosis of SMT of the large intestine and can have an important role in the choice of therapy.

ACKNOWLEDGEMENT

We thank Eisai Cho and Kenjiro Yasuda of the Department of Gastroenterology of Kyoto Second Red Cross Hospital (Japan) for their technical support to this study.

REFERENCES

1 **Stergiou N,** Haji-Kermani N, Schneider C, Menke D, Kockerling F, Wehrmann T. Staging of colonic neoplasms by colonoscopic miniprobe ultrasonography. *Int J Colorectal Dis* 2003; **18**: 445-449
2 **Waxman I,** Saitoh Y, Raju GS, Watari J, Yokota K, Reeves AL, Kohgo Y. High-frequency probe EUS-assisted endoscopic mucosal resection: a therapeutic strategy for submucosal tumors of the GI tract. *Gastrointest Endosc* 2002; **55**: 44-49
3 **Takada N,** Higashino M, Osugi H, Tokuhara T, Kinoshita H. Utility of endoscopic ultrasonography in assessing the indications for endoscopic surgery of submucosal esophageal tumors. *Surg Endosc* 1999; **13**: 228-230
4 **Xi WD**, Zhao C, Ren GS. Endoscopic ultrasonography in preoperative staging of gastric cancer: determination of tumor invasion depth, nodal involvement and surgical resectability. *World J Gastroenterol* 2003; **9**: 254-257
5 **Roseau G,** Dumontier I, Palazzo L, Chapron C, Dousset B, Chaussade S, Dubuisson JB, Couturier D. Rectosigmoid endometriosis: endoscopic ultrasound features and clinical implications. *Endoscopy* 2000; **32**: 525-530
6 **Shimizu S,** Myojo S, Nagashima M, Okuyama Y, Sugeta N, Sakamoto S, Kutsumi H, Otsuka H, Suyama Y, Fujimoto S. A patient with rectal cancer associated with ulcerative colitis in whom endoscopic ultrasonography was useful for diagnosis. *J Gastroenterol* 1999; **34**: 516-519
7 **Gast P,** Belaiche J. Rectal endosonography in inflammatory bowel disease: differential diagnosis and prediction of remission. *Endoscopy* 1999; **31**: 158-166
8 **Lew RJ,** Ginsberg GG. The role of endoscopic ultrasound in inflammatory bowel disease. *Gastrointest Endosc Clin N Am* 2002; **12**: 561-571
9 **Polkowski M,** Regula J, Wronska E, Pachlewski J, Rupinski M, Butruk E. Endoscopic ultrasonography for prediction of postpolypectomy bleeding in patients with large nonpedunculated rectosigmoid adenomas. *Endoscopy* 2003; **35**: 343-347
10 **Bhutani MS,** Nadella P. Utility of an upper echoendoscope for endoscopic ultrasonography of malignant and benign conditions of the sigmoid / left colon and the rectum. *Am J Gastroenterol* 2001; **96**: 3318-3322
11 **Mo LR,** Tseng LJ, Jao YT, Lin RC, Wey KC, Wang CH. Balloon sheath miniprobe compared to conventional EUS in the staging of colorectal cancer. *Hepatogastroenterology* 2002; **49**: 980-983
12 **Xu GQ,** Zhang BL, Li YM, Chen LH, Ji F, Chen WX, Cai SP. Diagnostic value of endoscopic ultrasonography for gastrointestinal leiomyoma. *World J Gastroenterol* 2003; **9**: 2088-2091
13 **Sun S,** Wang M, Sun S. Use of endoscopic ultrasound-guided injection in endoscopic resection of solid submucosal tumors. *Endoscopy* 2002; **34**: 82-85
14 **Watanabe F,** Honda S, Kubota H, Higuchi R, Sugimoto K, Iwasaki H, Yoshino G, Kanamaru H, Hanai H, Yoshii S, Kaneko E. Preoperative diagnosis of ileal lipoma by endoscopic ultrasonography probe. *J Clin Gastroenterol* 2000; **31**: 245-247
15 **Kinoshita K,** Isozaki K, Tsutsui S, Kitamura S, Hiraoka S, Watabe K, Nakahara M, Nagasawa Y, Kiyohara T, Miyazaki Y, Hirota S, Nishida T, Shinomura Y, Matsuzawa Y. Endoscopic ultrasonography-guided fine needle aspiration biopsy in follow-up patients with gastrointestinal stromal tumours. *Eur J Gastroenterol Hepatol* 2003; **15**: 1189-1193
16 **Ouchi J,** Araki Y, Chijiiwa Y, Kubo H, Hamada S, Ochiai T, Harada N, Nawata H. Endosonographic probe-guided endoscopic removal of colonic pedunculated leiomyoma. *Acta Gastroenterol Belg* 2000; **63**: 314-316

Edited by Kumar M and Zhu LH **Proofread by** Xu FM and Chen WW

PO Box 2345, Beijing 100023, China
Fax: +86-10-85381893
E-mail: wjg@wjgnet.com www.wjgnet.com

World J Gastroenterol 2004;10(16):2447-2451
World Journal of Gastroenterology
 ISSN 1007-9327

• CASE REPORT •

Gastrointestinal autonomic nerve tumors: A surgical point of view

Anton Stift, Josef Friedl, Michael Gnant, Friedrich Herbst, Raimund Jakesz, Etienne Wenzl

Anton Stift, Josef Friedl, Michael Gnant, Friedrich Herbst, Raimund Jakesz, Etienne Wenzl, Department of General Surgery, Medical University of Vienna, Vienna, Austria
Correspondence to: Dr. Anton Stift, Department of General Surgery, Medical University of Vienna, Waehringerguertel 18-20, A-1090 Vienna, Austria. a.stift@akh-wien.ac.at
Telephone: +43-1-40400-5621 **Fax:** +43-1-40400-6932
Received: 2003-11-12 **Accepted**: 2003-12-16

Abstract

AIM: Gastrointestinal autonomic nerve tumors are uncommon stromal tumors of the intestinal tract. Their histological appearance is similar to that of other gastrointestinal stromal tumors. We report two cases and performed an analysis of the literature by comparing our findings with the available case reports in the medical literature.

METHODS: Two patients were admitted with abdominal tumor masses. One occurred in the stomach with large multiple liver metastases and the second originated in Meckel´s diverticulum. The latter site has never been reported previously. Both patients underwent surgery. In one patient gastrectomy, right liver resection and colon transversum resection were performed to achieve aggressive tumor debulking. In the other patient the tumor bearing diverticulum was removed.

RESULTS: Postoperative recovery of both patients was uneventful. Histological examination, immunohistochemical analysis and electron microscopy revealed the diagnosis of a gastrointestinal autonomic nerve tumor. The patient with the tumor in Meckel's diverticulum died 6 mo after surgery because of pneumonia. The patient with liver metastases have been alive 13 years after initial tumor diagnosis and 7 years after surgery with no evidence of tumor progression. In light of our results, we performed a thorough comparison with available literature reports.

CONCLUSION: Radical surgical resection of gastrointestinal autonomic nerve tumors seems to be the only available curative approach to date, and long term survival is possible even in large metastasized tumors.

Stift A, Friedl J, Gnant M, Herbst F, Jakesz R, Wenzl E. Gastrointestinal autonomic nerve tumors: A surgical point of view. *World J Gastroenterol* 2004; 10(16): 2447-2451
http://www.wjgnet.com/1007-9327/10/2447.asp

INTRODUCTION

Gastrointestinal autonomic nerve tumors (GANTs) were first described by Herrera *et al.* in 1984. The authors used the term plexosarcoma to describe this entity[1]. In the last decade several investigators have recognized the distinct characteristics of this type of tumor[2-6]. It consists of a subgroup of gastrointestinal stromal tumors (GISTs) with a specific ultrastructural appearance, suggesting that it originates from neurons of the enteric plexus. Histologically, GANTs are usually low-grade spindle-cell neoplasms but cannot be definitely distinguished from stromal tumors or other neurogenic tumors by histological or immunohistochemical features. To date, the diagnosis of GIST is strongly suggested by immunostaining for the transmembrane tyrosine kinase receptor CD117 and c-kit gene mutations[7,8]. Partly based on these findings GISTs have been defined as tumors of the interstitial cells of Cajal[9]. Because GANTs also often showed CD117 staining some authors considered GISTs to be identical to GANTs[10]. Eyden *et al.* have recently studied 82 gastrointestinal stromal tumors in terms of their cellular differentiation by using electron microscopy. They demonstrated that electron microscopy was needed to establish the diagnosis of GANTs and to exclude other gastrointestinal stromal tumors[6]. We performed an analysis of the literature to compare our patients with the published data. The literature search yielded more than 120 published cases of GANTs, including the two cases presented in this report[1-6,11-38].

CASE REPORT

Case 1

This female patient was 22-year-old when she first noted fatigue, loss of appetite and epigastric discomfort in 1990. On physical examination she had a palpable epigastric mass. Upper gastrointestinal series and computed tomography (CT) suggested that the mass was a large gastric tumor. Endoscopy revealed several large masses protruding into the stomach without erosion of the overlying mucosa. Laparotomy showed that the entire stomach was infiltrated with nodular masses. In addition, the liver demonstrated multiple nodules. Intraoperatively obtained frozen sections revealed a leiomyosarcoma. Due to the poor prognosis of the disease and the extensive tumor burden the surgeon decided not to remove any tumor mass. The patient was discharged without any further treatment. Histological features and immunohistochemical characteristics were determined and found to be analogous to the results obtained six years later. Ultrastructural examination was not performed. At the time this case was diagnosed, only 10 GANTs had been documented in the literature.

Six years later the patient was still alive and was admitted to our hospital after an extensive weight loss (she weighed 38 kg at the time of admission). The patient complained of progressive abdominal discomfort and dyspnea. On physical examination the abdominal wall was extremely distended by a large palpable epigastric mass. Diagnostic studies including CT scan confirmed the known abdominal tumor. On the CT image the liver foci were partly solid and partly liquid (Figure 1).

Again, a laparotomy was performed. The intraoperative findings were similar to those obtained 6 years earlier. By then, the gastric tumor invaded the transverse mesocolon. Maximum debulking was achieved by total gastrectomy, transverse colon resection and right hepatectomy, leaving only small tumor deposits in the left liver. The resected gastric tumor mass measured approximately 40 cm×25 cm×20 cm in aggregate and the liver foci covered 25 cm×12 cm×12 cm (Figures 2, 3). After an uneventful recovery the patient was discharged after 3 wk and returned to work 5 wk later. CT series obtained 3, 6 and 12 mo after the operation showed no measurable expansion of the remaining foci in the left liver. A CT scan performed 24 mo

after the operation revealed spontaneous partial regression of the metastatic liver foci. Seven years after surgery, the patient was still in excellent clinical condition and free of discomfort. In addition, the patient delivered a healthy boy in 1997.

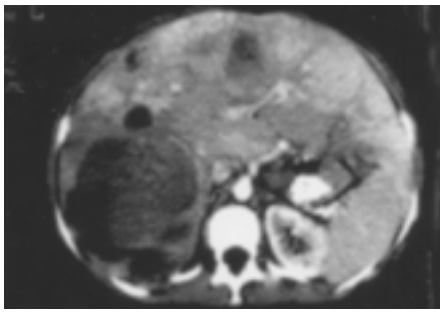

Figure 1 Preoperative CT-scan of diseased liver and stomach.

Figure 2 Stomach with infiltrating nodular masses.

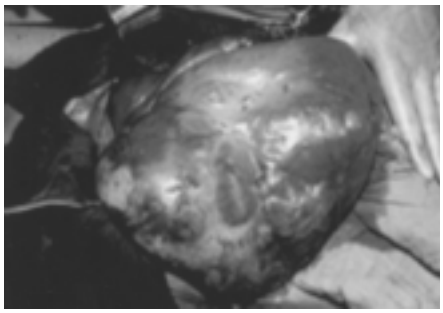

Figure 3 Right liver containing multiple metastatic nodules.

Microscopically, the resected gastric tumor chiefly consisted of plump spindle cells with distinct nuclear pleomorphism. In some areas 15 mitotic figures per 10 high power fields were identified. Immunohistochemical studies showed positive staining with antibodies to neuron specific enolase (NSE) and vimentin. There was also a weak focal staining for S 100 and HISL-19. No detectable staining for chromogranin A, 1 A 4, HHF 35, EMA, MNF 116, CAM 5.2, JC 70a and CD117 was observed. Just a small part of the tumor mass showed positive staining with an antibody to CD 34. Microscopically, the resected metastatic liver tumor also mainly consisted of plump spindle cells. In contrast to the original tumor mass, immunohistochemical studies showed 100 percent positive staining for CD 34 but negative staining for CD 117. CD 117 staining was performed a few weeks ago in order to take into account newest drug developments like tyrosine kinase inhibitors as a potential treatment option. Approximately 80% of the sampled tumors were necrotic. Ultrastructural examination showed neuron-like cells with long cytoplasmatic processes and dense core neurosecretory granules. Thus, the diagnosis of a gastrointestinal autonomic nerve tumor (GANT) was made.

Case 2

A 68-year-old man was admitted to the hospital with a one month history of fever and weight loss of 4 kg. No abnormal findings were registered on physical examination. Computerized tomography showed a decaying liver tumor. The Mendel-Mantoux reaction was highly positive. Therefore the liver focus was considered to be tuberculotic. Tuberculostatic triple-drug therapy was administered for 6 mo. After 12 mo, a CT scan of the abdomen and upper gastrointestinal series showed a normal liver with no pathological signs. An additional new finding was suggestive of a tumor of the ileum. Laparotomy revealed neoplastic nodular masses (9 cm×6 cm) originating from Meckel's diverticulum. The tumor was resected along with an ileal segment. The patient had an uneventful recovery and was discharged 10 d postoperatively. Light microscopy revealed that the tumor was composed of interlacing fascicles of plump, pleomorphic spindle cells, partly showing a storiform and epitheloid pattern. Less than one mitotic figure per 10 high-power fields was identified. Immunohistochemical stainings for vimentin, S-100 and neuron specific enolase (NSE) were positive, whereas staining for Lu 5, CAM 5.2, MNF 116, EMA, desmin, chromogranin, 1A4, Q-BENT10, JC70A, HMB-45, PGM1, HHF35 and CD117 was negative.

Ultrastructural examination showed neuron-like cells with long branching cytoplasmatic processes. Dense-core granules were scarce. No basal lamina, dense bodies, or pinocytotic vesicles were found.

Six months later the patient died of a severe pneumonia. A post-mortem examination showed no intestinal abnormalities or recurrence of disease.

DISCUSSION

Gastrointestinal autonomic nerve tumors represent a rare distinct subcategory of gastrointestinal stromal tumors. First described by Herrera *et al*. in 1984 as plexosarcoma supposedly originating from the enteric autonomic plexus, more than 120 cases including our own have been documented in the literature[1-6,11-38]. These tumors were found in patients of a wide age range (10 to 85 years) with a median age of 58 years. Seventy-nine per cent of patients were older than 50 years. The tumors were found slightly more often in males (62 males *vs* 58 females). The reported clinical signs and symptoms are shown in Table 1. In the majority of cases, the primary site of the tumor was the stomach, duodenum, jejunum and ileum, but the esophagus[21,22], rectum[26, 34], bladder[30] or colon[31] have also been reported in some cases (Table 2).

Table 1 Clinical symptoms of 78 reported GAN tumors

Clinical symptoms	No. of patients	Percent of patients
Abdominal pain	32	41
Meaena	19	24
Abdominal mass	10	13
Weight loss	10	13
Vomiting	9	12
Fatigue	7	9
Fever	5	6
Anemia	4	5
Obstructive jaundice	2	2
No clinical symptoms	5	6

On imaging studies, the tumor often presents as a large and lobulated solid mass, with areas of necrosis. It is locally invasive. Radiological techniques did not permit a distinction between GANTs and other gastrointestinal stromal tumors[28,33].

The greatest dimension of the tumor was determined in 81

cases, and ranged from 1.5 cm to 40 cm (median 10.4 cm). Eighty per cent was larger than 5 cm and 37% had one dimension larger than 10 cm. The bulky tumor masses were predominantly cystic and necrotic. In two cases an abscess was present in the tumor[17,29]. Some of these GANTs were observed in patients with Carney's triad (3 cases)[16,17], neurofibromatosis (3 cases)[15,20,25], and adrenal ganglioneuroma (1 case)[20].

Table 2 Anatomic sites of the primary tumors (n = 120)

Location	No. of patients	Percent of patients
Stomach	45	37.5
Jejunum	26	22.0
Ileum	21	17.5
Duodenum	12	10.0
Retroperitoneum	4	3.3
Mesentery	3	2.5
Esophagus	2	1.6
Peritoneum	2	1.6
Rectum	2	1.6
Colon	1	0.8
Bladder	1	0.8
Omentum	1	0.8

The tumors were usually intramuscular-intramural, well demarcated, but not encapsulated, unilocated or multilocated masses of variable consistency, with or without haemorrhage and necrosis.

Histologically, the reported tumors showed a variety of patterns, none of which was specifically diagnostic. Most lesions were spindle cell tumors with features resembling either smooth muscle tumors or neurogenic tumors. Epitheloid cells were also detected, usually as a minor population. The cellular arrangement was either whorled, patternless, fascicular, palisaded or storiform. Generally, the tumor cells had an eosinophilic cytoplasm. Pleomorphism was not significant and mitosis ranged from 1 to 23/10 high-power fields.

Results of immunohistochemical studies demonstrated that the tumor was most often reactive to vimentin and other markers of nerve tissues such as neuron-specific enolase (NSE), synaptophysin, S-100 protein, neurofilament, and chromogranin A (Table 3). These proteins are normally expressed by neurons from the autonomic enteric nerve plexus, supporting a histogenesis of GANTs from enteric autonomic plexuses of Meissner or Auerbach. The muscle marker desmin and muscle-specific actin could not be demonstrated, although focal alpha-SMA positivity was seen in 7 reported cases[24,27]. Except for one study (2 cases) focal staining for cytokeratins (CAM5.2) was found to be negative[26]. GANTs usually lacked smooth muscle cell features[1,2,11].

Table 3 Summary of immunohistochemical findings of 120 cases

Antigens	No. of cases studied	No. positive cases	Percent of positivity
Vimentin	103	95	92
Neuron-specific Enolase	117	105	90
Chromogranin A	92	10	11
Synaptophysin	105	33	31
S-100 protein	117	44	38
Neurofilaments	87	14	16
Vasoactive intestinal peptide	25	5	20

Over the last two years GANTs were also tested for CD117 and almost all of them were positive[10].

Ultrastructural studies of all the reported cases revealed features suggestive of myenteric plexus in origin. The diagnostic ultrastructural features included the presence of long, closely opposed cell processes containing intermediate filaments, dense-core neurosecretory granules, microtubules, and synapse-like structures with variable numbers of neurosecretory granules and small vesicles. The essential ultrastructural criteria applied for the diagnosis of GANT in all reported cases included neurosecretory granules and intermediate filaments. It should be noted that five reported GANTs showed weak signs of smooth-muscle morphology. Therefore, the presence of smooth muscle cell features might also suggest GANT[6].

The primary therapy in almost all reported cases was surgical resection or debulking, in 2 cases preceded by radiotherapy, and in nine cases preceded by chemotherapy. Three patients received chemotherapy alone. There was no evidence of clinical response using chemotherapy or radiation. As demonstrated in our report, aggressive tumor debulking without any further treatment could also be considered suitable in terms of prolonged survival and quality of life.

According to published reports, 8 patients out of 67 (12%) had metastases at clinical presentation and 18 patients (27%) developed metastases during follow up (Table 4). The estimated survival curve of the clinically documented cases (n = 67) is shown in Figure 4.

Table 4 Metastases of reported GANT cases (n = 67)

Metastases at clincal presentation			Metastases in clinical follow up		
	No. of patients	%		No. of patients	%
Location	8	12	Location	18	27
Liver	7	10	Liver	6	9
			Retroperitoneal 4	6	
Lymph node	2	3	Local recurrence	5	7
			Omentum	3	4
Omentum	2	3	Mesentery	2	3
			Peritoneum	2	3

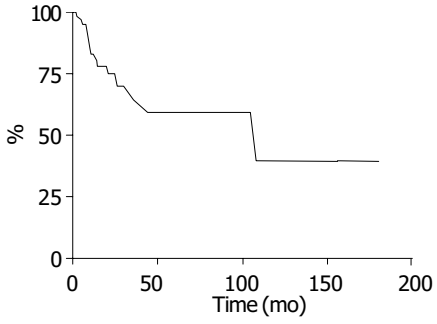

Figure 4 Estimated Kaplan-Meier survival curve of 67 reported patients.

Gastrointestinal autonomic nerve tumors occurred with an estimated frequency of 1% of all malignant gastrointestinal tumors and up to 25% of gastrointestinal stromal tumors[6]. In retrospective studies of collected pathological specimens, several investigators found that light microscopic studies yielded ambiguous results and ultrastructural examination was required in order to establish an accurate diagnosis of gastrointestinal autonomic nerve tumor[6,20,26].

Based on these observations we believe that GANTs are probably more common than previously thought. The rarity of GANT may therefore be a consequence of the unavailability of routine electron microscopic analysis. The exact biological behavior of GANTs is not fully elucidated because of the limited

number of reported cases, but it appears that, despite their low grade malignant histological appearance, most GANTs had an uncertain and a poor prognosis in case of metastases. With respect to one of our patients long term survival was possible even with metastatic diseases. Preliminary data indicated no significant correlation between treatment, tumor site and clinical outcomes[2,15].

Some authors suggested that GANTs should be regarded as a type of GISTs because of their mostly identical c-kit mutations[10,39]. Others argued that this common feature might not justify considering GIST and GANT as the same entity because of the neuronal nature of GANT[6]. The recent observation that most GANTs were CD117 positive could have an important clinical impact, since tyrosine kinase inhibitors have yielded good responses in other CD117 positive tumor entities. To date there are no reports on the use of tyrosine kinase inhibitors in CD 117 positive GANTs, but promising data for c-kit positive GISTs which were successfully treated with tyrosine kinase inhibitors have recently been published[39].

Radical surgical resection appears to be the most promising and solely curative treatment regimen for gastrointestinal autonomic nerve tumors. However, as demonstrated in case 1, patients with metastases might also survive for a long time. Some studies in the literature report had similar findings. We therefore suggest that even in cases of large tumor masses, non- curative, aggressive surgical tumor debulking is potentially useful to improve the patient's quality of life. For metastatic CD117 positive tumors tyrosine kinase inhibitors might be an appropriate palliative treatment approach. As demonstrated in case 2, GAN tumors could also involve unusual anatomic sites like Meckel's diverticulum.

To gain more information about this distinct type of GISTs, careful ultrastructural and immunohistochemical studies of all GIST cases would be beneficial. We are aware that ultrastructural examination is not available at every clinical pathology unit. However, we propose that pathologists harvest small specimens of the tumor for analysis at specialized institutions. An accurate histological diagnosis seems to be essential in order to ensure that all patients receive adequate and timely treatment and furthermore to learn more about this tumor and its biological behavior especially with respect to newly developed drugs like tyrosine kinase inhibitors. To date there is no difference in the surgical treatment of GANTs and GISTs. But there is some evidence that these tumors are from different origins and may therefore exhibit distinct biological behaviors. However, due to the limited number of reported GANTs further investigations would be necessary to fully characterize these tumors with respect to future treatment decisions.

ACKNOWLEDGMENT

We thank Christine Brostjan, PhD for critical review of the manuscript.

REFERENCES

1 **Herrera GA**, Pinto de Moraes H, Grizzle WE, Han SG. Malignant small bowel neoplasm of enteric plexus derivation (plexosarcoma). Light and electron microscopic study confirming the origin of the neoplasm. *Dig Dis Sci* 1984; **29**: 275-284
2 **Herrera GA**. Small bowel neoplasm. *Dig Dis Sci* 1985; **30**: 698
3 **Walker P**, Dvorak AM. Gastrointestinal autonomic nerve (GAN) tumor. Ultrastructural evidence for a newly recognized entity. *Arch Pathol Lab Med* 1986; **110**: 309-316
4 **Tortella BJ**, Matthews JB, Antonioli DA, Dvorak AM, Silen W. Gastric autonomic nerve (GAN) tumor and extra-adrenal paraganglioma in Carney's triad. A common origin. *Ann Surg* 1987; **205**: 221-225
5 **Dvorak AM**. Gut autonomic nerve (GAN) tumors. In: Watanabe S, Wolf M, Sommers SC, eds. Digestive disease pathology. Vol 2. *Philadelphia WB Saunders* 1989: 49-66
6 **Eyden B**, Chorneyko KA, Shanks JH, Menasce LP, Banerjee SS. Contribution of electron microscopy to understanding cellular differentiation in mesenchymal tumors of the gastrointestinal tract: a study of 82 tumors. *Ultrastruct Pathol* 2002; **26**: 269-285
7 **Miettinen M**, Sobin LH, Sarlomo-Rikala M. Immunohistochemical spectrum of GISTs at different sites and their differential diagnosis with a reference to CD117 (KIT). *Mod Pathol* 2000; **13**: 1134-1142
8 **Schmid S**, Wegmann W. Gastrointestinal pacemaker cell tumor: clinicopathological, immunohistochemical, and ultrastructural study with special reference to c-kit receptor antibody. *Virchows Arch* 2000; **436**: 234-242
9 **Kindblom LG**, Remotti HE, Aldenborg F, Meis-Kindblom JM. Gastrointestinal pacemaker cell tumor (GIPACT): gastrointestinal stromal tumors show phenotypic characteristics of the interstitial cells of Cajal. *Am J Pathol* 1998; **152**: 1259-1269
10 **Lee JR**, Joshi V, Griffin JW Jr, Lasota J, Miettinen M. Gastrointestinal autonomic nerve tumor: immunohistochemical and molecular identity with gastrointestinal stromal tumor. *Am J Surg Pathol* 2001; **25**: 979-987
11 **Herrera GA**, Cerezo L, Jones JE, Sack J, Grizzle WE, Pollack WJ, Lott RL. Gastrointestinal autonomic nerve tumors. 'Plexosarcomas'. *Arch Pathol Lab Med* 1989; **113**: 846-853
12 **Walsh NM**, Bodurtha A. Auerbach's myenteric plexus. A possible site of origin for gastrointestinal stromal tumors in von Recklinghausen's neurofibromatosis. *Arch Pathol Lab Med* 1990; **114**: 522-525
13 **MacLeod CB**, Tsokos M. Gastrointestinal autonomic nerve tumor. *Ultrastruct Pathol* 1991; **15**: 49-55
14 **Pinedo Moraleda F**, Martinez Gonzalez MA, Ballestin Carcavilla C, Vargas Castrillon J. Gastrointestinal autonomic nerve tumours: a case report with ultrastructural and immunohistochemical studies. *Histopathology* 1992; **20**: 323-329
15 **Lauwers GY**, Erlandson RA, Casper ES, Brennan MF, Woodruff JM. Gastrointestinal autonomic nerve tumors. A clinicopathological, immunohistochemical, and ultrastructural study of 12 cases. *Am J Surg Pathol* 1993; **17**: 887-897
16 **Perez-Atayde AR**, Shamberger RC, Kozakewich HW. Neuroectodermal differentiation of the gastrointestinal tumors in the Carney triad. An ultrastructural and immunohistochemical study. *Am J Surg Pathol* 1993; **17**: 706-714
17 **Thomas JR**, Mrak RE, Libuit N. Gastrointestinal autonomic nerve tumor presenting as high-grade sarcoma. Case report and review of the literature. *Dig Dis Sci* 1994; **39**: 2051-2055
18 **Segal A**, Carello S, Caterina P, Papadimitriou JM, Spagnolo DV. Gastrointestinal autonomic nerve tumors: a clinicopathological, immunohistochemical and ultrastructural study of 10 cases. *Pathology* 1994; **26**: 439-447
19 **Kodet R**, Snajdauf J, Smelhaus V. Gastrointestinal autonomic nerve tumor: a case report with electron microscopic and immunohistochemical analysis and review of the literature. *Pediatr Pathol* 1994; **14**: 1005-1016
20 **Dhimes P**, Lopez-Carreira M, Ortega-Serrano MP, Garcia-Munoz H, Martinez-Gonzalez MA, Ballestin C. Gastrointestinal autonomic nerve tumours and their separation from other gastrointestinal stromal tumours: an ultrastructural and immunohistochemical study of seven cases. *Virchows Arch* 1995; **426**: 27-35
21 **Lam KY**, Law SY, Chu KM, Ma LT. Gastrointestinal autonomic nerve tumor of the esophagus. A clinicopathologic, immunohistochemical, ultrastructural study of a case and review of the literature. *Cancer* 1996; **78**: 1651-1659
22 **Shek TW**, Luk IS, Loong F, Ip P, Ma L. Inflammatory cell-rich gastrointestinal autonomic nerve tumor. An expansion of its histologic spectrum. *Am J Surg Pathol* 1996; **20**: 325-331
23 **Ojanguren I**, Ariza A, Navas-Palacios JJ. Gastrointestinal autonomic nerve tumor: further observations regarding an ultrastructural and immunohistochemical analysis of six cases. *Hum Pathol* 1996; **27**: 1311-1318
24 **Shanks JH**, Harris M, Banerjee SS, Eyden BP, Joglekar VM, Nicol A, Hasleton PS, Nicholson AG. Mesotheliomas with deciduoid morphology: a morphologic spectrum and a variant

not confined to young females. *Am J Surg Pathol* 2000; **24**: 285-294
25 **Sakaguchi N**, Sano K, Ito M, Baba T, Fukuzawa M, Hotchi M. A case of von Recklinghausen's disease with bilateral pheochromocytoma-malignant peripheral nerve sheath tumors of the adrenal and gastrointestinal autonomic nerve tumors. *Am J Surg Pathol* 1996; **20**: 889-897
26 **Erlandson RA**, Klimstra DS, Woodruff JM. Subclassification of gastrointestinal stromal tumors based on evaluation by electron microscopy and immunohistochemistry. *Ultrastruct Pathol* 1996; **20**: 373-393
27 **Matsumoto K**, Min W, Yamada N, Asano G. Gastrointestinal autonomic nerve tumors: immunohistochemical and ultrastructural studies in cases of gastrointestinal stromal tumor. *Pathol Int* 1997; **47**: 308-314
28 **Jain KA**, Gerscovich EO, Goodnight JJ. Malignant autonomic nerve tumor of the duodenum. *Am J Roentgenol* 1997; **168**: 1461-1463
29 **Honda K**, Mikami T, Ohkusa T, Takashimizu I, Fujiki K, Araki A, Shimoi K, Enomoto Y, Ariake K, Miyasaka N, Nihei Z, Oda K, Terada T. Gastrointestinal autonomic nerve tumor with giant abscess. A case report and literature review. *J Clin Gastroenterol* 1997; **24**: 280-285
30 **Reid I**, Suvarna SK, Wagner BE, Rogers K. Plexosarcoma of the bladder. *Eur J Surg Oncol* 1997; **23**: 463-465
31 **Donner LR**. Gastrointestinal autonomic nerve tumor: a common type of gastrointestinal stromal neoplasm. *Ultrastruct Pathol* 1997; **21**: 419-424
32 **Minni F**, Casadei R, Santini D, Verdirame F, Zanelli M, Vesce G, Marrano D. Gastrointestinal autonomic nerve tumor of the jejunum. Case report and review of the literature. *Ital J Gastroenterol Hepatol* 1997; **29**: 558-563
33 **Rueda O**, Escribano J, Vicente JM, Garcia F, Villeta R. Gastrointestinal autonomic nerve tumors (plexosarcomas). is A radiological diagnosis possible? *Eur Radiol* 1998; **8**: 458-460
34 **Lev D**, Kariv Y, Messer GY, Isakov J, Gutman M. Gastrointestinal autonomic nerve (GAN) tumor of the rectum. *J Clin Gastroenterol* 2000; **30**: 438-440
35 **Kerr JZ**, Hicks MJ, Nuchtern JG, Saldivar V, Heim-Hall J, Shah S, Kelly DR, Cain WS, Chintagumpala MM. Gastrointestinal autonomic nerve tumors in the pediatric population: a report of four cases and a review of the literature. *Cancer* 1999; **85**: 220-230
36 **Tornoczky T**, Kalman E, Hegedus G, Horvath OP, Sapi Z, Antal L, Jakso P, Pajor L. High mitotic index associated with poor prognosis in gastrointestinal autonomic nerve tumour. *Histopathology* 1999; **35**: 121-128
37 **Giessling U**, Puffer E, Ludwig K. Gastrointestinal autonomic nerve tumor (GANT)—a rate tumor of the ileum. *Chirurg* 2001; **72**: 600-602
38 **Beck A**, Jonas J, Frenzel H, Bahr R. Gastrointestinal autonomic nerve tumor. *Zentralbl Chir* 2001; **126**: 702-706
39 **Joensuu H**, Fletcher C, Dimitrijevic S, Silberman S, Roberts P, Demetri G. Management of malignant gastrointestinal stromal tumours. *Lancet Oncol* 2002; **3**: 655-664

Edited by Wang XL **Proofread by** Zhu LH and Xu FM

PO Box 2345, Beijing 100023, China
Fax: +86-10-85381893
E-mail: wjg@wjgnet.com www.wjgnet.com

World J Gastroenterol 2004;10(16):2452-2454
World Journal of Gastroenterology
 ISSN 1007-9327

• CASE REPORT •

Granular cell tumor of colon: Report of a case and review of literature

Dae-Kyung Sohn, Hyo-Seong Choi, Yeon-Soo Chang, Jin-Myeong Huh, Dae-Hyun Kim, Dae-Yong Kim, Young-Hoon Kim, Hee-Jin Chang, Kyung-Hae Jung, Seung-Yong Jeong

Dae-Kyung Sohn, Hyo-Seong Choi, Yeon-Soo Chang, Jin-Myeong Huh, Dae-Hyun Kim, Dae-Yong Kim, Young-Hoon Kim, Hee-Jin Chang, Kyung-Hae Jung, Seung-Yong Jeong, Research Institute and Hospital, National Cancer Center, Goyang, Gyeonggi 411-769, Korea
Correspondence to: Dr. Seung-Yong Jeong, Center for Colorectal Cancer, Research Institute and Hospital, National Cancer Center, 809 Madu-dong, Ilsan-gu, Goyang, Gyeonggi 411-769, Korea. syjeong@ncc.re.kr
Telephone: +82-31-920-1632 **Fax:** +82-31-920-0002
Received: 2004-03-15 **Accepted:** 2004-04-09

Abstract

Granular cell tumor (GCT) is uncommon in the colon and rectum. Here we report a case of GCT in the transverse colon. A 48-year-old male patient underwent a screening colonoscopy. A yellowish sessile lesion, about 4 mm in diameter, was found in the transverse colon. An endoscopic snare resection was performed without complication. Histological examination revealed the tumor consisted of plump neoplastic cells with abundant granular eosinophilic cytoplasm containing acidophilic periodic acid Schiff-positive, diastase-resistant granules. Immunohistochemical analysis showed the tumor cells expressed S-100 protein and neuron-specific enolase. Thus, the resected tumor was diagnosed as a GCT. Since GCTs are usually benign, endoscopic resection constitutes an easy and safe treatment. Colonoscopists should consider the possibility of GCT in the differential diagnosis of submucosal tumors of the colon.

Sohn DK, Choi HS, Chang YS, Huh JM, Kim DH, Kim DY, Kim YH, Chang HJ, Jung KH, Jeong SY. Granular cell tumor of colon: Report of a case and review of literature. *World J Gastroenterol* 2004; 10(16): 2452-2454
http://www.wjgnet.com/1007-9327/10/2452.asp

INTRODUCTION

Granular cell tumor (GCT) is relatively rare soft tissue tumor that can be located anywhere in the body. It commonly occurs in oral cavities and subcutaneous tissues, but is uncommon in the colon and rectum[1,2]. In the gastrointestinal tract, the most common site for GCT is the esophagus, followed by the duodenum, anus and stomach[3,4]. This usually benign tumor appears as a submucosal nodule, measuring less than 2 cm in diameter, and is often found incidentally during colorectal examinations[2-6]. Here we report a case of a 48-year-old man diagnosed with a GCT arising in the transverse colon and treated by endoscopic resection.

CASE REPORT

A 48-year-old man was admitted for a screening colonoscopy. He had been healthy without specific complaints, family or past medical history. At the time of colonoscopy, a yellowish, hemispheric nodule 4 mm in diameter, was found in the transverse colon. It was a firm nodule covered by intact mucosa (Figure 1). The patient underwent an endoscopic snare resection, was observed for 30 min, and then discharged. There was no immediate or delayed complication.

Figure 1 A hemispheric, yellowish submucosal tumor with intact mucosa, about 4 mm in diameter in transverse colon revealed by endoscopy.

Histological examination of the resected tissue revealed a submucosal tumor composed of solid masses of plump histiocyte-like tumor cells with abundant granular eosinophilic cytoplasm containing acidophilic periodic acid Schiff (PAS)-positive, diastase-resistant granules (Figure 2). Immunohistochemical analysis showed the tumor cells

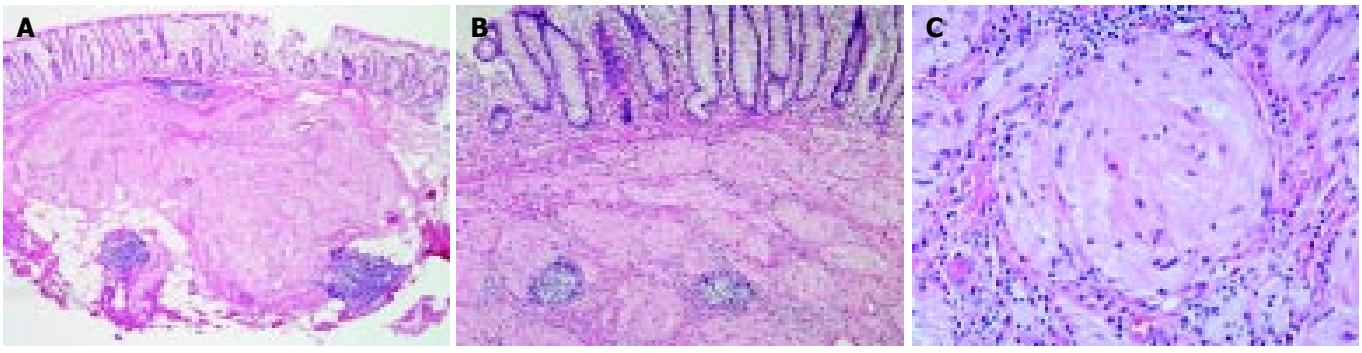

Figure 2 A submucosal tumor revealed by histological examination in resected tissue. A: Resected lesion showing a submucosal tumor covered with normal mucosa (HE staining, ×40). B: Higher magnification view of the tumor (HE staining, left: ×100; right: ×200).

Table 1 Summary of 7 cases of colorectal granular cell tumor reported in Korea

N	Year	Author	Sex / Age	Location	Size (cm)	Treatment
1	1982	Kim *et al*.[12]	F / 44	Cecum	1.5×1.5	Surgery
2	1983	Lee *et al*.[13]	F / 31	Cecum	1.0	Surgery
3	1991	Choi *et al*.[14]	F / 39	A-colon	0.9×0.8	Polypectomy
4	2000	Kim *et al*.[15]	M / 40	Appendix	0.7	Polypectomy
5	2003	Lee *et al*.[16]	F / 36	A-colon	1.5×0.6	Polypectomy
6	2003	Kim *et al*.[17]	M / 49	Rectum	0.7	Polypectomy
7	The present case		M / 48	T-colon	0.4×0.3	Polypectomy

expressed S-100 protein and neuron-specific enolase (NSE) (Figure 3), but were negative for desmin and cytokeratin. The resected tumor was diagnosed as a GCT occurring in the transverse colon.

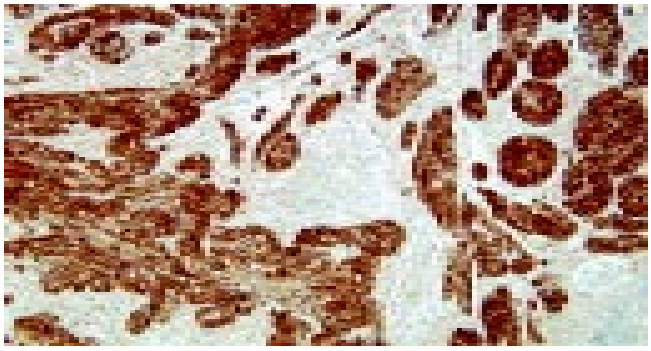

Figure 3 Diffuse and strong expression of S-100 protein in tumor shown by immunohistochemical examination (Original magnification: ×100).

DISCUSSION

GCT, first described by Abrikossoff in 1926[7], may arise virtually anywhere in the body, but was seldomly found in the gastrointestinal tract[1,2]. In most cases, gastrointestinal GCTs were found incidentally during endoscopy, and appeared as small, round submucosal nodules covered by normal mucosa[1-5,8-10]. GCTs have also been detected in the muscle layer of the gastrointestinal tract and in subserosal areas, although such findings were uncommon[2,4,11].

Endo *et al*.[10] reported 33 cases of colorectal GCT in Japan, and Rossi *et al*.[8] reported 55 patients diagnosed with GCTs of the colon. To date, 7 cases of colonic GCT have been reported in Korean literature (Table 1). This excludes two cases of perianal GCT which may have arisen from perianal skin rather than anal mucosa. Except for one rectal case, all 6 colonic GCTs reported in Korea were located in the proximal colon - ascending colon, transverse colon and cecum including the appendix. The male-to-female ratio was 1:1.3 and the mean age was 41.0±6.5 years (range 31-49 years). Bowel resection was the treatment administered for the 2 cases diagnosed before 1985, while endoscopic removal of the tumor was performed in the later cases. Advances in endoscopic diagnosis and resection probably led to the alteration in treatment approach for the latter cases.

GCT could seldomly be diagnosed based on macroscopic and endoscopic examination due to both its small size and its shape resembling a diminutive polyp[1]. Recently, endoscopic ultrasound has been frequently used for determining the depth of tumor invasion in the gastrointestinal wall, and is also useful for evaluating gastrointestinal submucosal tumors[9,10,18]. However, in the present case, it was difficult to suspect GCT because the endoscopic features of the tumor resembled those of a small sessile polyp. We performed one-stage endoscopic snare polypectomy during screening colonoscopy.

The final diagnosis of GCT depends on pathological findings. The histological markers for GCT are: (1) plump histiocyte-like, bland-looking neoplastic cells with abundant granular eosinophilic cytoplasm containing acidophilic, PAS-positive, diastase-resistant granules; (2) small, uniform nuclei, in which mitotic figures are absent; (3) neural markers, including S-100 protein or NSE expressed uniformly[10,19-22]. In the present patient, the histological findings on the resected specimen were typical of a GCT.

Although GCTs are usually benign, some malignant GCT cases have been reported. Malignancy has been found to correlate with tumor size, more than 60% of metastatic GCTs were larger than 4 cm in diameter[6,11,23]. However, in most colonic GCTs, the tumor size was less than 2 cm and the tumor was well separated from the muscularis propia. Since this tumor is considered to be usually benign, endoscopic removal has been the most appropriate choice of treatment for colonic GCT[2,8,10,24].

In conclusion, we report a case of GCT in the transverse colon. The tumor was removed by endoscopic resection and the patient was discharged without complication. GCTs of the colon can be found incidentally during colonoscopy, and endoscopic removal of the tumor is the safest and most feasible treatment. Colonoscopists should consider the possibility of GCT in the differential diagnosis of submucosal tumors of the colon.

REFERENCES

1 **Lack EE**, Worsham GF, Callihan MD, Crawford BE, Klappenbach S, Rowden G, Chun B. Granular cell tumor: a clinicopathological study of 110 patients. *J Surg Oncol* 1980;**13**: 301-316

2 **Yasuda I**, Tomita E, Nagura K, Nishigaki Y, Yamada O, Kachi H. Endoscopic removal of granular cell tumors. *Gastrointest Endosc* 1995; **41**: 163-167

3 **Melo CR**, Melo IS, Schmitt F, Fagundes R, Amendola D. Multicentric granular cell tumor of the colon: report of a patient with 52 tumors. *Am J Gastroenterol* 1993; **88**: 1785-1787

4 **Yamaguchi K**, Maeda S, Kitamura K. Granular cell tumor of the stomach coincident with two early gastric carcinomas. *Am J Gastroenterol* 1989; **84**: 656-659

5 **Kulaylat MN**. Granular cell tumor of the colon [letter]. *Dis Colon Rectum* 1996; **39**: 711

6 **Jardines L**, Cheung L, LiVolsi V, Hendrickson S, Brooks JJ. Malignant granular cell tumors: report of a case and review of the literature. *Surgery* 1994; **116**: 49-54

7 **Abrikossoff A**. Uber myoma ausgehend von der quergestreiften willkurlichen muskulatur. *Virchows Arch Pathol Anat* 1926; **260**: 215-233

8 **Rossi GB**, de Bellis M, Marone P, De Chiara A, Losito S, Tempesta A. Granular cell tumors of the colon: report of a case and review of the literature. *J Clin Gastroenterol* 2000; **30**: 197-199

9 **Nakachi A**, Miyazato H, Oshiro T, Shimoji H, Shiraishi M, Muto Y. Granular cell tumor of the rectum: a case report and review of the literature. *J Gastroenterol* 2000; **35**: 631-634

10 **Endo S**, Hirasaki S, Doi T, Endo H, Nishina T, Moriwaki T, Nakauchi M, Masumoto T, Tanimizu M, Hyodo I. Granular cell tumor occurring in the sigmoid colon treated by endo-

scopic mucosal resection using a transparent cap (EMR-C). *J Gastroenterol* 2003; **38**: 385-389
11 **Uzoaru I**, Firfer B, Ray V, Hubbard-Shepard M, Rhee H. Malignant granular cell tumor. *Arch Pathol Lab Med* 1992; **116**: 206-208
12 **Kim MJ**, Oh SH, Moon YM, Choi HJ, Kim BR, Park CI. A case of granular cell tumor of the colon. *J Korean Med Assoc* 1982; **25**: 765-769
13 **Lee SR**, Park EB. Granular cell myoblastoma of the colon. *Korean J Gastrointest Endosc* 1983; **3**: 103-107
14 **Choi JK**, Choi MG, Choi KY, Chung IS, Cha SB, Chung KW, Sun HS, Kim BS, Choi YJ, Lee AH. A case of colonoscopically removed granular cell tumor in the ascending colon. *Korean J Gastrointest Endosc* 1991; **11**: 383-386
15 **Kim HS**, Cho KA, Hwang DY, Kim KU, Kang YW, Park WK, Yoon SG, Lee KR, Lee JK, Lee JD, Kim KY. A case of granular cell tumor in the appendix. *Kor J Gastoenterol* 2000; **36**: 404-407
16 **Lee SH**, Kim SH, Kim BR, Kim HJ, Bhandari S, Jung IS, Hong SJ, Ryu CB, Kim JO, Cho JY, Lee JS, Lee MS, Shim CS, Kim BS, Jin SY. Granular cell tumor of the ascending colon: report of a case. *Intestinal Research* 2003; **1**: 59-63
17 **Kim DH**, Kim YH, Kwon NH, Song BG, Jung JH, Kim MH, Rhee PL, Kim JJ, Rhee JC. A case of granular cell tumor in the rectum. *Korean J Gastrointest Endosc* 2003; **27**: 88-91
18 **Orlowska J**, Pachlewski J, Gugulski A, Butruk E. A conservative approach to granular cell tumors of the esophagus: four case reports and literature review. *Am J Gastroenterol* 1993; **88**: 311-315
19 **Azzopardi JC**. Histogenesis of the granular cell "myoblastoma". *J Pathol* 1957; **71**: 85-94
20 **Joshi A**, Chandrasoma P, Kiyabu M. Multiple granular cell tumors of the gastrointestinal tract with subsequent development of esophageal squamous carcinoma. *Dig Dis Sci* 1992; **37**: 1612-1618
21 **Armin A**, Connelly EM, Rowden G. An immunoperoxidase investigation of S-100 protein in granular cell myoblastomas: evidence for Schwann cell derivation. *Am J Clin Pathol* 1983; **79**: 37-44
22 **Lisato L**, Bianchini E, Reale D. Granular cell tumor of the rectum: description of a case with unusual histological features. *Pathologica* 1995; **87**: 175-178
23 **Matsumoto H**, Kojima Y, Inoue T, Takegawa S, Tsuda H, Kobayashi A, Watanabe K. A malignant granular cell tumor of the stomach: report of a case. *Surg Today* 1996; **26**: 119-122
24 **Kawamoto K**, Yamada Y, Furukawa N, Utsunomiya T, Haraguchi Y, Mizuguchi M, Oiwa T, Takano H, Masuda K. Endoscopic submucosal tumorectomy for gastrointestinal submucosal tumors restricted to the submucosa: a new form of endoscopic minimal surgery. *Gastrointest Endosc* 1997; **46**: 311-317

Edited by Wang XL **Proofread by** Chen WW and Xu FM

PO Box 2345, Beijing 100023, China
Fax: +86-10-85381893
E-mail: wjg@wjgnet.com www.wjgnet.com

World J Gastroenterol 2004;10(16):2455-2456
World Journal of Gastroenterology
 ISSN 1007-9327

• CASE REPORT •

A case of leptospirosis simulating colon cancer with liver metastases

Alessandro Granito, Giorgio Ballardini, Marco Fusconi, Umberto Volta, Paolo Muratori, Vittorio Sambri, Giuseppe Battista, Francesco B. Bianchi

Alessandro Granito, Giorgio Ballardini, Marco Fusconi, Umberto Volta, Paolo Muratori, Francesco B. Bianchi, Departments of Internal Medicine, Cardioangiology, Hepatology, Alma Mater Studiorum - University of Bologna, Italy
Vittorio Sambri, Department of Clinical and Experimental Medicine, Section of icrobiology, Alma Mater Studiorum - University of Bologna, Italy
Giuseppe Battista, Department of Radiology, Alma Mater Studiorum-University of Bologna, Italy
Correspondence to: Alessandro Granito, MD, Dipartimento di Medicina Interna, Cardioangiologia, Epatologia, Policlinico S.Orsola-Malpighi, via Massarenti, 9, 40138 Bologna, Italy. gralex@libero.it
Telephone: +39-51-6363631 **Fax:** +39-51-340877
Received: 2003-12-10 **Accepted:** 2004-03-04

Abstract

We report a case of a 61-year-old man who presented with fatigue, abdominal pain and hepatomegaly. Computed tomography (CT) of the abdomen showed hepatomegaly and multiple hepatic lesions highly suggestive of metastatic diseases. Due to the endoscopic finding of colon ulcer, colon cancer with liver metastases was suspected. Biochemically a slight increase of transaminases, alkaline phosphatase and gammaglutamyl transpeptidase were present; α-fetoprotein, carcinoembryogenic antigen and carbohydrate 19-9 antigen serum levels were normal. Laboratory and instrumental investigations, including colon and liver biopsies revealed no signs of malignancy. In the light of spontaneous improvement of symptoms and CT findings, his personal history was revaluated revealing direct contact with pigs and their tissues. Diagnosis of leptospirosis was considered and confirmed by detection of an elevated titer of antibodies to leptospira. After two mo, biochemical data, CT and colonoscopy were totally normal.

Granito A, Ballardini G, Fusconi M, Volta U, Muratori P, Sambri V, Battista G, Bianchi FB. A case of leptospirosis simulating colon cancer with liver metastases. *World J Gastroenterol* 2004; 10(16): 2455-2456
http://www.wjgnet.com/1007-9327/10/2455.asp

INTRODUCTION

Leptospirosis is a zoonosis caused by spirochetes of the genus Leptospira. Humans are infected only occasionally by direct contact with infected animals or through contaminated water and soil. The clinical presentation ranges from occult infection to Weil's disease with fatal complications as hepatorenal failure. It remains underdiagnosed largely due to the broad spectrum of symptoms and signs.

CASE REPORT

A 61 year-old male farmer, non-smoker without a history of alcohol abuse or cancer, was admitted to a local hospital due to fatigue and pain in the right upper abdominal quadrant with discovery of enlarged liver over the past three days, Ultrasonography (US) showed many hypoechoic lesions scattered in all hepatic segments. A computed tomography (CT) scan of the abdomen showed substitution of the whole liver by multiple low-density lesions with mild ring enhancement highly suggestive of metastatic disease (Figure 1) and retroperitoneal small (< 1 cm) lymph nodes. Upper gastrointestinal endoscopy was negative and colonoscopy disclosed an ulcer of the transverse colon which hystologically revealed edema and necro-inflammatory damage without signs of malignancy.

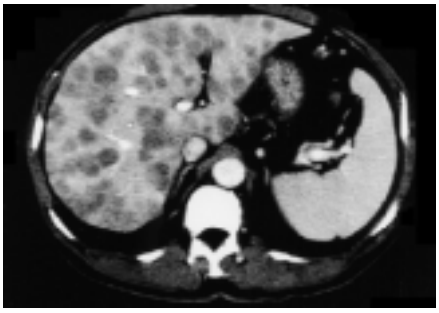

Figure 1 Contrast-enhanced abdominal CT scan (portal phase): multiple lesions appearing hypodense compared with normal liver parenchyma and showing mild ring enhancement.

Ultrasound guided liver biopsy of one of the lesions taken 10 d after admission excluded malignancy and was consistent with mild portal hepatitis and cholestasis. Laboratory tests showed alanine aminotransferase (ALT) 130 IU/l (normal<40), aspartate aminotransferase (AST) 76 IU/l (normal<37), alkaline phosphatase (ALP) 359 MU/mL (normal<280), gammaglutamyl transpeptidase (γ-GT) 252 MU/mL (normal<50). Normal serum levels of α-fetoprotein, carcinoembryogenic antigen (CEA) and carbohydrate 19-9 antigen (CA 19-9) were present. The patient refused further investigations and was discharged with the suspicion of misdiagnosed neoplastic disease. Four wk later, on admission to our Unit, the patient was in good general condition and denied a weight loss and gastrointestinal symptoms. Physical examination revealed only a mild indolent hepatomegaly. Laboratory investigations showed only ALP 443 MU/mL and γ-GT 77 MU/mL. Ultrasonography and abdominal CT scan (Figure 2) revealed a dramatic decrease both in number and volume of the hepatic lesions with unmodified vascularization pattern. Chest X-ray was unremarkable. Colonoscopy revealed an ulcer of the right colon (Figure 3) characterized under histological profile by edema and necro-inflammatory cells. Viral, autoimmune and metabolic liver diseases were excluded by appropriate tests as well as metastatic tumors, primary hepatoma, pyogenic liver abscess, parasitic liver and colon lesions and colon cancer. Due to spontaneous improvement of symptoms and CT findings, his personal history was revaluated. A direct contact with pigs and their tissues three days before the onset of symptoms was reported (the patient, living in rural areas, butchered a domestic pig). On specific request, transient hematuria before admittance was reported. The hypothesis of leptospirosis was considered and confirmed by the positive result of indirect immunofluorescence on cultured leptospires (*Leptospira interrogans* serovar icterohaemorraghiae), which showed a high titer of antibodies

to leptospira (titer 1:1024). No cross-reaction with other spirochetes (Treponema and Borrelia) was seen. In two wk' time biochemical alterations were almost subsided. Despite spontaneous recovery, treatment with tetracyclines was started and the patient was dismissed. Two mo later US, CT and colonoscopy were totally normal and after a 2-year follow-up the patient has been fine.

Figure 2 Contrast-enhanced abdominal CT scan (portal phase): after 46 d both number and volume of hepatic lesions were considerably decreased.

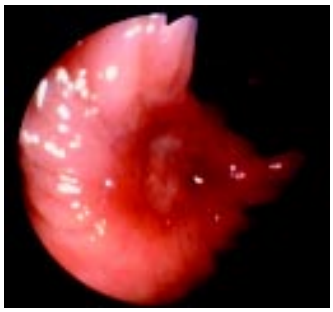

Figure 3 Endoscopic view of right colon showing an ulcerated lesion without signs of bleeding. A series of biopsies of the ulcer revealed only necro-inflammatory cells.

DISCUSSION

Leptospirosis is a worldwide zoonotic infection that commonly occurs in tropical and subtropical regions and in both urban and rural contexts. Human disease is acquired by contact with urine or tissues of an infected animal or through contaminated water and soil, whereas human-to-human transmission is rare. Diagnosis of leptospirosis is based either on isolation of the organism from the patient or on seroconversion. Antibodies generally do not appear until the second week of illness. The pathogenesis of leptospirosis is incompletely understood but it is well known that all forms of leptospires can damage small blood vessels, lead to vasculitis and spread to all organs[1]. The clinical presentation ranges from occult infection to Weil's disease with fatal complications as hepatorenal failure. The severity of disease reflects the severity of the underlying vasculitis. As a result of its protean clinical manifestations and non-specific presentations, leptospirosis has been underdiagnosed and frequently misdiagnosed as other diseases such as influenza, viral hepatitis, encephalitis, pneumonitis and acute renal failure[1-3]. The great majority of cases, as in this patient, were of mild severity (anicteric leptospirosis) and resolution coincided with the appearance of antibodies. Icteric leptospirosis, occurring between 5 and 10 % of patients, was a severe disease and often very rapidly progressive with multi-organ failure[4,5]. Treatment of leptospirosis depends on the severity of infection. Anicteric leptospirosis often requires hospital admission and close observation. Streptomycin, penicillins, cephem and tetracyclines are all effective anti-leptospiral antibiotics[4,5]. Radiological abnormalities, in particular pulmonary localization on high resolution CT (nodular densities, ground glass opacities, areas of consolidation) possibly related to haemorrhage, have been described in severe forms[6-8]. Although hepatomegaly is usual, CT evidence of multiple hepatic lesions, to our knowledge, has not yet been described in patients with leptospirosis. The histopathology of the liver in the course of leptospirosis was characterized by intrahepatic cholestasis, centrilobular necrosis with hypertrophy and hyperplasia of Kupffer cells but the architecture of parenchyma was not significantly disrupted and severe hepatic necrosis was not usual[4]. The presence of multiple hypoattenuated nodules in the liver was the most interesting feature of this case. The differential diagnosis of this CT appearance included hypovascular metastases, abscess, especially by angioinvasive organisms or lymphoma. However, the absence of a mass effect on the surrounding hepatic structures would be helpful in suggesting the possibility of an abscess correlated with damage of small blood vessels. The pathologic basis for this hypoattenuation may be correlated with a coagulative necrosis of the hepatic tissues caused by vasculitis of the hepatic vessels.

Gastrointestinal involvement with haemorrhage has been reported, mainly in the severe form of leptospirosis[2]. Interestingly, in this patient a colon ulcer was found at two different sites without any symptoms and signs of bleeding. The endoscopic and histological patterns of these colon lesions were consistent with ischemic colitis. Vascular disease of diverse etiologies and in particular vasculitis could be a cause of ischemic colitis[9].

In this patient, according to our experience, liver lesions were correlated with the endoscopic findings of colon ulcer therefore primary colon cancer with liver metastases was suspected initially. On the other hand, the CT pattern when seen in the appropriate clinical setting reduced the diagnostic suppositions of infectious disease.

In conclusion, this case, initially misdiagnosed as colon cancer with liver metastases, confirms clinical polymorphism of leptospirosis and high lights the role of a good knowledge of personal history and epidemiological data in the diagnosis of leptospirosis, especially in areas of relatively low endemicity as in western countries, where domestic animal contact is prominent sources of infection. This report also suggests that a diagnosis of leptospirosis should be considered in patients with laboratory and CT findings of liver involvement and a relevant history.

REFERENCES

1 **Plank R,** Dean D. Overview of the epidemiology, microbiology, and pathogenesis of Leptospira spp. In humans. *Microbes Infect* 2000; **2**: 1265-1276
2 **Lecour H,** Miranda M, Magro C, Rocha A, Goncalves V. Human leptospirosis-a review of 50 cases. *Infection* 1989; **17**: 8-12
3 **Katz AR,** Ansdell VE, Effler PV, Middleton CR, Sasaki DM. Assessment of the clinical presentation and treatment of 353 cases of laboratory-confirmed leptospirosis in Hawaii, 1974-1998. *Clin Infect Dis* 2001; **33**: 1834-1841
4 **Levett PN.** Leptospirosis. *Clin Microbiol Rev* 2001; **14**: 296-326
5 **Kobayashi Y.** Clinical observation and treatment of leptospirosis. *J Infect Chemother* 2001; **7**: 59-68
6 **Lee RE,** Terry SI, Walker TM, Urquhart AE. The chest radiograph in leptospirosis in Jamaica. *Br J Radiol* 1981; **54**: 939-943
7 **Henk CB,** Kramer L, Schoder M, Bankier AA, Ratheiser K, Mostbeck GH. Weil disease: importance of imaging findings for early diagnosis. *J Comput Assist Tomogr* 1996; **20**: 609-612
8 **Yiu MW,** Ooi GC, Yuen KY, Tsang KW, Lam WK, Chan FL. High resolution CT of Weil's disease. *Lancet* 2003; **362**: 117

Edited by Zhu LH **Proofread by** Xu FM

PO Box 2345, Beijing 100023, China
Fax: +86-10-85381893
E-mail: wjg@wjgnet.com www.wjgnet.com

World J Gastroenterol 2004;10(16):2457-2458
World Journal of Gastroenterology
 ISSN 1007-9327

• CASE REPORT •

Acute esophageal necrosis and liver pathology, a rare combination

Amir Maqbul Khan, Rangit Hundal, Vijaya Ramaswamy, Mark Korsten, Sunil Dhuper

Amir Maqbul Khan, Rangit Hundal, Vijaya Ramaswamy, Mark Korsten, Sunil Dhuper, North Central Bronx and Veterans Affair Hospital, New York 10710, USA
Correspondence to: Amir Maqbul Khan, 59 beaumont circle #3 Yonkers, NY 10710, USA. dramirkhan@hotmail.com
Telephone: +1-718-5849000 Ext. 6753
Received: 2003-12-12 **Accepted:** 2004-02-18

Abstract

Acute esophageal necrosis (AEN) or "black esophagus" is a clinical condition found at endoscopy. It is a rare entity the exact etiology of which remains unknown. We describe a case of 'black esophagus', first of its kind, in the setting of liver cirrhosis and hepatic encephalopathy.

Khan AM, Hundal R, Ramaswamy V, Korsten M, Dhuper S. Acute esophageal necrosis and liver pathology, a rare combination. *World J Gastroenterol* 2004; 10(16): 2457-2458
http://www.wjgnet.com/1007-9327/10/2457.asp

INTRODUCTION

Endoscopic discovery of a 'black esophagus' or 'acute esophageal necrosis' (AEN) that is unrelated to ingestion of caustic or corrosive agents is quite exceptional. It has been described only a few times in the past. Lacey *et al*. in 1991 reported 25 cases[1]. A similar report by Benoit *et al*.[2] in 1999 cited 27 cases after an extensive review of the literature. Since then there have been sporadic case reports. It is difficult to estimate its true incidence as we think this disease is largely underreported. The exact etiology of 'black esophagus' still remains unknown. We describe a case of 'black esophagus', first of its kind, in the setting of liver cirrhosis and hepatic encephalopathy.

CASE REPORT

A 59-year-old hispanic male with a known past medical history of hypertension, chronic alcohol abuse, liver cirrhosis, chronic pancreatitis and depression was admitted to the psychiatry service for aggressive behaviours, depression and suicidal ideation. On d 2, he was transferred to the medical floor after evaluation for a change in mental status with confusion, disorientation and impulsive behaviours.

A detailed history was elicited on further interrogation. Patient was known to have hypertension for 10 years for which he required monopril, metoprolol and clonidine. The history also revealed alcohol abuse for 45 years, still an active abuser, alcoholic liver cirrhosis diagnosed for 4 years and negative hepatitis B and C serologies. He had multiple previous admissions for hepatic encephalopathy and earlier in the same year underwent chemotherapy for a biopsy proven hepatocellular carcinoma. He denied smoking and illicit drug abuse.

On examination the patient was drowsy but arousable, responding to verbal commands, oriented to 'place and person', but not 'time'. He was afebrile and hemo-dynamically stable. General physical examination was normal. Cardiac, pulmonary, abdominal and neurological examinations did not show any abnormalities. Rectal examination was normal with a negative guaiac test.

Laboratory data on admission were: WBC 5.1 n/L with 48% granulocytes, hemoglobin (H)/ hematocrit (Hct) of 10.3/ 31, MCV of 80.3 fl, RDW of 15.4%, platelets of 174 /n.

Na 141 mE , K 4.5 mE, Cl 108 mE, CO_2 26.1 mE, BUN 32 mg/dL, Creatinine 2.1 mg, Gluc 134 mg, Total bili 0.6 (0.3 direct), albumin 2.8 gm, proteins 6.7 gm, alkaline phosp 217 U/L, SGOT 50 U/L, SGPT 39U/L, LD 225 U/L, PT 11.4, aPTT 27.6 s and INR 1.05 s, Ammonia 139.8 um.

Ethanol on admission was 56.2, serum Osm 312, normal TSH, syphilis(-), ferritin 593, TIBC 168, total iron 58 and iron saturation 35%, B12/folate 226/22.7. CT scan of the head was negative for bleed/metastasis or any mass. CT scan of the abdomen revealed a few scattered diverticuli and accessory spleen.

A diagnosis of hepatic encephalopathy, anemia and intra-vascular volume depletion was established based on the clinical and laboratory data. Hydration with normal saline at 125 cc/h and treatment with lactulose 445 cc qid (titrated to bowel movement) were given. The rest of the management included administration of resperidal, thiamine, folate and ativan (prn). His anti- hypertensive medications were continued and patient was placed under close observation for alcohol withdrawal.

During the following 2 d (d 4 and 5) the patient's mental status improved to full orientation without any signs of confusion, agitation and/or suicidal ideation. Ammonia level dropped to 85 um. A drop in H/Hct (9.7/29.7) was related to intravascular volume depletion.

On d 6 of admission, the patient's clinical status deteriorated with a recurrence of confusion and lethargy. Patient was found to have tachycardia (heart rate of 120/min), a blood pressure of 105/70, a positive stool guaiac test, BUN/Creatinine of 68/3, ammonia of 105 um and a drop in his H/Hct (7.8/22). His management at this point included continuous intravenous hydration, blood transfusion with 3 units of packed red blood cells and intravenous proton pump inhibitors. His anti-hypertensive medications were held. The patient was transferred to a monitored setting for further observation and an esophageal gastro-duodenoscopy (EGD) was scheduled.

EGD revealed a continuous segment (15-35 cm) of necrosis with exudates, ulcerations and friable mucosa in the middle and distal parts of the esophagus. The gastro-esophageal (GE) junction showed no evidence of varices, stomach and duodenum linings were normal. A biopsy taken from the necrotic area confirmed the findings of fibrinoid necrotic debris with hemosiderin deposits and acute inflammatory cells on pathological examination of the specimen. An ultrasound of the abdomen revealed a medical renal disease without obstruction, liver texture consistent with cirrhosis with reversal of portal venous flow and mild ascites.

The patient made an uneventful recovery over the next 3 d. He was transferred to the medical floor from where he was discharged with a follow up in the outpatient clinic. No recurrences of any GI symptoms were reported in his 3-mo-follow-up.

DISCUSSION

'Black esophagus' has been described primarily in post-mortem studies[3,4]. Goldenberg *et al*.[5] gave us a detailed endoscopic description of 2 cases in the early 1990s. In a one-year prospective study conducted in Rouen University Hospital,

France, 8 (0.2%) cases of 'acute esophageal necrosis' were identified among the 3 900 patients who underwent EGD[6]. Since then there have been only a handful of case reports. The numbers reported in the literature may highly underestimate the real incidence of this condition as suggested by this prospective trial. Acute esophageal bleeding is the most common presentation. The condition is generally seen in the elderly and those having co-morbid conditions.

A variety of mechanisms have been proposed to account for the development of this condition, and low systemic perfusion seems to play the dominant role. Other mechanisms cited include direct toxic effect[7,8], as well as indirect mucosal breakdown and acid effect[9], however, none of these have been proved. The frequent involvement of distal 1/3 esophagus[10], absence of gastric lesions, presence of necrosis of mucosal/submucosal necrosis, presence of thrombus microscopically and rapid regression of disease after hemodynamic stability were similar to ischemic colitis[11,12] and strongly support the ischemic basis for the insult.

Other conditions associated with this disease entity were prolonged hypertension[13], ischemia[5,14], hyperglycemia[1], hypersensitivity to antibiotics[15], herpetic infection[16], gastric volvulus[17], posterior mediastinal haematoma and aortic dissection[3,18], anti-cardiolipin antibodies[19] and Steven Johnson syndrome[20]. In short, a multi-factorial etiology to absence of any disease (idiopathic) is possible. The pathogenesis of ischemic insult in our case can be accounted for by the low systemic perfusion with reversal of portal venous flow and worsening of hepatic encephalopathy.

Diagnosis is established with endoscopy with or without biopsy. The differential diagnosis included melanosis[21], pseudo-melanosis[22], and acanthosis nigrans[23].

The main reported complications of AEN were esophageal stenosis and stricture formation[1,2]. Lacy *et al*.[1] reported a 15% complication rate, whereas other case series have reported very low to none. Recurrence was less than 10%[6,24] and mortality ranged between 0-33%[1,6,25]. The prognosis depends on the patient's general status rather than the extent of local esophageal necrotic lesions.

Generally there is no standardized treatment but the overall consensus favours conservative treatment with intra-venous proton pump inhibitors and short-term parenteral nutrition. The main aim is to avoid extension of insult with time for a spontaneous and aided recovery.

In short, AEN is still uncommon with exact etiology and pathogenesis largely unclear. The majority do not have any long-term sequel, only a few develop strictures and stenosis. Prognosis varies, and a majority recover with conservative treatment with death being an uncommon outcome.

REFERENCES

1 **Lacy BE,** Toor A, Benson SP, Rothstein RI, Maheshwari Y. Acute esophageal necrosis: report of two case ans a review of the literature. *Gastrointestinal Endoscopy* 1999; **49**: 527-532

2 **Benoit R,** Grobost O. Oesophage noir en rapport avec une nécrose aigue oesophagienne: un nouveau cas [French]. *Presse Med* 1999; **28**: 1509-1512

3 **Lee KR,** Stark E, Shaw FE. Esophageal infarction complicating spontaneous rupture of the thoracic aorta. *J AMA* 1977; **237**: 1233-1234

4 **Brennan JL.** Case of extensive necrosis of the esophageal mucosa following hypothermia. *J Clin Pathol* 1967; **20**: 581-584

5 **Goldenberg SP,** Wain SL, Marignani P. Acute necrotising esophagitis. *Gastroenterology* 1990; **98**: 493-496

6 **Emmanuel ES,** Savoye G, Hochain P, Herve S, Antonietti M, Lemoine F, Ducrotte P. Acute esophageal necrosis: a 1 year prospective study. *Gastrointestinal Endoscopy* 2002; **56**: 213-217

7 **Orlando RC,** Powell DW, Carney CN. Pathophysiology of acute acid injury in rabbit esophageal epithelium. *J Clin Invest* 1981; **68**: 286-293

8 **Tobey NA,** Orlando RC. Mechanisms of acid injury to rabbit esophageal epithelium: role of basolateral cell membrane acidification. *Gastroenterology* 1991; **101**: 1220-1228

9 **Bass BL,** Schweitzer EJ, Harmon JW, Kraimer J. H+back diffusion interferes with intrinsic reactive regulation of the esophageal mucosal blood flow. *Surgery* 1984; **96**: 404-413

10 **Swigart LL,** Siekert RG, Hambley WC, Anson BJ. The esophageal arteries: an anatomic study of 150 specimens. *Surg Gynecol Obstet* 1950; **90**: 234-243

11 **Marston A,** Pheils MT, Thomas ML, Morson BC. Ischaemic colitis. *Gut* 1966; **7**: 1-15

12 **Ottinger LW.** Mesenteric ischemia. *N Engl J Med* 1982; **307**: 535-537

13 **Haviv YS,** Reinus C, Zimmerman J. Black esophagus: a rare complication of shock. *Am J Gastroenterol* 1996; **91**: 2432-2434

14 **Goldenberg SP,** Wain SL, Marignani P. Acute necrotising esophagitis [letter]. *Gastroenterology* 1991; **101**: 281-282

15 **Mangan TF,** Colley AT, Wytock DH. Antibiotic-associated acute necrotising esophagitis [letter]. *Gastroenterology* 1990; **99**: 900

16 **Cattan P,** Cuillerier E, Cellier C. Black esophagus associated with herpes esophagitis. *Gastrointestinal Endoscopy* 1999; **49**: 105-107

17 **Kram M,** Gorenstein L, Eisen D, Cohen D. Acute esophageal necrosis associated with gastric volvulus. *Gastrointestinal Endoscopy* 2000; **51**: 610-612

18 **Minatoya K,** Okita Y, Tagusari O, Imakita M, Yutani C, Kitamura S. Transmural necrosis of the esophagus secondary to acute aortic dissection. *Ann Thorac Surg* 2000; **69**: 1584-1586

19 **Cappell MS.** Esophageal necrosis and perforation associated with the anticardiolipin antibody syndrome. *Am J Gastroenterol* 1994; **89**: 1241-1245

20 **Mahe A,** Keita S, Blanc L, Bobin P. Esophageal necrosis in the Stevens-Johnson syndrome. *J Am Acad Derm* 1993; **29**: 103-104

21 **Sharma S,** Venkateswaran S, Chacko A, Mathan M. Melanosis of the esophagus. *Gastroenterology* 1991; **100**: 13-16

22 **Kimball MW**. Pseudomelanosis of the esophagus. *Gastrointest Endosc* 1978; **24**: 121-122

23 **Geller A,** Aguilar H, Burgart L, Gostout CJ. The black esophagus. *Am J Gastroenterol* 1995; **90**: 2210-2212

24 **Nayyar AK**, Royston C, Slater D, Bardhan KD. Pseudomembranous esophagitis. *Gastrointestinal Endoscopy* 2001; **54**: 730-735

25 **Moreto M,** Ojembarrena E, Zabella M, Tanago JG, Ibanez S. Idiopathic acute esophageal necrosis: not necessarily a terminal event. *Endoscopy* 1993; **25**: 534-536

Edited by Zhu LH **Proofread by** Xu FM

PO Box 2345, Beijing 100023, China
Fax: +86-10-85381893
E-mail: wjg@wjgnet.com www.wjgnet.com

World J Gastroenterol 2004;10(16):2459-2460
World Journal of Gastroenterology
 ISSN 1007-9327

• CASE REPORT •

Dysphagia lusorium in elderly: A case report

Bulent Kantarceken, Ertan Bulbuloglu, Murvet Yuksel, Ali Cetinkaya

Bulent Kantarceken, Division of Gastroenterology, Medical Faculty, Sutcu Imam University, Kahramanmaras, Turkey
Ertan Bulbuloglu, Department of General Surgery, Medical Faculty, Sutcu Imam University, Kahramanmaras, Turkey
Murvet Yuksel, Department of Radiodiagnostic, Medical Faculty, Sutcu Imam University, Kahramanmaras, Turkey
Ali Cetinkaya, Department of Internal Medicine, Medical Faculty, Sutcu Imam University, Kahramanmaras, Turkey
Correspondence to: Bulent Kantarceken, Yenisehir Mah. 22. Sokak Ahenk Apt.No;17/5, Kahramanmaras, Turkey. bkantarceken@inonu.edu.tr
Telephone: +90-344-2210915 **Fax:** +90-344-2212371
Received: 2004-03-09 **Accepted:** 2004-04-09

Abstract

AIM: Late unset of dysphagia due to vascular abnormalities is a rare condition. We aimed to present a case of right subclavian artery abnormalities caused dysphagia in the elderly.

METHODS: A 68-year-old female was admitted with dysphagia seven months ago. Upper endoscopic procedures and routine examinations could not demonstrate any etiology. Multislice computed thorax tomography was performed for probable extra- esophagial lesions.

RESULTS: Multislice computed thorax tomography showed right subclavian artery abnormality and esophagial compression with this aberrant artery.

CONCLUSION: Causes of dysphagia in the elderly are commonly malignancies, strictures and/or motility disorders. If routine examinations and endoscopic procedures fail to show any etiology, rare vascular abnormalities can be considered in such patients. Multislice computed tomography is a usefull choice in such conditions.

Kantarceken B, Bulbuloglu E, Yuksel M, Cetinkaya A. Dysphagia lusorium in elderly: A case report. *World J Gastroenterol* 2004; 10(16): 2459-2460
http://www.wjgnet.com/1007-9327/10/2459.asp

INTRODUCTION

Dysphagia Lusoria was first described by Bayford in 1794 in a 62 year-old woman[1]. Postmortem examination of this case showed the abnormal origination of right subclavian artery from aortic arch and compression on the esophagus. Abnormalities of the thoracic aorta and great vessels are not uncommon and can result in esophageal compression and dysphagia. The most common congenital abnormality of the aorta is an isolated aberrant right subclavian artery[2]. Usually this abnormality does not lead to symptoms. However, sometimes dysphagia (dysphagia lusoria) develops. Mass effect on the esophagus can cause dysphagia. A right aortic arch with an aberrant left subclavian artery is less common but may also result in esophageal compression[3]. A pulmonary sliding occurs when an aberrant left pulmonary artery arises from the right pulmonary artery and passes between trachea and esophagus. Compression on both trachea and esophagus can occur. This abnormality can also be reliably detected with contrast-enhanced CT. We aimed to present a 68-year-old woman who had late onset dysphagia due to such a rare condition.

CASE REPORT

A 68-year-old female was admitted to our hospital with dysphagia nearly for seven months. Dysphagia was occuring both solid and liquids. There were no clear symptoms except dysphagia, such as loss of weight, fever, sweating at night, diarrhea, hematemesis, melena or hematochesia. She complained about odinophagia, bloating, regurgitation and epigastric pain especially after analgesic using. She also had chest pain radiating to the left arm with effort. She had a history of operation for discal hernia, ischemic heart disease and diabetes mellitus. She was using anti-ischemic drugs, analgesics (Including aspirin), beta blockers and diuretics.

In physical examination her general condition was good, thyroid was palpeable. She had mild epigastric pain with palpation and no other signs. Hgb was136 g/L, WBC (White blood cell count) was 77 000 μL, PLT was 290 000 μL in laboratory tests. Erythrocyte sedimentation rate was 10 /h, SGOT was 57 U/L, SGPT was 84 U/L, ALP was 245 U/L. Other biochemical parameters were normal (BUN, creatinine, glucose, *etc*). Markers for hepatitis A,B,C were negative. Thyroid function tests were normal. She had esophagus graphy with radiopaque two months ago showing slight compression on esophagus in lower levels. Esophagogastroduodenoscopy (EGD) 5 mo ago showed minimal hiatus hernia, reflux esophagitis and antral gastritis. Some drugs were given to the patient for these findings but her dysphagia symptoms did not relieve. EGD 3 mo after, only showed antral gastritis. Other drugs (PPIs, antiacids) were given also, but dysphagia of the patient did not relieve. After admission to our clinic, the major complaint of the patient was persistent dysphagia despite the treatments. Thorax CT was performed (Multislice spiral CT) to exclude thoracal lesion-dysphagia, it showed right subclavian artery abnormality and esophagal compression on this aberrant artery (Figures 1A, B). Multislice computed thorax tomography (MCT) showed the right subclavian artery originating from the posterior wall of the aortic arch as its last branch distal to the origin of the left subclavian artery and it passed obliquely between esophagus and vertebral column and then coursed upwards on the right side.

DISCUSSION

Dysphagia is a common problem that lowers quality of life for the elderly and a symptom that may originate from many different causes. Esophageal dysphagia could be caused by esophageal carcinoma, esophageal stricture and webs, achalasia, diffuse esophageal spasm and scleroderma, caustic esophagitis and infectious esophagitis[4]. The other rare cause of dysphagia in the elderly is vascular compression on the esophagus (Dysphagia lusoria). Based on autopsy findings, the lusorian artery had a prevalence of 0.7% in the general population[5]. Recently Fockens *et al*. found a prevalence of 0.4% in 1 629 patients who underwent endoscopy for various reasons[6]. Dysphagia lusoria might be seen in young adults[7], and in middle and/or elder ages as in our case[8]. Why it gives symptoms in

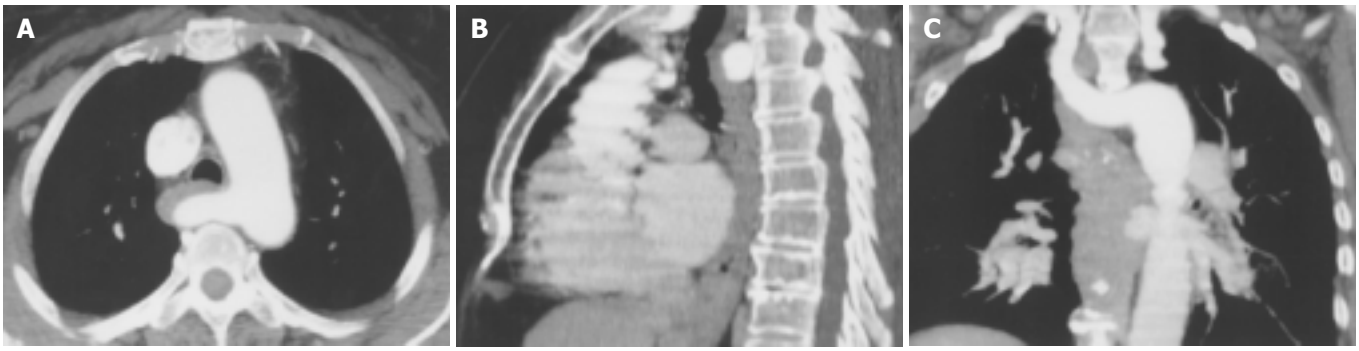

Figure 1 Axial (A) coronal (B) sagittal (C) MIP multislice CT images from the arterial phase showing right subclavian artery originating from the posterior wall of aortic arch, and compression with antreo-right lateral deplacement of esophagus by this right subclavian artery.

elderly is not clear. Some theories have been suggested, such as increased rigidity of the esophagus itself or the vessel wall, aneurysm formation, especially in the presence of a Kommerell's diverticulum[9], elongation of the aorta, and the combination of an aberrant artery and a truncus bicaroticus[10]. Interestingly in our patient, she had a history of dysphagia for 7 mo. She had not any lesion except minimal esophagitis in EGD. Reflux esophagitis can explain dysphagia sometimes. After the treatment of esophagitis with proton pump inhibitors (PPI), our patient's dysphagia symptom did not relieve. The late onset of dysphagia in our patient could be explained by the changes in vertebral column. Retrosternal goitre which may be responsable for dysphagia was not found in CT. Radiopaque graphy of the esophagus could be used to show the compression of aberrant artery on esophagus, but CT scanning and/or angiography can usually confirm the diagnosis of dysphagia lusoria. Aberrant artery could be shown with multislice CT as three dimension angiographic images were non-invasive without the need of invasive angiography[11]. Here, we also presented the multislice computed tomography angiography images of the patient with a symptomatic aberrant retro-esophagial subclavian artery compression (Figure 2).

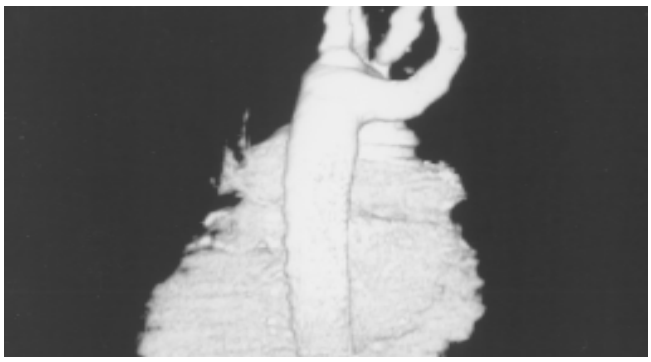

Figure 2 Volume-rendered three-dimensional image by computed tomography demonstrating aberrant artery right subclavian artery originating from the posterior wall of aortic arch.

We showed the aberrant right subclavian artery abnormality and compression on the esophagus clearly. That is why we did not repeat the radiopaque graphy of the esophagus. Coronary angiography was planned but the patient refused this procedure. So the patient was referred to a cardiovascular surgeon.

In conclusion, dysphagia in an elder patient can be caused by a rare abnormality of the subclavian artery insertion. Multislice CT can reveal this abnormality.

REFERENCES

1 **Bayford D.** An account of singular case of obstructed deglutition. *Memoires Med Soc London* 1794; **2:** 275–286
2 **McLoughlin MJ,** Weisbrod G, Wise DJ, Yeung HP. Computed tomography in congenital anomalies of the aortic arch and great vessels. *Radiology* 1981; **138:** 399-403
3 **Jaffe RB.** Radiographic manifestations of congenital anomalies of the aortic arch. *Radiol Clin North Am* 1991; **29:** 319-334
4 **Barloon TJ,** Bergus GR, Lu CC. Diagnostic imaging in the evaluation of dysphagia. *Am Fam Physician* 1996; **53:** 535-546
5 **Molz G,** Burri B. Aberrant subclavian artery (arteria lusoria): Sex differences in the prevalence of various forms of the malformations. Evaluation of 1378 observations. *Virch Arch A Pathol Anat Histol* 1978; **380:** 303–315
6 **Fockens P,** Kisman K, Tytgat GNJ. Endosonographic imaging of an aberrant right subclavian (lusorian) artery. *Gastrointest Endosc* 1996; **43:** 419
7 **Ballotta E,** Bardini R, Bottio T. Aberrant right subclavian artery. An original median cervical approach. *J Cardiovasc Surg* 1996; **37:** 571-573
8 **Cullen DM,** Kirk RK, Joseph IM. Late-onset dysphagia lusoria. *Ann Thorac Surg* 2001; **71:** 710-712
9 **Brown DL,** Chapman WC, Edwards WH, Coltharp WH, Stoney WS. Dysphagia lusoria: Aberrant right subclavian artery with a Kommerell's diverticulum. *Am Surg* 1993; **59:** 582-586
10 Janssen M, Baggen MG, Veen HF, Smout AJ, Bekkers JA, Jonkman JG, Ouwendijk RJ. Dysphagia lusoria: clinical aspects, manometric findings, diagnosis, and therapy. *Am J Gastroenterol* 2000; **95:** 1411-1416
11 **Gareth J MH,** Owens PE, Roobottom CA. Aberrant right subclavian artery and dysphagia lusoria. *N Engl J Med* 2002; **347:** 1532

Edited by Wang XL **Proofread by** Xu FM

PO Box 2345, Beijing 100023, China
Fax: +86-10-85381893
E-mail: wjg@wjgnet.com www.wjgnet.com

World J Gastroenterol 2004;10(16):2461-2463
World Journal of Gastroenterology
 ISSN 1007-9327

• CASE REPORT •

Minute gastric carcinoid tumor with regional lymph node metastasis: A case report and review of literature

Shu-Duo Xie, Lin-Bo Wang, Xiang-Yang Song, Tao Pan

Shu-Duo Xie, Lin-Bo Wang, Xiang-Yang Song, Tao Pan, Department of Oncologic Surgery, Sir Run Run Shaw Hospital, College of Medical Science, Zhejiang University, Hangzhou 310016, Zhejiang Province, China
Correspondence to: Dr. Shu-Duo Xie, Department of Oncologic Surgery, Sir Run Run Shaw Hospital, College of Medical Science, Zhejiang University, 3 Qingchun East Road, Hangzhou 310016, Zhejiang Province, China. jamestse@netease.com
Telephone: +86-571-86959492
Received: 2003-12-12 **Accepted:** 2004-02-18

Abstract

We have encountered an unusual case of gastric carcinoid tumor. Gastroscopic examination of this 32-year-old male patient showed a smooth protrusion at the greater curvature of the gastric body with a central depression, identified by subsequent biopsy as carcinoma. The patient had a normal serum gastrin level and was negative for anti-parietal cell antibody. Histological examination of the resected gastric tissues showed that the tumor was a carcinoid, 0.3 cm×0.3 cm in size with only one regional lymph node metastasis. We reviewed the pathogenesis, clinical presentation, diagnosis and treatment of gastric carcinoids and raise the possibility of being a lymph vessel-related metastasis even for a minute carcinoid tumor. Sentinel lymph node biopsy is recommended for surgery of minute carcinoid tumors.

Xie SD, Wang LB, Song XY, Pan T. Minute gastric carcinoid tumor with regional lymph node metastasis: A case report and review of literature. *World J Gastroenterol* 2004; 10 (16): 2461-2463
http://www.wjgnet.com/1007-9327/10/2461.asp

INTRODUCTION

Carcinoid tumors represent an unusual and complex disease spectrum with protean clinical manifestations. Gastric carcinoids account for 3 of every 1 000 gastric neoplasms. Gastric carcinoids types I and II generally follow a benign course, with 9% to 30% developing metastases, usually multiple and small characterized by infiltration restricted to the mucosa and submucosa. The third type of gastric carcinoids (type III, sporadic tumors) occurs without hypergastrinemia but often progresses in an aggressive course, 54% to 66% of which may develop metastases. Approximately 50% of these often large, single tumors have atypical histology, and some patients may develop carcinoid syndrome; but except for rare cases, carcinoid tumor of the stomach less than 1 cm in size generally does not give rise to regional metastasis.

CASE REPORT

The patient in question was male, aged 32 years old, admitted for upper gastric discomfort after dinner for six mo, which worsened in the past two mo prior to admission. The patient complained of epigastric distention, but this did not affect his normal diet. He had no vomiting, abdominal pain, melena or regurgitation. The symptoms waxed and waned, but clearly worsened in the last two mo. Physical examination revealed no obvious anemia, the lung and heart sounds were normal, the abdomen was soft and flat, and no hepatomegaly or splenomegaly was noted, nor was an abdominal mass palpated; rectal examination found no abnormalities, and no enlargement of the superficial lymph nodes was present. The patient was free of symptoms of hypergastrinemia or carcinoid. Gastroscopy identified a nodule on the greater curvature of the stomach, 0.6 cm by 0.6 cm in size, with erosive lesion above the nodule. Biopsy was done and the results indicated carcinoid. The patient received subsequently laparotomy in which a node was found near the pylorus, yellowish in color and 0.5 cm by 0.5 cm in size. The node was extensively resected along with the marginal area 2 cm in width. One enlarged lymph node below the pylorus was also resected. Post-operative histology revealed a 0.3 cm node, gray-white or gray-red, beneath the mucosa. Under microscope, tumor cells were seen in the submucosa and mucosa propria, uniform in shape and arranged in cribiform nests. A radical distal subtotal gastrectomy was subsequently performed, and the post-operative histology reported no residual cancer or additional metastasis in the 23 lymph nodes. The patient was then discharged and followed up for one year without findings indicative of recurrence or distant metastasis.

DISCUSSION

Carcinoid is also known as chromaffin cell carcinoma and belongs to an unusual type of tumor with relatively low malignant potential. The most frequent sites for carcinoid tumors in human are the gastrointestinal (GI) tract (74%) and the bronchopulmonary system (25%). Within the GI tract, most carcinoid tumors occur in the small bowel (29%), appendix (19%), and rectum (13%)[1]. However, the frequency of gastric carcinoid tumors has increased markedly due to endoscopic screening, performed in patients with chronic atrophic gastritis. In Japan, mass endoscopic screening for gastric lesions is common, which results in an identified frequency of gastric carcinoid tumor as high as 41% of all carcinoid tumors[2]. Zhen *et al.* reviewed 26 reports of carcinoid in China and reported 126 cases of carcinoid in the stomach from a total of 1 080 cases of GI tract carcinoid. Most gastric carcinoids occur in 40- to 60-year-old patients, irrespective of genders. Recently, a classification system was proposed to distinguish gastric carcinoid tumors into three types, namely, tumors associated with chronic atrophic gastritis (type I), tumors associated with Zollinger-Ellison syndrome (ZES, type II), and biologically more aggressive, sporadic lesions (type III)[3,4]. Currently little is known about the factors that may induce or promote the malignant growth of carcinoids[5]. For some gastric carcinoids, studies show that gastrin is an important growth factor[6], and an increased incidence of gastric carcinoids can be expected in disease states (pernicious anemia, atrophic gastritis, Zollinger-Ellison syndrome) that result in hypergastrinemia. In pernicious anemia and atrophic gastritis, 4% to 11% of the patients develop gastric carcinoids[7,8]. Patients with Zollinger-Ellison syndrome

also develop gastric carcinoids, although they are much more frequent in the subgroup with MEN 1[9]. Studies suggest that other important growth factors in some carcinoid tumors include transforming growth factor alpha (TGF-alpha) and TGF-beta[10,11], insulin-like growth factor-1 (IGF-1)[7,11], trefoid peptides (TFF1, TFF2, TFF3)[7], platelet-derived growth factor[10], vascular endothelial growth factor[12], acidic and basic fibroblast growth factor, and epidermal growth factor[10,11]. Mutations in common oncogenes, such as *K-ras*, are uncommon in GI carcinoids. Over amplification of HER2/*neu*, *c-myc*, and *c-jun* have been described in some cell lines derived from GI endocrine tumors and some carcinoids[13]. Alterations in the common tumor suppressor gene *p*53 are also uncommon in carcinoids. MEN 1 has been shown to be due to defects in the 10-exon gene on chromosome 11q13 that encodes a 610-amino acid nuclear protein[14,15]. Loss of heterozygosity at this locus has been reported to occur in 26% to 78% of cases of carcinoids, and mutations in the MEN I gene in 18%[16-18]. Microsatellite instability is rare in carcinoids[19]; however, by comparative genomic hybridization, both frequent gains (of chromosome 5, 14, 17q, 7) and losses (especially of chromosome 9p) are reported[20].

Gastric carcinoids originate from parachromaffin cells of the gastric mucosa. Tumor cells can occur virtually anywhere in the stomach, but mostly occur in the antrum. Gastric carcinoid is often difficult to diagnose due to the absence of specific symptoms or signs, especially in the early stage. When the tumor protrudes into the gastric cavity, the patient usually feels epigastric pain, suffers bloody vomiting, melena, epigastric burning, nausea or other digestive disorders. Carcinoid syndrome is seen in only a few gastric carcinoid cases where extensive dissemination or liver metastasis can be present. Gastric carcinoid in its early stage frequently escapes detection, and is usually found by gastroscopy. When the tumor grows to more than 2 cm, barium meal will help the diagnosis. The patient in this report was a young man who had only non-specific symptoms like epigastric distension without carcinoid syndrome and the tumor was near the antrum only 0.5 cm in size. The pathology was typical carcinoid. This patient did not have chronic gastritis or Zollinger-Ellison syndrome and the lesion was single, which belonged therefore to type III.

Surgical resection is the major strategy for treatment of gastric carcinoid, and chemotherapy and radiotherapy have not proved to produce obvious effects. For gastric carcinoids, the treatment is generally decided on the basis of the presence of hypergastrinemia[21-25]. Most researchers recommend that in patients with type I or II, in which hypergastrinemia is present with small lesions of less than 1 cm, the carcinoid should be removed endoscopically[22,24,25], while when the tumor exceeds 2 cm or local invasion is present, disputes over total gastrectomy[26] or only resection with antrectomy arise for type I (pernicious anemia) lesions[21]. For type I or II lesions of 1 to 2 cm, no agreement has been reached on the treatment. Some recommend that these lesions should be treated surgically[21], whereas others urge endoscopic treatment[25]. In type III gastric carcinoids not associated with hypergastrinemia, which tend to be larger and more aggressive, excision and regional lymph node clearance is recommended when the tumor grows to larger than 2 cm[21-23,25]. Some researchers prefer a similar approach for any carcinoid larger than 1 cm, whereas others consider such a resection be reserved for tumors in this size range showing histologic invasion. Most tumors smaller than 1 cm can be treated endoscopically. Tumors less than 1 cm in size are called minute carcinoids, which seldom give rise to regional lymph node metastasis, especially tumors less than 0.5 cm in size. But very rarely, minute carcinoids do have lymph node metastasis, as reported by a Japanese researcher Naitoh[27]. Such a case has not previously been reported in China. The case reported in this paper is similar to the case reported in Japan. The post-operative pathology showed only a single lesion 0.3 cm in size invading the submucosa. There was just one lymph node metastasis, which is also uncommon. Local resection of the stomach was done in the first operation, and one enlarged lymph node was resected that was identified as metastasis by histology, so subtotal gastrectomy and lymph node dissection were done in the second operation. The other lymph nodes were normal, however, we regarded this approach was appropriate.

Sentinel lymph node biopsy has been used widely for surgery of melanoma[28,29] and is currently receiving intensive study on its application for other malignant tumors such as breast, rectal and gastric cancer[30,31]. The sentinel node is the most likely lymph node that harbors metastasis. A negative sentinel lymph node (SLN) would suggest that metastatic disease has not occurred, whereas a positive SLN would indicate possible involvement of other nodes in the same basin. Therefore sentinel lymph node biopsy may be attempted in operations for minute carcinoid. If the sentinel lymph node is positive, excision and regional lymph node clearance is needed, otherwise, local resection of the stomach is sufficient.

The prognosis of gastric carcinoid is favorable and patients may expect long postoperative survival. In patients with localized disease, 5-year survival rate may reach 64%, and it was 40% for regional involvement. Postoperative chemotherapy or radiotherapy was not performed in this particular case and the one-year follow-up found no recurrence or distant metastasis.

REFERENCES

1 **Modlin IM,** Sandor A. An analysis of 8305 cases of carcinoid tumors. *Cancer* 1997; **79**: 813–829
2 **Mizuma K,** Shibuya H, Totsuka M, Hayasaka H. Carcinoid of the stomach: a case report and of 100 cases reported in Japan. *Ann Chir Gynaecol* 1983; **72**: 23–27
3 **Soreide JA,** van Heerden JA, Thompson GB, Schleck C, Ilstrup DM, Churchward M. Gastrointestinal carcinoid tumors: long-term prognosis for surgically treated patients. *World J Surg* 2000; **24**: 1431–1436
4 **Modlin IM,** Gilligan CJ, Lawton GP, Tang LH, West AB. Gastric carcinoids-the Yale experience. *Arch Surg* 1995; **130**: 250–256
5 **Oberg K.** Biology, diagnosis, and treatment of neuroendocrine tumors of the gastrointestinal tract. *Curr Opin Oncol* 1994; **6**: 441
6 **Rindi G,** Bordi C, Rappel S, La Rosa S, Stolte M, Solcia E. Gastric carcinoids and neuroendocrine carcinomas: pathogenesis, pathology, and behavior. *World J Surg* 1996; **20**: 168
7 **Modlin IM,** Tang LH. Cell and tumor biology of the gastric enterochromaffin-like cell. *Ital J Gastroenterol Hepatol* 1999; **31**: S117
8 **Kokkola A,** Sjoblom SM, Haapiainen R, Sipponen P, Puolakkainen P, Jarvinen H. The risk of gastric carcinoma and carcinoid tumours in patients with pernicious anaemia. *Scand J Gastroenterol* 1998; **33**: 88
9 **Lehy T,** Cadiot G, Mignon M, Ruszniewski P, Bonfils S. Influence of multiple endocrine neoplasia type 1 on gastric endocrine cells in patients with the Zollinger-Ellison syndrome. *Gut* 1992; **33**: 1275
10 **Oberg K.** Expression of growth factors and their receptors in neuroendocrine gut and pancreatic tumors, and prognostic factors for survival. *Ann N Y Acad Sci* 1994; **733**: 46
11 **Wulbrand U,** Wied M, Zofel P, Goke B, Arnold R, Fehmann H. Growth factor receptor expression in human gastroenteropancreatic neuroendocrine tumours. *Eur J Clin Invest* 1998; **28**: 1038
12 **Terris B,** Scoazeck JY, Rubbia L, Bregeaud L, Pepper MS, Ruszniewski P, Belghiti J, Flejou J, Degott C. Expression of vascular endothelial growth factor in digestive neuroendocrine tumours. *Histopathology* 1998; **32**: 133
13 **Evers BM,** Rady PL, Tyring SK, Sanchez RL, Rajaraman S, Townsend CM Jr, Thompson JC. Amplification of the HER-

2/neu protooncogene in human endocrine tumors. *Surgery* 1992; **112**: 211
14 **Guru SC,** Goldsmith PK, Burns AL, Marx SJ, Spiegel AM, Collins FS, Chandrasekharappa SC. Menin, the product of the MEN1 gene, is a nuclear protein. *Proc Natl Acad Sci U S A* 1998; **95**: 1630
15 **Chandrasekharappa SC,** Guru SC, Manickam P, Olufemi SE, Collins FS, Emmert-Buck MR, Debelenko LV, Zhuang Z, Lubensky IA, Liotta LA, Crabtree JS, Wang Y, Roe BA, Weisemann J, Boguski MS, Agarwal SK, Kester MB, Kim YS, Heppner C, Dong Q, Spiegel AM, Burns AL, Marx SJ. Positional cloning of the gene for multiple endocrine neoplasia-type 1. *Science* 1997; **276**: 404
16 **Jakobovitz O,** Nass D, DeMarco L, Barbosa AJ, Simoni FB, Rechavi G, Friedman E. Carcinoid tumors frequently display genetic abnormalities involving chromosome 11. *J Clin Endocrinol Metab* 1996; **81**: 3164
17 **Gortz B,** Roth J, Krahenmann A, de Krijger RR, Muletta-Feurer S, Rutimann K, Saremaslani P, Speel EJ, Heitz PU, Komminoth P. Mutations and allelic deletions of the MEN1 gene are associated with a subset of sporadic endocrine pancreatic and neuroendocrine tumors and not restricted to foregut neoplasms. *Am J Pathol* 1999; **154**: 429
18 **D'Adda T,** Keller G, Bordi C, Hofler H. Loss of heterozygosity in 11q13-14 regions in gastric neuroendocrine tumors not associated with multiple endocrine neoplasia type 1 syndrome. *Lab Invest* 1999; **79**: 671
19 **Ghimenti C,** Lonobile A, Campani D, Bevilacqua G, Caligo MA. Microsatellite instability and allelic losses in neuroendocrine tumors of the gastro-entero-pancreatic system. *Int J Oncol* 1999; **15**: 361
20 **Terris B,** Meddeb M, Marchio A, Danglot G, Flejou JF, Belghiti J, Ruszniewski P, Bernheim A. Comparative genomic hybridization analysis of sporadic neuroendocrine tumors of the digestive system. *Genes Chromosomes Cancer* 1998; **22**: 50
21 **Ahlman H,** Kolby L, Lundell L, Olbe L, Wangberg B, Granerus G, Grimelius L, Nilsson O. Clinical management of gastric carcinoid tumors. *Digestion* 1994; **55**: 77
22 **Gilligan CJ,** Lawton GP, Tang LH, West AB, Modlin IM. Gastric carcinoid tumors: the biology and therapy of an enigmatic and controversial lesion. *Am J Gastroenterol* 1995; **90**: 338
23 **Akerstrom G.** Management of carcinoid tumors of the stomach, duodenum, and pancreas. *World J Surg* 1996; **20**: 173
24 **Bordi C,** Falchetti A, Azzoni C, D'Adda T, Canavese G, Guariglia A, Santini D, Tomassetti P, Brandi ML. Aggressive forms of gastric neuroendocrine tumors in multiple endocrine neoplasia type I. *Am J Surg Pathol* 1997; **21**: 1075
25 **Ahlman H.** Surgical treatment of carcinoid tumours of the stomach and small intestine. *Ital J Gastroenterol Hepatol* 1999; **31**: S198
26 **Shi W,** Buchanan KD, Johnston CF, Larkin C, Ong YL, Ferguson R, Laird J. The octreotide suppression test and [**111In-DTPA-D-Phe]-octreotide scintigraphy in neuroendocrine tumours correlate with responsiveness to somatostatin analogue treatment. *Clin Endocrinol* 1998; **48**: 303
27 **Kumashiro R,** Naitoh H, Teshima K, Sakai T, Inutsuka S. Minute gastric carcinoid tumor with regional lymph node metastasis. *Int Surg* 1989; **74**: 198-200
28 **Shen J,** Wallace AM, Bouvet M. The role of sentinel lymph node biopsy for melanoma. *Semin Oncol* 2002; **29**: 341-352
29 **Leong SP.** Selective sentinel lymphadenectomy for malignant melanoma. *Surg Clin North Am* 2003; **83**: 157-185
30 **Tafra L.** Sentinel node biopsy for breast cancer. *Minerva Chir* 2002; **57**: 425-435
31 **Lin KM,** Rodriguez F, Ota DM. The sentinel node in colorectal carcinoma. Mapping technique, pathologic assessment, and clinical relevance. *Oncology* 2002; **16**: 567-575

Edited by Chen WW **Proofread by** Zhu LH and Xu FM